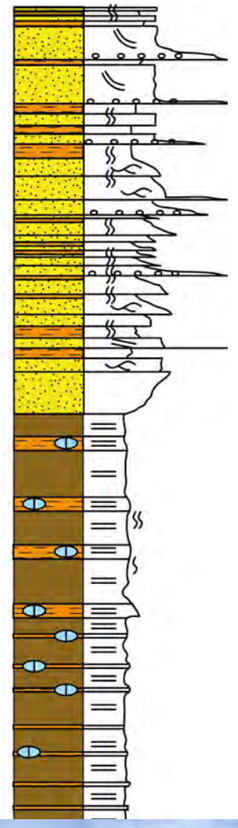

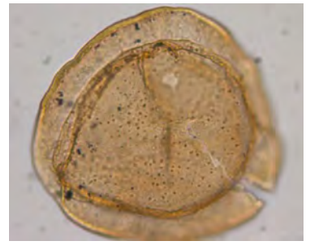

FOCUS Project

Upper Jurassic Sandstones: Detailed sedimentary facies analyses, correlation and stratigraphic architectures of hydrocarbon bearing shoreface complexes in the Dutch offshore

by Renaud Bouroullec, Roel Verreussel, Kees Geel, Dirk Munsterman, Geert de Bruin, Mart Zijp, Nico Janssen, Isabel Millán and Thijs Boxem

TNO innovation for life

TNO Report

FOCUS

Upper Jurassic Sandstones: Detailed sedimentary facies analyses, correlation and stratigraphic architectures of hydrocarbon bearing shoreface complexes in the Dutch offshore.

Date	January 2016
Author(s)	Renaud Bouroullec, Roel Verreussel, Kees Geel, Dirk Munsterman, Geert de Bruin, Mart Zijp, Nico Janssen, Isabel Millán and Thijs Boxem
No. of copies	25
Number of pages	270
Number of appendices	6 (149 pages)
Sponsors	EBN B.V., ENGIE E&P Nederland B.V., Oranje-Nassau Energie B.V., Sterling Resources Ltd and Wintershall Noordzee B.V.
Project name	FOCUS - Upper Jurassic Sandstones: Detailed sedimentary facies analyses, correlation and stratigraphic architectures of hydrocarbon bearing shoreface complexes in the Dutch offshore.

TKI FOCUS is a collaboration between

Ministry of Economic Affairs
EBN B.V.
ENGIE E&P Nederland B.V.
Oranje-Nassau Energie B.V.
Sterling Resources Ltd
Wintershall Noordzee B.V.

Management Summary

We investigated the Upper Jurassic and Lower Cretaceous in the Eastern part of the Dutch offshore to provide new insights on the regional and local stratigraphic, depositional and syn-depostional settings. Despite having numerous known reservoirs, this stratigraphic interval still holds key remaining questions regarding its depositional environments and the preservation of sandy strata. The local and regional correlation of these strata across the main structural provinces requires new analysis and insights that this project offers. The study area encompasses three main structural provinces, the Dutch Central Graben (DCG), the Terschelling Basin (TB) and the Step Graben (SG) and five platforms, namely the Cleaver Bank High (CBH), the Central Offshore Platform (COP), the Friesland Platform (FP), the Ameland Block (AB) and the Schill Grund High (SGH). The main stratigraphic interval of interest is the Upper Jurassic and Lower Cretaceous, which is divided into three sequences (Sequences 1, 2 and 3) that contain sand-rich reservoir intervals such as the Lower, Middle and Upper Graben Formations, the Friese Front Formation, the Terschelling Sandstone Member and the Scruff Greensand Formation.

This project includes sedimentological, biostratigraphic, geochemical, stratigraphic and structural analysis of subsurface data including cores, cuttings, wireline logs and seismic data. The project started in June 2014 and lasted until December 2015. The present report summarizes and compiles the results obtained by the TNO Research Team. It describes the multidisciplinary approach that was used to analyze the complex interplays between the depositional systems, active structures and paleotopographic reliefs.

1) The sedimentological analysis was achieved by detail interpretation of core data (twelve cores on eleven wells, totaling 617 m) and provided valuable information regarding the depositional environments present in the Upper Jurassic - Lower Cretaceous of the Dutch offshore. These depositional environments include continental, coastal, restricted marine and open marine settings.
2) The palynological analysis gave new constrain to better understand the depositional environments and the climatic variations during the Late Jurassic-Early Cretaceous in the study area. These palynological analyses help refining the chronostratigraphic controls of the sediments encountered at the locations of seven wells . These results were extremely valuable in constraining the regional stratigraphic correlations within such structurally complex basins that were affected by various tectonic events and growth structures (salt diapirs and active faults).
3) The geochemical analysis, carried out on nine wells, consisted of a C13 stable isotope analysis that was carried out to increase accuracy on stratigraphic age determination using a detailed reference curve compiled by the Geobiology Research Team of TNO.
4) The stratigraphic and tectonic analyses were carried out using an integrated approach. The stratigraphic correlation of key stratigraphic surfaces and intervals (including information from the new sedimentological, biostratigraphical and geochemical analyses) was achieved by correlating numerous wells along transects that were also used for regional seismic transects analysis. This combined approach allows to better constrain the structural and paleo-topographic variabilities between wells. This approach permits a robust stratigraphic analysis that includes seismically-controlled regional and local unconformities, that were often previously missed or underestimated, as well as better constrain on the complex interplays between active structures (salt bodies and faults) and syn-tectonically influenced depositional systems.

The results obtained from the combination and integration of these various analytical techniques are used to produce a new stratigraphic and tectono-stratigraphic model for the Upper Jurassic and Lower Cretaceous in the northern and eastern part of the Dutch offshore.

This project strongly improved the understanding of the Upper Jurassic and Lower Cretaceous in the Dutch offshore by providing a tectono-stratigraphic framework based on modern concepts of sequence stratigraphy and syn-depositional tectonic models. The use of regional seismic and well correlation panels helped to better constrain the three main depositional sequences identified in the study area as well as their varying preservation potential between the Dutch Central Graben, the Terschelling Basin, the Step Graben and their surrounding platforms.

Content

Recommendations on reading and accessing information in this report:

1) The report is built in a graphically heaving format with some figures that, locally, display small fonts and graphic details, For full appreciation of these graphics we recommend to use the digital version of this report in which the high resolution graphics are preserved and accessible.
2) There is a lot of cross referencing between chapters to avoid repetitions of figures and the reader will require to often turn few pages back and forth to follow some of the discussions.
3) The detailed core interpretation as well as the compiled seismic and correlation panels are displayed as single pages in the Appendices A1 and A4. These documents may be printed as stand alone A0 format posters.

1 INTRODUCTION

1 - Introduction

1.1 Research goals

- To update and increase knowledge on the distribution and stratigraphic architecture of Upper Jurassic to Lower Cretaceous reservoir sands in the Dutch Central Graben, Step Graben and Terschelling Basin.
- To decrease uncertainties related to the occurrence, spatial distribution (lateral and vertical trends) and facies of these sandstones.
- To build new and robust depositional, stratigraphic and tectono-stratigraphic models based on new biostratigraphic, facies, sequence stratigraphic and structural information.
- To relate reservoir/field scale results to key stratigraphic and tectono-stratigraphic events, by combining small-/medium-scale (laminae to reservoir scale) analysis (core, biostratigraphy, stable isotope) with sub-regional- and regional-scale wireline log and seismic analysis.

1.2 Objectives

The main objective of this project is to build a new stratigraphic framework for the Upper Jurassic and Lower Cretaceous in the Dutch Central Graben, Terschelling Basin and Step Graben by:

- interpreting core material to better understand the depositional environments encountered,
- obtaining new time lines from palynological and stable isotope techniques to better constrained the local and regional correlation between wells,
- and correlating key stratigraphic intervals throughout the study area using standard well correlation techniques combined with seismic interpretation along the same sections.

However, this project does not include any substantive seismic mapping such as time structure, isopach or attribute mapping. Such approach will be tackled in a follow up project.

1.3 Study area

The study area includes three main basins, namely the Dutch Central Graben (DCG), the Terschelling Basin (TB) and the Step Graben (SG) and five platforms, namely the Cleaver Bank High (CBH), the Central Offshore Platform (COP), the Friesland Platform (FP), the Ameland Block (AB) and the Schill Grund High (SGH). (Figure 1.1). This is an area roughly 270 km in length (in the NS direction) and an average of 120 km in width (in the EW direction), which covers the eastern part of the A, B and E blocks (east of 3° 20'), the entire B and F blocks, most of the L (L01-L09) and M (M01, M02, M04, M05, M07 and M08) blocks as well as part of the G block (G10, G13, G16 and G17).

1.4 Stratigraphic interval of interest

Three sandy stratigraphic intervals were originally proposed as main investigation targets for this project :

- Late Jurassic Lower Graben Fm./ Friese Front Fm.: Callovian to Oxfordian in age. Transgressive unit, fluvial to shoreface, N-S sediment transport direction.
- Late Jurassic Terschelling Sandstone Mb.: Early Tithonian (or Early/Middle Volgian) in age. Aggradational, barrier sandstones, parallel to the palaeo-shore lines.
- Late Jurassic/Early Cretaceous Scruff Greensand Fm./ Scruff Spiculite Mb.: Late Tithonian to Berriasian (Middle Volgian to Ryazanian) in age. Aggradational, shoreface, wide spread distribution.

These intervals are part of stratigraphic sequences studied in Munsterman *et al.* (2012), which set the stage for the present project. Each one of these sequences were deposited within a different stage of the basin's evolution (Verreussel *et al*., in prep).The project focuses on these three sandy intervals but also extends to all stratigraphic units (high and low net-to-gross units) of the Upper Jurassic to Lower Cretaceous in the study area.

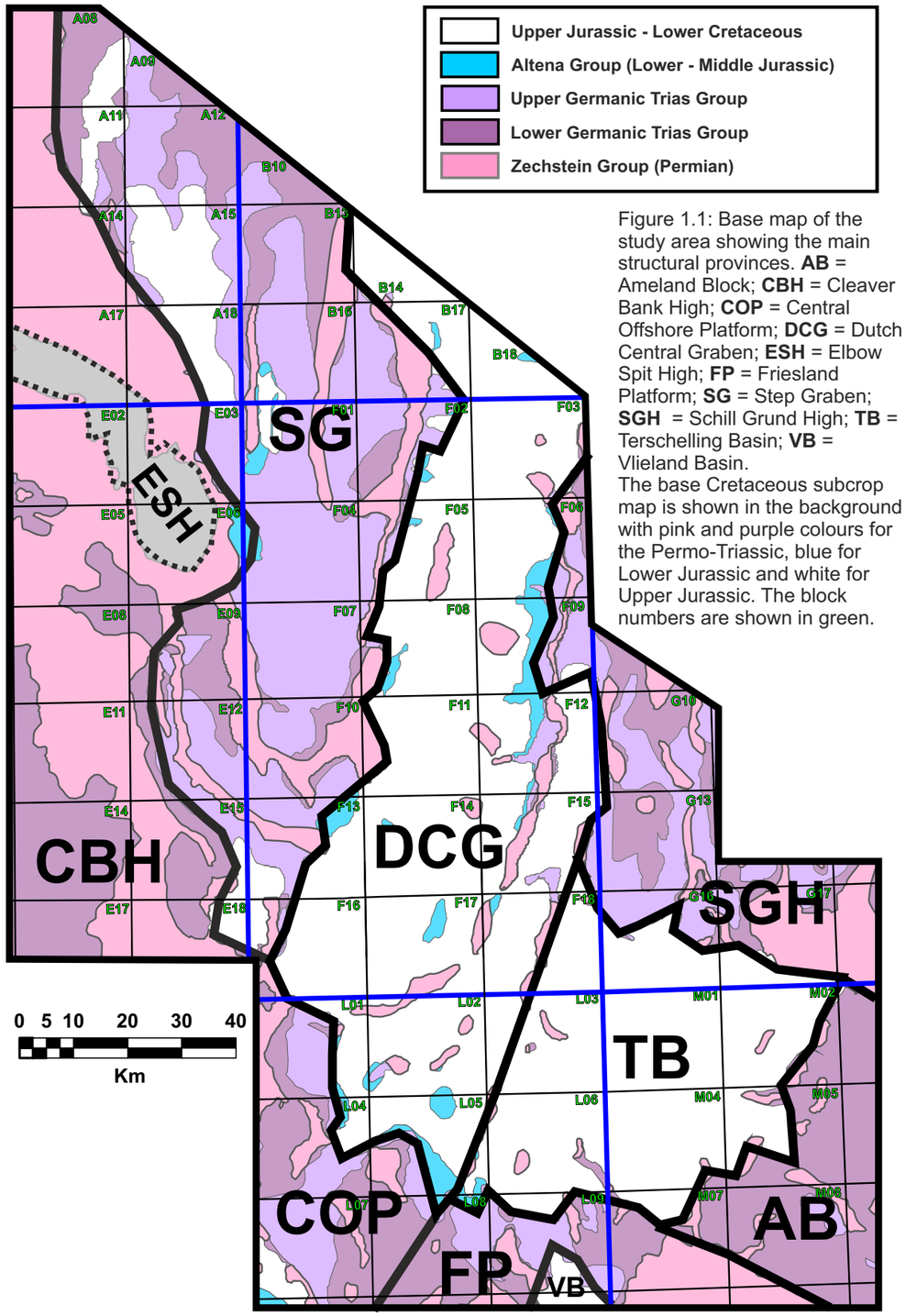

Figure 1.1: Base map of the study area showing the main structural provinces. **AB** = Ameland Block; **CBH** = Cleaver Bank High; **COP** = Central Offshore Platform; **DCG** = Dutch Central Graben; **ESH** = Elbow Spit High; **FP** = Friesland Platform; **SG** = Step Graben; **SGH** = Schill Grund High; **TB** = Terschelling Basin; **VB** = Vlieland Basin.
The base Cretaceous subcrop map is shown in the background with pink and purple colours for the Permo-Triassic, blue for Lower Jurassic and white for Upper Jurassic. The block numbers are shown in green.

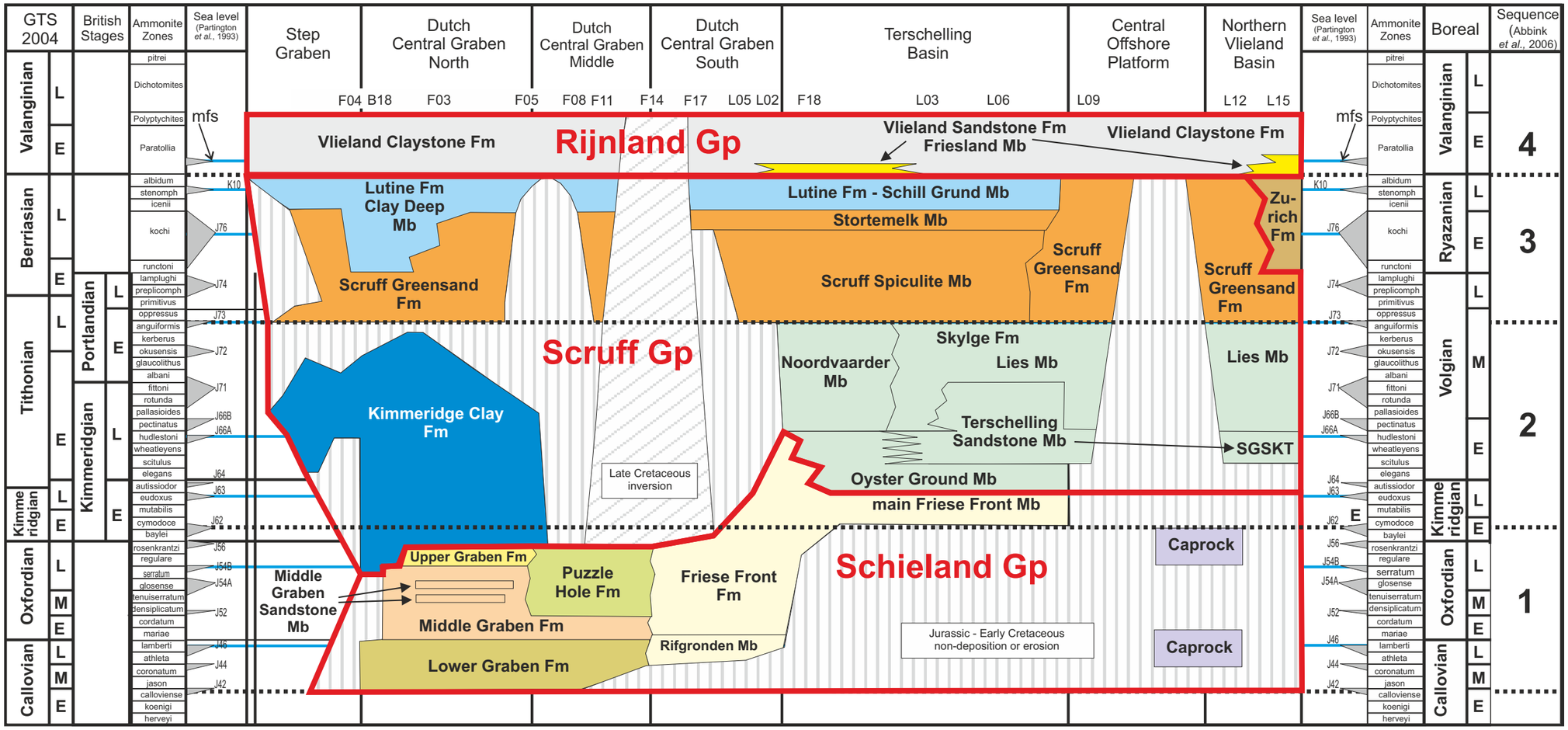

Figure 1.2: Lithostratigraphic framework of the Middle Jurassic - Early Cretaceous in the Dutch Central Graben and adjacent basins. N-S oriented section. Munsterman et *al.* (2012)

1.5 Focus Project core research team

Renaud Bouroullec	Senior Geologist (TNO)	Lead Scientist: Seismic interpretation, stratigraphic correlation, structural analysis and final integration.
Thijs Boxem	Geologist (TNO)	Project Manager.
Roel Verreussel	Senior Geologist (TNO)	Biostratigrapher: Palynological, C13 stable isotope analysis. Sequence stratigraphic interpretation and final integration.
Kees Geel	Senior Geologist (TNO)	Sedimentologist: Core description, facies and depositional system analysis.
Dirk Munsterman	Senior Geologist (TNO)	Biostratigrapher: Palynological analysis and lithostratigraphic analysis.
Geert de Bruin	Geologist (TNO)	Seismic interpretation.
Mart Zijp	Geologist (TNO)	Seismic interpretion, core description and data management.

1.6 Acknowledgments

We would like to thank Dario Ventra and Robin du Mée for their help on describing cores, Johan ten Veen for reviewing the final project report and giving valuable comments, Harmen Mijnlieff for enlightening us with his knowledge of the Upper Jurassic. A great appreciation goes to Isabelle Millan and Daniel Korosi for helping with the figures conception and the field guide preparation.
We also thank Alain Trentesaux and Freek Busschers for their help and insights during the field trip to the Boulonnais in June 2015.

We would like to thank all the industry sponsors for their financial support for the project but also for the valuable discussions we had during the various meetings, core and poster workshops as well as during the Boulonnais field trip in June 2015. We would especially like to thank Rob Lengkeek (ONE B.V.), Rutger Gras (ONE B.V.), Eveline Rosendaal (EBN B.V.), Lena Dauphin (ENGIE E&P Nederland B.V.), Ruud Lambert (Wintershall Noordzee B.V.) and Hugh Riches (Sterling Resources Ltd) for their active roles in this project.

1

GEOLOGICAL SETTING

2 - Geological Setting

The geological setting of the study area is complex since it involves several extensional, compressional and strike-slip deformation phases during the Meso-Cenozoic (Figure 2.1). The deposition settings encountered in the Upper Jurassic and Lower Cretaceous interval vary greatly and include continental, shallow marine to open marine depositional systems that are studied in the present project.

In this chapter we summarize key published geological information regarding the Mesozoic tectonic evolution and stratigraphy. The third part of this chapter summarizes the existing stratigraphic information of three sequences deposited within the study area during the Upper Jurassic and Lower Cretaceous.

2.1 Overview of the tectonic evolution of the study area and greater North Sea Region during the Mesozoic

The Mesozoic tectonic evolution of the studied part of the Dutch offshore has been summarized in several publications (Herngreen and Wong, 1989; van Adrichem *et al.,* 1997; de Jager, 2007; Geluk, 2007; Wong, 2007; Rosendaal *et al.*, 2014). It is important to place this tectonic evolution into a larger regional west-european context and various key publications are instrumental in that respect (e.g. the extensive work of Ziegler; the Millennium and Southern Permian Basin atlases).

During the Triassic and Jurassic the structural setting of the Netherlands changed from a single extensional basinal configuration (the Southern Permian Basin) to a series of smaller, fault-bounded basins and highs (De Jager, 2007). Two main tectonic events shaped the North Sea Basin during the Mesozoic: 1) the break-up of Pangea and the associated rifting during most of the Mesozoic, and 2) the closure of the Tethys Ocean/Alpine collision and the associated inversion tectonics during the late Mesozoic (culminating later during the Cenozoic).

A brief summary of the tectonic activity during the Mesozoic is presented below, with information regarding the overall North Sea region as well as specific information regarding the study area.

2.2.1 Early Triassic

The start of rifting during the Early Triassic was related to the break-up of Pangea in the proto-Atlantic between Greenland and the Fennoscandia High (Lott *et al.*, 2010) (Fig. 2.2). The southward propagation of the rift system toward the North Sea can be traced down into the northern part of the study area, breaching the Mid North Sea–Rinkøbing-Fyn High, with more prominent extensional faulting in the Northern part of the North Sea than in the study area (Zeigler, 1990; Roberts *et al.,* 1995; Coward *et al.*, 2003).

Farther south, into the study area as well as in the North German Basin, the subsidence (mainly thermal in origin) was uniform, with Buntsandstein and Muschelkalk reflectors apparently unaffected by syn-depositional faulting (Ziegler, 1990; Hoffmann & Stiewe, 1994; Geluk, 2007). The Dutch Central Graben subsided faster during the Bundsandstein depositional cycle than the platform areas (Terschelling and Vlieland basins) but not as rapidly as the Horn and Glückstadt Grabens farther to the east.

2.2.2 Middle Triassic

In response to continued thermal subsidence, the Muschelkalk strata were deposited over a wider area than the Bundsandstein series and onlap onto paleo-highs such as the London-Brabant and Bohemian massifs (Pharaoh *et al.,* 2010). Differential subsidence of the Central, Horn and Glückstadt grabens is reflected in synsedimentary faulting and increased thicknesses of Muschelkalk strata compared to areas outside the grabens (Geluk, 2005 and 2007).

Triassic sequences thicken into the newly-formed Dutch Central Graben and Broad Fourteens Basin (Fig. 2.2). The Zechstein salt was mobilized at this time with piercing salt domes and rim-syclines developing in later stages (De Jager, 2007).

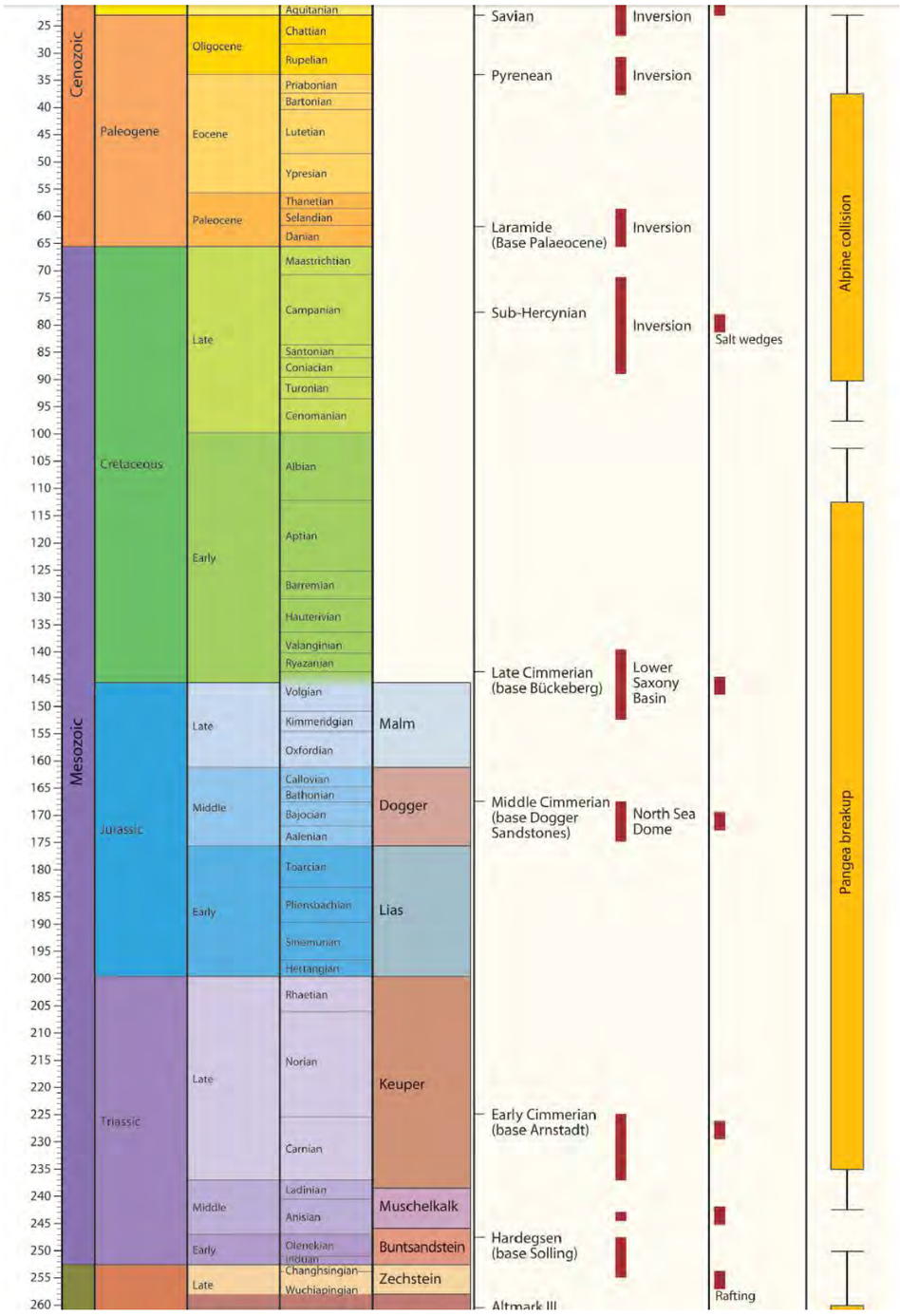

Figure 2.1: Main tectonic episodes and halokinetic episodes during the Mesozoic and Paleogene in the Southern Permian Basin (Pharaoh *et al.*, 2010).

2.2.3 Late Triassic

The North Atlantic rift system propagated southward into the Central Atlantic area (Fig. 2.2). Contemporaneous, uplift of the flanks of the rift is indicated by the increased clastic influx into the Southern Permian Basin from northern sources (Ziegler, 1988 and 1990a). In response to continued counter-clockwise rotation of Pangea, the Souther Permian Basin moved to latitudes of 30 to 40 degree N by Late Triassic times. In the Southern North Sea, the direction of extension was E-W during the Late Triassic (Pharaoh et al. 2010). The North Sea, Horn and Glückstadt grabens remained active during this period, with very minor associated volcanic activity (Ziegler, 1990a).

Stratigraphic sequences deposited during this period thicken northwards into the Dutch Central Graben and Broad Fourteens Basins, the only regions with active faulting. The faults affecting the Upper Triassic were produced by dextral transtension (Van Hoorn, 1987).The increased sediment loading upon the thick Zechstein salt in the northern Dutch offshore sector, triggered piercing of salt diapirs and the development of rim-synclines (Pharaoh et *al.*, 2010). It is important to notice that some salt structures extruded onto the basin floor to form large allochthonous overhangs onlapped by uppermost Triassic deposits (Krzywiec, 2004).

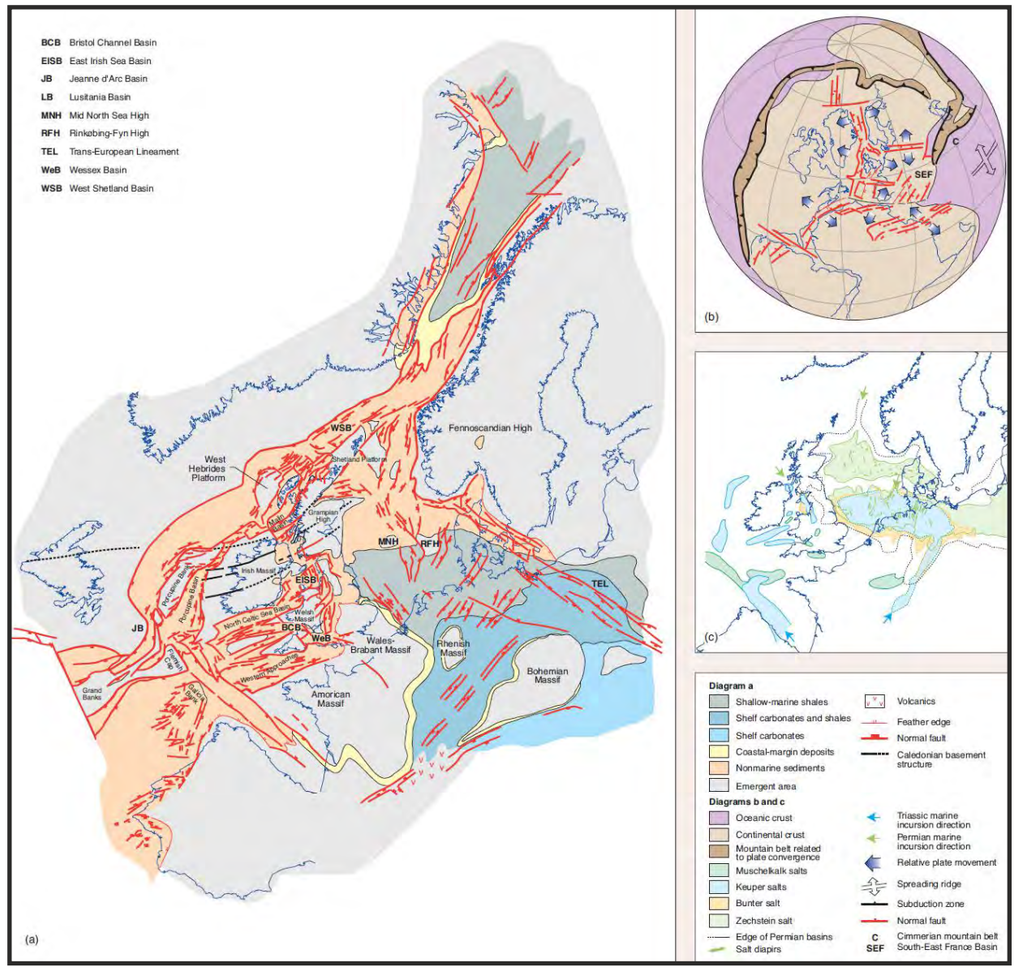

Figure 2.2: Triassic times in the North Sea Region. a) Palinspastic maps. b) Global views. c) Distribution of the basins and structures. From Coward *et al.*, 2003.

2.2.4 Early Jurassic

The North Atlantic rift propagated southwards into the Central Atlantic, with crustal separation achieved toward the end of the Early Jurassic. There seems to have been very little Early Jurassic rifting in the northern North Sea. The palaeogeography indicates infilling of the passively subsiding Triassic–Lower Jurassic rift (Coward et *al.*, 2003). Continued regional thermal subsidence of the Northern and Southern Permian basins during the Rhaetian and Hettangian, combined with a eustatic sea-level rise, controlled the development of a wide, open-marine basin. Clastics were shed into this broad, regionally subsiding basin from the Fennoscandian Shield, East European Platform and Bohemian Massif. Stagnant-water stratification led to the deposition of the Posidonia Shale Formation during the Toarcian, the principal source rock for the oil provinces of the southern North Sea and northern Germany (Ziegler, 1990a).

The Lower Jurassic series was later deeply truncated in the central North Sea during Mid- to Late Jurassic times. Nevertheless, it appears that the Early Jurassic was a period of relative tectonic quiescence, with faulting largely restricted to the Dutch Central Graben and locally to the Broad Fourteens Basin. The Cleaver Bank and Schill Grund Highs remained stable areas during much of the Early Jurassic and probably accumulated sediments hundreds of metres thick (Pharaoh et *al.*, 2010).

2.2.5 Middle Jurassic

The most important event during this period is the uplift of the central North Sea area that started towards the end of the Aalenian, presumably in response to the impingement of a transient mantle plume on the lithosphere, which continued during the Bajocian and Bathonian (Ziegler, 1990a; Underhill & Partington, 1993; Surlyk & Ineson, 2003). Development of this large thermal dome (700 × 1000 km), caused deep truncation of Lower Jurassic and even Triassic sediments and the development of the regional Mid Cimmerian Unconformity (also referred as the Intra-Aalenian Unconformity by Underhill and Partington,1993) in the central North Sea area (Fig. 2.3). This regional uplift closed the existing seaway, separating the Arctic Seas from the Tethys and Atlantic Oceans (Ziegler,1988 and 1990a). Crustal extension across the North Sea rift system persisted during the uplift of this thermal dome as shown by continued fault-controlled subsidence of the Viking Graben, the subsidence of deep half-grabens containing continental series in the Central Graben, and continued tectonic activity in the array of transtensional basins along the southern margin of the Southern Permian Basin (Ziegler, 1990a). Three major rift systems were active in the Netherlands during Mid to Late Jurassic (Figures 2.4 and 2.5): 1) the N-S oriented Dutch Central Graben-Vlieland Basin system, 2) the E-W oriented Lower Saxony Basin system, and 3) the NW-SE oriented Ruhr Valley Graben, West and Central Netherlands Basins, and Broad Fourteens Basin (extending to the UK to the Sole Pit Basin).

By late Mid-Jurassic times, the Central North Sea Dome had subsided sufficiently for open-marine conditions to be restored in the North Sea. Sedimentation resumed variably during the Callovian or Late Jurassic in areas uplifted during Mid-Jurassic times (Ziegler 1990a).

It is important to notice that the London-Brabant Massif was also uplifted during Mid-Jurassic times, its Triassic and Upper Paleozoic cover was removed to expose the Lower Carboniferous core. Fission-track data suggest that a thickness of 3000 m of sediments was removed (Van den Haute & Vercoutere, 1990).

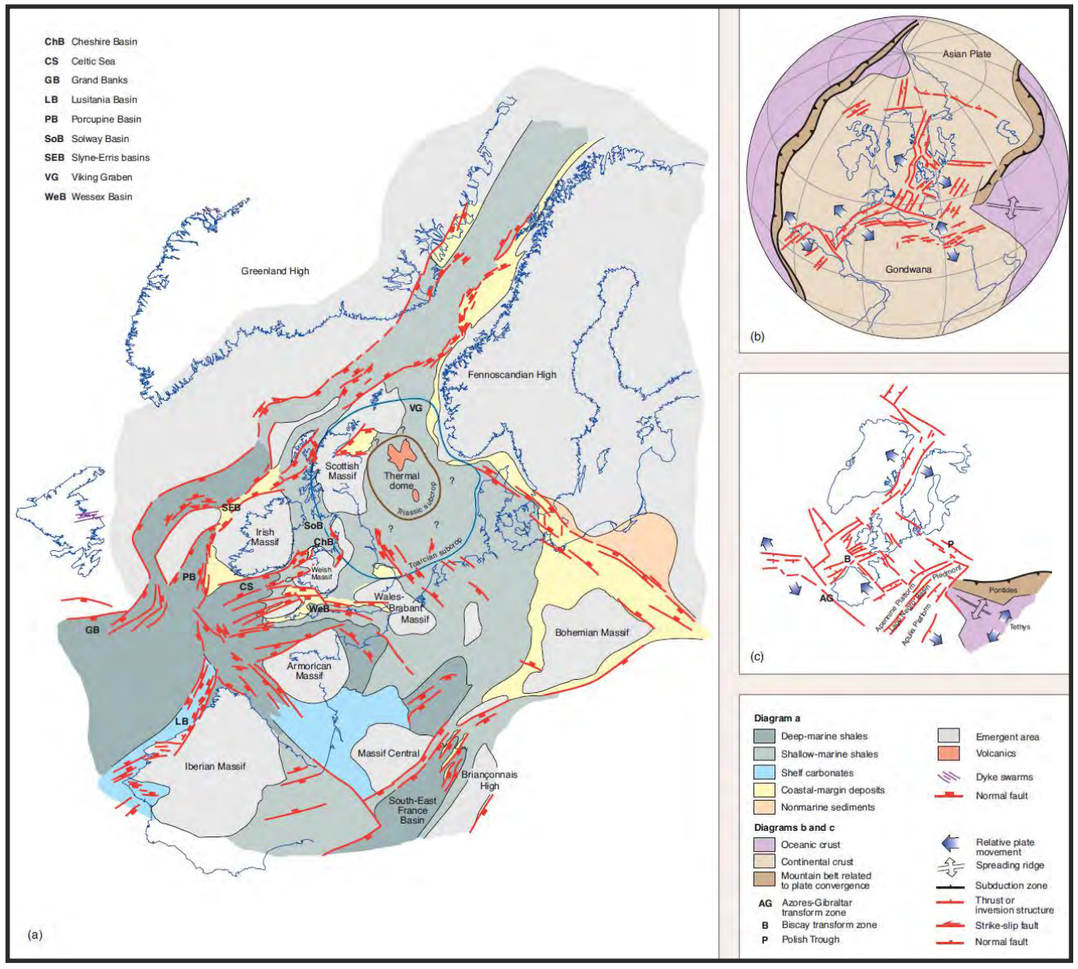

Figure 2.3: Mid-Jurassic times in the North Sea Region. a) Palinspastic maps. b) Global views. c) Distribution of the basins and structures. From Coward *et al.*, 2003.

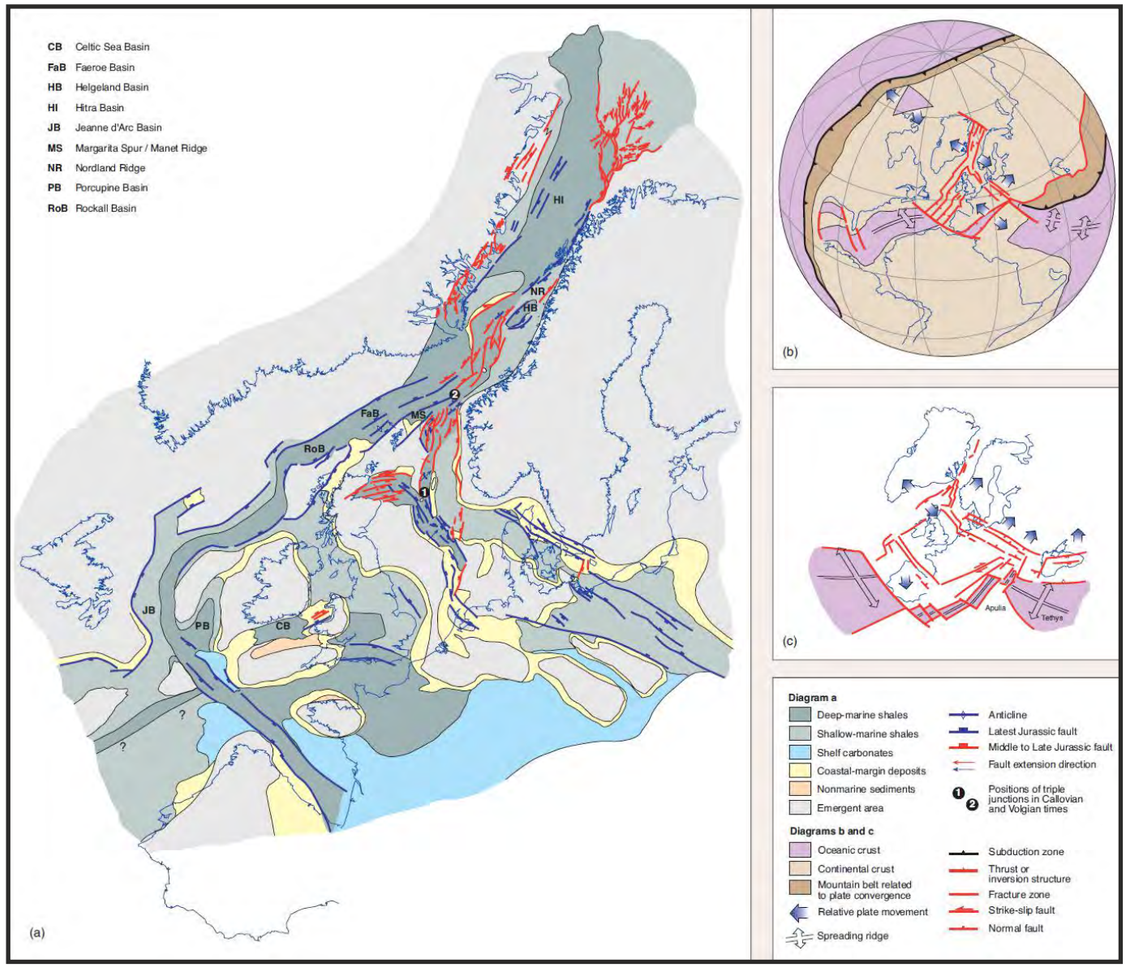

Figure 2.4: Late Jurassic times in the North Sea Region. a) Palinspastic maps. b) Global views. c) Distribution of the basins and main structures. From Coward *et al.*, 2003.

2.2.6 Late Jurassic to Early Cretaceous

Accelerated crustal extension across the North Sea rift system resulting in NW trending transtensional basins to form along the southern margin of the Southern Permian Basin (Figures 2.4, 2.5 and 2.6). This rifting phase allowed large areas to be exposed and subsequently eroded. During the Late Jurassic and Early Cretaceous transtensional subsidence occurred within northwest-oriented basins but also transpressional uplift of narrow highs along the southern margin of the Southern Permian Basin. The main tectonic elements of the Dutch sub-surface developed during the Late Jurassic and Early Cretaceous, comprising the late Cimmerian rift pulses. Extensional faulting and subsidence accelerated in the northerly trending Dutch Central Graben (Heybroek, 1975; Schroot, 1991).

A eustatic sea-level lowstand at the Jurassic-Cretaceous transition, combined with stress-induced deflection of the lithosphere, led to earliest Cretaceous emergence and erosion of large parts of western and central Europe (Ziegler, 1990a). Crustal extension across the North Sea graben system gradually decreased during the Early Cretaceous and essentially ended during the Aptian to Albian (Ziegler, 1990a; Torsvik *et al*., 2002; Coward et *al.*, 2003).

In the Dutch sector, thick fluviolacustrine to shallow-marine sequences accumulated in the Dutch Central Graben during Late Jurassic and Early Cretaceous times. Volgian to Ryazanian shales are kerogenous in the northern Dutch Central Graben (Herngreen & Wong, 1989). In the southern part of the graben, the provenance of clastic sediments was the Cleaver Bank-Broad Fourteens High, which was uplifted during Callovian times. Adjacent highs such as the Friesland Platform were uplifted and eroded at the same time. The Schill Grund High formed a stable platform area on the eastern flank of the Dutch Central Graben.

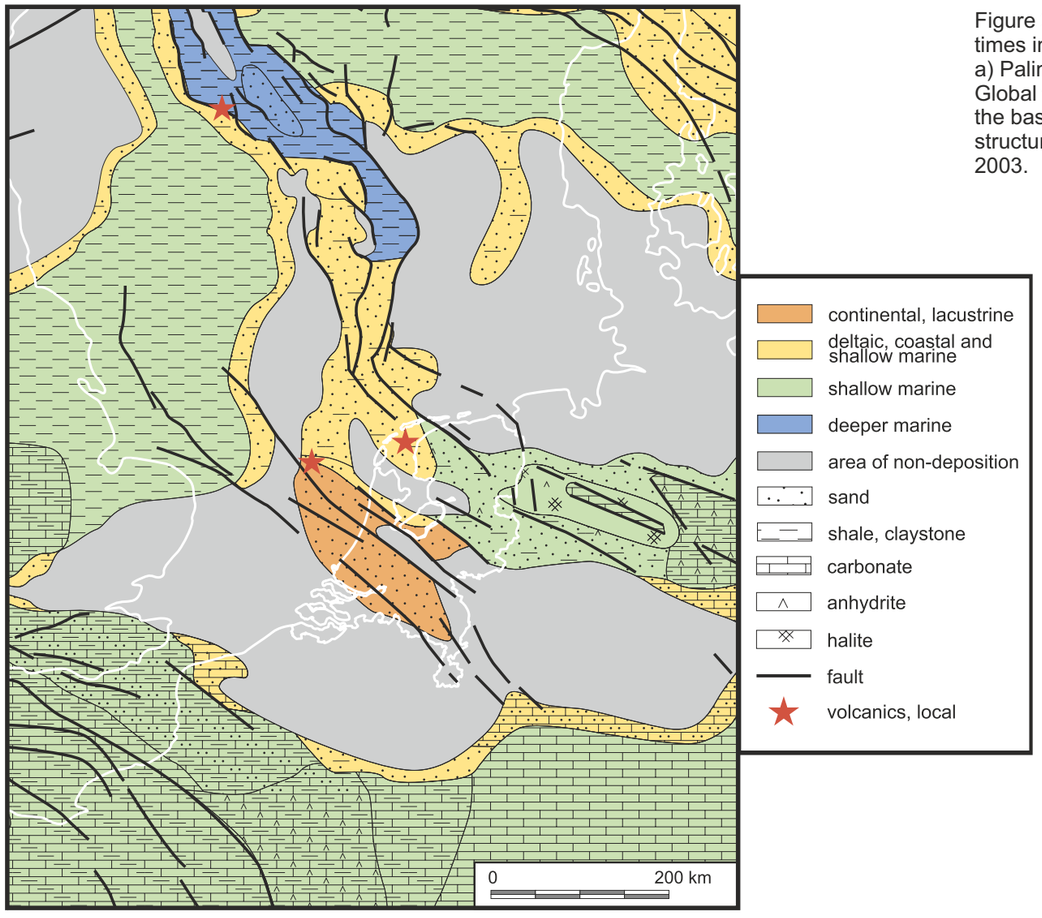

Figure 2.5: Paleogeographic map of the Netherlands and adjacent areas during the Kimmeridgian-Tithonian. Present day shorelines shown as white lines (after Ziegler, 1990; modified from Wong, 2007).

Figure 2.6: Early Cretaceous times in the North Sea Region. a) Palinspastic maps. b) Global views. c) Distribution of the basins and main structures. From Coward *et al.*, 2003.

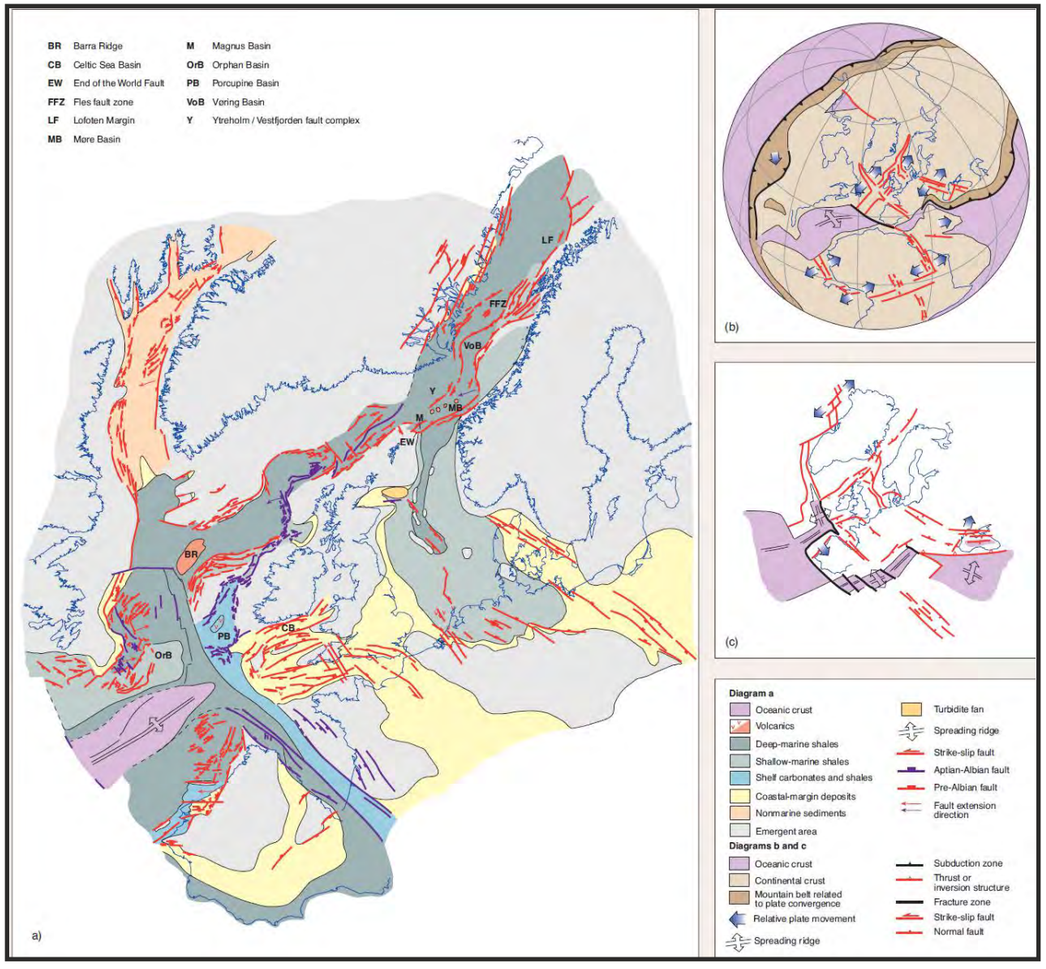

The Step Graben and Terschelling Basin subsided more slowly than the Central Graben during the Late Jurassic and accumulated thinner sequences. Salt walls developed along the main bounding faults of the Dutch Central Graben. Late Jurassic uplift of the Friesland Platform resulted in erosion down to Lower Triassic and, locally, to Zechstein levels (NITG-TNO, 2004). Basin-controlling faults accommodated the east–west extension in the Central Graben. However, due to the complex reactivation history, unambiguous evidence of dextral transtensional displacement is only available locally, for example, in the Rifgronden Fault Zone between the Terschelling Basin and the Schill Grund High (De Jager, 2007).

During Callovian to Oxfordian times, the uplift of structural highs such as the Broad Fourteens and Friesland highs shed clastics into the adjacent rapidly subsiding basins. The Zuidwal alkaline volcanic complex (Kimmeridgian) developed during the late Kimmerian rifting phase. In the Terschelling Basin, tectonic events were slightly delayed compared to the Dutch Central Graben; uplift occurred before the end of the Mid-Jurassic and a thin, younger, Upper Jurassic sequence rests on the Triassic, whereas the Lower Cretaceous sequence is thicker than in the Central Graben.

The Cleaver Bank High and Schill Grund High, which were platforms during much of Triassic to Early Jurassic times, were uplifted and eroded during the mid- to late Cimmerian rifting phases. Upper Jurassic and Lower Cretaceous syn-rift strata are consequently missing from these highs, where Triassic and Permian strata are unconformably overlain by thin post-rift Lower Cretaceous and thicker Upper Cretaceous rocks (De Jager, 2007). Hundreds of metres of Triassic to Middle Jurassic sediments were probably removed from these highs. The thick Rijnland Group (latest Ryazanian to Albian) succession, comprising mainly fine-grained clastics, was subsequently deposited across a large open-marine basin. (Pharaoh *et al.*, 2010).

2.2.7 Mid- to Late Cretaceous

The North Sea rift system became inactive and the North Atlantic Ocean started to open with rifting concentrated on areas between Europe and Greenland (Ziegler 1988 and 1990a). The Neo Tethys Ocean opened to the south of Europe during the Mid-Cretaceous and starting to close during the Late Cretaceous due to the convergence between the African and Eurasian plates (Ziegler, 1990a).

Regional thermal subsidence of the North Sea Basin started during the Hauterivian and Barremian in combination with gradually rising sea levels, and by Aptian-Albian times the southern Permian Basin was a vast shallow-marine basin. Transgression and thermal subsidence occurred during the Albian to Turonian. During the Late Cretaceous, this basin further expanded to reach its maximum extent in response to thermal subsidence and sea-level rise to about 100-200 m above the present-day level. The Upper Cretaceous Chalk series is up to 2000 m thick in the basin (Ziegler, 1990a).

In the southern Permian Basin, inversion tectonics due to the Alpine collision affected basement blocks during the late Turonian and intensified during the Senonian and the Paleocene (Ziegler, 1990a). This inversion was heterogenous with strain localized in narrow zones separated by undeformed regions (Pharaoh *et al.*, 2010). Inversion also produced decoupling on Zechstein salt and thin-skinned tectonics. The NW trend of early inverted basins and transpressional fault reactivation indicates N to NE oriented compressional stresses (Kley & Voigt, 2008).

2.2 Overview of structural elements affecting the study area since the Triassic

2.2.1 Strike slip deformation

The dominant NW-SE fault set in the Netherlands such as the Hantum and Rifgronden Fault Zones, probably dates back to the Caledonian orogeny when Laurentia and Avalonia collided (De Jager, 2007). Several of this early NW-SE faults were reactivated during the Permian (George and Berry, 1993 and 1997; Glennie, 1998; De Jager, 2007) as well as less prominent conjugate NE-SW to NNE-SSW oriented fault set which is the second most common fault set in the Dutch subsurface (Ziegler, 1988 and 1990). Reactivation of some of these NW-SE oriented structures also occurred during the Meso-Cenozoic.

2.2.2 Rifting

- Active rifting started in the north of the study area in the **Early Triassic** (e.g. Central and Horn Grabens) but only reached the study area in the Mid-Triassic. The Dutch Central Graben subsided slightly faster than adjacent platforms (Terschelling and Vlieland Basins) but not as rapidly as the Grabens farther east in Germany and Denmark. No rift-shoulder uplift has been documented during this period.

- During the **Mid-Triassic** the Dutch Central Graben and the Broad Fourteens Basin started to subside with Zechstein salt becoming mobile along bounding faults (Remmelts, 1995).

- During the **Late Triassic** the differential subsidence persisted between the basins and their shoulders. Locally, transtentional dextral strike slip structures (including flower structures) are involved (Van Hoom, 1987). Zechstein salt was also mobilized during this period.

- Rifting was still possibly active during the **Early Jurassic** in the Dutch Central Graben but little evidence of active faulting is observed in the Southern Permian Basin, especially in the study area where tectonic activity is focused in the Dutch Central Graben.

- The rift evolution during the **Mid-Jurassic** is broadly unknown due to the Central North Sea-related uplift that eroded all of the Middle Jurassic deposits in the study area. The erosion locally denudated the Dutch Central Graben down to the Carboniferous level such as in the northern part of the Cleaver Bank High. The exact amount of eroded strata on the eastern shoulder of the Dutch Central Graben is unknown, The Step Graben and the Terschelling Basin were also uplifted and erosion cut down to Lower Jurassic and Triassic levels (Van Hoorn, 1987). The Horn Graben became inactive during the Middle Jurassic.

- The rifting during the **Late Jurassic** and Early Cretaceous is dominantly expressed as wrench tectonics with NW-oriented transtensional basin subsidence and transpressional uplift of narrow zones. The main rifting pulses (Cimmerian rift pulses) in the study area occurred during this period. The Schill Grund High was a stable platform area and the Step Graben and Terschelling Basin subsided but relatively less than the Dutch Central Graben. Late Jurassic uplift of the Friesland Platform resulted in erosion down to Lower Triassic and, locally, to Zechstein levels (NITG-TNO, 2004). There are evidences of local dextral transtensional displacement in the Rifgronden Fault Zone between the Terschelling Basin and the Schill Grund High (De Jager, 2007). The Zuidwal alkaline volcanic complex (Kimmeridgian) developed during the late Cimmerian rifting phase. In the Terschelling Basin, tectonic events were slightly delayed relative to the Dutch Central Graben; uplift occurred before the end of the Mid-Jurassic and a thin, younger, Upper Jurassic sequence rests on the Triassic, whereas the Lower Cretaceous sequence is thicker than in the Dutch Central Graben (Doornenbal and Stevenson, 2010). The Cleaver Bank High and Schill Grund High were uplifted and eroded during the mid- to late Kimmerian rifting phases. Therefore, Upper Jurassic and Lower Cretaceous strata are often missing on these highs, where Triassic and Permian strata are unconformably overlain by thin post-rift Lower Cretaceous and thicker Upper Cretaceous rocks (De Jager, 2007).

2.2.3 Salt tectonics

The presence of Zechstein salt that was deposited during the Late Permian had a pronounced influence on the subsequent evolution of the North Sea Basin, beginning with its effects on Triassic sedimentation patterns.

The partitioning of the Southern Permian Basin into several basins and highs during the Triassic and Jurassic was accentuated by the intense salt tectonics, primarily along fault-bounded basin margins (Wong, 2007). Basin compartmentalization and minibasin formation were associated with salt withdrawal in much of the Dutch Central Graben. These basins are often bounded by listric growth faults. Mid-Triassic minibasins subsided into the Zechstein salt over much of the central North Sea.

Differential loading was important for minibasin development near sediment entry points, and thin-skinned extension on the platforms was balanced by basement extension in the central axis of the basin. Along the edges of the Triassic fault basins, the faults are commonly soft-linked and offset through the Zechstein salt (Pharao*h et al.*, 2010).

During the Mid-Triassic, thin-skinned normal faults formed on autochthonous Zechstein salt and large salt swells formed. Piercing salt bodies and rim-synclines developed later (Jager, 2007). With increased differential subsidence between the subsiding basins and their shoulders, salt bodies increasingly mobilized upward from the previously formed salt swells and initiated large rim-synclines.

2.3 Overview of the stratigraphy of the Upper Jurassic and Lower Cretaceous in the study area and in surrounding regions of the southern North Sea

The Upper Jurassic to Lower Cretaceous interval is composed of four groups (Schieland, Scruff, Niedersaksen and Rijnland Groups). Three of these groups are present within the study area, the Schieland, Scruff and Rijnland Groups. The first two groups (Schieland and Scruff Groups) are studied in detail in this project. Their strata were deposited on top of the Lower to Middle Jurassic Altena Group, mainly consisting of argillaceous sediments (including the well known Posidonia Shale Formation) with intercalation of calcareous units.

The sedimentary in filling of basins and adjacent regions in the Upper Jurassic – Lower Cretaceous is predominantly controlled by the structural evolution of the region (Figures 2.7 and 2.8).

2.3.1 Sequence 1

In the Callovian, rifting resumed and continued until the Early Cretaceous (Valanginian). At first, this rifting was oriented E-W and influenced the axis of the DCG and further to the southwest the Broad Fourteens Basin (BFB). Deposits of this phase are referred to as Sequence 1 by Abbink *et al.* (2006) and as Graben Axis in Verreussel *et al.* (in prep.) (Figure 2.8). These deposits are primiraly deposited in the DCG and in the western part of the TB. This sequence comprises the Lower Graben Fm., Puzzle Hole Fm. and Friese Front Fm. sands and coals. During the Kimmeridgian, a dramatic change in structural setting and structural style occurred.

2.3.2 Sequence 2

The direction of the extension regime changed from E-W to SW-NE. Numerous old NW-SE oriented lineaments and structures become rejuvenated, resulting in the opening of peripheral basins such as the Terschelling Basin, the Step Graben, and also lead to major basin development in the Broad Fourteens Basin. In some parts of the DCG, the opposite occurs: uplift and erosion. Most of the uplift and erosion in the DCG can be ascribed to salt movement. Salt is withdrawn from some parts (e.g. the F11 rim syncline), resulting in the formation of turtle structures (e.g. the F03-FB condensate Field) and diapirs (e.g. the F17-18 salt structure) in other part. This interval is referred to as Sequence 2 in Abbink *et al.* (2006) and Peripheral Basins in Verreussel *et al.* (in prep.) (Fig. 2.8). This phase provided accommodation space for siliciclastic deposits with hydrocarbon reservoir potential (non-marine Schieland Group and Scruff Group) in the peripheral basins. Towards the end of the phase, fault activity and salt movement reached a peak.

2.3.3 Sequence 3

During this third phase, adjacent platforms like the Schill Grund Platform and the Cleaver Bank High were flooded. In the Dutch Central Graben area, large accumulations of sandstone of the Scruff Greensand Fm. are associated with this phase. In the Danish Central Graben area, highly condensed organic-rich mudstones are associated with this phase. This phase, occurring around the Jurassic-Cretaceous boundary is referred to as Sequence 3 in Abbink *et al.* (2006) and as Adjacent Plateaus in Verreussel *et al.* (in prep.) (Fig. 2.8). Sequences 2 and 3 are relatively thick in the peripheral basins compared to the DCG. In the Broad Fourteen Basin, deposition continued in the axial region, whereas renewed tectonic activity in the Ryazanian led to major erosion on its margins.

At the end of the Ryazanian the rifting came to an halt. Fault activity in the DCG-area gradually ceased and the younger marine sandstones and shales of the Rijnland Group effectively cover the former graben and platform areas in the north of the Dutch offshore. As the basins continued to (thermally) differentially subside, characterizing **Sequence 4** (not analyzed in this project), the coastal Vlieland Sandstone and the Vlieland Claystone Formation were deposited.

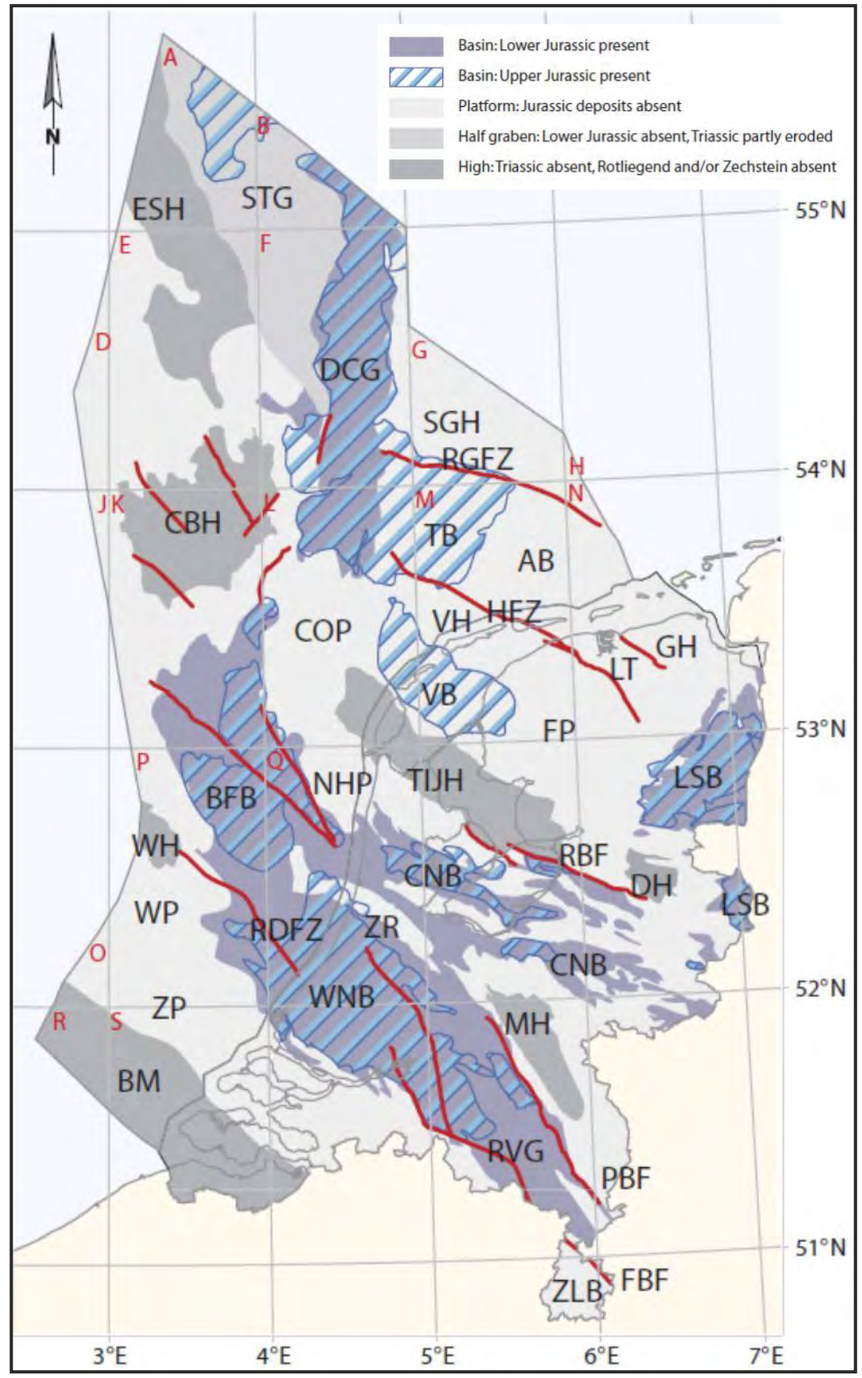

Figure 2.7: Late Jurassic-Early Cretaceous structural elements in the Netherlands. Adapted from Duin *et al.* (2006).

2.4 Overview of the depositional environments of the Upper Jurassic and Lower Cretaceous in the study area (from Munsterman *et al.*, 2012)

2.4.1 Sequence 1

Lower Graben Formation: Greyish brown, very fine to fine-grained, well-sorted sandstones, occurring in beds generally less than 10 m thick, with intercalations of thin greyish brown silty to sandy claystones. The formation is generally carbonaceous with some distinct coal layers. The individual sandstone bodies have a rather restricted lateral extent. Fluvio-deltaic and coastal plain.

Middle Graben Formation: Grey, locally very silty, carbonaceous claystones. In the northern part of the F-quadrant (e.g. F02, F03 and F05) one thick or locally two sandstone beds may be intercalated. At the base of the formation three thin but distinct coal seams occur. Lacustrine to marginal marine embayment.

Upper Graben Formation: Greyish brown, fine-grained, carbonaceous sandstones, separated by a silty clay succession. Marginal marine barrier-island system.

Puzzle Hole Formation: Light brownish-grey carbonaceous claystones with intercalations of siltstones and thin sandstones. Coal seams are frequent (10 to 20 seams per 100 m interval) and give the formation the typical seismic response. Lower delta plain; lagoonal tidal flats, estuary and tidal channels, bay head deltas and mouthbars.

Friese Front Formation: Alternating claystones, siltstones, sandstones and some minor coal. Non-marine (coastal) delta plain to lagoonal deposits.

Rifgronden Member: Dark-grey, carbonaceous, locally silty to sandy claystone, with thin intercalated beds of well-sorted, very fine to fine-grained sandstone, dolomite and coal. Lagoonal.

2.4.1 Sequence 2

Kimmeridge Clay Formation: The sediments of the Kimmeridge Clay Fm. were deposited in an outer shelf setting. Dolomitic beds and structureless organic matter (SOM) indicate times of decreased input of clastics and stagnant water conditions due to a stratified water column. The higher frequency of dolomitic beds and SOM in the northern realm reflects a slightly deeper environment .

Oyster Ground Member: Claystones, non- to slightly silty. Lithology, fossils, lignite and regional palaeogeography suggest that the Oyster Ground Member was deposited in restricted lagoon-like conditions with washover deposits. The monotypical thin-walled shell assemblages confirm a restricted marine setting.

Terschelling Sandstone Member: Fine- to medium-grained sandstone (occasionally up to coarse sand and gravel), well to poorly sorted. In most cases, e.g. in wells L06-02, L06-03 and M01-01, the sediments of this member are interpreted to be deposited as a barrier island complex, including shoreface to foreshore and washover fans environments, protecting the restricted marine (lagoonal) setting of the Oyster Ground.

Noordvaarder Member: Well-sorted, greenish-grey, slightly argillaceous, occasionally calcite cemented, glauconitic sandstones. The sands were deposited in a shallow marine environment, ranging from offshore to lower shore face.

Lies Member: Bioturbated silty to sandy claystones. The sediments are considered to be deposited in the offshore/shelf environment.

2.4.1 Sequence 3

Scruff Spiculite Member: Light green-grey, fine-grained, glauconitic and slightly argillaceous intensely bioturbated sandstones. The sediments of this formation were deposited in a (offshore to) shoreface environment. Facies change laterally from relatively clean 'bioclastic' sandstone to an argillaceous sandstone reflecting the position of the depositional area on the basin floor topography (Abbink *et al.*, 2006). A semi-enclosed shallow marine environment is envisaged.

Stortemelk Member: Fine- to very fine-grained, argillaceous sandstones with intense bioturbation. Shoreface to offshore.

Clay Deep Member: Grey to black claystone. Deposited in a shelf environment. Basin circulation stagnated which resulted in dysoxic to anoxic basin-floor conditions and in the deposition of bituminous claystones.

Schill Grund Member: Olive-grey to grey-brown claystones. Open-marine shelf conditions prevail. The slightly or non-bituminous nature of the sediments indicate near-normally oxygenated basin-floor circumstances.

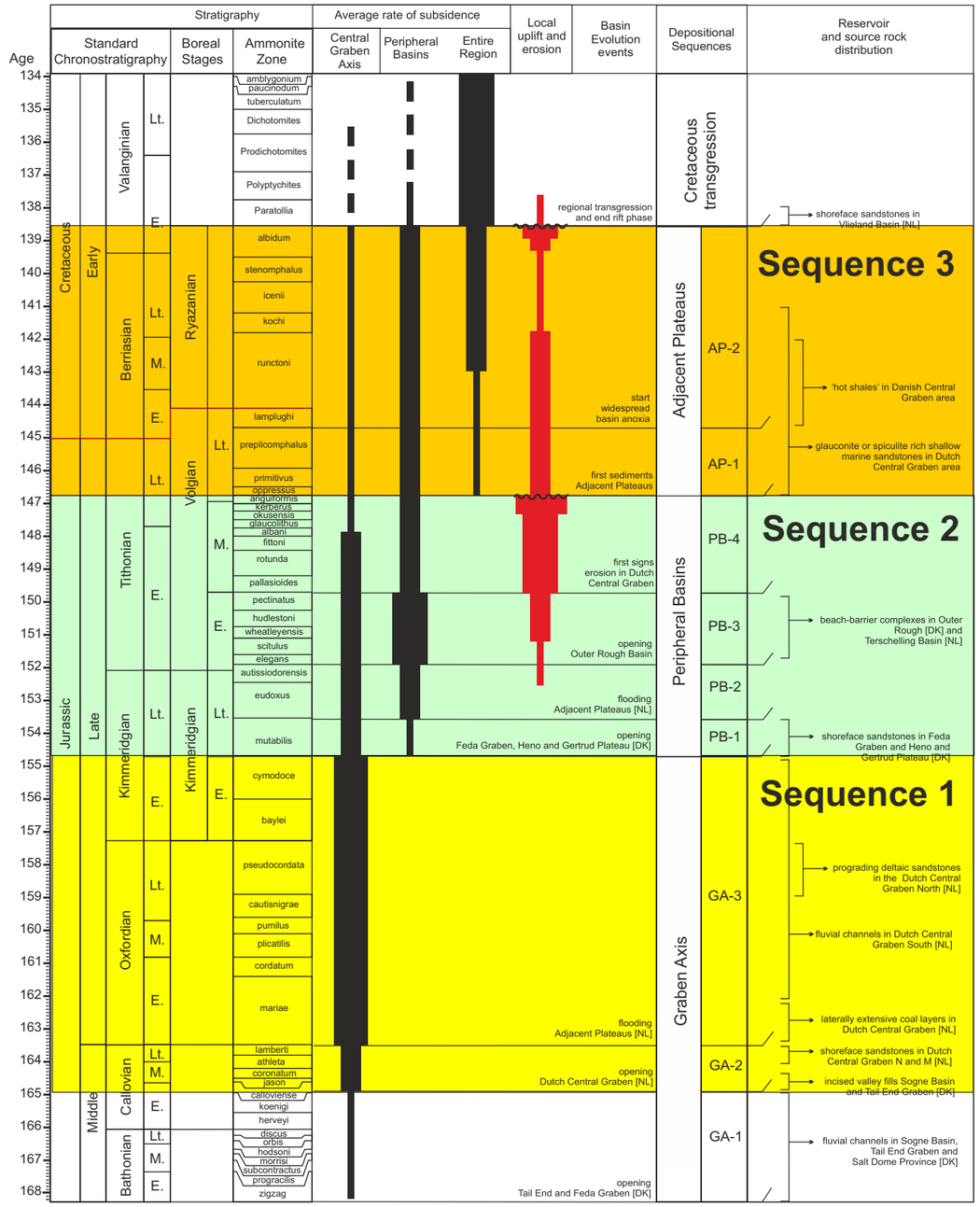

Figure 2.8: Schematic representation of the Late Jurassic to Early Cretaceous basin evolution of the Central Graben area from Denmark, Germany and The Netherlands (from Verreussel *et al.*, in prep.).

METHODOLOGY 3

3 - Methodology

Several analytical techniques were used in this multi-disciplinary project. In this chapter we describe concisely the methodology used.

Quad.	Wells	Panels								Core	Palyno.	Stable isotope
		A1	A2	B	C	D	E	F	G			
A	A08-01							■				
	A12-01								■			
	A12-02							■				
	A18-02-S1								■			
B	B13-02							■				
	B14-01							■				
	B14-02							■				
	B14-03							■				
	B18-02							■				
	B18-03				■			■				
E	E18-01					■						
	E18-07					■						
F	F01-01								■			
	F03-03				■							
	F03-05-S1				■					■	■	■
	F03-06				■							
	F03-07							■				
	F03-08				■							
	F04-02-A											
	F06-01				■					■	■	■
	F07-02						■					
	F08-01				■							
	F08-02				■							
	F09-01								■			
	F11-01				■							
	F11-02						■					
	F11-03						■					
	F12-03						■					
	F14-05				■					■	■	■
	F14-06				■							
	F15-A-01				■					■	■	■
	F16-A-05					■						
	F16-02					■						
	F16-04					■						
	F17-01				■							
	F07-03				■						■	
	F17-04					■					■	■
	F17-05	■	■		■	■						
	F17-06	■	■		■							
	F17-09				■	■				■	■	■
	F18-01					■						
	F18-02					■						
	F18-03					■					■	■
	F18-08					■						
	F18-09-S1					■						
G	G10-03						■					
	G13-02			■								
	G16-02					■						
	G16-03			■								
	G16-04			■		■						
	G16-05			■								
	G17-01					■						
	G17-02					■						
	G17-03					■						
L	L02-FA-101			■								
	L02-03				■							
	L02-05	■	■		■							
	L02-06-S1				■							
	L03-01	■	■									
	L03-03	■	■									
	L03-04	■	■	■								
	L04-01				■							
	L04-05				■							
	L05-04				■							
	L05-05				■					■		
	L06-02	■	■							■	*	
	L06-03			■						■	*	
	L09-01			■								
	L09-02			■								
M	M01-01			■						■	*	
	M04-01	■	■									
	M04-03	■	■									
	M04-04	■	■									
	M07-01	■										
	M07-03	■	■									
	M07-07	■	■							■	■	■
	M07-08		■							■	■	■
	M08-02	■										

Table 3.1 Wells used in the project for the regional panels, for core, palynological and stable isotope analysis. * Palynological data for wells L06-02, L06-03 and M01-01 are from Abbink *et al.*, 2006.

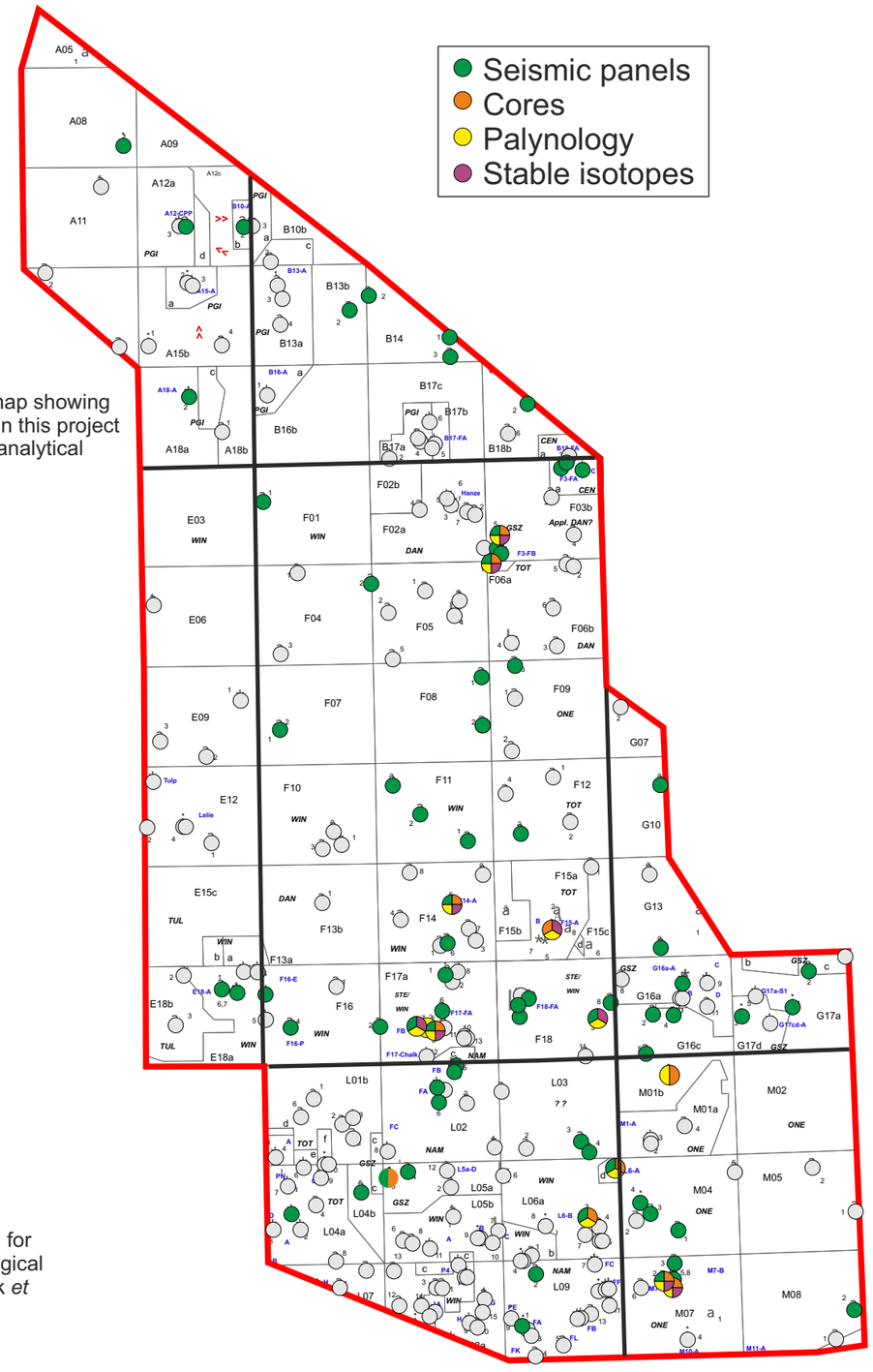

Fig. 3.1 Base map showing the wells used in this project for the various analytical techniques.

3.1 Palynology

3.1.1 Principles and application

Palynologists study acid-resistant organic matter from sedimentary rocks. Organic matter is classified into palynomorphs, organic microfossils within a certain size range, and palynodebris, all other organic material such as plant-tissue, wood fragments, structureless organic matter, and so on. The combination of palynomorphs and palynodebris is called palynofacies. Within the palynomorph category, two groups are considered the most important: the dinoflagellate cysts, or dinocysts, and the pollen and spores, or sporomorphs. Because palynology straddles both the marine and the terrestrial realm, it is ideally suited for the study of shallow to non-marine sedimentary rocks.

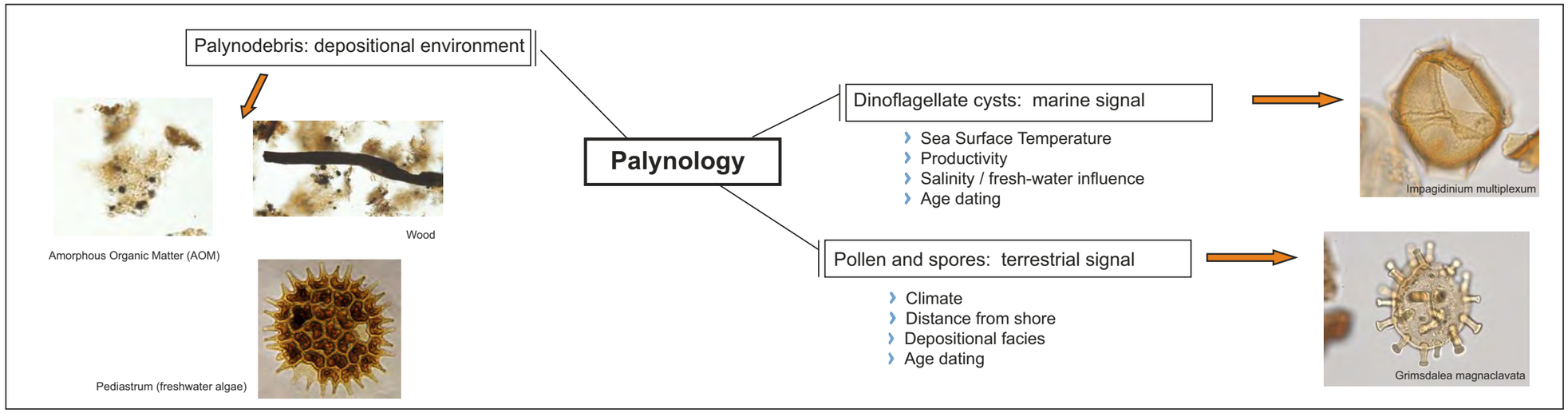

Figure 3.2: Principles and application of palynological analysis.

3.1.2 Workflow

The organic matter is extracted from the rock by a standard laboratory processing procedure. During the first step, the sedimentary rock is crushed and treated with HCl to digest the carbonate. After that, the mineral bonds of the silicates are destroyed by applying HF, which releases the acid-resistant organic matter. The organic residue is then concentrated by sieving over a 7 micron mesh. The organic matter particles larger than 7 micron are brought on a glass slide, fixed by a mounting medium such as glycerine jelly, and covered by a thin glass cover slip. The result is called a palynological preparation or slide. Its content is studied using a transmited light microscope with magnifications varying between 100 and 1000 microns. The microfossils such as dinoflagellate cysts and pollen and spores are identified on species level and counted. The occurrences of the different species are displayed on distribution charts. These charts are the basic modules for the age and palaeoenvironmental interpretation.

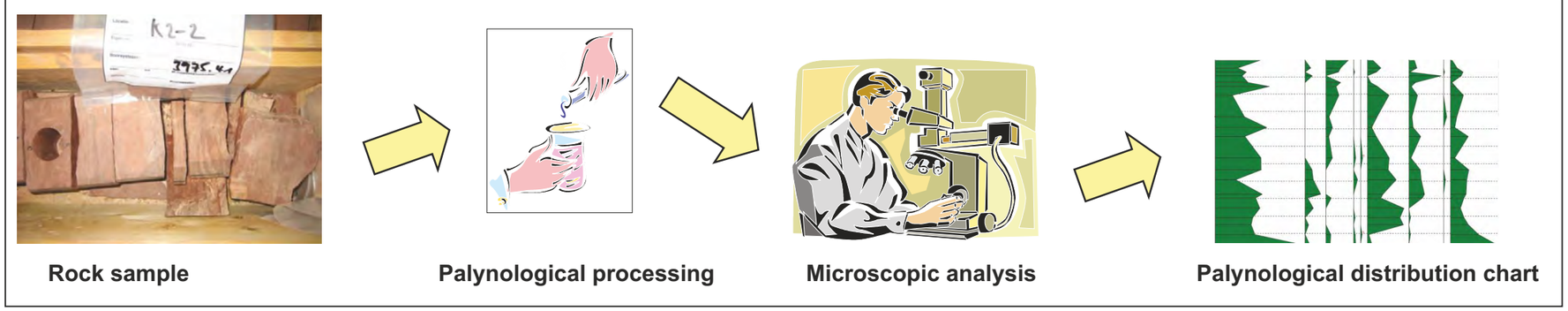

Figure 3.3: Typical workflow for palynological analysis: sample selection, processing, microscopy and distribution charts.

3.1.3 Age assessments

The TNO Zonation has been compiled over the past ten years and is based on palynological data from a vast number of exploration wells in the Dutch offshore. The four main zones defined in the TNO Zonation line up with the four sequences that are defined to describe the basin evolution (see Chapter 1). The TNO zonation is based on the LODs (Last Occurrence Datum) and FODs (First Occurrence Datum) of palynomorphs. The correlation to the international chronostratigraphic standard is achieved through comparison with key references such as Abbink (1998), Abbink *et al.* (2006), Bucefalo Palliani *et al.* (2002), Bucefalo Palliani & Riding (2000), Costa and Davey (1992), Davey (1979;1982), Duxbury *et al.* (1999), Heilmann-Clausen (1985), Herngreen *et al.* (1989, 2000), Koppelhus & Nielsen (1994), Partington *et al.* (1993a; b), Powell (1992), Riding and Thomas (1992) and Riding *et al.* (1999). The international geological timescale of Gradstein *et al.* (2012) is followed.

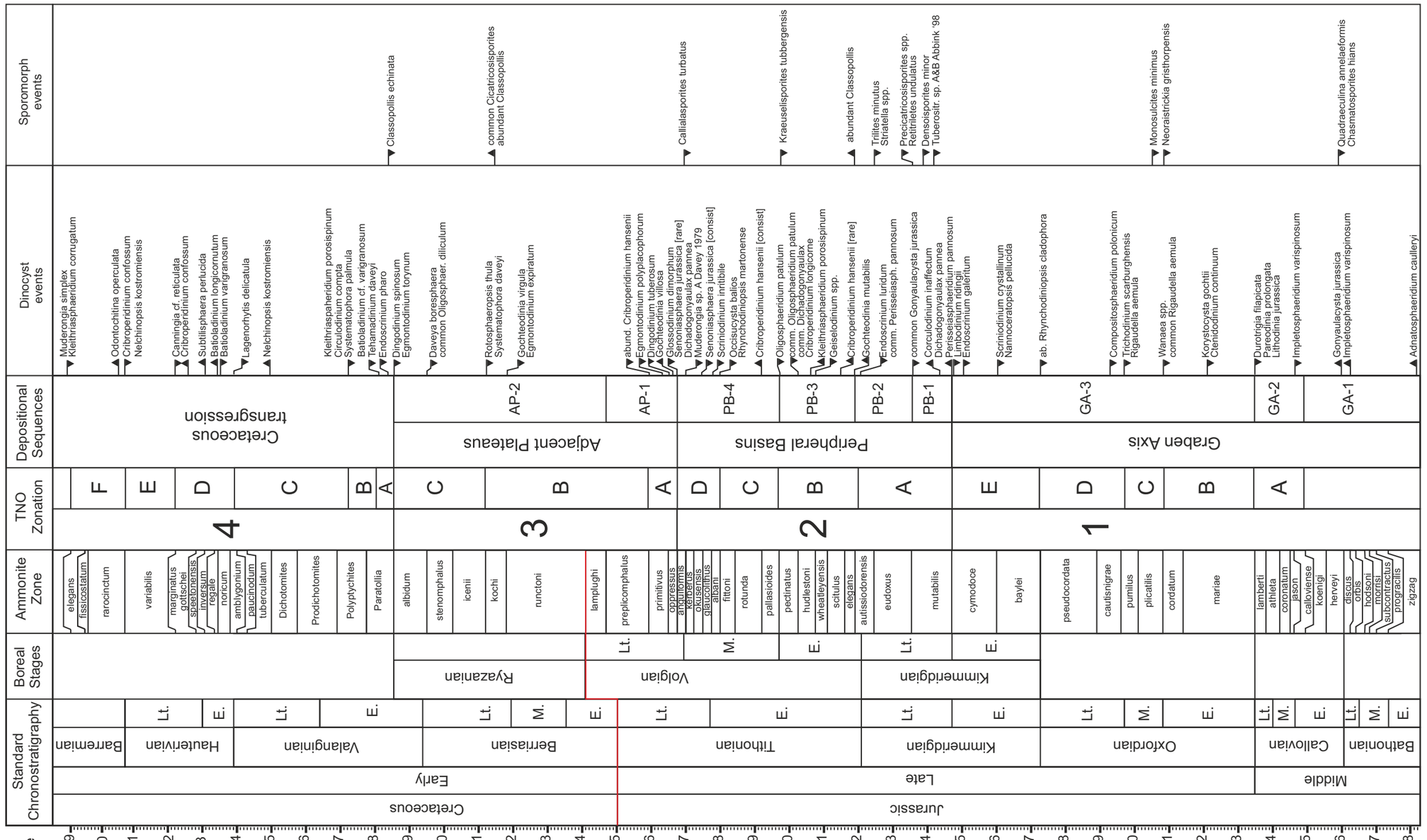

Figure 3.4: TNO Zonation.
The zonation is based on both dinoflagellate cyst and pollen and spore events. For the chronostratigraphic calibration, GTS 2012 is used (Grandstein et al., 2012). The oldest Jurassic deposits at the base of the "Late Jurassic rift phase", in the Central Graben area are Early to Middle Callovian, correlating to TNO Subzone 1A.

3.1.4 Palaeoenvironmental interpretation

The palaeoenvironmental interpretations based on palynology can not be compared one-on-one with the facies interpretations based on the core descriptions. Where the paleoenvironmental constraints from the core descriptions are based on *in-situ* features, such as ichnofossils or sedimentary structure, the palaeoenvironmental interpretations from the palynological analyses are biased by taphonomical processes, such as selectional preservation and transport. Therefore, a schematic representation of depostional environments is made where both worlds meet (Fig. 3.5). The palaeoenvironental interpretation resulting from the palynological analyses are based on a couple of general assumptions, which are listed below.

Open marine
Dominance of dinoflagellate cysts indicates open marine environments, in particular when the dinoflagellate cyst assemblages are highly diverse (many species).

Restricted marine
Dinoflagellate cyst associations of the type High Dominance – Low Diversity indicate a restricted marine environment, such as a lagoon, embayment or estuary.

Non-marine
Absence or near-absence of dinoflagellate cysts generally indicates non-marine or marginal marine environments.

Transgression
An increase in the ratio between dinoflagellate cysts and pollen and spores indicates a sea level rise.

Regression
A decrease in the ratio between dinoflagellate cysts and pollen and spores indicates a sea level fall.

Low energy conditions
Excellent physical preservation of palynomorphs and other organic matter particles may indicate low energy conditions such as for instance a lagoon or a lake.

High energy conditions
Poor physical preservation of palynomorphs may indicate high energy conditions such as for instance a river channel, basin floor fan or a beach.

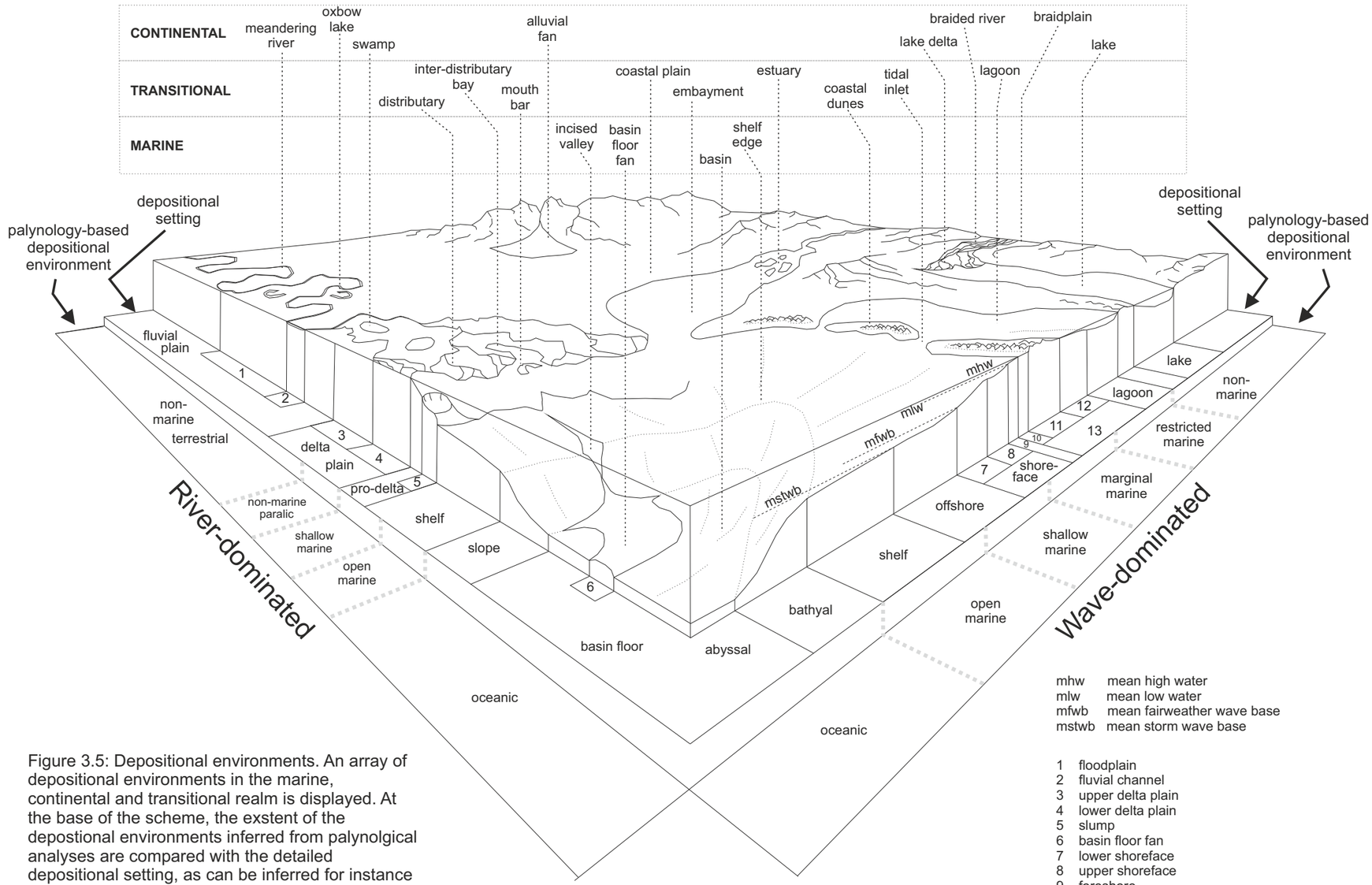

Figure 3.5: Depositional environments. An array of depositional environments in the marine, continental and transitional realm is displayed. At the base of the scheme, the exstent of the depostional environments inferred from palynolgical analyses are compared with the detailed depositional setting, as can be inferred for instance from core description analysis.

mhw mean high water
mlw mean low water
mfwb mean fairweather wave base
mstwb mean storm wave base

1 floodplain
2 fluvial channel
3 upper delta plain
4 lower delta plain
5 slump
6 basin floor fan
7 lower shoreface
8 upper shoreface
9 foreshore
10 beach
11 coastal dunes
12 washover
13 beach-barrier complex

3.2 Stable isotope analysis

Introduction

Isotopes are variants of a chemical element that differ in the amount of neutrons, but not in the amount of protons. Therefore, two isotopes of the same element display similar chemical behaviour, but differ in the molecular weight. Isotopes can be radioactive, like for instance carbon-14, or stable, like carbon-12 and carbon-13 (see Fig. 3.6). The type of stable isotope analysis applied in this project is organic Carbon-13 (δ13Corganic). In this type of stable isotope analysis, the numbers of two stable carbon isotopes, Carbon-13 and Carbon-12, are measured on the organic matter fraction that is contained in the sediment samples. The δ13Corganic ratio is then calculated by comparing the ratio against a standard. Note that it is also possible to assess δ13C on the calcite of fossils (e.g. belemnites) or on the bulk carbonate fraction of the sediment (δ13Ccarbonate).

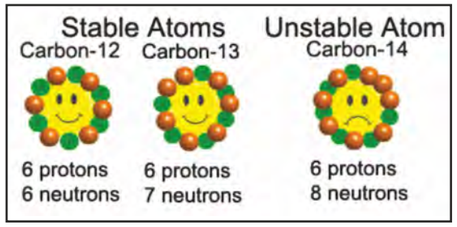

Figure 3.6: Isotopes of Carbon. Carbon-12 and Carbon-13 are stable isotopes, Carbon-14 is radio-active.

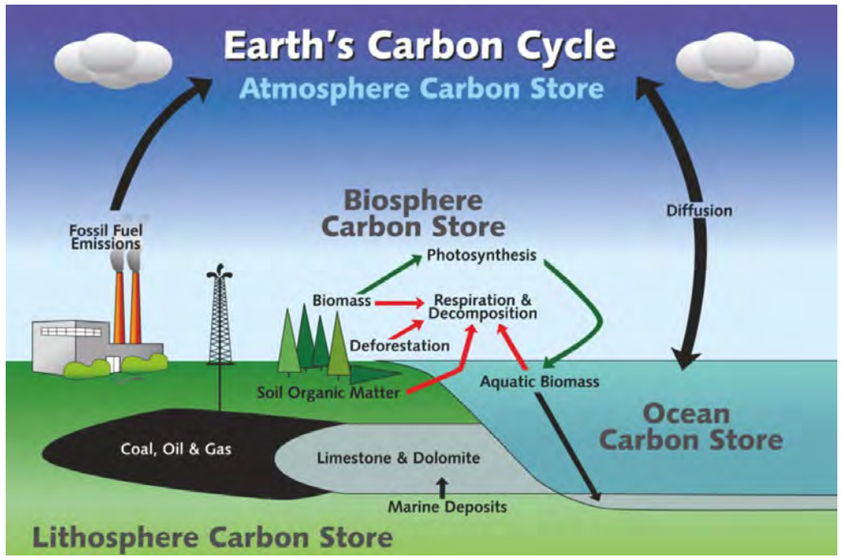

Figure 3.7: The carbon pools of the earth. Carbon may be stored in the lithosphere as rock, e.g. in limestone, or as fossil fuel, e.g. coal, oil or gas. Carbon is also stored in the atmosphere, as CO_2. When exchange of carbon occurs between pools, like for instance when excessive burial of organic matter occurs during Oceanic Anoxic Events, the atmospheric ratio between Carbon-12 and Carbon-13 will be affected.

Application

The application of stable isotope analysis is based on the assumption that the measured ratio between C12 and C13 in a sediment sample reflects the atmospheric ratio at the time of deposition. Variations in the stable carbon isotope composition reflect changes in the isotopic composition of the global carbon pool (i.e., the exchange between the oceanic, terrestrial and atmospheric reservoirs, see Fig. 3.7). Most organisms exhibit preferential uptake of light carbon (carbon-12), due to chemical interactions at molecule level. As a consequence, during geological times when excessive burial of organic matter occurs, such as in Oceanic Anoxic Events (OAE), the atmospheric background ratio will become enriched in heavy carbon (carbon-13). Therefore, OAE's are usually associated with positive excursions in δ13C. During times of excessive burning of fossil fuels, like it is occurring at the present-day, carbon-12 is brought back into the atmosphere, leading to enrichment in light carbon (carbon-12), associated with a negative excursion in δ13C. Negative excursions can also be provoked by volcanic out gassing, and in extreme cases to the dissociation of seafloor methane hydrates.

Reference curve

For our purpose in the present study, the aim is to record trends in δ13Corganic that can be used for stratigraphic correlation. Over the past couple of years, a large amount of stable isotope data was gathered from exploration wells of the Dutch offshore. Based on these data, a reference curve for the Upper Jurassic is compiled (see Fig. 3.8). The newly acquired isotope analyses from this study are correlated to this reference curve. At the same time, the reference curve is continuously updated and improved by incorporating new data in the existing stack. This task will also be carried out after the project using the newly obtained data.

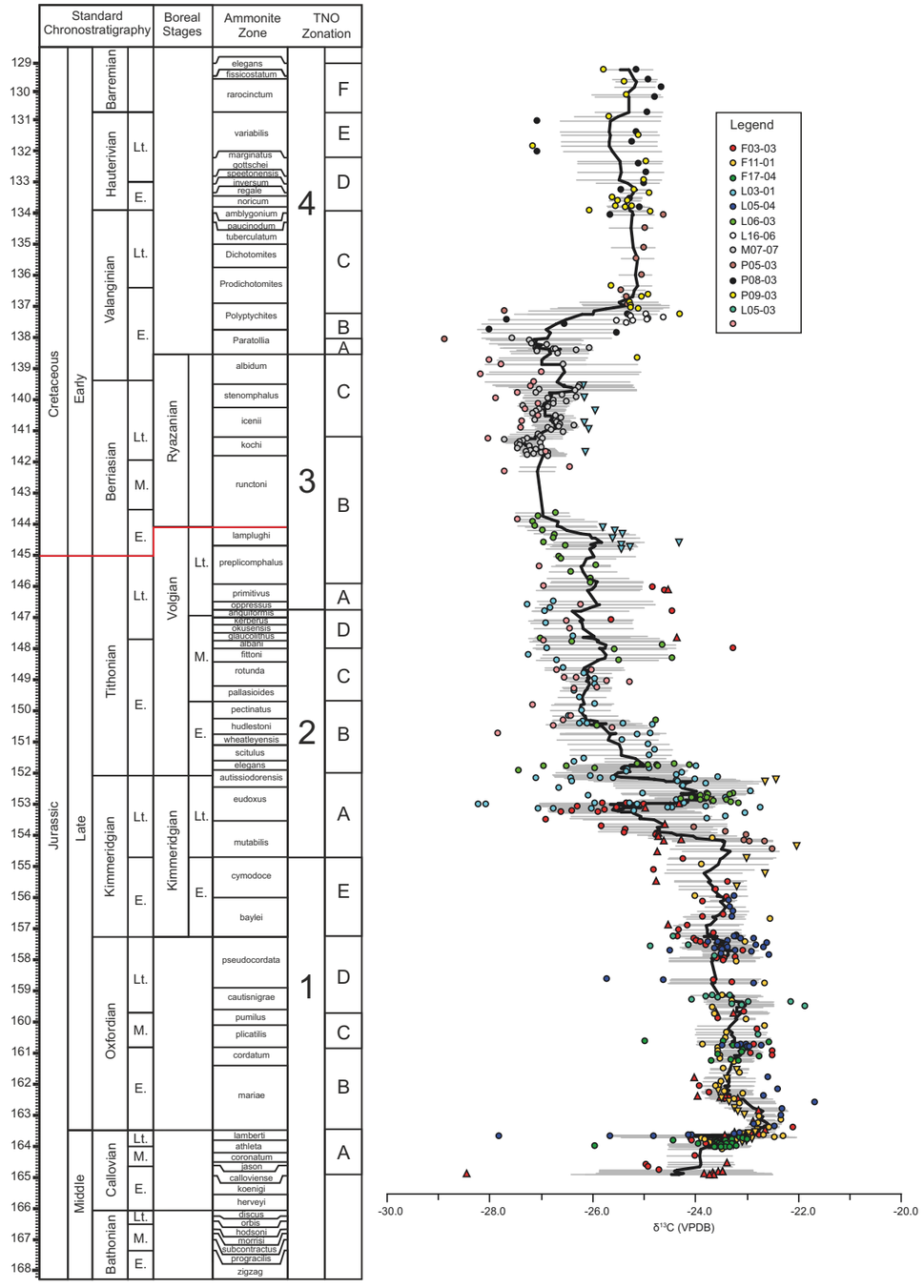

Figure 3.8: Stable isotope reference curve for the Upper Jurassic to Lower Cretaceous of the Dutch offshore (TNO report 2014 R10343). The record is compiled from numerous exploration wells.

3.3 Core description and analysis

A total of 617 m of core from eleven different wells was described (Table 3.2). Sequence 1 (Lower Graben / Friese Front) had most meters of core described: 329 m, followed by the Scruff Greensand from Sequence 3 (211 m), and finally the Terschelling Sandstone and Oyster Ground Shale from Sequence 2 (77 m).

All core descriptions were done in TNO's core repository in Zeist using core material from the repository itself (Fig. 3.9). Core quality varied considerably between the various cores. Some were well preserved and mounted in epoxy, whereas others consisted of pieces of rock still contained in plastic bags. But the overall quality of the core material was good to excellent.

Descriptions were made on a 1:20 or 1:100 scale using sedimentological logging paper. The following sedimentological parameters were logged: composition and texture, average grain size, sedimentary structures (lamination, cross-bedding, rip-up clasts, etc), diagenetic minerals and bioturbation. Since the majority of the rocks of interest in the FOCUS project were deposited in a shallow marine environment, special attention was paid to the description of the various ichnofacies that were present in the cores.

The trace fossil atlases from Pemberton *et al.* (2014) and Gerard & Bromley (2008) were of great help (see Appendix A6, Field Guide Appendix 1). The nomenclature of the various ichnogenera was mostly based on these publications. Generally, sedimentary structures and ichnogenera were easy to identify, thanks to the fact that most of the sand-sized fraction consists of relatively clean quartz grains whereas the shale laminae usually contain considerable amounts of dark micas and clays. A full legend of sedimentary structures and ichnogenera can be found in Appendix A1.

Sedimentary logging was aided by the use of well logs. Use was made of composite logs, drilling evaluation logs, and playbacks of the litho-porosity logs. Logs were used to determine core shifts, the formation's global lithology, cemented streaks, porosity, hardness (to detect cemented zones), and oil saturation.

Fig. 3.9. Core description at TNO's core repository in Zeist.

Table 3.2: Overview of cores described during the FOCUS TKI project.

Stratigraphic Unit	Well	Top [m]	Bottom [m]	Missing [m]	Core length [m]	Total [m]
Scruff Greensand	F15-A-01	2259	2284	5	20	211
	L06-02	2232	2263		31	
	M07-07	3936	3989		53	
	M07-08	4800	4907		107	
Terschelling Sandstone	L06-02	2464	2504		40	77
	L06-03	2095	2111		16	
	M01-01	2288	2309		21	
Lower Graben / Friese Front	F03-05-S1	3165	3302		137	329
	F06-01	3196	3317		121	
	F14-05	2148	2190		42	
	F17-09	2039	2052		13	
	L05-05	2704	2735	15	16	
Total meters of core described						**617**

3.4 Seismic interpretation

The main focus of the seismic analysis is on a series of regional scale seismic transects that were constructed to cover all of the main basins and structures observed in the study area. Seven regional seismic sections (A to G) have been constructed using a combination of 2D and 3D seismic lines (see location map, Fig. 4.3.1). Each of these seismic section were constructed to be parallel to seven well correlation panels and intercept the same series of wells. For each constructed composite seismic sections the key horizons and structures were interpreted in Petrel and exported to a drafting package for edits. Below is the list of horizons and structures interpreted.

Horizons

Ten main horizons have been interpreted on seven regional transects as well as in several additional seismic sections.

- Base of Zechstein.
- Top of Zechstein : Including salt bodies, either connected to the autochthonous salt or disconnected as allochthonous salt diapirs. The salt feeders (or stems) were also interpreted, as well as salt welds.
- Base of Upper Triassic (base Upper Trias Germanic Group).
- Base of Lower Jurassic (base Altena Group).
- Base of Sequence 1 of the Upper Jurassic.
- Base of Sequence 2 of the Upper Jurassic.
- Base of Sequence 3 of the Upper Jurassic.
- Base of Rijnland Group.
- Base of Chalk Group.
- Base of Cenozoic.

In the seismic transects shown, each key interval was later color-filled with transparencies to be able to identify the seismic amplitude characters of that particular zone. Some additional horizons were locally interpreted where they could be identified, these include:

- Key unconformities intra Upper Jurassic.
- Coal layers in Sequence 1 of the Upper Jurassic.
- Top of Terschelling Sandstone Mb.

Faults

Normal, reverse and strike slip faults where identified at the base Zechstein as well as throughout the post Zechstein sections. Particular attention was paid to faults intercepting the Upper Triassic to Cretaceous interval, and especially for the faults that show evidence of syn-depositional activity during the Late Jurassic and the Early Cretaceous.

Stratal termination interpretation

In addition to the interpretation of key horizons and structures, stratal terminations were identified and mapped within the Upper Jurassic Sequences 1, 2 and 3. These include truncations, onlaps and downlaps, which are represented as black half arrows on the interpreted seismic panels.

Seismic flattening technique

Each interpreted regional seismic sections was also flatten onto the top of Sequence 1 or Sequence 3 (depending on the required display) to be able to have a more realistic display of the depositional geometry during and at the end of the Late Jurassic. This technique, is purely vertical, and, therefore, is not perfect and does not replace a structural restoration approach, but still allows to observe more relevant geometry in basins where post-deposition deformation (in relation to Upper Jurassic) are intense. It also permits to better evaluate subtle stratigraphic thickness variation and stratal terminations by correcting for post-depositional folding and faulting. For these flattened sections, the main Upper Jurassic horizons, faults active during the Late Jurassic and salt bodies present within the Upper Jurassic were interpreted. Stratal terminations were also added to highlight the main unconformities, onlaps and downlaps associated with key horizons.

An additional technique, named extended flattened technique (Fig. 3.10), was used to compensate for the local erosions that truncated large portion of Upper Jurassic strata. The reference horizons (e.g. top of Sequence 3) was extended into younger strata to allow the underlying Upper Jurassic zone to be pushed down to a elevation level that is regionally realistic. This allow for a better appreciation of the original stratal geometries within basins that have been locally uplifted and eroded.

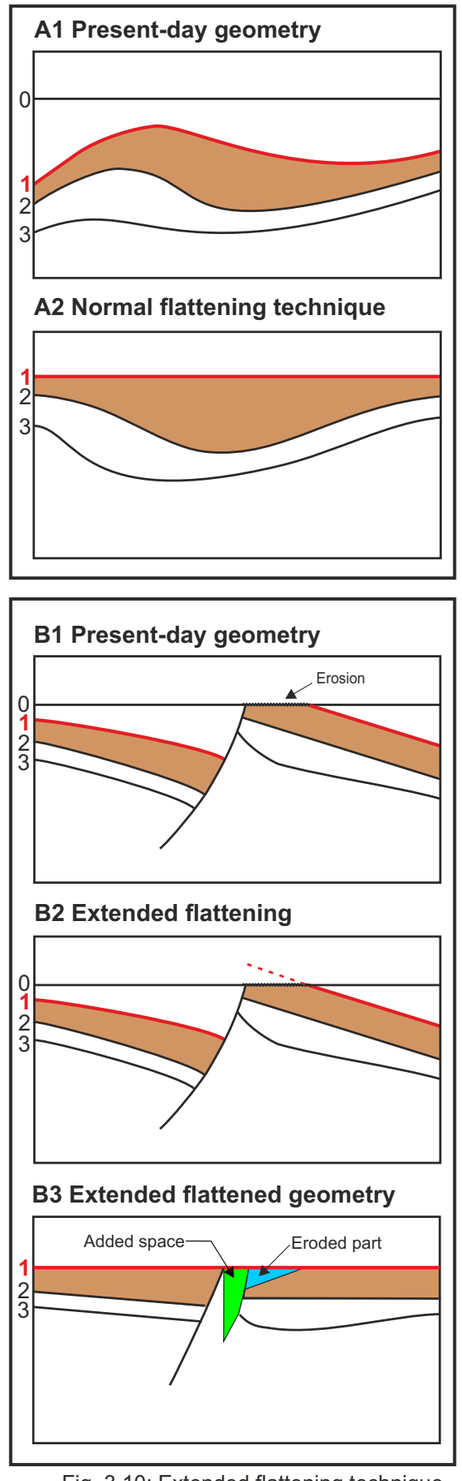

Fig. 3.10: Extended flattening technique

3.5 Stratigraphic correlation

In association with the regional seismic sections, regional stratigraphic correlations were constructed using the same wells shown in the corresponding seismic sections. The stratigraphic correlations are carried out for individual Upper Jurassic Sequences (1, 2 and 3) or in a combined way with all three sequences displayed in the same panels (depending on the structural complexity and the amount of erosion of individual sequences).The stratigraphic correlations were carried out exclusively for the Upper Jurassic, and include key surfaces and lithostratigraphic units listed below :

Sequence 1:
- Base of Sequence 1*
- Lower Graben Formation
- Rifgronden Member
- Friese Front Formation
- Middle Graben Formation
- Puzzle Hole Formation
- Upper Graben Formatiom
- Kimmeridge Clay Formation
- Top of Sequence 1

Sequence 2:
- Base of Sequence 2**
- Main Friese Front Member
- Oyster Ground Member
- Terschelling Sandstone Member
- Noordvaarder Member
- Lies Member
- Kimmeridge Clay Formation
- Top of Sequence 2

Sequence 3:
- Base of Sequence 3***
- Scruff Greensand Formation
- Scruff Spiculite Member
- Stortemelk Member
- Schill Grund Member
- Clay Deep Member
- Top of Sequence 3****

* Base of Sequence 1 is also referred as the Mid Cimmerian Uncorformity.
** Base of Sequence 2 is also referred as the J62 Unconformity (Partington *et al*., 1993a).
*** Base of Sequence 3 is also referred as the J73 Uncorformity (Partington *et a*l., 1993a).
**** Top of Sequence 3 is also referred as the Late Cimmerian Uncorformity.

Since some of this lithostratigraphic subdivisions are locally lateral and time equivalent of each other (e.g. Terschelling Sandstone Mb. transitions northward to the Lies Mb. within the TB), correlation heavily relies on age determination to identify primary correlation units. For work we used previously acquired palynological data (previous TNO reports) and new palynological data acquired in this study. Additionally, these palynological zones were locally validated and reinforced using previously acquired and new stable isotope data.

Standard well log correlation was applied using mainly GR and Sonic curves to correlate lithological variations between and within stratigraphic units. The main sandy intervals were highlighted for each well and correlated from well top when possible. Locally, this exercise is quite easy and strait forward. However, the uncertainties grow with increasing distances between wells and it is often difficult for proximal depositional setting such as fluvial deposits, where sandy thin units are often related to isolated channels and, therefore, unlikely to be easily correlatable across long distances. In this case, we used a different display to represent the thick (20 m +) sand-rich fluvially-dominated stratigraphic intervals, that are shown as orange fills instead of traditional yellow fills used for sandy strata. Locally some particular and easily recognizable stratigraphic units are also used as useful correlation units. This is the case of regionally and persistently present coal beds (2 or 3) within the Lower Graben Formation (Sequence 1).

In addition to the palynological and stable isotope data, other correlation techniques were used. The stratigraphic correlations greatly benefit from having the seismic section equivalents (including flattened versions) that give additional and valuable information regarding the stratal geometry between wells, such as:

- Stratal thickening and thinning,
- Stratal pinch outs and drapes,
- Identification of truncations, onlaps and downlaps for top and base of Sequences 1, 2 and 3, as well as internally in these sequences,
- Presence of syn-depositional faults that locally affect the thickness of stratigraphic units,
- Presence of salt bodies that were active during deposition of given stratigraphic units.

4.1

RESULTS

PALYNOLOGY AND STABLE ISOTOPES

4.1 Palynology and stable isotopes

4.1.1 Lower Graben Formation (Part 1/7)

Sequence stratigraphic interpretation of well F03-05-S1: The absolute abundance values of the marine dinoflagellate cysts and the terrestrial pollen and spores display a negative correlation. Where the absolute abundances of dinoflagellate cysts show a sudden increase, maximum flooding surfaces (MFS) are inferred. The pink lines in Fig. 4.1.1 are drawn where the frequencies of dinocysts are lowest, indicating the transition from regressive to transgressive. Based on the combination of these two proxies, four transgressive-regressive cycles are inferred. These cycles are indicated in Fig. 4.1.1 as CAL1 to CAL4. Because the entire cored interval stretches within one ammonite zone (the latest Callovian lamberti zone), it is assumed that these cycles are high-order sea level cycles. The Maximum Flooding Surface (MFS) around 3222m is correlated with the latest Callovian 3rd order MFS known in the literature as the J46 (e.g. Partington *et al.*, 1993a & b).

Palaeoclimatic and palaeoenvironmental interpretation of well F03-05-S1: The closed sum diagrams of the pollen and spores display the most abundant pollen and spore types (to the left) and a subdivision according to the presumed affinity with a certain type of environment (to the right). The environmental affinities are based on Abbink (1998) and co-workers (Abbink *et al.*, 2006). The most prominent types are smooth trilete spores, *Perinopollenites* and *Cerebropollenites. Classopollis* is rare, and even absent in the upper reaches of the core, indicating relatively cool and humid conditions. *Cerebropollenites* is quite abundant in the interval 3185m 3210m, interpreted to represent tidal channel and tidal shoal environments, according to the core description interpretation. The smooth trilete spores appear to be associated with brackish environments, such as embayments and lagoons. Note the ACME occurrences (super abundant) of the dinoflagellate cyst species *Rigaudella aemula* and *Evansia/Pareodinia.* These events are useful for short distance correlation.

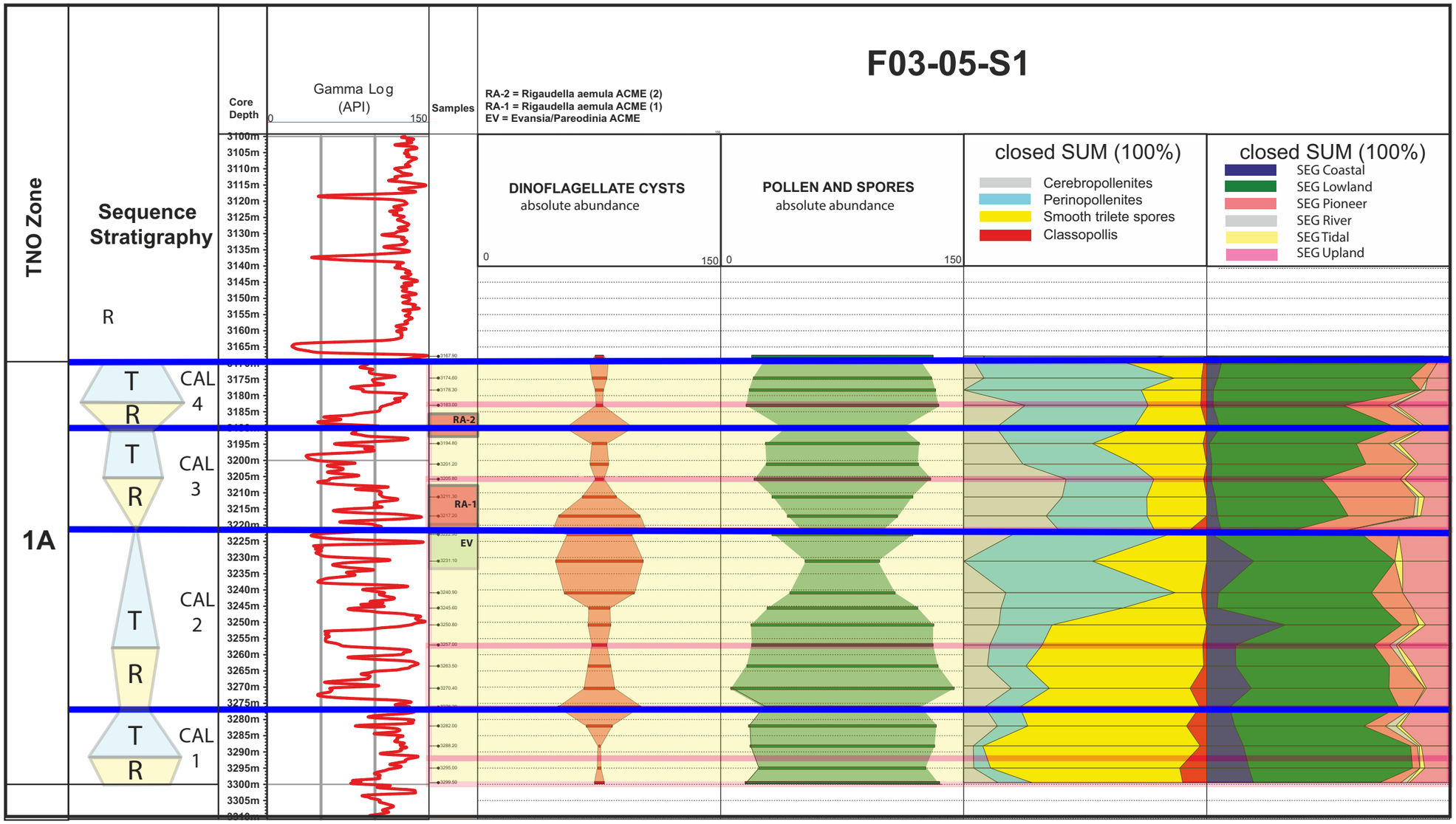

Figure 4.1.1 Palynology based summary chart of well F03-05-S1. A sequence stratigraphic interpretation is displayed on the left; T indicates Transgressive, R indicates Regressive. Blue lines are maximum flooding surfaces, pink lines represent the transition from regressive to transgressive trend.
SEG stands for Sporomorph Eco-Group (Abbink, 1998; Abbink et al. 2006).

4.1.1 Lower Graben Formation (Part 2/7)

Combined palynological and stable isotope results: The stable isotope results of well F03-05-S1 (Fig. 4.1.2) display a trend from relatively negative (-) towards positive (+), with a maximum at 3220m, and a gradual swing towards more negative again. The trend towards the positive maximum is very smooth with little scatter. The positive maximum more or less coincides with the J46 MFS. The trend above the positive maximum display more scatter. Note the extreme TOC values up to 70%, associated with coal bearing intervals.

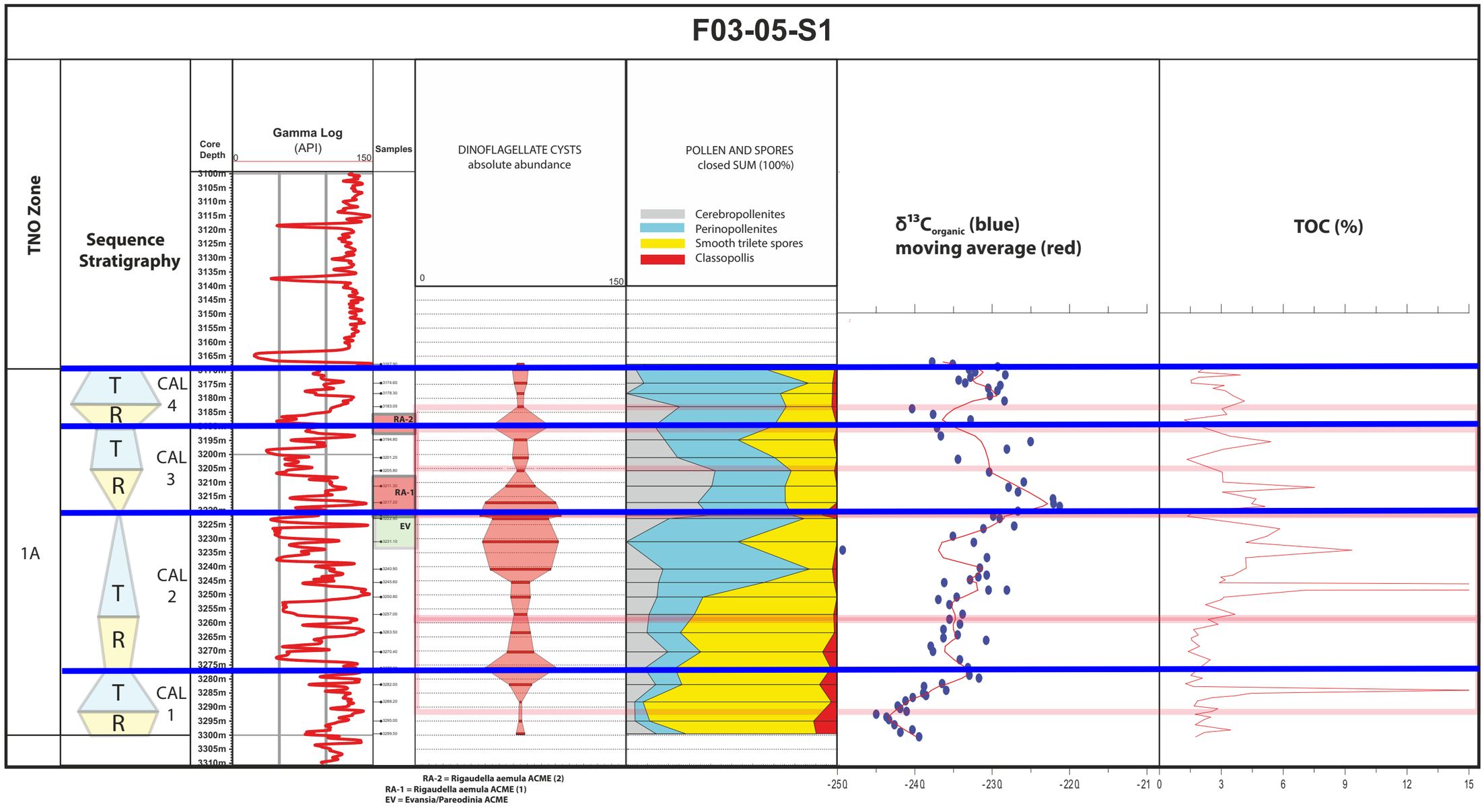

Figure 4.1.2. Combined palynological and stable isotope results of well F03-05-S1. Blue lines are maximum flooding surfaces, pink lines represent the transition from regressive to transgressive trend.

4.1.1 Lower Graben Formation (Part 3/7)

Sequence stratigraphic interpretation (Fig. 4.1.3)**:** the absolute abundance values of the marine dinoflagellate cysts and the terrestrial pollen and spores display a negative correlation. Where the absolute abundances of dinoflagellate cysts show a sudden increase, maximum flooding surfaces (MFS) are inferred. Where the absolute abundances of pollen and spores peak, sequence boundaries (SB) are inferred. Based on the combination of these two proxies, three maximum flooding surfaces and four (partial) transgressive-regressive cycles are inferred. Because the top part of the cored interval is assigned to the Oxfordian TNO Subzone 1B, the uppermost cycle is named OX-1. The MFS around 3290.8m is correlated with the latest Callovian 3rd order MFS known in the literature as the J46 MFS (e.g. Partington *et al*., 1993a; b).

Palaeoclimatic and palaeoenvironmental interpretation: The closed SUM diagrams of the pollen and spores display the most abundant pollen and spore types (to the left) and a subdivision according to the presumed affinity with a certain type of environment (to the right). The environmental affinities are based on Abbink (1998; Abbink *et al.*, 2006). The most prominent types are smooth trilete spores, *Perinopollenites* and *Cerebropollenites. Classopollis* is rare troughout, indicating relatively cool and humid conditions. *Cerebropollenites* is quite abundant in the interval 3254m 3290.8m, interpreted to represent tidal channel and tidal shoal environments, according to the core description interpretation. The top of the core, interval 3196m - 3207m, is dominated by smooth trilete spores. This part is characterized by thick coal development and interpreted as a swamp environment, based on the core descriptions.Note the ACME occurrences (super abundant) of the dinoflagellate cyst species *Rigaudella aemula* and *Evansia/Pareodinia.* These events are useful for short distance correlation.

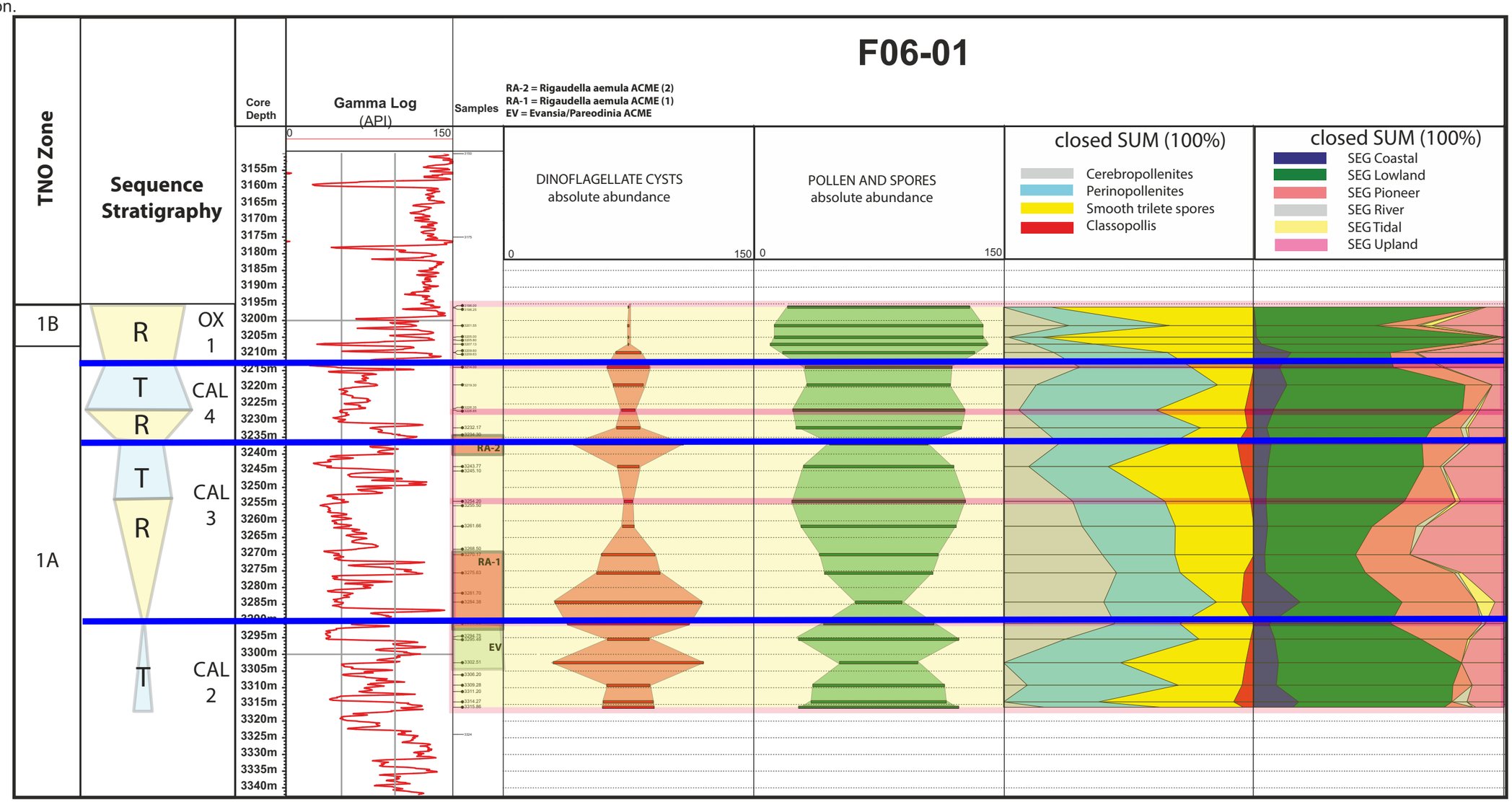

Figure 4.1.3 Palynology based summary chart of well F06-01. A sequence stratigraphic interpretation is displayed on the left; T indicates Transgressive, R indicates Regressive. Blue lines are maximum flooding surfaces.

4.1.1 Lower Graben Formation (Part 4/7)

Combined palynological and stable isotope results of well F06-01 (Fig. 4.1.4): The stable isotope results of well F06-01 display a trend from relatively negative (-) towards positive (+), with a maximum at 3272m, and a gradual swing towards more negative again. The trend towards the positive maximum is very smooth with little scatter. The positive maximum incepts just above the J46 MFS. The trend above the positive maximum display more scatter. Note the extreme TOC values (up to 70%), associated with coal bearing intervals.

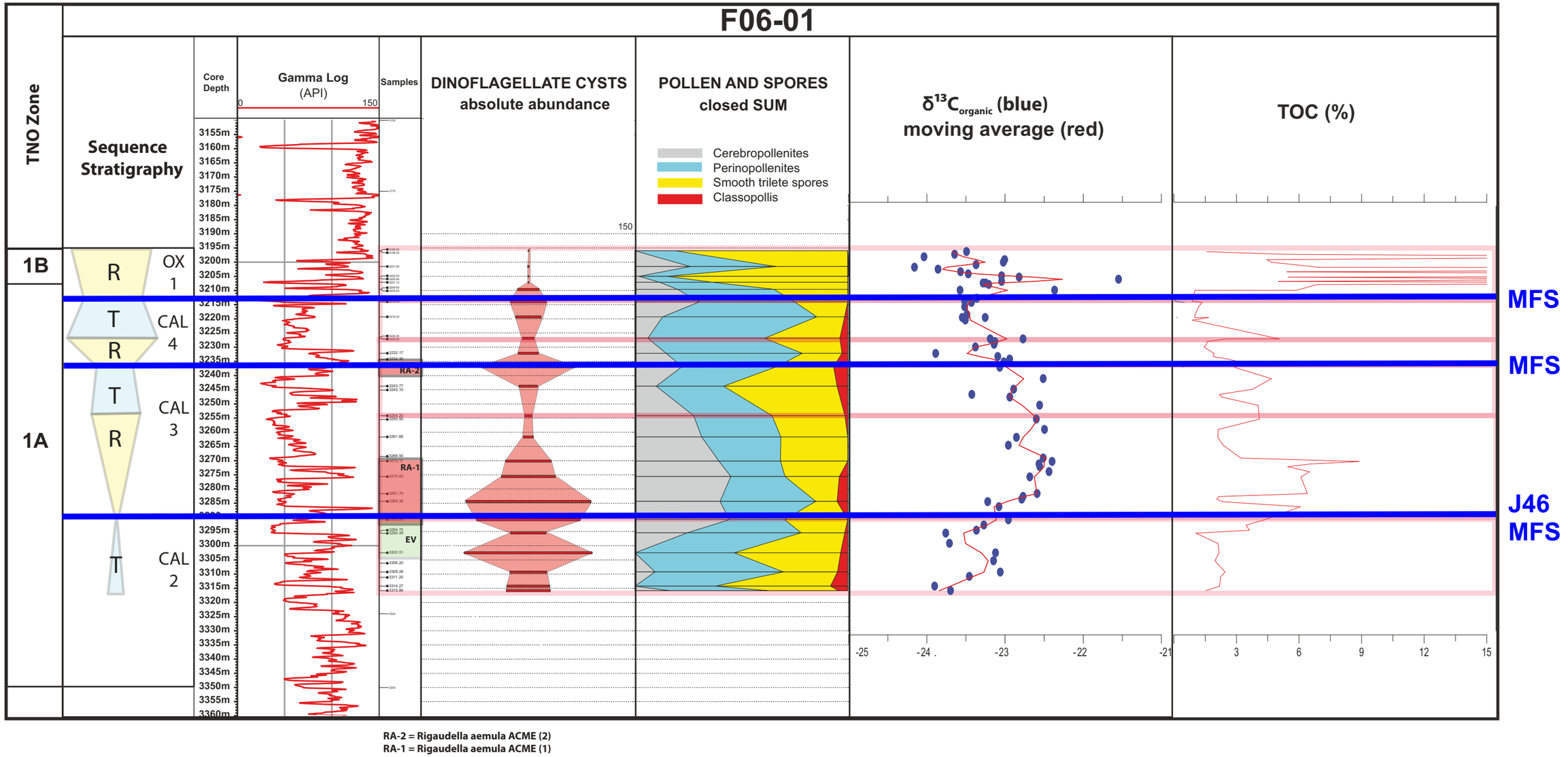

Figure 4.1.4 Combined palynological and stable isotope results of well F06-01. Blue lines are maximum flooding surfaces, pink lines indicate transtions from a regressive to a transgressive trend. The of-scale values

4.1.1 Lower Graben Formation (Part 5/7)

Correlation panel from well F03-05-S1 to well F06-01 (Fig. 4.1.5):
The Correlation panel is based on the combined palynological and stable isotope results. Based on the palynological results, four transgressive (T) - regressive (R) cycles are recognized in the late Callovian Subzone 1A. These sequences are named CAL1 to CAL4. The maximum flooding surfaces (MFS) are indicated in blue. The important 3rd order J46 MFS of Partington *et al.* (1993), incepts in the middle of the cored section in well F03-05-S1 and in the lower part of the cored section of well F06-01. Just above the J46 MFS, a positive peak (+) in the $\delta^{13}C$ stable isotope trend is observed in both wells, indicated with a dashed green line. The MFS associated with the second *Rigaulla aemula* ACME (RA-2), is accompanied by a negative peak (-) in the $\delta^{13}C$ stable isotope trend, represented with a red dashed line. Near the base of the cored section of well F03-05-S1, another negative (-) peak in the $\delta^{13}C$ stable isotope trend is recorded.

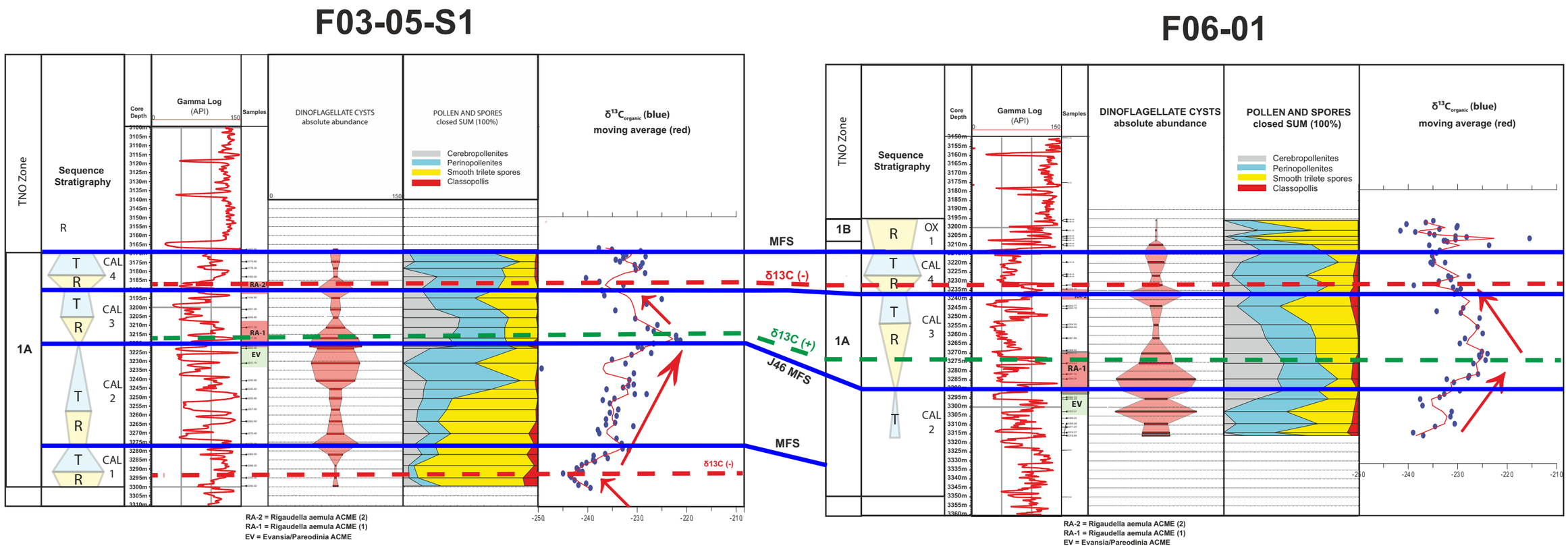

Figure 4.1.5 Correlation panel of well F03-05-S1 to F06-01. Blue lines represent Maximum Flooding Surfaces, derived from the palynological results. The dashed lines represent correllation lines based on the stable isotope analyses.

4.1.1 Lower Graben Formation (Part 6/7)

Sequence stratigraphic interpretation of well F14-05: the absolute abundance values of the marine dinoflagellate cysts are high troughout the entire cored section. A minor drop is noted in the interval 2155m - 2161m, concommittant with an increase in terrestrial pollen and spores (see Fig. 4.1.6). Two peak occurrences of specific dinocyst groups are observed: an ACME of *Rigaudella aemula,* in the interval 2164m - 2174m, and an ACME occurrence of the dinocyst group *Evansia/Glomodinium/Pareodinia,* in the interval 2180m - 2190m. In between these two peak abundances, at 2177m, a maximum flooding surface (MFS) is inferred (based on ACMEs). The MFS is correlated to the latest Callovian 3rd order MFS known in the literature as the J46 (e.g. Partington *et al.,* 1993).

Palaeoclimatic and palaeoenvironmental interpretation of well F14-05: The closed SUM diagrams of the pollen and spores display the most abundant pollen and spore types (to the left) and a subdivision according to the presumed affinity with a certain type of environment (to the right). The environmental affinities are based on Abbink (1998) and co-workers (Abbink *et al.*, 2006). The most prominent types are smooth trilete spores, *Perinopollenites* and *Cerebropollenites*.The warm and arid pollen type *Classopollis* is rare troughout the entire interval, indicating relatively cool and humid conditions. *Perinopollenites* is the most dominant pollen type and displays and increase towards the top, indicating increasing influence of relatively cool and wet lowland forests. *Cerebropollenites* is not very abundant, but it is more common near the base of the core, probably indicating some tidal influence. Smooth trilete spores are also not abundant, indicating the absence of real swamp environments. Note the ACME occurrences (super abundant) of the dinoflagellate cyst species *Rigaudella aemula* and *Evansia/Pareodinia.* These events are useful for short distance correlation.

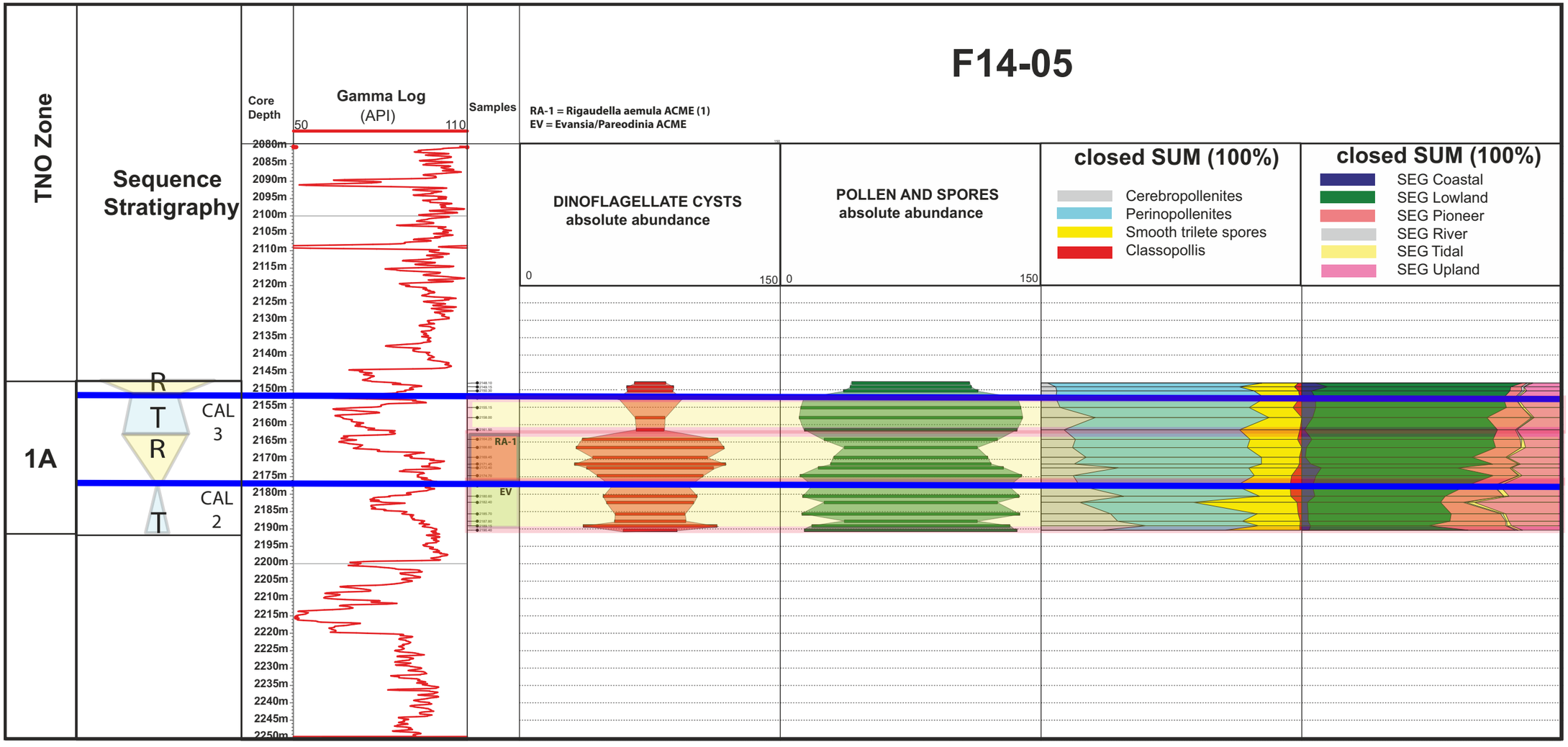

Figure 4.1.6 Palynology based summary chart of well F03-05-S1. A sequence stratigraphic interpretation is displayed on the left; T indicates Transgressive, R indicates Regressive. Blue lines are maximum flooding surfaces, pink lines represent transitions from regressive to transgressive trends.

4.1.1 Lower Graben Formation (Part 7/7)

Combined palynological and stable isotope results of well F14-05 (Fig. 4.1.7): Apart from the lower three samples, the stable isotope results of well F06-01 display a trend from relatively negative (-) towards positive (+), with a maximum at 2169m. Above 2169m, the values show a lot of scatter, but in general remain on the positive side.

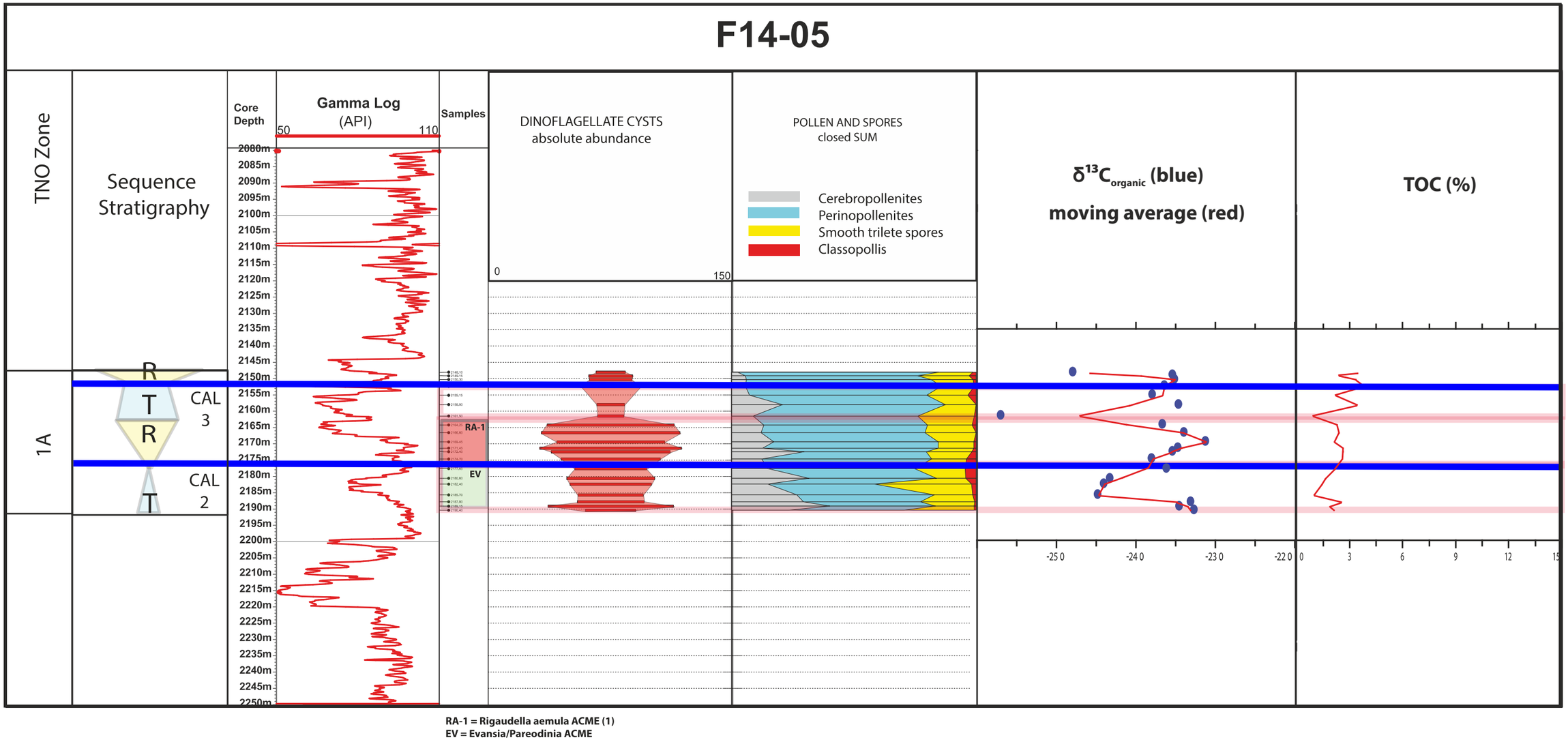

RA-1 = Rigaudella aemula ACME (1)
EV = Evansia/Pareodinia ACME

Figure 4.1.7 Combined palynological and stable isotope results of well F14-05. Blue lines are maximum flooding surfaces, pink lines represent transitions from regressive to transgressive trends.

4.1.2 Friese Front Formation (Part 1/3)

Biostratigraphy of well F17-03

Data source: Rijks Geologische Dienst, 1993, thirty four SWC samples between 1800-2070m
Lithostratigraphy (Table 4.1.1): New interpretation, differs from NLOG 2015
In the Upper Jurassic interval of well F17-03, Sequence 1 and Sequence 3 are represented, Sequence 2 is absent (Fig. 4.1.8).
Below the Upper Jurassic interval, The Posidonia Fm is present. It is expressed on the wireline logs by the combination of very high resistivity, very low density and widely varying GR. The Mid-Cimmerian unconformity, separating Lower from Upper Jurassic, is placed at 2038m, based on the palynological data. Below 2040m, dinocysts are absent, while *Chasmatosporites, Tasmanites* and freshwater palynomorphs are abundant, which is characteristic for the Werkendam Fm. The latest Callovian J46 MFS is recognized at 2035m, it is reflected by the common occurrence of Rigaudella aemula. Nothe that the lower part of the Friese Front, interval 197m - 2035m, is distinctly marine, indicated by the abundant occurrence of dinocysts. The regional (NW Europe) densiplicatum climate shift (Abbink *et al.* 2006) incepts between 1945m and 1959m and is inferred from the back-drop of Densoisporites, a pollen type charateristic for wet, lowland environments. The top of Subzone 1A is placed at 2005m and is based on the LOD of *Durotrigia filapicata.* The shaly interval between 1834m and 1854m, is assigned to the Late Ryazanian Subzone 3C, based on the occurrences of *Daveya boresphaera, Gochteodinia villosa,* Exeguisphaera phragma, and Tehamadinium daveyi. That age assignment is in line with a lithostratigraphic assignment to the Schill Grund Mb of the Lutine Fm. The overlying interval is rich in the dinocyst *Cymososphaeridium validum,* indicating a Valanginian age (Zone 4).

Table 4.1.1 Lithostratigraphy of well F17-03

F17-03 Lithostrat NLOG 2015	TOP	BASE
Vlieland Claystone Formation	1747	1847
Schill Grund Member	1847	1860
Stortemelk Member	1860	1870
main Friese Front member	1870	1975
Rifgronden Member	1975	2045
Lower Werkendam Member	2045	2071

F17-03 Lithostrat FOCUS project	TOP	BASE
Vlieland Claystone Formation	1747	1830
Schill Grund Member	1830	1857
Scruff Greensand Fm	1857	1870
Friese Front Fm	1870	2043
Werkendam Fm	2043	2071

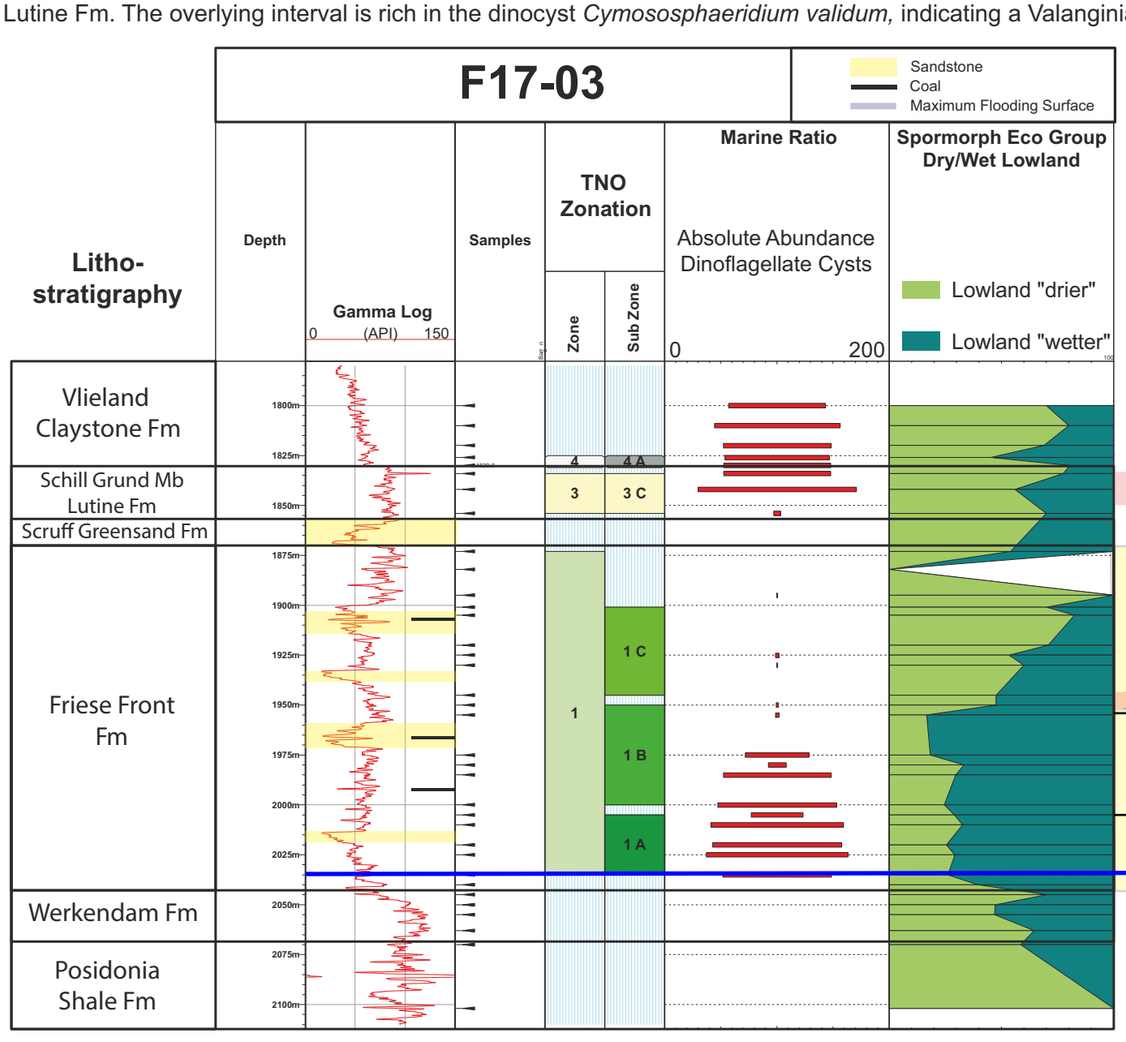

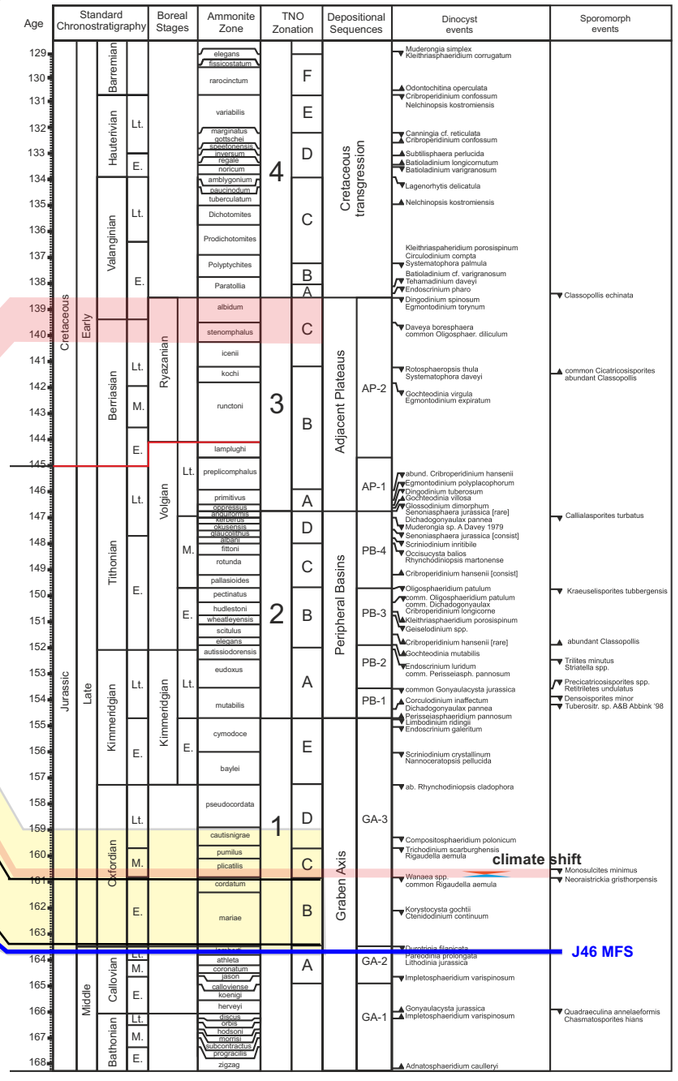

Figure 4.1.8 Biostratigraphy of well F17-03. The Upper Jurassic to Lower Cretaceous section is correlated to the TNO Zonation (see also Fig. 3.4 where the zonation is dislplayed in A3). The blue line represents the J46 maximum flooding surface (Partington *et al.*, 1993a; b).

4.1.2 Friese Front Formation (Part 2/3)

Biostratigraphy of well F17-04 (Fig. 4.1.9):
Data source: PhD Abbink (1998) and this study (FOCUS); thirty four core samples, fifteen SWC + ten cuttings
Lithostratigraphy (Table 4.1.2): this study (FOCUS project), slightly modified after NLOG 2015
The Upper Jurassic interval of well F17-04 comprises Sequence 1 and Sequence 3, while Sequence 2 is absent.
Immediately below the Upper Jurassic interval, the Posidonia Fm is present. It is expressed on the wireline logs by the combination of very high resistivity, very low density and widely varying GR. The latest Callovian J46 MFS is recognized at 2542m, based on the peak-abundance of marine dinoflagellate cysts. DInoflagellate cysts occur throughout the entire Friese Front, but the lower part shows elevated abundances. In the past, the enhanced marine influence of the lower Friese Front was used to split off a separate member, the Rifgronden Member. In this study, it is argued that the presence of dinoflagellate cysts is not an appropriate criterion to split off a separate member from the Friese Front Fm. Therefore, the entire Upper Jurassic section is assigned to the Friese Front Fm. The densiplicatum climate shift is recognized in the cored section at 2453.65m. The shift is inferred from the sudden decrease in Densoisporites, a pollen type charateristic for wet, lowland environments. The top of Subzone 1A is placed at 2533m, based on the LOD common Dichadogonyaulax sellwoodi and the LOD Durotrigia filapicata at 2542. The shaly interval above the Scruff Greensand Fm is assigned to the Late Ryazanian Subzone 3C, in line with a lithostratigraphic assignment to the Schill Grund Mb of the Lutine Fm.

Table 4.1.2 Lithostratigraphy of well F17-04

F17-04 Lithostrat NLOG 2015	Top MD	Base MD
Vlieland Claystone Formation	2150	2302
Schill Grund Member	2302	2398
Stortemelk Member	2398	2411
main Friese Front member	2411	2497
Rifgronden Member	2497	2572
Posidonia Shale Formation	2572	2624

F17-04 Lithostrat FOCUS project	Top MD	Base MD
Vlieland Claystone Formation	2150	2302
Schill Grund Member	2302	2398
Scruff Greensand Fm	2398	2411
Friese Front Fm	2411	2572
Posidonia Shale Formation	2572	2624

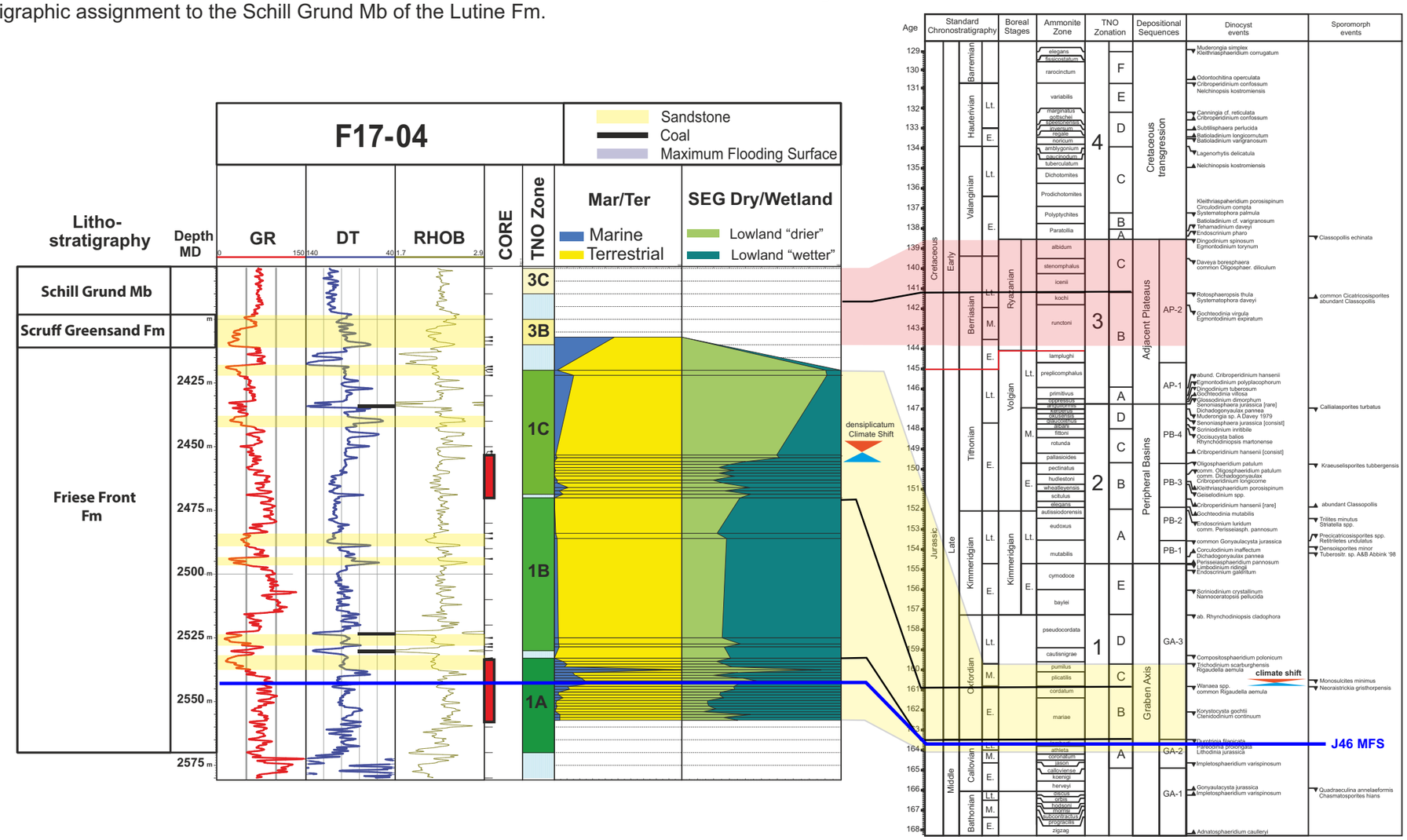

Figure 4.1.9 Biostratigraphy of well F17-04.
The Upper Jurassic to Lower Cretaceous section is correlated to the TNO Zonation (see also Fig. 3.4, where the zonation is displayed in A3 format). The blue line represents the J46 maximum flooding surface (Partington *et al.*, 1993a; b).

4.1.2 Friese Front Formation (Part 3/3)

Biostratigraphy of well F17-09 (Fig. 4.1.10):
Data source: Consultancy report provided by Sterling Resources (twenty cuttings samples), new analyses this study (seven cuttings samples, eight core samples)
Lithostratigraphy: this study, well F17-09 is not released yet
In the Upper Jurassic interval of well F17-09, Sequence 1 and Sequence 3 are represented, Sequence 2 is absent.
The base of the Upper Jurassic, the Mid-Cimmerian unconformity is placed at 2138m, based on the comparison and correlation with the nearby well F17-03. The cuttings samples in that interval are characterized by abundant caving. The top of TNO Subzone 1A is placed at 2113mCU, based on the LOD Pareodinia prolongata. The densiplicatum climate shift is inferred between 2014m and 2039.5m, based on the change from Densoisporites dominated assemblaged, to Callialasporites dominated assemblages.

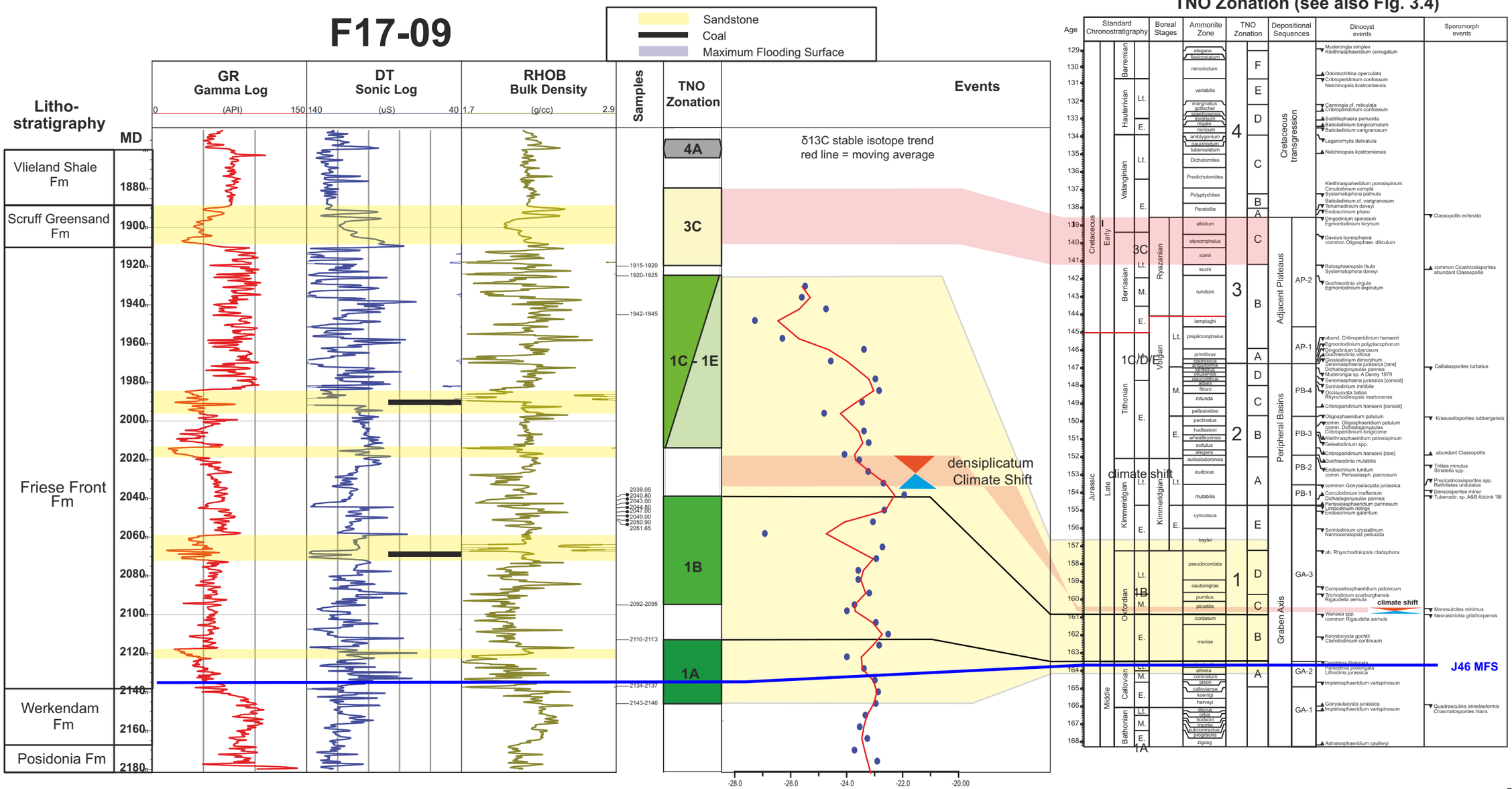

Figure 4.1.10 Biostratigraphy of well F17-09. The Upper Jurassic to Lower Cretaceous section is correlated to the TNO Zonation (see also Fig. 3.4 where the zonation is displayed in A3). The blue line represents the J46 maximum flooding surface (Partington *et al.*, 1993a; b).

4.1.3 Scruff Greensand and Skylge Formations (Part 1/4)

Biostratigraphy of well F15-A-01

Data source: new analyses, twenty one core samples for palyno & stable isotopes; existing data (Herngreen et al., 2001), thirty five SWC samples for palynology & stable isotopes

Age assessment (Fig .4.1.11)**:** In the Upper Jurassic interval of well F15-A-01, Sequence 2 and Sequence 3 are present, Sequence 1 is absent. The kick in the GR and Sonic around 2480m represent the base of the Rijnland Group, and is correlated to the Valanginian TNO Subzone 4A. The cored section between 2559m - 2584m is correlated to the Early Ryazanian - Late Volgian TNO Subzone 3B. The top of TNO Subzone 3A is inferred at 2588m.

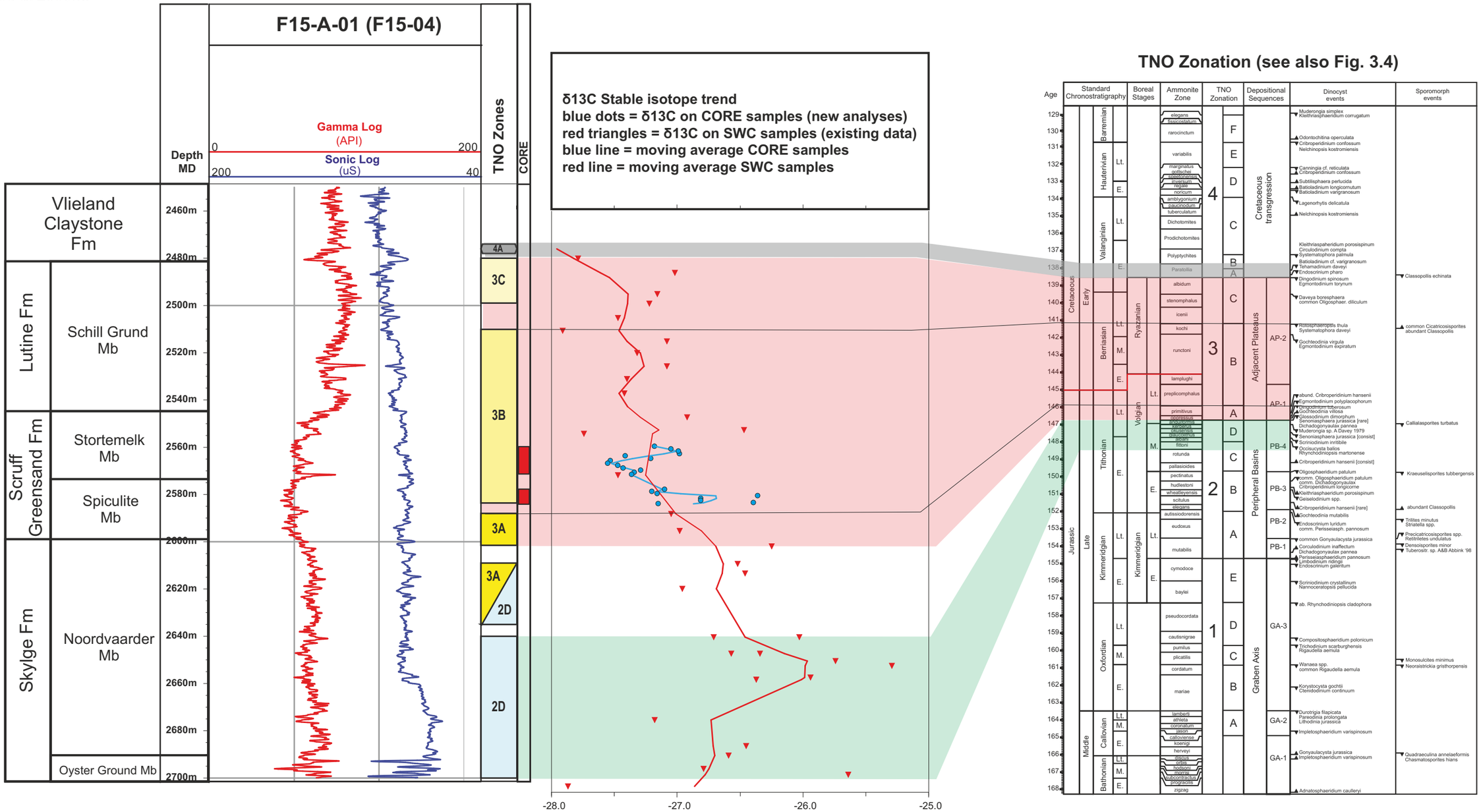

Figure 4.1.11 Biostratigraphy of well F15-A-01. The Upper Jurassic to Lower Cretaceous section is correlated to the TNO Zonation (see also Fig. 3.4 where the zonation is displayed in A3). The lithostratigraphy is after NLOG 2015.

4.1.3 Scruff Greensand and Skylge Formations (Part 2/4)

Biostratigraphy of well F18-03

Data source: new analyses, this study (quick scan, no detailed record). Twenty five cuttings samples for palyno and one hundred seventy three cuttings samples for stable isotopes.
Lithostratigraphy (Table 4.1.3): after NLOG 2015
Age assessment (Fig. 4.1.12): In the Upper Jurassic interval of well F18-03, Sequence 2 and Sequence 3 are present, Sequence 1 is absent. The kick in the GR and Sonic around 2425 represents the base of the Rijnland Group, and is correlated to the Valanginian TNO Subzone 4A.

Table 4.1.3 Lithostratiphy of well F18-03

Lithostratigraphy (NLOG 2015)	Top (MD)	Base (MD)
Vlieland Claystone Formation	2207	2400
Schill Grund Member	2400	2465
Stortemelk Member	2465	2558
Scruff Spiculite Member	2558	2652
Noordvaarder Member	2652	2827
Oyster Ground Member	2827	2923

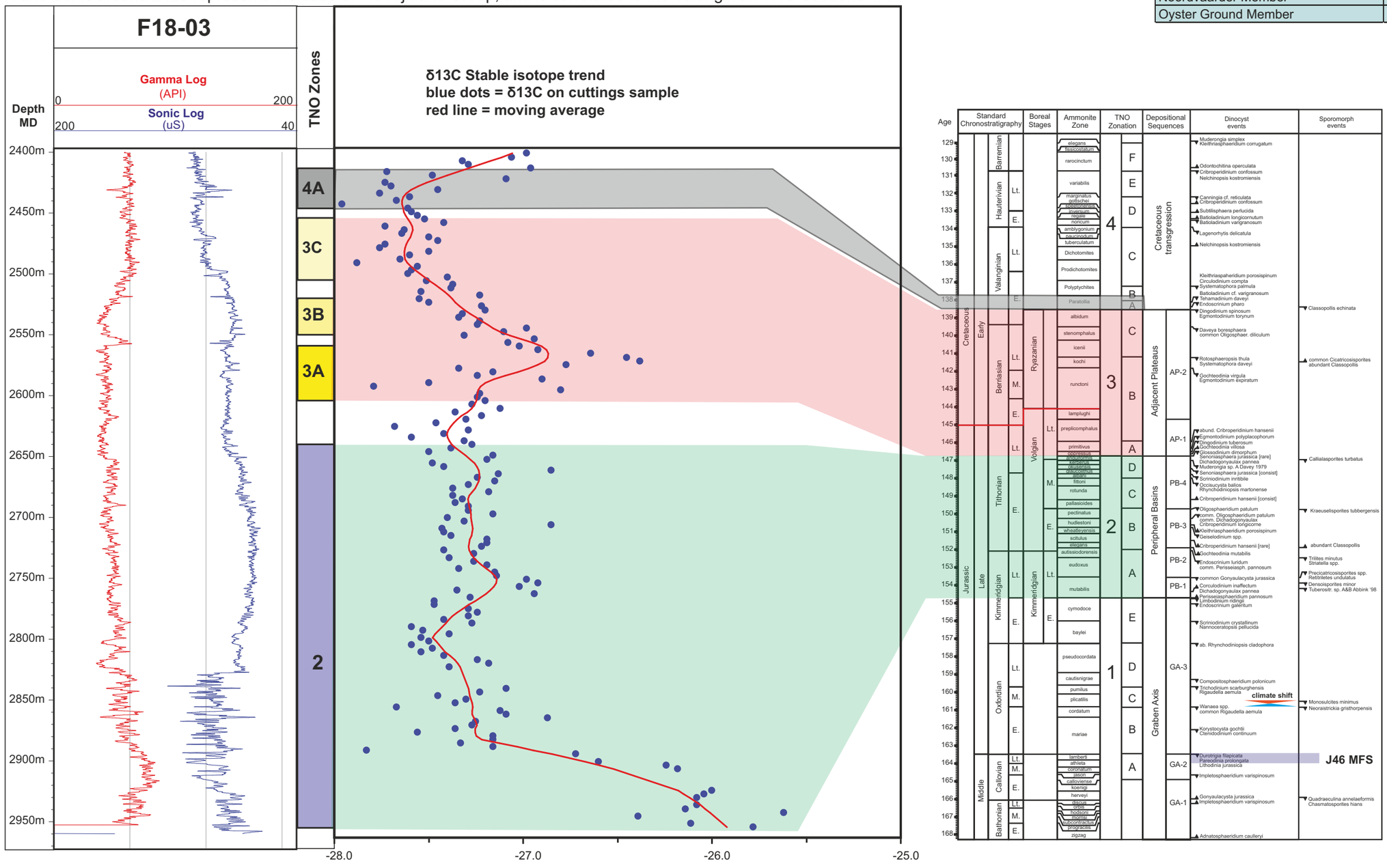

Figure 4.1.12
Biostratigraphy of well F18-03.
The Upper Jurassic to Lower Cretaceous section is correlated to the TNO Zonation (see also Fig. 3.4, where the zonation is displayed in A3).
The blue line represents the J46 maximum flooding surface (Partington *et al.*,1993).

4.1.3 Scruff Greensand and Skylge Formations (Part 3/4)

Age assignment (Fig. 4.1.13): TNO Subzones 4A, 3C and 3B are recognized in the cored interval and displayed on the left. The zonal assignments are based on LODs and FODs (see Chapter 2, Methodology). In addition, some important palynological events are indicated in the chart with the capitals A to E. These events are suited for local correlation, e.g. to well M07-08.
Sequence stratigraphy: A sequence stratigraphic interpretation based on the palynological results is not easy, because of the strong and continuous input of sand during deposition of the cored interval. Nevertheless, a conspicuous “hour glass” narrow in the dinocyst abundance curve is observed at 3980.5m, probably indicating a sequence boundary at this level. In addition, the interval between event A and B is very rich in dinocysts, indicating high relative sea levels for this interval.
Stable isotope trends: The stable isotope results display a gentle but convincing trend. From base to top, two and a halve cycles may be observed. These cycles are summarized by the following events: a negative maximum (-) at 3975m, inflection point at 3968m, positive max (+) at 3965m, inflection point at 3960m, negative max (-) at 3957m, inflection point at 3952m and positive max (+) at 3943m are observed.

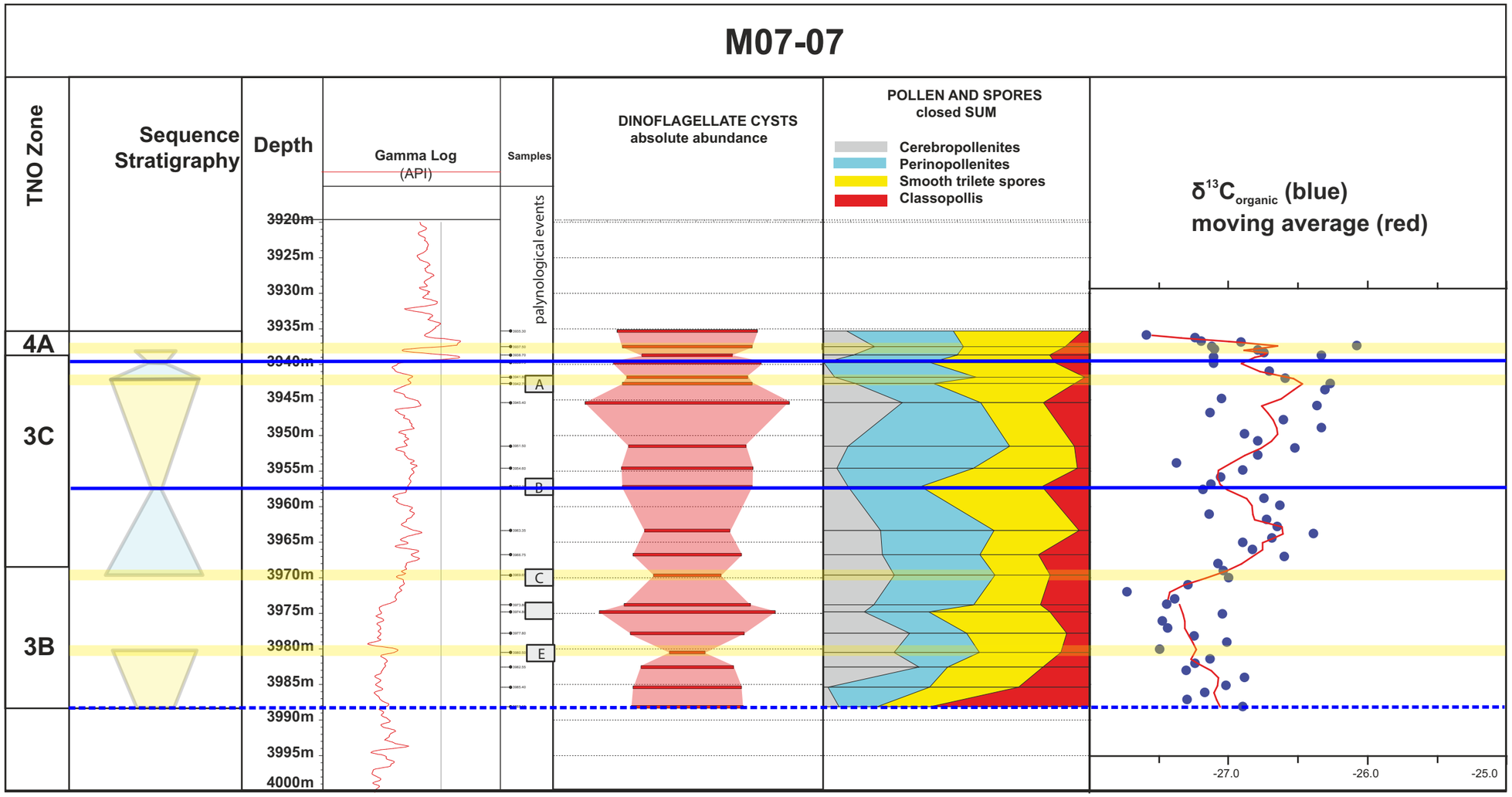

A = LCOD Oligosphaeridium diluculum
B = FCOD Oligosphaeridium diluculum
C = LOD Rotosphaeropsis thula
D = Cicatricosisporites/Classopollis break
E = FCOD Stiphrosphaeridium dictyophorum

Figure 4.1.13 Palynology and stable isotope results of well M07-07. Blue lines are maximum flooding surfaces.

4.1.3 Scruff Greensand and Skylge Formations (Part 4/4)

Combined palynological and stable isotope results of well M07-08 (Fig. 4.1.14)

Age assignment: Displayed on the left column are the TNO Subzones 3C and 3B that were assigned by interpreting the dinocyst and pollen and spore distribution charts. The zonal assignments are based on LODs and FODs (see Chapter 2, Methodology). In addition, some important palynological events could be recognized that are indicated in the chart with the captials A to D. These events are particularly useful for local correlation to well M07-08.

Sequence stratigraphy: The palynological results are hard to interpret in terms of sequence stratigraphy, the clastic supply was continuously high during deposition of the cored interval. The interval between events A and B is the most rich in dinocysts, indicating that the highest sea levels were probably reached during deposition of this interval. Probable sea level lows or sequence boundaries are inferred at 4855m and 4903m, where the absolute abundance values of the dinocysts reach an all time low.

Stable isotope trends: The stable isotope results display a gentle trend, with the moving average showing perhaps three cycles from more positive to more more negative values. These cycles are summarized as follows: a positive max (+) at 4898m, inflection point at 4890m, a negative max (-) at 4881m, inflection point at 4870m, a positive max (+) at 4956m, inflection point at 4845m, negative max (-) at 4833m, inflection point at 4820m, and a positive maximum (+) at 4805m.

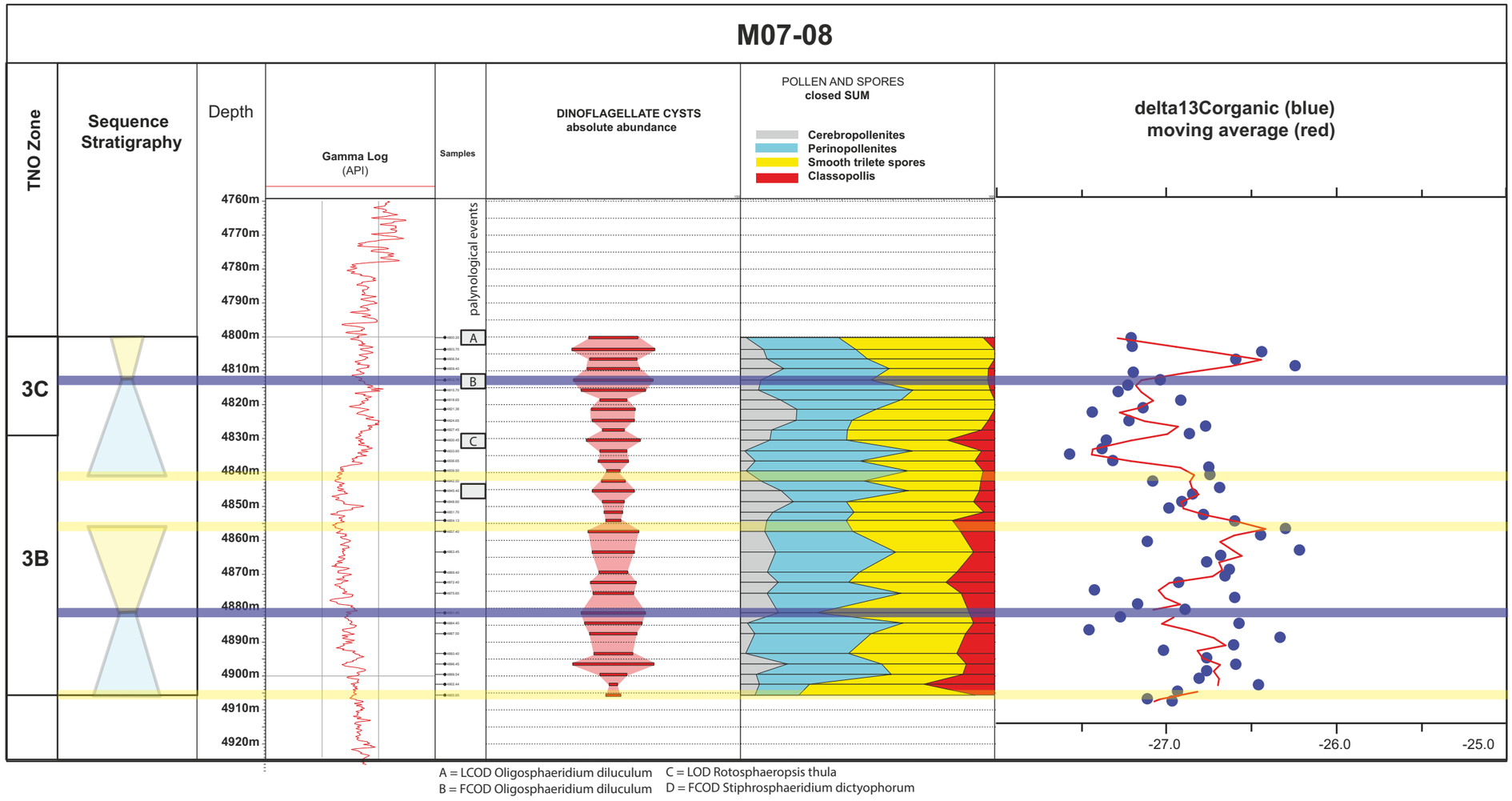

Figure 4.1.14 Palynology and stable isotope results of well M07-08

4.2

RESULTS
CORE ANALYSIS

4.2 Core Analysis

4.2.1 Summary

The threefold stratigraphic division that formed the starting point of the project, *viz.* Sequence 1, 2, and 3, is clearly visible in the distribution of the depositional environments that were established after the core descriptions were made (Table 4.2.1 and Figure 4.2.1).

Sequence 1, with cores from the Lower Graben and Friese Front formations, contains the most diverse environments of deposition: from swamps and freshwater lake fills to fully open marine deposits. This is also the sequence which has most meters of core described, mostly due to two very long cores: 137 m from F03-05-S1, and 121 m from F06-01. Figure 4.2.1 shows that the northern wells (F03-F06 area) have the most estuarine deposits and the southern wells (F14-F17-L05) the most marine deposits. This is remarkable in view of the basin topography, which is generally proximal in the South and distal in the North. The next chapters will discuss this subject in more detail (Verreussel et al, in prep).

Sequence 2 (Terschelling and Oyster Ground Formations) contains cores with lower and upper shoreface and estuarine deposits. The upper shoreface depositional environment is the dominant environment, the other two are more or less evenly distributed.

Sequence 3 (Scruff Greensand) is the most marine one, with facies that belong to shoreface depositional environment in M07-07 to shelf deposits in L06-02. The most proximal facies is found in M07-07, the most distal facies in L06-02.

Table 4.2.1: Cumulative amount (in m) of sedimentary facies identified in the cores for each of the three sequences.

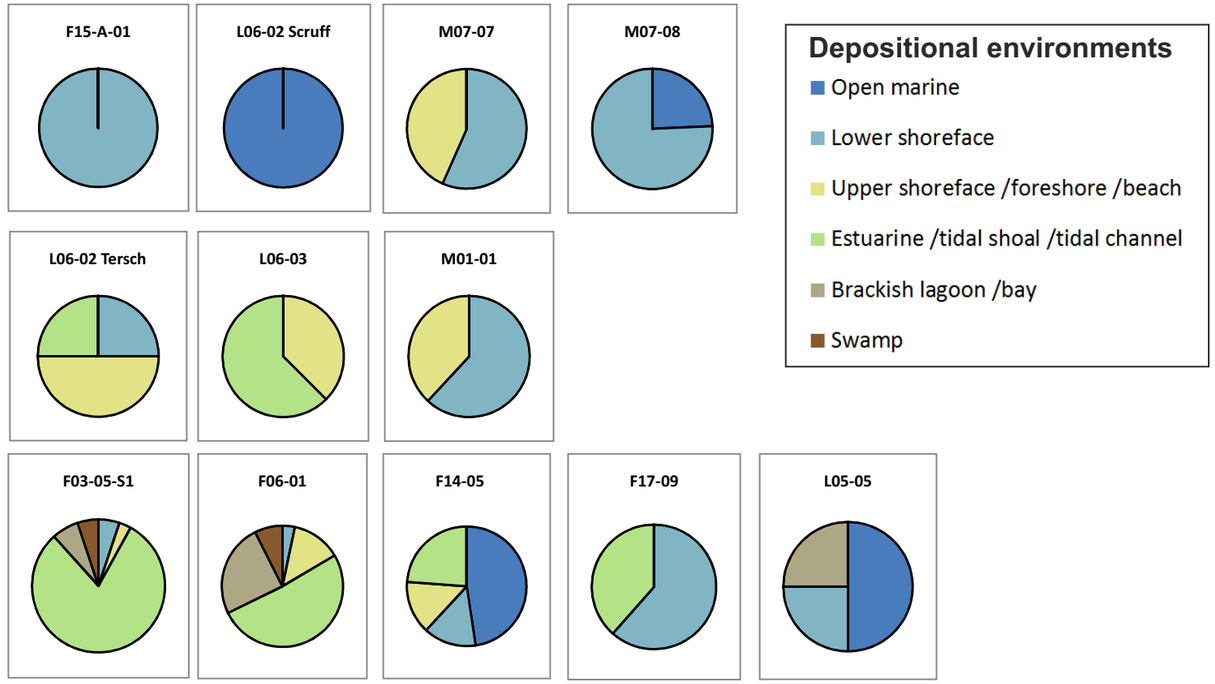

Stratigraphic Unit	Well	Open marine	Lower shoreface	Upper shoreface /foreshore /beach	Estuarine /tidal shoal /tidal channel	Brackish lagoon /bay	Swamp	
Sequence 3 Scruff Greensand Fm.	F15-A-01		20					20
	L06-02	31						31
	M07-07		30	23				53
	M07-08	26	81					107
Sequence 2 Terschelling Sandstone and Oyster ground Members	L06-02		10	20	10			40
	L06-03			6	10			16
	M01-01		13	8				21
Sequence 1 Lower Graben and Friese Front Formations	F03-05-S1		7	4	110	9	7	137
	F06-01		4	16	62	30	9	121
	F14-05	20	6	6	10			42
	F17-09		8		5			13
	L05-05	8	4			4		16
		85	183	83	207	43	16	617

Figure 4.2.1: Relative proportions of sedimentary facies identified in the cores for each of the three sequences. Top row: Sequence 3; middle row: Sequence 2; bottom row: Sequence 1.

4 - Results - Core Analysis

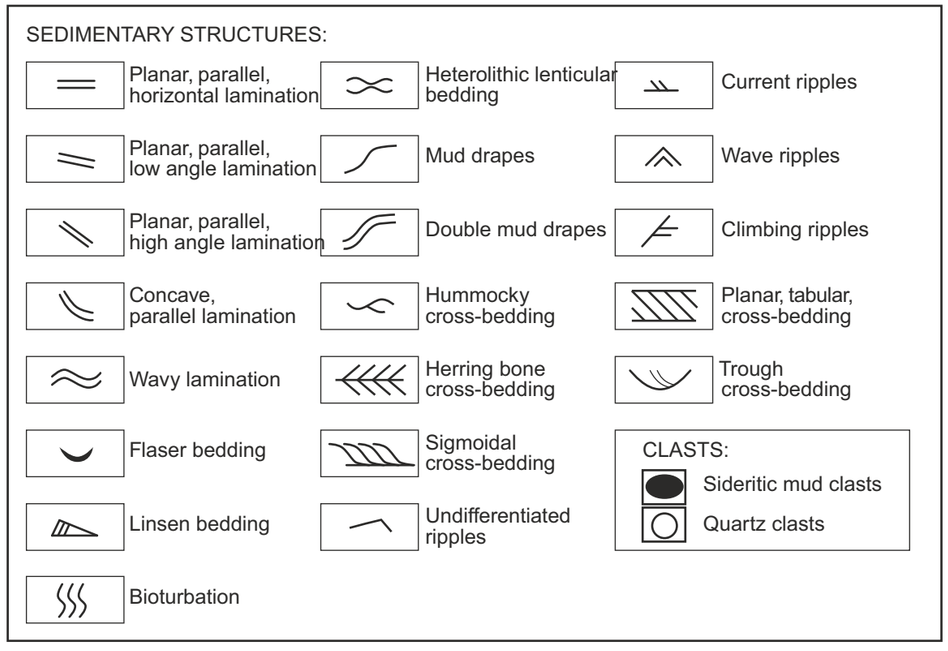

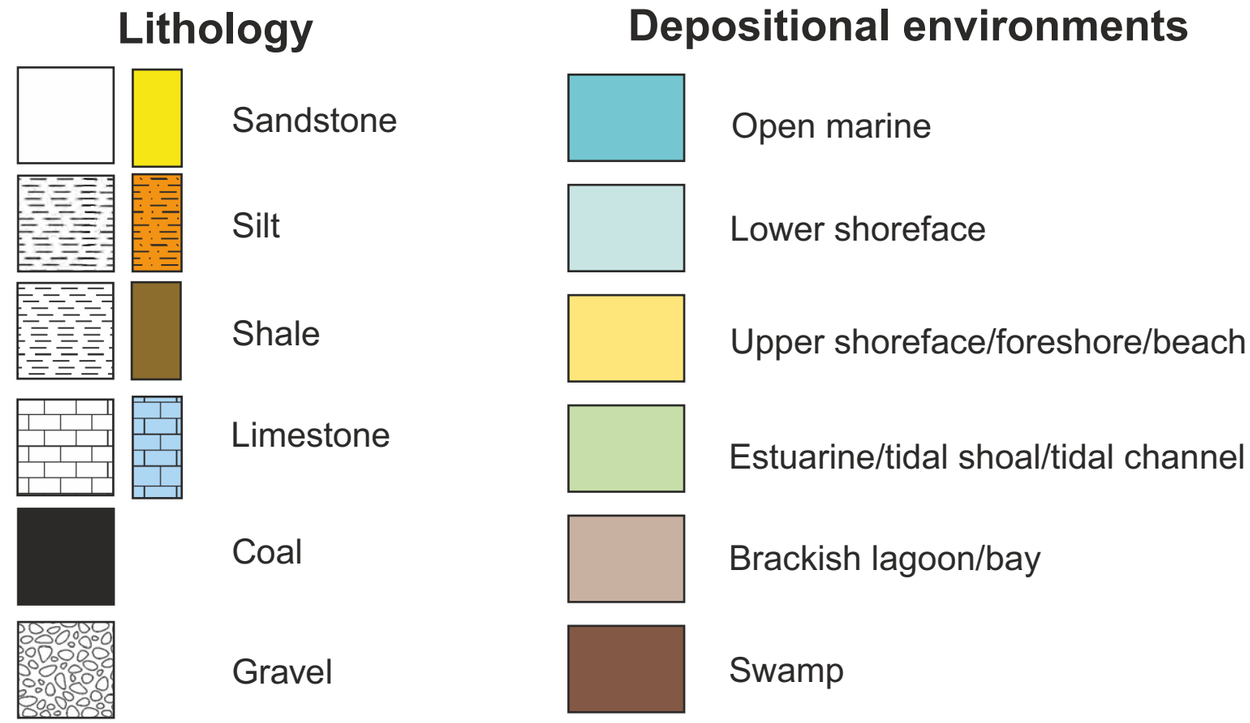

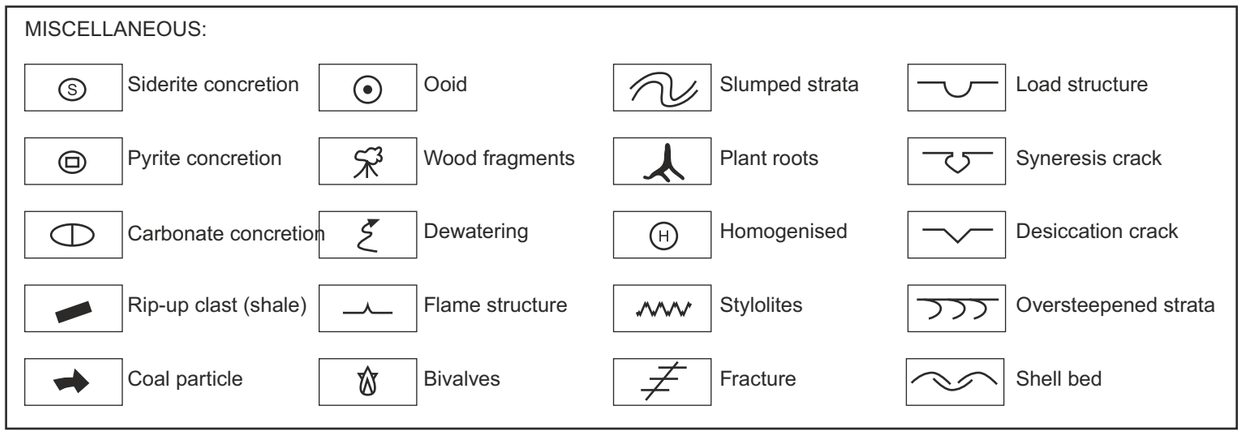

Figure 4.2.2: Legend for the core descriptions.

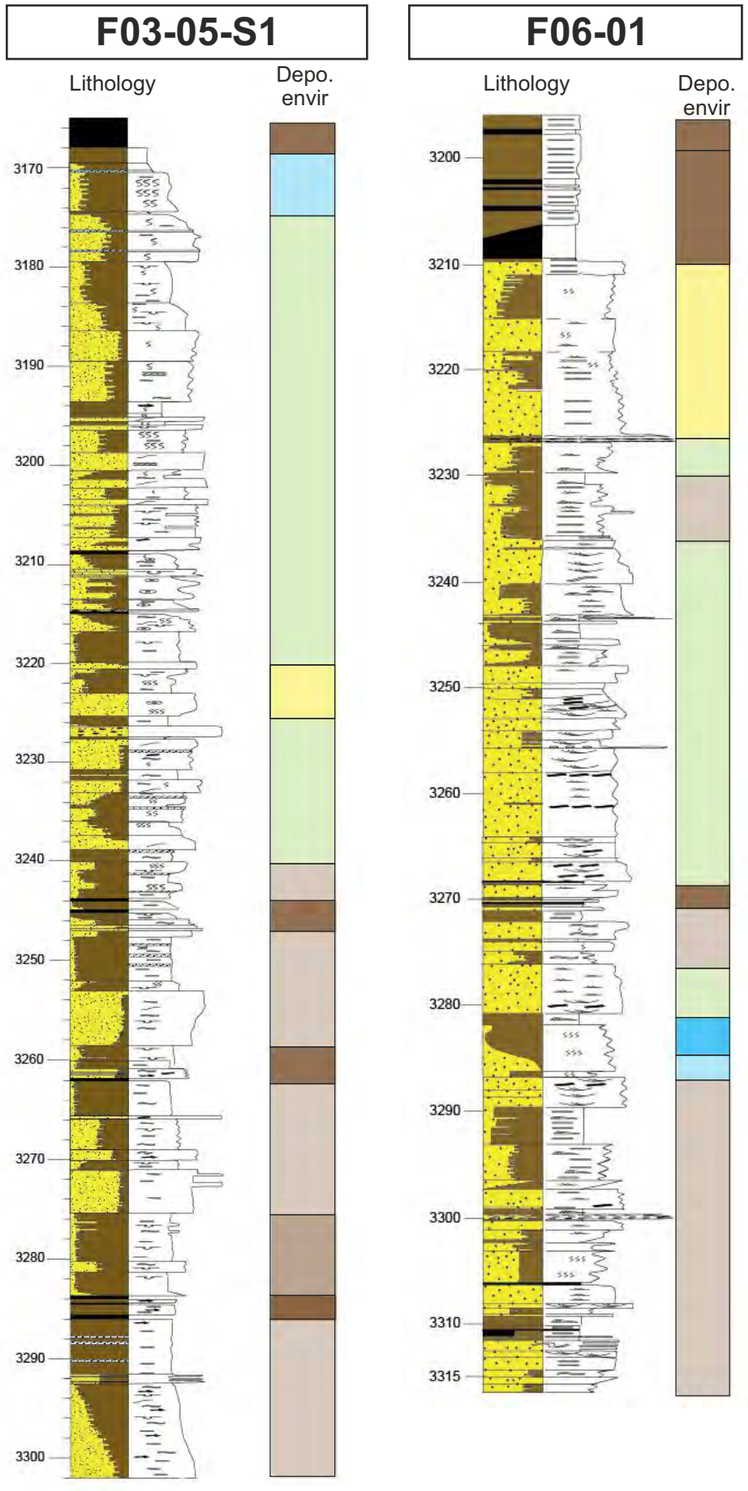

F03-05-S1, 3292.5 m - Finely laminated fresh water bay deposits with siderite cement and coal fragments

F06-01, 3239 m - Cross bedding with mud drapes deposited in a tidal channel

F06-01, 3222 m - Well sorted upper shoreface sands with large *Ophiomorpha*

F03-05-S1, 3166.5 m - Very thick (5 m) and extensive coal at the base of the Middle Graben Fm.

- Estuarine /tidal shoal /tidal channel
- Brackish lagoon /bay
- Swamp
- Open marine
- Lower shoreface
- Upper shoreface /foreshore /beach

4.2.2 - Sequence 1

Description of F03-05-S1 and F06-01
(see Fig. 4.2.2 for legend)

The cores from Sequence 1 have the widest variety in sedimentary facies of all three sequences. The depositional environments range from the lower reaches of the lower shoreface through upper shoreface and estuarine deposits to fluvial channel deposits. The longest cores were cut in the F3-FB Field, with F03-05-S1 and F06-01 as the most prominent ones. These two cores were cut in approximately the same stratigraphic interval and show a similar, overall transgressive development, roughly from freshwater bay via estuarine to marine shoreface. The Callovian-Oxfordian boundary near the top of the cores heralds the onset of a non-marine lake and swamp environment, virtually without any coarse grained sediment.

The lowermost few tens of meters of F03-05-S1 and F06-01 consist of very finely laminated, fine grained sandstones, siltstones and claystones. Thin (10 to 30 cm) coal layers are present, as are abundant siderite bands and nodules. Siderite is also present as an accessory cementing mineral within the sandstones. The sequence is further characterized by the almost complete absence of burrows, apart from some rootles (mostly in the seat earths underlying the coal seams) and some tiny *Planolites.* These sediments are interpreted to have been deposited in a very quiet fresh water to very low saline environment, where occasionally peats formed.

Gradually the sediments record more bioturbation, and many synaeresis cracks, pointing to mixed or varying water salinities. Sandy intervals of 1 to 4 m thick with cross bedding, mud drapes (occasionally double mud drapes) are thought to represent tidal channel deposits in a muddy estuarine environment. Centimeter-scale heterolithic bedding might represent tidal flat deposits.

The estuarine sequence is interrupted twice by a marine incursion. These marine intervals are primarily recognized by a sudden abundance of large and varied ichnogenera that are typical for a fully marine environment. Species include *Ophiomorpha, Asterosoma, Rosselia, and Zoophycos.*

The cored sequence in these two wells is topped by a non-marine coals and shale interval, starting at the Callovian-Oxfordian boundary.

4 - Results - Core Analysis

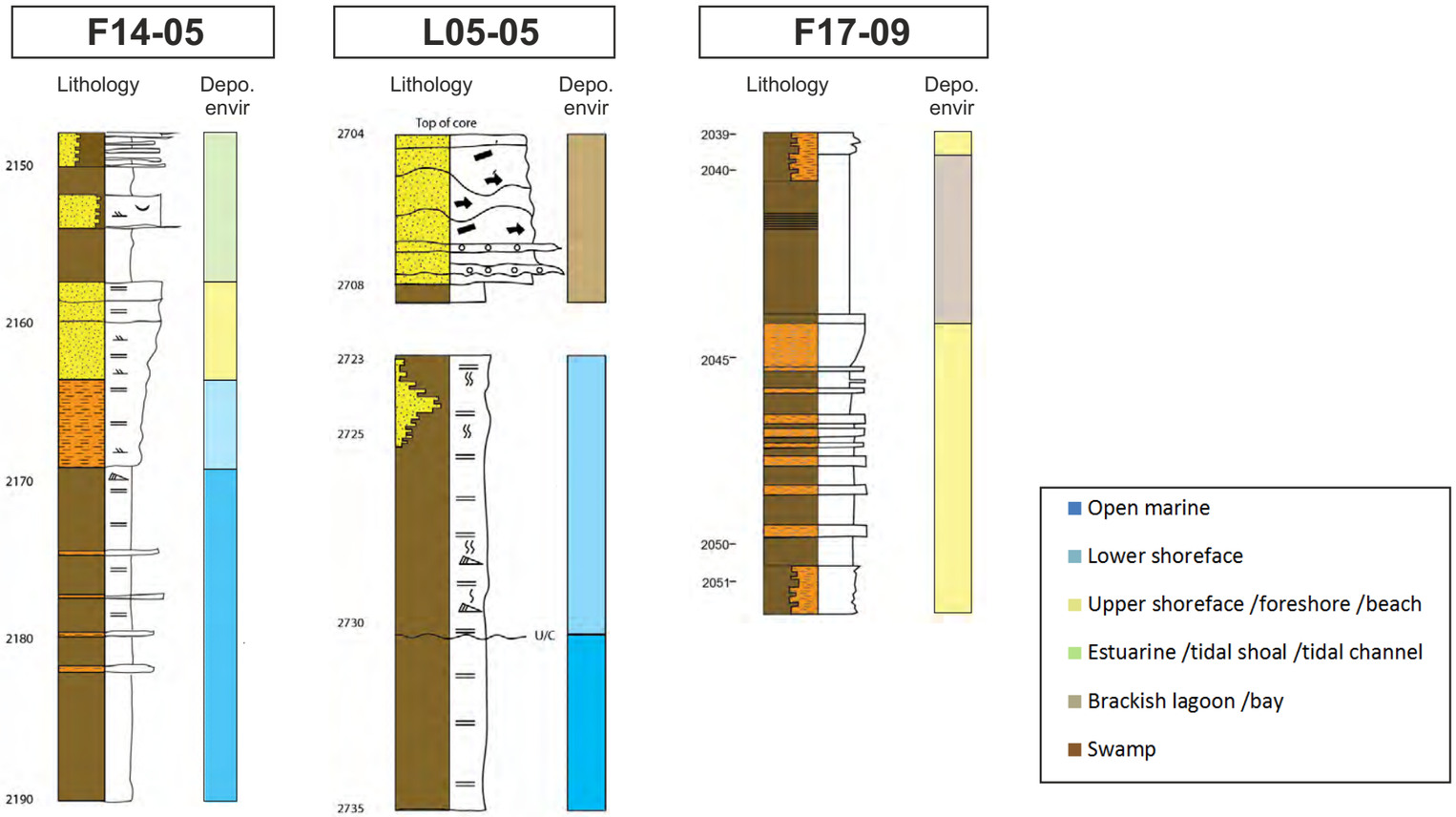

F14-05, 2173 m - Offshore / shelf muds

F14-05, 2167 m - Bioturbated b cross-bedded siltone and claystone interpreted as with Lower shoreface

L05-05, 2729.6 m - Lower shoreface muds with storm sands, cemented by pyrite and dolomite cement)

L05-05, 2704.4 m - Fluvial channel sands with coal fragments

F17-09, 2051 m - Lower shoreface with *Rhizocorallium*

Description of F14-05, F17-09 and L05-05
(see Fig. 4.2.2 for legend)

The three cores from wells F14-05, F17-09 and L05-05 are a few tens of meters long, and, therefore, only provide a glimpse of the depositional environment of Sequence 1 in the Southern part of the study area.

Well F14-05 shows a classic regressive shoreface sequence of in total 40 m thick. The sequence has offshore muds at its base, with some thin, silt-sized beds, interpreted as distal storm deposits. Gradually the amount of clay diminishes, and lower shoreface environment prevails with more and thicker , more proximal storm deposits. Via a series of upper shoreface sands, characterized by medium to coarse grained, cross-bedded *Ophiomorpha*-bearing sands, the top of the sequence is interpreted as a tidal lagoon, mud dominated, with occasional tidal creeks or tidal flats. Fauna is a typical impoverished one, with very few genera (mainly Planolites) which have very small diameters.

The core from Well F17-09 has an overall fine grain size. The twelve meter long core contains only mud and silt. The lower silt-dominated part is interpreted as lower shoreface, the upper part as lagoonal. The latter has no visible bioturbation. It does show some parallel lamination and several siderite streaks and nodules. The top part of the core sees a return to marine conditions, with heterolithic silt-shale bedding and marine burrows, such as *Scolicia.*

Well L05-05 has some five meters of Lower Jurassic shales (Altena Gp.) at its base, unconformably overlain by a mud-dominated sequence, interpreted as lower shoreface deposits. Sedimentary structures include fine-grained starved ripples, very thin parallel laminated silt streaks, varying degrees of bioturbation *(Scolicia* or *Psilonichnus).* Pyrite, dolomite, and siderite cements and nodules are common.The uppermost 5 meters are characterized by coarse grained cross beds, mostly contorted, and have erosional bases. Pebble lags are common, and the entire sequence has a large amount of coal fragments. This sequence is interpreted as a fluvial channel deposit.

4 - Results - Core Analysis

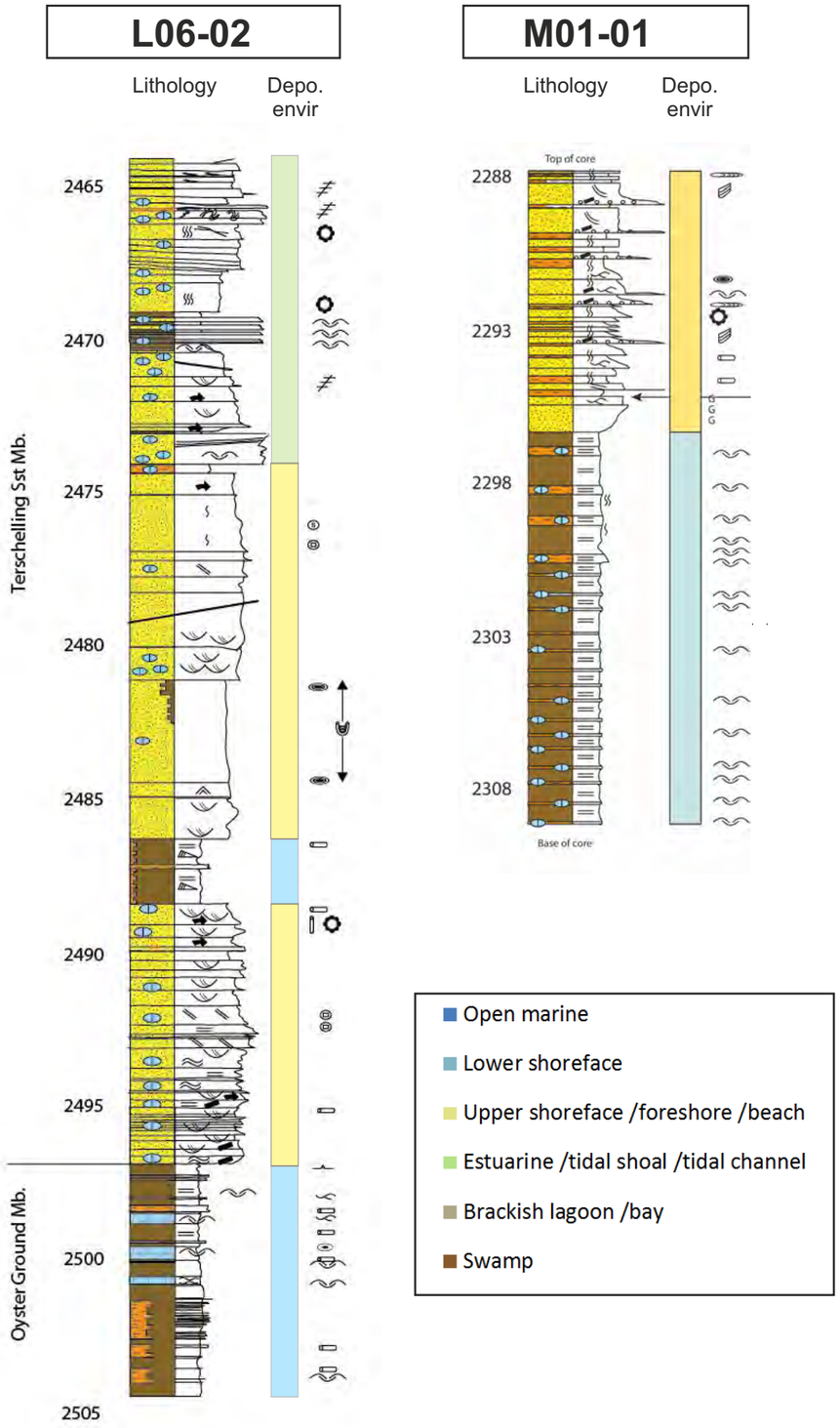

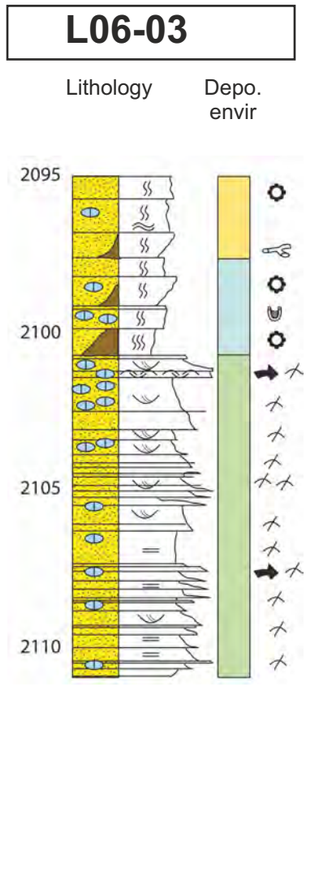

4.2.3 - Sequence 2

Description of L06-02, L06-03, and M01-01
(see Fig. 4.2.2 for legend)

Three cores were investigated that penetrated sediments from Sequence 2: L06-02 (40 m), L06-03 (16 m), and M01-01 (21 m).
In the L06-M01 area Sequence 2 is represented by the Oyster Ground Member and the overlying Terschelling Sandstone Member of the Skylge Group.

The Oyster Ground Mb has a similar appearance in L06-02 and M01-01: parallel laminated claystone with numerous thin, silt-sized storm beds. The thickness of these storm beds increases upward, from a cm or less at the base of the cores to 20 cm near the top of the Oyster Ground Mb. In L06-02 some small-scale hummocky cross-stratification can be observed in the thicker beds. Many of these storm beds contain shell hashes, which appear to form the nuclei of severe calcite cementation in these beds.

The Terschelling Sst. contains a variety of lithofacies in the three wells. The most frequently occurring facies consists of middle to coarse-grained sand, massive or cross bedded, with varying degrees of bioturbation. Ichnogenera include predominantly *Ophiomorpha, Asterosoma, Diplocraterion,* and *Teichichnus.* This facies is interpreted as upper shoreface deposits.

A second facies manifests itself in L06-02 in the interval 2488 to 2497 m. This sequence consists of numerous trough cross-bed sets of some 5-10 cm, is generally poorly sorted, and contains many rip-up clasts. The interval shows an overall fining upward trend and contains almost no trace fossils, apart from a single *Ophiomorpha* and *Skolithos* at the top.

The third facies is found only in L06-03. The lowermost 10 m of the core is made up of this facies. It consists of a stack of strongly fining upward beds (very coarse to medium-fine) with abundant shell hashes. Mostly parallel laminated, but cross bedding also occurs. This facies shows a conspicuous absence of trace fossils. It is interpreted as a series of washover fans deposited in a back barrier environment.

L06-03, 2204.9 m - Calcite-cemented shell bed interpreted as a washover deposit

L06-02, 2496.8 m - Contact between the offshore/lower shoreface muds of the Oyster Grn Mb and the overlying calcite-cemented Terschelling Sst.

L06-02, 2483.5 m - Well sorted upper shoreface sands with abundant *Ophiomorpha*

L06-02, 2495 m - Poorly sorted, coarse-grained cross-bedded sands interpreted as tidal inlet deposits.

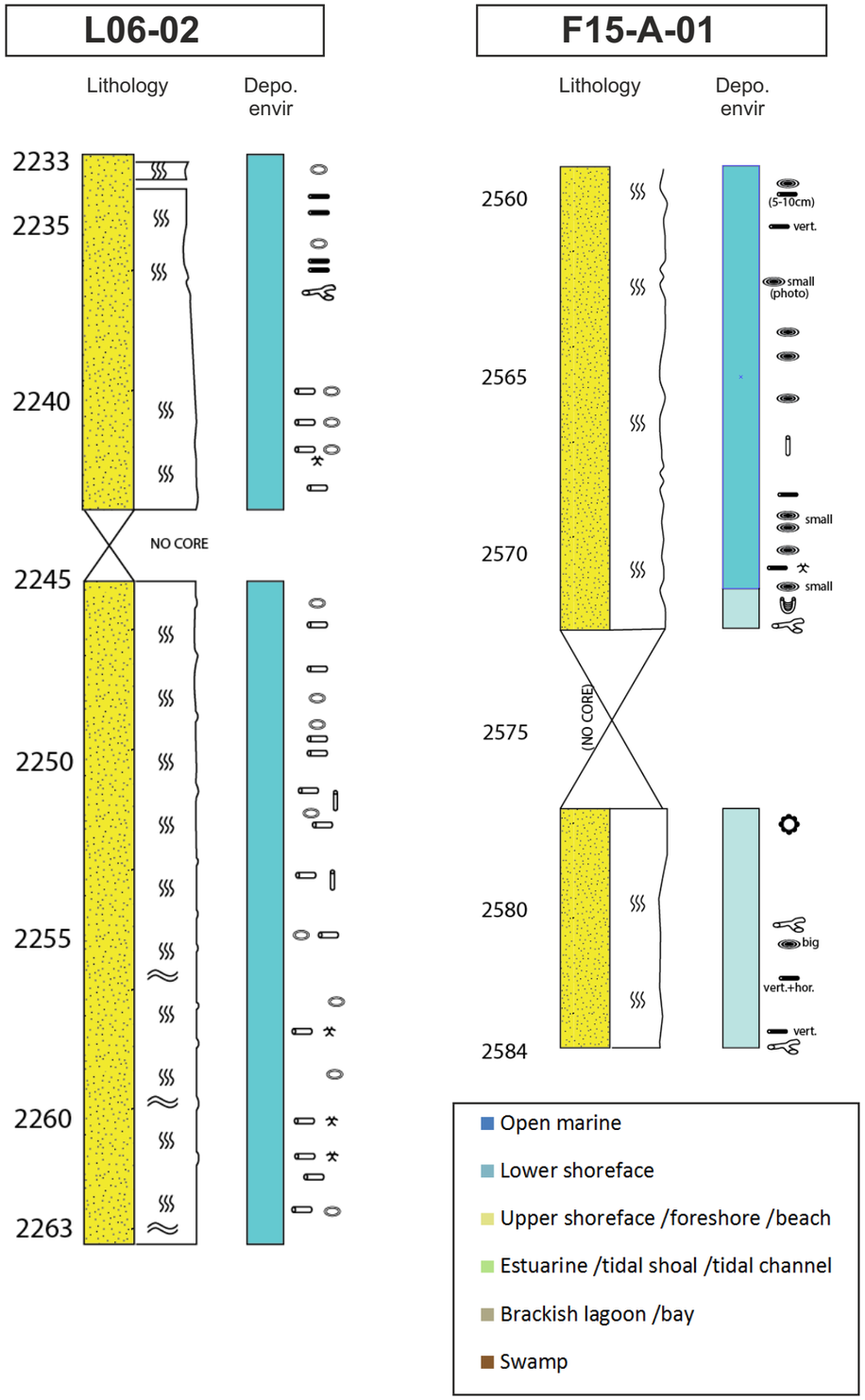

4.2.4 - Sequence 3

Description of F15-A-01, L06-02, M07-07, and M07-08 (Part 1)
(see Fig. 4.2.2 for legend)

Sequence 3 has been investigated in cores from four wells: F15-A-01, L06-02, M07-07, and M07-08. It is represented by the Scruff Greensand Formation.

The Scruff Greensand is a green-coloured, mostly completely bioturbated sand. The green colour is caused by the presence of glauconite, mostly as grains. The amount of glauconite is variable throughout the sequence. In M07-08 for example, the percentage of glauconite grains varies from 12 to 28%. The dark green colour is also partly caused by the large amount of clay present, mostly in the form of dispersed clay in between the quartz and glauconite greens, or as faecal pellets.

Sedimentary structures are almost completely destroyed by the intense burrowing. Sometimes some parallel or wavy lamination can be seen, but most of the Scruff Greensand has been homogenised by the burrowing organisms.

Grain size varies from well to well. The smallest grain sizes are found in L06-02 (very fine sand), while M07-08 shows coarse to very coarse sand in its upper 30 m.

Wells M07-07 and M07-08 show a conspicuous lithofacies which is not present in L06-02 and F15-A-01. Several thin layers of very coarse material (gravel, with pebbles up to a few cm in diameter) are found in otherwise fairly homogeneous sediments. These layers are 5-10 cm thick and often show a reverse grading. Most of the clasts are intraclasts (including phosphate-cemented sandstone), but some Zechstein and Trias pebbles are present. Apparently, the regular sedimentation was interrupted from time to time by an event shed very coarse clasts into the basin. These events were most likely gravity flows, as grain flows and debris flows are known to deposit inversely graded beds.

The Scruff Greensand was deposited in a fully marine environment, as testified by the *Cruziana* and *Zoophycos* ichnological assemblages. The depositional environment varies a bit between the four wells. L06-02 has the most distal sediments which were deposited in the largest water depths, typically in a lower offshore to shelf environment.

F15-A-01 - Overview of a part of the Scruff Greensand (2570-2583.6m) showing its conspicuous green appearance

F15-A-01 - Complete bioturbation and secondary re-bioturbation. The youngest burrows are *Phicosiphon*

L06-02 - Belemnite in a fine-grained shelf facies

4 - Results - Core Analysis

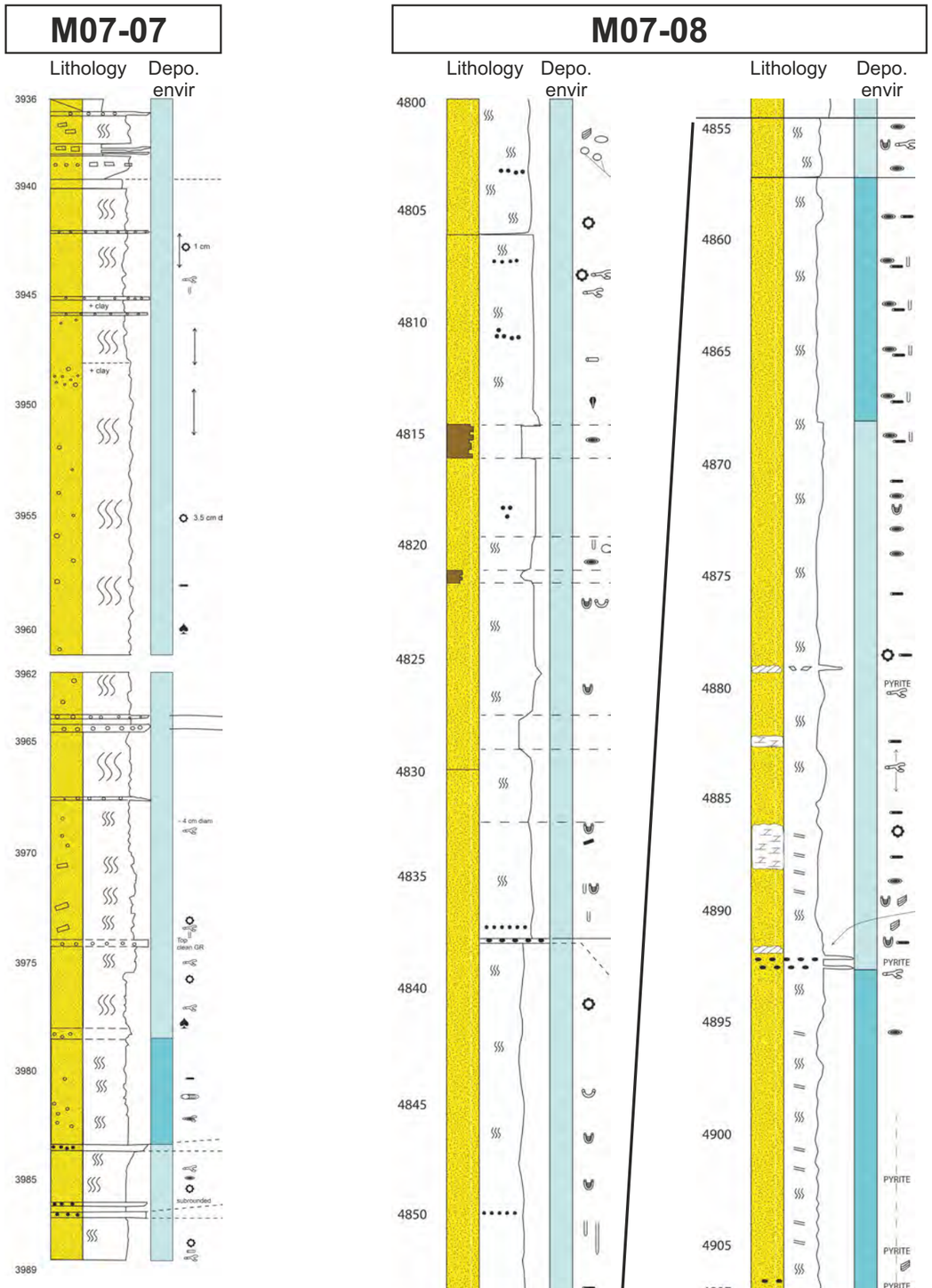

Description of F15-A-01, L06-02, M07-07, and M07-08 (Part 2)
(see Fig. 4.2.2 for legend)

F15-A-01 was deposited in slightly shallower water depths and closer to the shore, as suggested by its larger grain size and shallower ichnogenera, such as Asterosoma and *Paleophycos.*

M07-07 and M07-08 were deposited in an even shallower environment. Ichnogenera such as *Ophiomorpha, Diplocraterion, Rosselia, Asterosoma,* and *Thalassinoides* all point to lower shoreface environments. Also, grain sizes are coarser in these two wells. Especially the upper 35 m of M07-08 is coarse to very coarse. The fact that both wells are punctuated by very coarse grained gravity flows, where some of the extraclasts are very angular, suggests that shoreline slopes could have been very steep, and that emerging land masses (i.e. diapirs) were actively eroded.

M07-07 - Gravel beds in a lower shoreface environment, probably deposited by gravity flows. Most of the clasts are intraclasts, but some Zechstein and Trias pebbles are present. Note the high angle of deviation of the well.

M07-07 - Extraclasts floating in a sand matrix, probably Zechstein and Trias pebbles.

M07-08 - Lower shoreface deposits with *Diplocraterion* as the dominant burrow. Some floating pebbles seem to have been trapped in a spherical burrow, possibly *Psilonichnus*

4.3

RESULTS

SEISMIC INTERPRETATION

4 - Results: Seismic interpretation

The next two chapters (4.3 and 4.4), present the results of the seismic interpretation and the results for the stratigraphic correlation panels (displayed in association with the flattened interpreted seismic sections). The complete compilation of each regional panels that include the interpreted seismic sections, the flattened seismic sections and the stratigraphic correlation sections are found in Appendix A4.

4.3 Seismic interpretation

Seven regional panels that include interpreted seismic sections, flatten seismic section and corresponding stratigraphic correlation have been constructed (Fig. 4.3.1). Each seismic section and its corresponding well correlation panels where analyzed at the same time, by the same interpreter. This allowed for a integrated interpretations of seismic and well data.

Note that Panel A has two versions (A1 and A2) with the southeastern part of the seismic panels following a different trend: 1) Panel A1, from M04-01 to the southeast toward M08-02; Panel A2 (dotted blue line in Fig. 4.3.1) from M04-01 to the south toward M07-03, M07-07, M07-08 and M07-01. The location maps (Figure 4.3.1) shows the location of each of the regional panels presented in Figures 4.3.3 to 4.3.10 and 4.4.1 to 4.4.10. The structural and stratigraphic frameworks of each of the seismic panels shown on Figure 4.3.1 are described in this chapter.

Below is the list of wells that are included for each panel:

Panel A1

F17-06, F17-05, L02-05, L03-01, L03-03, L03-04, L06-02, M04-04, M04-03, M04-01,(M08-02), M07-03, M07-07 and M07-01.

Panel A2

F17-06, F17-05, L02-05, L03-01, L03-03, L03-04, L06-02, M04-04, M04-03, M04-01, M07-03, M07-07, M07-08, M07-01

Panel B

G13-02, G16-03, G16-04, G16-05, L03-04, L06-03, L09-02, L09-01

Panel C

B18-03, F03-08, F03-05-S1, F03-06, F03-03, F06-01, F08-01, F08-02, F11-01, F14-05, F14-06, F17-01, F17-06, F17-09, L02-05, L02-03, L02-FA-101, L02-06-S1, L05-04, L05-05, L04-05, L04-01

Panel D

E18-01, E18-07, F16-A-05, F16-04, F16-02, F17-04, F17-09, F17-05, F18-02, F18-01, F18-09-S1, F18-03, F18-08, G16-02, G16-04, G17-03, G17-01, G17-02

Panel E

F07-02, F11-03, F11-02, F11-01- F12-03, G10-03

Panel F

A08-01, A12-02, B13-02, B14-02, B14-01, B14-03, B18-02, B18-03, F03-07

Panel G

A12-01, A18-02-S1, F01-01, F04-02-A, F09-01

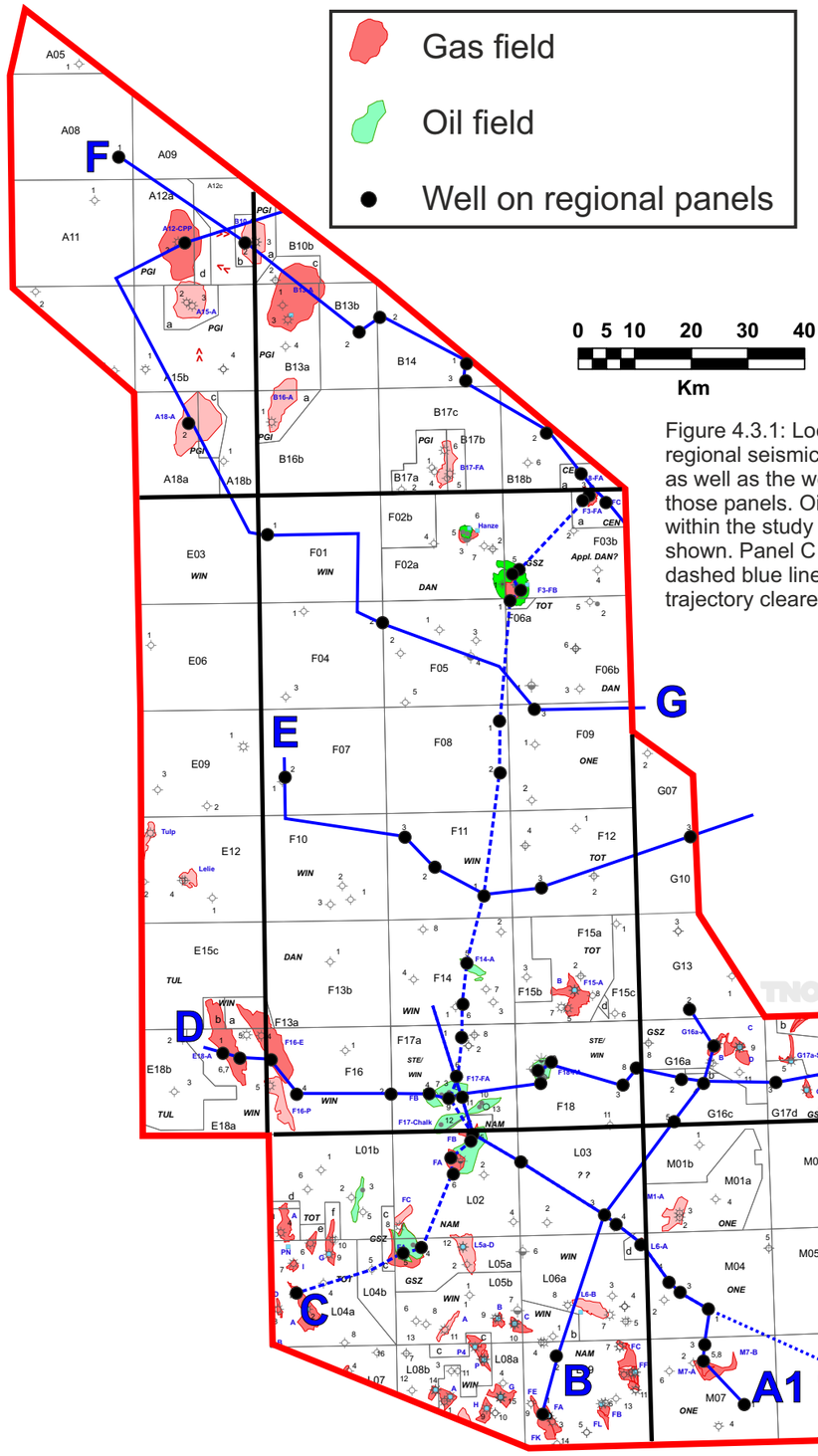

Figure 4.3.1: Location map of the regional seismic panels (blue lines) as well as the wells intercepted by those panels. Oil and gas fields within the study area are also shown. Panel C is shown as a dashed blue line to make its trajectory clearer.

Seismic profiles

- Fault
- Anticline
- Salt body
- Salt feeder
- Salt weld

- Cenozoic
- Chalk Group (Upper Cretaceous)
- Rijnland Group (Lower Cretaceous)
- Sequence 3 (Upper Jurassic-Lower Cretaceous)
- Sequence 2 (Upper Jurassic)
- Sequence 1 (Upper Jurassic)
- Altena Group (Lower Jurassic)
- Upper Triassic (Upper Germanic Trias Group)
- Lower Triassic (Lower Germanic Trias Group)
- Zechstein (Lower Germanic Trias Group)

- Unconformity
- Onlap
- Truncation
- Downlap
- Internal horizon
- Coal rich-unit (Middle Graben Fm.)

Stratigraphic Correlations

- Sand-rich interval
- Thick sand-rich interval (stacked channels)
- Thick sandstone and siltstone (Noordvaarder Mb.)
- S3 / S2 / S1 — Shale-rich intervals
- Coal rich-unit (Middle Graben Fm.)
- Volcanoclastics
- Volcanics

- Base of Sequence 3
- Base of Sequence 2
- Base of Sequence 1

- Fault
- Salt body

- Cored interval

- Unconformity
- Onlap
- Truncation
- Downlap

Figure 4.3.2: Legend for seismic panels (Figures 4.3.3 to 4.3.10) and correlation panels (Figures 4.4.1 to 4.4.10).

4 - Results: Panel A1 - DCG, Terschelling Basin & Friesland Plaform

TNO innovation for life

4.3 Seismic interpretation

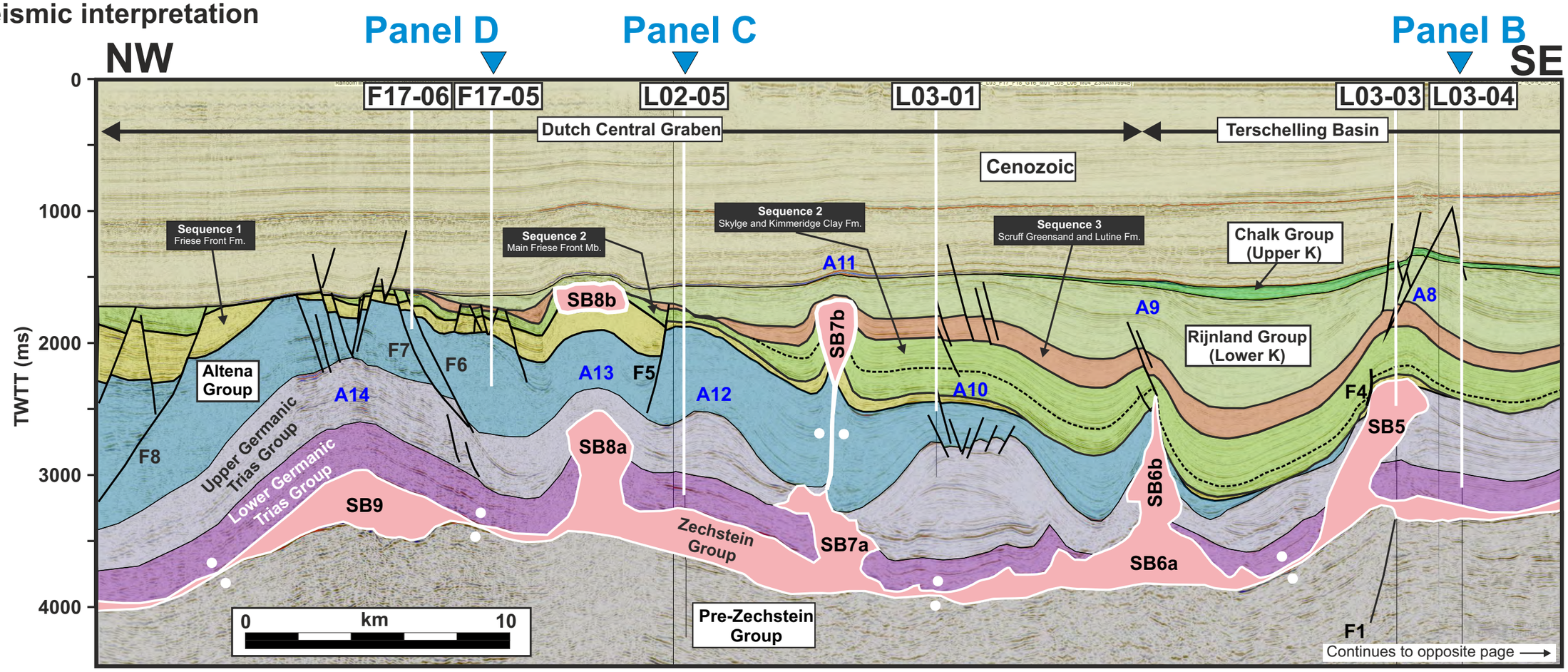

Figure 4.3.3 (Part 1): Interpreted seismic section A is trending SE-NW and is located across three structural provinces, namely from SE to NW, the Friesland Platform, the Terschelling Basin and the southern part of the Dutch Central Graben. This seismic section is 111,5 km long and intercepts four wells in the DCG (F17-06, F17-05, L02-05, L03-01), six wells in the TB (L03-03, L03-04, L06-02, M04-04 and M04-01) and one well on the Friesland Platform (M08-02). See Fig. 4.3.1 for location map and Fig. 4.3.2 for legend.

Base Zechstein (BZ) configuration

- Gently dipping from the SE (2,5 sec. TWTT) to the NW (3,5 sec. TWTT) between the southern side of the section to the L03-03 area.
- Bounding fault (F1), located below salt body 5 (SB5), separates the southern gently dipping BZ to a deeper (0,5 sec., TWTT) flat zone located between salt bodies SB5 and SB7.
- Shallowing up BZ between salt bodies SB7 and salt pillow SB9 .
- Deepening BZ from salt pillow SB9 north westward, down to 4 sec (TWTT).
- Small faults locally offset the BZ in central and southeastern part of the section and possibly below salt pillow SB9).

Zechstein salt bodies

- Nine salt bodies observed (SB1-9) that include two salt pillows (SB1 and SB9) and seven salt diapirs (SB2-8).
- Note that most of the salt bodies are decapitated at the base of major unconformities: 1) SB1a and SB2 at the base of the Chalk Group, 2) SB4, SB5 and SB6b at the base of the Upper Jurassic, and 3) SB8 at the base of the Rijnland Group.
- Salt body SB1 is an elongated salt pillow that is located on the northern part of the Friesland Platform. It is showing a small salt diapir (SB1a) at its northwestern extremity, in the core of a large anticline (A1).
- Salt body SB2 is a salt diapir with a narrow feeder and a diamond shaped body. It sits over a base Zechstein fault. Its wider part is located within Cretaceous strata and is located within anticline (A4).
- Salt body SB3 has a similar shape as SB2 but is observed in a deeper section, in the Upper Triassic. It also located in the core of a compressional anticline (A6)
- Salt body SB4 is similar to SB3 but is wider and has a thick feeder. It is associated with a thick autochthonous salt pillow (SB4a) to the SE. SB4 is a good example of a decapitated piercement.
- Salt body SB5 is also encased in Upper Triassic strata but has a wide and tilted (to the SE) salt feeder. It is located above the largest base Zechstein fault F1.
- Salt body SB6 is similar to SB3 and SB4 except its elongated, arrow-shaped, upper part that extend into the Jurassic (Lower and Upper Jurassic). It also has a large associated deformed salt pillow (SB6a).
- Salt Body SB7 is composed of a deep salt body (SB7a) and a shallow salt body (SB7b) connected by a very narrow salt feeder (stem). SB7a has a complex shape that suggest that this salt feature may have been initially remobilized during the Late Triassic before being again remobilized during the Jurassic. SB7b is a tear drop-shape salt diapir draped by the younger part of Sequence 3 but style deformed due to Cretaceous and Cenozoic compression.
- Salt body SB8 is also composed of a deep and shallow part. In this section, the feeder linking both those salt feature is not seen, and is located off section. The deeper salt body (SB8a) is wide within the Upper Triassic section. The shallow salt body SB8b is encased within the Upper Jurassic and is draped by Rijnland Group strata.
- Salt body SB9 is a large salt pillow located at the base of a large anticline (A14).

Note that the autochthonous Zechstein salt is welded out at several locations along the section (see salt weld symbols, two white dots).

Faults

Several faults are observed in this section. Below is a list of the main fault families.

- Deep faults located below the Zechstein (e.g. F1).
- Crestal faults above deep (e.g. A10, A14) and shallow (e.g. A4) anticlines.
- Large growth faults that detached above allochthonous salt, such as faults F2, F3 and F4 or within Triassic strata, such as F5, F6, F7 and F8. These latest faults may have detached on Triassic in situ salt layers (e.g. Röt Salt) or on remobilized upward, and now welded out, Zechstein salt.
- Numerous small faults are also observed around salt bodies and within the Jurassic, Cretaceous and Cenozoic sections.

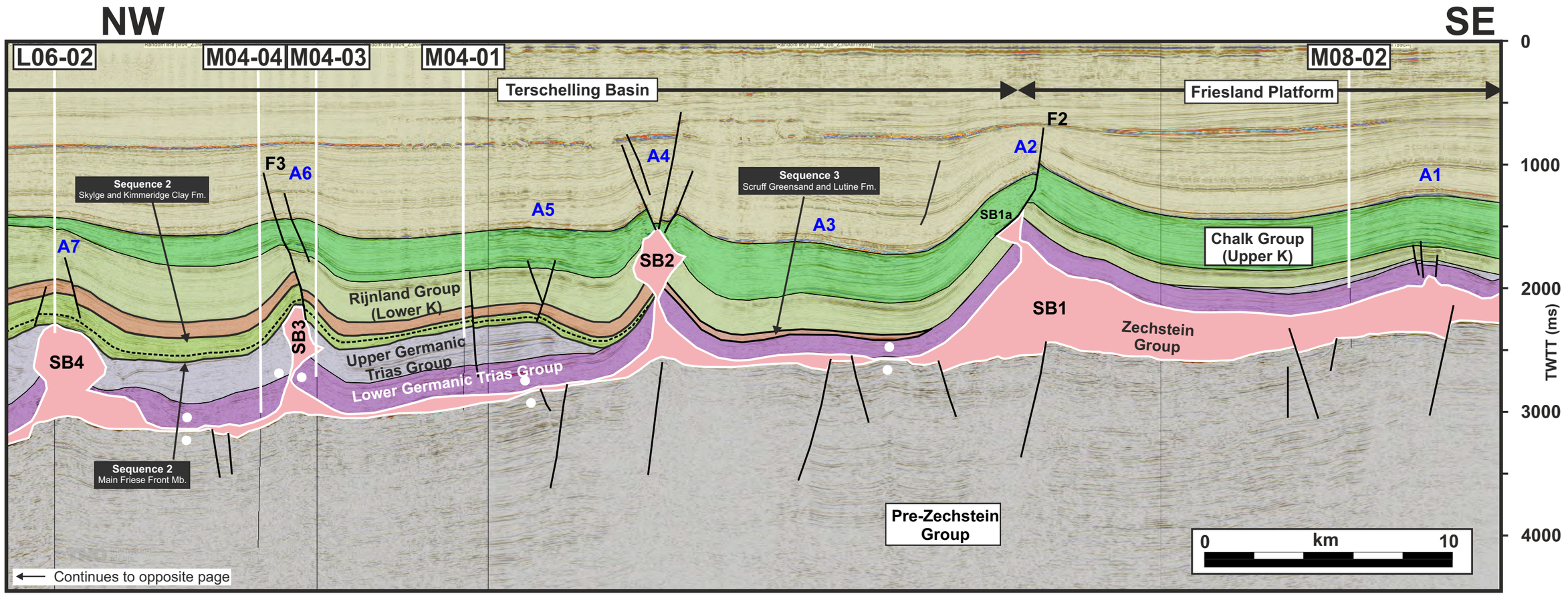

Figure 4.3.3 (Part 2):

Folds

Fourteen anticlines are observed within this seismic section. Most of these anticlines are compressional features related to Cretaceous and Cenozoic shortening but three anticlines (A10, A12 and A14) are extensional features at the base of turtles structures (Trusheim, 1960; Seni and Jackson, 1983). These features are similar to well know turtle structures such as the Mensa and Thunder Horse turtles in the Deep Gulf of Mexico and are related to autochthonous salt moving laterally due to sediment loading during the Late Triassic, that later "inverted" (sensus turtle structure kinematics), with their flanks subsiding while wedge-shape stratigraphic external forms (sensus Rowan and Weimer, 1998) developed on both sides (in this case Altena Group wedges).

Stratigraphy

Lower Triassic

The Lower Triassic is thin (200 ms. TWWT) on the Friesland Platform and slightly thicker (between 300 and 400 ms. TWTT) elsewhere. It presents a typical seismic amplitude configuration with continuous high and low amplitudes and a lack of noticeable internal unconformities. The thinner part of the Upper Triassic on the Ameland Platform is interpreted as being related to later erosional events during the Jurassic and the Cretaceous (with Rijnland Group strata sitting directly over the Lower Triassic strata). Note that the Lower Triassic is locally absent on the SW side of the salt body SB6a. This can be either due to the presence of a large salt body at this location during the Early Triassic, or due to a later translation of this Lower Triassic block toward the NW (rafting).

Upper Triassic

This interval present a great variability in stratigraphic thickness along the section. It is locally absent, such on the Friesland Platform and NW of salt body SB2. Its time-thickness varies between 0 and 850 ms. (TWTT.s). Its thickest area are within the three turtles structures described above (A10, A12 and A14).

Its seismic amplitude configuration is highly variable and is continuous to chaotic. Numerous internal unconformities are observed as well as internal stratigraphic wedging and dipping that are often associated with stratigraphic downlaps, toplaps and onlaps. The top of the Upper Triassic is often erosional, with Lower Jurassic, Upper Jurassic and Cretaceous strata cutting down into this stratigraphic interval.

Lower Jurassic (Altena Group)

This stratigraphic interval is only observed in the northwestern half of the seismic section, northwest of salt body SB5. Its thickness varies greatly from 0 to 1.2 sec. (TWWT.), the thickest areas being the wedges along the side of the turtles structures A10 and A14. Note the characteristic high amplitude of the Posidonia shales locally observed in the upper part of the Lower Jurassic section, such as SE of salt body SB7a.

Upper Jurassic

Along this seismic section, this stratigraphic interval is only present in the TB and the DCG. It was likely deposited on the Friesland Platform but was later eroded during the Cretaceous. Detailed description of this interval is given in Chapter 4.4 (Figures 4.4.1 and 4.4.2).

Rijnland Group

This stratigraphic interval is present along most of the section, except northwest of well F17-06. It is the thickest in the northwestern part of the TB (800 sec. TWTT) and thins to the NW and SE, where it becomes locally highly erosional (e.g. at the location of well L02-05 and SE of salt body SB2).

Chalk Group

This interval is only observed in the southeastern part of the seismic section, SE of well L03-01. It is very thin (less than 100 ms. TWTT) toward the NW, between wells L03-01 and L06-02, and thickens southeastward to a maximum of 500 ms (TWTT). Its base is locally erosional.

Cenozoic

The Cenozoic interval is thick (up to 1,8 sec. TWTT.) and shows thickness variation related to Alpine inversion of several salt features, such as SB1a, SB2, SB3, SB5 and SB8.

4 - Results: Panel A2 - Terschelling Basin & Friesland Platform

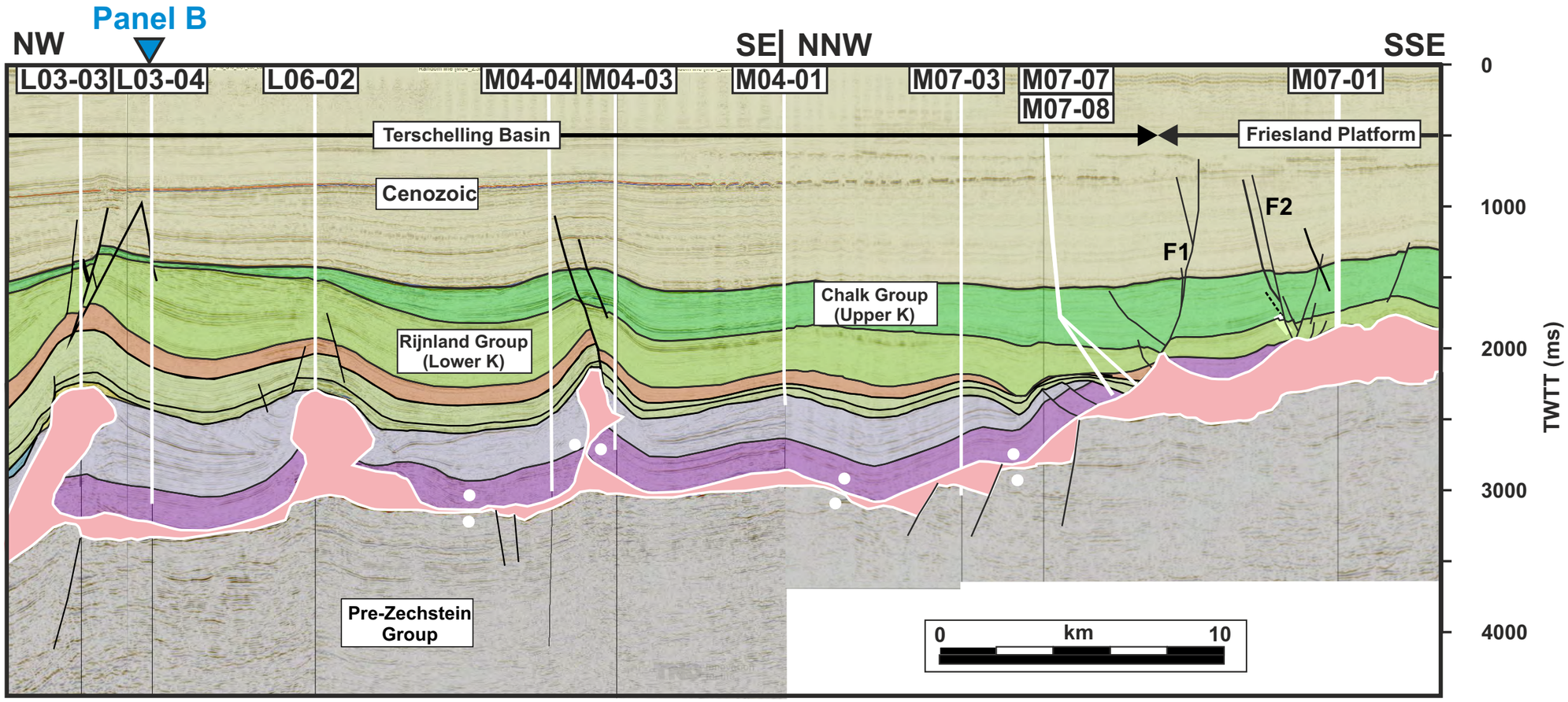

Figure 4.3.4: Interpreted seismic section A2 trending SE-NW, with a NNW-SSE section from well M04-01. This seismic section is nearly the same section as the southeastern part of section A1, but diverges to the SSE from well M04-01. This seismic section is 50 km long and intercepts, nine wells in the TB (L03-03, L03-04, L06-02, M04-04, M04-03, M04-01, M07-3, M07-07 and M07-08) and one well on the Friesland Platform (M07-01). This seismic section is partially similar to the seismic section presented in Figure 4.3.3, except the southeastern part, from well M04-01 to the SSE. Therefore, only the southeastern part of the section is described here. Please refer to Figure 4.3.3 for description of the northwestern part of the section (NW of well M04-01). See Fig. 4.3.1 for location map and Fig. 4.3.2 for legend.

Base Zechstein (BZ) configuration:

The BZ ramps up rapidly from well M04-01 toward the SSE. Several NNW dipping faults accommodate this elevation difference between the Friesland Platform and the TB.

Zechstein salt bodies:

- No allochthonous salt bodies are observed to the SSE of well M04-01 along this seismic section.
- The autochthonous Zechstein salt is the thickest on the Friesland Platform and in the hanging walls of the three "basement" faults described above.

Faults:

Several faults are observed in the SSE part of this section. Below is a list of the main fault families.

- Deep faults located below the Zechstein (see description above).
- A large growth fault (F1) is observed at the limit between, the Friesland Platform and the TB. F1 detached along the dipping top Zechstein surface and was active during the Late Jurassic and Chalk depositional times. The thinning of the Rijnland Group on the hanging wall side of F1 indicates that this fault may have also been active as a strike slip fault. However, the timing of these strike slip movement is not well understood. The geometry of the upper part of F1, as well as the presence of fault array F2, is also indicative of wrench tectonics (flower structures).

Folds

No major anticlinal structures are observed SSE of well M04-01, but a small syncline can be observed between well M07-03 and wells M07-07/08. The origin of this syncline is not well understood, but seems to involve a local erosional feature, with deep incision into the Upper Triassic interval.

Stratigraphy

Lower Triassic:
The Lower Triassic is only present between well M04-01 and M07-07/08 (where it is mainly isopachous) and is missing on the Friesland Platform. At its SSE extent, it is faulted and truncated (with a high angle unconformity) at the base of the Upper Jurassic.

Upper Triassic:
The Upper Jurassic interval presents more thickness variation than the Lower Triassic and is also truncated at the SSE edge (margin) of the TB; however, it is observed above the Zechstein salt on the Friesland Platform.

Lower Jurassic (Altena Group)
Absent in this part of the Basin

Upper Jurassic
Along this part of the seismic section (SSE of well M04-01), this stratigraphic interval is only present in the TB. It was likely deposited on the Friesland Platform but was later eroded during the Cretaceous. Detailed description of this interval is given in Figures 4.4.1 and 4.4.2.

Rijnland Group
The Rijnland Group thins toward the SSE and locally drapes (cut into?) the autochthonous Zechstein Group on the Friesland Platform. It also locally eroded part of the Upper Jurassic, between wells M07-03 and M07-07/08.

Chalk Group
The Chalk Group time-thickness varies locally in this part of the seismic section (SSE of well M04-01), mainly around active faults (e.g. F1), and cut increasingly farther down into the Rijnland Group toward the SSE, from the location of well M07-03.

Cenozoic
The Cenozoic interval is thick and a few normal and strike slip faults (e.g. F1 and F2) were active during this period.

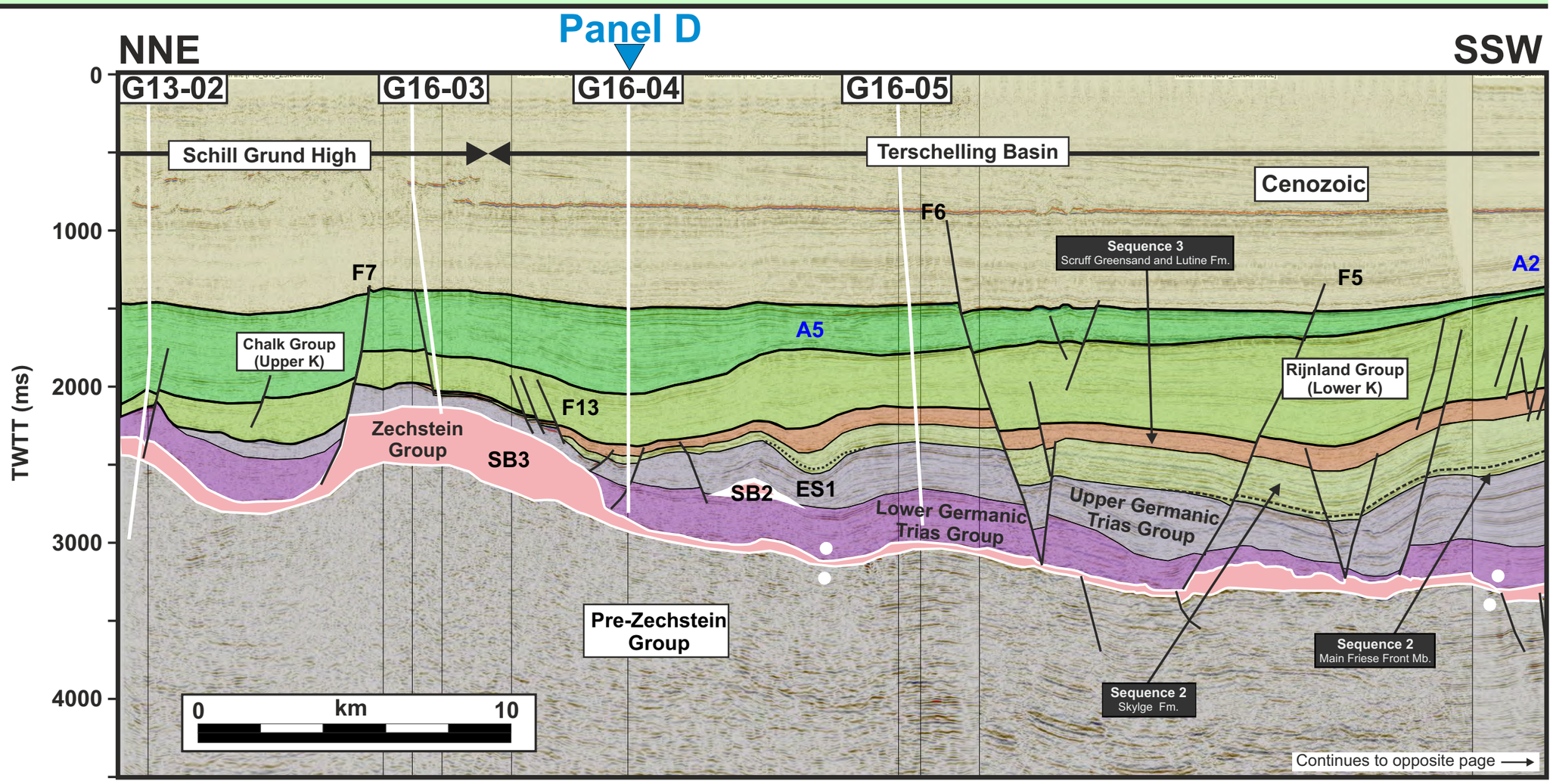

Figure 4.3.5 (Part 1):
Interpreted seismic section B1 trends NNE-SSW and is located across four structural provinces, namely from north to south, the SGH, the TB, the Friesland Platform and the Vlieland Basin. This seismic section is 91,5 km long and intercepts one well on the Friesland Platform (L09-01), four wells in the TB (L09-02, L03-04, G16-05 and G 16-04) and two wells on the SGH (G16-03 and G13-02). See Fig. 4.3.1 for location map and Fig. 4.3.2 for legend.

Base Zechstein (BZ) configuration

- Gently dipping from the SSW and the NNE (2.6 sec. TWWT), toward the central part of the section (3.3 sec. TWTT), with the deepest part around well L03-04.
- The large monocline (A1) can be observed at the BZ level in the southern part of the section, between faults F1 and F2, with faults mainly dipping northward in the south and southward in the north (the hinge point (H1) is shown). A1 is located along the Hantum Fault Zone.

Zechstein salt bodies

- Only three noticeable salt bodies can be observed in this section (SB1-3).
- SB1 and SB3 are large salt pillows located on the Friesland Platform and the SGH, respectively. These salt bodies are draped by thin Upper Triassic strata and, locally, by Cretaceous Rijnland Group strata. They both have box-shaped geometry and are located at the northern and southern basin margins of the TB.
- Salt body SB2 is located at the top of the Lower Triassic and is draped by Upper Triassic strata. The presence of an evacuation syncline to the south of SB2 suggests that this salt body was likely larger during the Late Triassic, but was evacuated during the Late Jurassic, as proved by the over-thickened Upper Jurassic interval just south of SB2.

Faults

- Numerous faults are observed in this section. Below is a list of the main fault families.
  - Several deep faults intercept the BZ but are mainly observed on the southern part of the section, with eighteen normal faults (three of them with more than 300 ms. (TWTT) of vertical offset, namely F1, F2 and F3) identified south of well L03-04. Only five faults are located to the north of that location. Note that the largest Meso-Cenozoic fault (F4) is located above the largest BZ fault (F3), while detaching in a shallower level (likely intra Upper Triassic).
  - Large crestal faults are located above the large central anticline (A2), which has its axis at well L03-04 location. These faults were active during the Lower Cretaceous.
  - Four large growth faults (F4-7) active during the Late Cretaceous and Cenozoic (possibly earlier for some of them). Most of them sole onto the autochthonous Zechstein salt, with only F4 that seems to detached on a shallow level, which can be an in-situ Upper Triassic salt layer (e.g. Röt Salt) or a remobilized upward allochthonous Zechstein salt sheet that was later welded out.
  - Smaller growth faults, which were active during the Jurassic and Early Cretaceous, can also be observed. Faults F8-13 have Upper Jurassic and Lower Cretaceous growth strata on their hanging wall sides.

Folds

Four main anticlines are observed within this seismic section. The largest is anticline A2 that is centered at the axis of the TB. According to stratal thickness configuration, we interpret this feature has having been active during the deposition of the Chalk Group and during the Cenozoic.

4 - Results: Panel B1 - SGH, TB, FP & VB

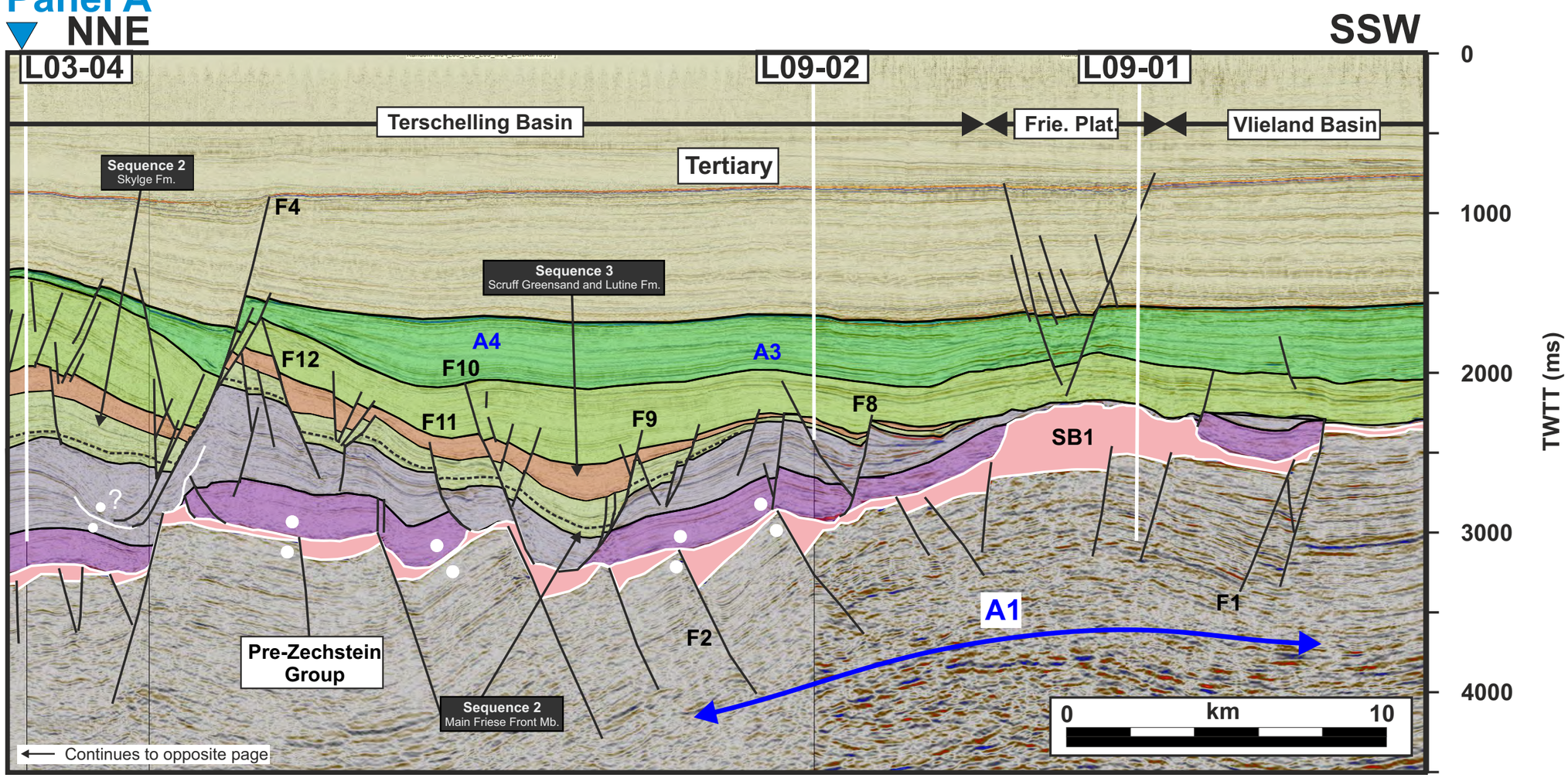

Figure 4.3.5 (Part 2):
Three smaller anticlines (A3-5) are also observed. A3 is a deep anticline that has little expression above the Rijnland Group / base Chalk Group. It forms the southern basin margin of the TB and had a important impact of the distribution of the Upper Jurassic that onlaps and laps onto it. A4 is also a deep anticline that was active during the Late Jurassic and remained active until the early Late Cretaceous. A5 is locate to the north between wells G16-05 and G16-04. It sits above the evacuation syncline (ES1) and the salt body SB2. This anticline formed during the Late Jurassic and remained active until the early part of the Cenozoic.

Stratigraphy

Lower Triassic

The Lower Triassic is very interesting in this section. It shows some great thickness variation and is locally absent. This interval is not present at four locations, two of them above the thick Zechstein salt pillows SB1 and SB3, and two of them in the central part of the section, above faults F2 and F3. Above fault F2, a 4 km-wide area doesn't have any Lower Triassic at Present-day. This can be explained in two ways: 1) either a large salt body was present during the deposition of the Lower Triassic, creating a topographic high on which little to no Lower Triassic was deposited. This salt body may have been later evacuated, bringing the Upper Triassic strata down into its current position; 2) or the Lower Triassic strata was originally deposited at this location, but was later rafted away due to some lateral translation of stratal block, similar to gravitational gliding systems as seen along the Congo Margin (Rouby et al, 2002). The first model may be valid since another thinner Lower Triassic zone is observed over a remnant thin salt pillow below fault F5. However, the presence of large growth faults (F9 and F11) favors a growth fault/raft model to explain this absent Lower Triassic at this location.

Upper Triassic

This interval thickness greatly varies along this section. It is very thin to absent on the platforms and thickens from the TB margins toward the axis of the basin (greater thickness around well L03-04). Its thickness also locally varies across some of the growth faults observed (e.g. F8 and F9) and around the allochthonous salt body SB2 where the Upper Triassic is onlapping.

Lower Jurassic (Altena Group)

Not present along this section

Upper Jurassic

Along this seismic section, this stratigraphic interval principally occurs in the TB and within very thin remnant accumulations on the SGH. It was likely deposited on both southern and northern platforms but was later eroded during the Cretaceous. Detailed description of this interval is given in Figures 4.4.3 and 4.4.4.

Rijnland Group

This stratigraphic interval is present along the entire section. Its thickness trend mimics those of the Upper Triassic and Upper Jurassic, with the thickest areas in the axis of the TB and thinning toward the north and south. It is worse noticing that the thickest part of the Rijnland Group is shifted to the north (by 6 km) compared to those of older intervals.

Chalk Group

The Chalk Group has a very different (quasi inverse) thickness trend than older intervals. It is very thin at the axis of the TB and thickens toward the North and South.

Cenozoic

As for the Chalk Group, the Cenozoic also thickens southward and northward from a thin area at the basin axis.

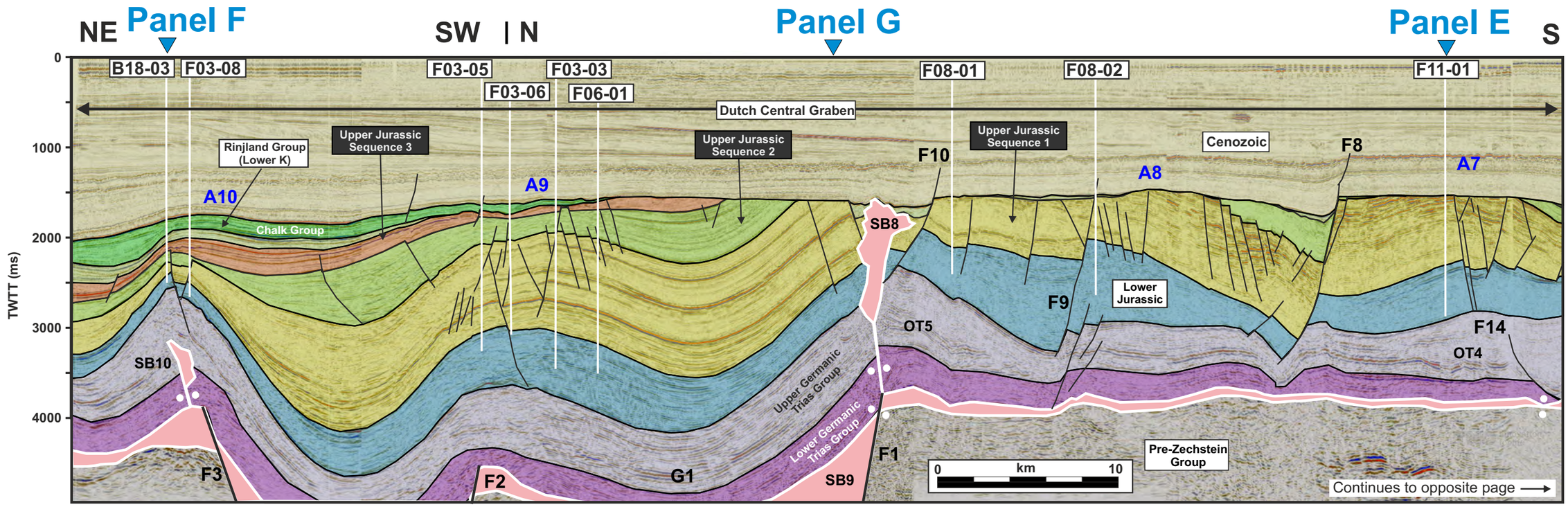

Figure 4.3.6 (Part 1)

Interpreted seismic section C, located in the axis of the DCG and extends southward to the southern part of the COP. It trends N-S, with locally two SW-NE trends at its extremities. This seismic section is 170 km long and intercept twenty one wells. See Fig. 4.3.1 for location map and Fig. 4.3.2 for legend.

Base Zechstein (BZ) configuration

The base Zechstein is overall dipping to the north from a highly faulted southern zone (around the monocline A1) to the fault F1, which has a 1,5 sec. TWTT. throw to the north. This large fault bounds the deepest part of the DCG (G1) and is synthetic to another large fault F2 farther north below well F03-05 and an antithetic fault F3 that bound the other side of the deeper part of the graben.

A large monoclinal feature A1, which can be observed at the base Zechstein, is the eastern continuation of the monocline A1 observe in the southern part of TB (Panel B). It is highly faulted and has two secondary grabens (G2 and G3) separated by a large horst underneath the salt Body SB2.

In the central part of the section, a few faults bound smaller grabens, half grabens and horsts and are often located below shallow salt bodies.

Zechstein salt bodies

- Ten noticeable salt bodies (SB1-10) are recognized along this section
- SB1 is a small diapir located in the core of anticline A3 that was active during the Late Cretaceous and the Cenozoic.
- SB2 is located between wells L04-01 and L04-05 is one of the shallowest salt body in the Dutch offshore (900 ms. TWTT. deep). It separate the COP from the DCG and sits over a “basement” horst at the hinge of the large anticlinal flexure A1.
- SB3 is a salt feature composed of two disconnected salt bodies (SB3a and SB3b). These two salt bodies were likely connected prior to the activity of fault F4 during the Jurassic and Early Cretaceous.
- SB4 is a large salt diapirs with two lateral wings along a thick salt feeder. These salt wings extend between the Upper Triassic and the Lower Jurassic. Their nature can be debated, as intrusive or extrusive features. The extrusive nature (welded out Zechstein salt sheet emplaced during the Late Triassic) is the favored hypothesis of the TNO geological team. However, no detailed analysis has been carried out yet but will be tested in a following project at TNO. SB4 was active during the Jurassic and Early Cretaceous as seen by the stratal thickness variation across the salt body.
- SB8 is a salt diapir with a narrow salt feed (vertical weld) and is located above the large base Zechstein fault F1. This salt body reaches upward the Cenozoic and may have been highly dissolved and/or eroded during the Jurassic, Cretaceous and Cenozoic.
- SB9 is a thick autochthonous salt pillow bounded to the south by the large F1 fault.
- SB10 is in the core of anticline A3 and is encased in the Upper Triassic.

Faults:

Numerous faults are observed in this section. Below is a list of the main fault families.

Several deep faults intercept the base Zechstein and were described above.

Seven large listric growth faults(F4-F10) are observed in the DCG. They are all normal faults dipping to the north. Some of them may have been inverted during Cretaceous and Cenozoic .

- F4 is located between well L05-04 and L02-06-S1 and was active during the Early Cretaceous. This fault detached at the top of salt body SB3a.
- F5 is located between wells L02-05 and F17-09 and was active during the Early Jurassic, Late Jurassic and early Cenozoic . Its activity during the Cretaceous is unknown due to erosion of Cretaceous strata at the base of the Cenozoic. This salt likely detached within or at the base of the Lower Jurassic.
- F6 is located between wells F10-05 and F11-01. The period of activity of this fault is unclear due to the erosion at the base Cenozoic. This fault detach intra Upper Triassic.
- Faults F7-9 are located in the central part of the section and were active during the Cretaceous and Cenozoic. These faults detached intra Upper Triassic.
- Fault 10 was active during the early Cenozoic and likely detached intra-Triassic.
-
- SB5 and SB6 are two small salt pillows encased within the Upper Triassic. We interpret those features to be remobilized Zechstein salt rather that over thicken in situ Triassic salt. It is likely that those features were once part of an allochthonous salt sheet system, possibly locally amalgamated prior to a secondary salt evacuation and the formation of salt welds (possibly connected SB4 and SB4 at the base of Lower Jurassic.
- SB7 is a large salt pillow located below the F17 anticline A2 and is located above a base Zechstein graben.

Smaller syn-depositional faults are observed on this section (e.g. F11-13). They were mainly active during the Late Jurassic and Early Cretaceous. They are listric and dip either southward or northward. Some of faults detached intra-Upper Triassic or at the base of the Lower Triassic. Note that some of the faults are located on the flanks of anticline A2, dipping southward on the southern flank and northward on the northern flank.

Crestal faulting can be observed between faults F8 and F9 and below the F03-05/F06-01 wells.

4 - Results: Panel C - Dutch Central Graben

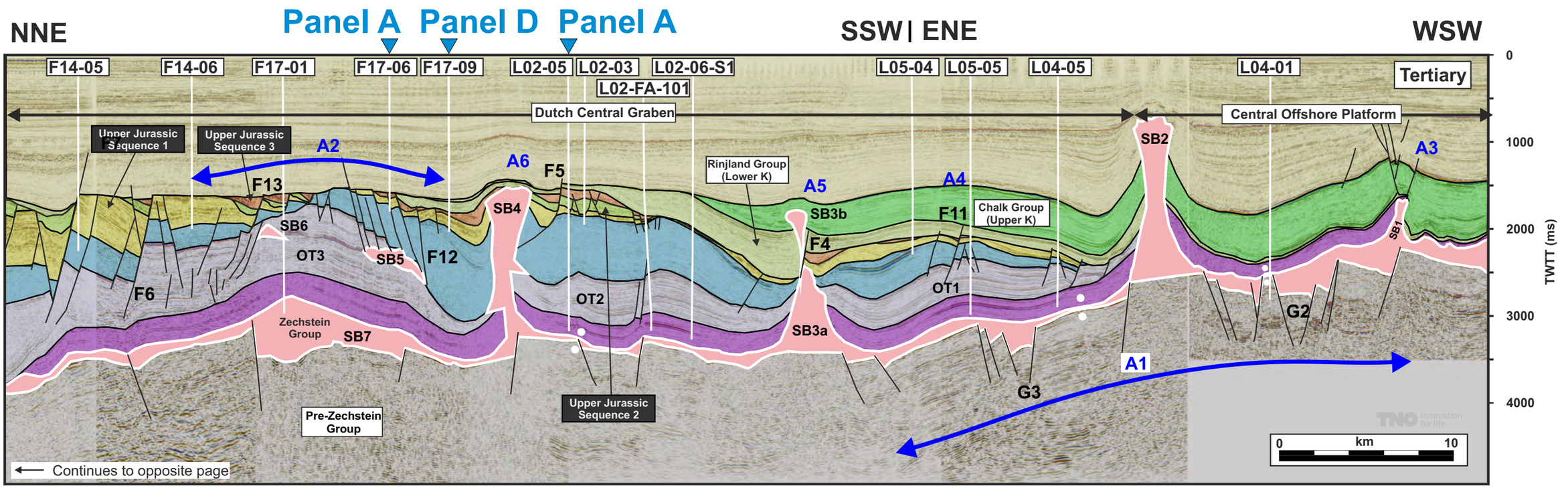

Figure 4.3.6 (Part 2)

Folds

Ten main anticlines and monoclines are observed within this seismic section.

- A1, A2 and A3 were described above.
- A4 is a broad anticline that for due to salt migration and diapiric growth on SB2 and SB3.
- A5 and A6 are small anticlines related to compressional tectonics during the Cenozoic.
- A7 and A8 are large asymmetric turtles structures that have been highly truncated on their northern flanks during the Cenozoic.
- A9 is a large anticline that was active during the Early and Late Jurassic.

Stratigraphy

Lower Triassic

- The Lower Triassic is quite isopachous along this section with an regular thickening northward. However, at two locations it present some particular characteristics.
- On the COP, on the southern side of SB1, the Lower Triassic is very thin due to Cretaceous erosion. At this location is only consists of a thin drape over the Zechstein.
- The Lower Triassic is missing over a 1km area on the southern side of fault F14. It was likely translated southward as a raft related to the F14 faults (growth fault/raft system).

Upper Triassic

- The Upper Triassic greatly varies in thicknesses along this seismic section.
- It is only present in the DCG and was eroded on the COP.
- It shows a cyclical thinning and thickening trends across the Dutch Central Graben, suggesting some early salt movement during this period in the Graben, with local subsidence and minibasins formation.
- Five main over thickened zones can be observed (OT 1-OT5) that can be interpreted as Upper Triassic paleo-depocenters. These depocenters can also be interpreted as bowl- or trough-shape stratigraphic external forms (Rowan and Weimer, 1998) at the base of turtle structures, therefore defining 5 large turtle structures in the DCG.
- Some of the Upper Triassic thickness variations can also be attributed to salt (in situ or remobilized), such as the salt bodies SB5 and SB4 and erosion at the base of Lower Jurassic.

Lower Jurassic (Altena Group)

- The Altena Group varies greatly in thicknesses often as a mirror image of the Upper Triassic interval (e.g. over thinned Lower Jurassic above over thickened Upper Triassic)
- The Lower Jurassic is not present to the south of well L04-05 due to Early Cretaceous erosion.
- Note the presence of high amplitude horizons toward the top of the Altena Group (e.g. F11-01) that correspond to the Posidonia Shale Formation.
- Note also the over thickening of the Lower Jurassic below well F17-09 that was likely due the withdrawal of salt, autochthonous or most likely allochthonous sin origin.

Upper Jurassic

- The Upper Jurassic increases dramatically from the south of the section (where it is even absent on the COP) and the northern part of the section where it is locally up to 2.5 sec. (TWTT.) thick.
- This interval is locally eroded by subsequent events (Cretaceous and Cenozoic). Detailed description of this interval is given in Figure 4.4.5 and 4.4.6.

Rijnland Group

- This stratigraphic interval is only present in the southern part of the section (between wells L04-01 to well F17-06) and as small and thin remnants on the footwall of faults F7, F8, F9 and F10, and finally as a thin draping interval to the northeast of well F03-05.

Chalk Group

- The Chalk Group is quite thick in the southern part of the section and is only draping salt bodies SB4 and SB8 farther north.
- It is also present as a thin interval that thickens north-westward from F06-01 to the northwestern edge of the section.

Cenozoic

- The Cenozoic has roughly similar thickness along the seismic section, except locally near growth anticlines (often related to squeezing of salt bodies during Alpine inversion) and across a few of the large growth faults (F5-10).

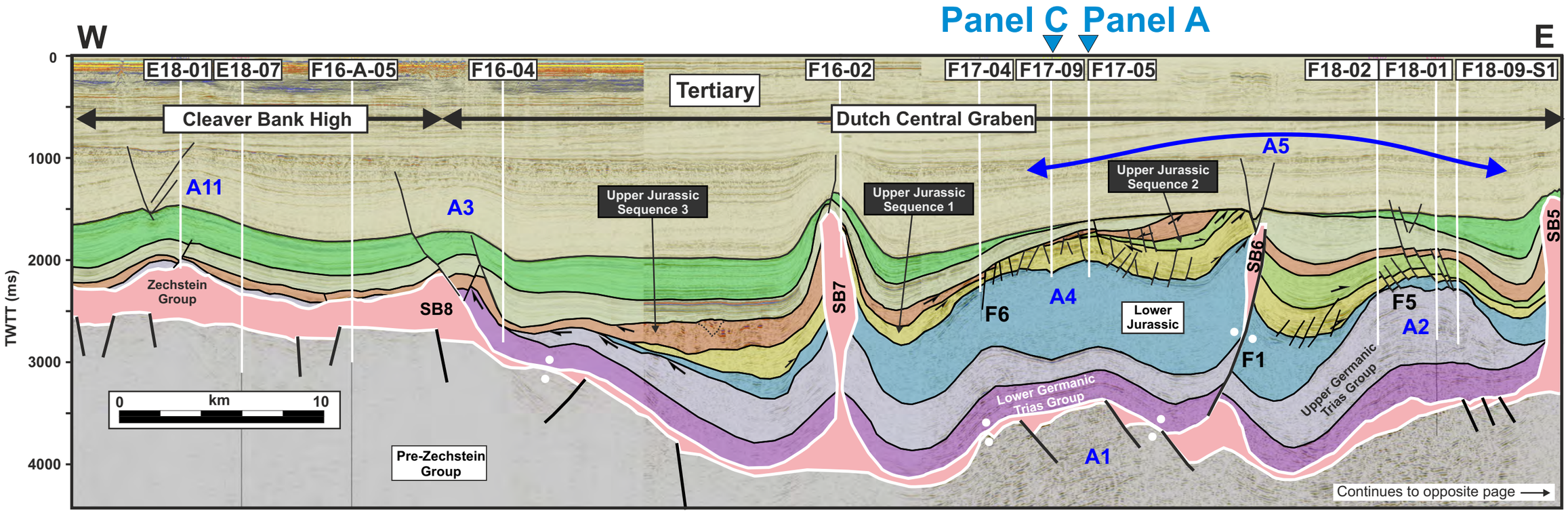

Figure 4.3.7 (Part 1)

Section D is located across four structural provinces, namely from east to west, the SGH, the TB, the DCG and the CBH. This panel is trending E-W, except in its eastern extremity where it is oriented to the NE, from well G17-01. This seismic section is 171,6 km long and intercepts eighteen wells. See Fig. 4.3.1 for location map and Fig. 4.3.2 for legend.

Base Zechstein (BZ) configuration

The base Zechstein is relatively shallow (around 2,5 sec. TWTT) on the platforms (CBH and SGH. It deepens along a gentle slope in the TB, toward the DCG, and rises again from 4 sec. (TWTT) toward the west from well F18-02. Many faults offset the BZ and define a series of grabens, half grabens and horsts.

Note the presence of a large anticline (A1) below well F17-09.

Zechstein salt bodies

Eight noticeable salt bodies (SB1-8) are recognized along this section.

- SB1-4 and SB8 are large salt pillows with thin to no Triassic cover, and locally thin drapes of Upper Jurassic strata.
- SB5 is located in the F18 block and is a tall pillar-shaped salt diapir that reaches the Chalk Group. It defines the eastern limit of the Lower Jurassic and Sequence 1 of the Upper Jurassic. It controlled the eastern part of the F18 turtle structure (A2) during those periods.
- SB6 is a highly deform salt diapir, which has an oblique salt feeder connected to the deep autochthonous salt. This feeder was likely reactivated as a reverse fault (F1) during the Cretaceous. The present day geometry of this salt diapir was influenced by Alpine compression and may have been much larger and wider during the Triassic and Jurassic. It can be summarized as the core of a large reverse fault. It was also likely controlling the western part of the F18 turtle structure (A2).
- SB7 is a narrow, tear-shaped salt body that was highly squeezed during the Cretaceous and Cenozoic compression (as seen by the steepness of the Cretaceous strata on the flanks of the diapir).

Faults:

Numerous faults are observed in this section. Below is a list of the main fault families.

- Several deep faults intercept the base Zechstein and are described above.
- A small pop-up structure (F2-F3) can be observed between wells G17-03 and G16-04. This feature was likely initially a graben, which was subsequently inverted.
- Numerous syn-depositional faults (e.g. F4-6) are observed, especially in the DCG. They were active during the Late Jurassic and Early Cretaceous.
- Crestal faulting can be observed in the F18 and F17 turtle structures. They were mainly active during the Late Jurassic (as seen by the unfaulted Rijnland Group strata on the western flank of the F17 turtle structure).
- Inverted fault F1 is discuss above. The probability that this fault was also active as a strike slip structure is high but this interpretation will require additional analysis.
- A large fault (F7) is present at the western boundary of the DCG. It was likely active as a normal fault during the Jurassic (may be Triassic) but was later inverted during the Late Cretaceous and Cenozoic, as proved by the presence of anticline A3 on its hanging wall side.

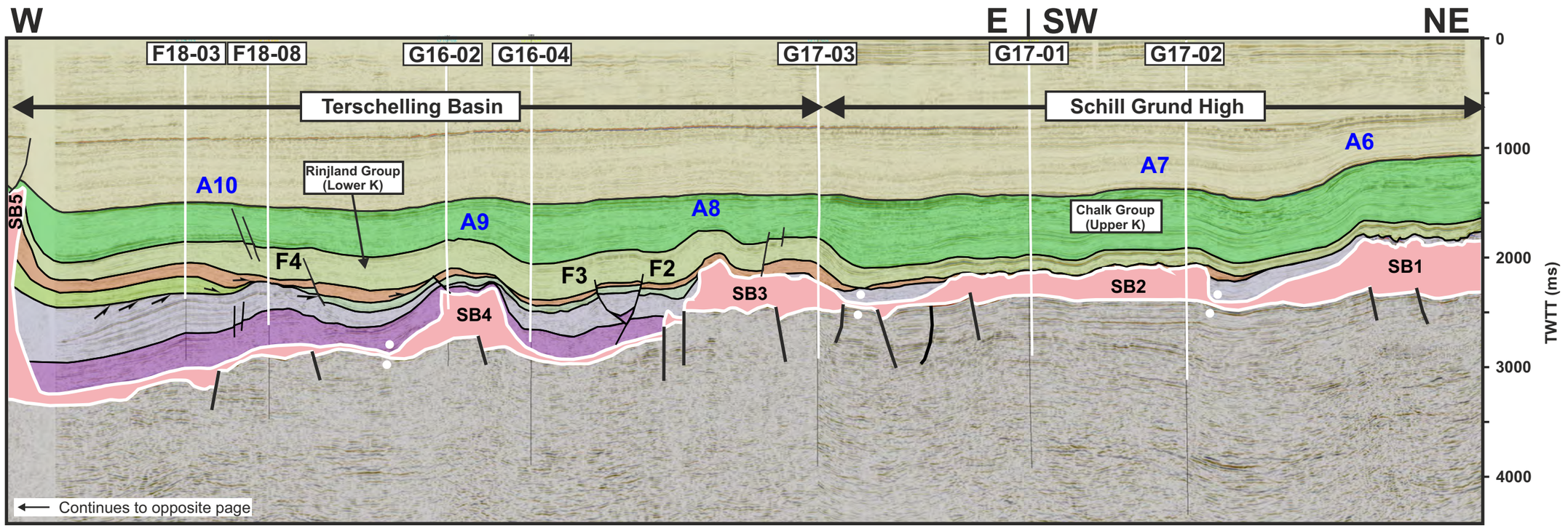

Figure 4.3.7 (Part 2)

Folds

Ten main anticlines and monoclines are observed within this seismic section.

- A1 is described above.
- A2 and A4 are related to the F18 and F17 turtle structures, respectively.
- A3 was described above.
- A5 is a large anticlinal structure that encompasses both the deep F17 and F18 turtle structures. It was active primarily during the Cenozoic and is related to the Alpine compression (in contrast to the A2 and A4 anticlines that are related to turtle structures and, therefore, extensional features.
- Smaller anticlines (A6-11) can be seen on the platforms and are related to Upper Cretaceous and Cenozoic compression.

Stratigraphy

Lower Triassic

The Lower Triassic is well preserved in the DCG and the TB, but its very thin or missing on the platforms. It is locally truncated by Lower Jurassic, Upper Jurassic and Rijnland Group strata.

Upper Triassic

The Upper Triassic is only present in the DCG and TB where it varies greatly in thickness. It is thickest in the F18 turtle structure and on the eastern side of salt body SB5.

Lower Jurassic (Altena Group)

The Altena Group is only present in the DCG and is thickest in the F17 turtle structure and in the western flank of the F18 turtle structure. This indicates that the timing of deformation of both turtle structures (F17 and F18) is different, with F18 turtle structure inverting during the early part of the Early Jurassic and the F18 turtle inverting during the Late Jurassic.

Note that the lower part of Sequence 1 (Upper Jurassic) (yellow) onlaps at high angle on the Lower Jurassic west of well F18-02. This is not the case for the F17 turtle structure. This also indicates different timing of activity for both turtle structures.

Upper Jurassic

The Upper Jurassic is present in all four provinces but is very thin on the SGH and the CBH, where only Sequence 3 is present. In the TB the Upper Jurassic is still thin but both Sequence 2 and 3 are present. In the DCG all three Upper Jurassic sequences are present and are thickest around salt body SB6. Detailed description of this interval is given in Figure 4.4.7.

Rijnland Group

This stratigraphic interval is present throughout the section, except on the western side of the salt body SB6, where it was eroded at the base of the Cenozoic. It is relatively thicker in the TB and the DCG than on the surrounding platforms

Chalk Group

The Chalk Group is thicker on the eastern side of the section and is eroded (as the Rijnland Group) on the western side of the salt body SB6.

Cenozoic

The Cenozoic is thinnest on the eastern edge of the seismic section and thickest between wells F16-04 and F16-02 (2,1 sec. TWTT).

4 - Results: Panel E - SG, DCG and SGH

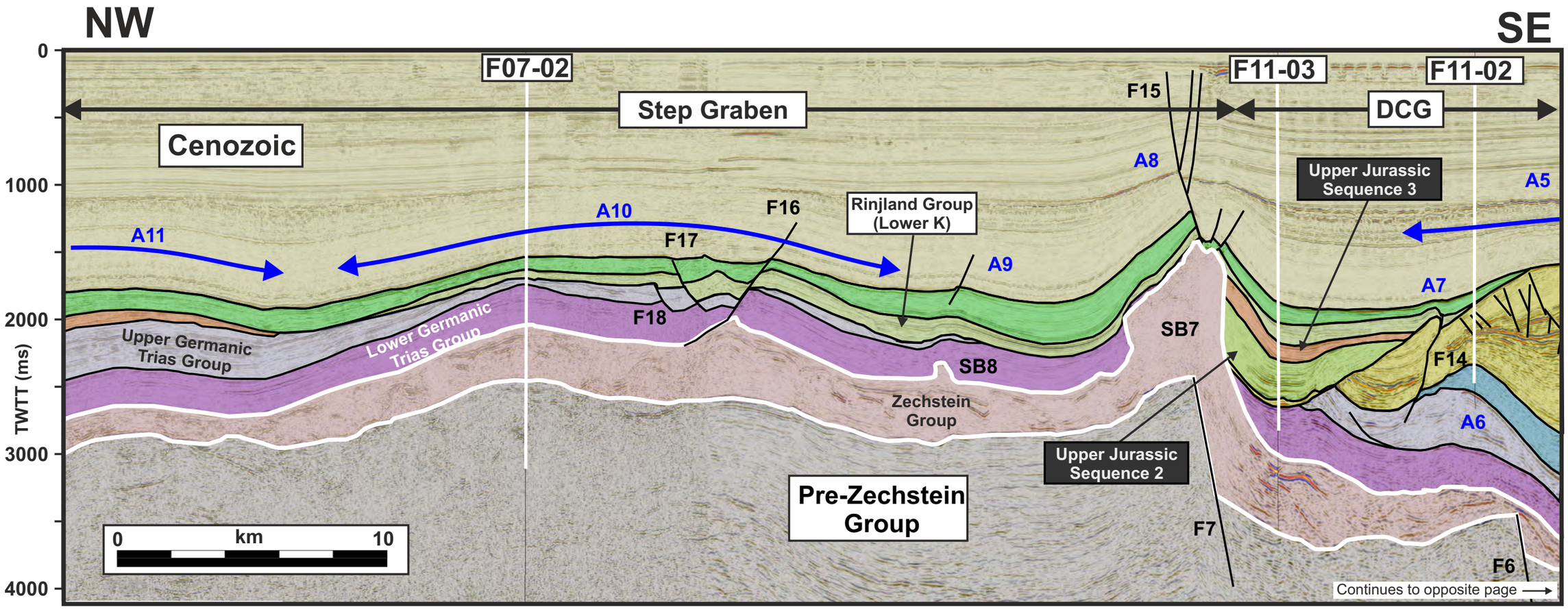

Figure 4.3.8 (Part 1)
Section E is located across three structural provinces, namely from east to west, the Schill Grund High (SGH), the Terschelling Basin (TB) and the Step Graben (SG). This panel trends NW-SE and E-W, except in its western extremity where it is oriented to the NW from well F07-02. This section is 100,5 km long and intercepts 6 wells. See Fig. 4.3.1 for location map and Fig. 4.3.2 for legend.

Base Zechstein (BZ) configuration

The BZ is relatively shallow (around 3 sec. TWTT) on the platforms (CBH and SG). It deepens within the DCG to a maximum of 3.8 sec. (TWTT). The fault pattern in the DCG consists of two half grabens (F2-3 and F6-F7) on both sides of a deep central graben (F4-F5) beneath well F11-01.

Note a slightly elevated BZ in the area below well F07-02.

Zechstein salt bodies

Eight noticeable salt bodies (SB1-8) are recognized along this section. Note that the Zechstein stays quite thick (300-600 ms. TZTT) from the location of well F11-02 toward the west.

- SB1 and SB2 are two salt bodies in the cores of two thrusts (A1 and A2) that were active during the Late Cretaceous and the early Cenozoic. These two thrusts have different vergence. SB1 was likely a detachment for fault F8 that acted as a growth fault during the Late Jurassic (similar to the Fat Sand setting; De Jager, 2012).
- SB3 (a and b) is also located within a Upper Cretaceous and early Cenozoic compressional feature that is a salt cored popup structure (A3). A part of the salt body (SB3b) is encased in the upper part of the popup and is overlay by a small graben.
- SB4 is a small salt diapir sitting at the eastern boundary of the DCG. It has a steep and elevated Lower Triassic eastern flank.
- SB5 is a small and deep diapir encassed in Triassic strata. Fault set F11 soles onto this salt body.
- SB6 is located above the “basement” fault F3 and reaches upward into Upper Jurassic strata.
- SB7 is a wide stocky salt body sitting on the western boundary of the DCG.
- SB8 is a small salt diapir that is located at the core of a low amplitude anticline (A9).

Faults

Numerous faults are observed in this section. Below is a list of the main fault families.

- Several deep faults (F1-7) intercept the base Zechstein and are described above.
- Several reverse faults are observed on the eastern part of the section. F8 was originally a growth fault active during the Late Triassic (Fat Sand type), and was reactivated as a reverse fault during the Late Jurassic. This fault was not connected to any deep-seated fault. F9 is also a reverse fault set (two faults involved) but no evidence of early normal motion during the Triassic is observed. A popup structure located below A3 is composed of three reverse faults and is salt cored.
- Several faults were active during the Late Jurassic in the DCG. They are crestal faults within the A5 (F11) turtle structure but are also locally situated on the eastern flank of the turtle, such as F11-13 faults that are syn-depositional and active until the Cenozoic.
- F14 is also an interesting fault. In its present-day configuration this fault is a reverse fault that was likely active during the Late Jurassic. However, this fault was likely a normal fault during the deposition of Sequence 1 (Upper Jurassic).
- Fault set F15 is one of the youngest fault system observed in this part of the Basin. These faults likely accommodate late motions of the salt diapir SB7 and/or differential compaction between the DCG and the SG.

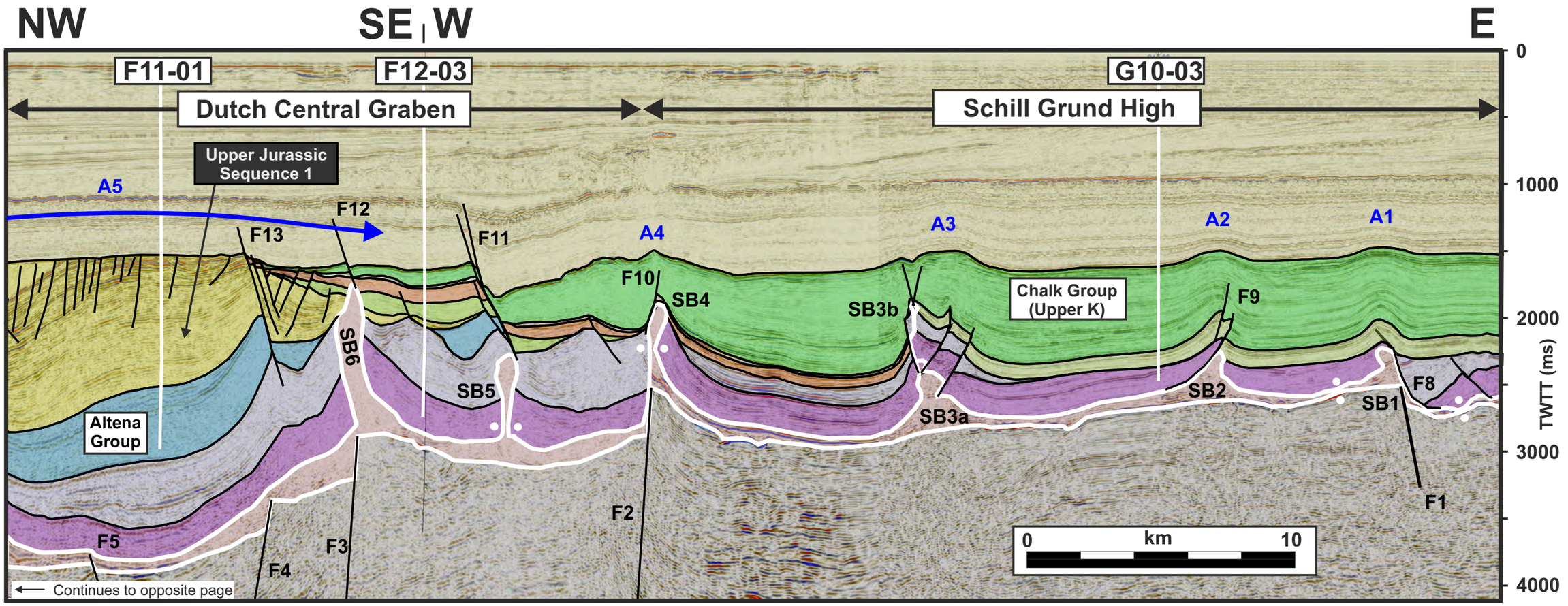

Figure 4.3.8 (Part 2)

- Faults F16-18 define a small Cretaceous and early Cenozoic graben. Grabens can form in compressional settings (e.g. Oligocene grabens in the Alps) but only if they are oriented perpendicular from the main direction of shortening. This graben can also be interpreted as a crestal feature at the top of anticline A10 .

Folds

Eleven main anticlines are observed within this seismic section.

- A1-3 are described above. They are active during the Late Cretaceous and early Cenozoic.
- A4 is a anticline related to the anticlockwise rotation of the hanging wall of fault F11.
- A5 is the DCG axial anticline that is related to the Alpine compression within the graben.
- A6 is a monocline related to the “basement step” over fault F6. It is formed by the differential withdrawal of Zechstein salt on both side of fault F6.
- A7 is described above.
- A8 is a young (early to late Cenozoic) structure that formed over the western boundary of the DCG.
- A9-11 are Late Cretaceous and early Cenozoic structures.

Stratigraphy

Lower Triassic

The Lower Triassic is preserved across the entire section. It is rafted toward the east on the eastern side of salt body SB1 due to the Late Triassic growth faulting (F8).

Upper Triassic

The Upper Triassic is very thin to absent on the SG. It is overall thin but thickens westward toward the CBH. In the DCG, it varies in thickness and is locally eroded at the position of well F11-03.

Lower Jurassic (Altena Group)

The Altena Group is only present in the DCG, in two different zones, in a small area located east of well F12-03 and in the axis of the DCG (F11-02/F11-01 area). In this second zone, it is thick at the axis of the DCG but thins and pinches out toward the east and west. This interval does reach the eastern boundary of the DCG but not the western boundary.

Upper Jurassic

The Upper Jurassic is present in all three provinces and is described in detail in Fig. 4.4.8.

Rijnland Group

This stratigraphic interval is present throughout most of this seismic section, except on the western side of the SB6 salt body and on the SG, west of the anticline A10. It is overall quite thin (less than 200 ms. TWTT)

Chalk Group

The Chalk Group is thicker on the eastern side of the section and is also eroded away (as the Rijnland Group) on the western side of the salt body SB6 (apex of anticline A5). Its thickness varies rapidly around the anticlines A1-3.

Cenozoic

The Cenozoic is the thinnest on the eastern edge of the seismic section and thickest between wells F16-04 and F16-2 (2,1 sec. TWTT).

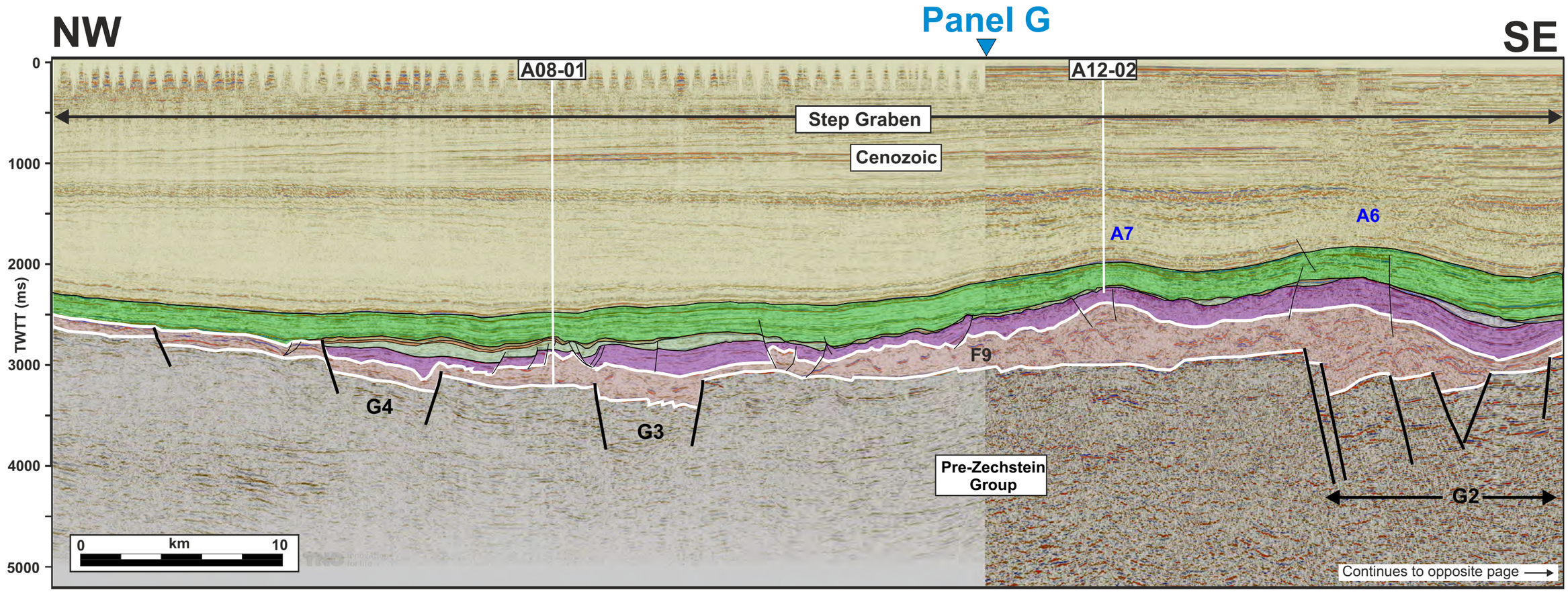

Figure 4.3.9 (Part 1)

Interpreted seismic section F, located in the northern part of the study area, trends SE-NW from the DCG (F03 block) to the northern part of the SG (A05 block), parallel the Dutch-German offshore boundary. 144,2 km long interpreted seismic section that intercepts nine wells. See Fig. 4.3.1 for location map and Fig. 4.3.2 for legend.

Base Zechstein (BZ) configuration

- The BZ varies greatly from the SG where it is relatively shallow (2,5 to 3 sec TWTT) and flat, until it reaches the location of well B13-02 at the edge of the DCG. At this location the BZ dips to the southeast until it reaches 4,9 sec. (TWTT), just SE of well B14-03. From this location it stay deep but is offset by large faults (F1 and F2). From this location it regularly rises to the SE.
- Several faults are observed at the BZ, F1 and F2 being the largest within the DCG. Other faults defined a series of half grabens on the NW side of the DCG between wells B14-02 and B14-01, one small graben (G1) in the DCG and three grabens (G2-4) on the SG.

Zechstein salt bodies

Four salt bodies are identified along this seismic section.

- SB1 is a salt diapirs with two lateral wings. This salt body is encased within the Upper Triassic and has a feeder connected to the autochthonous Zechstein salt.
- SB2 is a large salt pillow in the core of anticlinal A3.
- SB3 is a thin and deformed salt sheet that is not connected to SB4. It is connected to a allochthonous salt system toward the south. This feature is quite spectacular, with the base of the salt sheet truncating intra Upper Triassic strata and the overlying Upper Triassic thin and highly deformed by syn-depositional faults that detached on this allochthonous salt sheet.
- SB4 is a triangular shape salt pillow in the core of anticline A5. Its southeastern flank is used as a detachment by a large growth fault (F7) that was active during the Late Jurassic (Sequence 2).

Faults

Numerous faults are observed in this section. Below is a list of the main fault families.

- Several deep faults intercept the BZ and are described above.
- Several faults are interpreted as strike slip faults. F4, F5, and all the smaller faults located between them, are defined a flower structure between anticlines A1 and A2. The timing of activity of this strike slip structure is difficult to estimate but is likely Late Jurassic to Cenozoic.
- Crestal faulting can be observed at the crest of anticlines A1 and A2.
- The small growth faultslocated above the allochthonous salt sheet SB3 are mainly dipping to the SE and were active during the Early Jurassic.
- Two large growth faults (F6 and F7) are observed in the B14-02 area B13-02 but have different growth periods. F6 was active during the early Cenozoic, while F7 (and a few of its conjugates) was active during the Late Jurassic (Sequence 2).
- F9 is also a growth fault that detached on the NW flank of salt pillow SB4. This fault was active during most of the Cenozoic.
- Small faults can be seen in the over thinned pre-Chalk Group strata on the SG. These faults are mainly normal but one inverse fault (F9) can be seen.

4 - Results: Panel F - Dutch Central Graben and Step Graben

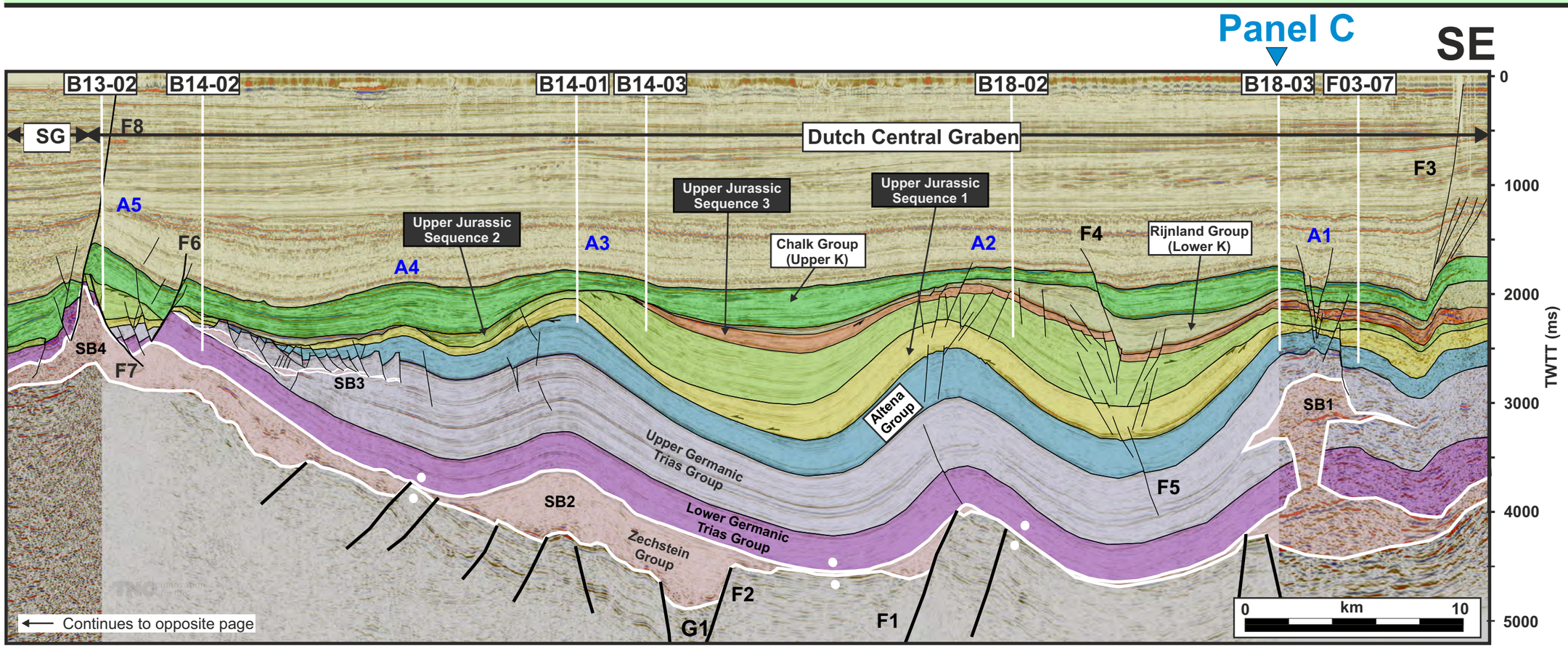

Figure 4.3.9 (Part 2)

Folds
Seven anticlines (A1-A7) are located on this section. Four are located in the DCG (A1-4) and three on the SG (A5-7).

- A1, A2 and A3 are large anticlines that were active during the Late Jurassic and Cretaceous, with minor growth during the early Cenozoic.
- A4 is interpreted as being related to the deflation (withdrawal) of the SB3 allochthonous salt sheet that occurred during the Early Jurassic (and possibly during the Late Jurassic).
- A5 is located at the boundary between the DCG and the SG and is related to the differential subsidence between the two structural provinces.

Stratigraphy

Lower Triassic:
The lower Triassic is present over most of the section F. It is missing in the last 15 km in the northwestern edge of the section due to the base Chalk group erosion that truncated down into the Zechstein level. The Lower Triassic is over-thinned on the SG as well as above salt body SB4. This indicates that this salt body likely started to rise during this period with only a thin and faulted Lower Triassic drape located above.

Upper Triassic
The Upper Jurassic shows high thickness variability along this section. This interval is thick in the DCG (in average 700-900 ms. TWTT), and shows some local thickening below anticlines A1-3. However, these over-thickened areas are interpreted as artifacts due to the fact that we are using time seismic data. This interpretation will have to be tested with depth data. The Upper Triassic is only observed as thin lenses on the SG due to later erosional events.

Lower Jurassic (Altena Group)
The Lower Jurassic is only present with the DCG along this section. It's thickness varies only slightly until it reaches well B14-0t where it rapidly thins and pinches out toward the NW. This rapid thinning is attributed to the salt sheet SB3 that was thicker and created a topographic high, but was later withdrawn, deforming the over-thinned Lower Jurassic and faulting this interval intensely.

Upper Jurassic
The Upper Jurassic greatly varies in thickness along section F. It is thick in the axis of the DCG and thins toward its margins. In the DCG it accumulated within two small minibasins (MB1 and MB2) that are divided by the anticline A2 that was active. The Upper Jurassic is only present as thin drapes (due to later erosion) on the SG. See Fig. 4.4.9 for more detailed interpretation of the Upper Jurassic interval along this section.

Rijnland Group
This stratigraphic interval is only present along the southeastern part of the DCG and disappears before reaching well B14-03. It is thickest in the syncline between anticline A1 and A2.

Chalk Group
The Chalk Group is present along the entire section but presents some thickness variation. It is overall slightly thicker northwest of well B14-01 and varies in thickness due to folding toward the southeast.

Cenozoic
The Cenozoic thickens toward the NW.

4 - Results: Panel G - Step Graben and Dutch Central Graben

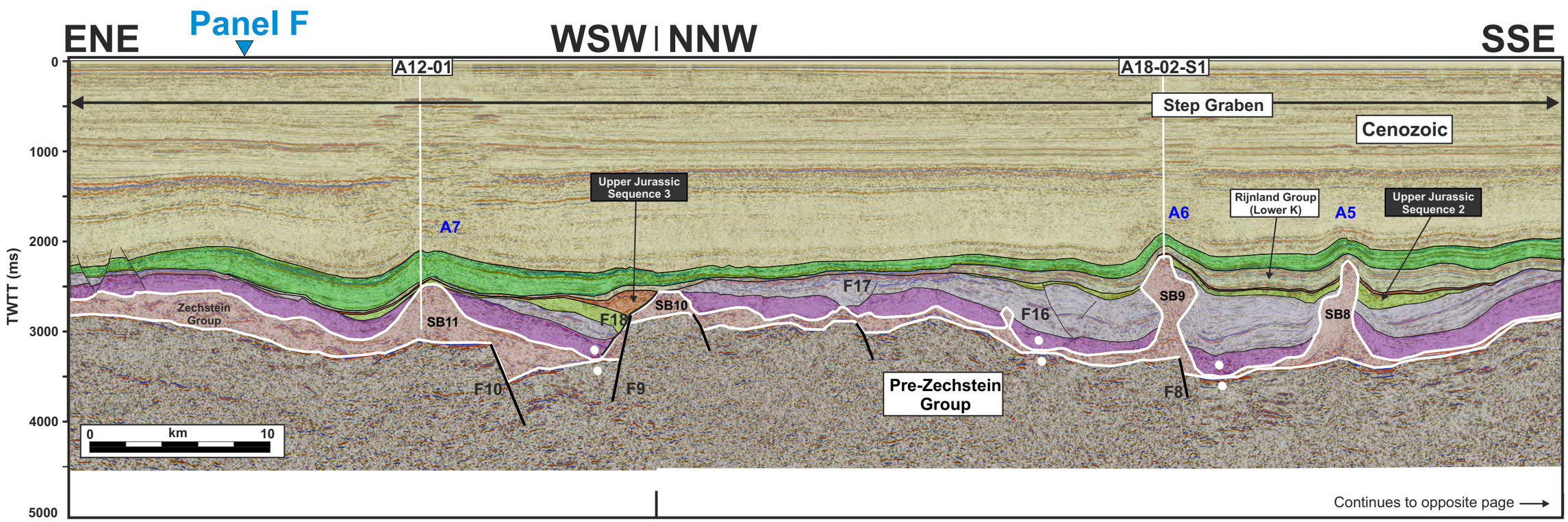

Figure 4.3.10 (Part 1)

Interpreted seismic section G is located on the Step Graben and the DCG. This section has a C-shape on a map view and changes trend several time from ENE-WSW to NNW-SSE to W-E to N-S to NW-SE and finally W-E across the DCG. This irregular trend was chosen to capture as many wells as possible on the SG that have Upper Jurassic strata. This section is 144,2 km long interpreted seismic section that intercepts nine wells. See Fig. 4.3.1 for location map and Fig. 4.3.2 for legend.

Base Zechstein (BZ) configuration

The base Zechstein is irregular but relatively shallow (around 3 sec. TWTT) on the SG and deepens from Fault F4, at the edge of the DCG, to reach 4.6 sec. (TWTT) at its deepest. In the eastern side of the DCG the BZ rises in a stepped fashion to reach 2.5 sec. (TWTT) on the eastern and right side of the section.

Zechstein salt bodies

Eleven salt bodies are observed along this section. Each of these salt bodies display very different geometry and timing of movement.

- SB1 is a small salt pillow at the autochthonous salt level. It is likely connected to the salt sheet SB2 by a vertical feeder.
- SB2 is a very interesting salt feature. The quality of the seismic data doesn't allow for a clear imaging of this feature. Our interpretation is that of an amalgamated allochthonous salt sheet, which has at least two salt feeders. This salt sheet was deflated (withdrawn) during the Early Jurassic (potentially the Late Jurassic and even Cretaceous) as proved by the large growth faults (F11, 12, 13 and 14; possibly F15) that were active and detached on this feature. This salt system is a Roho salt system (as defined by Schuster, 1995).
- SB3 is a tall tear drop-shape salt diapir sitting on fault F2. It was active from the Late Jurassic to the Cenozoic .
- SB4 is a small narrow salt diapir at the western boundary of the DCG. It may have had a very different shape before the Alpine compression since it is now located in the core of an east verging thrust, with Lower Triassic to Upper Jurassic being thrusted up toward the west.
- SB5 is a very deformed and complex salt structure with three associated salt diapirs connected to a autochthonous salt pillow over a BZ fault (F5). Its geometry suggests a overall compressional structure but additional detail work would be required to fully understand this feature.
- SB6 to SB9 are four salt diapirs with similar geometry. The difference between these four diapirs are located within the strata located on their flanks. SB6 doesn't have any Jurassic on its eastern flank; SB7 shows a small Lower Jurassic rim syncline draped by Upper Jurassic-Lower Cretaceous (Sequence 3); SB8 and SB9 have thin Upper Jurassic Sequence 2 strata on their flanks.
- SB10 is a salt roller sitting on the footwall side of fault F19.
- SB11 is a salt pillow in the core of anticline A7).

Faults

Numerous faults are observed in this section. Below is a list of the main fault families.

- Several deep faults (F1-10) intercept the BZ and are described above.
- Several growth faults (F11-14) are detaching on shallow salt body SB2 and are part of the Roho salt system.
- F16 is part of a popup structure on the SG.
- F17 and F18 are growth fault detaching on the autochthonous salt. F18 is large and presents an Upper Jurassic growth wedge in its hanging wall side.

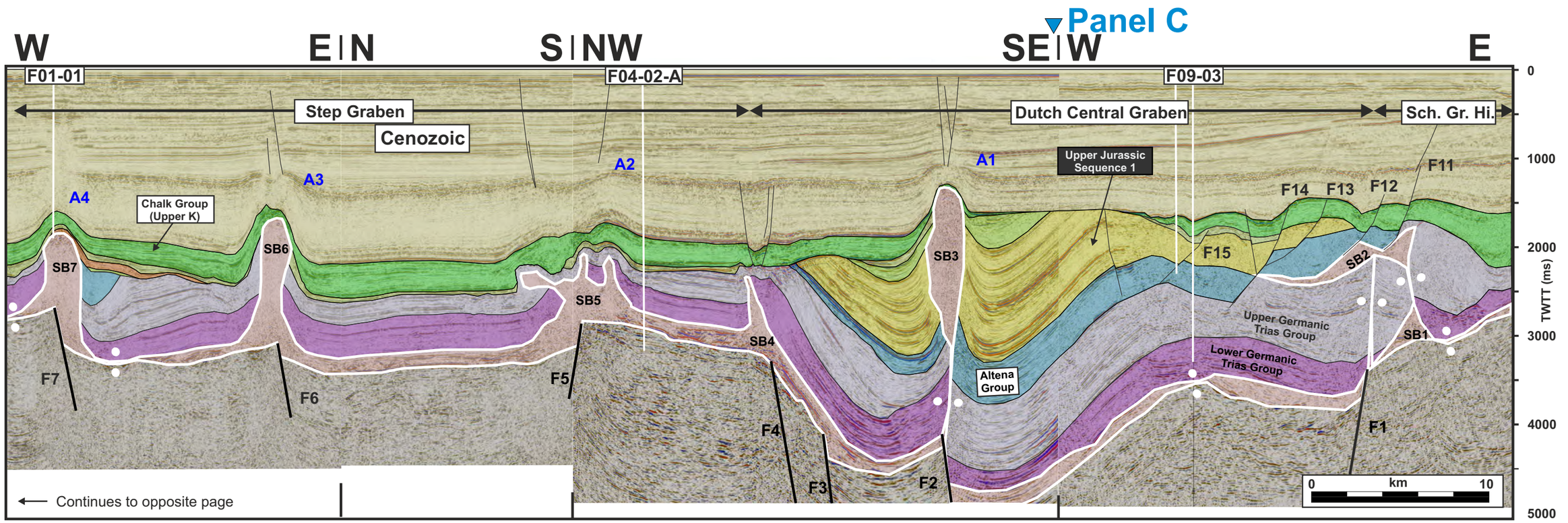

Figure 4.3.10 (Part 2)

Folds

Seven anticlines (A1-A7) are located on this section. One is located in the DCG (A1) and six on the SG (A2-7).

- All seven anticlines were active, mainly, during the Cenozoic (Alpine compression) and some of them (A1-A3) possibly earlier during the Cretaceous.
- All seven anticlines are salt cored.
- Note the uplifted Triassic section above salt body SB4, with the presence of a thrust verging toward the west. This structure inverted during Alpine compression.

Stratigraphy

Lower Triassic

The Lower Triassic is present over most of the section G. It is missing west of salt pillow SB1 and is faulted down along fault F18. The Lower Triassic is thinner on the western part of the SG than on the eastern part and in the DCG.

Upper Triassic

The Upper Jurassic shows high thickness variability along this section. In the DCG it is thick (in average 700-1100 ms. TWTT). This interval is locally eroded (e.g. on the western flank of the DCG). Along the SG it shows high variability in thickness, with thicks above “basement” lows (e.g. east of SB7) and thins in the vicinity of some of the salt bodies (e.g. SB5-6) and on the eastern part of the profile. The Upper Triassic is even missing in the ENE side of well A12-01.

Lower Jurassic (Altena Group)

The Lower Jurassic is mainly present with the DCG along this section. It is thinner on the western side of the DCG and thickens toward the east. It is also present within a small rim syncline located east of salt body SB7.

Upper Jurassic

The Upper Jurassic greatly varies in thickness along section G. It is thick in the axis of the DCG and thins toward its margins. In the DCG it accumulates within two small sub-basins separated by salt body SB3. The Upper Jurassic is also present on the SG (except to the ENE end of the profile), mainly as a thin remnant drape. It is relatively thicker around salt bodies SB7 and SB8, as well as in the hanging wall of fault F18.

Rijnland Group

This stratigraphic interval is present in the western part of the DCG and in the SG as a relatively thin interval. It is slightly thicker in the vicinity of well A18-02-S1.

Chalk Group

The Chalk Group is present everywhere except on the middle of the DCG, over a 7 km-wide zone. It varies greatly in thickness along the profile.

Cenozoic

The Cenozoic thickens toward the right side of the panel (W and ENE).

4.4

RESULTS

STRATIGRAPHIC CORRELATION

4.4 Stratigraphic correlations

The stratigraphic correlations for each regional panel is presented in this chapter.

Figure 4.4.1 (see next page)

This section A1 trends SE to NW through the Terschelling Basin and the southern part of the Dutch Central Graben. See Fig. 4.3.1 for location map and Fig. 4.3.2 for legend.

A) Flatten seismic section showing the Upper Jurassic and Lower Cretaceous interval

This section is flattened of top of Sequence 3. Sequence 1 (lower part of Friese Front Fm.) in yellow, Sequence 2 in green (with slightly different shade of green for the upper part of Friese Front Fm. and the Skylge Fm.), and Sequence 3 in orange. Sequences 1, 2 and 3 of the Upper Jurassic-Lower Cretaceous (UJ-lLC) are present in this section. The UJ-lLC was deposited in an asymmetric fashion in the TB. The southeastern part of the basin slope was low angle (up to well L03-01) and the northwestern part had a high angle slope and was syn-depositionally deformed by a large active fault (F5). The basal surface of the UJ-lLC is erosional and covers an irregular topography. This erosional surface cut down into Lower Jurassic strata in the NW part of the section and in Triassic (Upper and even Lower) in the SE part of the section (Fig. 4.3.3).

B) Stratigraphic well correlation of Sequence 1 and lower part of Sequence 2

Section flattened on the base of the Skylge Formation.

Sequence 1:

This depositional sequence is deposited in four locations (L1-4) that are 800 m to 10 km wide and 50 to 230 m deep topographic lows. These topographic lows are interpreted as incised valleys that are filled with lownet-to-gross strata of the Friese Front Formation. It is still unclear if these incised valleys are still connected in map view and if they can be mapped and connected to a larger depositional systems toward the DCG. The Friese Front Formation is composed of delta plain and lagoonal deposits (Munsterman et al, 2012). The strata onlaps at high angle along the margins of the incised valleys (see L1-L7 in Figs. 4.4.1A and B) .

Lower part of Sequence 2:

This stratigraphic interval is divided into two parts along this section. The lower part is composed of the Main Friese Front Mb. (Fig. 4.4.1 B) and the upper part is composed of Skylge Fm., which include the Oyster Ground, the Terschelling Sandstone, and the Lies Members. Note that the upper part of the Lies Mb. is not shown on Figure 4.4.1C since this section is flattened on a easily recognized MFS present in the lower part of the Lies Member. The base of S2 is also erosional and S2 fills three topographic lows (L5-7) in the southeastern half of the section. These three topographic lows are 4 to 10 km wide and 30 to 140 m deep. They are increasingly shallower and have decreased confinement toward the southeast (from L5 to L7). As for the incised valleys described above (Sequence 1), these S2 incised valleys are also filled with strata from the Main Friese Front Mb. (delta plain and lagoonal deposits) that have, for this interval, higher net-to-gross, with deltaic sands up to 5-7 m thick (possibly thicker in the topographic lows?). The lower part of Sequence 2 (Fig. 4.4.1B) is sandier than Sequence 1, with interbedded sandstones (up to 15 m), siltstones and mudstones. From the SE to the NW, this lower part of Sequence 2 shows an increase in net sand, with the highest net sand and individual thickest sands located around wells L06-2, L03-04 and L03-03. This may be also related to active salt structures (salt bodies and faults) around those wells that may have provided local sources of redeposited sediments. Possible low angle clinoforms can also be observed on Fig. 4.4.1B between wells L03-03 and L03-01. This part of Sequence 2 onlaps onto Sequence 1 to the NW.

C) Stratigraphic well correlation of upper part of Sequence 2

Section flattened on a easily recognizable MFS intra Lies Mb. net-to-gross interval deposited restricted marine settings; the TSM has a high net-to-gross and is interpreted as tidal inlets, tidal channels and shoreface deposits; and the LM is a low net-to-gross interval deposited in offshore setting. The following discussion will be carried at Skylge Fm. level since the upper part of the OGM is lateral time equivalent of the lower part of the TSM and the upper part of the TSM is lateral time equivalent of the lower part of the LM. The upper part of Sequence 2 filled up a asymmetric basin (low angle to the SE, high angle to the NW), which had three topographic steps (ToS 1-3), with local minor onlaps onto previously generated topographies. The net-to-gross varies greatly from SE to NW, with the highest net-to-gross at the location of wells M04-01, M04-3 and M04-04, which corresponds to the thickest and sandiest Terschelling Sandstone Member. The lower part of this sandy strata can be correlated to the NW toward wells L06-02, L03-04, L03-03 and L03-01. The upper part of the sandy strata observed at M04-01, M045-03 and M04-04 rapidly transition toward the NW to a low net-to-gross interval (in well L06-02, L03-04 and L03-03), that are interpreted as offshore mudstones (Lies Member). Note that, based on the GR logs analysis, the sandy interval (TSM) is showing progradational to retrogradational trends between well M04-04 and L06-02.

4 - Results: Panel A1 - TB and DCG - Sequences 1 & 2

TNO innovation for life

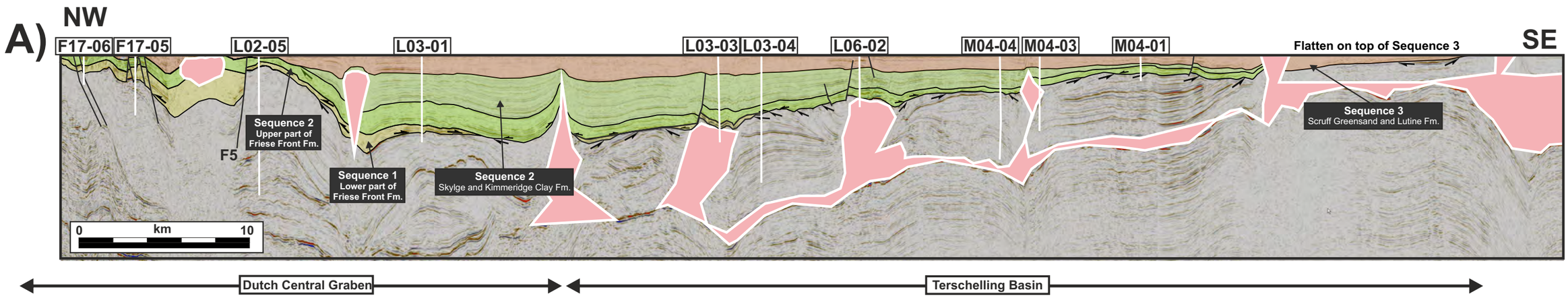

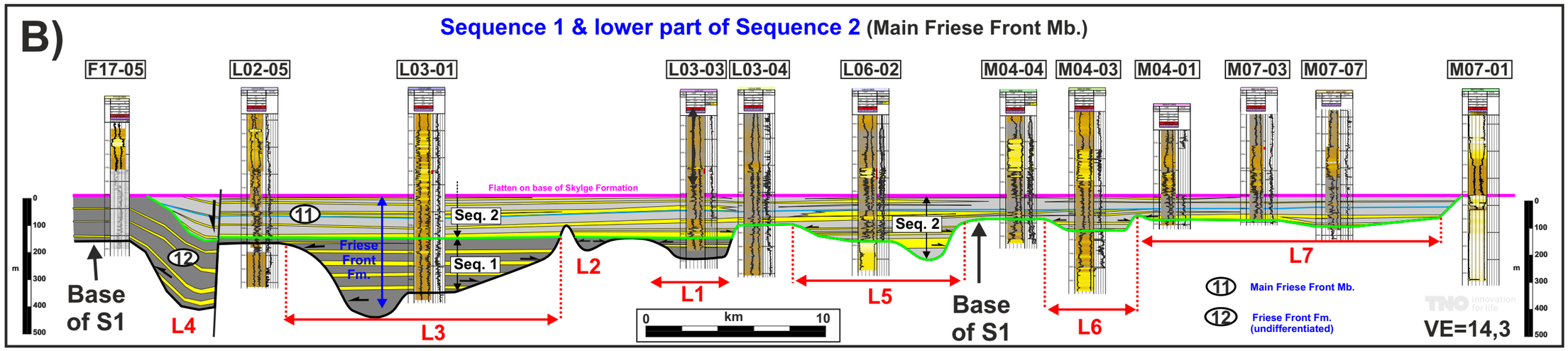

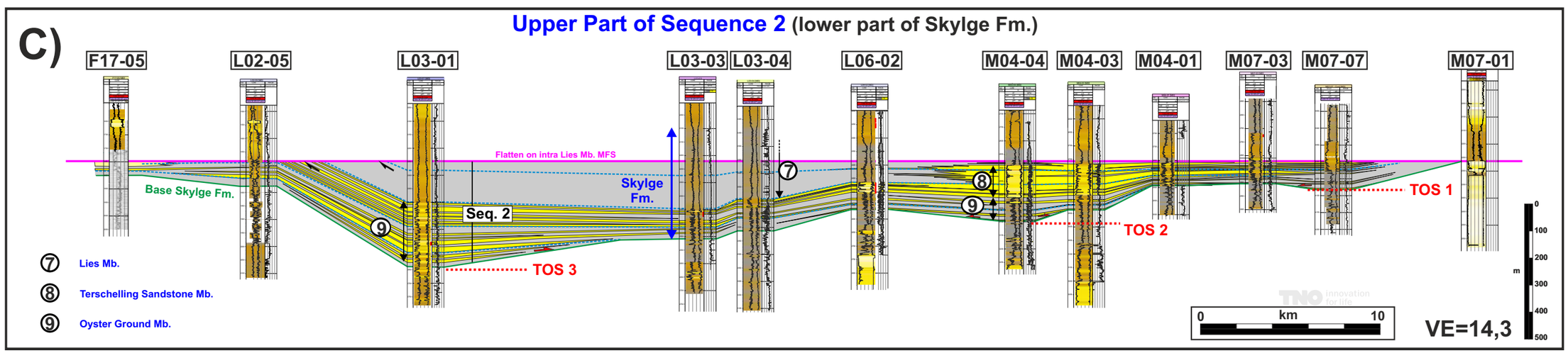

Figure 4.4.1 (See previous page for figure caption)

4 - Results: Panel A1 - TB and DCG - Sequence 3

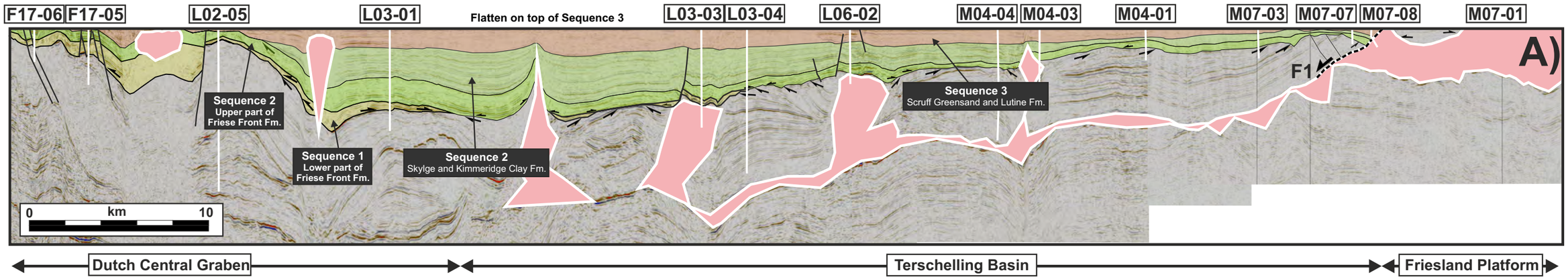

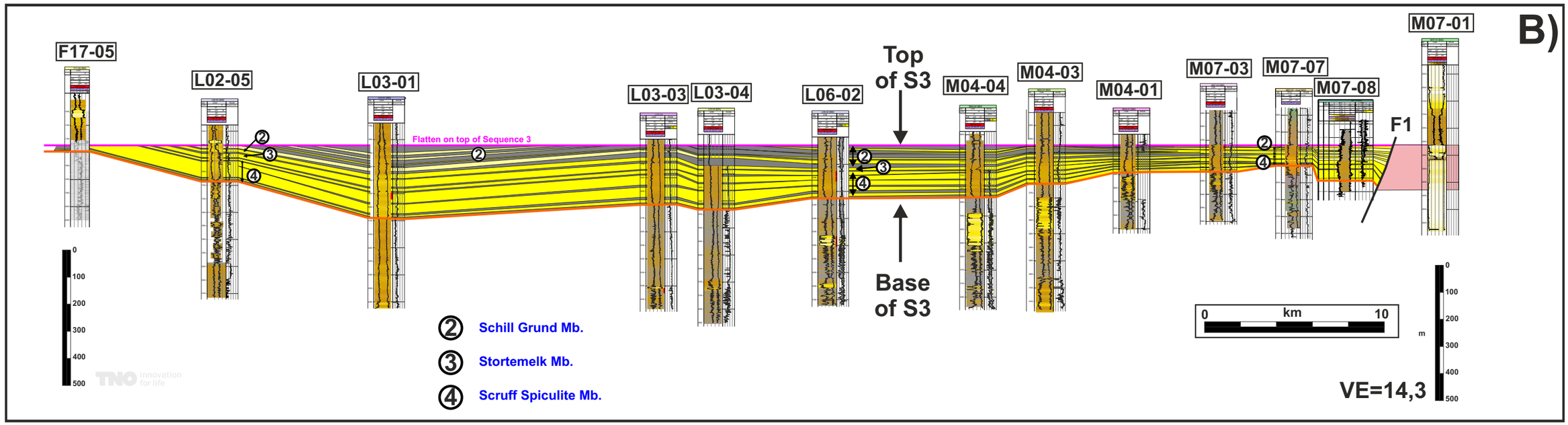

Figure 4.4.2
This section A1 trends SE to NW through the Terschelling Basin and the southern part of the Dutch Central Graben. See Fig. 4.3.1 for location map and Fig. 4.3.2 for legend.

A) Flattened seismic section showing the Upper Jurassic and Lower Cretaceous intervals.
This section is flattened on top of Sequence 3. Sequence 1 (lower part of Friese Front Fm.) is shown in yellow, Sequence 2 in green (with slightly different shade of green for the upper part of Friese Front Fm. and the Skylge Fm.), and Sequence 3 in orange.

B) Stratigraphic well correlation of Sequence 3. Section flatten on the top of Sequence 3
The overall basin fill for Sequence 3 is asymmetric (as for S1 and S2) with a low angle to the SE and a high angle to the NW (toward the F17 Field). Sequence 3 consists of the Scruff Greensand Fm., which is composed of the Scruff Spiculite, the Stortemelk and the Schill Grund Members in this part of the Dutch offshore. The Scruff Spiculite Mb. is interpreted as offshore sandstones (offshore bars); the Stortemelk Mb. is interpreted as shoreface to offshore deposits; and the Schill Grund Mb. is interpreted as bituminous claystones deposited in anoxic to dysoxic basin-floor setting. In this section the stratigraphy of S3 can be divided in two different depositional systems:

1) A regional basin fill that shows a fining upward trend (from Scruff Spiculite to Schill Grund Members) between well M04-01 and L02-05. The sandiest part of the depositional system is located around well L03-01 and gets more interbedded, with thin low net-to-gross strata, toward the SE. The depositional system is transitional upward from a sandy offshore setting to a muddy offshore setting that is interpreted as being related to changes in sediment supply, or proximity to the sediment source, rather than a significant deepening of the basin.
2) A second local depositional system can be observed in the SE part of the section, between well M07-03 and the southern basin margin. This depositional system is sandy and increasingly thicker, and sandier, toward the southern basin margin. At this location this depositional system is interpreted as being highly controlled by basin margin processes that include redeposition of sediments from the Friesland Platform to the south and syn-depositional faulting. This interpretation is also supported by core description of the M07-07 and 07-08 wells that show numerous extra-formational angular clasts that are likely originating from the eroded Triassic strata on the bounding platform. This sandy basin margin is also controlled by active syn-depositional structures such as fault F1 (Fig. 4.4.2A) that was active during deposition of S3 (possibly also S2) and detaches on the basin margin Zechstein salt, forming a growth stratal wedge.

4 - Results: Panel B1 - TB and DCG - Sequences 1 & 2

TNO innovation for life

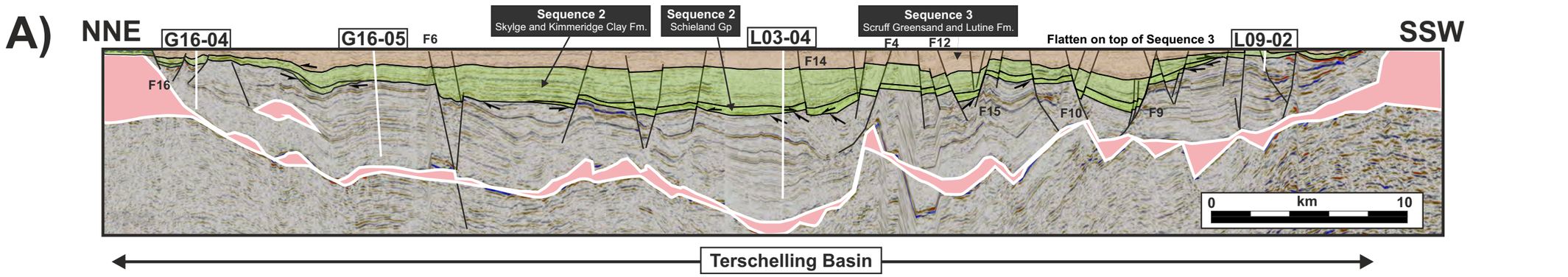

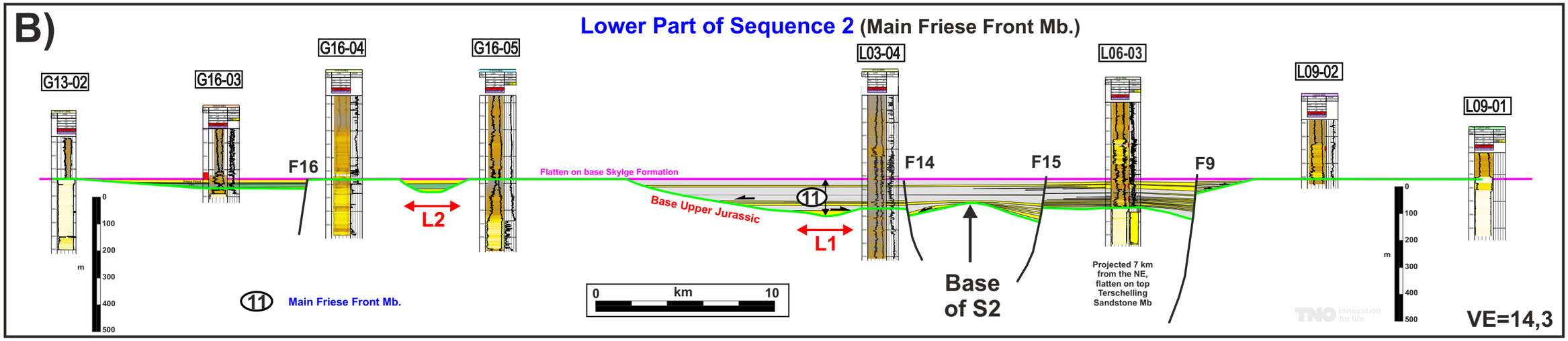

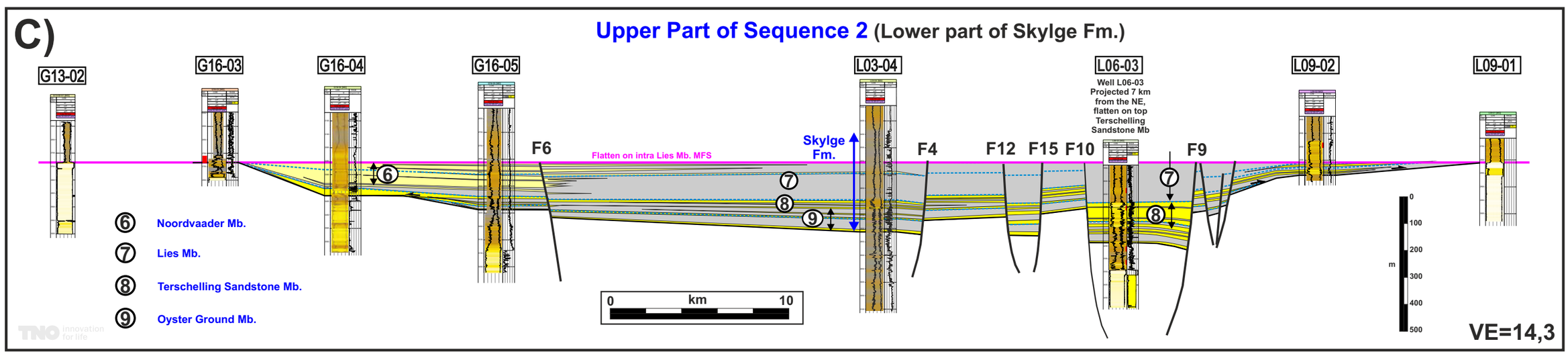

Figure 4.4.3 (previous page)

This section B1 trends NNE to SSE through the Terschelling Basin. See Fig. 4.3.1 for location map and Fig. 4.3.2 for legend.

A) Flatten seismic section showing the Upper Jurassic and Lower Cretaceous intervals

This section is flattened of top of Sequence 3. Sequence 2 shown in green (with slightly different shade of green for the upper part of Friese Front Fm. and the Skylge Fm.), and Sequence 3 in orange.

B) Stratigraphic well correlation of the lower part of Sequence 2

Section flattened on the base of the Skylge Fm. The depositional geometry is similar to the other Terschelling Basin section (Section A, Fig. 4.4.1) with relatively sandy strata filling up topographic lows (4 to 11 km wide and 50 to 70 m thick incised valleys) on the northern side of the section (between wells G16-05 and G16-04; around well G16-03).

The central part of the section consist of a 34 km wide basin that is highly controlled by paleo-topographic relieves in the axis and margins (NNE and SSW). The northern margin is low angle and muddy while the southern margin is at a higher angle and sandier. Several syn-depositional normal faults are also observed (F9, F14-16) that offset the base of S2 by 30 to 90 m. The sequence thickens into these faults, and it is likely, yet speculative, that the sandy strata are more abundantly developed close to the faults.

C) Stratigraphic well correlation of upper part of Sequence 2

Section flattened on an easily recognizable MFS intra Lies Mb. This upper part of S2 also shows a asymmetric basin fill, as for the lower part of S2, but is deposited over a larger zone, from well G16-04 to well L09-02. Several other similarities exist between the lower and upper parts of Sequence 2: 1) The southern part of the basin is affected by syn-depositional normal faults and is sandier (especially the lower section (e.g. Terschelling Sandstone Mb. Around well L06-03); 2) the southern margin is at an higher angle than the northern margin.

An additional sandy and silty depositional system is observed in the upper part of the Skyge Fm. in this northern part of the Terschelling Basin, namely the Noordvaarder Mb. Note that a 27 m thick sandy interval is present at the base of the Skylge Fm. at the location of well G16-04, which indicates that good quality sands can also be found on low angle northern basin margin in the Terschelling Basin. This member is observed at the locations of wells G16-04 and G16-05 and is interpreted as pinching out southward.

Several syn-depositional normal faults are also observed (F4, F6, F9, F10, F12 and F15).

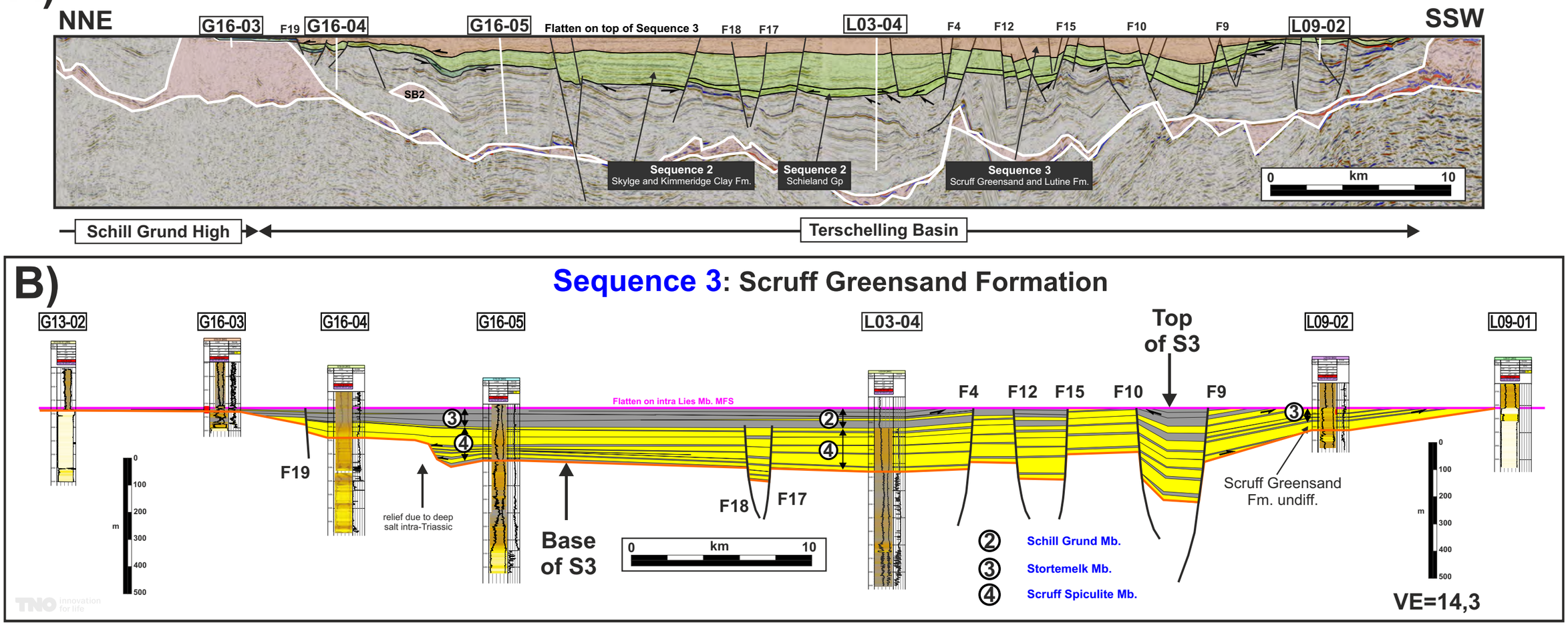

Figure 4.4.4

This section B1 shows the stratigraphic correlation of Sequence 3 in a NNE to SSE trend in the Terschelling Basin. See Figure 4.3.1 for location map and Fig. 4.3.2 for legend.

A) Flattened seismic section showing the Upper Jurassic and Lower Cretaceous intervals.
This section is flattened of top of Sequence 3. Sequence 2 shown in green (with slightly different shade of green for the upper part of Friese Front Fm. and the Skylge Fm.), and Sequence 3 in orange.

B) Stratigraphic well correlation of Sequence 3. Section flattened on the top of Sequence 3
The Terschelling Basin was also asymmetric during the deposition of S3, with a low angle basal slope to the north and a high angle to the south. However, the northern basin margin is slightly more complex than for S2, with a topographic high that bounds the lower part of S3 between wells G16-05 and G16-04. These topographic relief is interpreted as being related to an allochthonous salt body (SB2) intra Triassic (likely remobilzed Zechstein than Röt salt), that was withdrawn during the Upper Jurassic , defining the northern basin margin of the TB during S2 and the early part of S3. This topographic relief was over-stepped during the deposition of the younger part of S3. Note that the over-stepping S3 strata are sandier that the underlying S3 strata between wells G16-05 and G16-04. Several syn-depositional normal faults are also observed (F4, F9, F10, F12 F15, and F17-19).

The overall stratigraphy of S3 in this section is showing fining upward (Scruff Spiculite to Schill Grund Members) and a northward fining trends. Several syn-depositional faults were still active during this period, especially in the southern part of the basin. Locally S3 was eroded (between wells L03-04 and L09-02).

4 - Results: Panel C - Dutch Central Graben - Sequence 1

TNO innovation for life

N B18-03 F03-08 F03-05 F03-06 F03-03 F06-01 F11-01 S

A)

Flatten on top of Sequence 1

Zone added to restore stratigraphy

F08-01 F08-02

Middle and Upper Graben Formation

Lower Graben Formation

Lower Jurassic

0 km 10

Continues to opposite page →

Dutch Central Graben

B)

B18-03 F03-08 F03-05-S1 F03-06 F03-03 F06-01 F11-01

Flatten on top of Sequence 1

S1-UC2

S1-UC1

Zone added to restore stratigraphy

F08-01 F08-02

Coal Beds, Middle Graben Formation

m 0 100 200 300 400 500

0 km 10

F9

Base of S1

10 Kimmeridge Clay Fm.

14 Puzzle Hole Fm. Mb.

15 Upper Graben Fm.

16 Middle Graben Fm.

17 Lower Graben Fm.

4 - Results: Panel C - Dutch Central Graben - Sequence 1

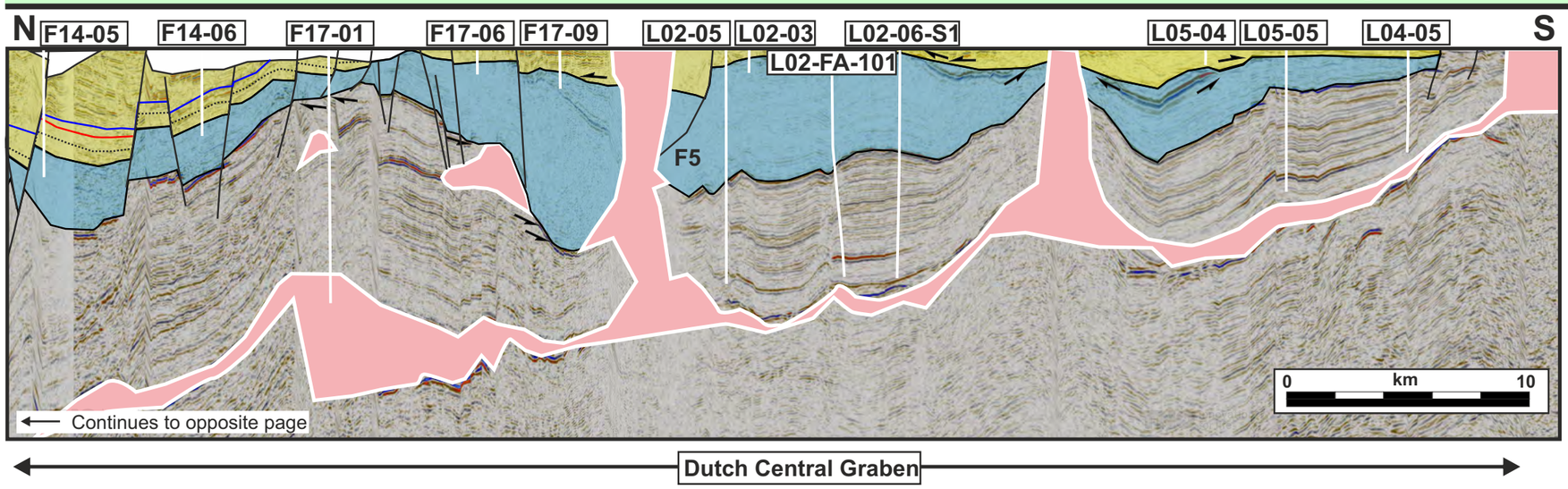

Dutch Central Graben

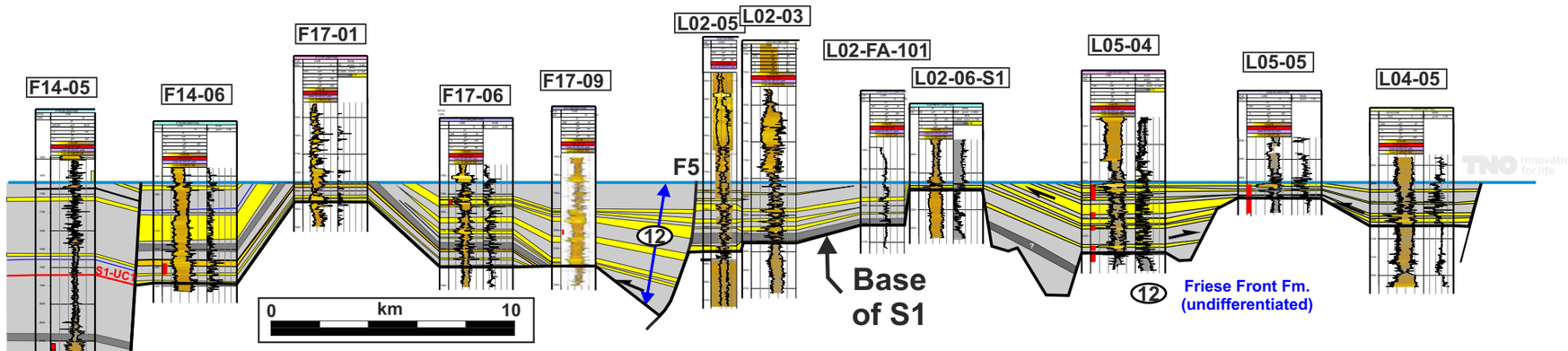

Figure 4.4.5 (over two adjacent pages)
This section C is located in the axis of the Dutch Central Graben and trends NNW-NNE. See Fig. 4.3.1 for location map and Fig. 4.3.2 for legend.

A) Flatten seismic section showing the Lower Jurassic and the Sequence 1 of the Upper Jurassic

The extended flattened technique was used in four location to compensate for the large portions of Sequence 1 that were eroded at the base of the Cenozoic (e.g. Zone 1). This seismic section is flattened on the top of Sequence 1.

The Altena Group varies greatly in thickness. Note the presence of high amplitudes toward the top of the Altena Group (e.g. well F11-01) that correspond to the Posidonia Shale Formation. Note the over thickening of the Lower Jurassic below well F17-09 that was likely due the withdrawal of salt, autochthonous or most likely allochthonous in origin.

The Upper Jurassic basin fill is asymmetric with a low angle southern slope and a steeper northern slope, between wells F03-05-S1 and F03-08. The steeper northern slope is partially due to the seismic section being positioned closer to the eastern margin of the DCG at this location. S1 is thin in the southern part of the section due to post-depositional erosion in this part of the DCG. S1 is thick in the central and northern parts of this section and locally shows internal erosional surfaces that are described below.

B) Stratigraphic well correlation of Sequence 1

This section is flattened on the top of Sequence 1. At its thickest point (at the location of well F06-01) S1 is 1615 m thick (five time the height of the Eiffel Tower!). Along this section several lithostratigraphic units are present: Friese Front, Lower Graben, Middle Graben, Upper Graben, Puzzle Hole and Kimmeridge Clay Formations. Three stratigraphic intervals (lower S1, middle S1 and upper S1) are described below. Note that several faults are shown on this section. One of them (F5) is interpreted as being active during the deposition of S1. The other faults may also have been active during this period but more detailed work is necessary to get a definite answer.

1) The lower stratigraphic interval of S1 is composed of the lower part of the Friese Front Fm. in the south and the Lower Graben Fm. in the central and northern part of the section. It is easily identified thanks to a well recognizable series of coal beds (2 to 3 beds, shown as grey interval with dashed outlines on the figure), located near the base of the Middle Graben Fm., that can be correlated throughout the DCG from well L02-03 to B18-03. This lower stratigraphic interval has the highest net-to-gross in S1.

It is composed of fluvio-deltaic and coast plain deposits, with locally fluvial channel stacking vertically to form thick (up to 100 m) sandy units (orange units in this figure). The base of S1 is irregular and locally onlaps on paleo-topographic highs that are observed in the F03-F06 blocks as well as the F11 block. This indicate that individual sub-basins were present during this period in the DCG, likely due to differential subsidence that was related to variable deep salt migration amount and locations. The northern sub-basin (F06-F03) subsided the fastest with up to 550 m of S1 strata accommodated, compared to the 290 m in the F11-01 area and 50 m in the F17 area. The highest net sand is found in the F06-F03 area, but the highest net-to-gross is observed is in the F08-02 well, which is located between the two sub-basins and where the sandstone units amalgamation is the greatest.

2) The middle part of Sequence 1 is composed of the upper part of the Friese Front Fm. in the south of the section, and the Middle Graben Fm. in the central and northern parts of the section. This stratigraphic unit is low net-to-gross and presents two particularly interesting events in the form of the basin-wide coal rich unit (dark grey interval with black dashed line in the figure) and an internal erosional surface (S1-UC1, shown as a red line) in the middle of the Middle Graben Fm. Locally some sandy strata are observed in this interval such as in the F03-F06 area, which rapidly pinch out to the south. These deposits may be related to local input from the eastern basin margin. The upper part of this interval also shows some sandstone units deposited in the hanging wall of fault F9 (well F08-01).

3) The upper part of Sequence 1 is composed of the Puzzle Hole, Upper Graben and Kimmeridge Clay formations. The lower part of the Puzzle Hole Fm. in well F11-01 correlates northward to the Upper Graben Fm. at well F08-01 and in the F06-F03 area. The upper part of the Puzzle Hole Fm. correlates northward to the Kimmeridge Clay Fm.. The Puzzle Hole Fm. is composed of various shallow water depositional environments (lower delta plain, lagoonal and tidal). The lower stratigraphic interval of the Puzzle Hole Fm. correlates northward to in the marginal marine, shoreface deposits of the Upper Graben Fm. The upper stratigraphic interval of the Puzzle Hole Fm. correlates northward to the depositionally deeper outer shelf silty claystones of the Kimmeridge Clay Fm.. Note that the internal correlation between well F11-01 and the F06-F03 area is difficult due to the post-depositional erosion of S1 in the F08 area. Also note the higher net-to-gross of the upper part of the Kimmeridge Clay Fm. in the F03-F06 area with 5 to 15 m thick silty and sandy units that pinch out southward. These deposits can also be related to local secondary sediment sources from the DCG lateral margins.

4 - Results: Panel C - Dutch Central Graben - Sequences 2 & 3

TNO innovation for life

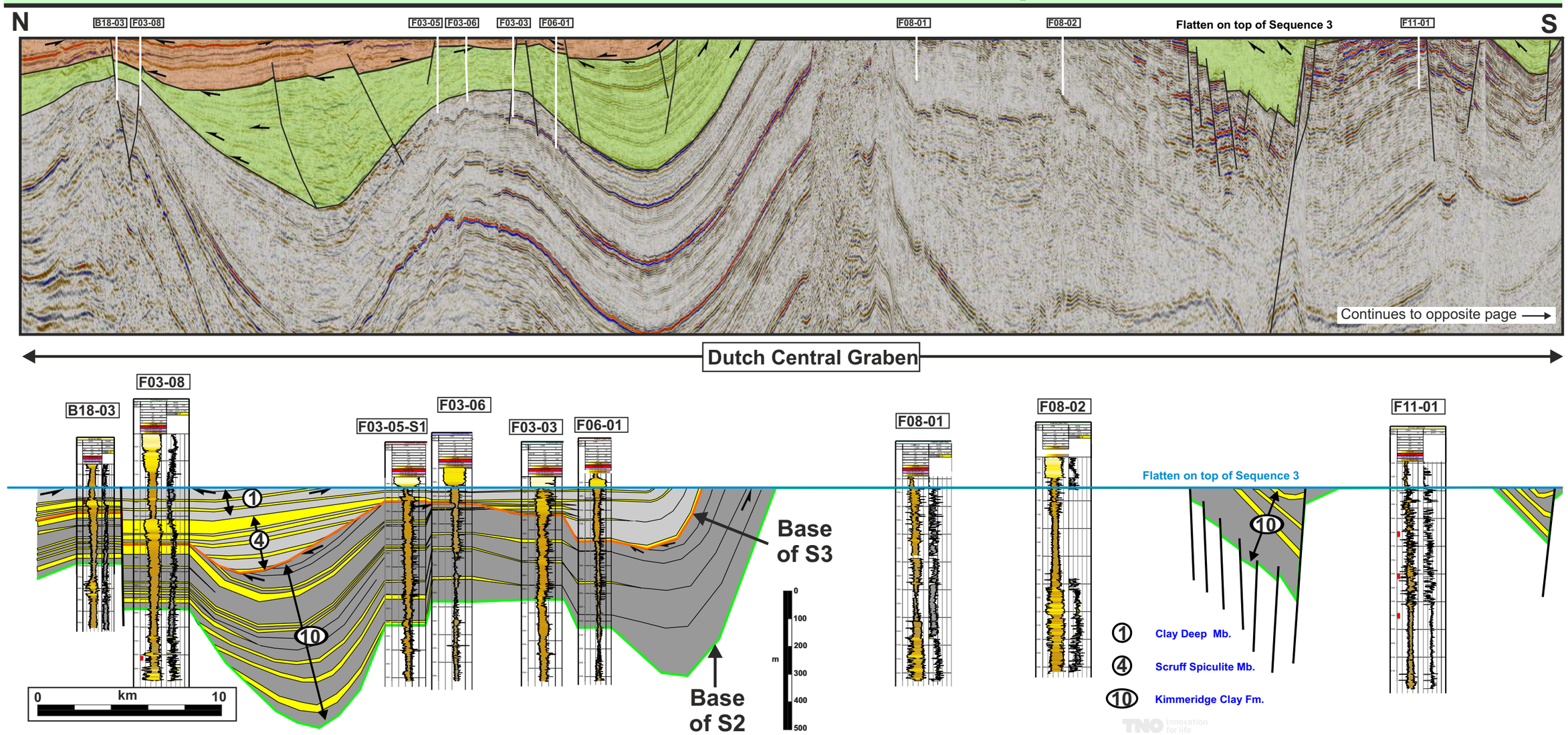

Figure 4.4.6 (Part 1)
This section is located in the axis of the Dutch Central Graben and trends NNW-NNE. See Fig. 4.3.1 for location map and Fig. 4.3.2 for legend.

A) Flattened seismic section showing the Sequence 2 and 3 of the Upper Jurassic
Sequences 2 and 3 are only locally present along this section, with only small preserved areas remaining after post-depositional erosional events, often in the hanging walls of normal faults and in a larger sub-basin in the north of the section (F03-F06 area). In this northern sub-basin, S2 and S3 are deposited in two syn-depositional synclines separated by the F03 paleo-high.

B) Stratigraphic well correlation of Sequences 2 and 3

Sequence 2
S2 is interpreted in thin and discontinuous accumulations from well L02-FA-101 to the northern part of the section. Six small zones and the larger northern sub-basin have S2 strata preserved. The lithostratigraphic units encountered are the Main Friese Front Mb. (L02-FA-101, F17-01), the Oyster Ground Mb. (L02-05), the Terschelling Sandstone Mb.(L02-05) and the Kimmeridge Clay Fm. in the northern part of the section where it is up to 550 m thick. S2 has overall a relatively low net-to-gross, except at the locations of wells L02-03, L02-05 and F17-01, where the Terschelling Sandstone Mb. (or Noordvaarder Mb.?)-type strata are observed.
To the north, the Kimmeridge Clay Fm. is more sandy than for S1 at the same location, and shows southward pinch-outs toward the F06-F03 area. Thicker sands are observed in the upper part of F03-08 and B18-03 wells and are interpreted as Noordvaarder Mb.-type deposits.

Sequence 3
S3 is observed in the southern and northern parts of the section. In the south S3 is relatively thin and only present in small area in the L05, L02 and F17 blocks. In this part of the basin S3 is the thickest in the L02 block with 120 m of Scruff Greensand Fm. To the north of the section, S3 deposited (as for S2) in two syn-depositional synclines and shows a sandier lower section (e.g. F03-08, F03-05-S1 and F03-03 wells). S3 also show in this part of the basin a southward decrease of sand occurrences with pinch outs of individual sandy units observed for example between wells F03-03 and F06-01.

4 - Results: Panel C - Dutch Central Graben - Sequences 2 & 3

TNO innovation for life

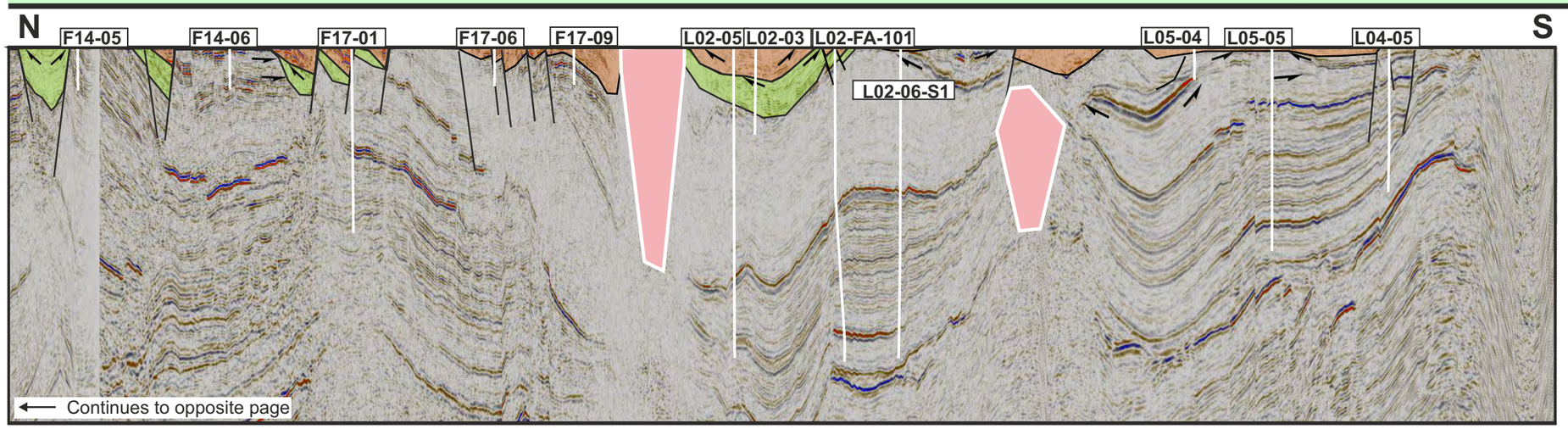

Dutch Central Graben

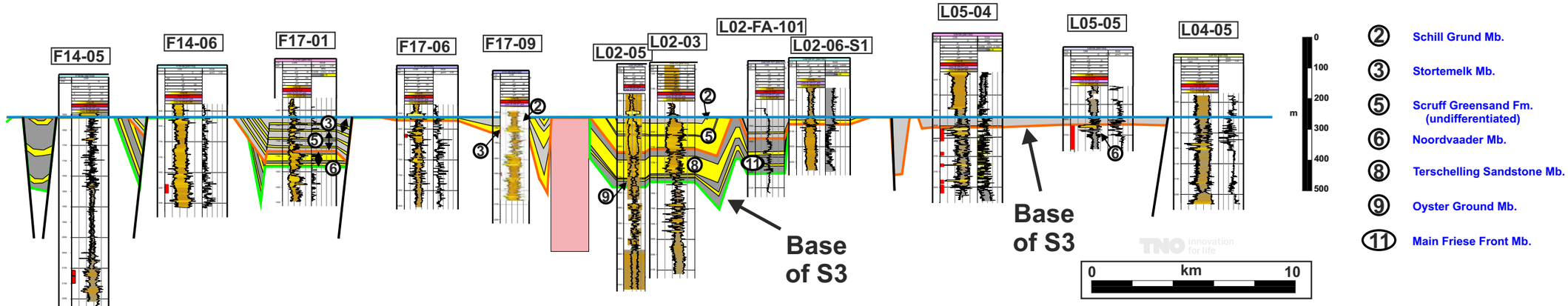

② Schill Grund Mb.
③ Stortemelk Mb.
⑤ Scruff Greensand Fm. (undifferentiated)
⑥ Noordvaader Mb.
⑧ Terschelling Sandstone Mb.
⑨ Oyster Ground Mb.
⑪ Main Friese Front Mb.

4 - Results: Panel D - CBH, DCG, TB and SGH - Sequences 1, 2 & 3

TNO innovation for life

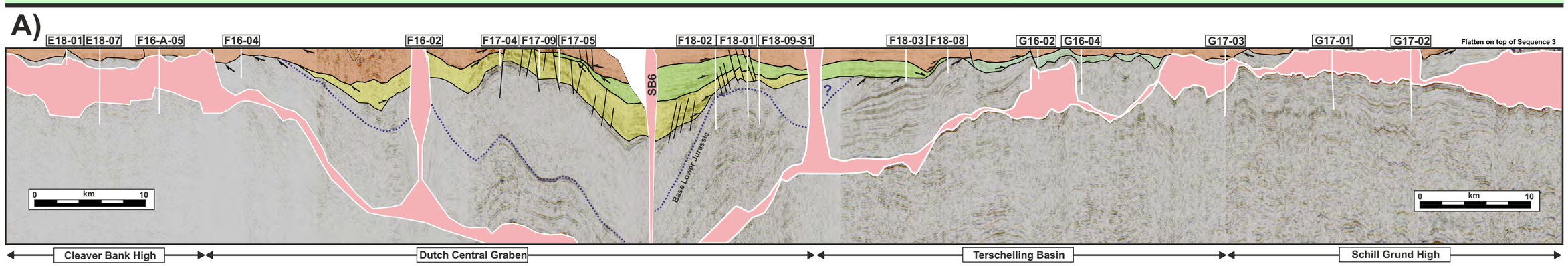

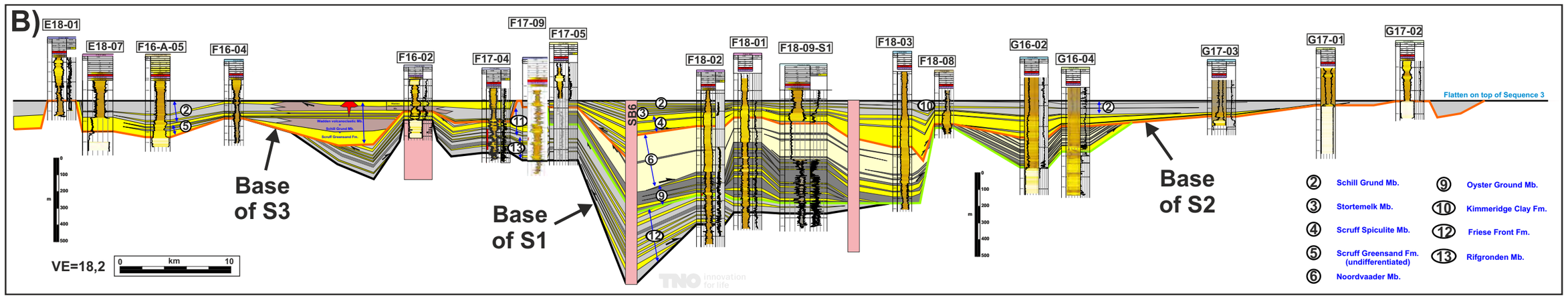

Figure 4.4.7
This section D trends E-W and is located over four structural provinces, the southern part of the Cleaver Bank High, the Dutch Central Graben, the northern side of the Terschelling Basin and the Schill Grund High. See Fig. 4.3.1 for location map and Fig. 4.3.2 for legend.

A) Flattened seismic section showing the Upper Jurassic and Lower Cretaceous intervals
This section is flattened on top of Sequence 3, with Sequence 1 shown in yellow, Sequence 2 in green and Sequence 3 in orange. Sequence 1 is present in most of the DCG while Sequence 2 is observed in the eastern part of the DCG and in the TB. Sequence 3 is present in all four structural provinces.

B) Stratigraphic well correlation of Sequences 1, 2 and 3
Sequence 1
S1 is thickest (430 m) in the middle of the DCG at the location of the salt diapir SB6 between wells F18-02 and F17-05. The sequence thins eastward and pinches out between wells F18-09-S1 and F18-03, and westward between wells F16-02 and F16-04. The stratigraphic interval is mainly composed of deposits from the Friese Front Fm. (including Rifgronden Mb.). The recognizable coal beds are also observed in the Rifgronden Mb. (that correlates northward to the Middle Graben Fm.). The strata are mainly composed of interbedded sandstones, siltstones and claystones deposited in delta plains and lagoons. The upper part of S1 is sandier toward the west (e.g. wells F17-04 and F16-02).

Sequence 2
S2 is thickest (550 m) to the west in the F18-01 and F18-09-S1 area. This sequence thins rapidly westward onto the eastern flank of the F17 turtle structure. The F18 turtle structure inverted earlier than F17 turtle structure, and was a locus of deposition during S2. This sequence is present in the northern part of the Terschelling Basin and onlaps on the Terschelling basin's northern margin east of well G16-04. The lower boundary of S2 is mainly concordant in the DCB but highly erosional in the TB where it truncates Upper Triassic strata and was deposited in confined settings, likely similar to the configuration (incised valleys) seen in panels A and B in the TB. Two different stratigraphic intervals can be distinguished: 1) the lower part of S2 is composed of interbedded sandstone, siltstones and claystones of the upper part of the Friese Front Fm. (which is filling up paleo-topographies) and the Oyster Ground Member. Note that these deposits are locally sandier close to paleo-topographic reliefs (e.g. well F18-03 close to the paleo-high located to the east) the upper part of S2 is composed of siltstone and sandstones of the Noordvaarder Mb. that is exceptionally thick in this part of the basin (up to 300m). The entire S2stratigraphic succession onlaps at high angle on the paleo-topographic high that was present between F18-03 and F18-08.

Sequence 3
S3 is present along most of the section D (except at its extreme NE side). The lower part of S3 is sandy and composed of Scruff Spiculite and Stortemelk Members that onlap at low angle onto the eastern basin margin and have their thickest location at the F18-03 well. The Schill Grund Mb. is a low net-to-gross interval that becomes even more sand poor laterally toward the east (e.g. well G17-03). Note the presence of the Wadden Volcanoclastic Mb. in well F16-02. We interpret a seismically chaotic zone, located to the east of this well, as the position of the volcano(es) (shown as a red polygon) that produced these volcanoclastic sediments (shown as a brown unit). Note that S3 is becoming lower net-to-gross also to the west.

4 - Results: Panel E - SG, DCG, and SGH - Sequences 1, 2 & 3

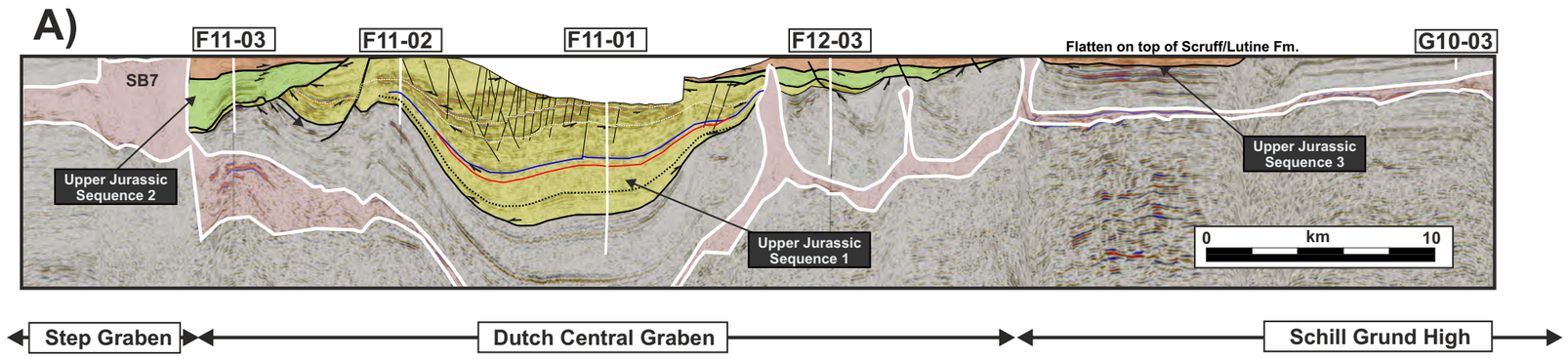

Figure 4.4.8
Section E trends NW-SE and crosses three structural provinces, the southern part of the Step Graben, the Dutch central Graben and the Schill Grund High. Note that the western part of the regional panel is not shown here since little Upper Jurassic is found to the extreme west of the regional Panel (see. Fig. 4.3.8). See Fig. 4.3.1 for location map and Fig. 4.3.2 for legend.

A) Flattened seismic section showing the Upper Jurassic and Lower Cretaceous intervals.
This section is flattened on top of Sequence 3, with Sequence 1 shown in yellow, Sequence 2 in green and Sequence 3 in orange. Sequence 1 is present in the axis of the DCG while Sequences 2 and 3 are only present on the lateral margins as rim-syncline (in the west) or a eastward thinning succession in the east. Note that the extended seismic flattening technique was used to compensate for the post-depositional erosion that occurred between wells F11-03 and F 12-03.

B) Stratigraphic well correlation of Sequences 1, 2 and 3

Sequence 1
This sequence is thick in the axis of the DCG (980 m) and was probably thicker (up to 1300 m) prior to later erosional events. The basin was a relatively narrow (25 km in width) during the deposition of S1 and was rapidly subsiding, as shown by the through shaped geometry of the basin. This trough had a U-shape in the axis and two smaller “plateaux” at the location of well F11-02 and half way between wells F11-01 and F12-03. The eastern and western part of the S1 basin were later eroded (see high angle truncation on the west side and lower angle on the east side) and these zones became later the loci of deposition for Sequences 2 and 3. The lower part of S1 is composed of sandy Lower Graben Fm. strata that onlapped onto the lateral margins of the basin. The Middle Graben Fm. remains low net-to-gross and holds an significant internal unconformity (S1-UC1). The Puzzle Hole Fm. shows dramatic thickness variations in this strike view, and holds several internal unconformities and onlap surfaces. These surfaces are due to the differential subsidence between the axis of the basin and its lateral margins that created rapid rotations and dipping of the lateral margins, with associated erosions and, possibly redeposition into the basin. Note that a thin sheet-like accumulation of S1 is still present at the base of well F11-03, sitting on a thick salt unit, which is interpreted as a Zechstein salt weld.

Sequence 2
This sequence is deposited in two zones on the side of the DCG. In the east S2 is deposited in a lens-shape geometry with evidence of erosion on the top surface. At this location S2 is relatively sandy (possibly Noordvaarder Mb.). On the western side of the DCG S2 is very thick and accumulated within a rim syncline on the side of salt body SB7. At this location S2 is higher N:G in its lower section and fine upward. Internal onlap surfaces are also observed.

Sequence 3
S3 is also only present on the lateral basin margins (wells F11-03 and F12-03). A thin zone of S3 strata is observed to the east, west of well G10-03.

4 - Results: Panel F - Step Graben and DCG - Sequences 1, 2 & 3

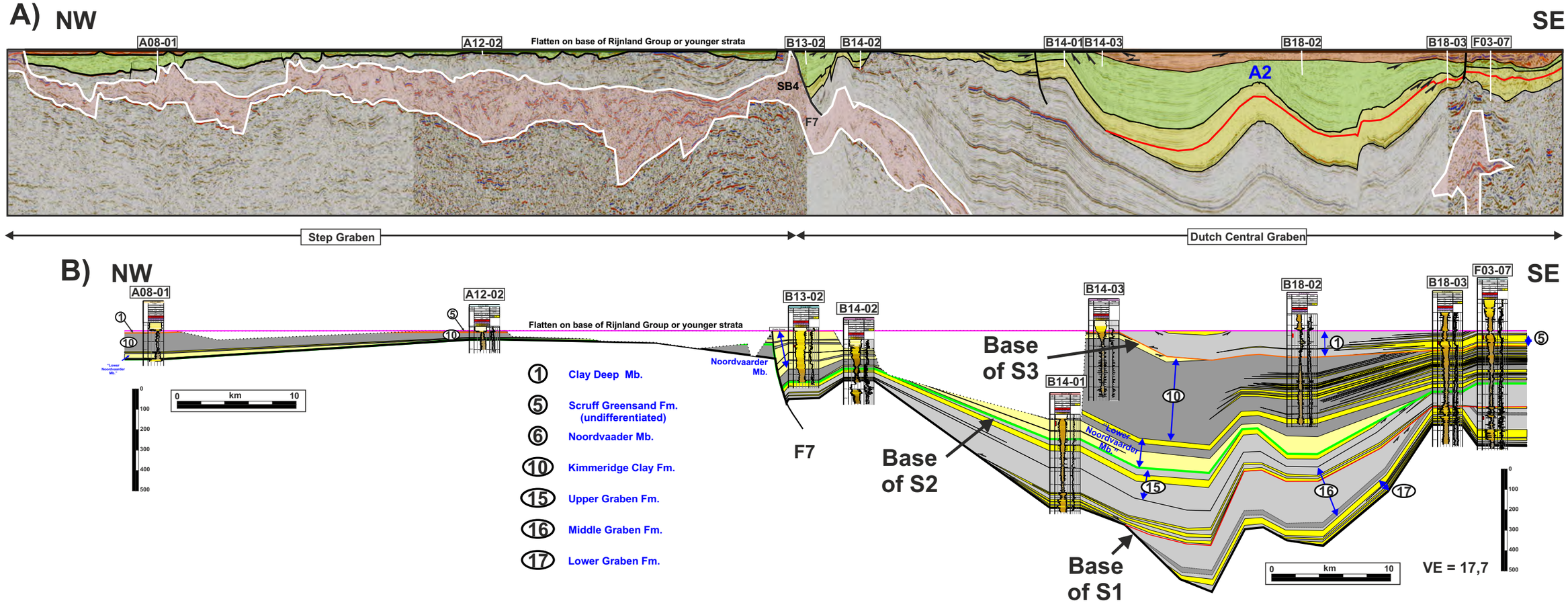

Figure 4.4.9
This section trends NW-SE and is located over two structural provinces, the Step Graben and the Dutch Central Graben. See Fig. 4.3.1 for location map and Fig. 4.3.2 for legend.

A) Flattened seismic section showing the Upper Jurassic and Lower Cretaceous intervals.
The Upper Jurassic and Lower Cretaceous have very different geometry in the SG and DCG provinces with thick accumulations in the DCG and only this remnants on the Step Graben. S1 and S2 are deposited in the DCG in two sun-basins while S3 is deposited as a thin sheet-like succession in the DCG.

B) Stratigraphic well correlation of Sequences 1, 2 and 3
Sequence 1
The lower part of S1 (Lower and Middle Graben Formations) is deposited in a narrow (25 km in width) zone that is eroded to the SE and onlaps on the contemporaneous basin margin to the NW. An significant unconformity is observed at the base of the Upper Graben Fm. that reshaped and widened the basin. The upper part of S1 is composed of Kimmeridge Clay Fm.-type facies that is itself truncated to the south by the base of Sequence 2. Note that the anticline A2 was likely active during the deposition of S1 (as well as S2) as seen by the thickness variation above A2's crest and flanks.

Sequence 2
S2 is present in both the DCG and the SG. In the DCG S2 is composed of Noordvaarder Mb.-type deposits and of Kimmeridge Clay Fm.-type deposits. The Noordvaarder Mb. sandy strata are located at the base of S2 in this part of the DCG, which indicates that these deposits may be part of a younger sandy depositional system than the one seen in the southern-central part of the DCG and in the northern part of TB. Silty and sandy deposits are observed in the Kimmeridge Clay Fm. in the southeastern part of the section in the DCG. These deposits pinch out toward the NW. They could be interpreted as deep water thin-bedded turbidites with sediment gravity flow coming from the SW or the W. Sequence 2 becomes very sandy at the northwestern margin the DCG at the locations of wells B14-02 and B13-02. These Noorvaarder Mb.-type deposits are interpreted here as growth strata on the hanging wall (roll over) side of the growth fault F7 that detached on the salt body SB4. S2 is present on the Step Graben but little sand is observed in these remnant Upper Jurassic accumulations.

Sequence 3
S3 is only present in the DCG as a relatively thin (140m) depositional system that shows a clear lateral facies change between the SE (wells F03-07 and B18-03) and the axis of the DCG (well B18-02), where Scruff Spiculite Mb. laterally transitioning to Clay Deep Mb.

4 - Results: Panel G - SG and DCG - Sequences 1, 2 & 3

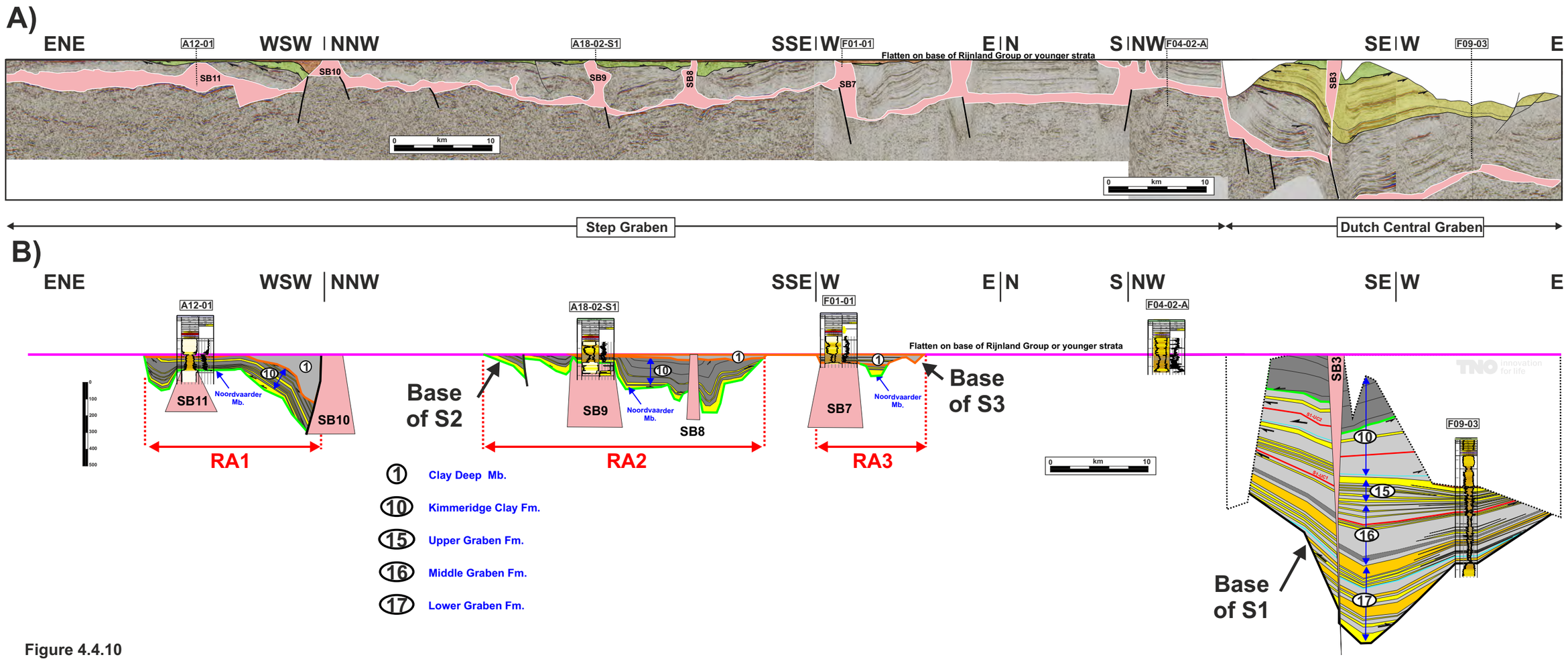

Figure 4.4.10

This section G is located on the Step Graben and the Dutch Central Graben. This section has a C-shape on a map view and changes trends several time from ENE-WSW to NNW-SSE to W-E to N-S to NW-SE and finally W-E across the DCG. This irregular trend was chosen to capture the as many well on the SG that have Upper Jurassic strata. See Fig. 4.3.1 for location map and Fig. 4.3.2 for legend.

A) Flattened seismic section showing the Upper Jurassic and Lower Cretaceous intervals

The Upper Jurassic and Lower Cretaceous have very different geometry in the SG and DCG, with a thick S1 and S2 succession in the DCG and three thinner successions of S2 and S3 on the SG. This seismic section is flattened on the top of S3.

B) Stratigraphic well correlation of Sequences 1, 2 and 3

Sequence 1
Along this section S1 is only present in the DCG. The lower part of S1 (lower 2/3 of Lower Graben Fm.) is onlapping at high angle on both lateral basin margins. The basin then was only 16 km wide but widens upward to more than 30 km by the end of the depositional time of the Lower Graben Fm. The Middle and Upper Graben Formations are also present in this section in the DCG.

Sequence 2
S2 is present in the DCG and in three smaller remnant accumulations (RA1-3)on the SG:
- RA1 is a 17 km wide remnant accumulation of Upper Jurassic (S2 and S3). S2 is 70 to 100 m thick in RA1 and is present in the A12-01 well. To the WSW of this well some S2 basal onlap is observed.
- RA2 is a 29 km wide remnant accumulation. Two salt bodies (SB8 and SB9) are present in this area, which locally affect the S2 stratigraphy, with local onlaps on SB9 and a small rim syncline on the SSE side of SB8. The lower part of S2 shows some onlaps on the lower S2 surface (in similar fashion as S1 and S2 in the Terschelling Basin (interpreted as incised valleys in the TB).
- RA3 is a deep (60 m thick) and narrow (2 km wide) conduit (incised valley?).

Sequence 3
Sequence 3 is only present on the Step Graben in the three remnant accumulations (RA1-3).
- In RA1 Sequence 3 is controlled by a growth fault that detached on the western flank of salt body SB10. This fault was slightly inverted during the Late Cretaceous and lower Cenozoic.
- In RA2 and RA3 S3 is thin (20-50 m thick). A thin zone of S3 strata is observed to the east, west of well G10-03.

DISCUSSION

5.1 Reservoir occurrence & depositional environment LOWER GRABEN FORMATION (F03-05-S1)

In Figure 5.1.1 the integrated results of the core description and palynology of well F03-05-S1 are displayed. The upper part of the Lower Graben Fm. (sea level cycle CAL1 and the lower half CAL2) starts off with marginal marine and freshwater environments, such as brackish lagoon, bay and swamp. This succession is dominated by smooth trilete spores, also pointing to freshwater influence, notably from rivers. The sea level gradually rises and reaches a maximum at the top of CAL2. Concomitant with the sea level rise, the amount of sand also increases. In the sea level cycles CAL3, CAL4 and the upper part of CAL2, tidal environments, such as tidal channels and shoals, are most abundant. Shoreface and open marine conditions are reached in the at the J46 Maximum Flooding Surface and just below the top of the Lower Graben Fm. The J46 MFS is characterized by successive peak abundances of the dinoflagellate cyst groups Evansia/Pareodina and Rigaudella aemula. The tidal environments of CAL3 are characterized by the abundant occurrence of the pollen type Cerebropollenites.

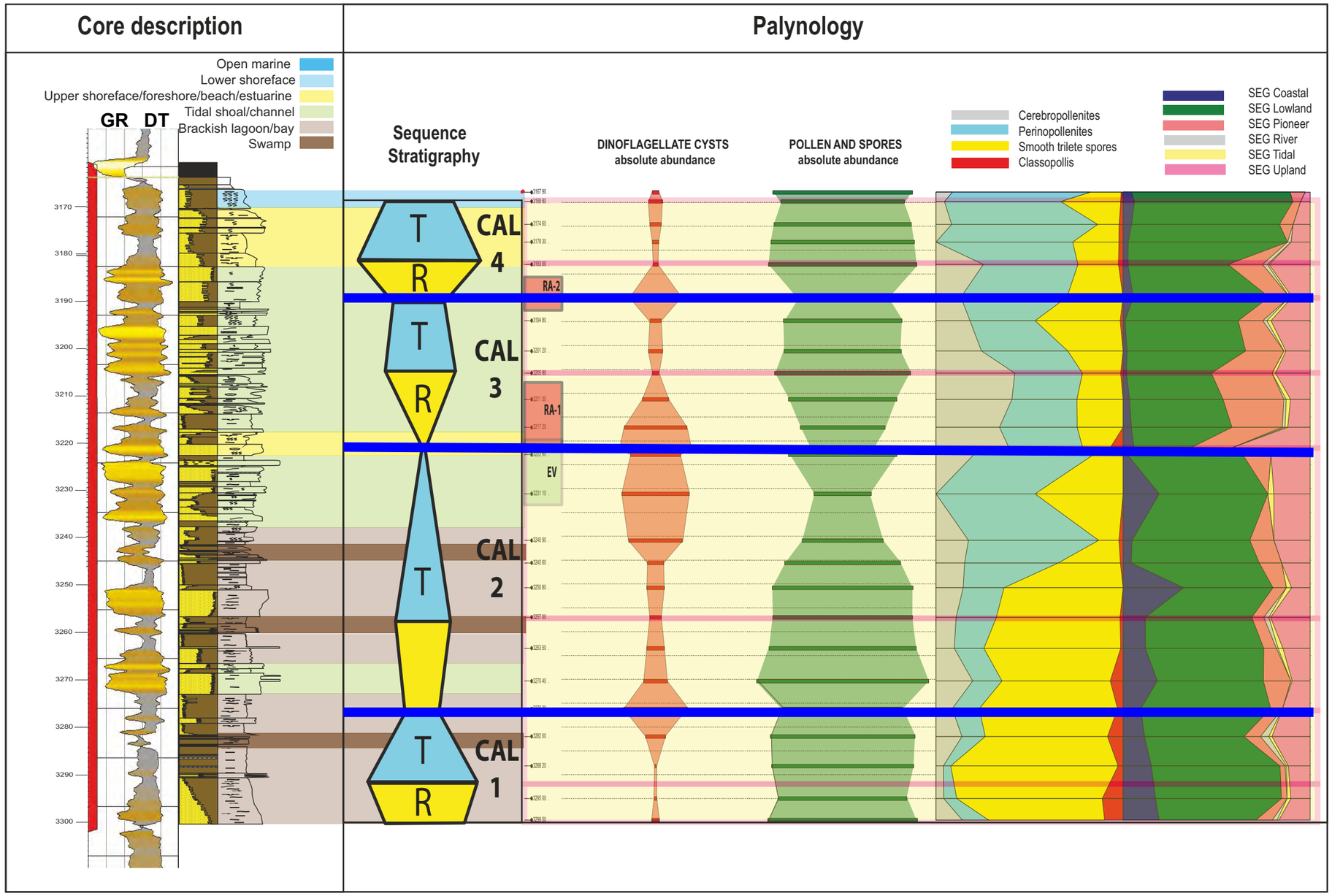

Figure 5.1.1: Core description and palynology of well F03-05-S1

LOWER GRABEN FORMATION (F06-01)

In Figure 5.1.2 the integrated results of the core description and palynology of well F06-01 are displayed. The upper part of the Lower Graben Fm. (sea level cycles CAL2, CAL3 and CAL4) and the very base of the Middle Graben Fm. (sea level cycle Ox1) are represented in the core. The base (upper half CAL2) starts off with brackish lagoon and bay environments. Open marine conditions are then reached at the J46 MFS, coinciding with a maximum in the abundance of dinoflagellate cysts. The sea level cycles CAL3 and CAL4 display a variety of marginal marine environments, such as tidal channels, shoals and lagoons, and reach offshore conditions at the top fo CAL4. Sea level cycles CAL3 and 4 display a high nett-to-gross. This all changes across the Callovian-Oxfordian boundary. At the base of the Middle Graben Fm. a thick coal bed is present, indicating sediment starvation in a swamp environment. Smooth trilete spores are abundant here.

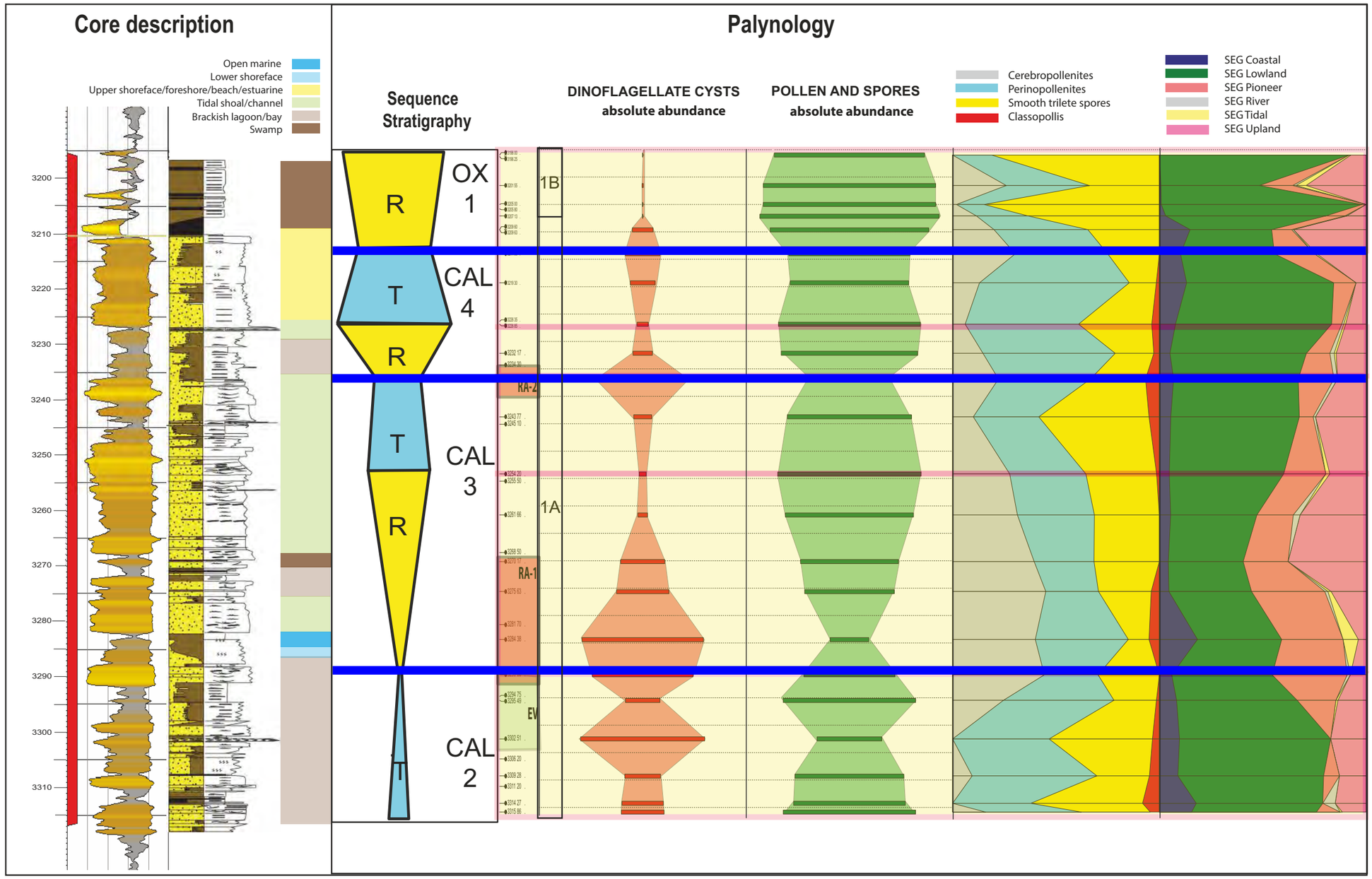

Figure 5.1.2: Core description and palynology of well F06-01

LOWER GRABEN FORMATION

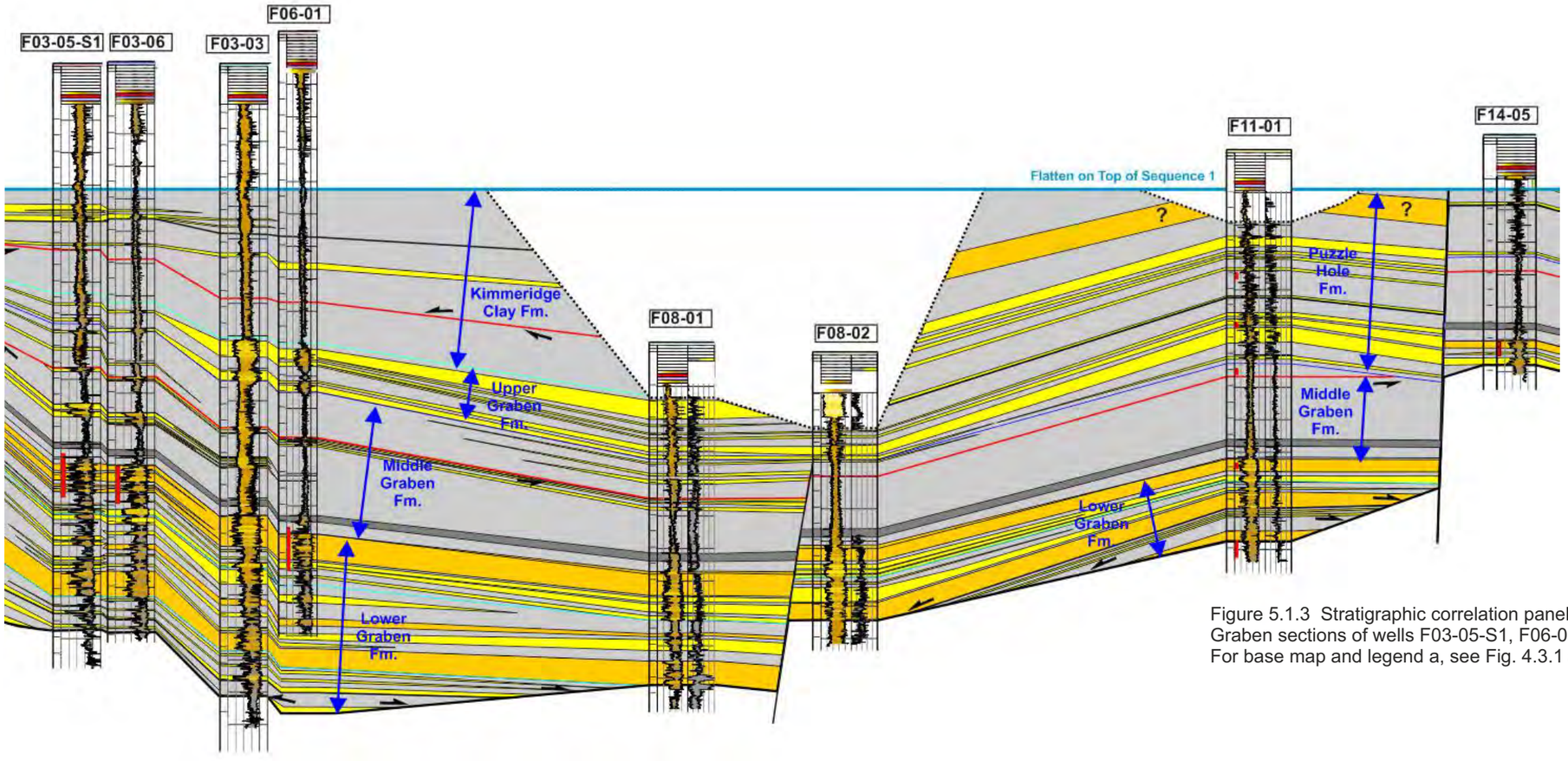

Figure 5.1.3 Stratigraphic correlation panel showing the position of the cored Lower Graben sections of wells F03-05-S1, F06-01 and F14-05 (insert from Fig. 4.4.5). For base map and legend a, see Fig. 4.3.1 and 4.3.2.

Figure 5.1.4 (next page)

The Lower Graben Fm. is characterized by sandstones, shales and intermittent coal layers and may reach 300 m in thickness. The studied cored sections are from the upper part of the Lower Graben Fm. In well F06-01 the transition to the Middle Graben Fm. is included. The depositional environment of the cored intervals ranges from continental (swamp), to transitional (estuarine, lagoon) to marine (shoreface, open marine). The combined palynological and stable isotope results provide an excellent stratigraphic framework for correlation of the three cores. From both the core descriptions and the palynological analyses, a large scale transgression to a distinctly marine interval in the middle of the cores is observed. The large scale transgression is punctuated by smaller scale sea level cycles. The maximum flooding surface associated with the large-scale transgression is referred to as the J46 MFS (Partington et al., 1993a; b), and is correlated to the latest Callovian. The relative sea level rise must have been significant, judged from the transgressive facies onlapping for instance the L05 and F17 areas, and from the open, offshore marine facies in F14-05. In the F03 and F06 areas, the sediment supply, in particular sand, must have been high because offshore, deep marine conditions were never established. Nevertheless, while the relative sea level continued to rise, the transition to the Middle Graben Fm. records a change to freshwater environments. In addition, the thick coal developments in the Middle Graben Fm. reflect a dramatic decrease in clastic supply. This apparent contradiction can be explained by assuming a relatively flat, pizza-like shape of the area surrounding the graben axis at the time of the transgression. The transgressing sea would have pushed back the marginal marine environments, away from the graben axis that then would stay virtually devoid of clastic supply. The very wet climate that characterizes the Callovian-Oxfordian transition, would then render the graben axis area in a freshwater swamp with occasional influence from the nearby sea.

LOWER GRABEN FORMATION

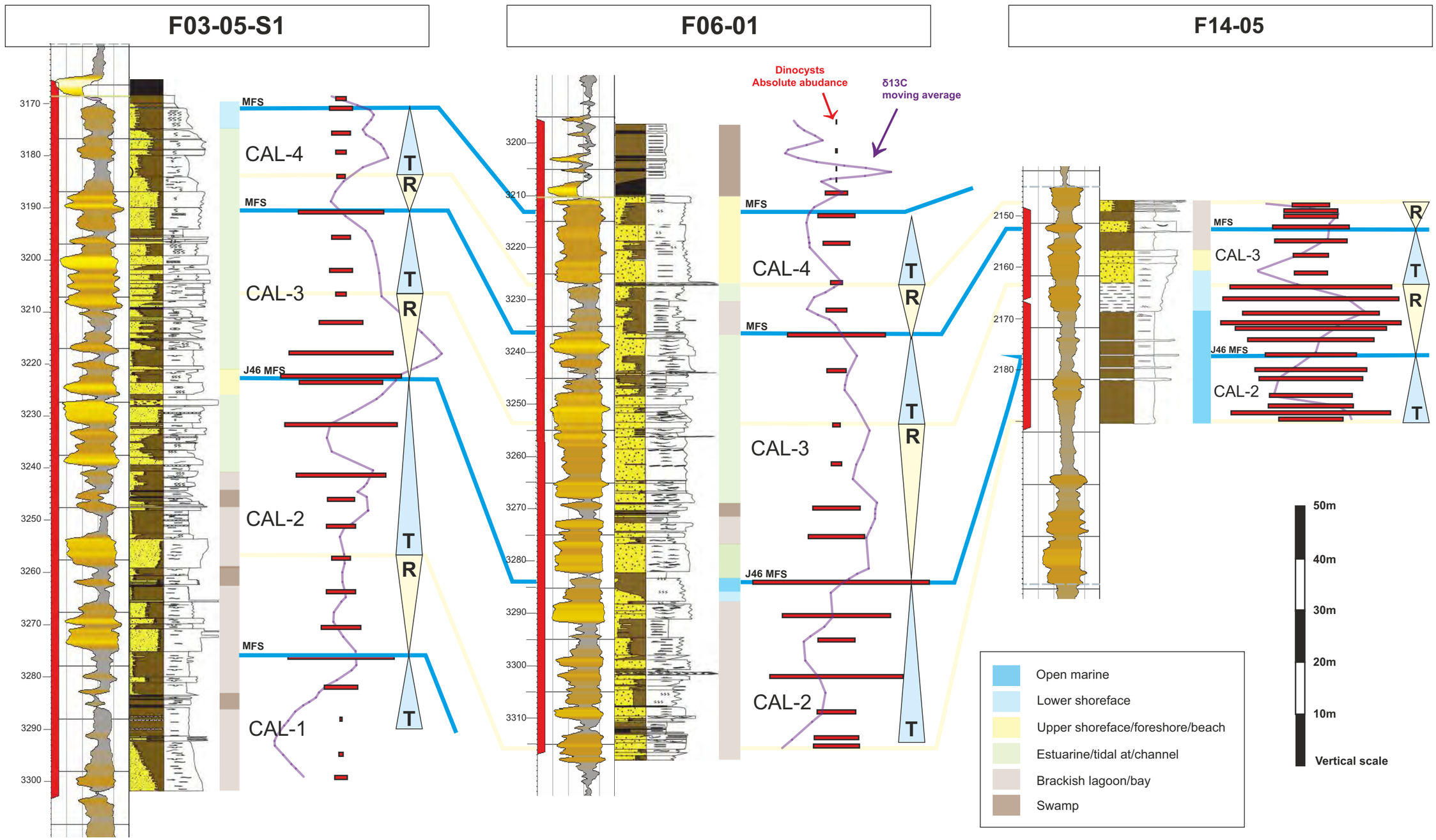

Figure 5.1.4 Correlation panel displaying the integrated core description, palynological and stable isotope results of the cored Lower Graben intervals from wells F03-05-S1, F06-01 and F14-05.

FRIESE FRONT FORMATION

Occurrences of sandstone complexes in the Friese Front Fm. of the Korvet (F17-FA) Field

The correlation panel (Fig. 5.1.7) displays the Upper Jurassic Friese Front Fm. of 5 wells from the Korvet Field. The panel is leveled on the densiplicatum climate shift; a change in climate from relatively cool and wet to slightly warmer and more arid conditions (Abbink, 1998). The shift is recognized in the palynological records of the wells as a change in the composition of the pollen and spore assemblages. In case the data density and quality allows, the zonal assignments to the TNO zonation are displayed next to the lithostratigraphy. The Friese Front Fm. in the Korvet Field consists of multi-storey sandstone complexes, shales and coal layers, in a typically paralic setting.

The succession starts with a marine transgression in the latest Callovian, the so called J46 MFS of Partington *et al.,* (1993). The top of the Friese Front Fm. is an erosional surface; in most wells the Oxfordian Friese Front Fm. is overlain by the Ryazanian Scruff Greensand Fm. In well F17-05, a section of Skylge Fm., probably Early Kimmeridgian, is present, but the biostratigraphic control in the uppermost parts of the Friese Front Fm. is mediocre, at best. Note that well F16-02 is completely dominated by shale, sandstones are virtually absent.

In the other wells, the sandstone complexes are separated by shaly intervals, probably representing relatively high sea levels. Marine influence is present throughout the entire Friese Front interval, but it is strongest in the lower part, below the densiplicatum climate shift. Note, that in well F17-07, the stratigraphic distance between the Friese Front sandstone complex unit B and unit C is relatively small, due to a fault that cuts out a small section. This fault is visible on the seismic cross-section. Note that the green seismic horizon (base of S2) displayed on the seismic cross-section in the upper part of the Friese Front Fm. probably correlates to the sandstone complex unit D. A distinct change in the wireline log patterns occurs at that level.

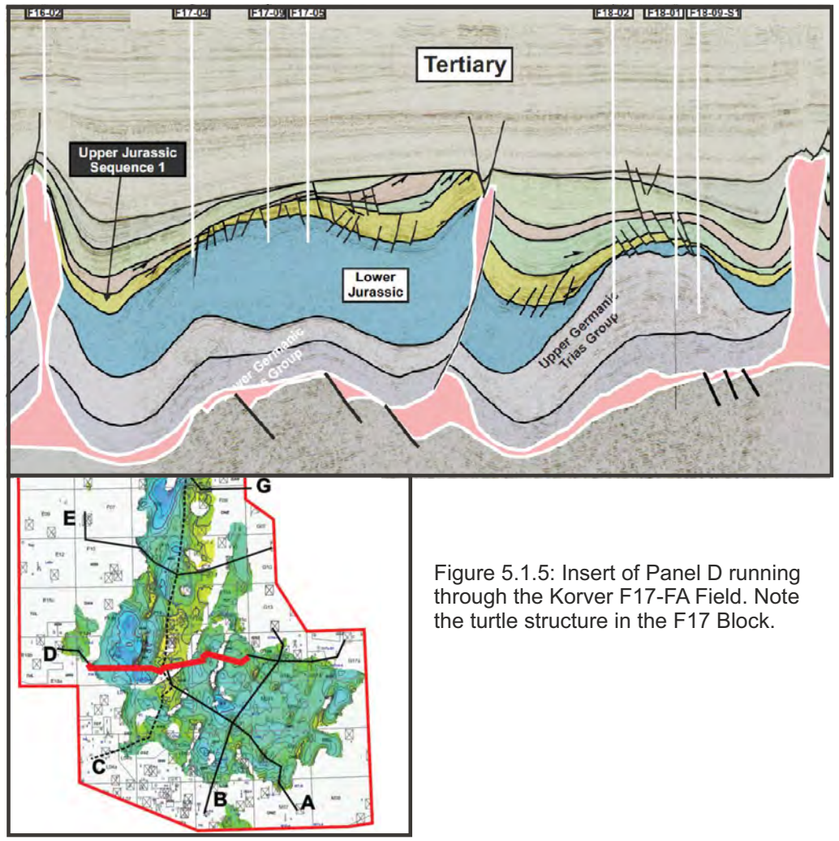

Figure 5.1.5: Insert of Panel D running through the Korver F17-FA Field. Note the turtle structure in the F17 Block.

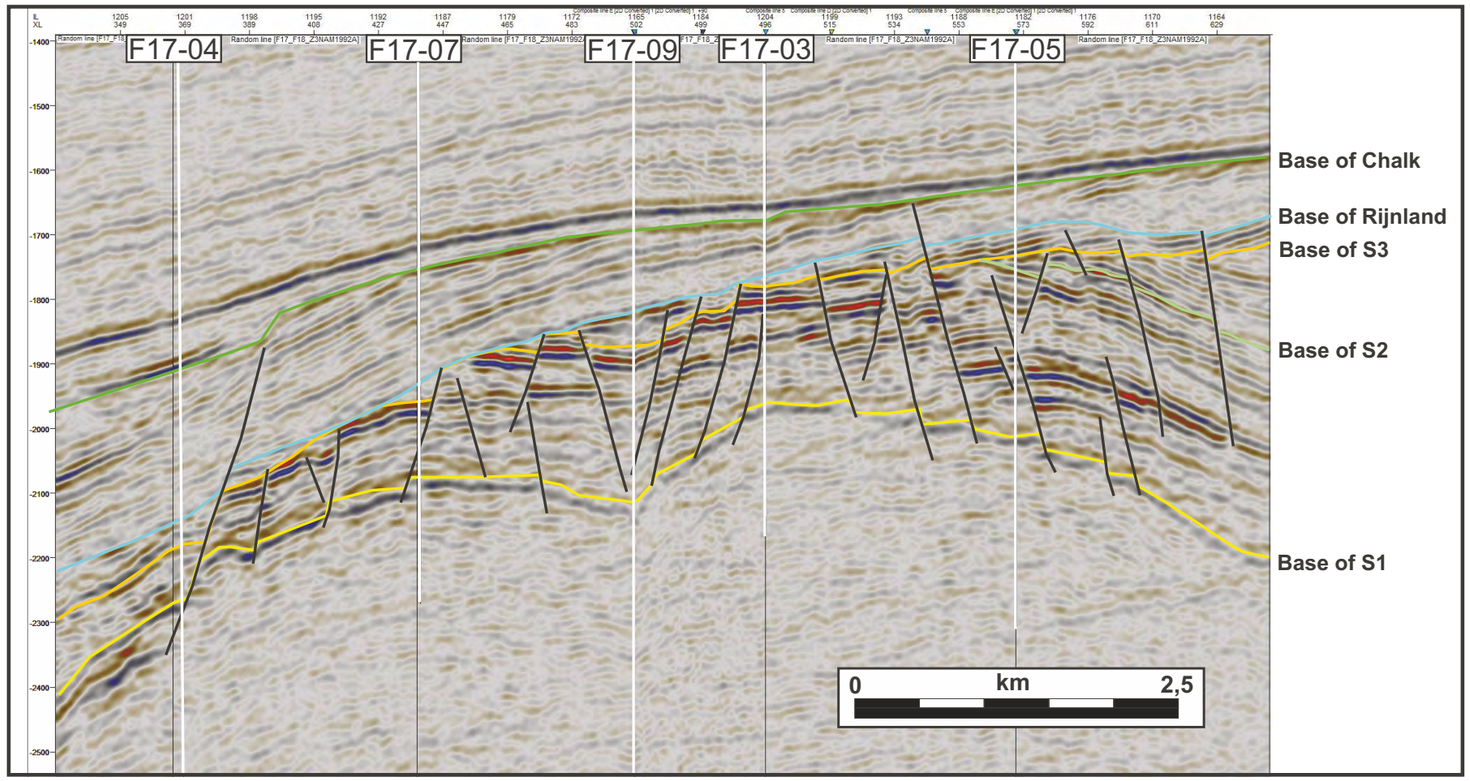

Figure 5.1.6: Seismic cross section through the F17 Korvet Field. The line display wells F17-04, F17-07, F17-09, F17-03 and F17-05 from West to East, in the same order as on Fig. 5.1.7.

FRIESE FRONT FORMATION

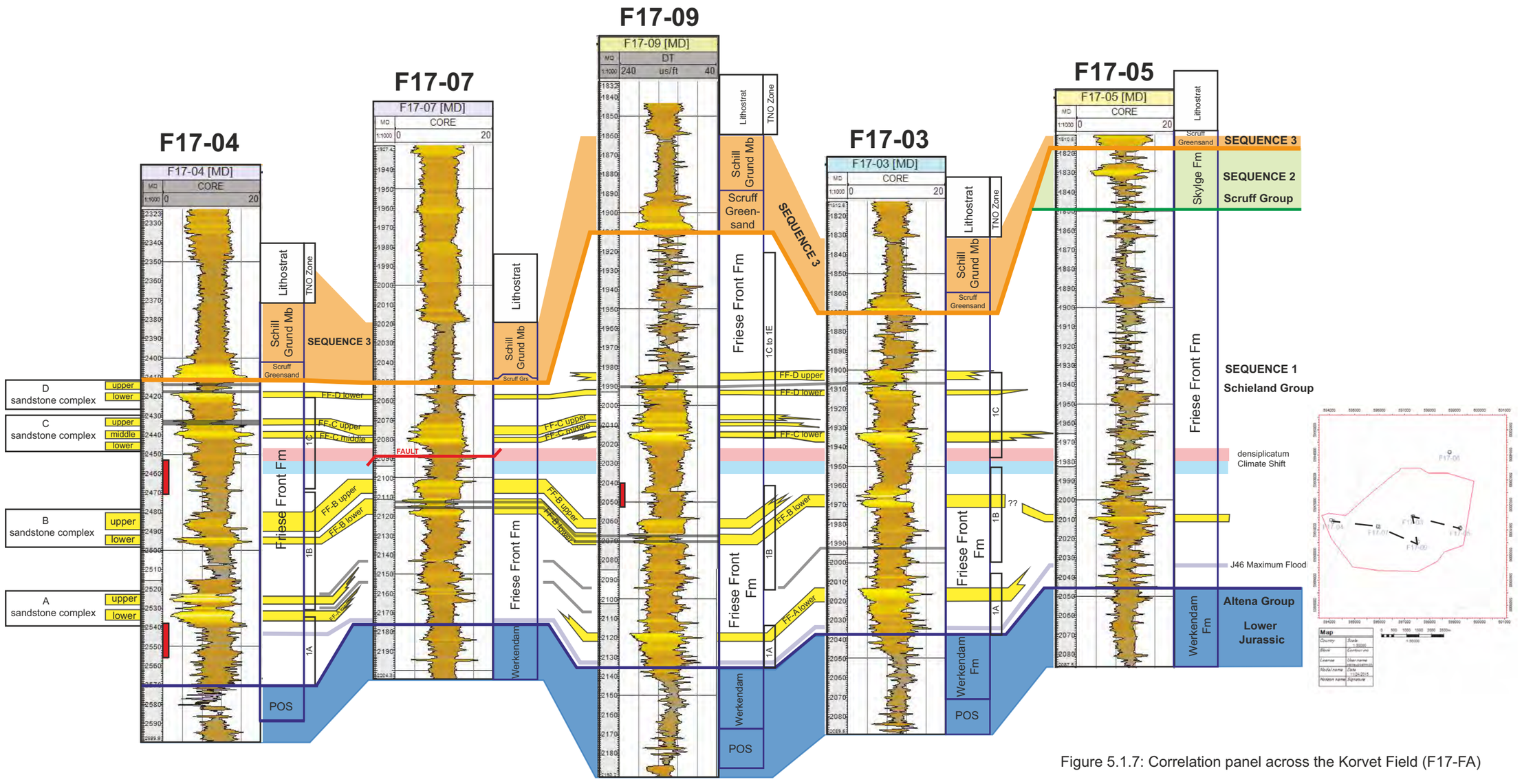

Figure 5.1.7: Correlation panel across the Korvet Field (F17-FA)

Sandstone complex unit A consists of a lower and upper unit, separated by a coal layer and a shale. The lower unit belongs to TNO Subzone 1A and is Late Callovian in age. The upper unit belongs to TNO Subzone 1B and is Early Oxfordian in age. Complex A upper is only present in the westernmost well F17-04. The two units in that well display a coarsening upward pattern, followed by a significant coal layer and thin shale layer. The coals probably reflect the transgressive surface. Note that the two coal layers at the base of Subzone 1B are probably correlative equivalents of the two lowermost coal layers of the Middle Graben Fm. as it occurs for example in wells F03-05-S1, F06-01 and F14-05

Sandstone complex unit B consists of a lower and upper unit, separated by a shale. Both units belong to TNO Subzone 1B and are Early Oxfordian in age. The lower unit is thin, less than 9 m in thickness, but it is quite clean. In addition, it is the only one that occurs in all five wells, although the correlation to the easternmost well F17-05 is tentative. In most wells, particularly in well F17-07 and F17-09, the lower unit of B is associated with two closely spaced coal layers. The upper unit of B is thicker, but not very clean. It displays a coarsening upward base and a fining upward top. Towards the East the lower unit of B shales out.

Sandstone complex Unit C consists of a lower, a middle and an upper unit, separated by thin shales. All units belong to TNO Subzone 1C and are Middle Oxfordian in age. The lower unit is a coarsening upward, very clean sandstone, with a maximum thickness of 5 meters. It only occurs in F17-09 and F17-03. The middle unit of C is a thin sheet sandstone that gradually grades into shale towards the east. The upper unit of C is more heterogenous and is associated with two closely spaced coal layers in well F17-04. The upper unit of C shales out towards the Northeast (F17-03) and East (F17-05).

Sandstone complex unit D consists of a lower and an upper unit, separated by a very thin shale (less than a meter) or by a coal layer. Sandstone complex D is indistinct, the lower unit is only well developed as a clean sandstone in well F17-04, where it displays a coarsening upward trend. The upper unit only occurs in wells F17-09 and F17-03, where it marks the end of the sandstone complexes. Above sandstone complex D, the wireline log patterns change: only shales are present from D to the top of the Friese Front Fm.

NOORDVAARDER MEMBER

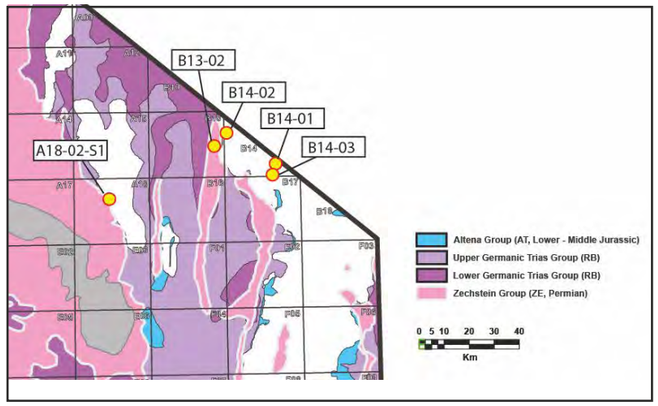

Figure 5.1.9: Base map

The graben axis of the Dutch Central Graben generally runs North-South. In the B13/B14 Blocks, a small graben branches off from the main graben towards the northwest (Fig. 5.1.9). In this NW-SE oriented mini-graben, the Kimmeridge Clay Fm. onlaps on the Lower Graben Fm. (B14-01) or on the Triassic (B14-02). With the increase in tectonic activity during “Sequence 2”, a time when especially NW-SE oriented normal faults become very active, the fine-grained siliciclastics of the Kimmeridge Clay Fm. are gradually replaced by a coarsening upward sandstone sequence of the Noordvaarder Mb. (Fig. 5.1.10). Where exactly these sands are coming from is difficult to establish, but an origin to the West (B13) and/or to the South (B16 and B17) of the mini-graben seems most likely. Well B13-02 displays the thickest Noordvaarder Mb. succession. This well is located near a fault that marks the boundary of a salt structure. The fault must have been very active at the time of deposition of the Noordvaarder Mb., which is a perfect parallel to the Noordvaarder Mb. occurrences in the Terschelling Basin. In the Terschelling Basin the thickest Noordvaarder Mb. occurrences are next to major salt structures in the F15 and F18 quadrants and on the footwall of the Rifgronden Fault Zone.

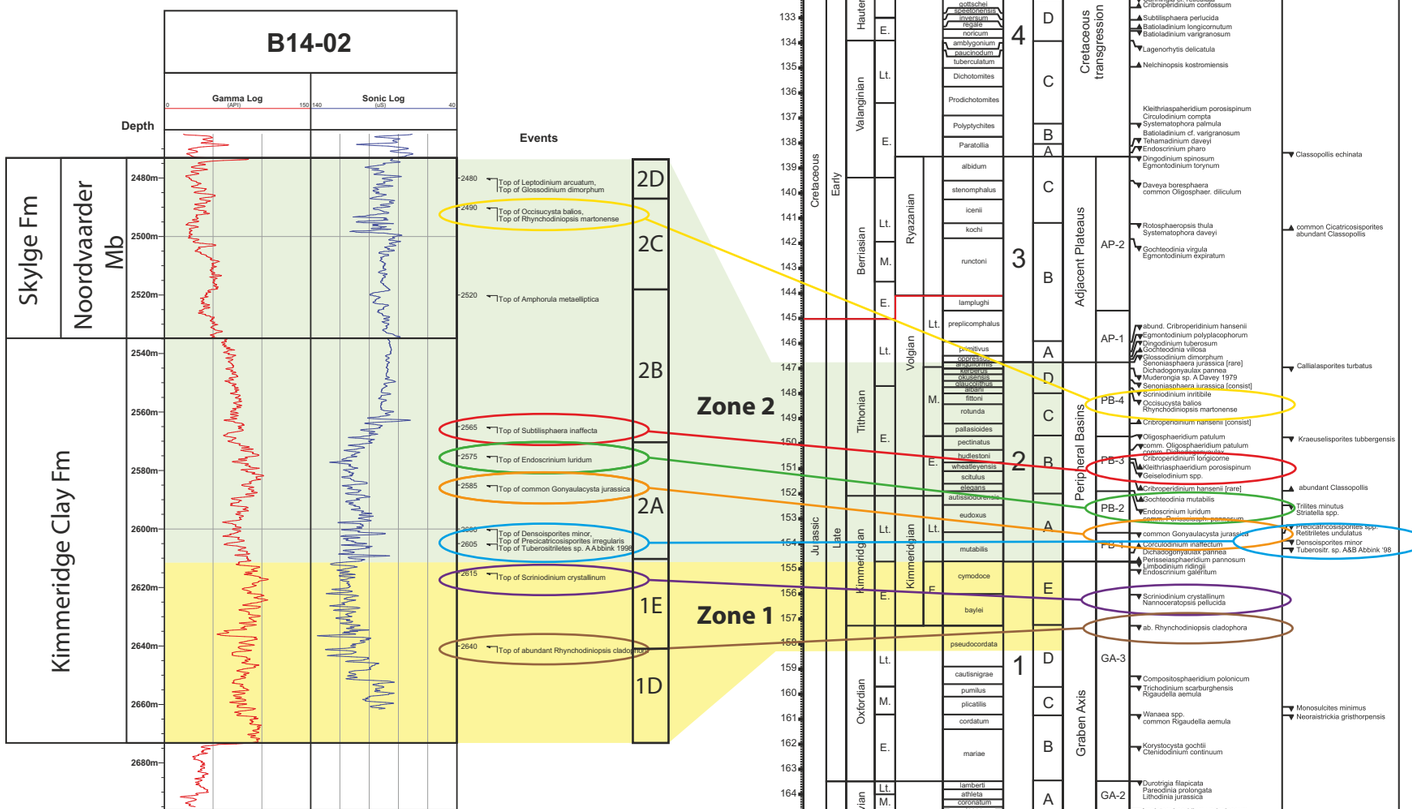

Figure 5.1.10: Chronostratigraphic calibration of the Noordvaarder Mb. of the Skylge Fm. and the Kimmeridge Clay Fm. Palynological events are used for correlation to the global standard of the Geological Time Scale (2012). The TNO Zonation is displayed in A3 format on Fig. 3.4.

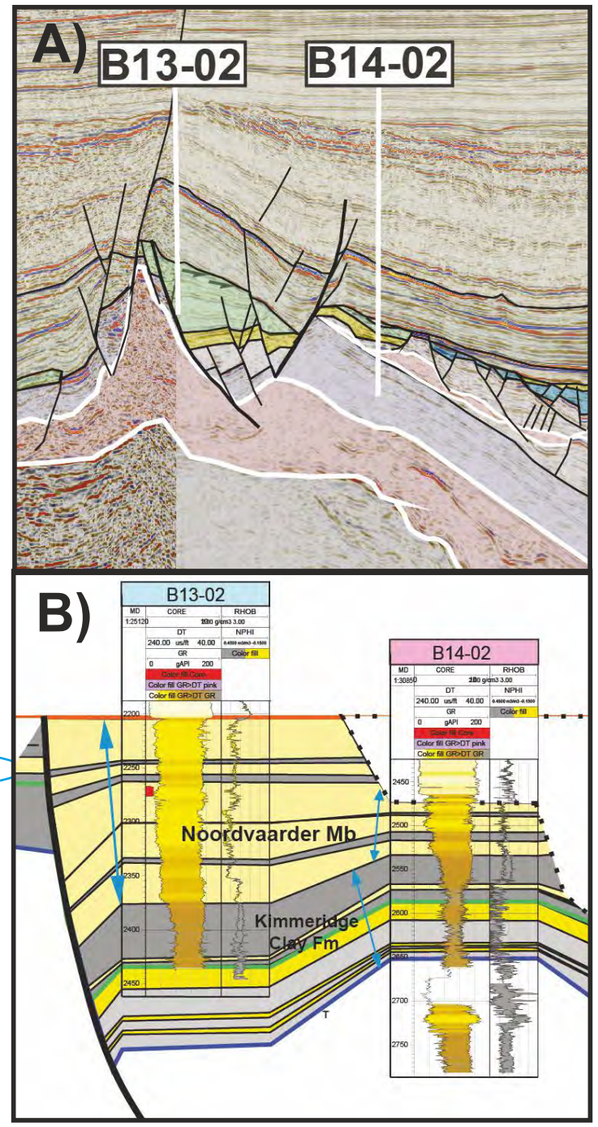

Figure 5.1.11: Seismic and geological cross section through the mini-graben in the B13/B14 area. Note the thick Noordvaarder Mb. occurrences indicating tectonic activity at the time of deposition.

NOORDVAARDER MEMBER

The Noordvaarder Mb. is a glauconitic sandstone and is part of the Late Kimmeridgian to Volgian Skylge Fm. The member is described and defined in the Terschelling Basin (see Munsterman *et al.,* 2012). The unit consists of greenish-grey, slightly argillaceous glauconitic sandstones, sometimes calcite cemented. The sandy sediments reflect the increase in tectonic activity that is associated with "Sequence 2" from the Late Jurassic rift phase in the Dutch Central Graben area (Verreussel et al., in prep.). As such, the Noordvaarder Mb. is the prelude to the imminent erosional phase in the Late Volgian and Early Ryazanian that led to the deposition of the thick sandstone succession of the Scruff Greensand Fm. The Noordvaarder Mb. is widely distributed in the Terschelling Basin, particularly around the crests of salt diapirs and close to the Rifgronden Fault Zone in the northwestern and northern corners of the basin. At the time of the definition of the member, there were no known occurrences of Noordvaarder outside the Terschelling Basin. In the JUSTRAT and FOCUS projects, it became apparent that the same mechanism that caused the shedding of sands in the Terschelling Basin, was also responsible for the now known occurrences of the Noordvaarder Mb. in the Step Graben.

Noordvaarder occurrence in the A18 quadrant

In the A18-02-S1 core, the Noordvaarder Mb. typically contains erosional products from the underlying Zechstein. In that part of the Step Graben, subsidence started in the Volgian (Sequence 2), creating accommodation space that lead to a transgression which eroded the top of the Zechstein diapir. The resulting sediment stack is a marine fining upward breccia and sandstone, followed by a marine shale.

Well A18-02-S1
interval 2064.40m- 064.65m

The lower part of the Noordvaarder Mb. is a breccia. The matrix consists of green, glauconite bearing sand and siltstone. The large, angular clasts consist of limestone, dolomite and shale. Higher up in the core, the breccia is succeeded by a fining-upward grey sandstone. The sandy Noordvaarder Mb. is succeeded by shales of the Lies Mb (Skylge Fm.).
(Photo of the opposite half of the core)

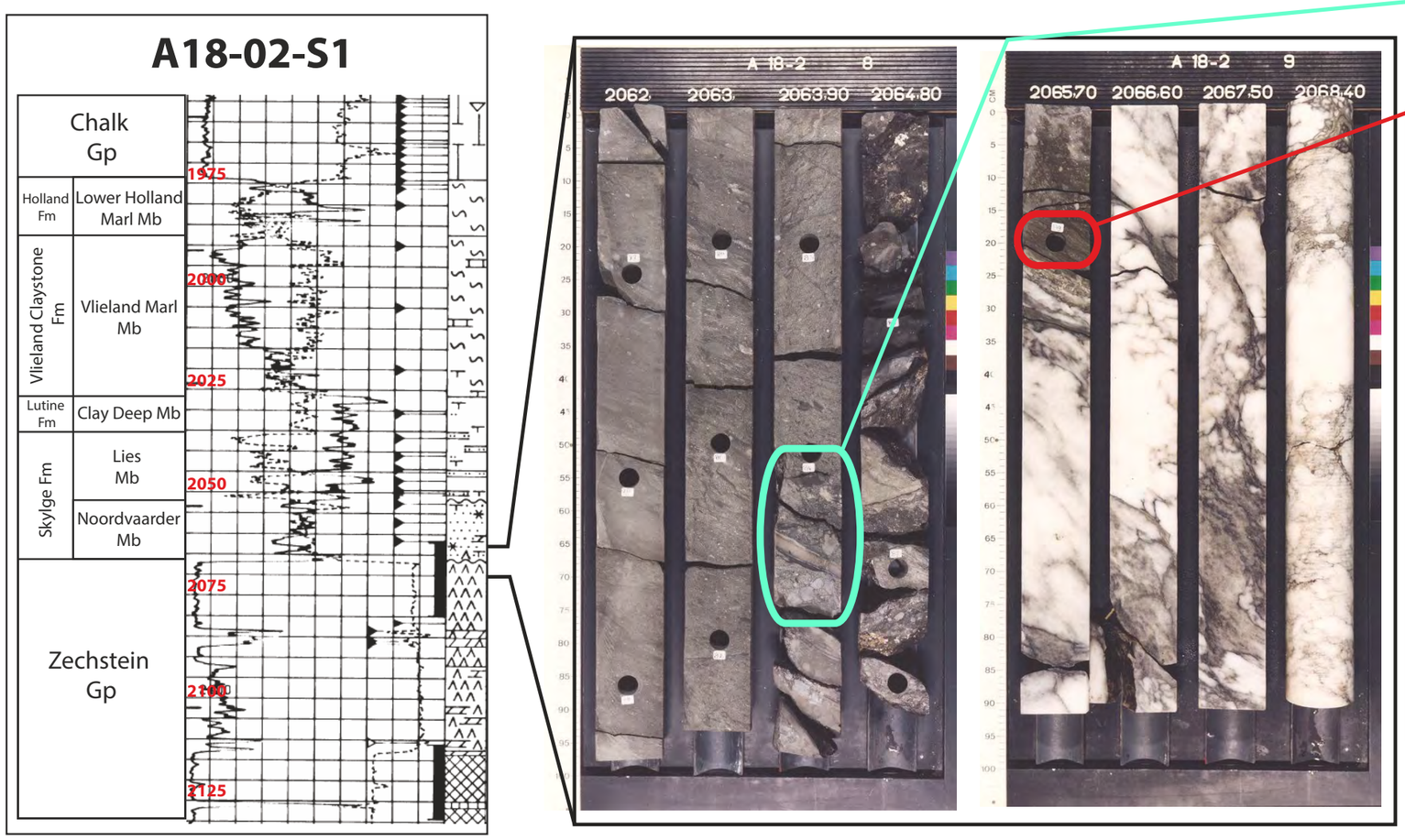

Well A18-02-S1
Sample 2065.9m;
base of the Noordvaarder Mb

The assemblage consists for more than 90% of well-preserved Permian reworking, together with Late Jurassic sporomorphs. Reworked Late Permian constituents are: Lueckisporites virkae, Vittatina spp., Lunatisporites spp. and Jugasporites delasaucei. The in-situ Jurassic assemblage consists of Callialasporites dampieri, Striatella jurassica and Classopollis spp.

Lueckisporites virkae

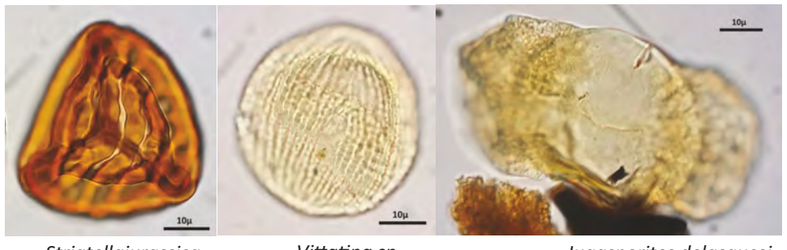

Striatellajurassica *Vittatina sp.* *Jugasporites delasaucei*

Figure 5.1.8: Noordvaarder Mb. occurrence in the A18 Block. Breccia and sandstones of the (lower) Noordvaarder Mb. of the Skylge Fm. lie directly on top of evaporites of the Zechstein Group.

SCRUFF FORMATION (M07-07)

Integrated palynological and core description results of well M07-07 (Fig. 5.1.11):
Core descriptions: The Scruff Greensand Fm. displays a trend of coarsening upward and fining upward. Particularly the interval between 3948m - 3976m is coarse grained. At the top of the core, shales (belonging to the Vlieland Claystone Fm.) are present. Pebble strings are common, indicating that the depositional environment was inclined (a slope).
Palynology: The palynological results are hard to interpret in terms of sequence stratigraphy, the clastic supply was continuously high during deposition of the cored interval. The interval between events A and B is very rich in dinocysts, indicating quite open marine conditions.

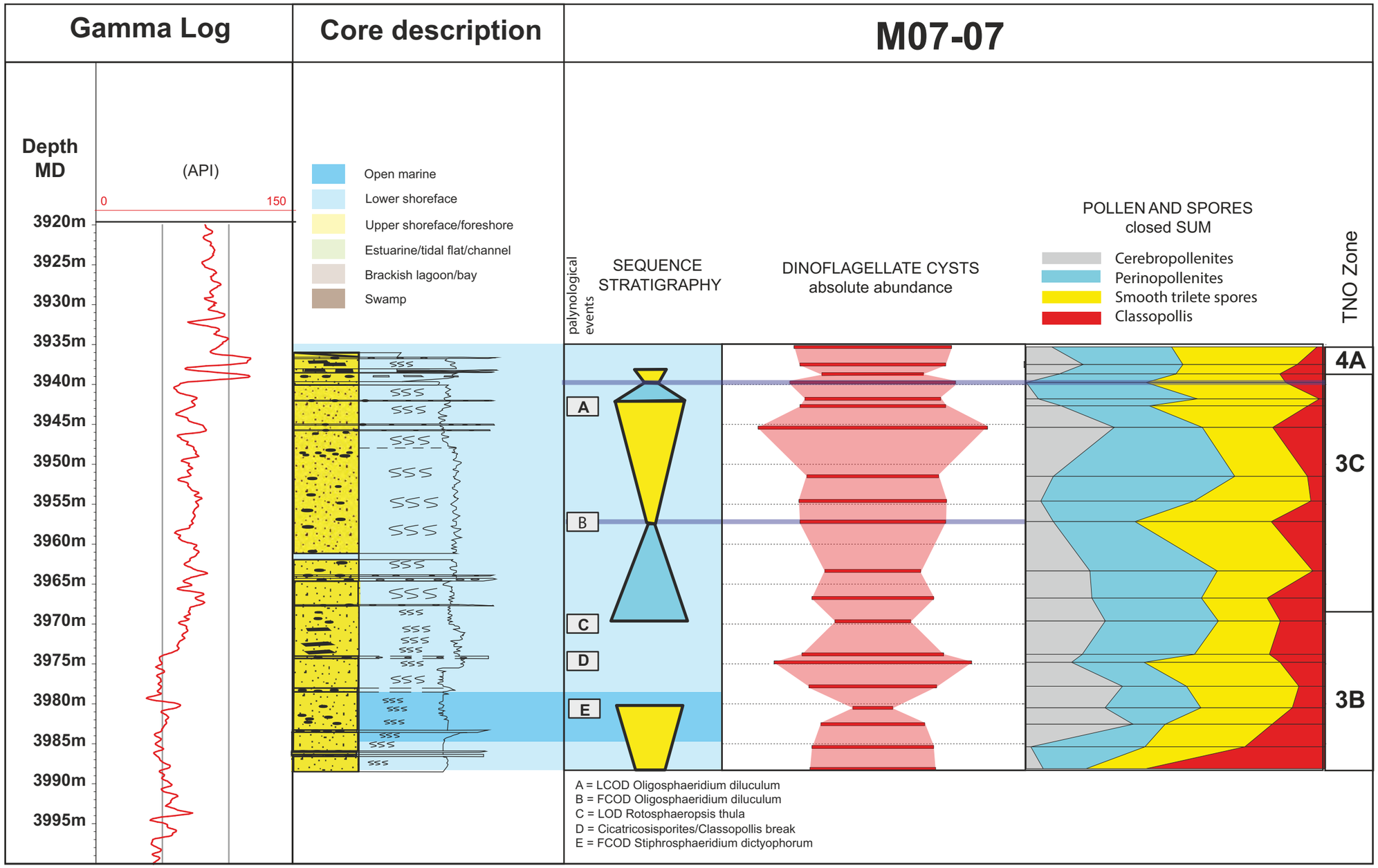

Figure 5.1.12: Core description and palynology of well M07-07

SCRUFF FORMATION (M07-08)

Integrated palynological and core description results of well M07-08 (Fig. 5.1.13):
Core descriptions: The Scruff Greensand Fm. displays a coarsening upward trend. Particularly above 4838m, the grainsize changes from predominantly fine/middle to coarse. Along with the change in grainsize, also the glauconite content increases. A lower shoreface environment is inferred for most of the cored section.

Palynology: The palynological results are hard to interpret in terms of sequence stratigraphy, the clastic supply was continuously high during deposition of the cored interval. The interval between events A and B is very rich in dinocysts, indicating quite open marine conditions. Probably low sea levels are inferred between 4835 and 4850m, where the absolute abundance values of the dinocysts reach an all time low.

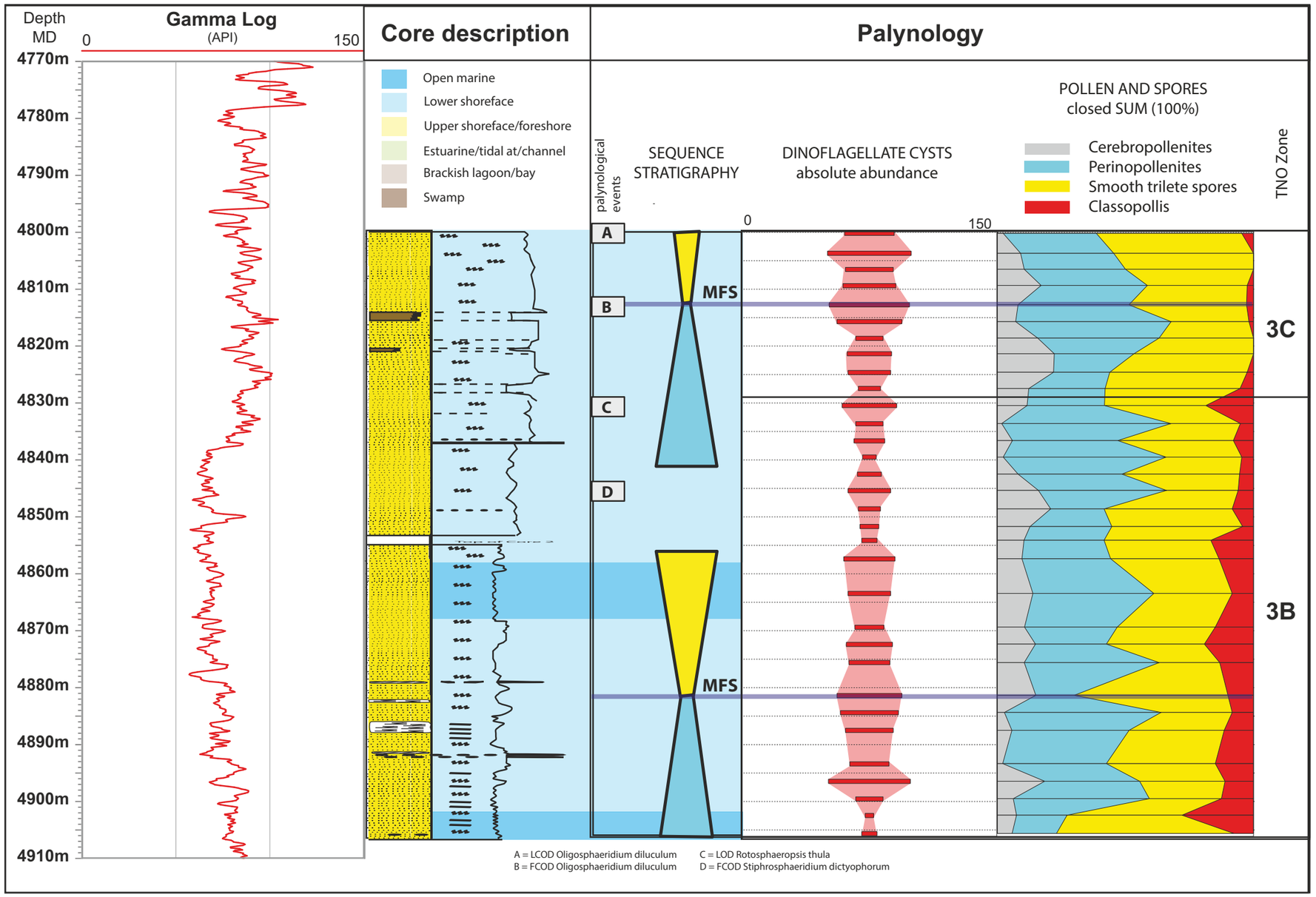

M07-08

Figure 5.1.13: Core description and palynology of well M07-08.

SCRUFF FORMATION

Sequence 3 is regarded as the final stage of the Late Jurassic rift phase and is mainly represented by the Scruff Greensand Fm. (Fig, 5.1.14). In most cases, the base of Sequence 3 is an unconformity, for example on adjacent Plateau areas such as the Schill Grund High, where the Scruff Greensand Fm. constitutes the base of the Upper Jurassic - Early Cretaceous sediment pile. In the Terschelling Basin, the base of Sequence 3 is conformable and marks the base of the Scruff Greensand Fm. The transition from Sequence 2 to 3 is a rapid coarsening upward, reflecting the onset of abundant sand supply. Sand dominated depositional environments persist until the end of Sequence 3 and is interpreted to reflect uplift and erosion in the hinterland. The wireline log patterns of the wells display a repetitive pattern of large-scale fining upward sequences that can be correlated across large distances. These cycles may be induced by tectonic pulses in the hinterland, or merely by eustatic sea level changes. Whatever the reason, the depositional system is clearly aggradational and not progradational. The top of Sequence 3 is represented by fine-grained deposits of the Schill Grund Mb. in the basin center (L06-02, M04-04, M04-03, M04-01), and by relatively coarse-grained sandstones of the Scruff Greensand Fm. at the basin margin (M07-07, M07-08).

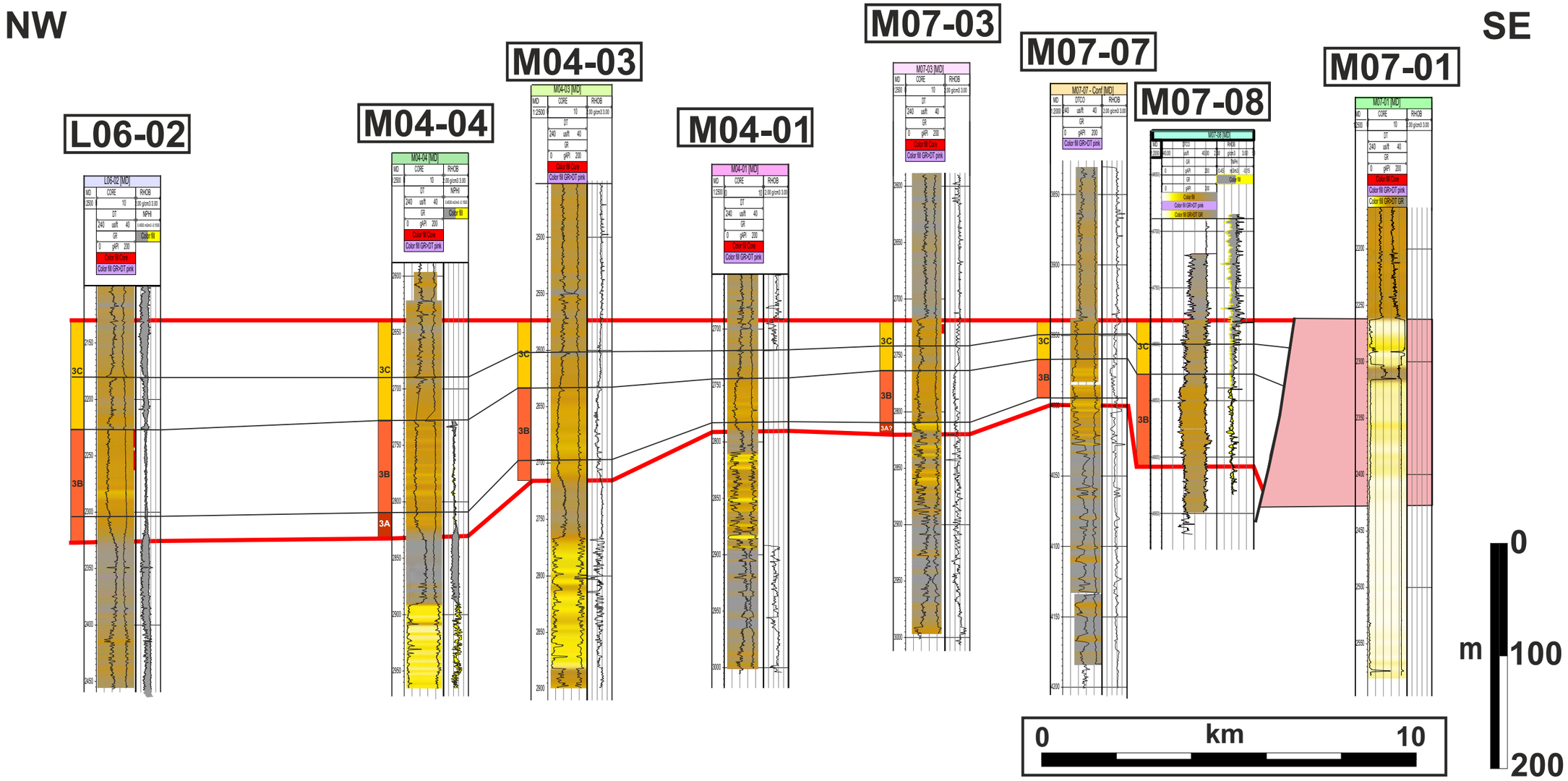

Figure 5.1.14: Correlation panel of the Scruff Greensand Fm. in the Terschelling Basin.
Zones 3B and 3C are identified on six of the seven wells. Note that zone 3A is identified only in well M04-04 and is inferred in wells L06-02, M04-03, M04-01, M07-03 and M07-07, based on the distinctive coarsening upward trend, typical for the base of Sequence 3. The Scruff Greensand Fm. displays a large-scale fining upward trend in the basin center (NW), but a large-scale coarsening upward trend at the basin margin (SE). Note the GR trend is biased by the glauconite content of the sandstone.

5.2 Tectono-Stratigraphy

Understanding the effect of active structures on the depositional record is often important to better constrain the stratigraphy and stratigraphic evolution of sedimentary basins. In the North Sea basins the complex structural evolution has to be well understood to unravel the complex stratigraphy that is highly affected by active structures.

The study area of the Focus project has experienced numerous basin-scale tectonics events, including the Triassic and Jurassic rifting (and its temporal variations in direction of extension), and the Late Cretaceous and Cenozoic Alpine compression associated with complex reactivation and shortening of pre-existing structures. The study area also experienced locally thin-skinned deformation occasionally related to the basin-scale tectonic events. Active faults and salt diapirism often relate to basin-scale adjustments but can also react to local-scale phenomena such as sediment input (an loading), gravity gliding, salt migration, basin margin steepening and differential subsidence over deep structures.

In this chapter we discuss the tectono-stratigraphy of the study area during the Late Jurassic and Early Cretaceous, and in particular the kinematic of salt bodies and syn-depositional faults.

5.2.1 Halokinetics and stratigraphy

The autochthonous Zechstein salt has been actively remobilized since the Late Triassic (and to a minor extent since the Early Triassic) in the study area. Note that salt diapirism during the Triassic is not the focus of the present study but is crucial to understand the structural setting of the basin prior to the Jurassic. This topic is a subject of an upcoming TNO study (STEM, for Salt Tectonics, Early Movements) in 2016. Salt tectonics is often complex and several aspects are discuss below, from the migration and withdrawal of autochthonous (Zechstein) salt, to the relationship between deep structures and shallow salt bodies, and to the specific relationship between shallow salt bodies and Upper Jurassic/Lower Cretaceous stratigraphy.

5.2.1.1 Autochthonous salt withdrawal

During the Late Jurassic and Early Cretaceous, Zechstein salt was actively migrating and withdrawing from its autochthonous level, creating locally high subsidence zone notably in the DCG. Several sub-basins, such as for example in the F17, F18 and F03/06 areas, experienced high accommodation at their axis (axial depocenters) due to salt withdrawal originally from the central part of the graben. With the autochthonous salt welding out, the active subsiding zones moved outward to the sides of the basin or sub-basins, forming stratigraphic wedges and troughs (rim synclines) that formed along the DCG lateral margins, increasing the upward migration of the salt into marginal salt diapirs. This type of structures are turtle structures that are often found in salt basins such as the Gulf of Mexico, the Brazilian margin and the west African margins. This dynamic is an extremely efficient way to create increased accommodation in basins by squeezing autochthonous salt toward the basin's lateral margins and increasing salt migration toward shallower levels in the form of allochthonous salt bodies (including salt stocks and salt sheets).

5.2.1.2 Relationship between deep structures and shallow salt bodies

The interaction between deep structures, such as base Zechstein faults, and shallow salt features is also an important aspect of the basin evolution. Numerous salt bodies are located above large base Zechstein faults. The relationship between salt bodies and adjacent basement structures has been studied by several authors (Vendeville and Jackson, 1992; Foster and Rattey, 1993; Dooley *et al*., 2003, 2005). Foster and Rattey (1993) show North Sea diapirs located above basement faults with stems up to 2 km high. Using physical modeling, Dooley et al. (2005) showed that salt diapirs form and rise in the footwall side of basement faults, due to greater extension in this structural position. At first, salt starts to move on both sides of the basement faults, but later, diapiric growth is related to salt moving exclusively from the footwall side into the diapir. Dooley *et al.* (2005) indicate that these diapirs are typically located at the apex of the extensional faults. Additionally, footwall strata tilt upward and adjacent areas subside due to salt flowing into the growing diapir. If this deformation continues, the structurally thinned sediment cover may be pushed up, so that the surrounding strata tilt. The pre-kinematic and deeper syn-kinematic strata are tilted around the basement-controlled diapirs, due to drag adjacent to the diapir walls and to down-building as the source salt moves towards the growing diapir. Continued extension or subsequent shortening can remobilize the diapir.

Table 5.2.1: Salt terms and definitions. From Bouroullec *et al*,. (in press).

Term	Definition
Autochthonous salt	A salt layer, surface (weld) or body resting in the original stratigraphic position.
Allochthonous salt	A sheet like salt body remobilized upward and emplaced within stratigraphically younger strata.
Expulsion rollover	A tectono-stratigraphic feature that forms over a flat layer of salt. This feature forms by a succession of basinward shifting depocenters that follow basinward spreading salt, giving the overall feature a progradational geometry.
Roho	A salt system that soles onto a shallow salt nappe and has updip extensional and downdip contractional structures. A roho system is characterized by large listric basinward-dipping growth faults that sole into a horizontal flat salt weld and are balanced by reverse faulting in the down dip area (Schuster,1995).
Salt body	General term referring to any individual salt feature. A salt body can autochthonous (e.g. salt roller) or allochthonous (e.g. salt stock). An autochthonous salt body is composed of a salt stem and salt bulb. A salt body can be partially or completely welded out.
Salt canopy	A composite salt structure formed by partial or complete coalescence of salt bodies or salt sheets.
Salt diapir	A mass of salt that has flowed ductiley and appears to have discordantly pierced or intruded the overburden. Alternative definition: A relatively mobile mass of salt that intrudes into preexisting rocks. Salt diapirs commonly intrude vertically through denser rocks because of buoyancy forces associated with the relatively low-density salt.
Salt pillow	A subcircular upwelling of salt that has a concordant overburden (Trusheim, 1960) .
Salt roller	A low-amplitude, asymmetric salt structure composed of two flanks, a gently dipping flank with a conformable stratigraphic contact with the overburden, and a steeply dipping flank with a normal-faulted contact with the overburden (Bally, 1981).
Salt sheet	A subhorizontal salt body that originally forms, by salt expansion at or near the seafloor, from a salt-diapir configuration.
Salt stem (or feeder)	The narrow part of salt body connecting the source salt to the allochthonous salt body.
Salt stock	A mushroom/bubble-shaped salt body that can have various shapes but own a deep feeder underneath connected to the mother salt (autochthonous salt) and a larger salt volume upward.
Salt tongue	A unconformable salt body that intrude obliquely into the overburden at the basinward limit of the salt layer. This term often refers to salt that is overthrusting the distal sediments at the basinward limit of the salt tectonic system.
Salt suture	Limit of precursor salt bodies within the canopy are called suture.
Salt system	The term “salt system” was defined by Jackson et al. (1994) as a system comprising a source salt layer and its overburden and subsalt strata. In the present study, an “allochthonous salt system” is defined as a group of structures that comprises (1) an allochthonous salt body (or genetically linked allochthonous salt bodies), (2) a source salt (autochthonous or deeper allochthonous salt layer), (3) salt-related stratigraphic forms, and (4) genetically-related faults and folds.
Salt wall	An elongate upwelling of diapiric salt that forms in parallel, sinuous rows (Trusheim, 1960).
Salt weld	A thin or narrow salt interval that form when a salt layer becomes very thin due to salt movement, dissolution or removal by faulting, and when the overburden and the underlying sub-salt strata become effectively welded together. Salt welds may also develop in the vertical direction by putting the sides of a former diapir in contact.

5 - Discussion - Tectono-Stratigraphy

Deep allochthonous salt bodies and Jurassic/Lower Cretaceous stratigraphy

Some of the salt bodies located within the Triassic and Lower Jurassic interval influenced the deposition of the Upper Jurassic and Lower Cretaceous. This is the case for salt bodies SB4-6 in Panel A (see Figs 4.3.5 and 5.2.2) around and over which Sequence 1 and 2 strata (Main Friese Front Mb.) are present. These strata were deposited in topographic lows that were created in the vicinity of salt bodies, either by continued upward salt movement (positive relief) in the case of SB6, or due to salt erosion or dissolution that created negative reliefs, in the case of SB5 and SB6.

In some cases the allochthonous salt bodies that were emplaced intra Triassic were remobilized again, locally creating (or suppressing) accommodation during the Late Jurassic. This is the case of one feature located in the northern part of the Terschelling Basin (SB3, located between wells G16-04 and G16-05, Fig. 5.2.2). At this location the thickness of the Upper Jurassic increases within a small syncline that is interpreted as being formed by the withdrawal of allochthonous salt within the SB2 salt body. This interpretation is based on the fact that the base of the Upper Triassic is not folded below the syncline. This structure is an evacuation syncline that was active during the Late Jurassic.

Locally extensive allochthonous salt sheets were emplaced into the Triassic, such as on the western margin (near the B14-02 well) (see Figures 5.2.3 and 5.2.4). At both these locations allochthonous Zechstein salt was emplaced as intrusive, or more likely extrusive, salt sheets (possibly locally formed by the amalgamation of several allochthonous salt bodies into salt canopies) and were later deformed and evacuated due to loading and faulting. The Late Jurassic was affected by these allochthonous salt system since the salt evacuation was mainly occurring during the Early Jurassic and Late Jurassic.

Shallow allochthonous salt bodies and Jurassic/Lower Cretaceous stratigraphy

Twenty three shallow allochthonous salt bodies are emplaced within the Upper Jurassic/Cretaceous or younger intervals. They often greatly impact the depositional style and the stratal thickness (and preservation) of the Upper Jurassic and Lower Cretaceous. Numerous growth stratigraphic wedges and troughs are observed on the sides of upward migrating salt bodies (e.g. around SB7b in Panel A, Fig. 4.4.3; around SB5-7 in Panel D, Fig. 4.4.7; east of SB7 in Panel E, Fig. 4.4.8; around SB3 in Panel G, Fig. 4.4.10). The evolution of these salt bodies often affected the geometry of surrounding stratigraphic units by forcing the rotation and tilt of neighboring stratal blocks that were later often eroded, creating complex progressive unconformities. One of the most extreme examples of complex relationship between salt body growth and Upper Jurassic/Lower Cretaceous stratigraphy is located in the western margin of the DCG in the F11 block (Fig. 4.4.8). In this example S1 is highly eroded at the base of S2 due, likely, to a earlier rotation of S1 stratal block on the flank of SB7, followed by erosion prior to the deposition of S2 and S3 within stratigraphic growth wedge. A more detailed 3D interpretation of this tectono-stratigraphic feature is required to fully understand the dynamic of this part of the DCG. A detailed structural restoration would also be required to capture the complex interplay between basin margin salt deformation and stratal geometry. Note that a thin salt unit is present at the base of the Upper Jurassic in well F11-03, which could be a Triassic in situ salt level (e.g. Triassic Röt Salt) or an allochthonous salt weld, remnant of a larger allochthonous salt sheet that was emplaced during the Late Triassic and later withdrawn, created high accommodation at this location and explaining the over-thickened S2 and S3 in well F11-03.

Figure 5.2.2: Close up seismic view of an evacuation syncline located in the northern part of the Terschelling Basin (also shown in regional panel B). The top of the Lower Triassic is a downlap surface south of the SB2 salt and is interpreted as a salt weld resulting from the evacuation of the salt that was previously there (likely allochthonous salt). The depocenters (yellow arrows) for S2, S3 and the Rijnland Group are located in the evacuation syncline ES1. The structure was also inverted during the Chalk Group (anticline A5).
The upper part of the anticline located above the salt body SB2 is eroded.

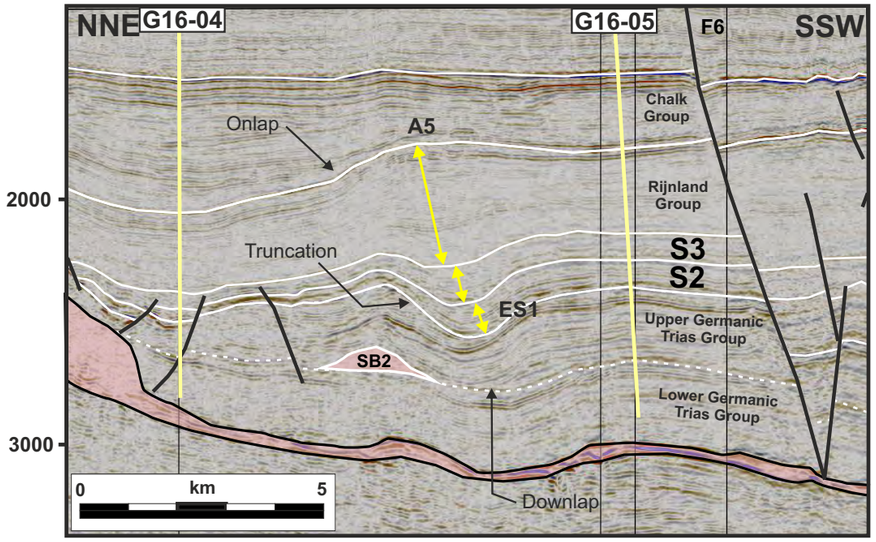

Figure 5.2.3: Close up seismic view of the Dutch Central Graben margin in the B13 and B14. Note the deflated salt body SB3 (dashed red outline) that is interpreted as a allochthonous salt body. This salt body is connected to a large salt system to the south (see Fig. 5.2.4 below)

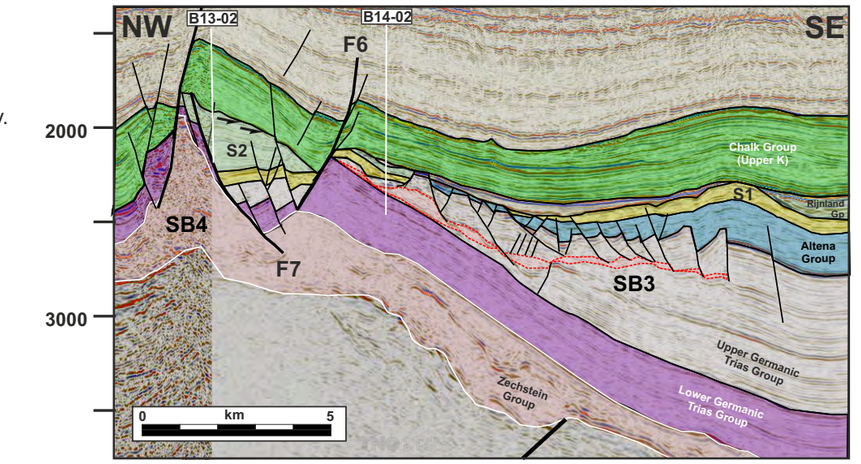

Figure 5.2.4: NS trending interpreted seismic line in the northern part of the Dutch Central Graben (DCG) and the Step Graben (SG). A large allochthonous salt system is interpreted. The allochthonous salt was emplaced during the Late Triassic and later loaded by younger Upper Triassic strata as well as Jurassic strata. Note that the salt present in the B14-02 well (Fig. 5.2.3) extends southward to this large allochthonous salt system (that is 21 km long (NS) and 12 km wide (EW)). From Bouroullec et al, unpublished.

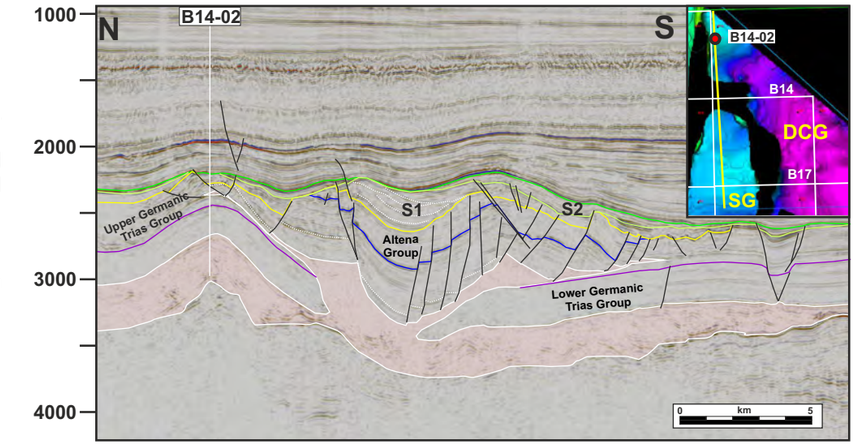

A conceptual kinematic model from Bouroullec *et al.* (in press) illustrates the evolution of a basement-controlled salt body from its original position (Fig. 5.2.1A), as an autochthonous salt layer, to its final position as an allochthonous salt body with a closed stem (Fig. 5.2.1E). Initially, a diapir and shallow graben develop above a basement fault (Fig. 5.2.1A and B); the diapir grows while the autochthonous salt layer starts to weld out (Fig. 5.2.1B and C). Next, the diapir expands at a shallow level while the stem is squeezed due to some shortening (Fig. 5.2.1D). Finally, the deep stratigraphic in Fig. 5.2.1E). This differential subsidence of the overburden was controlled by differential thickness of original autochthonous salt across the basement fault.

Several salt bodies in the study area are located above “basement” faults:
· Panel A: SB2 and SB5
· Panel C: SB1, SB2, SB3, SB4, SB8 and SB10
· Panel E: SB1, SB4, SB6 and SB7
· Panel G: SB2, SB3, SB4, SB5, SB6, SB7 and SB9

5.2.1.3 Relationship between salt bodies and Upper Jurassic/Lower Cretaceous stratigraphy

A total of 63 salt bodies have been interpreted in this study. Even if the scope of this project is not specifically on the salt tectonics of the study area, some valuable observations and some new insights on the relationship between salt tectonics and the stratigraphic record are presented here. Out of those 63 salt bodies, 28 are autochthonous pillows and rollers, 12 are allochthonous salt pillows and sheets within Triassic and Lower Jurassic strata, and 23 are located within Jurassic to Cenozoic interval.

<u>Autochthonous salt and Jurassic/Lower Cretaceous stratigraphy</u>

Some of the autochthonous salt bodies affected the stratigraphy of the Upper Jurassic and Lower Cretaceous, such as the salt pillows located in the southern and northern edges of the Terschelling Basin.

This is the case fo autochthonous salt bodies:

- SB1 in Section A, Fig. 4.4.3;
- SB1 and SB3 in Section B, Fig. 4.4.5;
- SB2-4 in Section D, Fig. 4.4.7;
- SB10 and SB11 in Section G, Fig. 4.4.10.

In many cases, the autochthonous salt bodies formed (often in association with overlying Triassic strata) the physical limits upon which the Upper Jurassic and Lower Cretaceous depositional system are confined (e.g. M7-07 area in the Terschelling Basin). Locally, the Upper Jurassic and Lower Cretaceous strata overstepped these autochthonous salt features and thin stratal drapes were deposited over these salt bodies or over their thin Triassic covers, such as for:

- S3 over salt body SB3 on Panel B (Fig. 4.4.5);
- western and eastern parts of panel D around wells F16-A-05, E18-07, E18-01, G16-02, G16-04, G17-03 and G17-01 (Fig. 4.4.7);
- Panel F at well A18-01; and Panel G at well A12-01(Fig. 4.4.10).

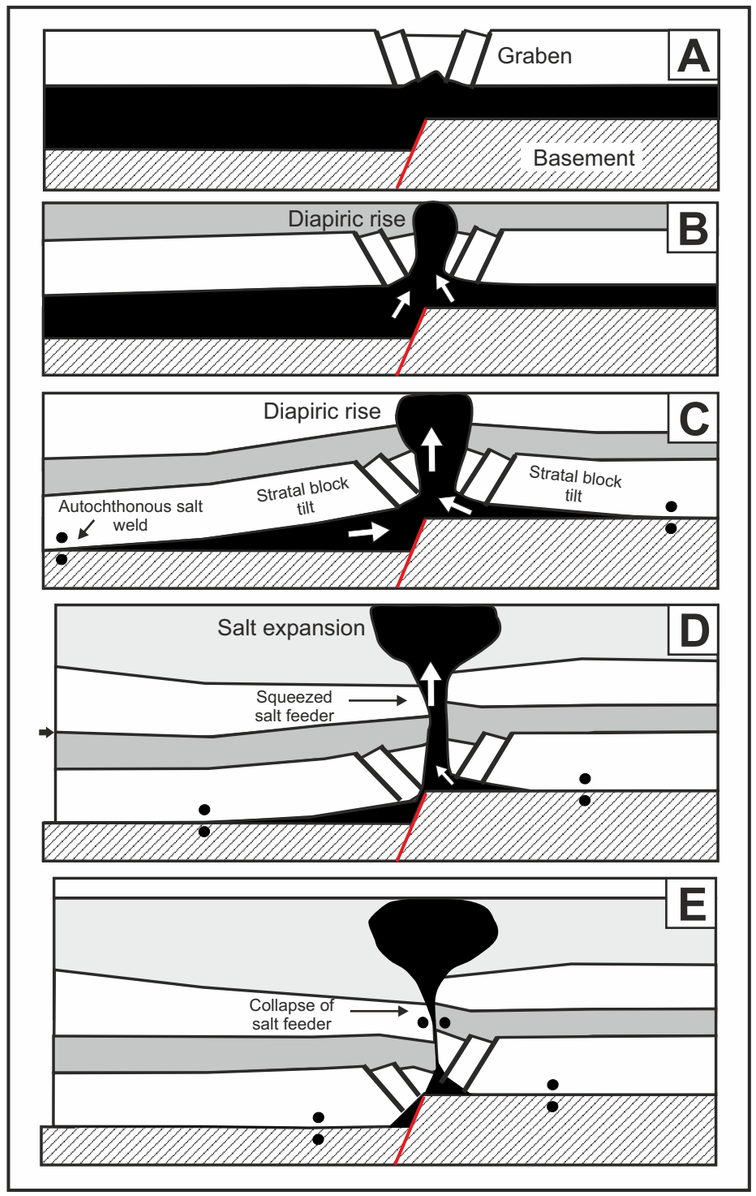

Figure 5.2.1: Evolution of a salt diapir over a basement step. From Bouroullec *et al.,* (in press).

5.2.2 Syn-depositional faulting and Jurassic/Lower Cretaceous stratigraphy

Numerous syn-depositional faults have been interpreted as having been active during the deposition of the Upper Jurassic and Lower Cretaceous in the study area. These faults varies in size and geometry and detached in various intervals, including on the autochthonous Zechstein, over or along allochthonous salt bodies, at the top or within the Upper Triassic and within the Lower Jurassic. These faults locally are listric growth faults that thicken significantly the Upper Jurassic/Lower Cretaceous, forming large roll over structure in the hanging wall sides of the faults.

Several listric growth faults are observed in the TB, SG and DCG.
The listric growth faults observed in the Terschelling Basin, such as the large fault F4 that is located in the axis of the TB, detached intra Triassic (Fig. 4.3.5). This fault was active during the Late Jurassic (S1, S2 and S3), during the Cretaceous and remained active until the Cenozoic. Several other growth faults are observed in the southern part of the TB, such as faults F8-F12 that greatly over thickens S2 and S3. It is difficult to estimate the lithology of the over thickened strata in the hanging walls of those faults however, it is common to find increased net sand in the hanging walls of growth faults such as in the Niger Delta (Bouroullec, 2002), the Gulf Coast in Texas (Bouroullec, 2002) or the Triassic of Svalbard (Edwards, 1978), and even in the study area, such as with the Triassic Solling Fat Sand (De Jager, 2012).

Another growth fault (F1) is located in the southern part of the TB, south of the M07-07 and M07-08 wells (Fig. 5.2.5). This fault has a complex history since it behaved: 1) as a normal growth fault during the Late Jurassic and Early Cretaceous, as shown by the stratigraphic wedge of S2 and S3 in its hanging wall side, 2) then potentially acted as a reverse fault during the deposition of the Rijnland Group, as shown by the thinner stratigraphy on the hanging wall side, 3) the again as a normal fault during the Late Cretaceous, as shown by the over thickened Chalk Group on the hanging wall side, 4) and finally as a reverse fault during the early Cenozoic, as shown by the uplifted top Chalk surface on the hanging wall side. This fault was likely also involved in wrench tectonics that affect the Hantum Fault Zone. Such complex tectonic history can create very good combined traps (stratigraphic/ structural traps) bringing over thickened and, likely sand rich strata, upward into a 3D or 4D closure. Other similar features have been observed in the TB and will be studied in a new TNO project in 2016 (TNO ComMa Project, standing for Complex Margin). Another similar growth fault (F18 or 19) that was subject to a later inversion is observed in the SG to the WSW of well 18-01. F18-19 was active during the deposition of S3 (possibly S2) and was later inverted, creating an interesting combined trap that is still undrilled.

The largest growth faults are observed in the DCG. Faults F5, F8-10 (Fig. 4.3.6) were active during the Early Jurassic and Early Cretaceous but the post depositional erosion of their footwall often doesn't allow to clearly establish the total kinematics of those extensional faults. However, some evidence of over thickening of the hanging wall strata can be observed, such as between wells F08-02 and F08-01 (Fig. 4.3.6) where the Lower and Middle Graben Formation's interval is 230 m thicker on the hanging wall side of fault F9 (more than 40 percent of stratigraphic thickening). Other noticeable listric growth faults in the DCG are faults F12 (and associates) located in the south of the F17 turtle structure (Fig. 4.3.6) that was active during the deposition of S1, and fault F7 (Fig. 5.2.3) located in the B13 block, that detached on an autochthonous salt body (SB4) and was active during the deposition of S2. In the latter example, the hanging wall side of fault F7 is clearly sandier with up to 160 m meters of Noordvaarder Mb. sandy strata observed in the hanging wall at well B13-02.

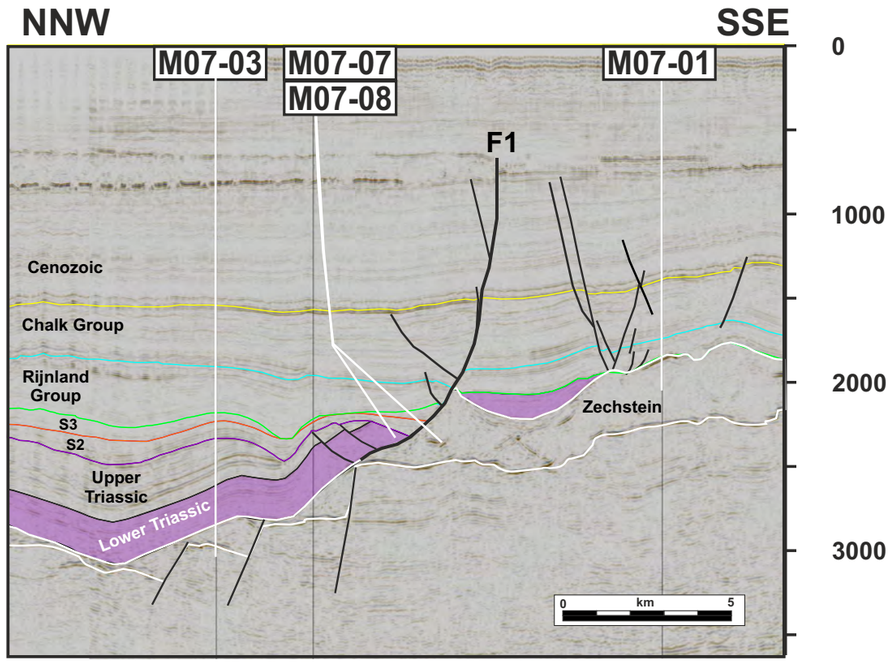

Figure 5.2.5: Interpreted seismic line in the southern part of the Terschelling Basin showing syn-depositional fault F1.

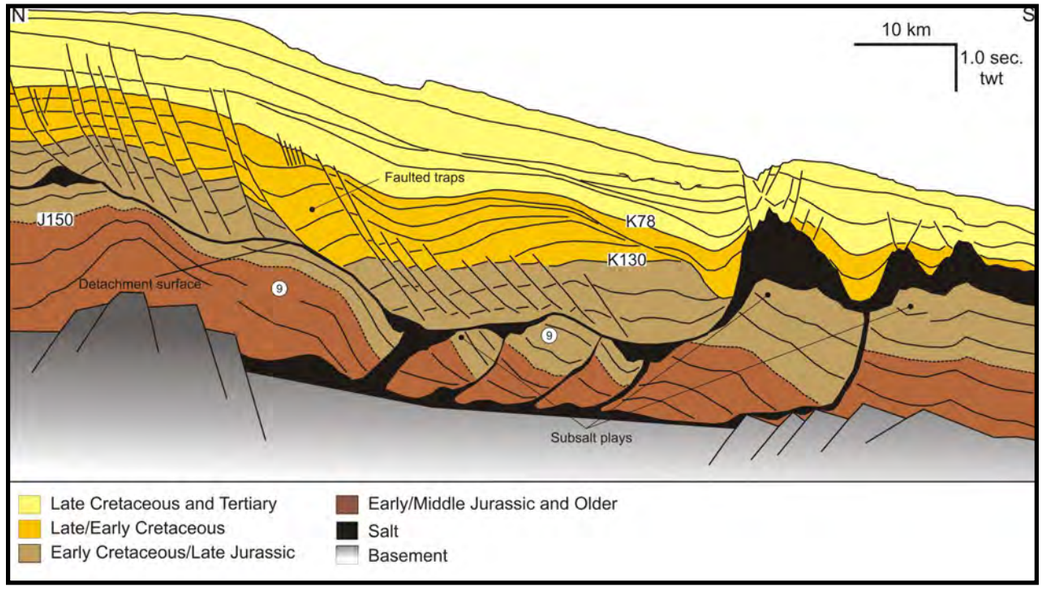

Figure 5.2.6: Seismic line in the Scotia Margin showing a Roho salt system with numerous normal faulting detaching on an allochthonous salt detachment. From www.callforbids.cnsopb.ns.ca.

` Other smaller listric and planar growth faults are observed in the DCG in two different settings 1) as shallow thin-skinned extensional systems along turtle structure flanks, and 2) as shallow thin-skinned extensional system above allochthonous salt sheets.

1) Small syn-depositional faults are observed on the flanks of turtle structure F17 (Panel A, Fig. 4.3.3) and detached in the Upper Triassic and at the base of the Lower Jurassic. These features are likely related to the over-steepening of the turtle flank sand the sliding of stratal block northward on the northern turtle flank and southward on the southern turtle flank during the Late Jurassic. Similar faults are observed on the eastern flank of F17 turtle structure (Panel D, Fig. 4.3.7) and were active during the deposition of S2 and S3. Syn-depositional faults F11-13 (Panel E, Fig. 4.3.8) are also dipping away from the axial turtle structure F11 and show over thicken of S2 strata.

2) The deformation and withdrawal of allochthonous salt sheets in B13 and F06 areas are also accommodated by syn-depositional extensional faulting during the Late Jurassic. Several faults (e.g. small faults above salt body SB3 in Fig. 4.3.9; faults F11-14 in F9 block, Panel G, Fig. 4.3.10) detached on the withdrawn and thinned allochthonous salt, geometry often seen in other salt basin with extensive allochthonous salt systems such as the Deep Gulf of Mexico in the USA or the Scotia margin (Fig. 5.2.6). These system are referred as Roho systems and have often a compressional downdip zones that are not clearly observed in the study area. More detailed work will be required to fully understand these salt systems of Noordvaarder Mb. sandy strata observed in the hanging wall at well B13-02 location.

5.3 Paleotopography

Depositional systems react to various external parameters, including sediment supply, eustatic variations and subsidence (or uplift). Another important control parameter in basins that are subject to intense syn-depositional deformation, are the effect of paleo-topographic features on the distribution and accumulation of sediments. Several locations within the study areas show evidence of paleo-topographic relief affecting the stratigraphy of the Upper Jurassic and Lower Cretaceous. The paleo-topography can be related to 1) active faults, 2) active salt structures , 3) growth anticlines and active basin margins, and 4) incisions within low to negative accommodation zones (e.g. in the Terschelling Basin prior to the deposition of S1 and S2 with incised valleys development).

5.3.1 Active faults

Faults can create topographic relief on the seafloor or at the free surface in continental settings. Fault scarps develop and affect the distribution of sediment pathways, the contemporaneous depositional systems and even the stacking pattern of depositional sequences (Fig. 5.2.7). In the study area several locations show noticeable stratigraphic variations between the footwalls and the hanging walls of syn-depositional faults during the Late Jurassic and Early Cretaceous. In the case of faults F8 and F9 in the Panel C (Fig. 4.3.6) the Lower Graben Fm. is not only thicker on their down thrown sides but also show a lower net-to-gross on their downthrown sides (even if the net sand is higher on the downthrown sides). This is often observed in growth fault settings where lower net-to-gross sediments are preferentially preserved in the high accommodation hanging walls and are preferentially eroded on the footwall sides (similar observations are made in the Niger Delta (Bouroullec, 2002). This creates a dilemma when drilling around syn-depositional faults, from either drilling the footwall where the sands are thinner but more amalgamated, or drilling the hanging wall s and get thicker sands but separated by thicker low net-to-gross interbeds. More detailed analysis of syn-depositional faults present in the study area would be required to evaluate precisely their impact on the stratigraphic record.

5.3.2 Active salt structures

Active salt features situated close or at the seafloor (or free surface in continental settings) are observed in several locations within the study area. Salt bodies that are close or at the seafloor are subject to several processes. They are easily eroded, often subject to increased dissolution, and they are often overlain by caprocks composed of deformed and cemented younger strata that were transported upward with the migrating salt. No detailed analysis of the topographic effects of salt bodies was carried out in this study since it requires detailed mapping and reconstruction of the surrounding area in 3D.

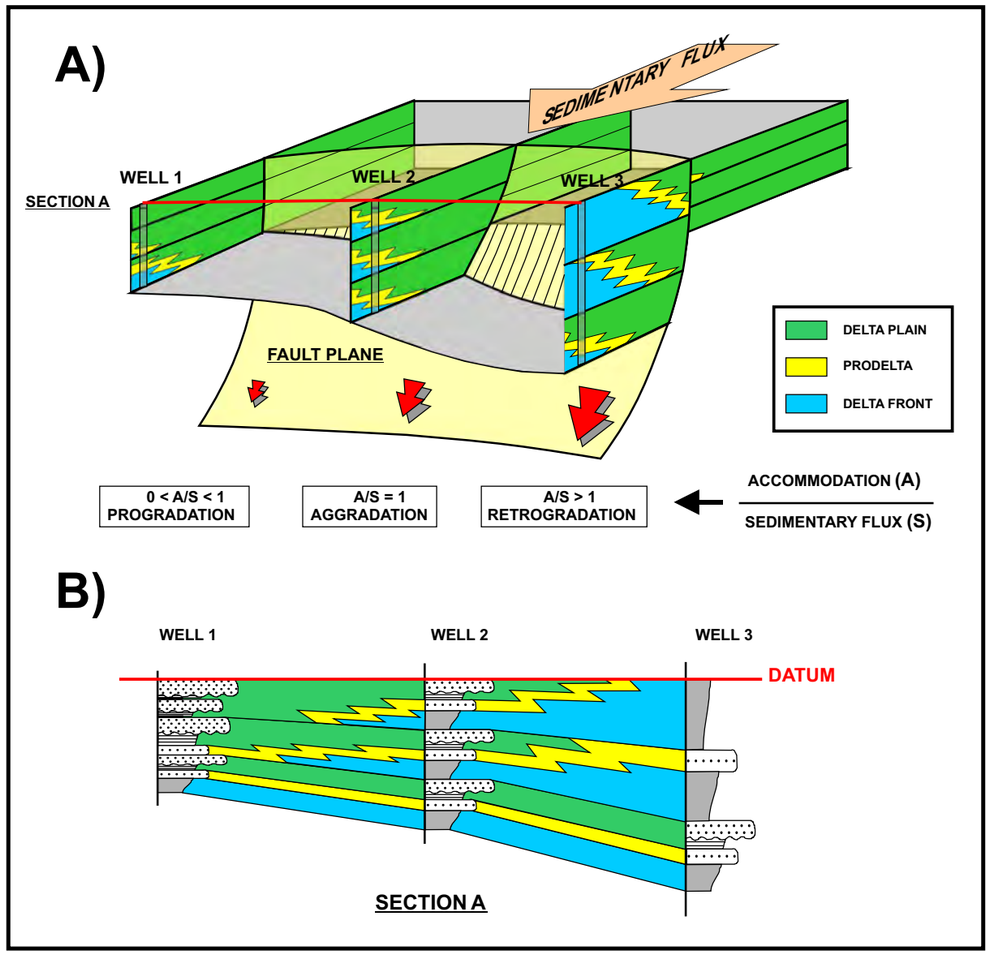

Figure 5.2.7: Effect of syn-depositional faulting on sequence stacking pattern. Active faults that reach the seafloor of the free surface can have an along strike variation in the amount of throw involved. The stacking pattern is influenced by the accommodation that is itself influenced by the amount of subsidence. Therefore, along a fault, the stacking pattern can change, from a progradational system to a retrogradational system (also deforming the coast line trends in result). From Bouroullec (1996).

5.3.3 Growth anticlines and active basin margins

Several growth anticlines were active during the Late Jurassic and the Early Cretaceous are observed along the studied regional transects Note that these growth anticline are not compressional structures but rather extensional that are due to differential subsidence created by salt migration that steepens the overlying strata.

- Anticlines A10 and A12 in Panel A (Fig. 4.3.3), which are the “L02" and “L03 turtle structures”, impact greatly the deposition of S1 that onlaps toward the NW and SE (on both sides of well L03-01) onto the growing structures. This indicate that these anticlines had positive reliefs during this period and were partially eroded. These growing structures provided increased confinements during this period that likely affected the depositional systems in the vicinity.
- Anticline A5 and the associated evacuation syncline ES1 controlled the deposition of S3 (and to a minor extent the lower part of S2) in the northern part of the TB (Fig. 5.2.2). This growth structure formed a significant positive topographic relief during the depositional of the lower part S3, with up to an estimated 85 m high slope that formed the contemporaneous northern Terschelling Basin margin. These feature was later being corrected by the continued depositio of the Scruff Spiculite Mb. and the over stepping of the sediment that widened the depositional area of the TB.
- Anticline A10 in Panel C (Fig. 4.3.6) was also growing during the deposition of S1, with the Lower Graben Fm. lapping onto this positive paleo-topography at a relatively high angle at first and then shallows up, even draping, the growing anticline toward the end of the Lower Graben Fm. Note that the intra Middle Graben Fm. unconformity S1-UC1 cuts into younger strata at the crest of the growth anticline, which indicates that a significant amount of strata was eroded at the crest and on the flank of the structure, possibly redeposited sediments into S1 farther north (see sands at the base of B14-01 in Panel F, Fig. 4.3.9). Note that another similar unconformity (S1-UC2) is recognized on seismic (Fig. 4.4.5) within the Kimmeridge Clay Fm., indicating that the growth anticline was growing more rapidly, and in response eroded, during those periods.
- Anticline A4 in Panel D (Fig. 4.3.7), which is the F17 turtle structure, shows truncation of S2 into S1 at the crest of the structure. S3 also later cut into S2 as shown by the local unconformity at the base of S3 on the eastern flank of the growth anticline.
- Another good example of the complex interplay between growth anticline and the stratigraphic record is shown on the panel E where S1 present multiple internal onlap surfaces and unconformities on the eastern flank of the A5 anticline (Fig. 4.3.8). This shows that the depositional area within the DCG changed constantly during the Late Jurassic and Early Cretaceous, sometime enlarging, sometimes narrowing, depending on the slowing down or acceleration of the rifting and of the salt migration within the graben.

Note that several growth anticline were likely shorten during the Late Cretaceous and Cenozoic compression. This shortening may have also been increased if the anticlines were salt cored, since the salt is more easily deformed and remobilized upward.

5.3.4 Incisions within low-to negative-accommodation zones

The southwestern part of the Terschelling Basin, the Step Graben and other low accommodation zones (e.g. Schill Grund High, Cleaver Bank High, Ameland Block and the Central Offshore Platform) were subject to little to no deposition of S1 and S2 during the Late Jurassic and the Early Cretaceous. Only small zones on the platforms and on the TB have strata from that age. When it is the case, they are often located within topographic lows. These topographic lows (L1-6 in Panel A, Fig. 4.4.1; L1-2 in Panel B1, Fig. 4.4.3; RA1-3 in Panel G, Fig. 4.4.10) are interpreted as incised valleys that developed during the early part of S1, providing sediment conduits into the DCG. However, his depositional model has not been tested using 3D mapping. To prove that this model of incised valley network located on the platforms and in the TB, possibly leading to the DCG (and possibly elsewhere) is accurate, a mapping exercise should be undertaken to reveal the paleogeography of this period. The sediment fills of those paleo-topographic features are likely much younger that the incisions since they mainly acted as sediment pathways in low accommodation zones and were only filled when the base level was corrected between the DCG and the surrounding platforms. It is also important to notice that the platform areas have suffered great amount of erosion (likely even multiple erosional phases) during the early fill of the DCG and the early phases of Late Jurassic rifting, which likely elevated the rift shoulders, increasing erosion of the footwalls of major bounding structures. Therefore, the preservation of these incised valley networks is low, which may possibly makes the mapping of these features difficult with only the deepest and/or youngest incised valleys preserved.

5.4 Basin Evolution

In this section we discuss the geological evolution of the study area during the Mid to Late Jurassic and Early Cretaceous, from Callovian to Ryazanian. The interval of interest is divided into three sequences, Sequence 1 (Middle Callovian - Early Kimmeridgian), Sequence 2 (Late Kimmeridgian to Middle Volgian) and Sequence 3 (Late Volgian to Ryazanian). A new stratigraphic framework (Figure 5.2.8) and stratigraphic distribution maps (Fig. 5.2.9) are presented in this chapter and are key document for the discussion presented below.

5.4.1 Sequence 1:

- In general, the distribution of Sequence 1 deposits is limited to the axis of the DCG. The basin development in the DCG area reflects renewed rifting, following the thermal doming event in the early Middle Jurassic. The first Middle Callovian deposits, situated on top of the Mid Cimmerian Unconformity, accumulate in a narrow (less than 10 km wide) zone in the central/northern part of the DCG (F11 to F03 blocks) (Fig. 5.2.8 and 5.2.9A). The sandstones and shales belong to the **Lower Graben Fm.** The deposits onlap onto the basin margins formed by Lower Jurassic strata that form a large trough shape basin. The basin configuration was confined by salt withdrawal in the axis of the DCG.
- The proximal sediment pathways for the Sequence 1 deposits have not yet been clearly identified. They may have been eroded away during later phases of the basin evolution or could be the incised valleys observed in the TB and the SG. More detailed work will be required in a follow up project (Focus 2) to get the final answer.
- The Late Callovian strata of the upper part of the Lower Graben Fm. covers a wider (15-20 km wide, Fig. 5.2.9B) zone than the Middle Callovian strata and extends farther south, into the F14 block and farther north to the B14 block. These deposits are very sandy and display sedimentary features consistent with a tidally influenced environment. Features pointing to alternating freshwater and salt water environments, such as synaeresis cracks, are abundant. A prominent relative sea level rise is associated with these deposits.
- The sediment stack in the F03 and F06 Blocks keeps up very well with the sea level rise, indicating a high sediment supply in that area. In the F14 Block, the presence of fine-grained offshore mudstones in the Late Callovian indicate drowning, pointing to a relatively low sediment supply.
- The Late Callovian transgression spills over the basin margins onto e.g. the F17 and LO5 areas. In these areas, a relatively thin, silty or sandy, coarsening upward sequence marks the base of the Upper Jurassic sediment stack.
- The Early Oxfordian deposits of the **Middle Graben Fm.** accumulated in a 40 km (in the south) to 22 km (in the north) wide zone within the DCG (Fig. 5.2.9C). This zone extends from the F14 block in the south to the B13 block in the north. Three regionally extensive coal beds, up to 3 m thick, are identified in the lower part of the Middle Graben Fm. (Fig. 5.2.8).
- The coal beds reflect a humid climate at the time of deposition. The relatively wet climate is inferred from the pollen and spore record by the dominance of wet, lowland types during this time interval.
- The coals beds also reflect sediment starvation in the DCG axis. The sudden disappearance of sand can be ascribed to the overstepping of the basin margins, pushing back the sandy shoreline by tens of kilometers. The axis of the DCG was left with a poor connection to the sea, rendering the actively subsiding basin as a freshwater dominated embayment with occasional marine incursions.
- The Early and Middle Oxfordian deposits in the southern part of the Dutch Central Graben, the F17, L02 and L05 Blocks, belong to the **Friese Front Fm**. In the F17 and L02 Blocks, the Friese Front Fm. is characterized by three to four sandy units (units A to D), associated with locally developed coal layers. The coarsening upward character of the sandstone complexes indicates a probable marginal marine origin (prograding delta?). More to the South, in the L05 Block, the Friese Front Fm. is characterized by an unknown number of sandy units, but these sandstone units are clearly non-marine, fluvial channels.
- A regional unconformity (S1-UC1) of Middle Oxfordian age has been identified in the DCG axis. This unconformity eroded through Lower Jurassic strata as well as older intervals, enlarging the depositional area of basin prior to the deposition of the upper part of the Middle Graben Formation (Middle Oxfordian).
- The upper part of Sequence 1 is composed of three formations that are time equivalent of each other's, from the proximal Friese Front Formation (from blocks L05 to F17), to the **Puzzle Hole Fm.** (from blocks F14 to F11), to the distal **Upper Graben Fm.** (from blocks F11 to B13). The depositional area is 22 (in the north) to 38 (in the south) km wide and extend from F05 to B13 blocks (Fig. 5.2.9D and E). The Friese Front Fm. in L05 is composed of mainly fluvial deposits, while the Puzzle Hole Fm. consists of fluvio-deltaic deposits. The Upper Graben Fm. is composed of higher net-to-gross strata deposited in deeper water, likely in prodeltaic to shelfal environments.
- A lateral sandy sediment input (unit E, Fig. 5.2.8) is observed at the top of the Upper Graben Fm. in Block B14, likely related to local basin sediment input from the basin margin(s).
- The upper limit of Sequence 1 is a regional unconformity.

5.4.2 Sequence 2:

- Sequence 2 is characterized by an increase in tectonic activity, e.g. vertical movement along NW-SE trending faults and salt movement. The TB and other peripheral basins outside the DCG axis become active during Sequence 2. The Sequence 2 stack of deposits in the TB reflects a mega-scale transgressive trend.
- Sequence 2 is characterized by a mosaic of different time equivalent lithostratigraphic units. For example the **Kimmeridge Clay Fm.** is lateral equivalent to 1) the **Main Friese Front Mb.**, 2) **the Oyster Ground Mb.**, 3) the T**erschelling Sandstone Mb.**, 4) **the Lies Mb.** , and 5) **the Noordvaarder Mb.** Therefore, the Kimmeridge Clay Fm. should be used and considered with great care when discussing the basin evolution in a sequence stratigraphic approach.
- The Kimmeridge Clay Fm. is limited in occurrence to the northern part of the Dutch Central Graben. This formation exhibits a low net-to-gross and displays cyclicity on the wireline logs. Unfortunately the Dutch Kimmeridge Clay Fm. fails as a source rock, unlike other localities..
- The older deposits of Sequence 2 are composed of continental strata of the Main Friese Front Mb. in the southeastern part of the study area (from M07 to F11) and of marine deposits (oldest part of the Kimmeridge Clay Fm.) in the northern part of the study area (from block F11 to A18). The Main Friese Front Mb. is present in the south and western part of the TB (blocks M07, M04, L06, L03) in the northern part of the TB (blocks G16, eastern F18) and in the southeastern part of the DCG (blocks L02, western part of F18, and in the southeastern part of F17) (Fig. 5.2.9F).

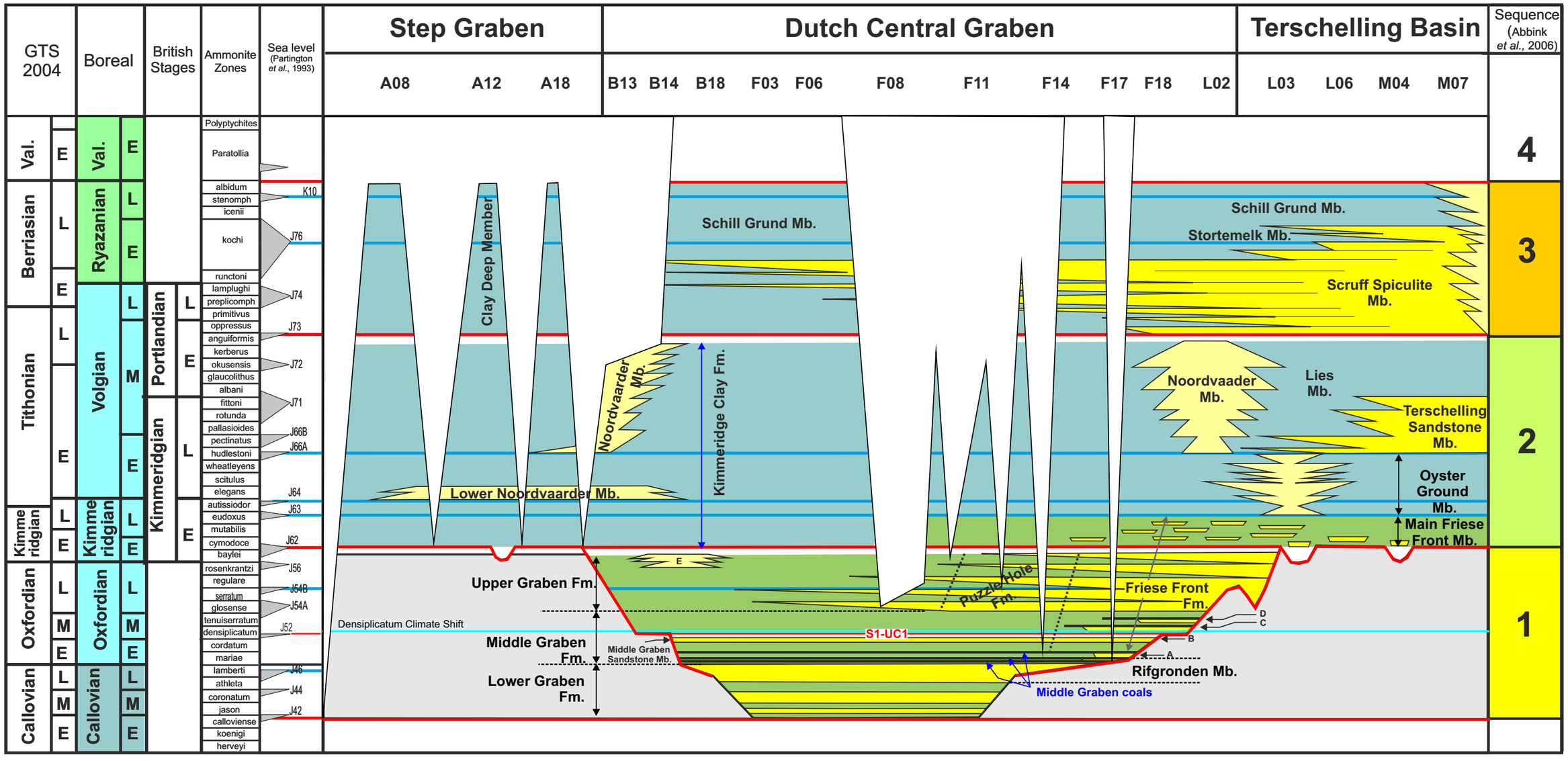

Figure 5.2.8: New stratigraphic framework of the uppermost Middle Jurassic - Lower Cretaceous in the Terschelling Basin, Dutch Central Graben and Step Graben in the Dutch offshore
The sand-rich intervals are shown as yellow polygons, with dark yellow polygons for regional depositional systems and light yellow for locally derived depositional systems (e.g. Noordvaarder Mb.). Fluvial, delta plain and esturarine/lagoonal claystones are shown in green. Marine claystones are shown in blue. Unconformities are shown as red lines and maximum flooding surfaces as blue lines. The three Middle Graben Formation coals are shown as three black lines. Densiplicatum Climate Shift shown as a light blue line. Dash black line show the lithostratigraphic limits if some of the upper Sequence 1 formations. Sandy units A-E refer to five sandy units in the Friese Front Fm. in the L02, F18, F17 and B14 areas.

- A significant flooding occurred in the basin at the onset of the Late Kimmeridgian (MFS J63) that set up marine conditions that persisted until the end of the Early Cretaceous (rest of S2 and S3). In the TB, the flooding is expressed by the occurrence of organic rich, fossiliferous, laminated shales belonging to the Oyster Ground Mb. of the Skylge Fm.
- After a second flooding event (MFS J64) two laterally-sourced sandy systems are identified in: 1) the L02-L06 area (focused around L03 block) and originated from the northwestern part of the TB and the eastern part of the DCG (Block F18), and 2) in the A08-B14 area, in the northern part of the DCG and in the SG (**lower Noordvaarder Mb.**). The southern sediment source persists throughout the Oyster Ground Mb. depositional time, while the northern sediment source (lower Noordvaarder Mb.) was only active during the lowest Late Kimmeridgian (Elegans and Scitulus ammonites zones).
- The upper part of Sequence 2 is composed of three sandy depositional systems, the Terschelling Sandstone Mb., and two geographically separated Noordvaarder Mb. accumulations (Figs. 5.2.8 and 5.2.9G). These sandy depositional systems are separated by the low net-to-gross Lies Mb. in the TB and the Kimmeridge Clay Fm. in the DCG. The Lies Mb. and the Kimmeridge Clay Fm. are lithologically undistinguishable and were likely deposited in a similar setting (deeper water). The Terschelling Sandstone Mb. is observed in the southeastern part of the TB (blocks M07, M04, L06 and L03) and is interpreted as a regional sediment input. The southern Noordvaarder Mb. is observed in the northern part of the TB (blocks G16, northern M01 and eastern F18) and in the southeastern part of the DCG (blocks western F18 and eastern F17) and is interpreted as a local sediment source originated from the local erosion and redeposition of sediment from the Schill Grund High. The northern Noordvaarder Mb. is deposited in the northwestern part of the DCG (blocks B17, B14 and B13) area. It is the thickest in the hanging wall side of the fault F7 (Fig. 5.2.3). It is interpreted as being related to the erosion and redeposition of the DCG northwestern flank (SG). Its lateral extent is unknown at this point and further seismic mapping will be required in a follow up project (Focus 2) to fully capture its potential as a new possible reservoir target.
- The Upper part of Sequence 2 is erosive.

5.4.3 Sequence 3:

- The base of Sequence 3 is a regional unconformity in the DCG and SGH. In the DCG the base of Sequence 3 erodes into Sequence 2, in the SGH, the base of Sequence 3 separates older strata, such as the Triassic or Permian, from Upper Jurassic. In the TB, the transition from Sequence 2 to Sequence 3 is conformable, usually expressed by a coarsening upward trend in the wireline logs.
- Sequence 3 is observed in the entire TB, the southern part of the DCG (Blocks L02, F18, F17, F16, E18), on the margin of the central DCG (blocks F12 and western F11), in the northern part of the DCG (blocks F05, F02, F03, B18 and B17), as well as locally on the SG (blocks F01, E03, A18, A15 and A12) (Fig. 5.2.9H)
- The vast volumes of sand held by Sequence 3 indicate substantial erosion in the hinterland and intrabasinal, undoubtedly related to local or even regional uplift.
- In the most actively subsiding parts of the basin (L03, F06, M04), Sequence 3 displays a coarsening upward base, followed by an overall fining upward trend. The large scale fining upward trend is punctuated by separate fining upward cycles. The sandy parts include the **Scruff Spiculite Mb.** and the **Stortemelk Mb.**, the fine-grained parts belong to the **Schill Grund Mb.** of the **Lutine Fm.**
- Spatially, Sequence 3 can be subdivided into three sandy depositional systems, separated by low net-to-gross strata.
- The aforementioned Scruff Spiculite Mb. is a regionally sourced unit that is found in the TB and the southern part of the DCG. It is a progradational system during the Late Volgian and earliest Ryazanian (Oppressus to early Kochi ammonite zones) and retrogradational during the middle part of the Kochi ammonite zone). The presence of ammonites, belemnites and *Zoophycos* ichnofacies in the cored interval of L06-02 indicates relatively open marine, offshore conditions in that part of the basin.
- The Stortemelk Mb. is confined to the TB and is progradational sandy systems deposited during the latest part of the Kochi Ammonite zone..
- The third sandy system of Sequence 3 is observed in the southern part of the TB in the M07 block and was active during the entire Sequence 3. It is interpreted as being related to the erosion and redeposition of the Ameland Block and Vlieland Platform (Zechstein and Triassic strata eroded and redeposited) as shown by the intra-formational clasts observed in the M07-08 core. A shoreface depositional environment is inferred. Pebble stringers are interpreted as debris flows, indicating an inclined depositional surface. Overall, the unit expresses a coarsening upward trend. Note that the Gamma Ray trend is heavily biased by glauconite content.
- The Schill Grund Mb. and the **Clay Deep M**b. are the distal low net-to-gross equivalent of the sandy depositional systems described above.

5 - Discussion - Basin Evolution

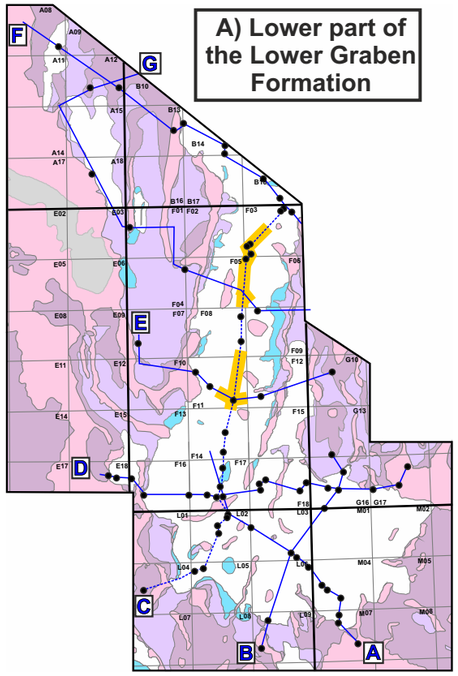

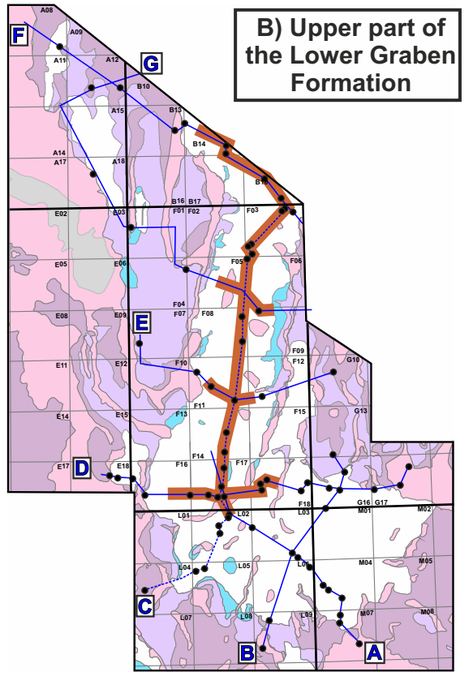

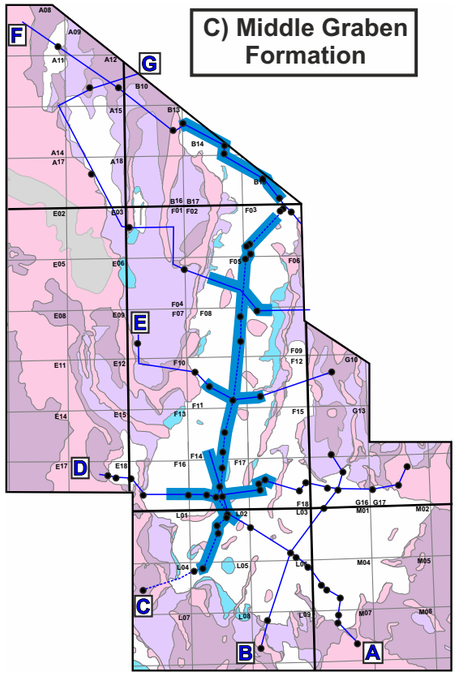

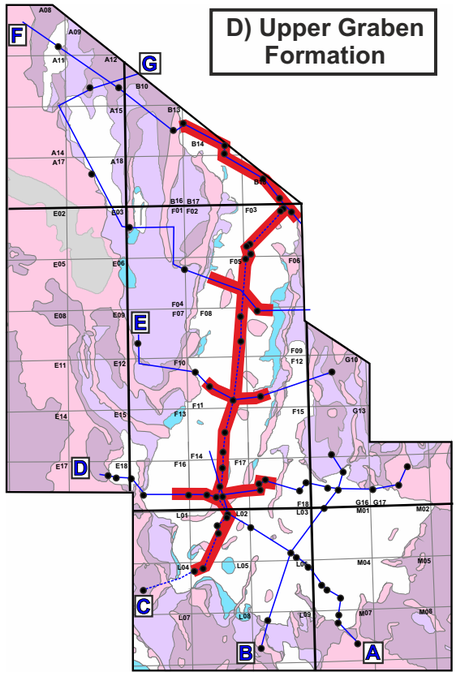

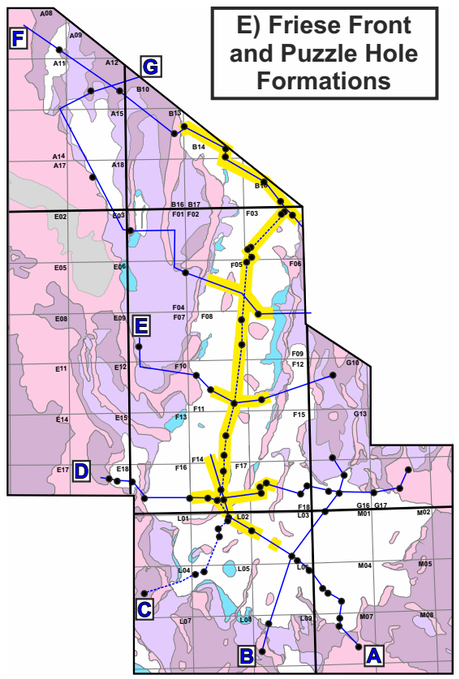

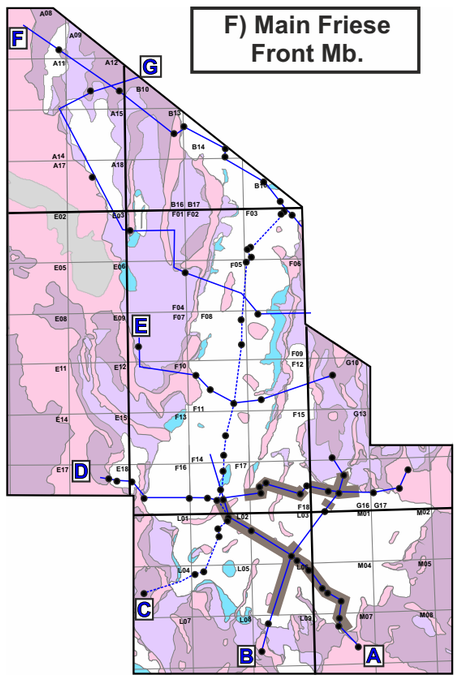

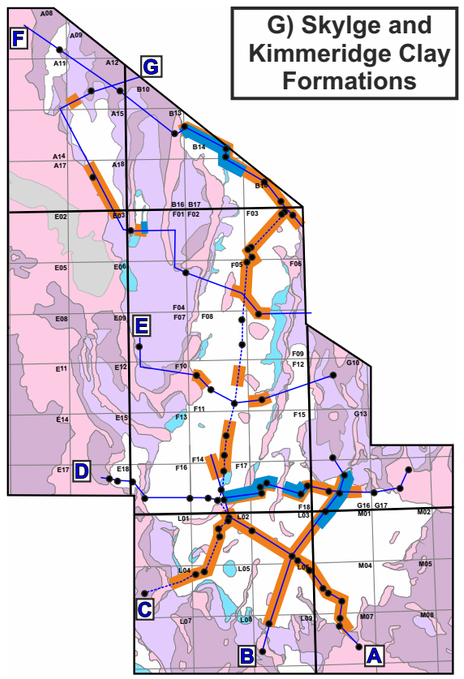

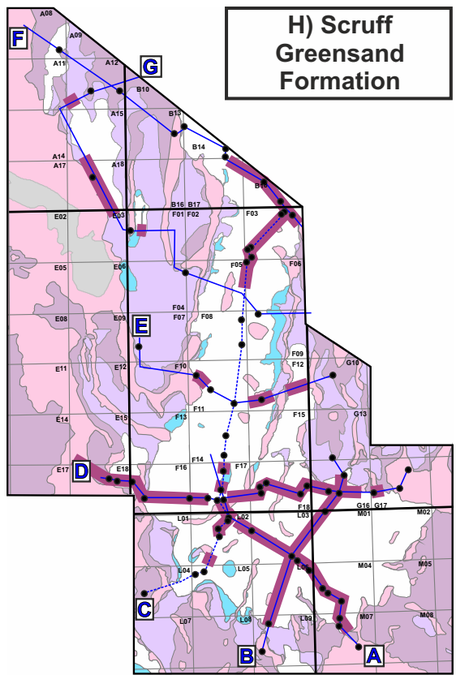

Figure 5.2.9: Distribution maps of the main stratigraphic formations and members of the Upper Jurassic and Lower Cretaceous in the study area. Each map shows the distribution of the strata as colored thick lines along the regional panels. No detailed mapping away from the panels were performed in this project. Note that the marginal sandy-rich Noordvaarder Member is also shown (as dark blue zones) in map G.

CONCLUSION
FUTURE RESEARCH
REFERENCES

Conclusions

Based on the integrated results of the seismic, core description, palynological and stable isotope analyses, the following conclusions are reached:

General

For the first time the Upper Jurassic to Lower Cretaceous of the Dutch Central Graben (DCG) was studied in such a detailed and integrated way. The outcome of the study acknowledges and strengthens the recently developed tectono-stratigraphic subdivision for the Upper Jurassic of the DCG. The basin evolution of the DCG evolves in three steps that reflect changes in basin configuration, invoked by regional changes in the tectonic regime.

Lower Graben Formation

The regionally traceable maximum flooding surface of the latest Callovian (the J46 MFS of Partington et *al.*, 1993a; 1993b) is an important event in the basin evolution of the DCG. The J46 MFS steps over the margins of the (until that time, relatively small and confined) basin and forms the base of the Upper Jurassic succession in i.e. the F17 and L05 Blocks. The basin fill in the F03/F06 area kept up with the J46 eustatic sea level rise, due to a high supply of sediment. The F14 area was more effected by the J46 sea level rise because of a lower sediment supply. The J46 MFS is associated with sandy, tidally influenced deposits in the F03/F06 Blocks (high net-to-gross), and with more fine-grained, open marine deposits in the F14 Block (low net-to-gross).

Friese Front Formation

The reservoir sandstones in the Friese Front Fm. of the F17 Block occur in 10 to 20 meter thick complexes, consisting of two or three coarsening upward cycles, capped by shale and/or coal. Four complexes are distinguished, two in the latest Callovian and Early Oxfordian and two in the Middle and Late Oxfordian. The reservoir sandstones in the Friese Front Fm. of the L05 Block occur as 5 meter thick fining upward units, depositing in a non-marine (swamp) environment.

Terschelling Sandstone Member

The reservoir sandstones of the Terschelling Sandstone Mb. of the Skylge Fm. occur as multi-storey sandstone bodies, reflecting transgressive-regressive cycles. The sandstones are deposited in a variety of environments ranging from lower shoreface to tidal channels, rather than barrier sandstones as previously described, with occasional freshwater influence.

Scruff Greensand Formation

The Scruff Greensand Fm. displays a thickening towards the center of the Terschelling Basin (TB). In the center of the basin, the Scruff Greensand Fm. is composed of a series of fining-upward cycles, terminating in the shales of the Schill Grund Mb. of the Lutine Fm. From the basin margin in the M07 Block to the basin center in the L06 Block, a general deepening trend is observed, from upper shoreface to open marine. At the basin margin, the Scruff Greensand Fm. is developed as a coarsening upward sequence. The Late Ryazanian coarse sandstones of the Scruff Greensand Fm. near the basin margin, correlate to the Schill Grund Mb. in the TB basin center. The M07-07 core shows intra-formational clasts that are interpreted as Triassic material shedding for the neighboring platform as debris flow deposits.

Noordvaarder Member

The Noordvaarder Mb. of the Skylge Fm. reflects the increase in tectonic activity, characteristic for Sequence 2, which is for instance expressed in the coarsening upward Noorvaarder successions in the B14 and B13 Blocks. In the western part of the Step Graben (SG), sandy deposits of the Noordvaarder Mb. may constitute the base of the Upper Jurassic sediment pile. In the eastern part of the SG, deposits belonging to Sequence 2 are absent.

Tectono-stratigraphy

The Upper Jurassic - Lower Cretaceous interval was deposited during a period of intense extensional deformation. Deep-skinned and thin-skinned tectonic structures were active during this period and resulted to a highly fragmented basinal configuration.

The seismic analysis, coupled to the stratigraphic correlation, shows that numerous autochthonous and allochthonous salt systems and their associated syn-depositional faults were active within the studied basins and along their margins, often affecting the deposition into sub-basins that had variable structural evolution. The withdrawal of Zechstein salt in the axis DCG, and to a lesser extend the TB, was the primary parameter affecting the high accommodation and the accumulation of thick Upper Jurassic strata (e.g. 1,6 km of Sequence 1 in the F03 block). The salt migrated from the axis of the basins toward their lateral margins and formed salt pillows (often above large pre-Zechstein normal faults) that frequently evolved into salt shallow bodies. These salt bodies played a critical role on the heterogeneous nature of the Upper Jurassic - Lower Cretaceous stratigraphy by creating zones of differential subsidence that experienced variable stratigraphic accumulation and preservation.

Two regionally significant unconformities (S1-UC1 and S1-UC2) have been identified in the northern part of the DCG. The S1-UC1 is observed in the upper part of the Middle Graben Fm. and the S1-UC2 in the lower part of the Kimmeridge Clay Fm. Their origins are still unclear but the fact that they can be traced form the basin margins to its axis reveals that they are related to either a significant relative sea level drop or a basin-scale tectonic uplift affecting the entire region.

The Late Cretaceous - Cenozoic Alpine shortening added an even greater level of complexity by increasing the heterogeneous nature of the basinal configuration due to differentially uplift, erosion, and preservation of Upper Jurassic and Lower Cretaceous strata.

Basin evolution

A new stratigraphic framework was established for the Upper Jurassic - Lower Cretaceous of the DCG, SG and TB (Fig. 5.2.8). This framework clarifies the lateral equivalencies of lithostratigraphic units in the basin by providing additional and robust time lines established using palynological, stable isotope, seismic and stratigraphic results.

Project Focus 2 (2016 – 2018)

Three-Dimensional Sequence Stratigraphic and Tectono-stratigraphic Analysis of the Upper Jurassic and Lower Cretaceous in the Dutch Offshore and Neighboring Regions

The research results obtained in the Focus 1 project (2014-2015) are setting the stage for additional research on the Upper Jurassic and Lower Cretaceous stratigraphic interval. The newly built knowledge on the depositional systems, stratigraphy and tectono-stratigraphy of the basin during this period can now be significantly increased by investigating, in even greater detail, the geology of the Dutch offshore as well as the neighboring regions.

Four interdependent lines of research are proposed:

1) A detailed sequence stratigraphic and tectono-stratigraphic analysis in the Dutch offshore

The research will be carried out by incorporating additional available wells, cores and seismic data. Key seismic horizons identified during the Focus 1 project ,as well as newly defined horizons, will mapped in 3D to produce isopach maps as well as detailed depositional systems maps based on new sequence stratigraphic framework and attribute analysis. These stratigraphic analysis will be carried out parallel to structural analysis, as it was done in the project Focus 1. This a crucial aspect of studying the Upper Jurassic and Lower Cretaceous stratigraphy of the study area, as highlighted by the results of the Focus 1 project. New biostratigraphic analysis will be carried out to increase control of the evolution of the basin. The analysis of the marginal stratigraphic settings along the studied basins will be carried in detailed using OpendTect software from dGB to better understand the interplay between the depositional systems and the ever changing margins. This will allow for an increased predictability of sandy deposits that are highly controlled by paleo-topographic features that often affect the accommodation rates and the preservation ratios.

The selection of stratigraphic interval of interest will be done in accordance with industry partners but several depositional systems are already high on our list.

a. Sequence 1.1: The Lower Graben Fm. depositional systems.
b. Sequence 1.3: The Friese Front/Puzzle Hole/Upper Graben Formations depositional systems.
c. Sequence 2.2: The Noordvaarder Mb. depositional systems.
d. Sequence 3: The Scruff Spiculite Mb. depositional system.
e. Marginal depositional systems in Sequences 1, 2 and 3.

2) A provenance study of the Upper Jurassic and Lower Cretaceous sand-rich depositional systems in the Dutch offshore

The sources of the sand entering the Terschelling Basin, Dutch Central Graben and the Step Graben are still remaining unclear. A provenance study carried out by the geochemistry team of TNO in close collaboration with the TNO geology team will be carried out to attempt to increase knowledge on the regional and local sediment sources. This study will allow for an increase controlled on the ever changing paleogeography of the study area during the Late Jurassic and Early Cretaceous.

3) Structural restorations within the Dutch Central Graben and neighboring platforms

Several interpreted 2D seismic sections obtained during the Focus 1 Project will be used for palinspastic restoration. These sections will be refined (if required), depth converted, and restored using 2D Move software from Midland Valley. The results will allow to ascertain in greater detailed and quantitatively the structural evolution of key structural features (including salt bodies and faults) in the study area, as well as evaluate with more accuracy the amount of erosion, redeposition and stratal preservation in the basins, along their margins and on the surrounding platforms during the Late Jurassic and Early Cretaceous. The results will also give new insight into the basin evolution during the Permo-Triassic, the Early and Middle Jurassic as well as the Late Cretaceous and Cenozoic.

4) Cross border stratigraphic analysis of the Upper Jurassic and Lower Cretaceous.

The increased knowledge obtained during the Focus 1 project on depositional systems, stratigraphy and tectono-stratigraphy of the Upper Jurassic and Lower Cretaceous within the Dutch offshore could be used to analyze this interval in the German, Danish and British sectors, as well as father south in the Dutch sector. Such research will be highly dependent on accessing valuable data in those areas to be able to develop accurate stratigraphic framework. We propose to start this study in a manner similar to Focus 1 research, by incorporating core description, new biostratigraphic analysis, 2D seismic analysis and well correlations.

References

Abbink, O.A., 1998, Palynological investigations in the Jurassic of the North Sea region. LPP Contribution Series, 8: 192 pp.

Abbink, O.A., Mijnlieff, H.F., Munsterman, D.K. and Verreussel, R.M.C.H., 2006, New stratigraphic insights in the “Late Jurassic” of the southern central North Sea Graben and Terschelling Basin (Dutch offshore) and related exploration potential. Netherlands Journal of Geosciences – Geologie en Mijnbouw 85(3): p. 221-238.

Bouroullec, R. and Weimer, P., in press, Geometry and Kinematics of Neogene Allochthonous Salt Systems in the Mississippi Canyon, Atwater Valley, western Lloyd Ridge and western DeSoto Canyon Protraction areas, Northern Deepwater Gulf of Mexico, AAPG Bulletin.

Bouroullec, R., de Bruin, G. and Zijp, M., 2015, Triassic Allochthonous Salt Emplacement and Associated Upper Jurassic-Cretaceous Deformation in the Dutch Offshore Southern North Sea, TNO report, unpublished.

Bouroullec, R., 1996, Growth Fault Raft system in the Congo Margin, Master Thesis, Rennes University.

Bouroullec, R., 2001, Growth fault kinematics and stratigraphic implications. PhD Thesis, Imperial College, London, 389 pp.

B**ucefalo Palliani, R.B., Mattioli, E. and Riding, J.B.**, 2002, The response of marine phytoplankton and sedimentary organic matter to the early Toarcian (Lower Jurassic) oceanic anoxic event in northern England. Mar Micropaleontol 46: p. 223–245.

Bucefalo Palliani, R. and Riding, J.B., 2000, A palynological investigation of the Lower and lowermost Middle Jurassic strata (Sinemurian to Aalenian) from North Yorkshire, UK. - Proceedings of the Yorkshire Geological Society, 53 (1): p. 1-16. Manchester.

Costa, L.I. and Davey, R.J., 1992, Dinoflagellate cysts of the Cretaceous System. In: Powell, A.J. (ed.), A Stratigraphic Index of Dinoflagellate Cysts: p. 99-154.

Coward, M.P., Dewey, J., Hempton, M. and Holroyd, J., 2003, Tectonic evolution. In: Evans, D.J., Graham, C., Armour, A. and Bathurst, P. (Eds): The Millenium Atlas: Petroleum Geology of the Central and Northern North Sea. The Geological Society (London), p. 17-33.

De Jager, J., 2007, Geological Development. In: Geology of the Netherlands, Eds Wong, Th., Batjes D.A.J. and De Jager, J. Publ. by the Royal Academy of Art and Sciences (KNAW). ISBN 978-90-6984-481-7.

De Jager, J., 2012, The discovery of the Fat Sand Play (Solling Formation, Triassic), Northern Dutch offshore – a case of serendipity. Netherlands Journal of Geosciences, v. 91, Is. 04, pp 609-619.

Davey, R.J., 1979, The stratigraphic distribiution of dinocysts in the Portlandian (latest Jurassic) to Barremian (Early Cretaceous) of northwest Europe. – AASP Contributions Series, 5B: 48-81. Dallas, Texas.

Davey, R.J., 1982, Dinocyst stratigraphy of the latest Jurassic to Early Cretaceous of the Haldager No. 1 borehole, Denmark. Geol. Surv. Denm. Ser. B, 6: 58pp.

De Jager, J., 2007, Geological development. In: Wong, T.E., Batjes, D.A.J. and De Jager, J. (Eds): Geology of the Netherlands. Royal Netherlands Academy of Arts and Sciences (Amsterdam): p. 5-26.

Dooley, T., McClay, K. R. and Pascoe, R., 2003, 3D modeling of the Revfallet fault system, offshore Norway, in D.A. Nieuwland, ed., New Insights into Structural Interpretation and Modeling: Geological Society of London, Special Publication No. 212, p. 151–168.

Dooley, T., McClay, K.R., Hempton, M. and Smit, D., 2005, Salt tectonics above complex basement extensional fault systems: results from analogue modeling, in A.G. Dore and B.A. Vining, eds., Petroleum Geology: North-West Europe and Global Perspectives: Proceedings of the 6th Petroleum Geology Conference, Geological Society of London, p. 1631–1648.

Doornenbal, H. and Stevenson, A, 2010, Petroleum geological atlas of the Southern Permian Basin area. EAGE, 342 pp.

Duin E.J.T., Doornenbal, J.C., Rijkers, R.H.B. Verbeek, J.W. and Wong, Th,E., 2006, Subsurface structure of the Netherlands - Results of recent onshore and offshore mapping, Netherlands Jopurnal of Geosciences - Geologie en Mijnbouw, 85, 4, pp. 245-276.

Duxbury, S., Kadolsky, D. and Johansen, S., 1999, Sequence stratigraphic subdivision for the Humber Group in the Outer Moray Firth area (UKCS, North Sea). In: Jones, R.W. and Simmons, M.D. (eds) Biostratigraphy in Production and Development Geology. Geol. Soc. Spec. Pub., 152: p. 23-54.

Edwards, C. W., 1976, Growth faults in the Upper Triassic deltaic sediments, Svalbard, Bulletin of American Association of Petroleum Geologists, 60, p. 341-355.

Foster, P.T. and Rattey, P.R., 1993, The evolution of a fractured chalk reservoir: Machar Oilfield, UK North Sea, in J.R. Parker, ed., Petroleum geology of northwest Europe: Proceedings of the 4th Conference: Geological Society of London, p. 1445–1452.

Geluk, M.C., 2005, Stratigraphy and tectonics of Permo-Triassic basins in the Netherland and surrounding areas. Thesis. Utrecht University (Utrecht): 171 pp.

Geluk, M.C., 2007, Triassic. In: Wong, T.E., Batjes, D.A.J. and de Jager, J. (Eds): Geology of the Netherlands. Royal Netherlands
Academy of Arts and Sciences (Amsterdam): p. 85-106.

George, G.T. and Berry, J.K., 1993, A new lithostratigraphy and depositional model for the Upper Rotliegend of the UK sector of the southern North Sea. In: North, C.P. and Prosser, D.J. (Eds): Characterization of Fluvial and Aeolian Reservoirs. Geological Society Special Publication (London) 73: p. 291-319.

George, G.T. and Berry, J.K., 1997, Permian (Upper Rotliegend) synsedimentary tectonics, basin development and palaeogeography of the southern North Sea. In: Ziegler, K., Turner, P. and Daines, S.R. (Eds): Petroleum Geology of the Southern North Sea: Future Potential. Geological Society Special Publication (London) 123: p. 31-61.

Gerard, J. and Bromley, R., 2008, Ichnofabrics in clastic sediments. Madrid, Spain, 97 pp.

Glennie, K.W. (Ed), 1998, Petroleum Geology of the North Sea, Basic concepts and recent advances. Blackwell (Oxford): 636 pp.

Gradstein, F.M., Ogg, J.G., Schmitz, M.D. and Ogg, G.M., 2012. The geological time scale 2012, Volume 2, 1144 pp.

Heilmann-Clausen, C., 1987, Lower Cretaceous dinoflagellate biostratigraphy in the Danish Central Trough. Danmarks Geol. Unders. Ser. A (17): p. 1-90.

Herngreen, G.F.W., Kerstholt, S.J. and Munsterman, D.K., 2000, Callovian - Ryazanian ('Upper Jurassic') palynostratigraphy of the Central North Sea Graben and Vlieland Basin, The Netherlands. Mededelingen Nederlands Instituut voor Toegepaste Geowetenschappen TNO, 63: 99 pp.

Heybroek, P., 1975, On the structure of the Dutch part of the Central North Sea Graben. In: Woodland, A.W. (Ed.): Petroleum and the Continental Shelf of North-West Europe. Applied Science Publishers Ltd (London): p. 339-349.

Hoffmann, N. and Stiewe, H., 1994, Neuerkenntnisse zur geologisch-geophysikalischen Modellierung der Pritzwalker Anomalie im Bereich des Ostelbischen Massivs. Zeitschrift geologischer Wissenschaften 22: p. 161-171.

Herngreen, G.F.W. and Wong, T.E., 1989, Revision of the Late Jurassic stratigraphy of the Dutch Central North Sea Graben. Geologie en Mijnbouw 68: p. 73-105.

References

Kley, J. & Voigt, T., 2008, Late Cretaceous intraplate thrusting in central Europe: Effect of Africa-Europe-Iberia convergence, not Alpine collision. Geology 36: p. 839-842.

Koppelhus, E.B. and Nielsen, L.H., 1994, Palynostratigraphy and palaeoenvironments of the Lower to Middle Jurassic Bagå Formation of Bornhorm, Denmark. Palynology, v.18, p.139-194, pl.1-5.

Krzywiec, P., 2004, Triassic evolution of the Kłodawa salt structure: basement-controlled salt tectonics within the Mid-Polish Trough (central Poland). Geological Quarterly 48 (2): p.123-134.

Lott, G.K., Wong, T.E., Dusar, M., Andsbjerg, J., Mönnig, E., Feldman-Olszewska, A. and Verreussel, R.M.C.H., 2010. Jurassic. In: Doornenbal, J.C. and Stevenson, A.G. (editors): Petroleum Geological Atlas of the Southern Permian Basin Area. EAGE Publications b.v. (Houten): p. 175-193.

Munsterman, D.K., Verreussel, R.M.C.H., Mijnlieff, H.F., Witmans, N., Kerstholt-Boegehold, S. and Abbink, O.A., 2012, Revision and update of the Callovian-Ryazanian Stratigraphic Nomenclature in the northern Dutch Offshore, i.e. Central Graben Subgroup and Scruff Group. Netherlands Journal of Geosciences-Geologie en Mijnbouw, 91 (4): p. 555-590.

Partington, M.A., Mitchener, B.C., Milton, N.J. and Fraser, A.J., 1993a, Genetic sequence stratigraphy for the North Sea Late Jurassic and Early Cretaceous: distribution and prediction of Kimmeridgian-Late Ryazanian reservoirs in the North Sea and adjacent areas. In: Parker, J.R. (ed.), Petroleum geology of northwest Europe: Proceedings of the 4th Conference, p. 347-370. London (Geological Society).

Partington, M.A., Copestake, P., Mitchener, B.C. and Underhill, .J.R., 1993b, Biostratigraphic calibration of genetic stratigraphic sequences in the Jurassic-lowermost Cretaceous (Hettangian to Ryazanian) of the North Sea and adjacent areas. In: Parker, J.R. (ed.), Petroleum geology of northwest Europe: Proceedings of the 4th Conference, p. 371-386. London (Geological Society).

Pharaoh, T. C., Dusar, M., Geluk M., Kockel F., KrawczykC., Krzywiec P., Scheck-Wenderoth, M., Thybo H., Vejbæk O. and van Wees, J. D., 2010, Tectonic evolution . in Doornenbal, H. and Stevenson, A. G, eds. Petroleum geological atlas of the Southern Permian Basin area. Houten, the Netherlands, EAGE, p. 25-57.

Powell, A.J., 1992, Dinoflagellate cysts of the Triassic system. In: Powell, A.J. (ed.), A Stratigraphic Index of Dinoflagellate Cysts: p. 1-6.

Remmelts, G., 1995, Fault-related salt tectonics in the southern North Sea, the Netherlands. In: Jackson, M.P.A., Roberts, D.G. and Snelson, S. (Eds): Salt tectonics: a global perspective. American Association of Petroleum Geologists Memoir 65: p. 261-272.

Riding, J.B. and Thomas, J.E., 1992, Dinoflagellate cysts of the Jurassic System. In: Powell, A.J. (ed.), A Stratigraphic Index of Dinoflagellate Cysts: p. 7-98.

Riding, J.B., Fedorova, VA. and Ilyna, V.I., 1999, Jurassic and Lowermost Cretaceous dinoflagellate cyst biostratigraphy of the Russian Platform and Northern Siberia, Russia. AASP Contribution 36, p. 3-180.

Pemberton, S.G., MacEachern, J.A. Gingras, M.K. and Bann, K.L., 2014,Trace fossil atlas – The recognition of common trace fossils in cores. 157 pp.

Roberts, A.M., Yielding, G., Kuznier, N.J., Walker, I.M. and Dorn-Lopez, D., 1995, Quantitative analysis of Triassic extension in the northern Viking Graben. Journal of the Geological Society 152: p. 15-27.

Rosendaal, E., Kaymakci, N., Wijker, D. and Schroot, B.M., 2014, Structural development of the Dutch Central Graben: new ideas from recent 3D seismic. Abstract, EAGE Meeting Amsterdam.

Rouby, D., Raillard, S., Guillocheau, F., Bouroullec, R. and Nalpas, T., 2002, Kinematics of a growth fault/raft system of the West African margin using 3-D Restoration, J. Struct. Geol., 24, p. 783-796.

Rowan, M. G., and P. Weimer, 1998, Salt-sediment interaction, northern Green canyon and Ewing Bank (offshore Louisiana), northern Gulf of Mexico: AAPG Bulletin, v. 82, p. 1055-1082.

Seni, S. J. and Jackson, M. P. A., 1983, Evolution of salt structures, East Texas diapir province, part 2: patterns and rates of halokinesis. Am. Assoc. Petrol. GeoL Bull. 67, p. 1245-1274

Trusheim, F., 1960, Mechanism of salt migration in northern Germany. Am. Assoc. Petrol. GeoL Bull. 44, p. 1519-1540.

Schroot, B.M., 1991, Structural development of the Dutch Central Graben. In: Michelsen, O. and Frandsen, F. (Eds): The Jurassic in the Southern Central Trough. Danmarks Geologiske Undersøgelse series B 16: p. 32-35.

Schuster, D.C., 1995, Deformation of allochthonous salt and evolution of related salt-structural systems, eastern Louisiana Gulf Coast, in M.P.A. Jackson, D.G. Roberts, and S. Snelson, eds., Salt tectonics, a global perspective: AAPG Memoir 65, p. 177-198.

Surlyk, F. and Ineson, J.R., 2003, The Jurassic of Denmark and Greenland: key elements in the reconstruction of the North Atlantic Jurassic rift system. In: Ineson, J.R. and Surlyk, F. (Eds): The Jurassic of Denmark and Greenland. Geological Survey of Denmark and Greenland Bulletin 1: 9-20.

Houben, A., Munsterman, D., Verreussel, R.M.C.H and Kerstholt-Boegehold, S., 2015, The JUSTRAT project – New stratigraphic framework for the Upper Jurassic to Lower Cretaceous in the Southern North Sea using integrated novel techniques. TNO report TNO 2015 R10343.

T**orsvik, T.H., Carlos, D., Mosar, J., Cocks, L.R.M. and Malme, T.N.M.,** 2002, Global reconstructions and North Atlantic paleogeography 440 Ma to recent. In: Eide, E.A. (Ed.): Batlas – Mid Norway plate reconstruction atlas with global and Atlantic perspectives. Geological Survey of Norway (Trondheim): p. 18-39.

Underhill, J.R. and Partington, M.A., 1993, Jurassic thermal doming and deflation in the North Sea: implications of the sequence stratigraphic evidence. In: Parker, J.R. (Ed.): Petroleum Geology of Northwest Europe: Proceedings of the 4th Conference. The Geological Society (London): p. 37-345.

Van den Haute, P. and Vercoutere, C., 1990, Apatite fission track evidence for a Mesozoic uplift of the Brabant Massif – preliminary results. Annales Société Géologique de Belgique 112: p. 443-452.

Van Hoorn, B., 1987, Structural evolution, timing and tectonic style of the Sole Pit inversion. Tectonophysics 137: p. 239-284.

Van Adrichem Boogaert, H.A. & Kouwe, W.F.P., 1997, Stratigraphic nomenclature of the Netherlands, revision and update by RGD and NOGEPA. Mededelingen Rijks Geologische Dienst, nieuwe serie, vol. 50, section a - j.

Vendeville, B.C. and Jackson, M.P.A., 1992, The rise of diapirs during thin-skinned extension: Marine and Petroleum Geology, v. 9, p. 331-371.

Verreussel, R.M.C.H., Dybkjaer, K., Johannessen, P.N., Munsterman, D.K., Ten Veen, J.H. and Van de Weerd, A., in prep., Late Jurassic basin evolution of the Central Graben area from Denmark and the Netherlands.

Wong, T.E., 2007. Jurassic. In: Wong, T.E., Batjes, D.A.J. and de Jager, J. (Eds): Geology of the Netherlands. Royal Netherlands Academy of Arts and Sciences (Amsterdam): p. 107-126.

Wong, T.E., Batjes, D.A.J. and De Jager, J. (Eds), 2007, Geology of the Netherlands. Royal Netherlands Academy of Arts and Sciences (Amsterdam): 354 pp.

Ziegler, P.A., 1988, Evolution of the Arctic, North Atlantic and western Tethys. American Association of Petroleum Geologists: 198 pp.

Ziegler, P.A., 1990a, Geological Atlas of Western and Central Europe (2nd edition). Shell Internationale Petroleum Maatschappij B.V.; Geological Society Publishing House (Bath): 239 pp.

Ziegler, P.A., 1990b, Tectonic and palaeogeographic development of the North Sea rift system. In: Blundell, D.J. and Gibbs, A.D. (Eds): Tectonic evolution of the North Sea rifts. Oxford Science Publications (Oxford): p. 1-36.

APPENDIX A1
CORE DESCRIPTION

Appendix A1.1 - Legend to core descriptions

TNO innovation for life

Legend to core descriptions

SEDIMENTARY STRUCTURES:

- Planar, parallel, horizontal lamination
- Planar, parallel, low angle lamination
- Planar, parallel, high angle lamination
- Concave, parallel lamination
- Wavy lamination
- Flaser bedding
- Linsen bedding
- Bioturbation
- Heterolithic lenticular bedding
- Mud drapes
- Double mud drapes
- Hummocky cross-bedding
- Herring bone cross-bedding
- Sigmoidal cross-bedding
- Undifferentiated ripples
- Current ripples
- Wave ripples
- Climbing ripples
- Planar, tabular, cross-bedding
- Trough cross-bedding

CLASTS:

- Sideritic mud clasts
- Quartz clasts

TRACE FOSSILS:

- *Chondrites*
- *Diplocraterion*
- *Phycosiphon*
- *Ophiomorpha*
- *Planolites*
- *Paleophycos*
- *Rhizocorallium*
- *Skolithos*
- *Teichichnus*
- *Schaubcylindrichnus*
- *Thalassinoides*
- *Zoophycus*
- *Asterosoma*
- *Conichnus*
- *Arenicolites*
- *Scolicia*
- *Monocraterion*
- *Rosselia*
- *Cylindrichnus*
- *Siphonites*
- Escape burrow

- Sandstone
- Silt
- Shale
- Limestone
- Coal
- Gravel

- Open marine
- Lower shoreface
- Upper shoreface/foreshore/beach
- Estuarine/tidal shoal/tidal channel
- Brackish lagoon/bay
- Swamp

MISCELLANEOUS:

- Siderite concretion
- Pyrite concretion
- Carbonate concretion
- Rip-up clast (shale)
- Coal particle
- Ooid
- Wood fragments
- Dewatering
- Flame structure
- Bivalves
- Slumped strata
- Plant roots
- Homogenised
- Stylolites
- Fracture
- Load structure
- Syneresis crack
- Desiccation crack
- Oversteepened strata
- Shell bed

Appendix A1.2 - F03-05-S1 Lower Graben Fm.

TNO innovation for life

Core photos

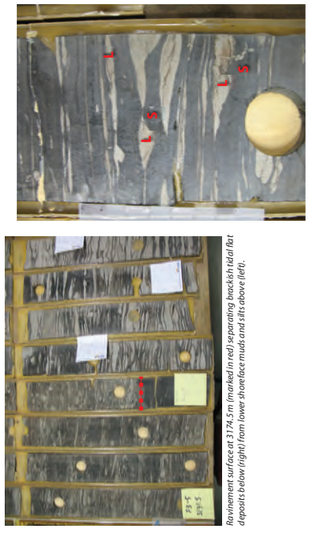
Ravinement surface at 3174.5m (marked in red) separating brackish tidal flat deposits below (right) from lower shoreface muds and silts above (left).

Near 3180 m. Lagoonal muds with isolated ripples or Linsen (L) and synaeresis cracks (S)


3231 - 3238 m. Tidal channel deposits (C) with cross-bedded sands and tidal flat deposits (F) characterised by heterolithic bedding

3210.9m. Soft-sediment deformation in tidal channel deposits

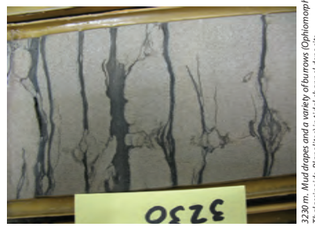
3230 m. Mud drapes and a variety of burrows (Ophiomorpha, Thalassinoids, Planolites) in tidal channel deposits.


3246 - 3253 m. Sand deposited as a bar in a channel (B), overlain by lagoonal muds (M) with very large synaeresis cracks (S) and tidal flats (F).


3253 m. Very large synaeresis cracks in lagoonal muds suggest large variations in water salinity.


3266 - 3273 m. Tidal channel deposits (C), overlain by lagoonal muds (M) and tidal flats (F).


3302 m. Thinly laminated fine sands with an abundance of coal fragments deposited in a freshwater lagoonal environment.

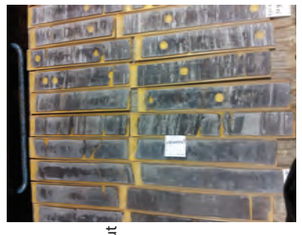
3290 - 3296 m. Lagoonal muds with a strongly impoverished and diminuitive fauna, suggesting a low salinity / fresh water environment.

Interpretation

Swamp	
Lower shoreface to shelf	
Ravinement surface	
Estuarine	
Tidal bars in channel	
Tidal flat	
Tidal flats	
Shoreface	
Tidal channel	
Tidal channel & tidal flat	
Subtidal brackish lagoon	
Swamp	
Subtidal brackish lagoon	
Sandy bar / small delta	
Swamps	
Subtidal brackish lagoon	
Tidal channel	
Subtidal brackish lagoon	
Swamp	
Bay / Lagoon with no sand input	
Deltaic: fresh to brackish, very quiet bay fill with occasional peat formation, occasional marine influence, and no tidal influence	

Core log

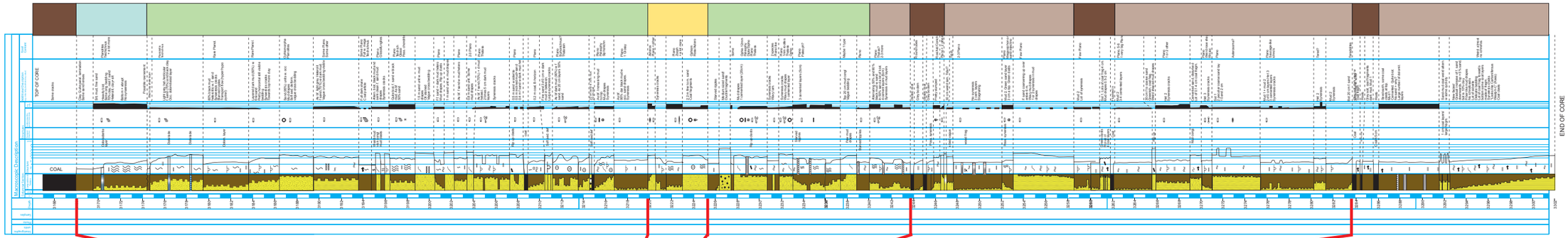

Well logs

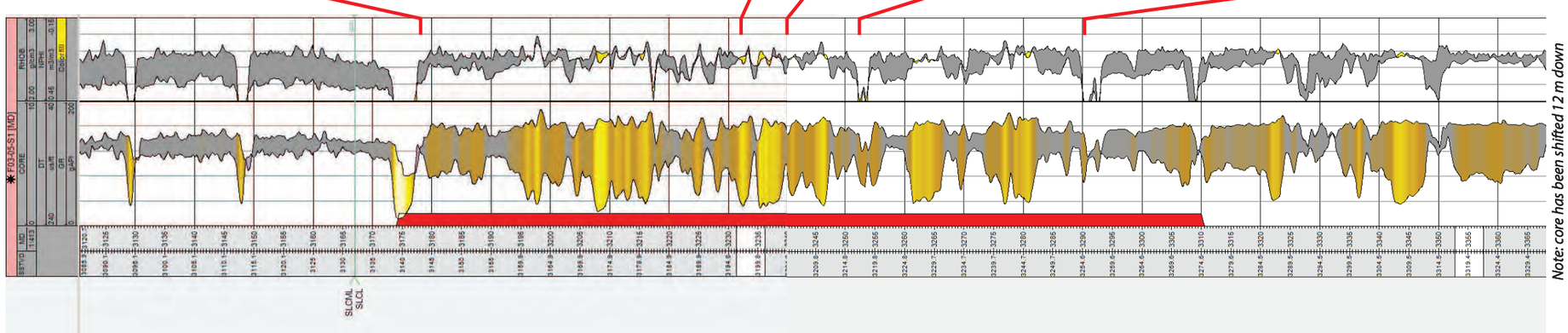

Note: core has been shifted 12 m down to match log depth

Facies Legend

- Open marine
- Lower shoreface
- Upper shoreface/foreshore/beach
- Estuarine/tidal shoal/tidal channel
- Backish lagoon/bay
- Swamp

Appendix A1.3 F06-01 Lower Graben Fm.

TNO innovation for life

Core photos

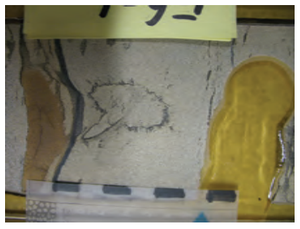

F06-01, 3222 m - Well sorted upper shoreface sands with *Ophiomorpha*

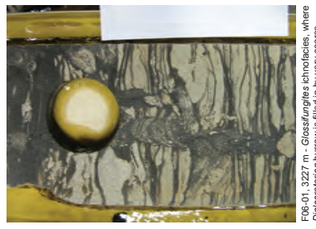

F06-01, 3227 m - *Glossifungites* ichnofacies, where *Diplocraterion barrowi* is filled in by very coarse material derived from the overlying sediment.

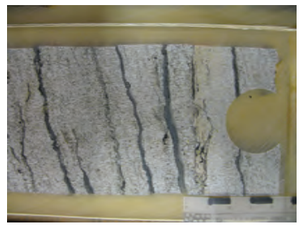

F06-01, 3239 m - Cross bedding with mud drapes deposited in a tidal channel

F06-01, 3260 m - Channel lag of a tidal channel consisting of rip-up mud clasts

F06-01, 3282m - Marine shaly sand overlain by lagoonal muds

F06-01, 3210-3217 m, Uppermost 8 m of the Lower Graben Fm. overlain by a thick coal layer of the Middle Graben Fm.

F06-01, 3225-3232 m, Lagoonal muds alternated with heterolithic tidal flat deposits.

F06-01, 3254-3260 m, Sand dominated tidal channel deposits with abundant (double) mud drapes, x-bedding, rip-up clasts.

F06-01, 3281-3288 m, Tidal channel deposits overlain by marine shales, which are in turn overlain by tidal, lagoonal muds. Boundaries are indicated by red lines.

F06-01, 3310-3316 m, Deltaic deposition: fresh to brackish, very quiet bay fill with occasional peat formation, occasional marine influence.

Interpretation

Fresh water environment: Lake and swamp deposits	
Callovian-Oxfordian boundary	
Storm sands	
Marine, shoreface	
Ravinement surface	
(sub) tidal shoal	
Subtidal brackish lagoon	
Tidal channel	
(sub) tidal shoal	
Subtidal brackish lagoon	
(sub) tidal shoal	
Tidal channel	
Tidal channel	
Tidal channel	
Swamps	
Subtidal brackish lagoon	
Tidal channel	
Marine incursion	
Tidal channel	
Subtidal brackish lagoon	
Deltaic: fresh to brackish, very quiet bay fill with occasional peat formation, occasional marine influence, and no tidal influence	

Core log

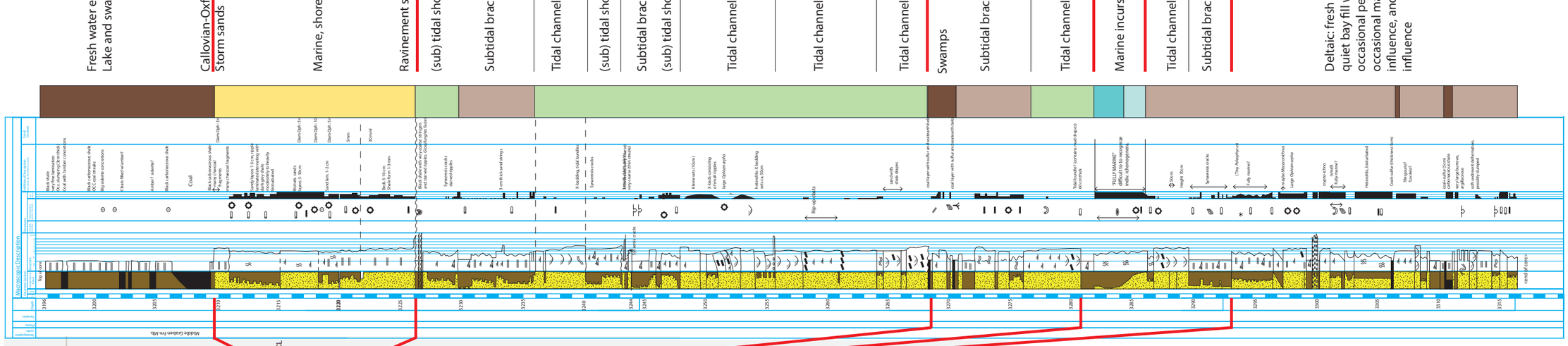

Well logs

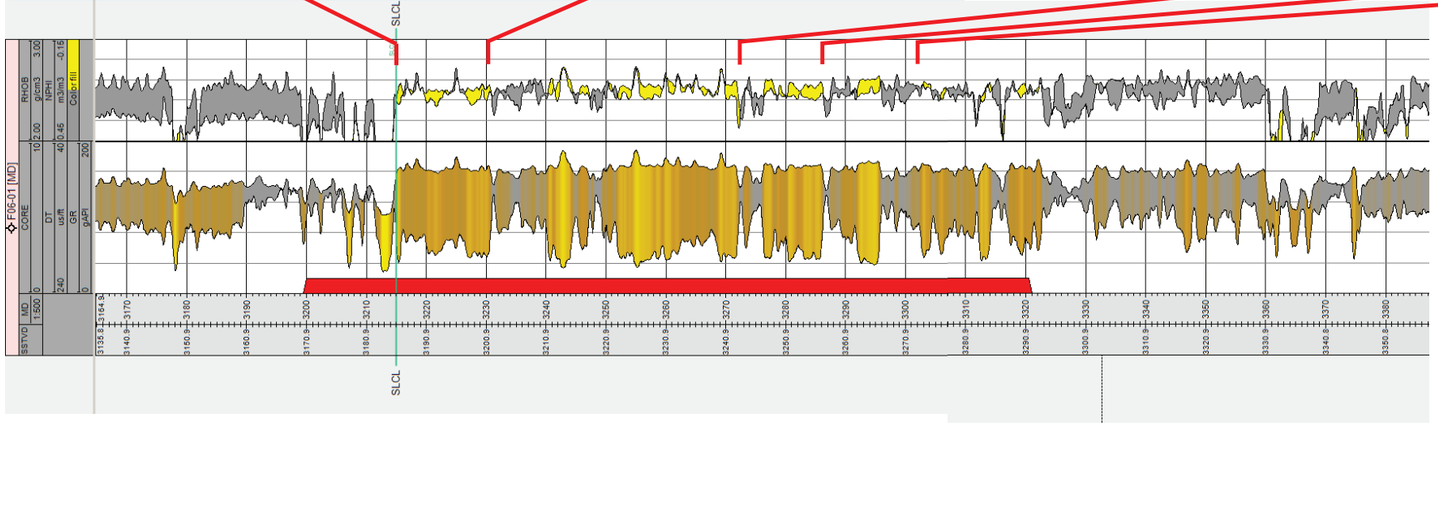

Note: core has been shifted 4 m down to match log depth

Facies Legend

- Open marine
- Lower shoreface
- Upper shoreface/foreshore/beach
- Estuarine/tidal shoal/tidal channel
- Brackish lagoon/bay
- Swamp

Appendix A1.4 - F14-05 Lower Graben Fm

TNO innovation for life

Well logs

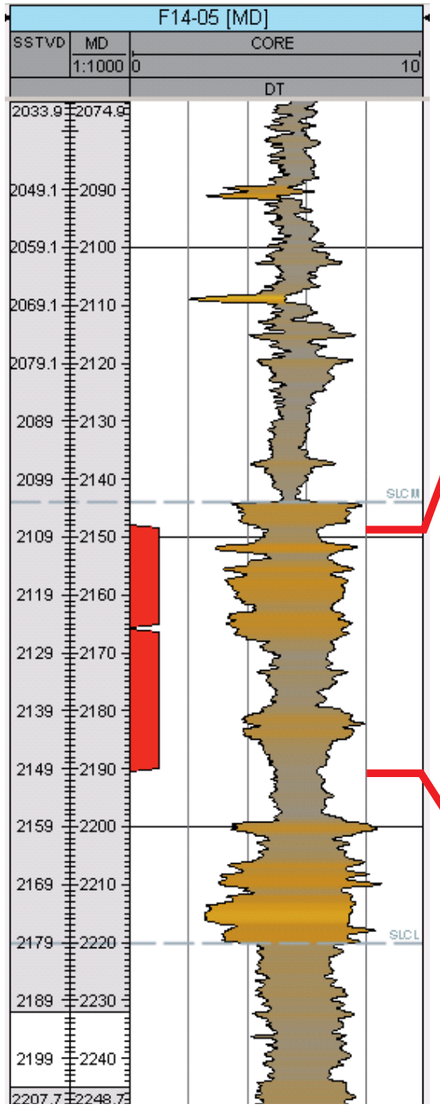

Sedimentary log

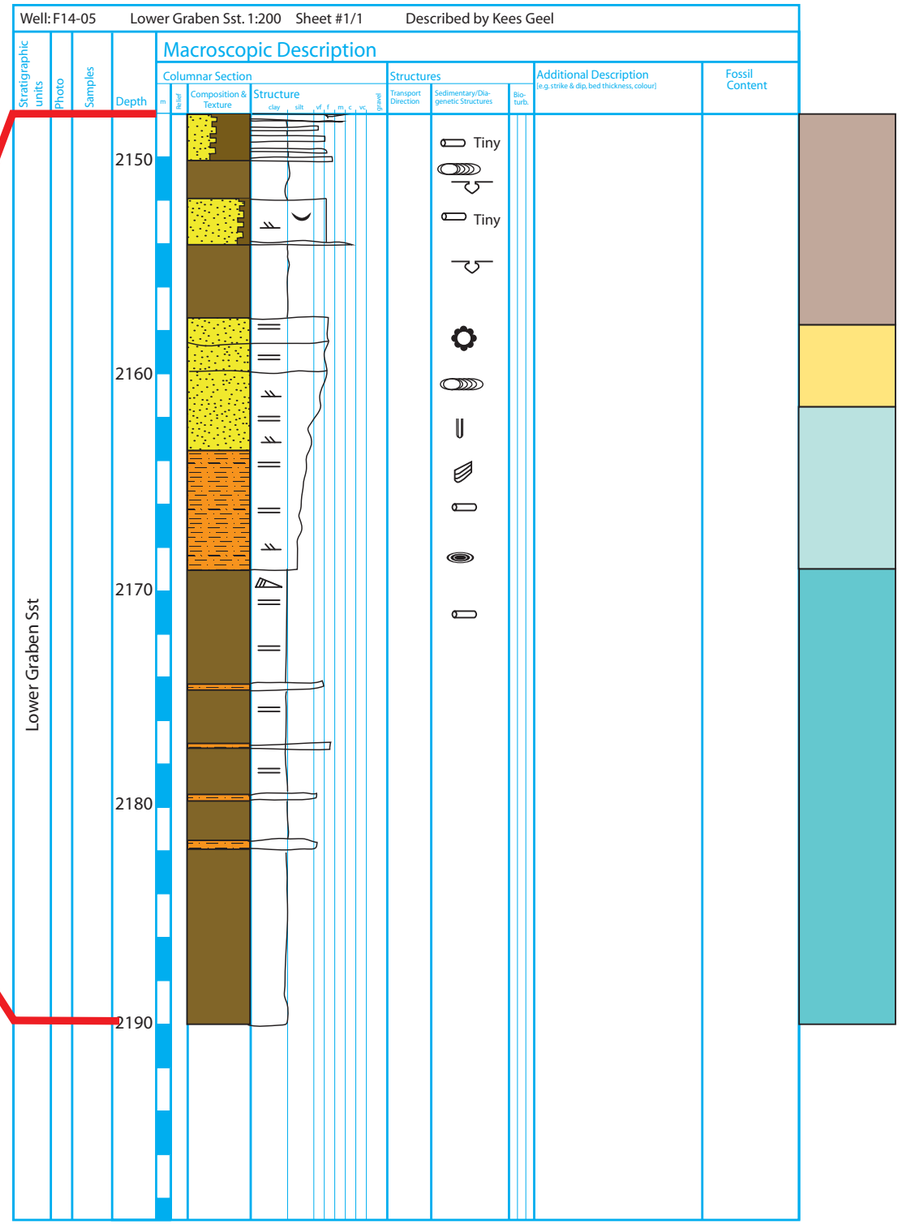

Interpretation

Subtidal Lagoon

Upper shoreface

Lower shoreface

Offshore

Facies Legend

- Open marine
- Lower shoreface
- Upper shoreface/foreshore/beach
- Estuarine/tidal shoal/tidal channel
- Brackish lagoon/bay
- Swamp

Appendix A1.5 - F17-09 Lower Graben Fm

TNO innovation for life

Well logs

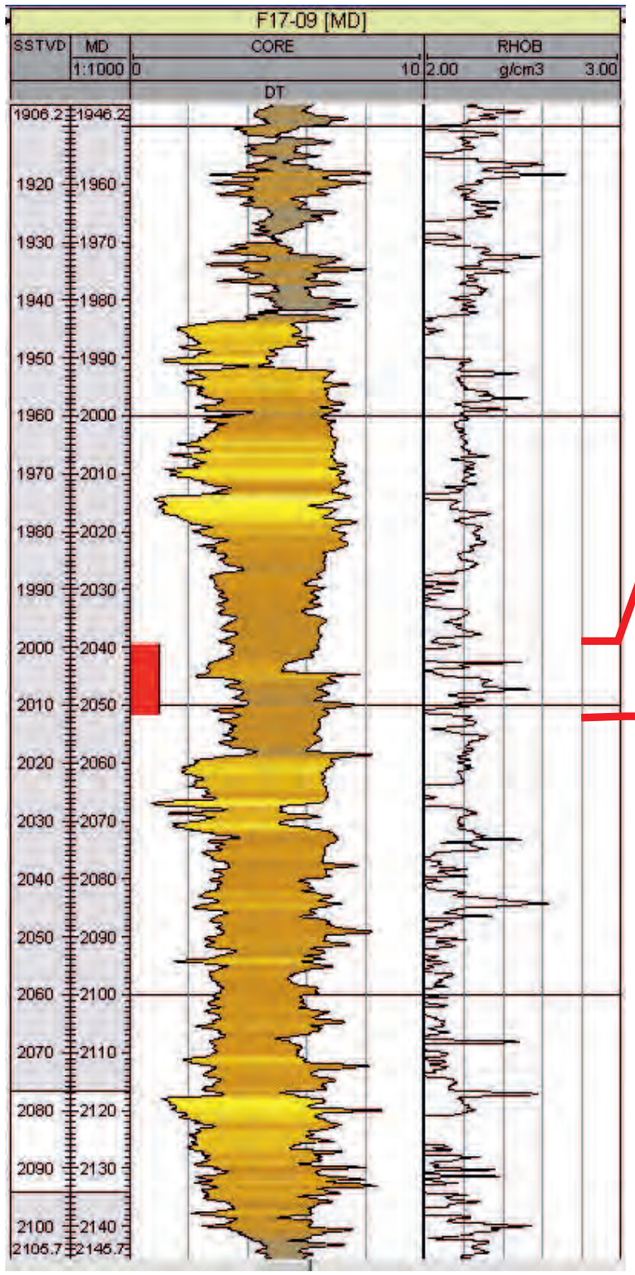

Sedimentary log

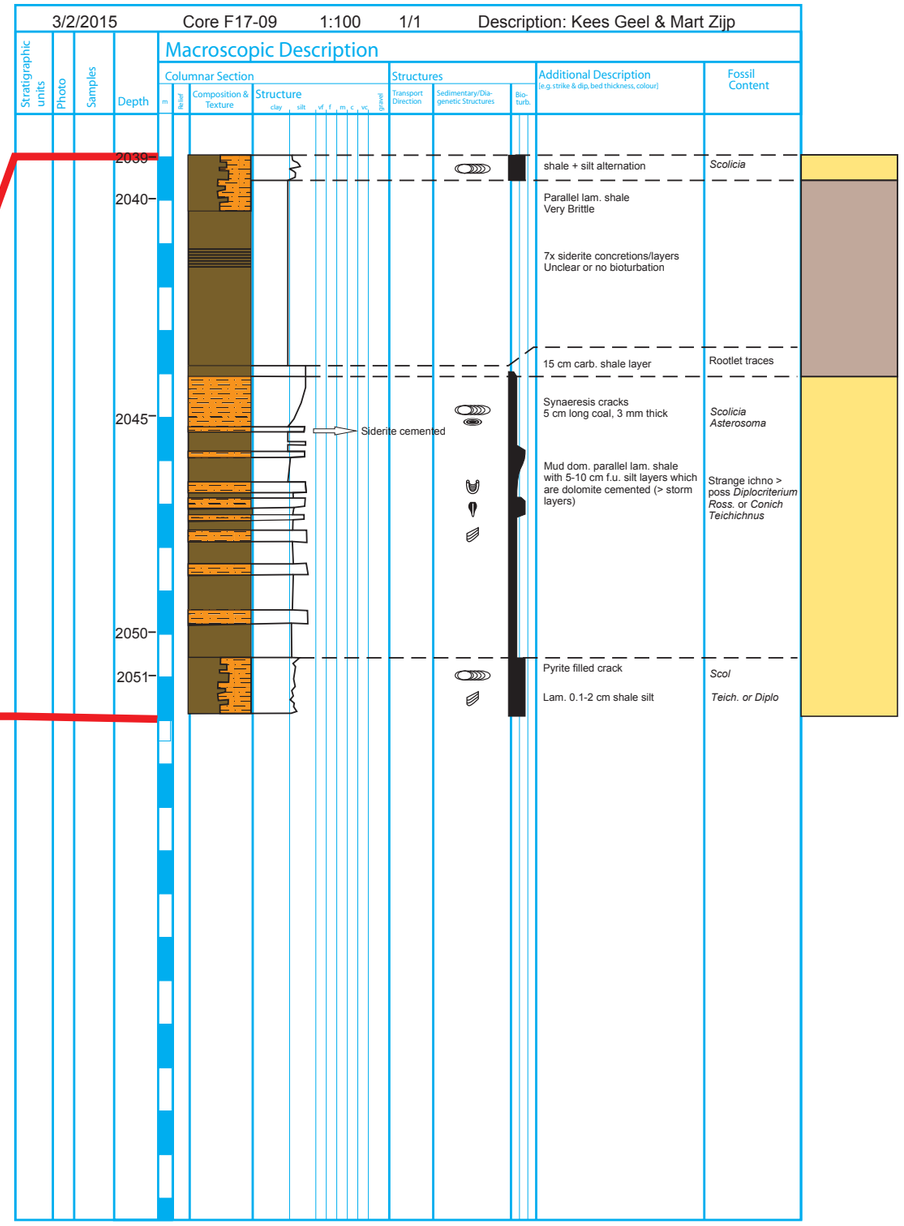

Interpretation

Upper shoreface

Subtidal Lagoon

Upper shoreface

Appendix A1.6 - L05-05 Friese Front Fm

TNO innovation for life

Well logs

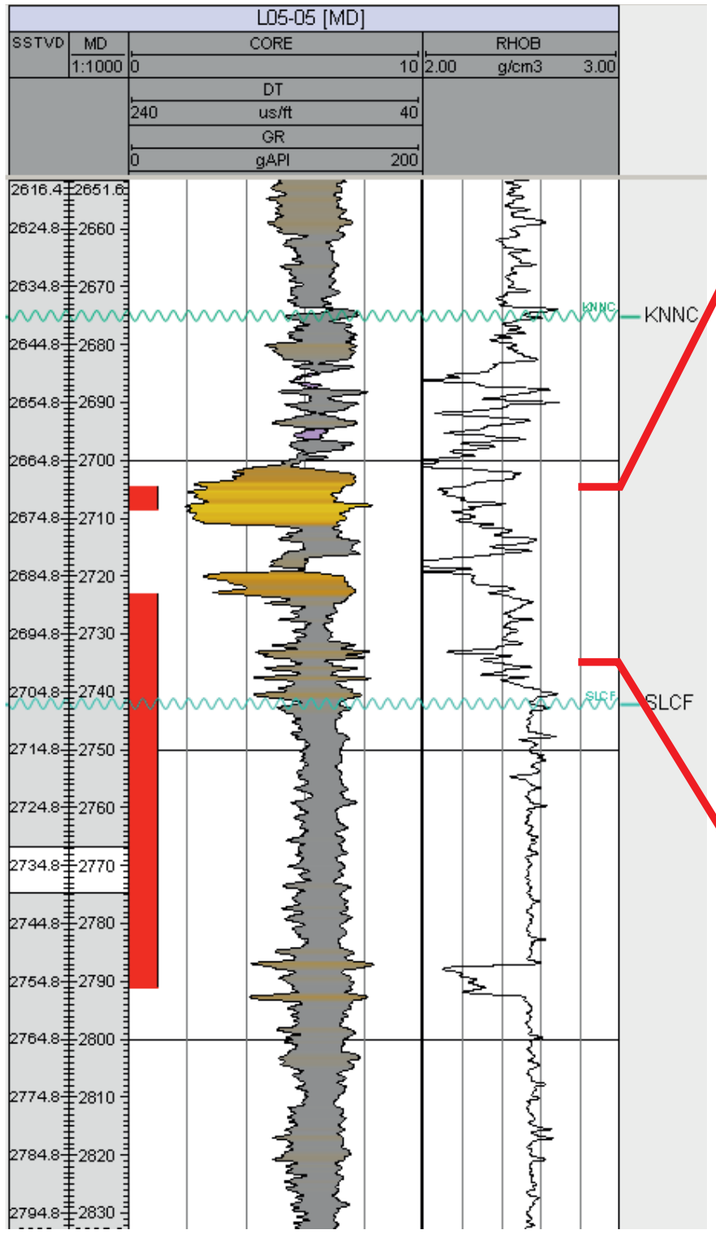

Sedimentary log

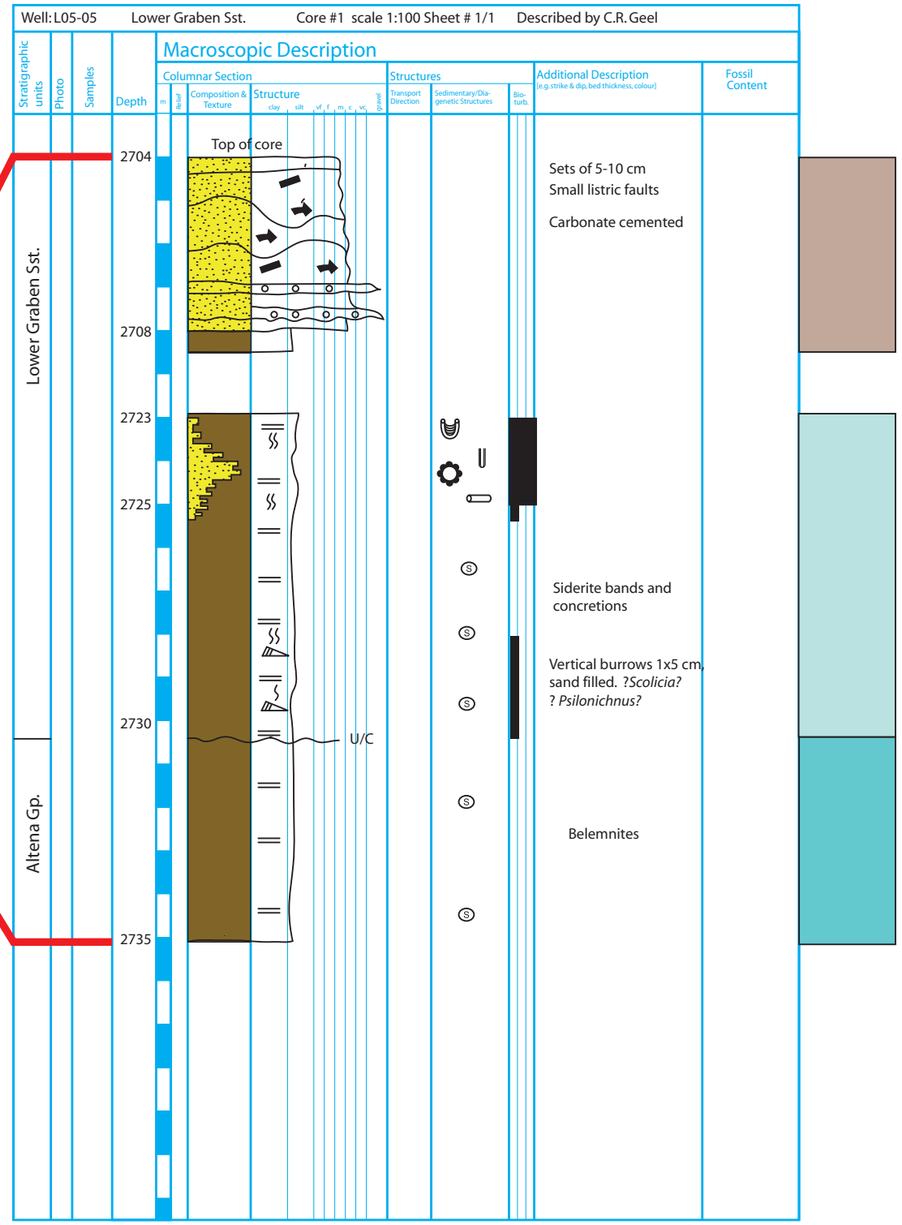

Interpretation

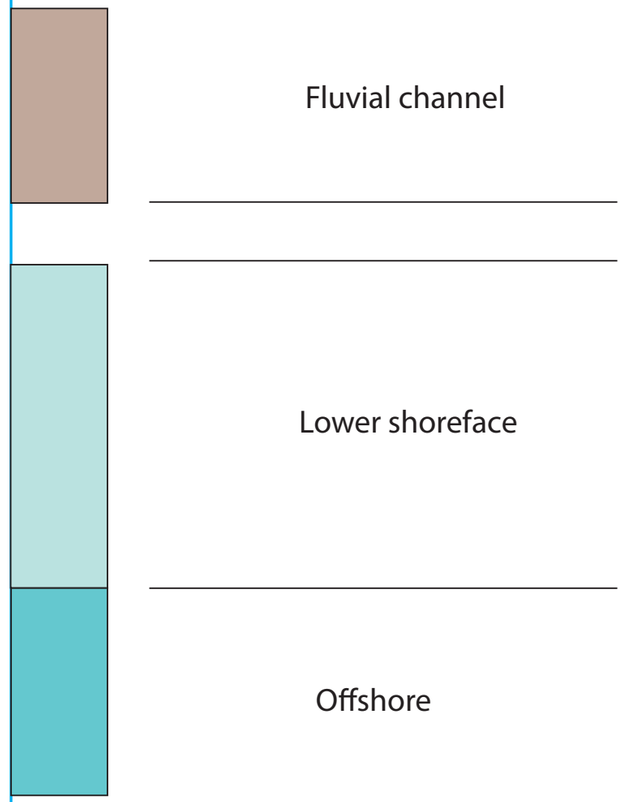

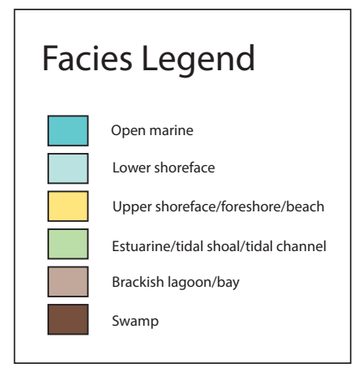

Appendix A1.7 - L06-02 Terschelling Sst

Well logs

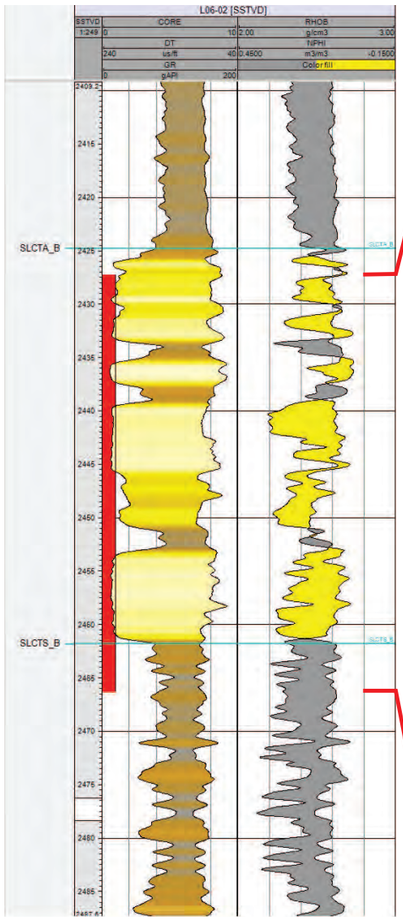

Sedimentary log

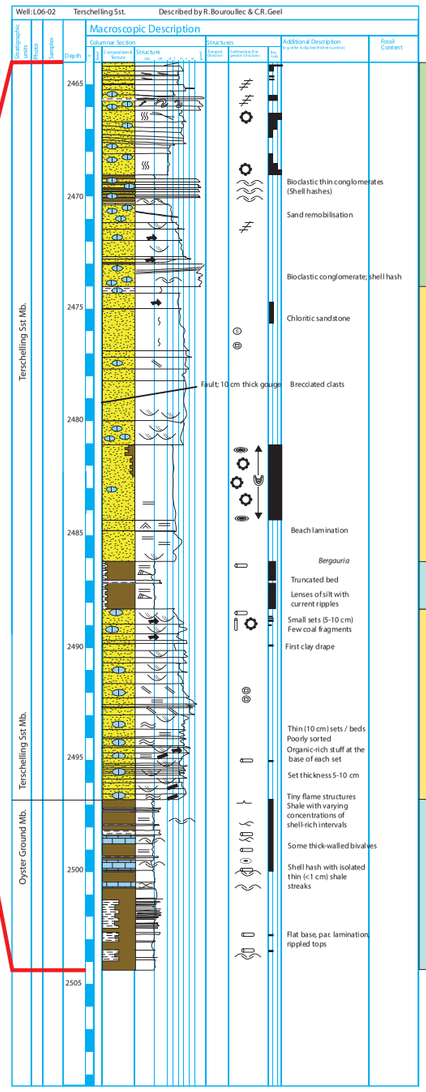

Interpretation

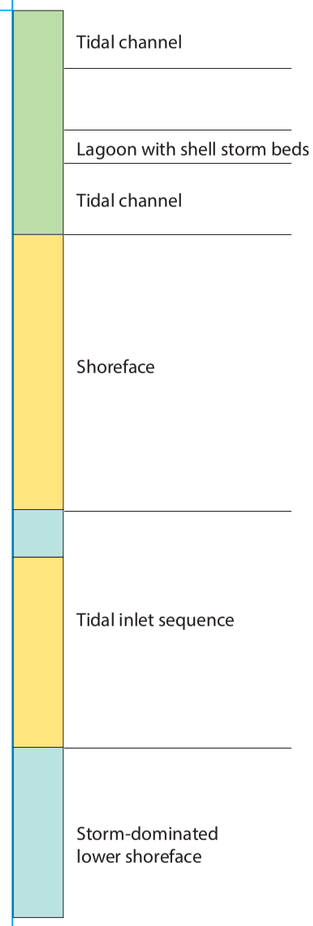

Core photos

2466 m. Hash of thick-walled bivalves deposited as cross beds

2484.5 m. Upper shoreface sands with abundant *Diplocraterion* and *Asterosoma*

2488 m. Bioturbated marine mudstones, forming the top of tidal inlet sequence

2495 m. Poorly sorted, coarse-grained crossbedded sands interpreted as tidal inlet deposits.

2464-2468 m. Cross-bedded sands, partly calcite-cemented overlying an Ophiomorpha-dominated structureless sandstone. Sequence is interpreted as a tidal channel. Note the abundant fractures and faults.

2469-2470 m. Alternation of shell-hash beds and shale layers. Lagoonal muds with washover fans.

2472-2474 m. Cross-beds rich in shell hash, and tidal bundles with mud drapes .

2481-2486 m. Upper shoreface sediments: parallel, low-angle beach lamination overlain by *Skolithos* ichnofacies with abundant *Ophiomorpha* and *Diplocraterion*.

2481-2486 m. At the right: contact between the offshore/lower shoreface muds of the Oyster Ground Mb and the overlying calcite-cemented Terschelling Sst. The Terschelling Sst has abundant coal rip-up clasts, cross-bedding, and is interpreted as a tidal inlet sequence.

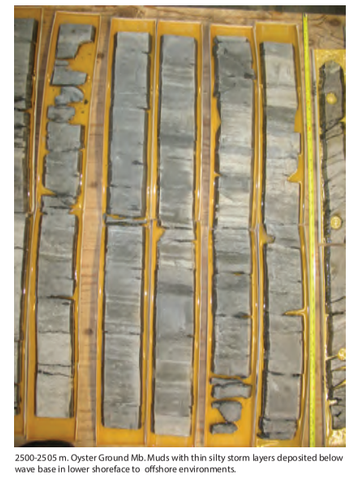

2500-2505 m. Oyster Ground Mb. Muds with thin silty storm layers deposited below wave base in lower shoreface to offshore environments.

Facies Legend

- Open marine
- Lower shoreface
- Upper shoreface/foreshore/beach
- Estuarine/tidal shoal/tidal channel
- Brackish lagoon/bay
- Swamp

TNO innovation for life

Appendix A1.8 - L06-03 Terschelling Sst

TNO innovation for life

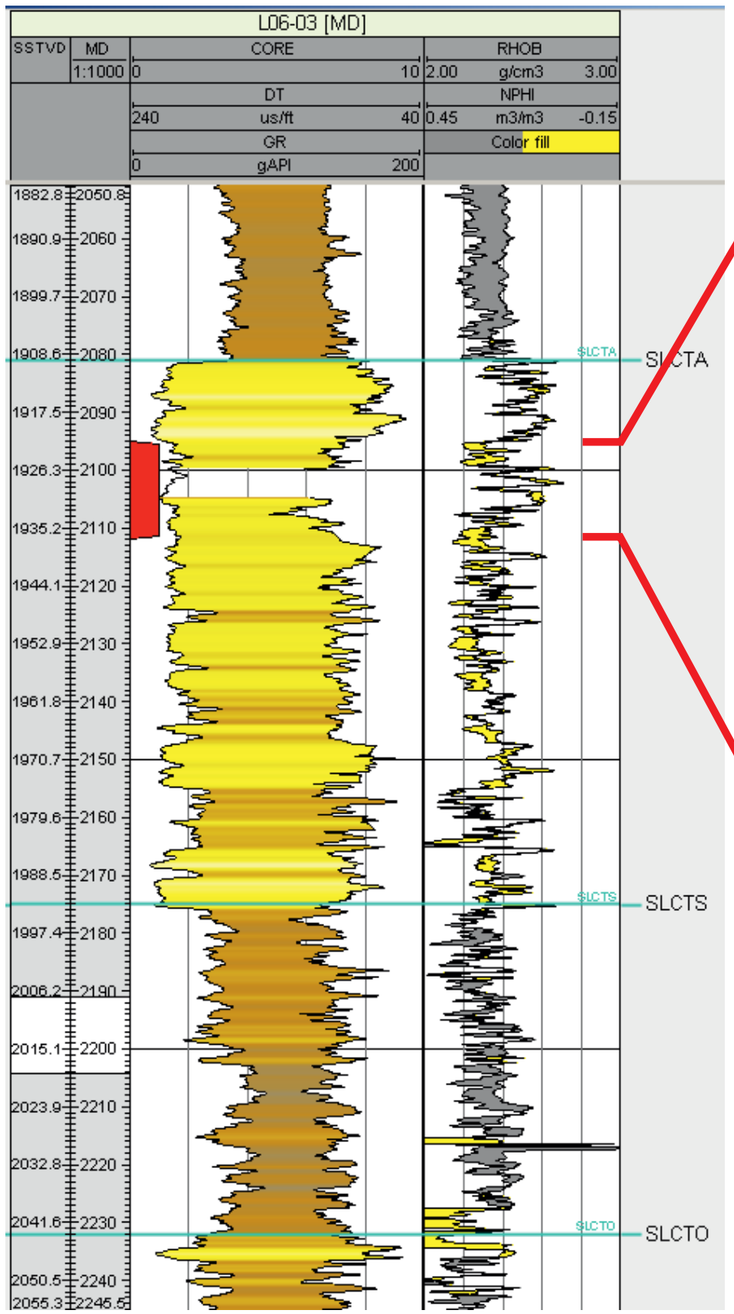

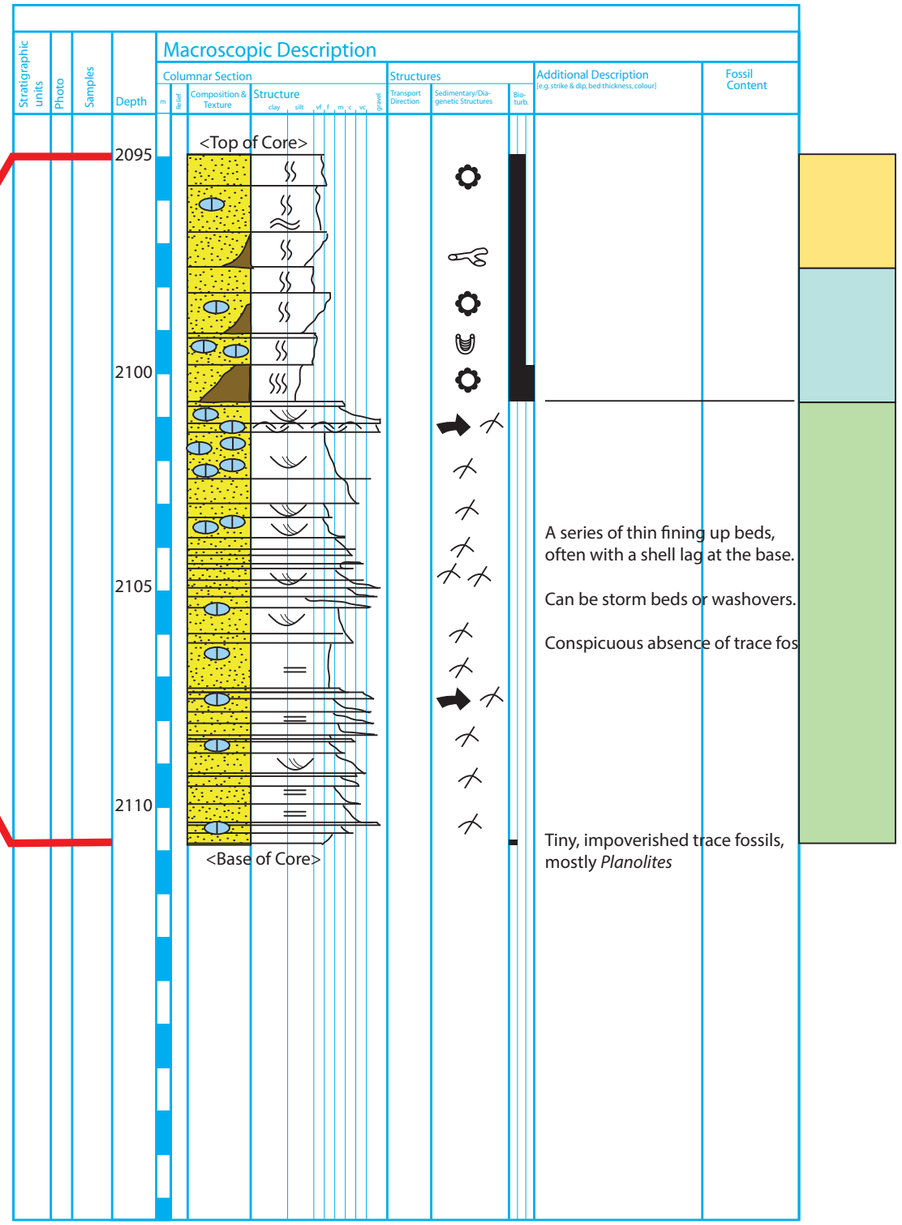

Upper shoreface

Lower shoreface

Ravinement surface

Back-barrier washover fans

Facies Legend

- Open marine
- Lower shoreface
- Upper shoreface/foreshore/beach
- Estuarine/tidal shoal/tidal channel
- Brackish lagoon/bay
- Swamp

Appendix A1.9 - M01-01 Terschelling Sst

TNO innovation for life

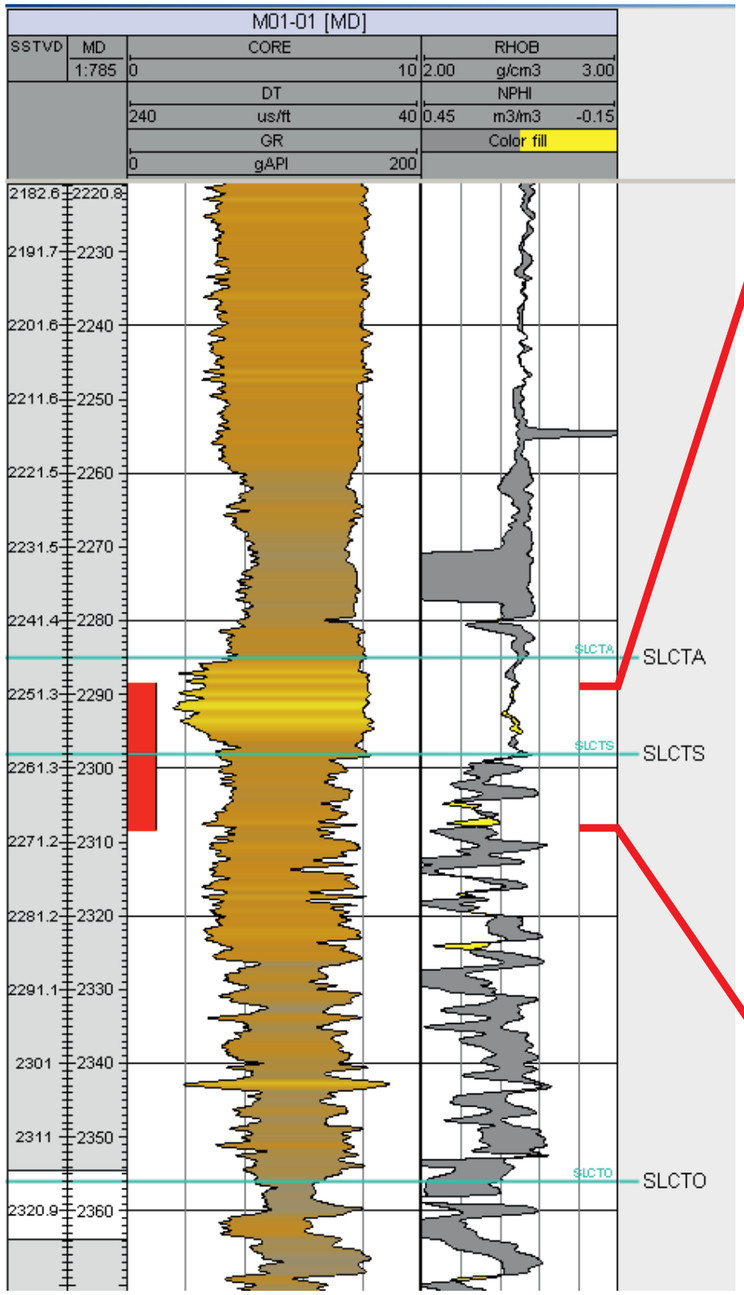

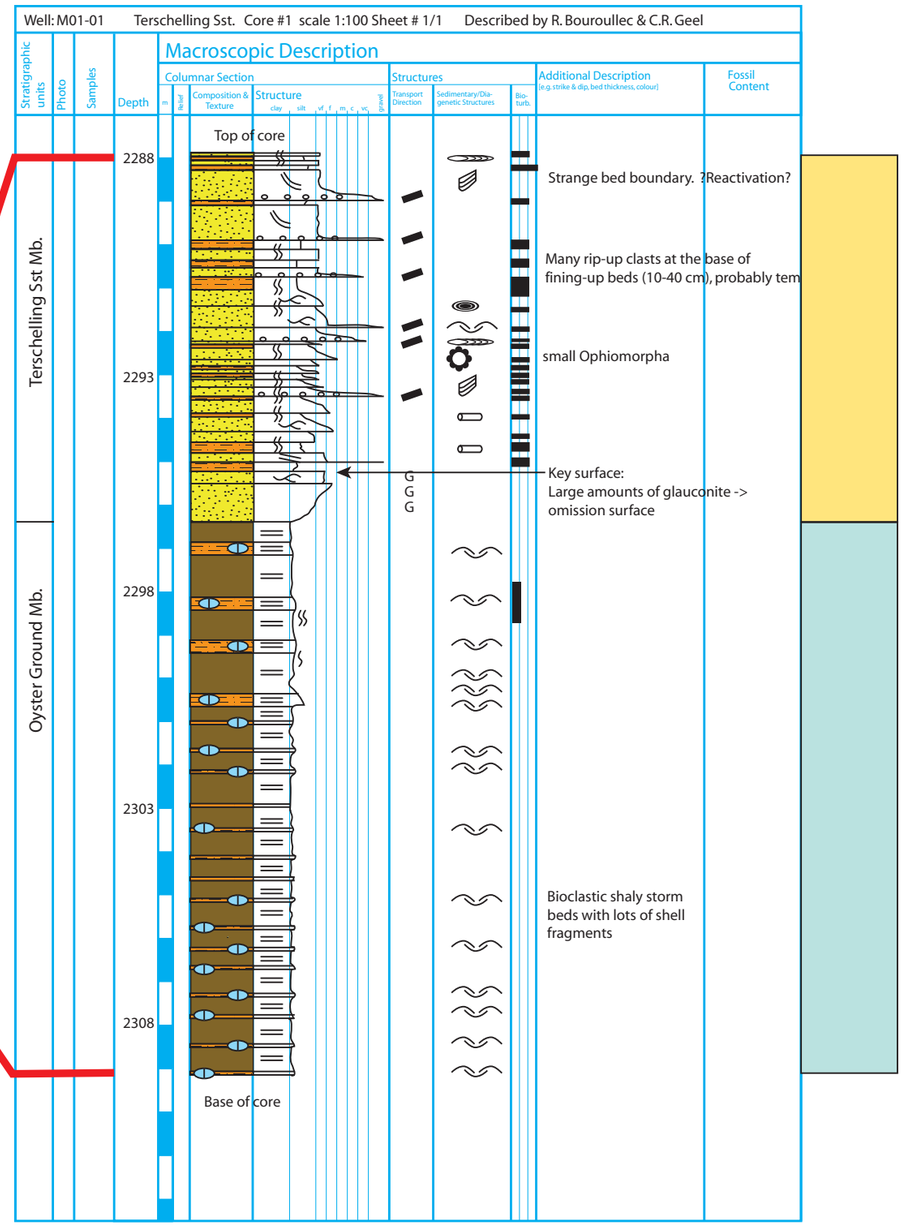

Upper shoreface

Lower shoreface

Facies Legend

- Open marine
- Lower shoreface
- Upper shoreface/foreshore/beach
- Estuarine/tidal shoal/tidal channel
- Brackish lagoon/bay
- Swamp

Appendix A1.10 - L06-02 Scruff Greensand

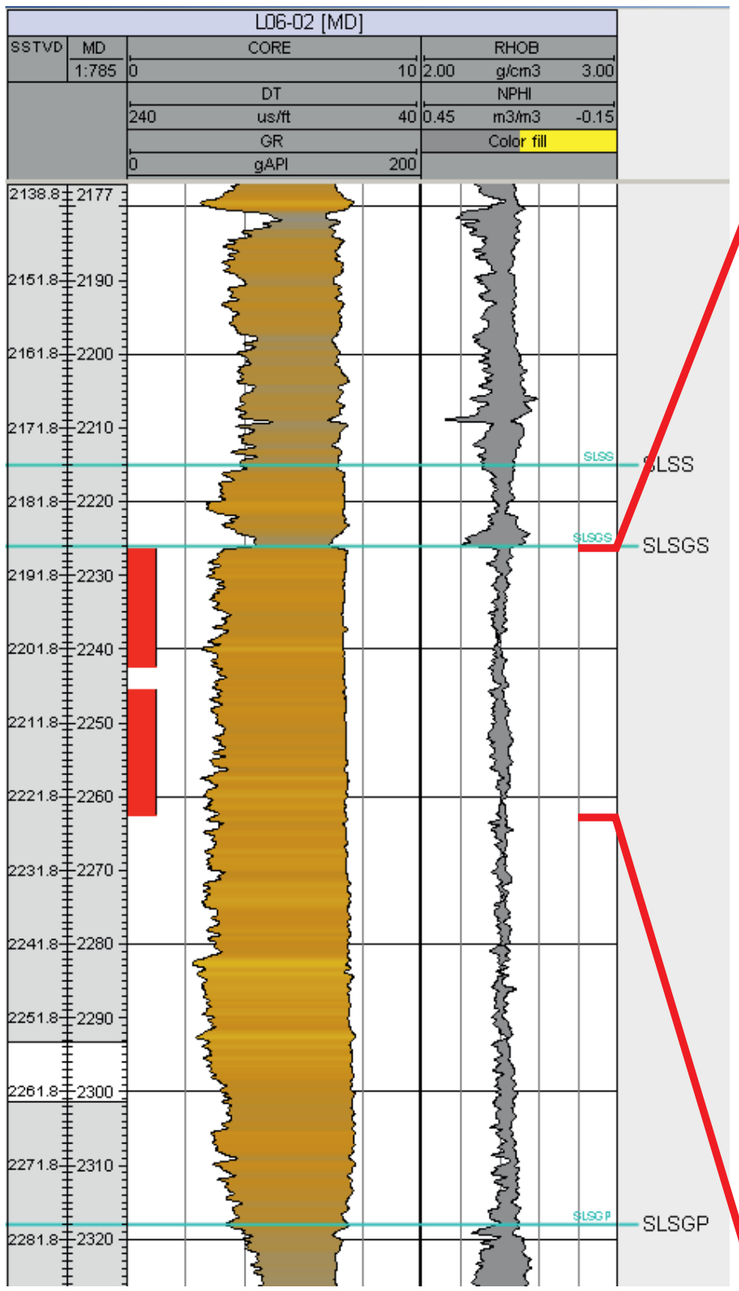

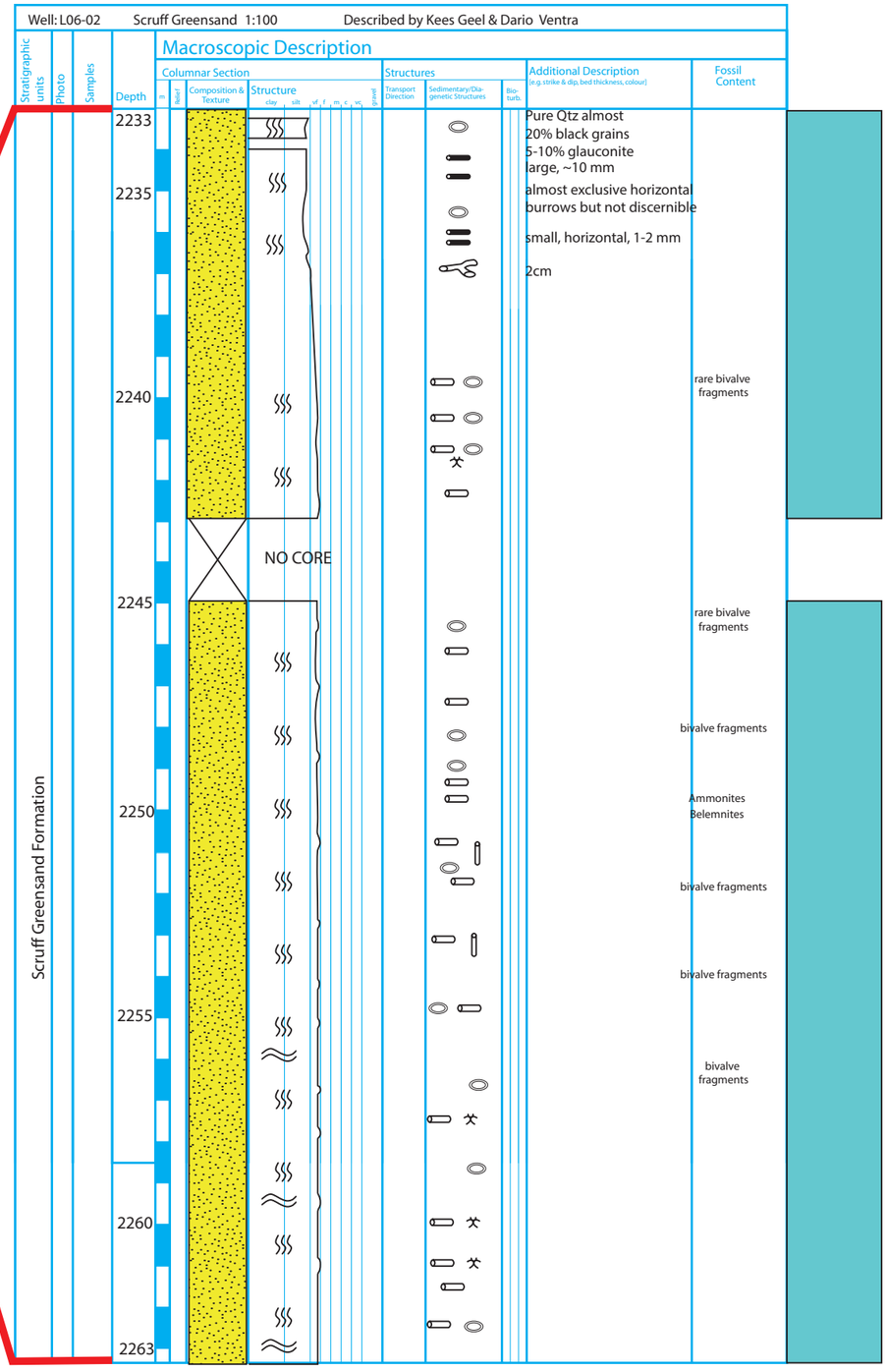

Offshore lower shoreface succession, below wave base

Facies Legend

- Open marine
- Lower shoreface
- Upper shoreface/foreshore/beach
- Estuarine/tidal shoal/tidal channel
- Brackish lagoon/bay
- Swamp

Appendix A1.11 - F15-A-01 Scruff Greensand

TNO innovation for life

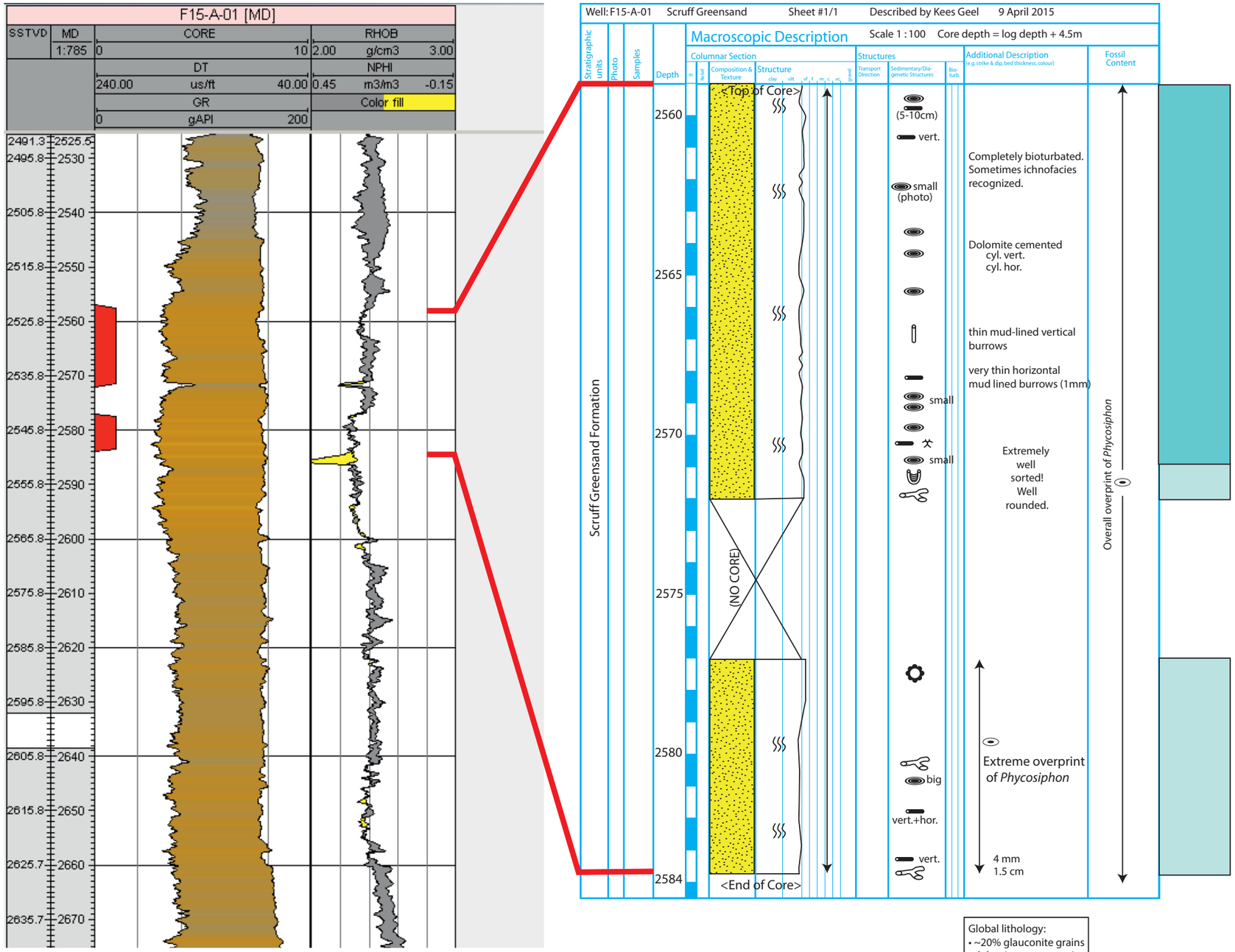

Open marine

Lower shoreface

Facies Legend

- Open marine
- Lower shoreface
- Upper shoreface/foreshore/beach
- Estuarine/tidal shoal/tidal channel
- Brackish lagoon/bay
- Swamp

Appendix A1.12 - M07-07 Scruff Greensand

TNO innovation for life

Sedimentary log

Interpretation

Lower shoreface | Offshore | Lower shoreface

Well logs

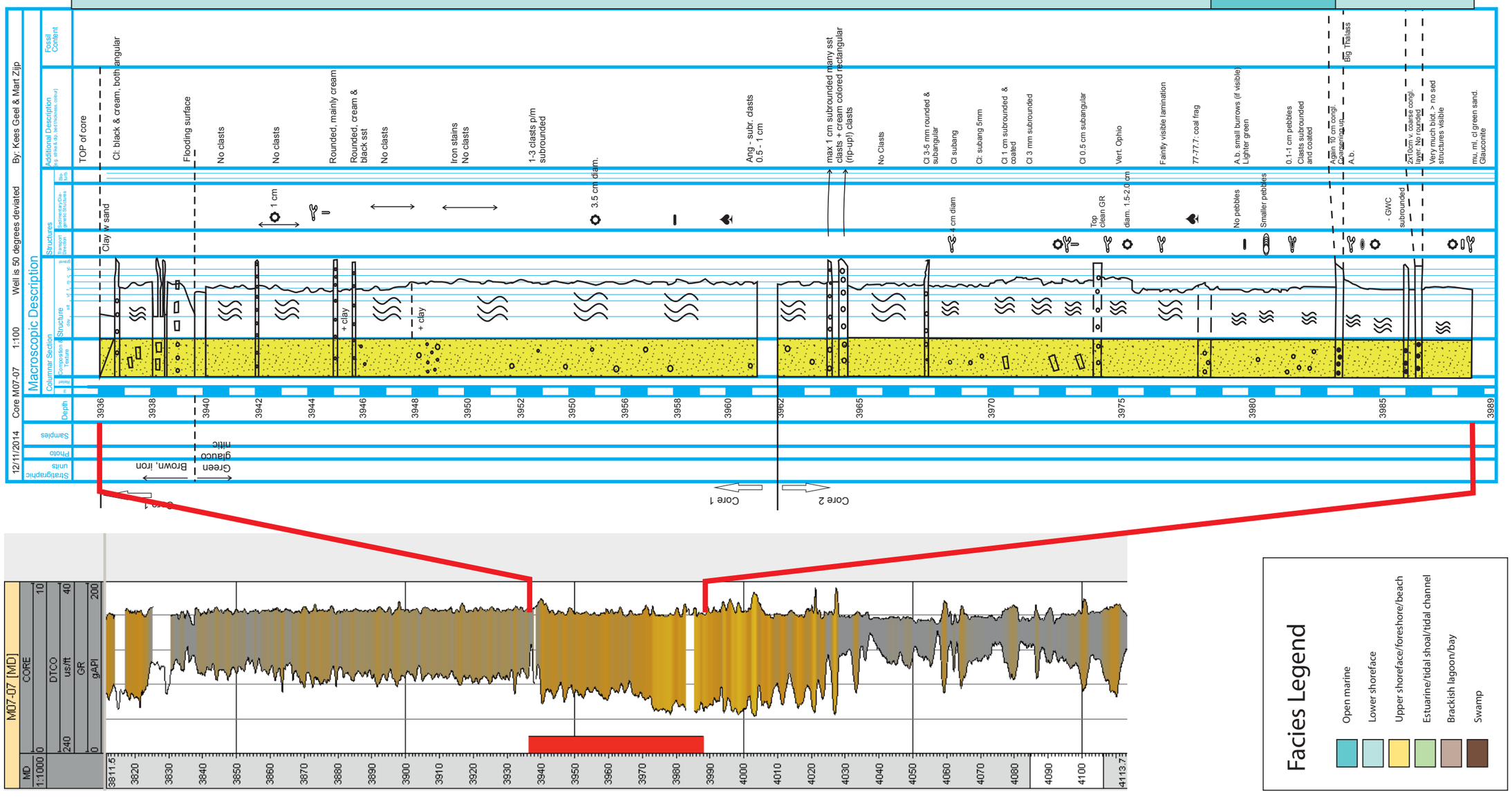

Facies Legend

- Open marine
- Lower shoreface
- Upper shoreface/foreshore/beach
- Estuarine/tidal shoal/tidal channel
- Brackish lagoon/bay
- Swamp

Appendix A1.13 - M07-08 Scruff Greensand

TNO innovation for life

Interpretation

Lower shoreface

Offshore

Lower shoreface

Offshore

Sedimentary log

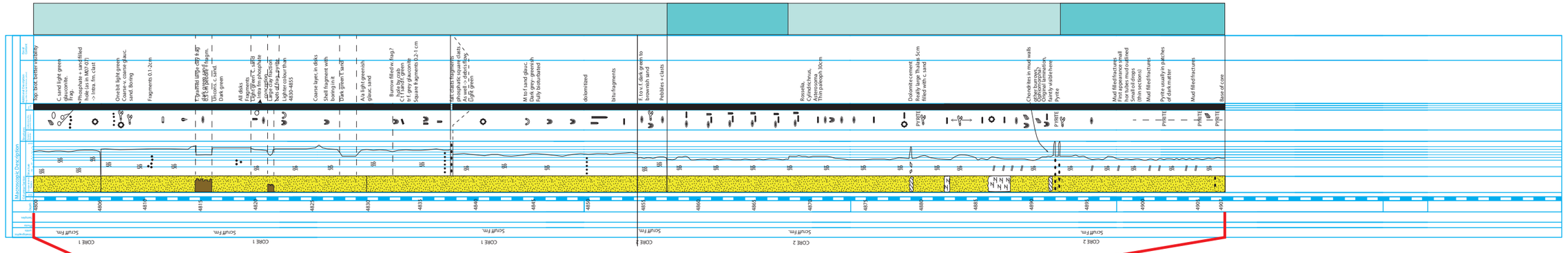

Well logs

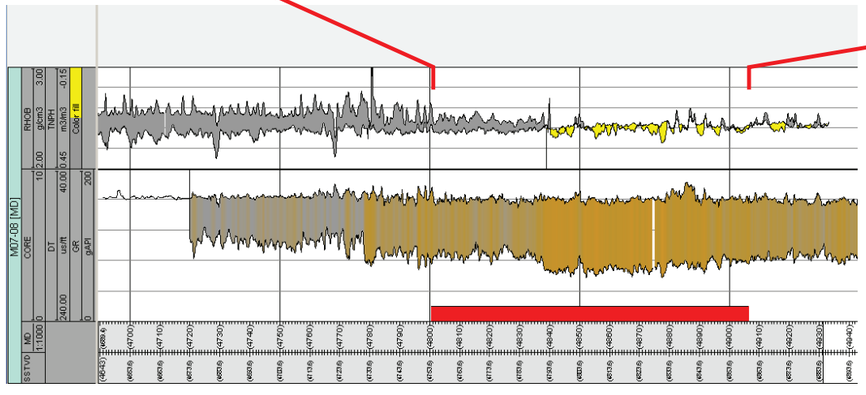

Facies Legend

- Open marine
- Lower shoreface
- Upper shoreface/foreshore/beach
- Estuarine/tidal shoal/tidal channel
- Brackish lagoon/bay
- Swamp

APPENDIX A2
PALYNOLOGY

Appendix A2 - Palynology

TNO innovation for life

Dinoflagellate cysts distribution chart of the cored Lower Graben interval from well F03-05-S1

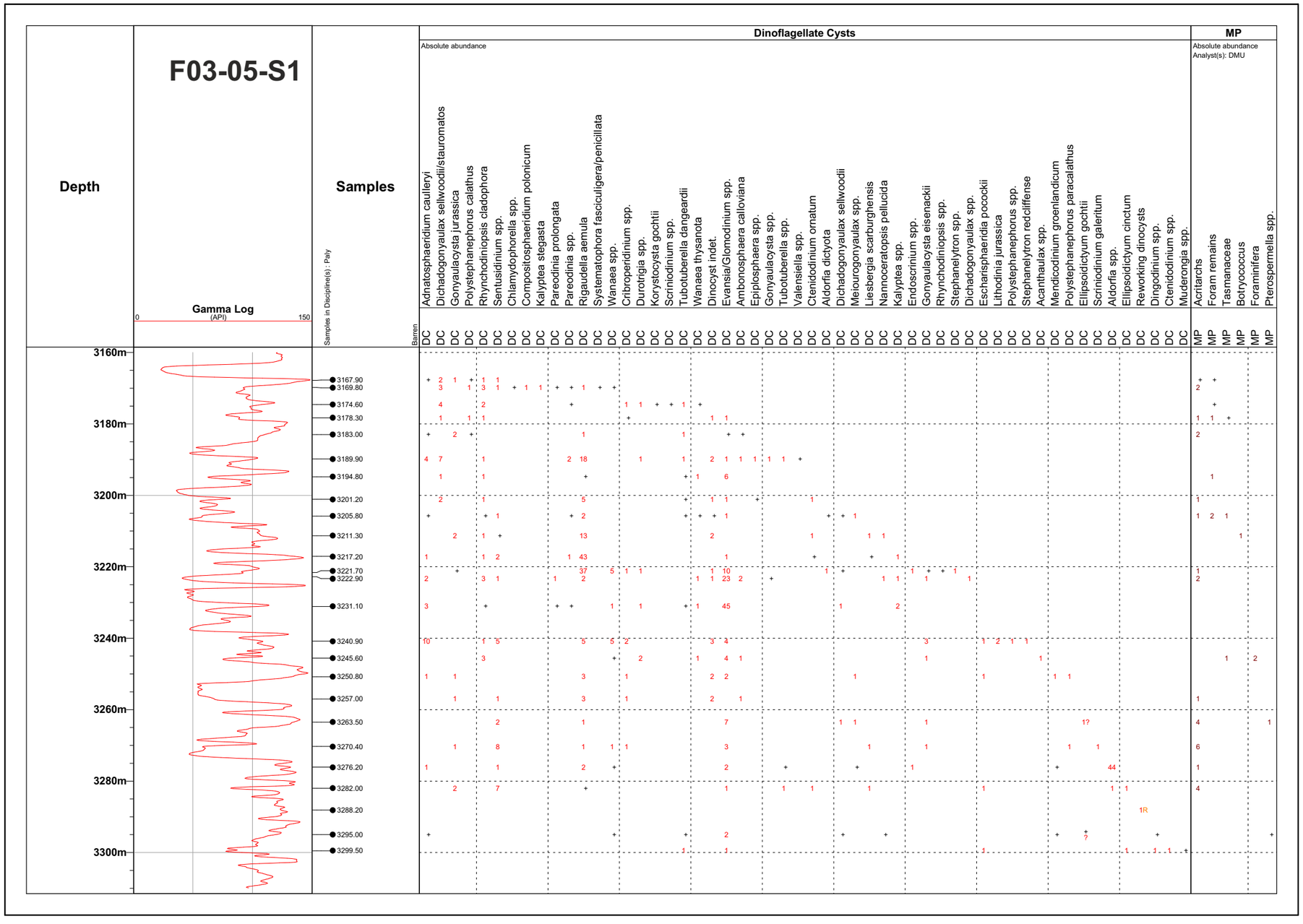

Appendix A2 - Palynology

TNO innovation for life

Pollen and spore distribution chart of the cored Lower Graben interval from well F03-05-S1

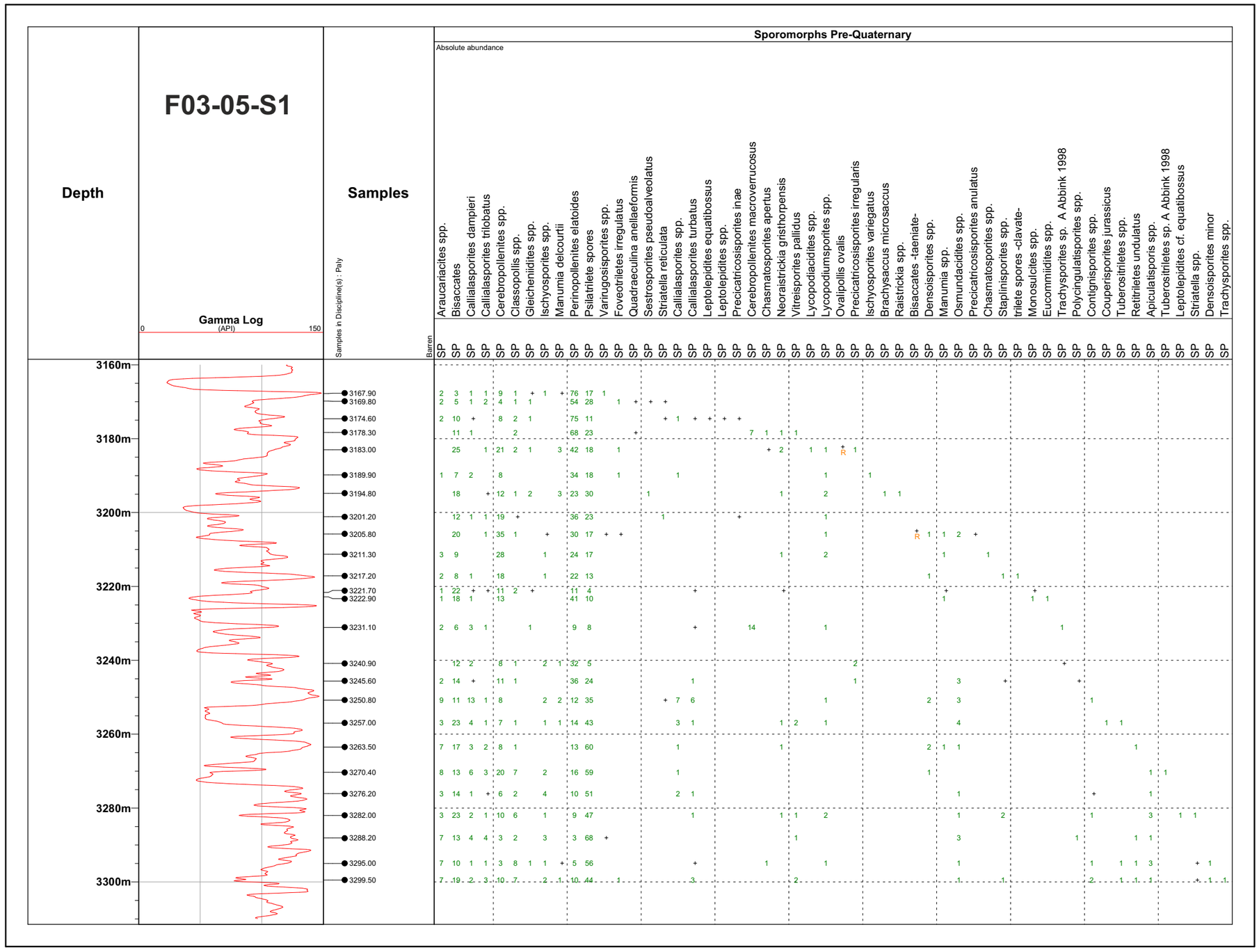

Appendix A2 - Palynology

TNO innovation for life

Dinoflagellate cyst distribution chart of the cored Lower Graben interval from well F06-01

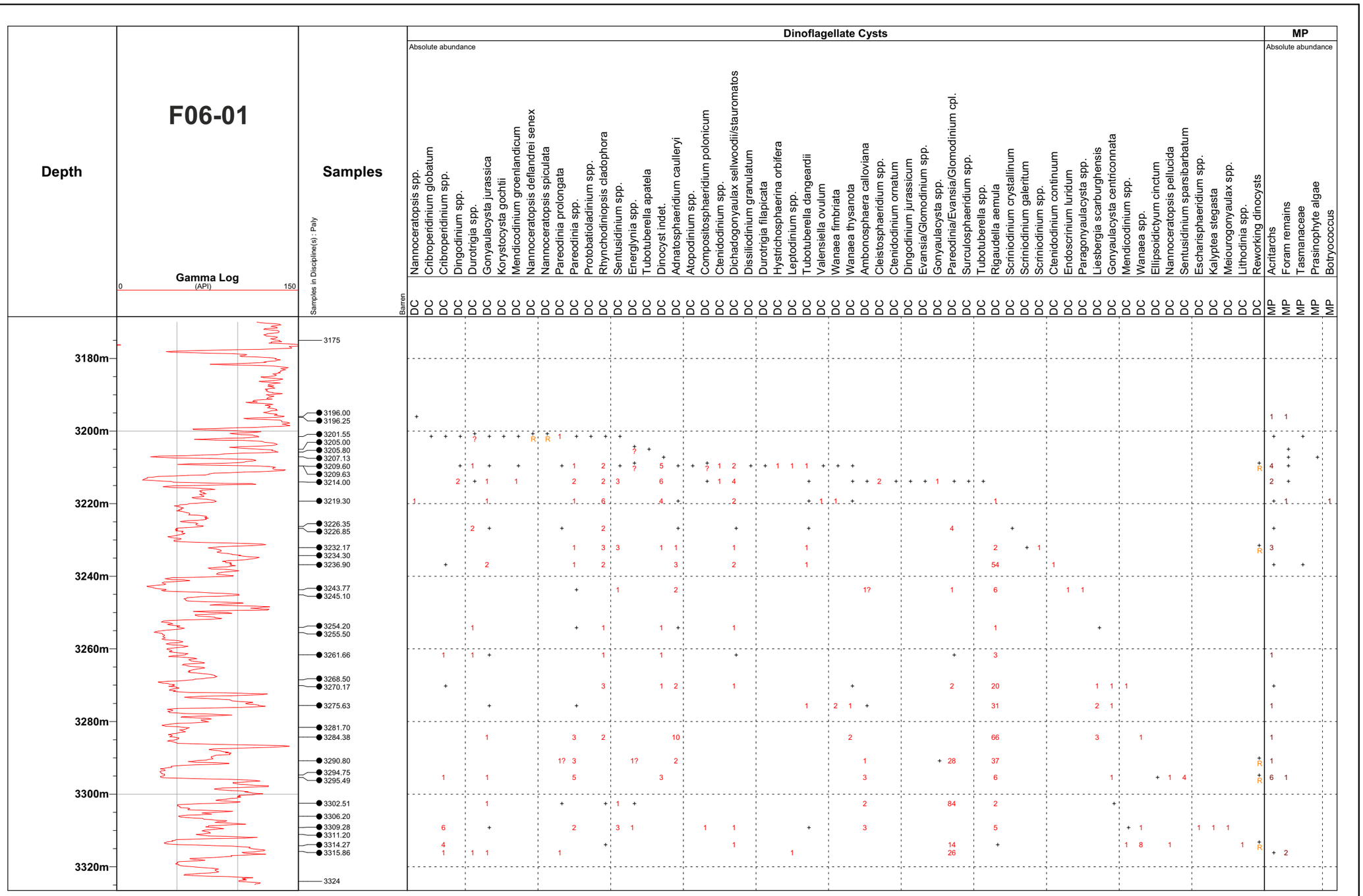

Appendix A2 - Palynology

TNO innovation for life

Pollen and spore distribution chart of the cored Lower Graben interval from well F06-01

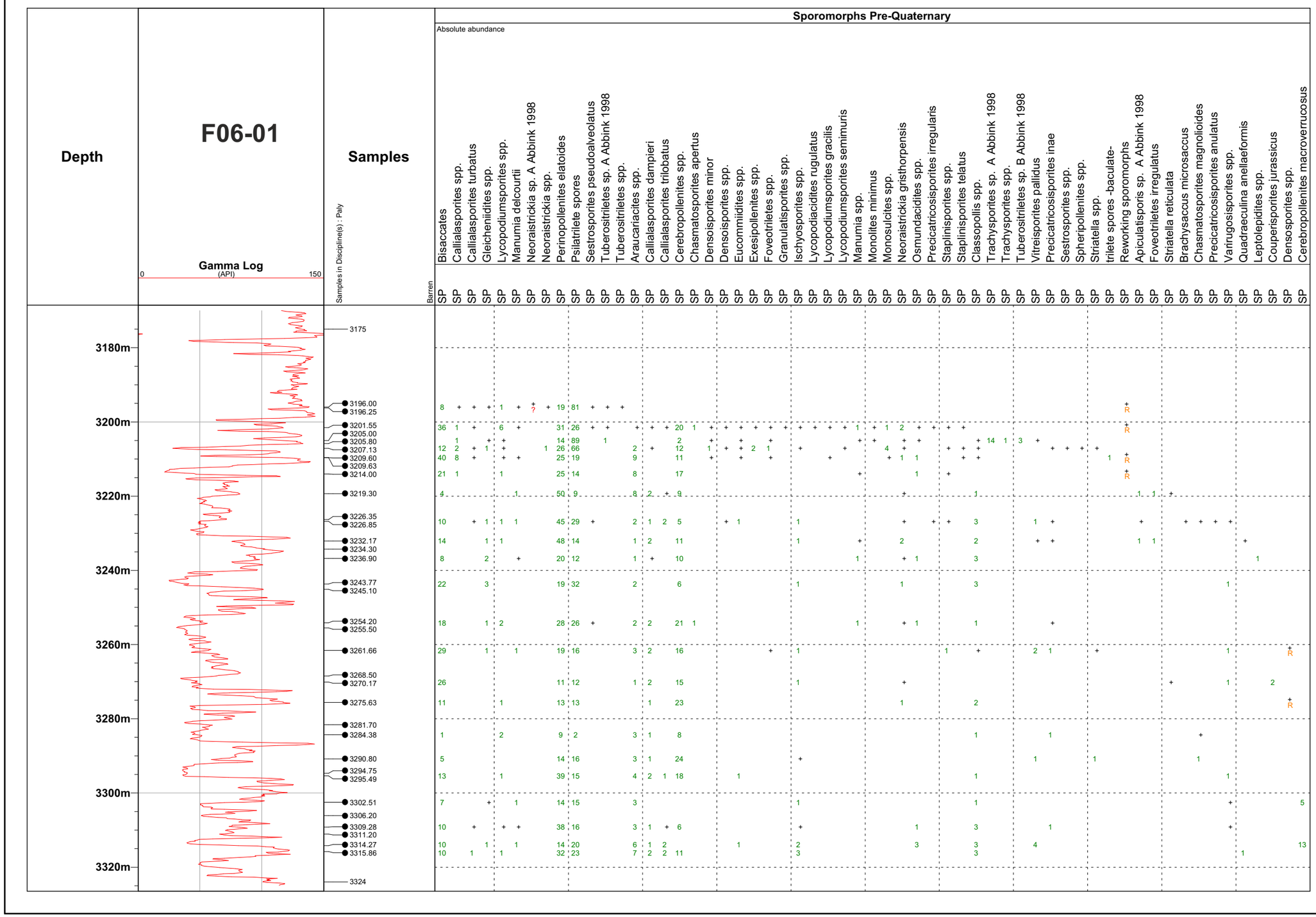

Appendix A2 - Palynology

TNO innovation for life

Dinoflagellate cyst distribution chart of the cored Lower Graben interval from well F14-05

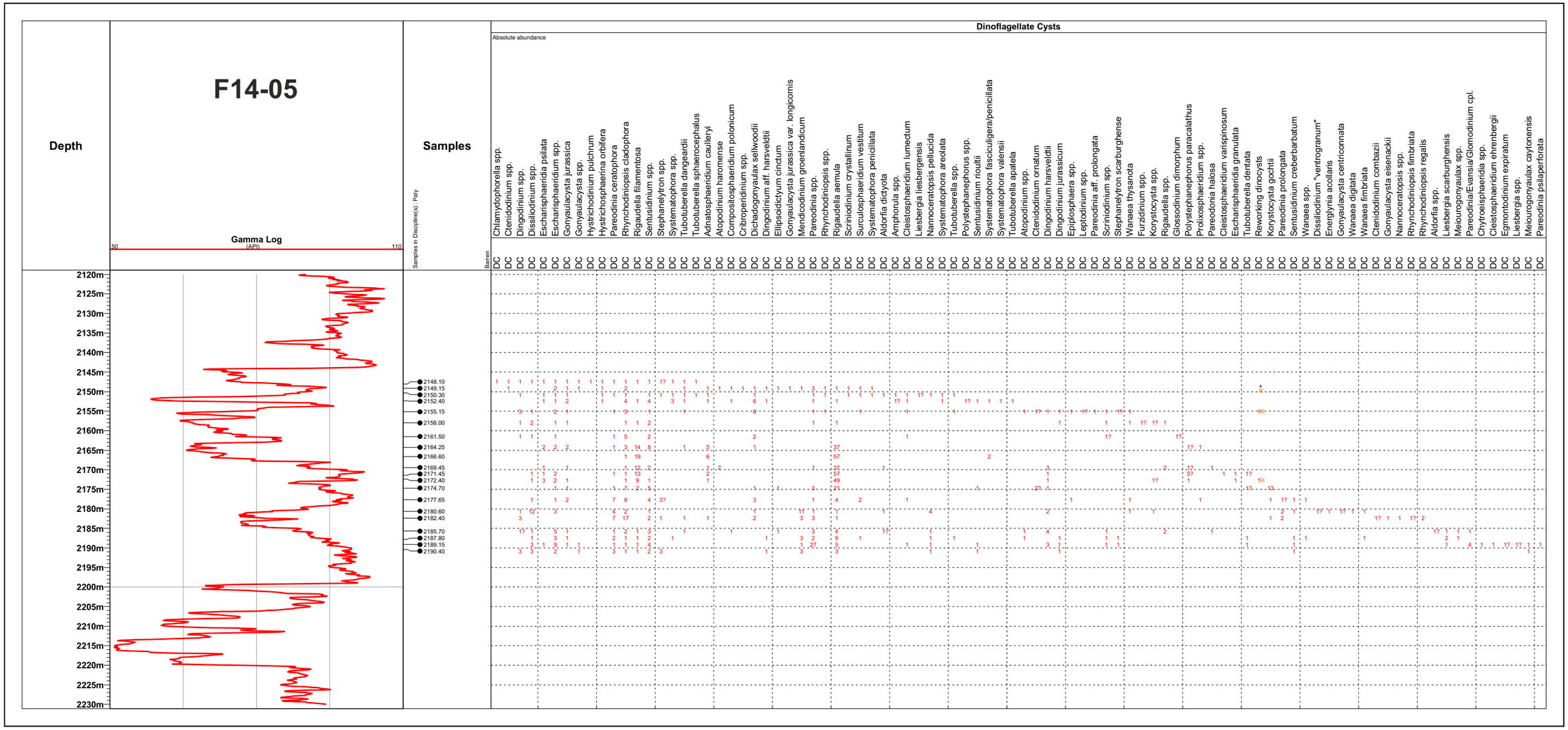

Appendix A2 - Palynology

TNO innovation for life

Pollen and spore distribution chart of the cored Lower Graben interval from well F14-05

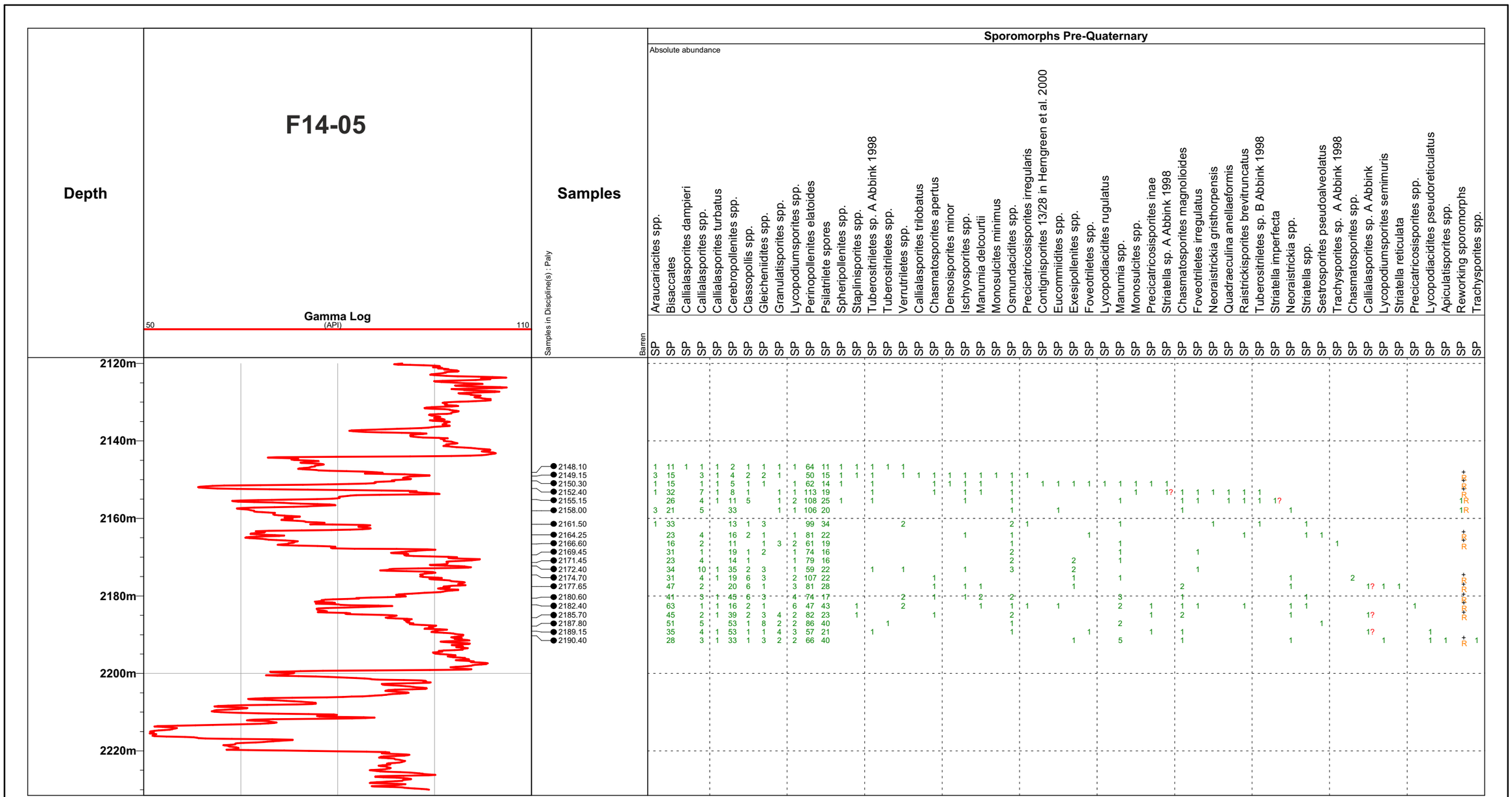

Appendix A2 - Palynology

TNO innovation for life

Dinoflagellate cyst distribution chart of the cored Scruff Greensand interval from well F15-A-01 (F15-04)

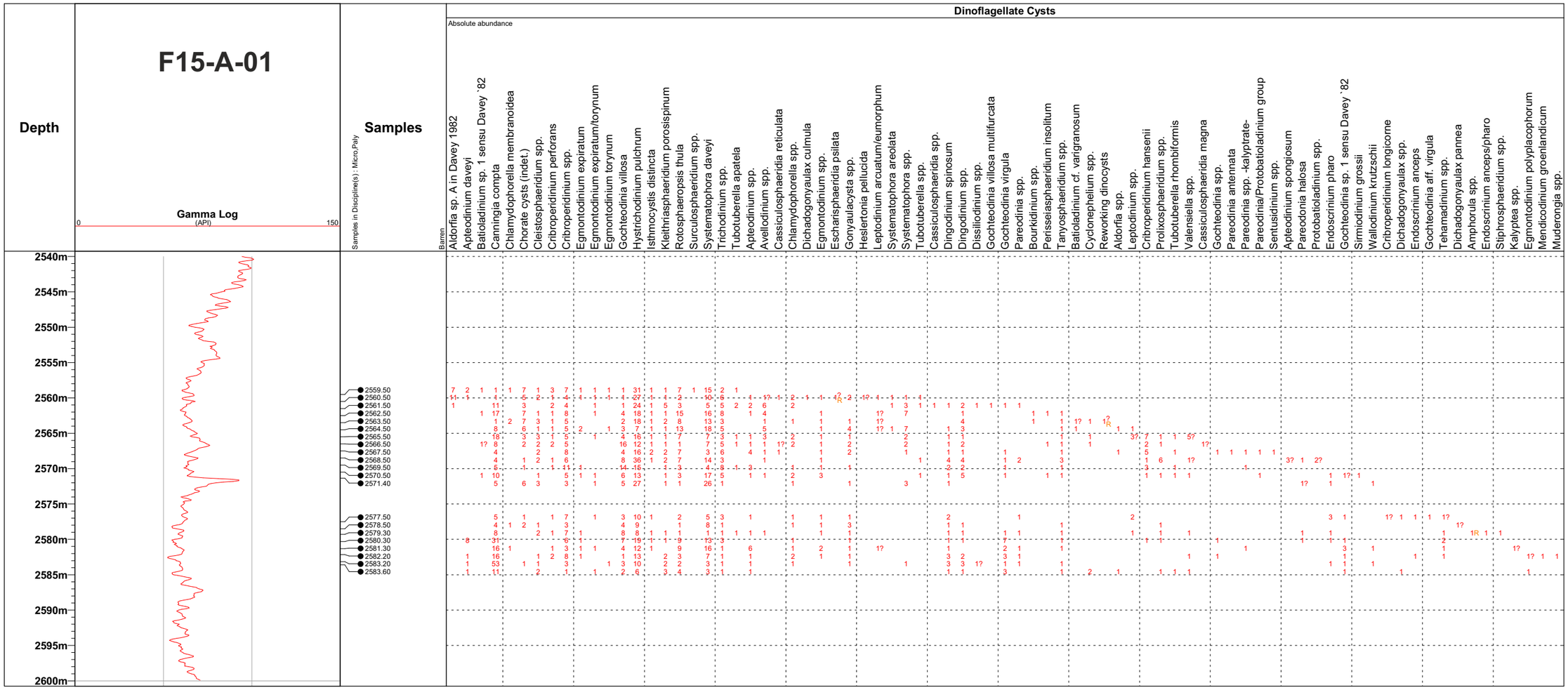

Appendix A2 - Palynology

TNO innovation for life

Pollen and spore distribution chart of the cored Scruff Greensand interval from well F15-A-01 (F15-04)

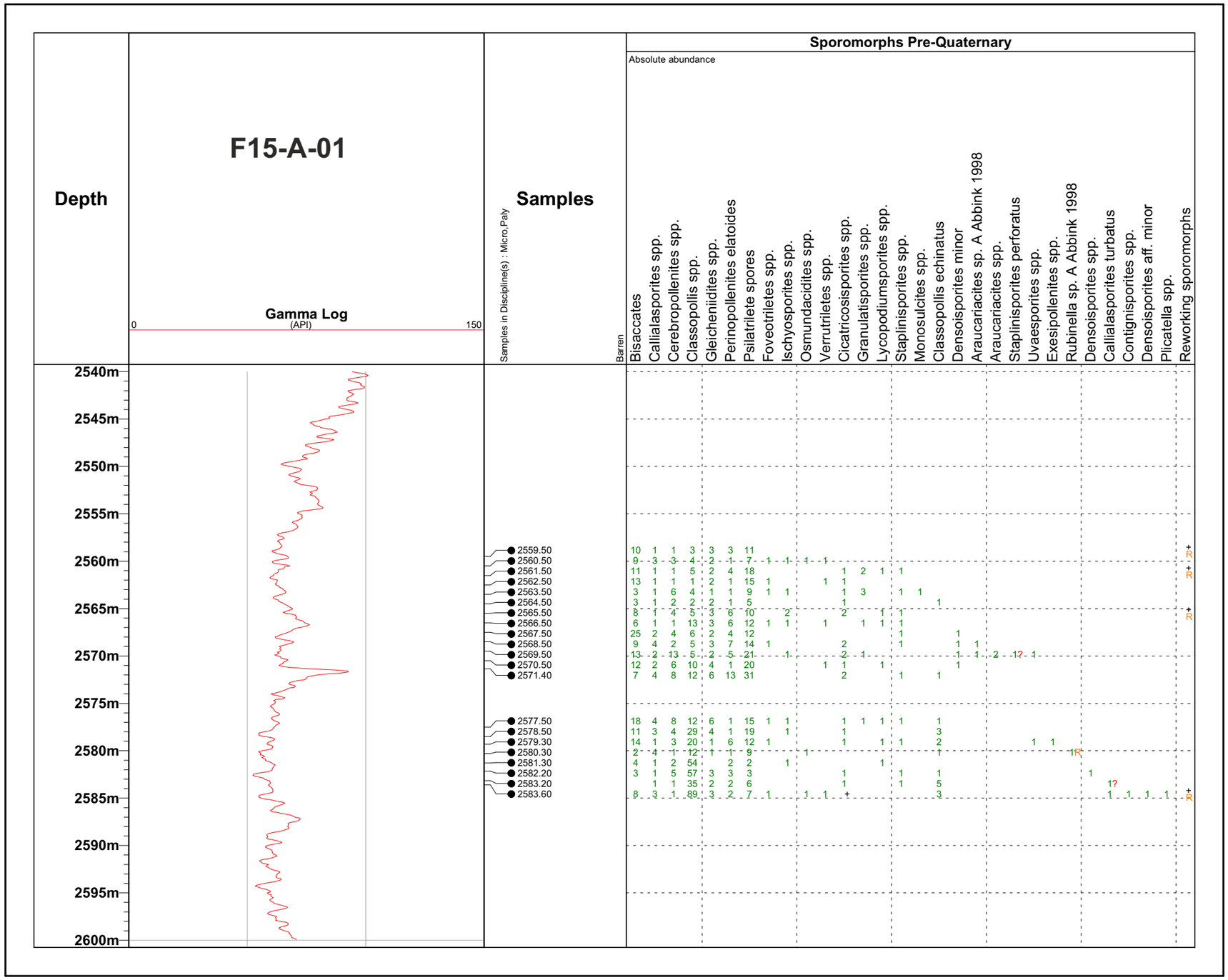

Appendix A2 - Palynology

TNO innovation for life

Dinoflagellate cyst distribution chart of the cored Scruff Greensand interval from well M07-07

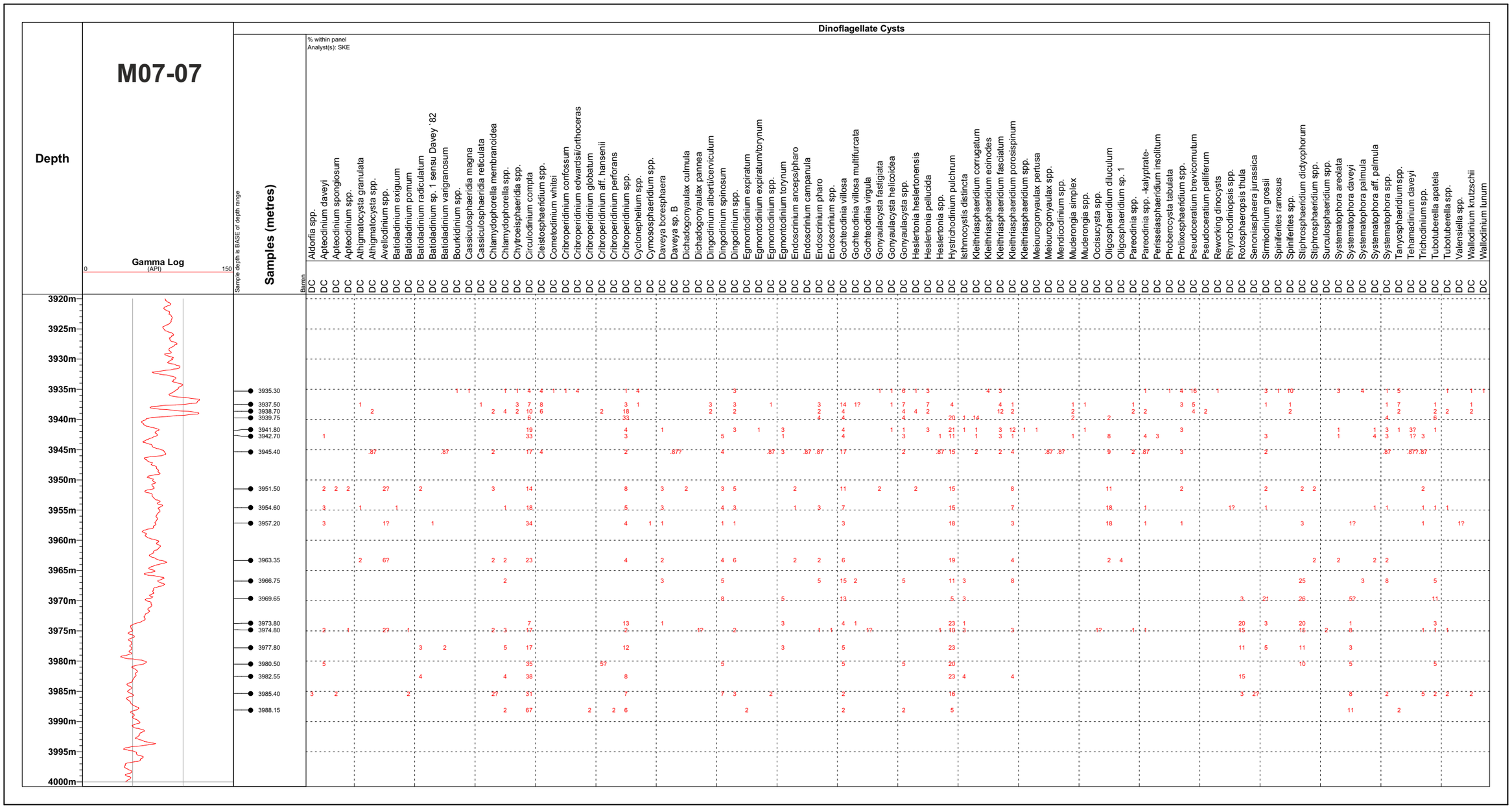

Appendix A2 - Palynology

TNO innovation for life

Pollen and spore distribution chart of the cored Scruff Greensand interval from well M07-07

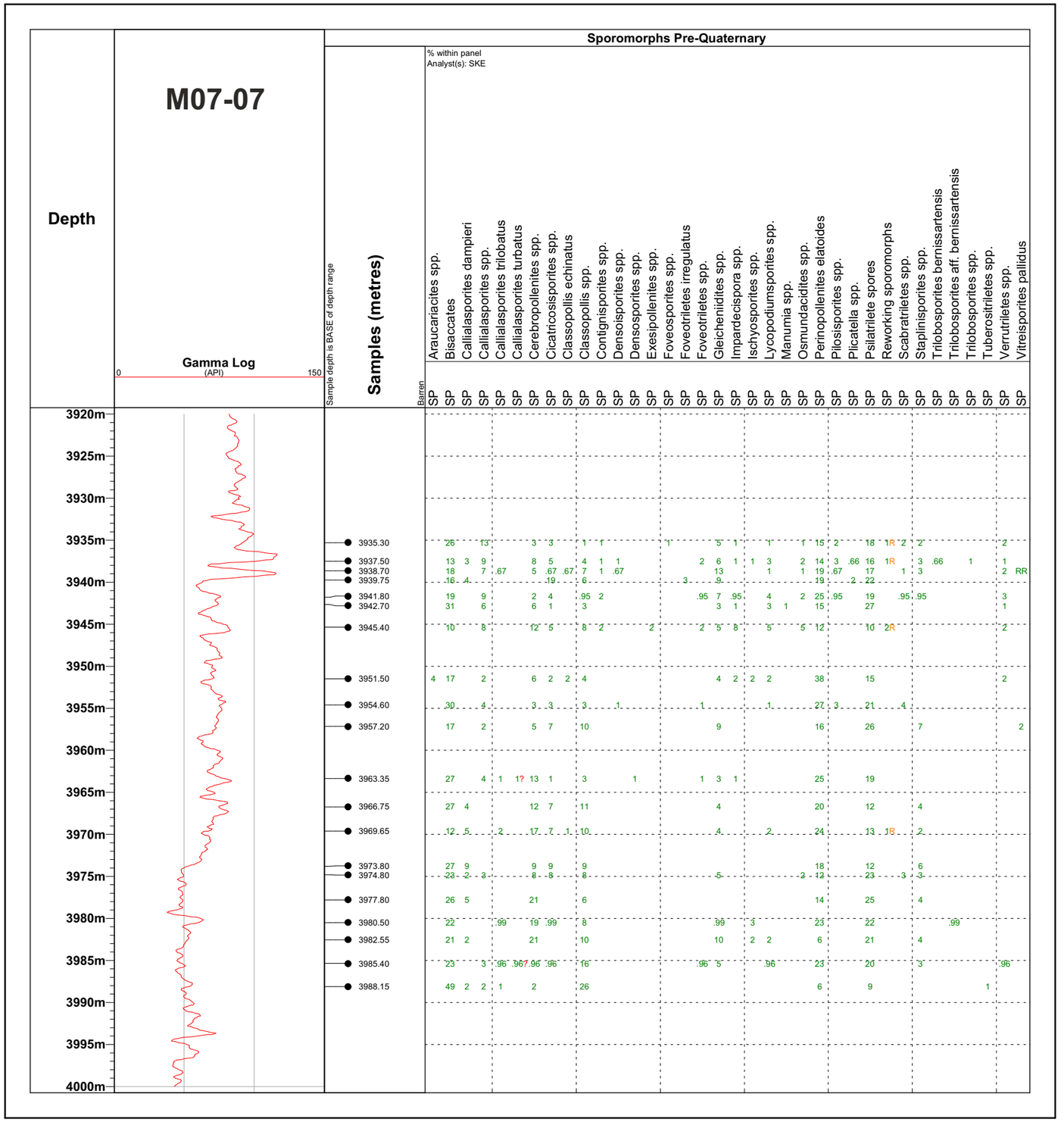

Appendix A2 - Palynology

TNO innovation for life

Pollen and spore distribution chart of the cored Scruff Greensand interval from well M07-08

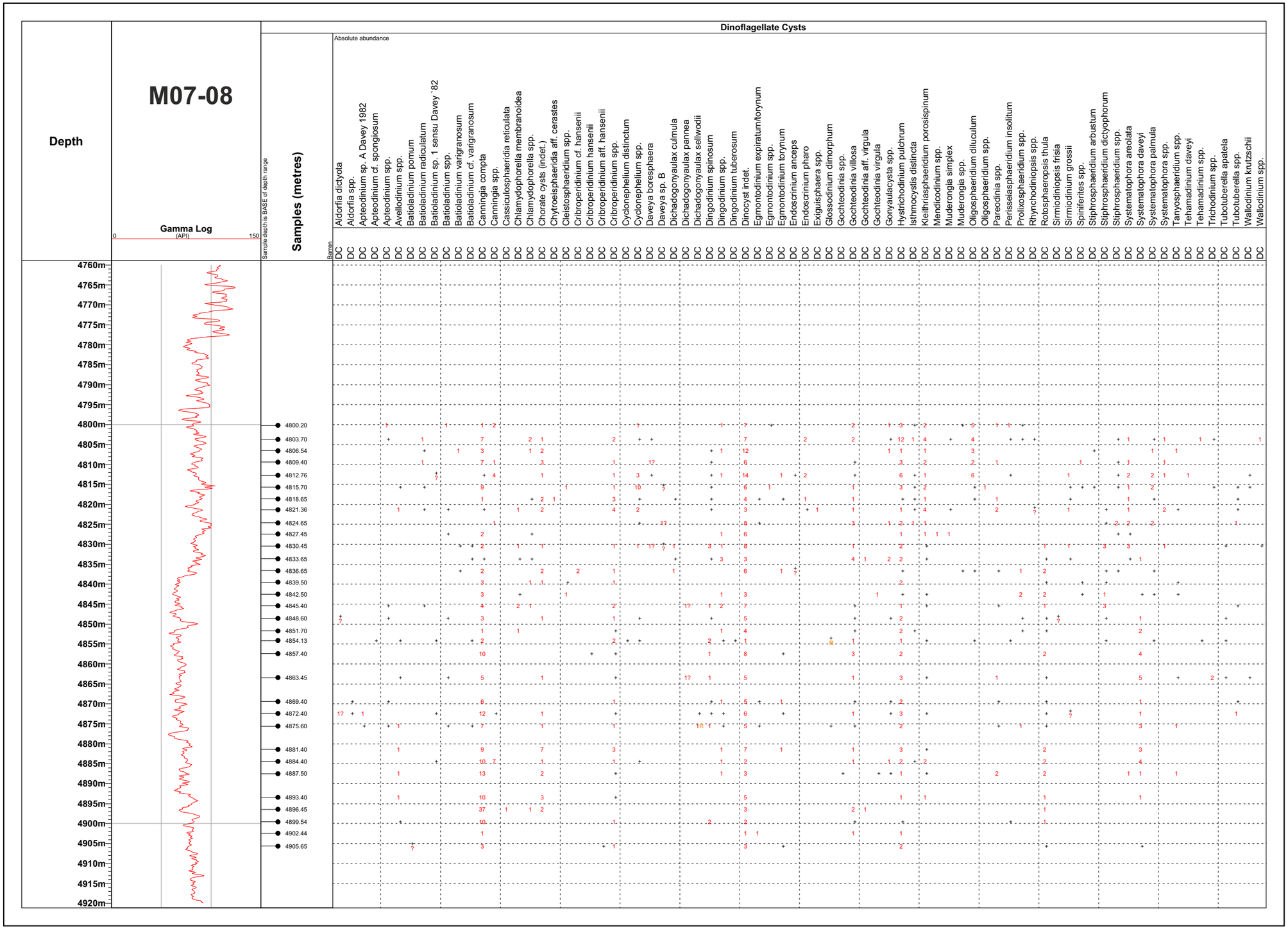

Appendix A2 - Palynology

TNO innovation for life

Pollen and spore distribution chart of the cored Scruff Greensand interval from well M07-08

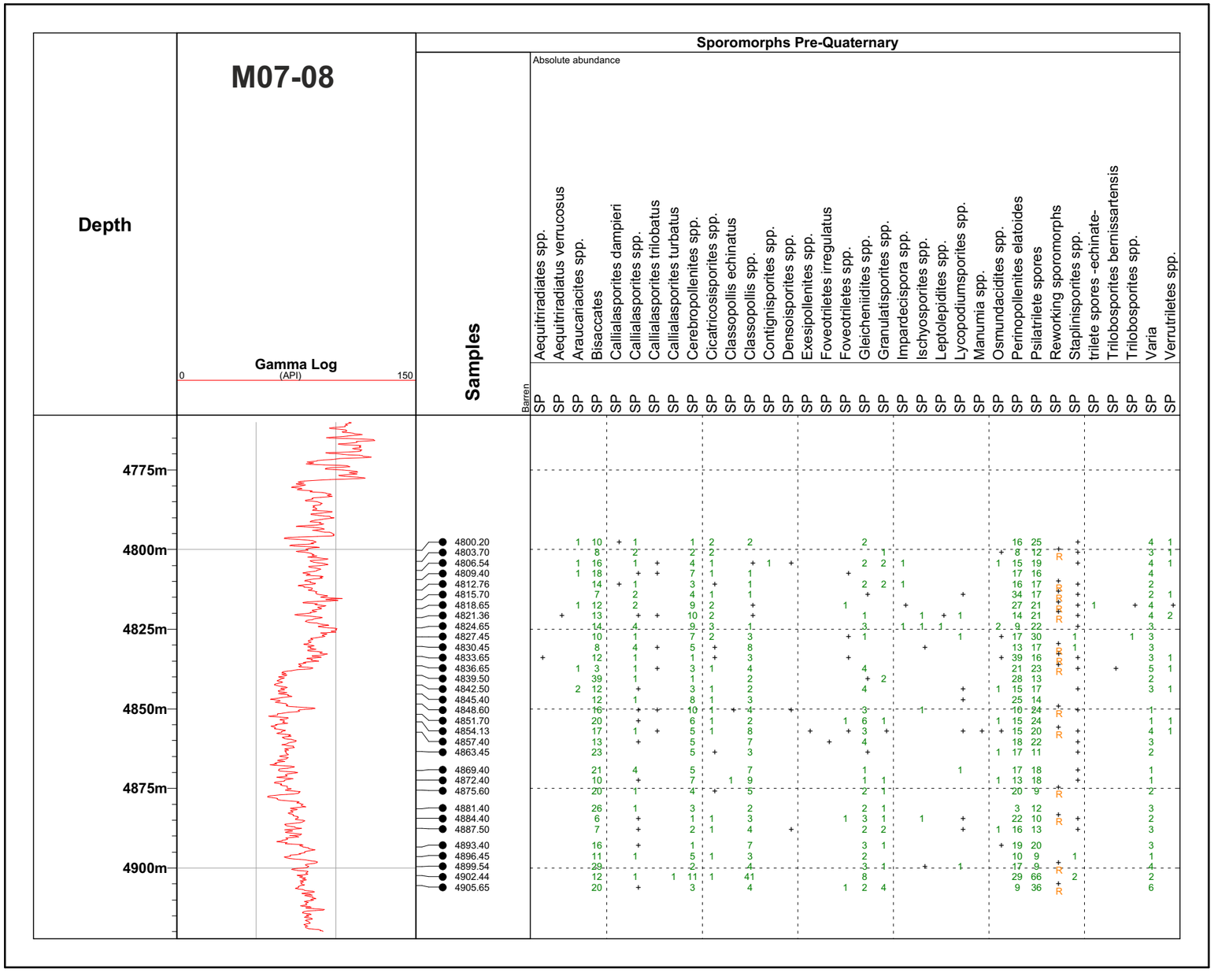

APPENDIX A3
STABLE ISOTOPES

Appendix A3 - Stable isotopes

Appendix A3-1 Stable isotope records

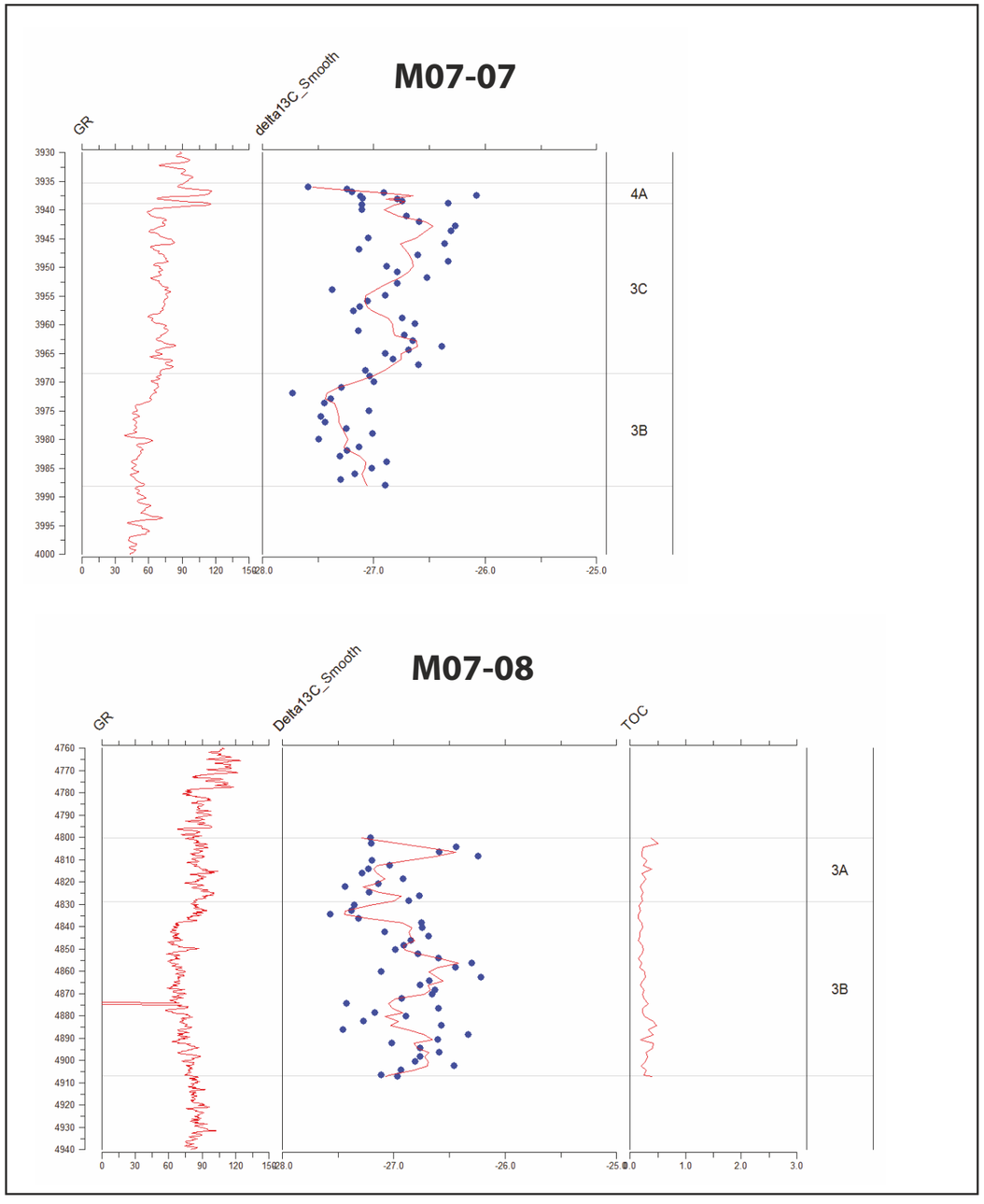

Sequence 3: Scruff Greensand Fm

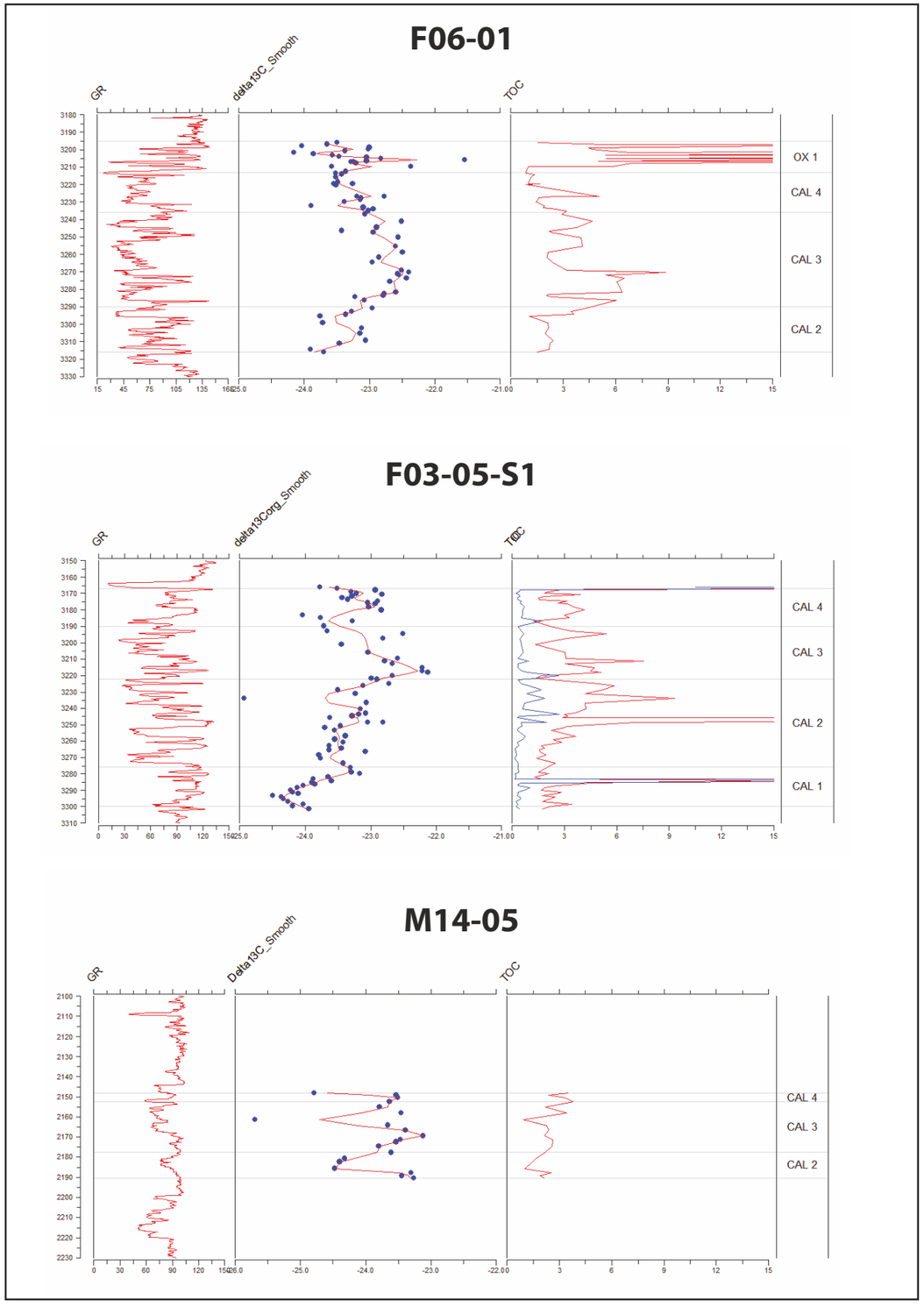

Sequence 1: Lower Graben Fm

Appendix A3 - Stable isotopes

TNO innovation for life

Appendix A3-2 Stable isotope records

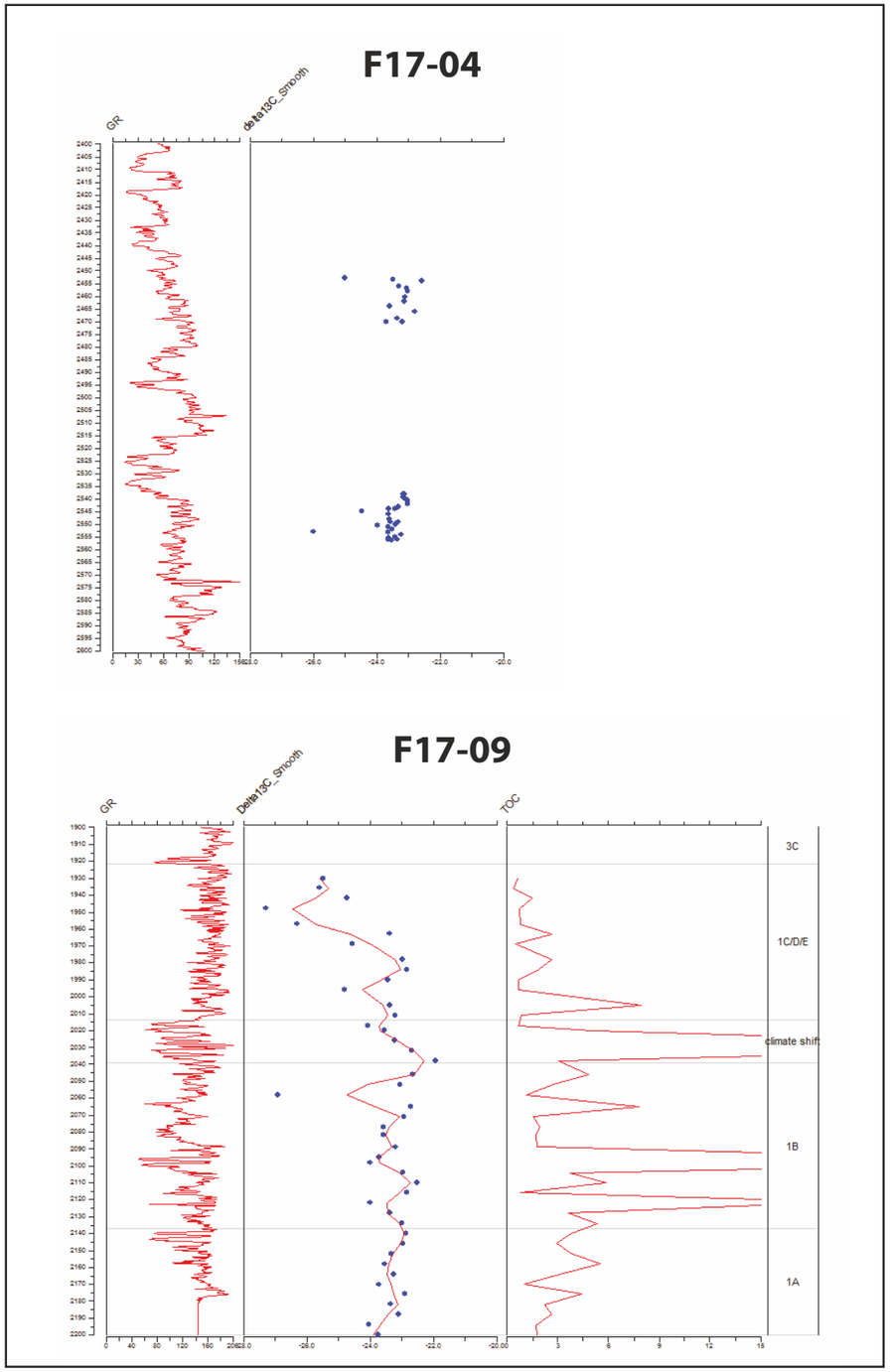

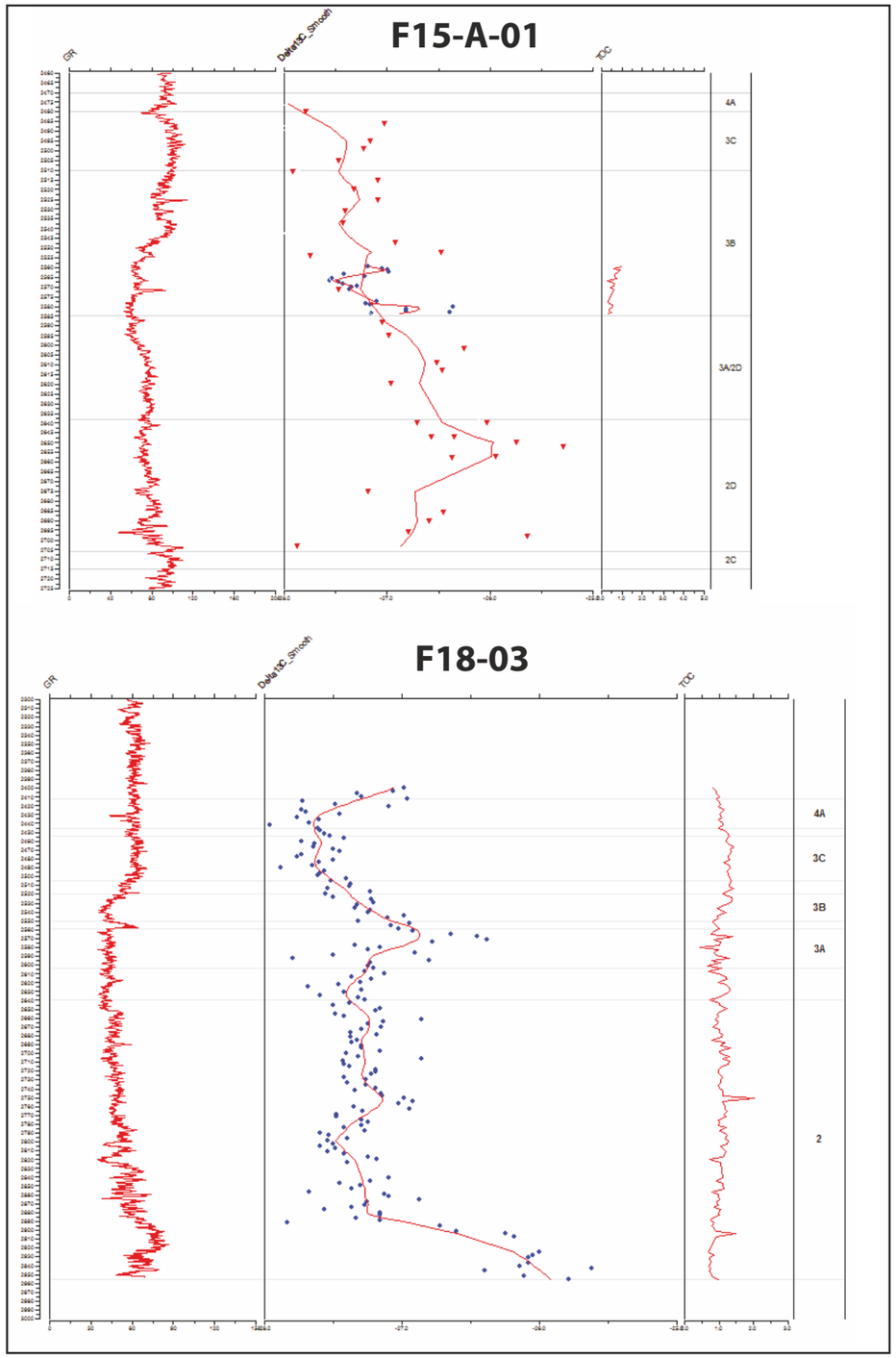

APPENDIX A4: SEISMIC INTERPRETATION and STRATIGRAPHIC CORRELATION

Appendix A4.1 - Seismic interpretation and stratigraphic correlation

TNO innovation for life

Seven regional panels that include interpreted seismic sections, flatten seismic section and corresponding stratigraphic correlation have been constructed. Each seismic section and its corresponding well correlation panels where analyzed at the same time, by the same interpreter (Fig. A4.1). This allowed for a integrated interpretations of seismic and well data.

Note that Panel A has two versions (A1 and A2) with the southeastern part of the seismic panels following a different trend: 1) Panel A1, from M04-01 to the southeast toward M08-02; Panel A2 (dashed in Fig. A4.1) from M04-01 to the south toward M07-03, M07-07, M07-08 and M07-01. The location maps (Figure A4.1) shows the location of each of the regional panels presented.

Below is the list of wells that are included for each panel:

Panel A1

F17-06, F17-05, L02-05, L03-01, L03-03, L03-04, L06-02, M04-04, M04-03, M04-01,(M08-02), M07-03, M07-07 and M07-01.

Panel A2

F17-06, F17-05, L02-05, L03-01, L03-03, L03-04, L06-02, M04-04, M04-03, M04-01, M07-03, M07-07, M07-08, M07-01

Panel B

G13-02, G16-03, G16-04, G16-05, L03-04, L06-03, L09-02, L09-01

Panel C

B18-03, F03-08, F03-05-S1, F03-06, F03-03, F06-01, F08-01, F08-02, F11-01, F14-05, F14-06, F17-01, F17-06, F17-09, L02-05, L02-03, L02-FA-101, L02-06-S1, L05-04, L05-05, L04-05, L04-01

Panel D

E18-01, E18-07, F16-A-05, F16-04, F16-02, F17-04, F17-09, F17-05, F18-02, F18-01, F18-09-S1, F18-03, F18-08, G16-02, G16-04, G17-03, G17-01, G17-02

Panel E

F07-02, F11-03, F11-02, F11-01- F12-03, G10-03

Panel F

A08-01, A12-02, B13-02, B14-02, B14-01, B14-03, B18-02, B18-03, F03-07

Panel G

A12-01, A18-02-S1, F01-01, F04-02-A, F09-01

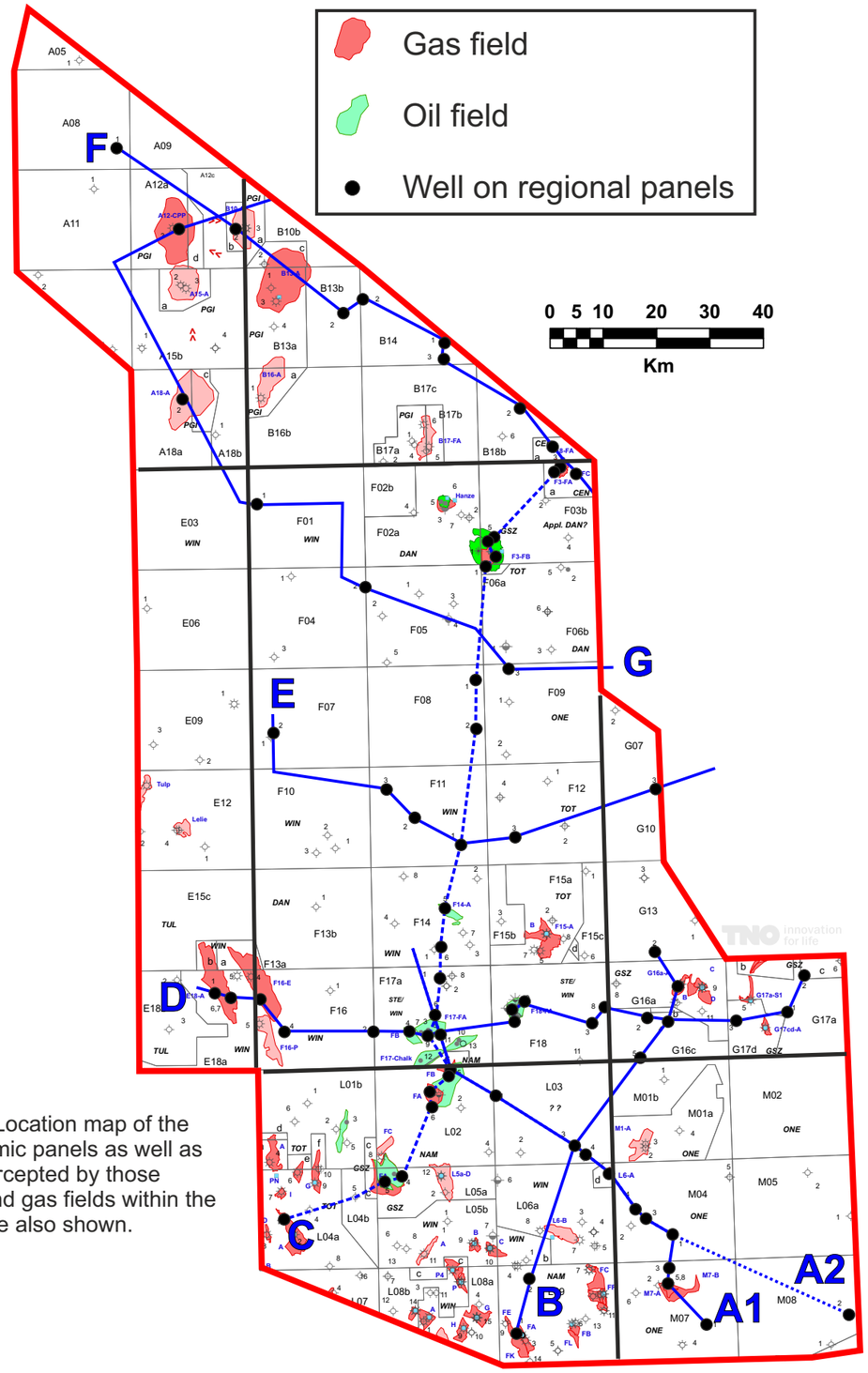

Figure A4.1: Location map of the regional seismic panels as well as the wells intercepted by those panels. Oil and gas fields within the study area are also shown.

Appendix A4.2 - Seismic interpretation and stratigraphic correlation

TNO innovation for life

Seismic profiles

- Fault
- Anticline (A)
- Salt body
- Salt feeder
- Salt weld

- Cenozoic
- Chalk Group (Upper Cretaceous)
- Rijnland Group (Lower Cretaceous)
- Sequence 3 (Upper Jurassic-Lower Cretaceous)
- Sequence 2 (Upper Jurassic)
- Sequence 1 (Upper Jurassic)
- Altena Group (Lower Jurassic)
- Upper Triassic (Upper Germanic Trias Group)
- Lower Triassic (Lower Germanic Trias Group)
- Zechstein (Lower Germanic Trias Group)

- Unconformity
- Onlap
- Truncation
- Downlap
- Internal horizon
- Coal rich-unit (Middle Graben Fm.)

Stratigraphic Correlations

- Sand-rich interval
- Thick sand-rich interval (stacked channels)
- Thick sandstone and siltstone (Noordvaarder Mb.)
- S3 / S2 / S1 — Shale-rich intervals
- Coal rich-unit (Middle Graben Fm.)
- Volcanoclastics
- Volcanics

- Base of Sequence 3
- Base of Sequence 2
- Base of Sequence 1

- Fault
- Salt body

- Cored interval

- Unconformity
- Onlap
- Truncation
- Downlap

Lithostratigraphy

1. Clay Deep Mb.
2. Schill Grund Mb.
3. Stortemelk Mb.
4. Scruff Spiculite Mb.
5. Scruff Greensand Fm. (undifferentiated)
6. Noordvaader Mb.
7. Lies Mb.
8. Terschelling Sandstone Mb.
9. Oyster Ground Mb.
10. Kimmeridge Clay Fm.
11. Main Friese Front Mb.
12. Friese Front Fm. (undifferentiated)
13. Rifgronden Mb.
14. Puzzle Hole Fm. Mb.
15. Upper Graben Fm.
16. Middle Graben Fm.
17. Lower Graben Fm.

Figure A4.2: Legend for seismic and correlation panels

Appendix A4.3 - Panel A1 - Terschelling Basin & Dutch Central Graben - Sequ. 1 & 2

TNO innovation for life

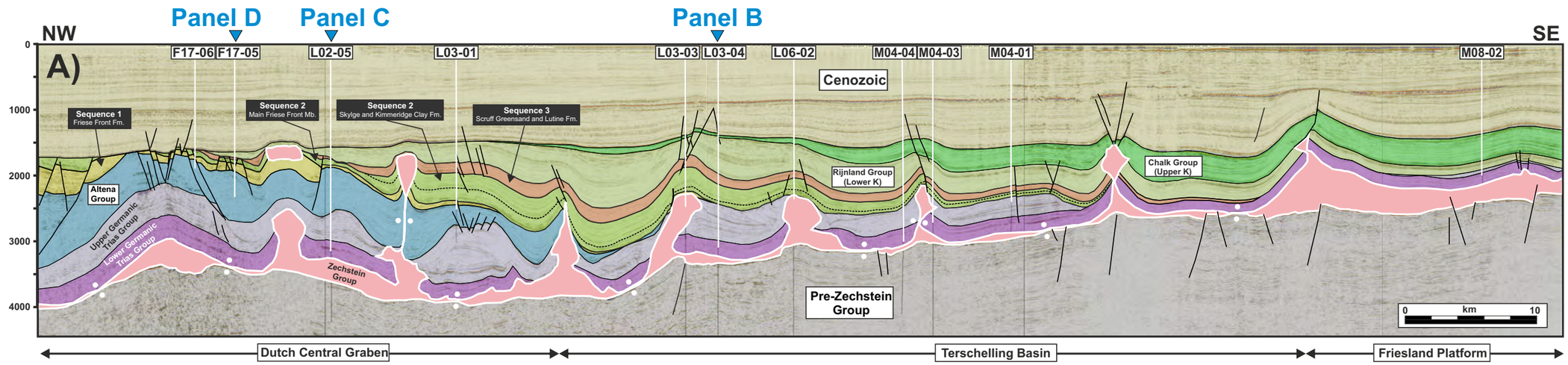

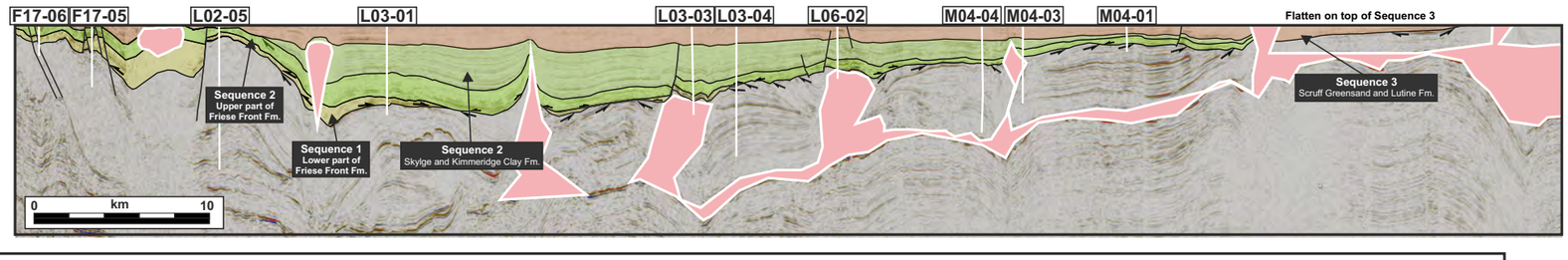

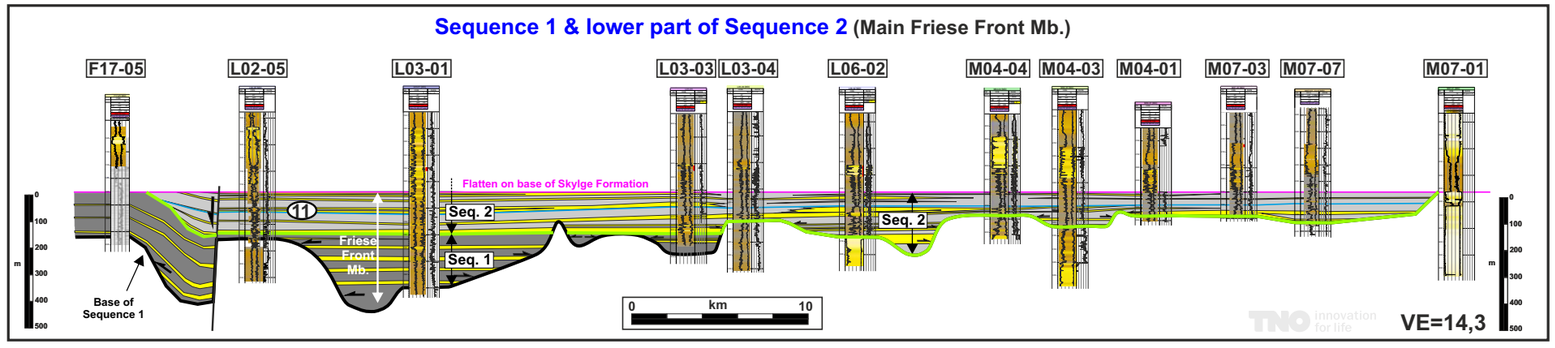

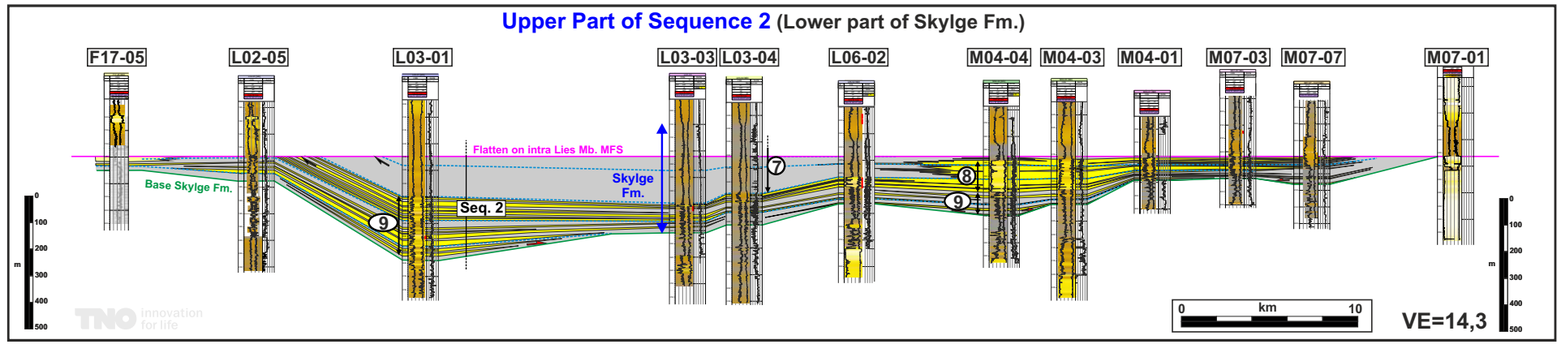

Panel A1 is located across three structural provinces, namely from SE to NW, the Friesland Platform, the Terschelling Basin and the southern part of the DCG, and is trending SE-NW. **A)** 111,5 km long interpreted seismic section that intercepts 11 wells. **B)** 87,5 km long, flattened and interpreted seismic section. The section is flattened on the Top of Sequence 3 (top of the Skylge Formation) and intercepts 10 wells. This seismic profile is the same as the one shown above but slightly shorten to the NW and SE. **C)** Well correlation section for Sequence 1 and the lower part of Sequence 2. This section is flattened on the base of Sequence 3 (Skylge Formation). This section intercepts 12 wells in total and is slightly different from the seismic section A and B in the SE part (from well M04-01) where a SSE trend is used to add wells M07-03, M07-07 and M07-01 to the section. The vertical exaggeration is 14.3. **D)** Well correlation section for the upper part of Sequence 2. This section is flattened on a well recognizable on GR and Sonic logs maximum flooding surface of the Lies Member. The vertical exaggeration is 14.3. See Fig. A4.1 for location map and Fig. A4.2 for legend.

⑦ Lies Mb.

⑧ Terschelling Sandstone Mb.

⑨ Oyster Ground Mb.

⑪ Main Friese Front Mb.

Appendix A4.4 - Panel A2 - Terschelling Basin & Central Graben - Sequence 3

TNO innovation for life

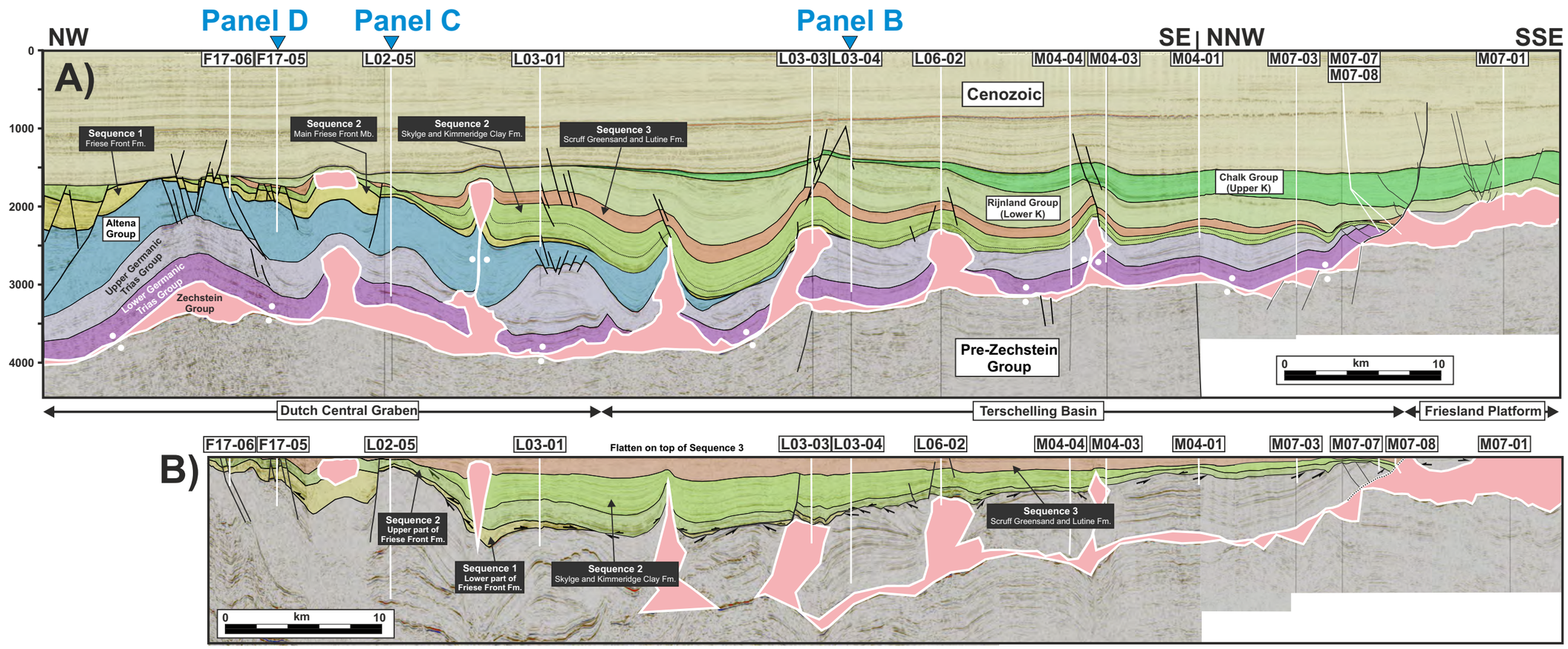

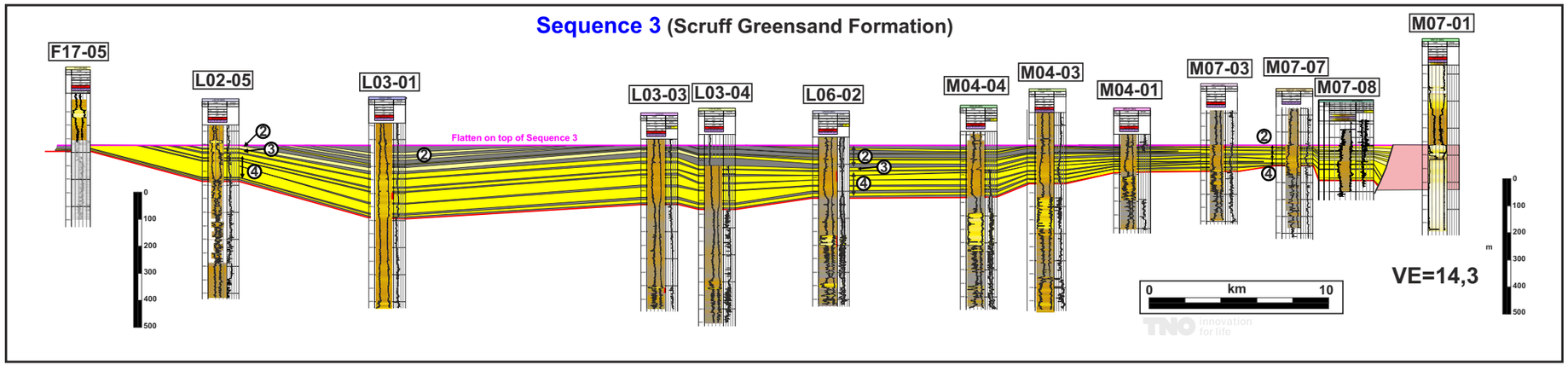

② Schill Grund Mb.

③ Stortemelk Mb.

④ Scruff Spiculite Mb.

Panel A2 is trending SE-NW and is located across three structural province, namely from SE to NW, the Friesland Platform, the Terschelling Basin and the southern part of the Dutch Central Graben. It is composed of three figures. **A)** 98,4 km long interpreted seismic section that intercept 14 wells. **B)** 86,4 km long, flattened and interpreted seismic section. The section is flattened on the top of Sequence 3 (top of the Skylge Formation) and intercepts 14 wells. This seismic profile is the same as the one shown above (A) but slightly shorten to the NW. **C)** Well correlation section for Sequence 3. This section intercepts 13 wells and is flattened on the top of Sequence 3 (Skylge Formation). The vertical exaggeration is 14.3. See Fig. A4.1 for location map and Fig. A4.2 for legend.

Appendix A4.5 - Panel B1 - Terschelling Basin - Sequence 2

TNO innovation for life

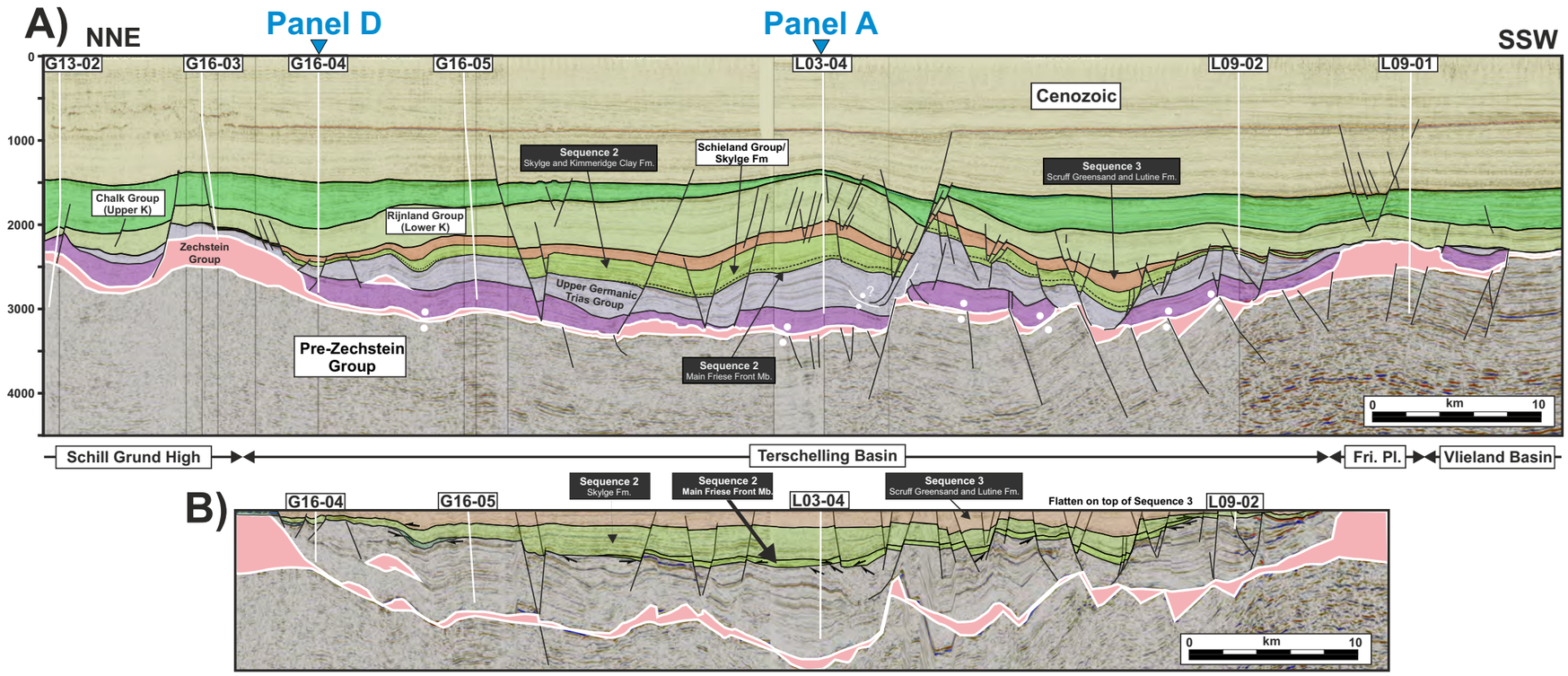

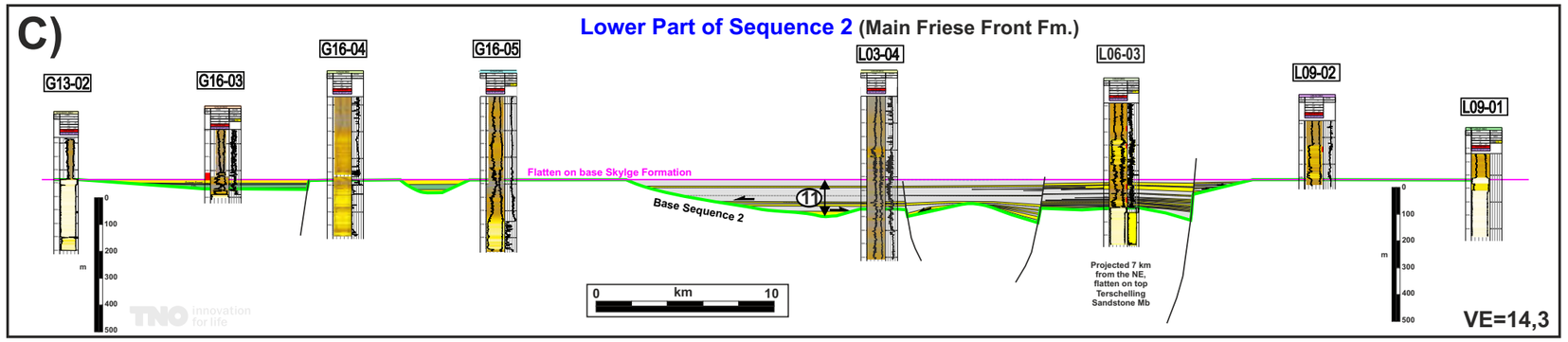

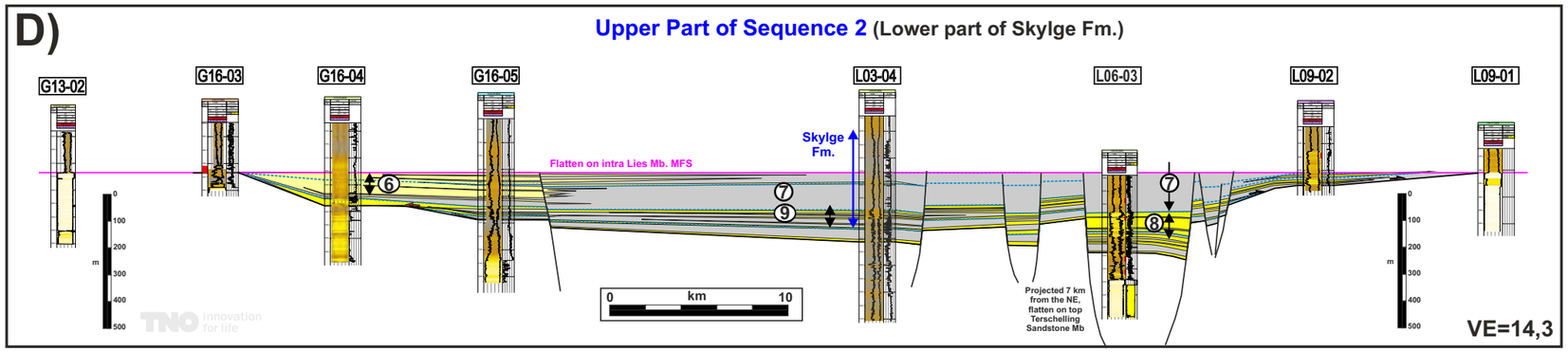

Panel B1 is located across four structural provinces, namely from north to south, the Schill Grund High, the Terschelling Basin, the Friesland Platform and the Vlieland Basin. This panel trends NNE-SSW and is composed of four figures. See Fig. A4.1 for location map and Fig. A4.2 for legend.

A) 91,5 km long interpreted seismic section that intercept 7 wells.

B) 69,5 km long, flattened and interpreted seismic section. The section is flattened on the top of Sequence 3 (top of the Skylge Formation) and intercept 4 wells. This seismic profile is the same as the one shown above (A) but slightly shorten to the NNE and SSW.

C) Well correlation section for the lower part of Sequence 2. This section is flattened on the base of Sequence 3 (base of Skyge Formation). Note that Sequence 1 is not observed in this part of the basin. This section intercepts 7 wells, with the addition of well L06-03 that is projected 7 km from the NW. The vertical exaggeration is 14.3.

D) Well correlation section for the upper part of Sequence 2. This section is flattened on a recognizable maximum flooding surface in the lower part of the Lies Member. This section intercepts the same wells as in (C). The vertical exaggeration is 14.3.

⑥ Noordvaader Mb.

⑦ Lies Mb.

⑧ Terschelling Sandstone Mb.

⑨ Oyster Ground Mb.

Appendix A4.6 - Panel B1 - Terschelling Basin - Sequence 3

TNO innovation for life

A)

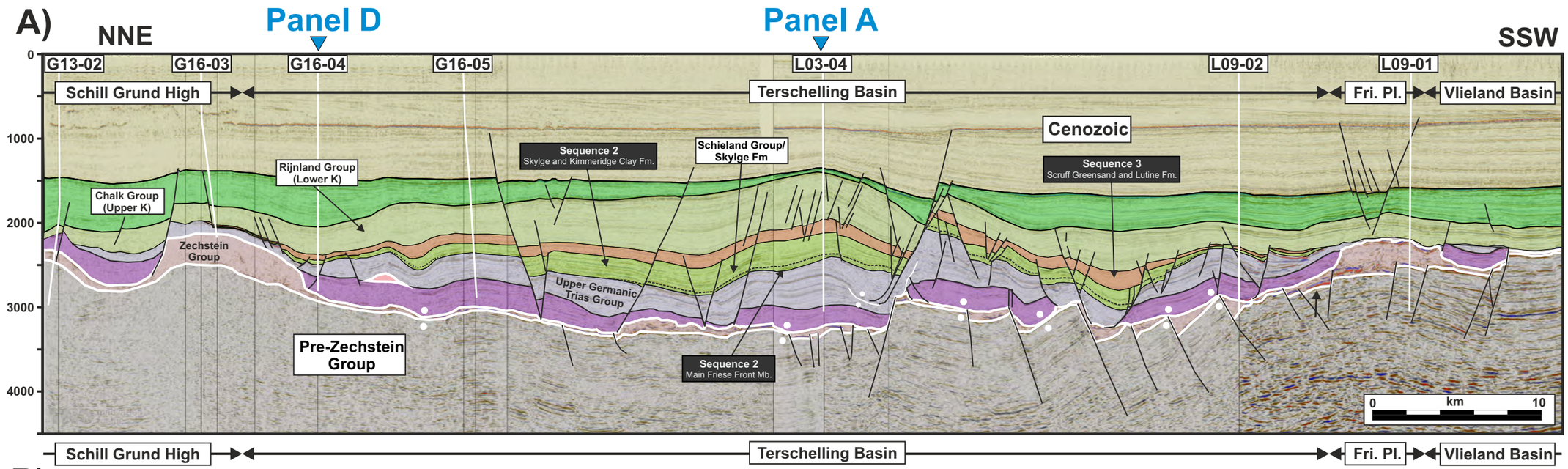

B)

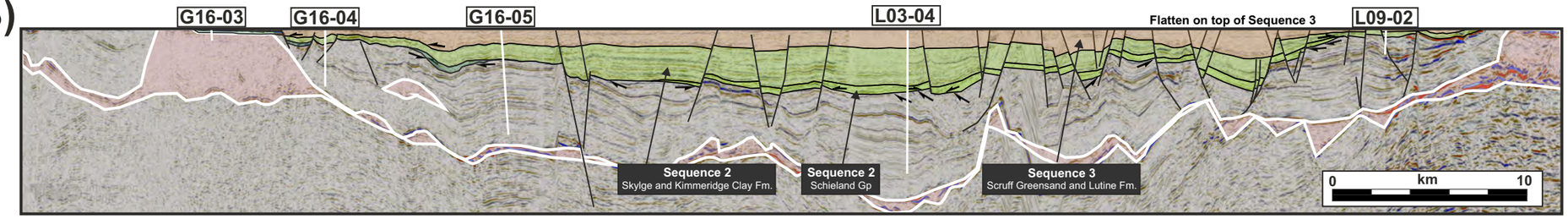

C)

Sequence 3 (Scruff Greensand Formation)

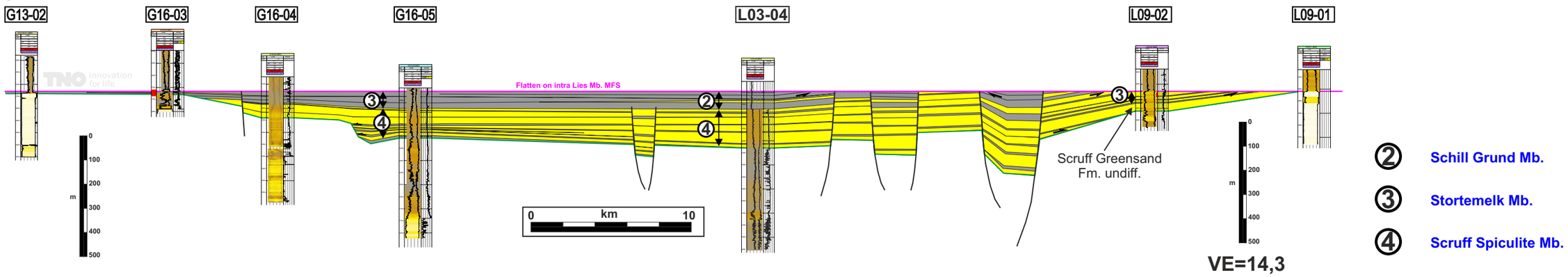

Panel B2 is located across four structural provinces, namely from north to south, the Schill Grund High, the Terschelling Basin, the Friesland Platform and the Vlieland Basin. This panel trends NNE-SSW and is composed of three figures. **A)** 91,5 km long interpreted seismic section that intercept 7 wells. **B)** 69,5 km long, flattened and interpreted seismic section. The section is flattened on the top of Sequence 3 (top of the Skylge Formation) and intercept 4 wells. This seismic profile is the same as the one shown above (A) but slightly shorten to the NNE and SSW. **C)** Well correlation section for Sequence 3. This section is flattened on the top of Sequence 3 (top of Skylge Formation). This section intercepts 7 wells. The vertical exaggeration is 14.3. See Fig. A4.1 for location map and Fig. A4.2 for legend.

Appendix A4.7 - Panel C1 - Dutch Central Graben - Sequence 1

TNO innovation for life

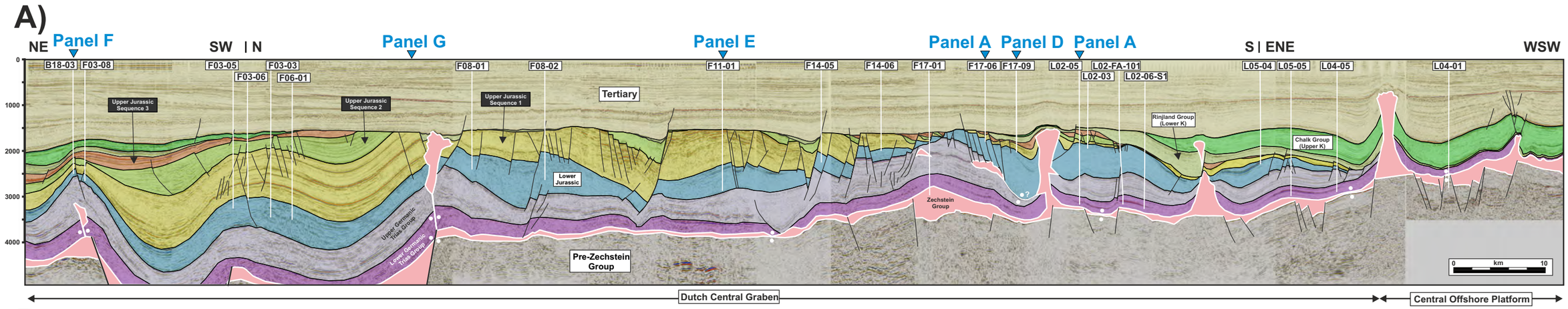

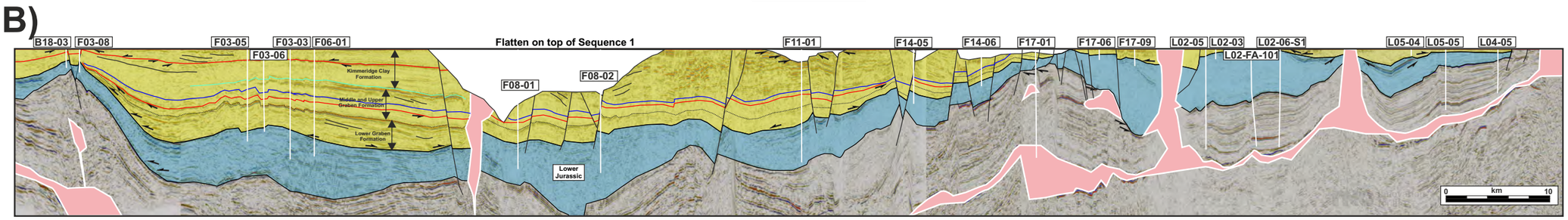

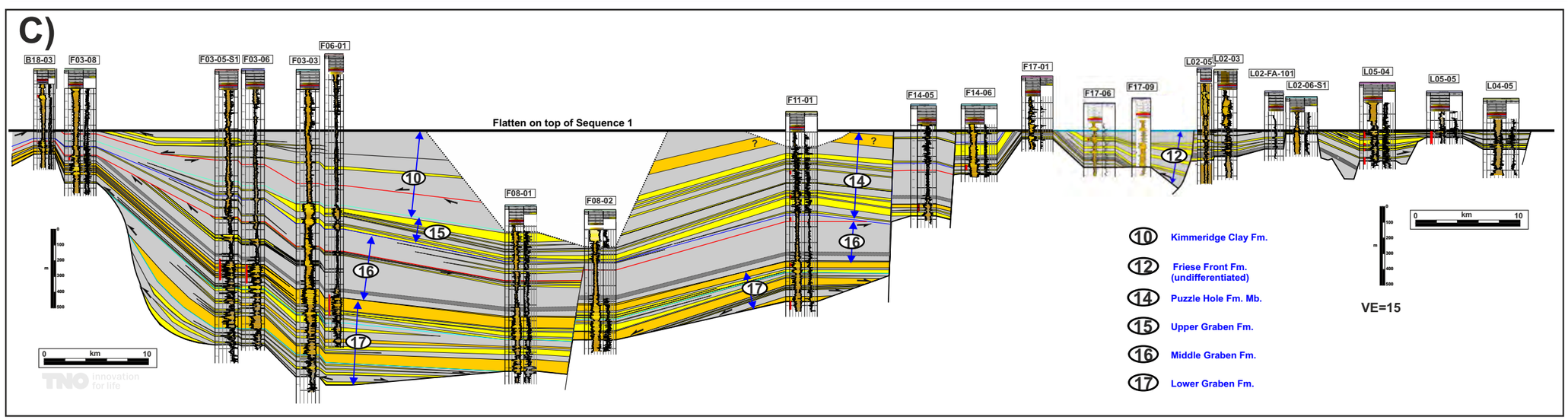

Panel C1 is located in the axis of the Dutch Central Graben and extends southward to the southern part of the Central Offshore Platform (COP). It trends N-S, with locally two SW-NE trends at its extremities. This panel is composed of three figures. **A)** 170 km long interpreted seismic section that intercept 21 wells. **B)** 152 km long, flattened and interpreted seismic section. The section is flattened on the top of Sequence 1 and intercept 19 wells. This seismic profile is the same as the one shown above (A) but slightly shorten to the South. Note that the modified flattened approached (four white polygons in the central part of the display; see methodology section for explanation of the technique) is locally used to obtain a more realistic geometry of Sequence 1. **C)** Well correlation section for Sequence 1. This section is flattened on the top of Sequence 1, intercepts 21 wells and has a vertical exaggeration of 15. See Fig. A4.1 for location map and Fig. A4.2 for legend.

Appendix A4.8 - Panel C2 - Dutch Central Graben - Sequences 2 & 3

TNO innovation for life

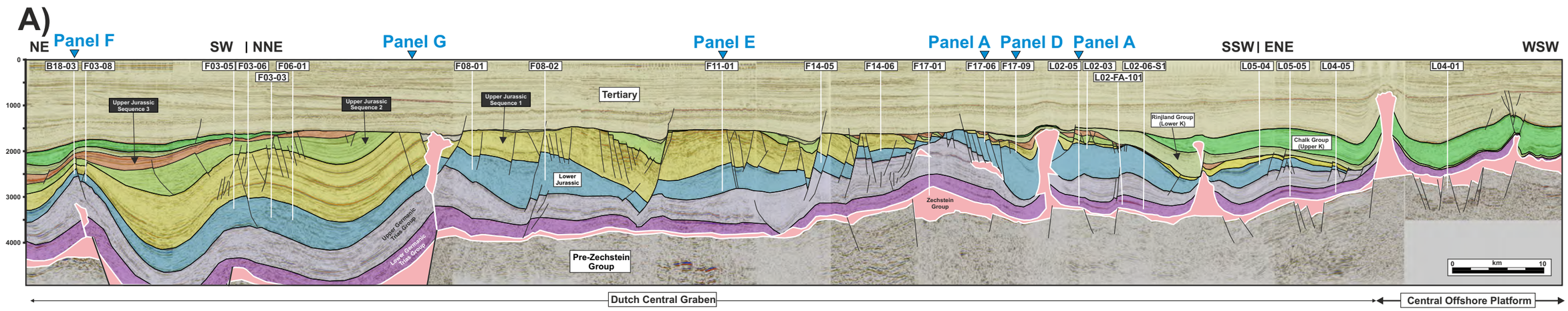

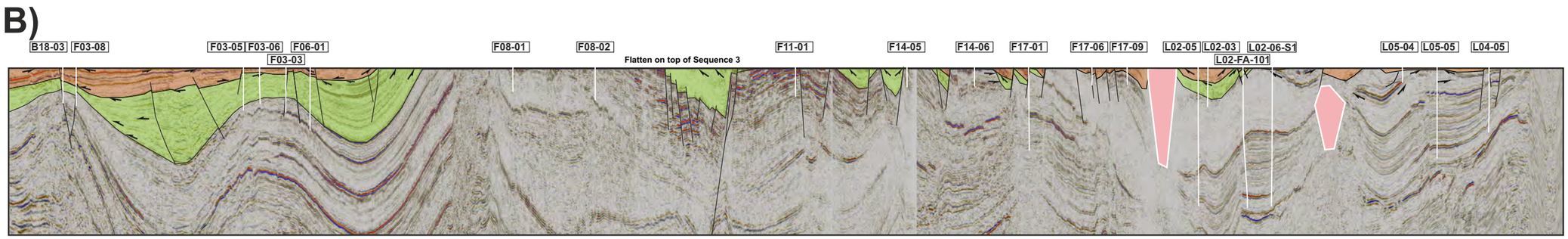

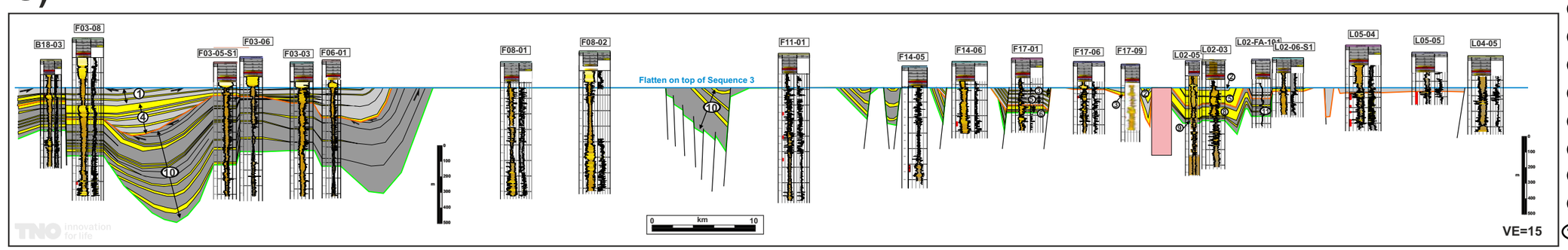

Panel C2 is located in the axis of the Dutch Central Graben and extends southward to the southern part of the Central Offshore Platform. It trends N-S, with locally two SW-NE trends at its extremities. This panel is composed of three figures. **A)** 170 km long interpreted seismic section that intercept 21 wells. **B)** 153,5 km long, flattened and interpreted seismic section. The section is flattened on the top of Sequence 3 and intercept 21 wells. This seismic profile is the same as the one shown above (A) but slightly shorten to the South. **C)** Well correlation section for Sequences 2 and 3. This section is flattened on the top of Sequence 3, intercepts 21 wells and has a vertical exaggeration of 15.
See Fig. A4.1 for location map and Fig. A4.2 for legend.

Appendix A4.9 - Panel D - CGH / DCG / TB / SGH

TNO innovation for life

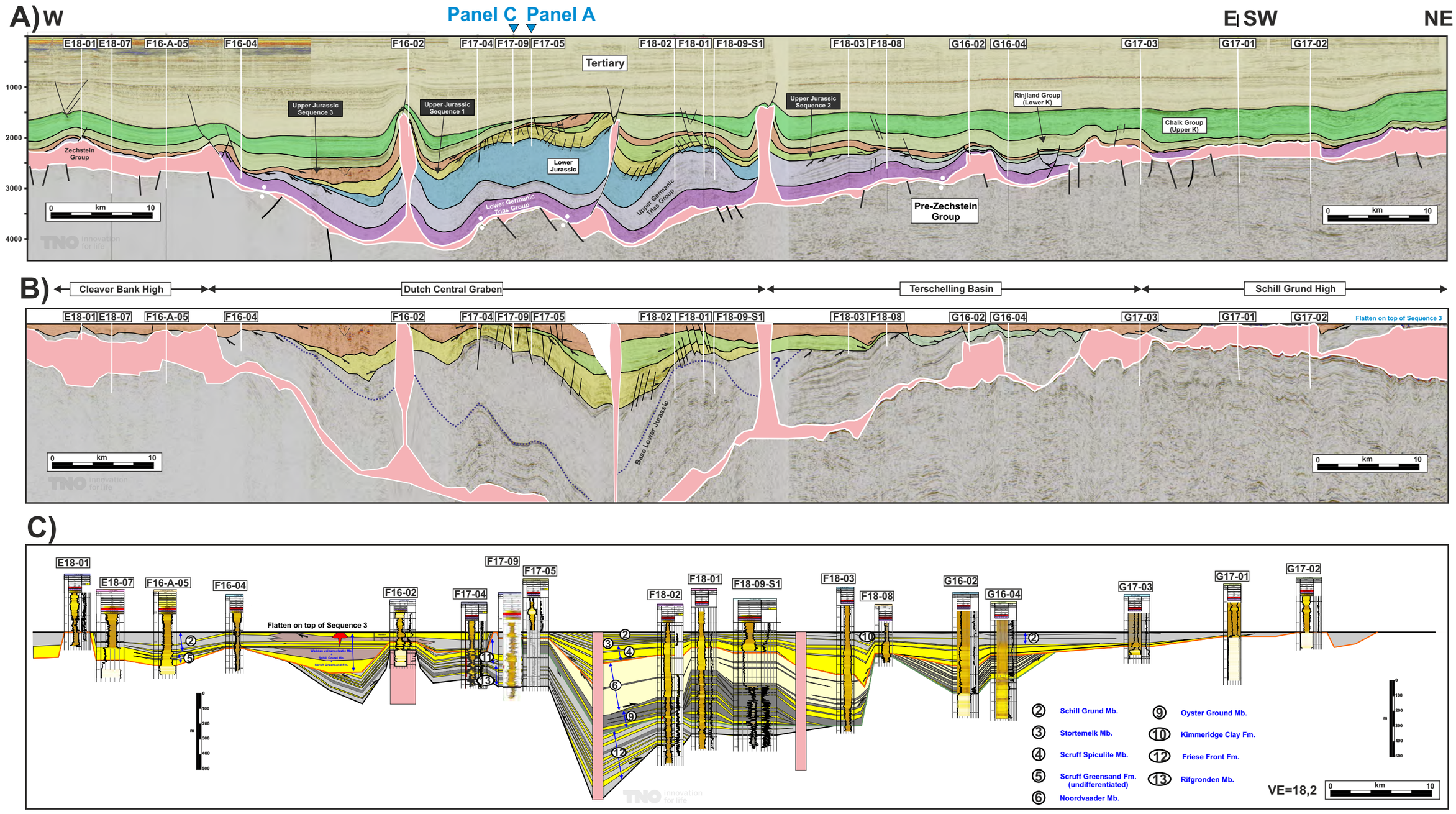

Panel F is located across four structural provinces, namely from east to west, the Cleaver Bank High, the Dutch Central Graben, the Terschelling Basin and the Schill Grund High.. This panel is trending NW-SE. This panel is composed of three figures: **A)** 144,2 km long interpreted seismic section that intercept 9 wells. **B)** 144,2 km long, flattened and interpreted seismic section. The section is flattened on the top of Sequence 3 and intercept 9 wells. This seismic profile is the same as the one shown above (A). **C)** Well correlation section for Sequences 1, 2 and 3. This section is flattened on the top of Sequence 3, intercepts 9 wells and has a vertical exaggeration of 17,7. See Fig. A4.1 for location map and Fig. A4.2 for legend.

Appendix A4.10 - Panel E - CGH / DCG / TB / SGH

TNO innovation for life

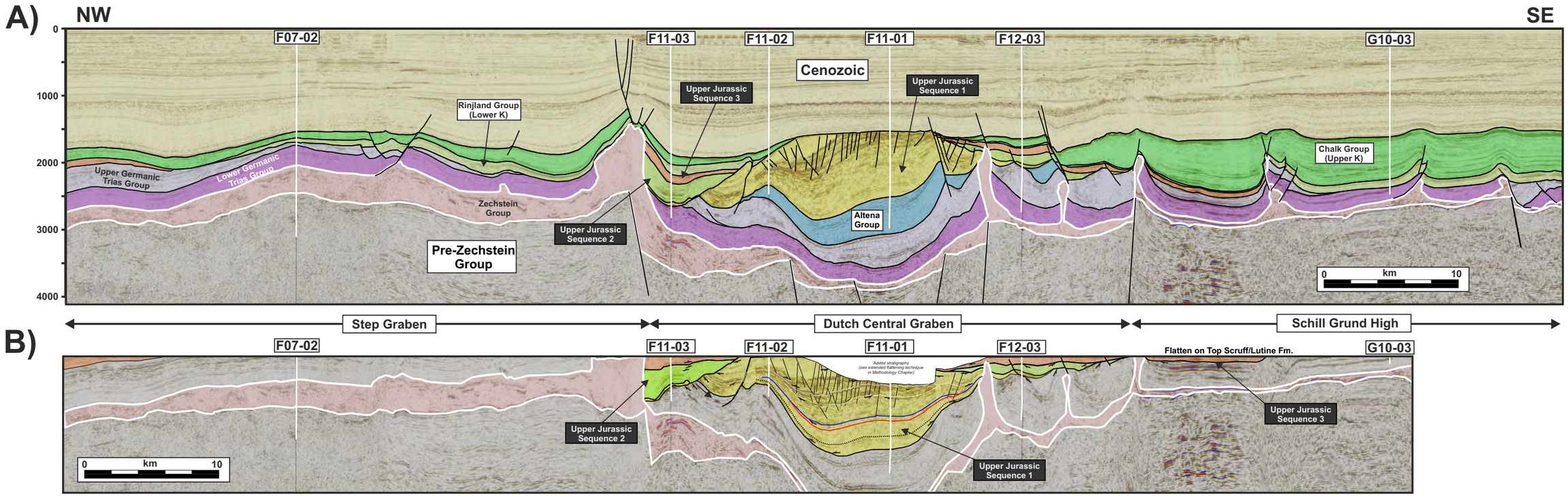

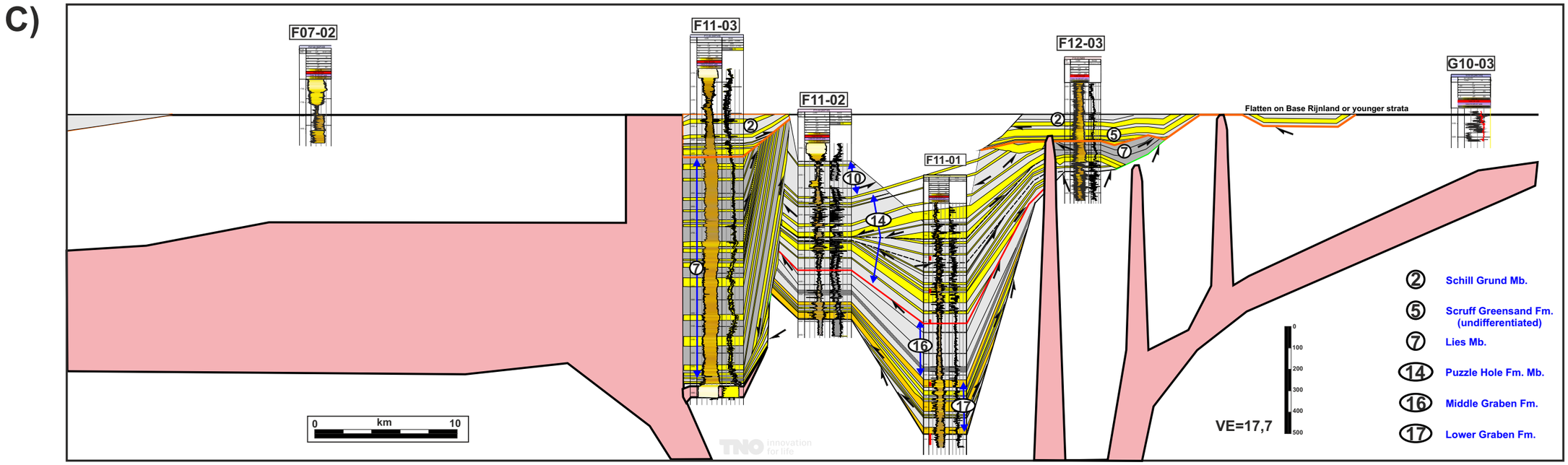

Panel E is located across three structural provinces, namely from east to west, the Schill Grund High (SGH), the Terschelling Basin (TB) and the Step Graben (SG). This panel is trending E-W, except in its western extremity where it is oriented to the NW from well F07-02. This panel is composed of three figures: **A)** 112 km long interpreted seismic section that intercept 6 wells. **B)** 100,5 km long, flattened and interpreted seismic section. The section is flattened on the top of Sequence 3 and intercept 6 wells. This seismic profile is the same as the one shown above (A). **C)** Well correlation section for Sequences 1, 2 and 3. This section is flattened on the top of Sequence 3, intercepts 6 wells and has a vertical exaggeration of 14,9. See Fig. A4.1 for location map and Fig. A4.2 for legend.

Appendix A4.11 - Panel F - Step Graben and Dutch Centra Graben

TNO innovation for life

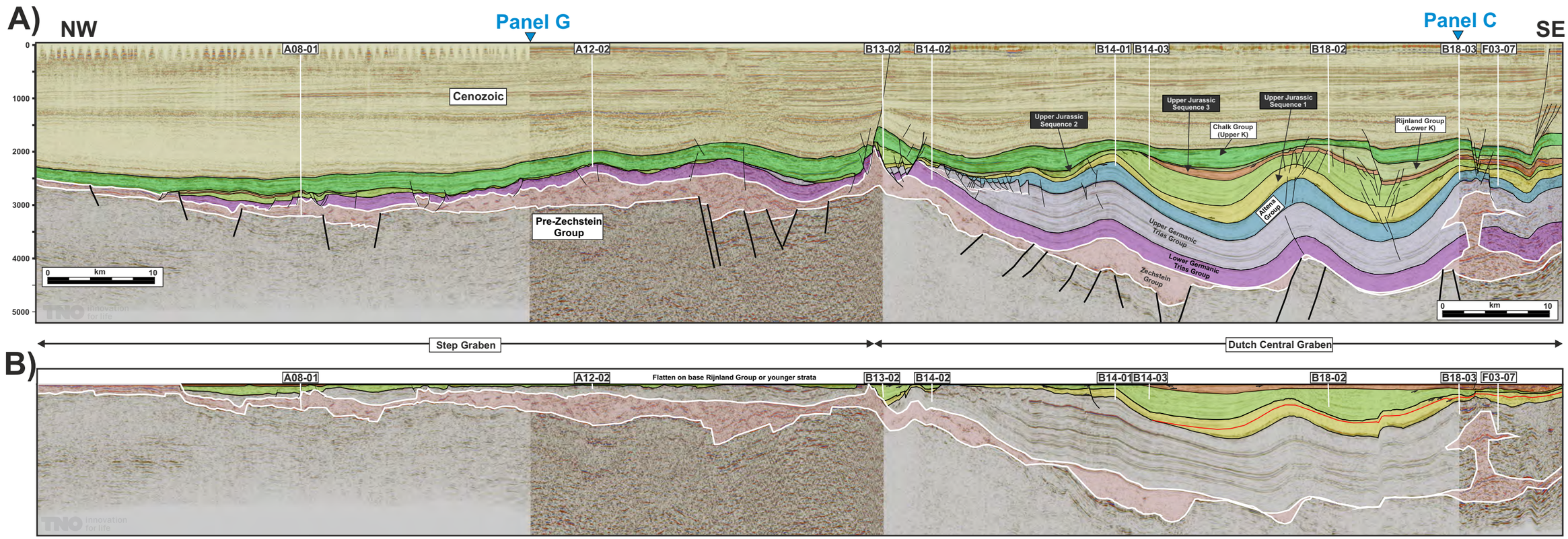

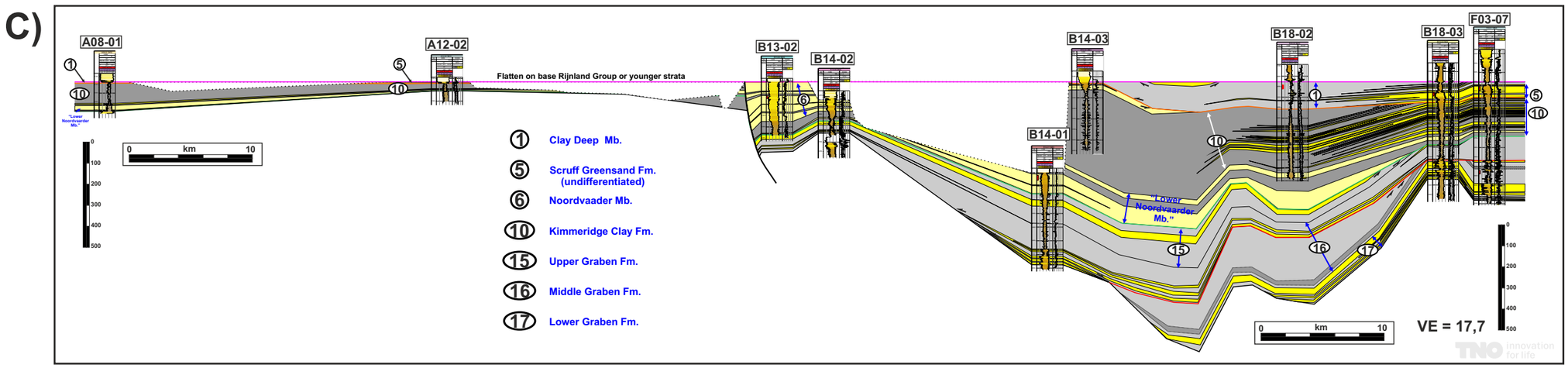

Panel F is located across two structural provinces, namely from east to west, the Step Graben and the Dutch Central Graben. This panel is trending NW-SE. This panel is composed of three figures. **A)** 144,2 km long interpreted seismic section that intercept 9 wells. **B)** 144,2 km long, flattened and interpreted seismic section. The section is flattened on the top of Sequence 3 and intercept 9 wells. This seismic profile is the same as the one shown above (A). **C)** Well correlation section for Sequences 1, 2 and 3. This section is flattened on the top of Sequence 3, intercepts 9 wells and has a vertical exaggeration of 17,7. See Fig. A4.1 for location map and Fig. A4.2 for legend.

Appendix A4.12 - Panel F - Step Graben and Dutch Central Graben

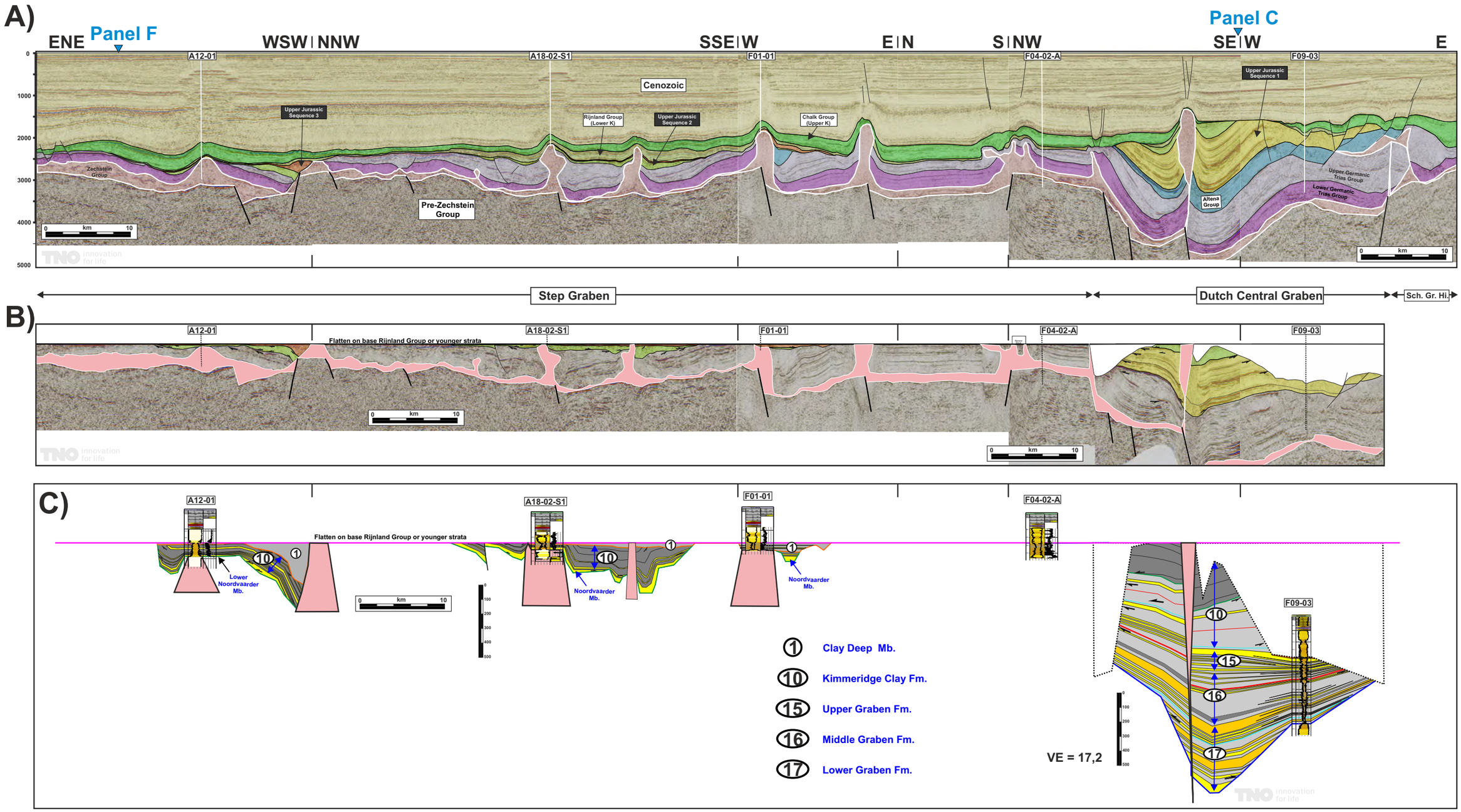

Panel G is located across two structural provinces, namely from northwest to southeast, the Step Graben and the TB. This panel is trending mainly NW-SE, except in its northwestern extremity where it turns to the WNW form well A12-01. This panel is composed of three figures. **A)** 169,6 km long interpreted seismic section that intercept 5 wells. **B)** 169,6 km long, flattened and interpreted seismic section. The section is flattened on the top of Sequence 3 and intercept 5 wells. This seismic profile is the same as the one shown above (A). **C)** Well correlation section for Sequences 1, 2 and 3. This section is flattened on the top of Sequence 3, intercepts 5 wells and has a vertical exaggeration of 17,2. See Fig. A4.1 for location map and Fig. A4.2 for legend.

APPENDIX A5:
THESIS ROBIN DU MEE

Tectono-stratigraphic and structural analysis of siliciclastic growth strata related to salt migration

Upper Jurassic-Lower Cretaceous in the Dutch Central Graben, Terschelling Basin and Step Graben

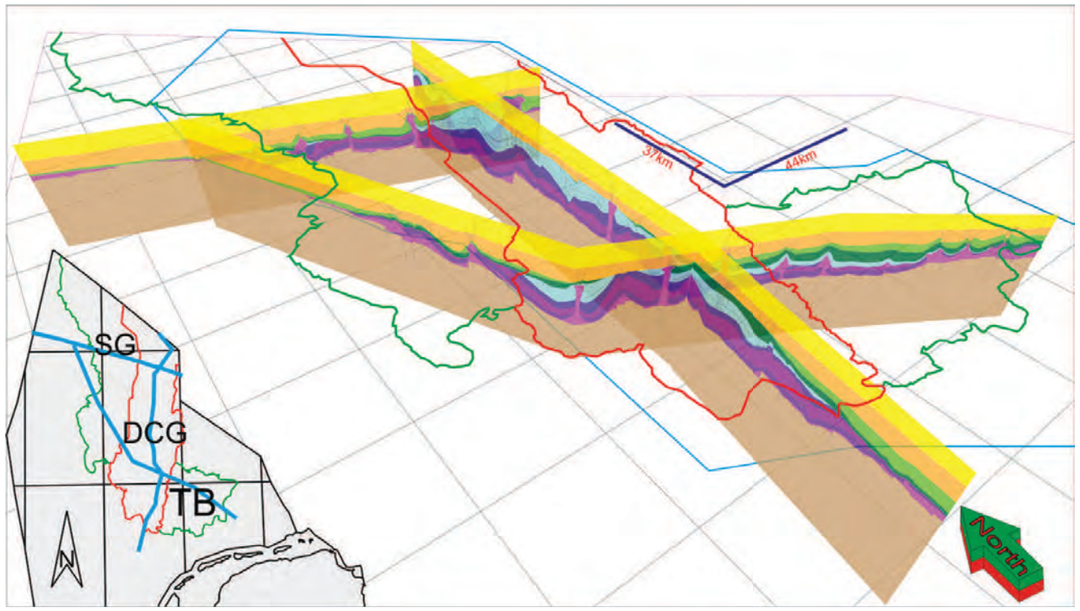

Author: Robin F. du Mée, Bsc. (1658263)
Date: 08-08-2015

Supervisors: Dr. Renaud Bouroullec (TNO Utrecht)
Prof. Dr. Jan d e Jager (VU University Amsterdam)

Master thesis: Earth Sciences, Solid Earth

Cover picture:
A 3-dimensional representation of three interpreted transects through the subsurface of the northern part of the Dutch offshore. SG: Step Graben, DCG: Dutch Central Graben, TB: Terschelling Basin

Abstract

This report summarizes the work of a Master Thesis carried out for the Earth Sciences program at the Faculty of Earth and Life Sciences of the VU University Amsterdam. This project has been carried out during a research internship at TNO in Utrecht between September 2014 and April 2015.

The timing, triggering and driving mechanisms of salt movement in the North Sea are still the subject of debate, even after half a century of research on this topic. Some of the main structural domains and elements in the Dutch subsurface were formed during the Kimmerian tectonic phase (Late Jurassic - Early Cretaceous), when rifting occurred and even accelerated. Several extensional areas were active during the Kimmerian, such as the Dutch Central Graben, the Step Graben and the Terschelling Basin, where up to 2500 m of sediments accumulated. The studied sediments are of Upper Jurassic to Lower Cretaceous age and belong to the largely continental Schieland Group, the predominantly marine Scruff Group and the coastal, shallow- to fairly deep- and open –marine Rijnland Group. Some additional results are provided about the Triassic, especially in regards to early salt tectonics. The understanding of the depositional systems of the Upper Jurassic to Lower Cretaceous hydrocarbon bearing siliciclastic reservoir facies is still incomplete. This research aims at improving our understanding on key processes that influenced the deposition and the thickness distribution of the Upper Jurassic to Lower Cretaceous sequences within the three basins. During this period tectonic processes such as salt flow, diapirism and faulting were induced by regional extension. The hydrocarbon exploration and production in the North Sea involving these reservoirs will benefit from a better understanding of the distribution and the geometry of these facies.

The interpretation and analysis of basin-wide seismic transects provided insights into the overall evolution of the Dutch North Sea. The main focus of this interpretation was to determine the structural style and the interplay between salt tectonics of the Zechstein Group and the deposition of the Upper Jurassic strata during active salt migration and faulting. A detailed analysis of a 3D seismic dataset in combination with well data was carried out in the area of the L5 and L6 blocks, at the boundary between the Dutch Central Graben and the Terschelling Basin. The research question of this work is: “How have the distribution and the geometry of the syn- tectonically deposited Upper Jurassic-Lower Cretaceous clastic growth strata in the Dutch North Sea evolved”. Interpreted seismic sections, time-structure maps and time-thickness maps were compiled to gain insights into the timing and direction of salt migration and the related diapirism during this period of active tectonism. Within the Upper Jurassic interval, two main sedimentary sequences were identified. Structural analysis of these two sequences demonstrates that a number of salt bodies deformed during these periods. The main features in the area are: 1) a NE-SW trending elongated salt wall, that primarily formed during deposition of the oldest Upper Jurassic sequence that is present in the study area, and was fed by salt flow from the Dutch Central Graben area to the west, 2) a large isolated salt diapir is also present in the study area, which formed during deposition of both Upper Jurassic sequences that are present in the study area, and was fed by salt from various locations. Additionally, signs of early salt migration are recognized for the Late Triassic period.

Table of Contents:

Introduction

This report presents the work of a research project carried out in the context of an internship at the Petroleum Geosciences team of the Dutch Organization for Applied Scientific Research (TNO) located in Utrecht. It is related to a Master thesis of the Earth Sciences MSc-program of the Faculty of Earth and Life Sciences of the VU University Amsterdam (MSc-specialization: Solid Earth, Course number 450199, 39 ECTS).

This research internship ran parallel to the 'Focus' research project and fed ideas and results into that project. The 'Focus' research is carried out by TNO and focusses on the Upper Jurassic reservoir facies that are also studied for this thesis. Stakeholders of the 'Focus' project are: TNO, EBN B.V., Oranje Nassau Energie B.V., Sterling Resources Ltd. and, Wintershall Noordzee B.V., GDF Suez E&P Nederland B.V.

Research aims

The area of the Terschelling Basin, the Dutch Central Graben and the Step Graben in the northern Dutch offshore is an important area of interest for the Dutch offshore oil and gas industry. Most of the easily traceable oil- and gas fields have been developed and most simple and obvious hydrocarbon plays have been identified, therefore a better understanding of the distribution of syn-tectonically deposited Upper Jurassic and Lower Cretaceous clastic reservoirs is essential for further exploration success. The presence of hydrocarbon accumulations in Upper Jurassic reservoir rocks is well known, but the influence of salt movement on the Upper Jurassic strata and the depositional systems, during this tectonic active period, is still not completely understood. A better understanding of the distribution of these sequences and the active structures is needed in order to generate new exploration prospects.

The purpose of this study is to investigate the distribution of the Upper Jurassic-Lower Cretaceous reservoir facies and their relationship to active rifting and salt migration in the Dutch Central Graben, Terschelling Basin and Step Graben. During the course of this research project the decision was made to focus on the margin of the western side of the Terschelling Basin and the southernmost part of the Dutch Central Graben. High resolution 3D seismic data is used to study a few selected salt bodies and their relationship to surrounding areas. The main part of this report deals with a structural and seismic study that has been conducted in the area of the L5 and L6 blocks in the Dutch exclusive economic zone (Figure 1 and 2). The main aim is to explain the evolution of these observed, and often very localized, features such as sub-basins or salt diapirs in relation to the regional geological development.

In order to achieve the research aims it was necessary to:

- Perform a literature study that comprises the general geological evolution of the North Sea area, previous work on the study area and the principles of salt tectonics.
- Conduct a basin-wide seismic interpretation study in order to find a suitable area that could be studied in greater detail. Three large basin-wide transects were interpreted in order to identify such an area and to get familiar with the structural style of the Dutch Northern Offshore.
- Analyze well-logs of most of the wells within the study area, to determine the signature of the different facies that are present within the Upper Jurassic interval in the study area, to verify a preexisting well marker dataset.
- Conduct seismic-to-well ties.
- Structurally interpret horizons and faults in 2D and 3D seismic data, to create time-structure maps and time-thickness maps using modeling software and to visually edit the results using a drafting software.
- Use the seismic interpretations to determine the distribution and the geometry of growth strata present in the study area.
- Study cored intervals of Upper Jurassic strata from selected wells in order to determine some of the depositional environments in the study area.

This research is relevant for the oil and gas industry since a greater understanding of the distribution, structure and evolution of the proven Upper Jurassic hydrocarbon reservoirs can aid future explorations of hydrocarbons in the study area.

Research area

In the Dutch Offshore the syn-tectonically deposited Upper Jurassic and Lower Cretaceous clastic reservoir rocks, such as the Terschelling Sandstone Formation or the Scruff Greensand Formation, are located in the Kimmerian rift basins of the southern North Sea. These clastic sediments were deposited at the same times as the formation of NNE-SSW and NW-SE trending salt bodies. These salt bodies possibly formed as a result of reactive diapirism triggered during the Kimmerian period of extension (E-W and later NE-SW). The direction of extension was oriented perpendicular to the orientation of the salt walls. Late Cretaceous to Early Cenozoic compression pulses inverted the rift basins and rejuvenated the salt structures. The study area of this research project is shown in Figure 1 and 2. The position of three regional transects, that were interpreted for this work are shown in Figure 2. Figure 1 gives an overview of the hydrocarbon fields and the economic activity in the vicinity of the study area.

Report structure

This report starts with a brief introduction of the scope and context of this research, including an introduction to the research area. In the next chapter the geological setting and the structural evolution of the Dutch North Sea including background on salt tectonics is provided. The dataset used and the methods employed in this study are then presented. Subsequently, the detailed results of this study are presented: 1) three basin-wide cross sections are presented; and 2) the results of the more detailed analysis in the L5 and L6 area are described. Time-structure and time-thickness maps are presented as well as six interpreted seismic lines. In the later section, the results are presented and their implications discussed. The discussion focuses on the events that structurally affected the Upper Jurassic. The last section summarizes the results and the conclusions, which can be drawn from this study. Recommendations for future work are then proposed. A digital copy of this report, including all figures and appendices, can be found here:
https://www.dropbox.com/sh/om2l8sjlzmrkjr8/AABkqMLcDvqsBxp3jc6VKU4aa?dl=0
High resolution versions of the figures presented in this report can be found online at that location.

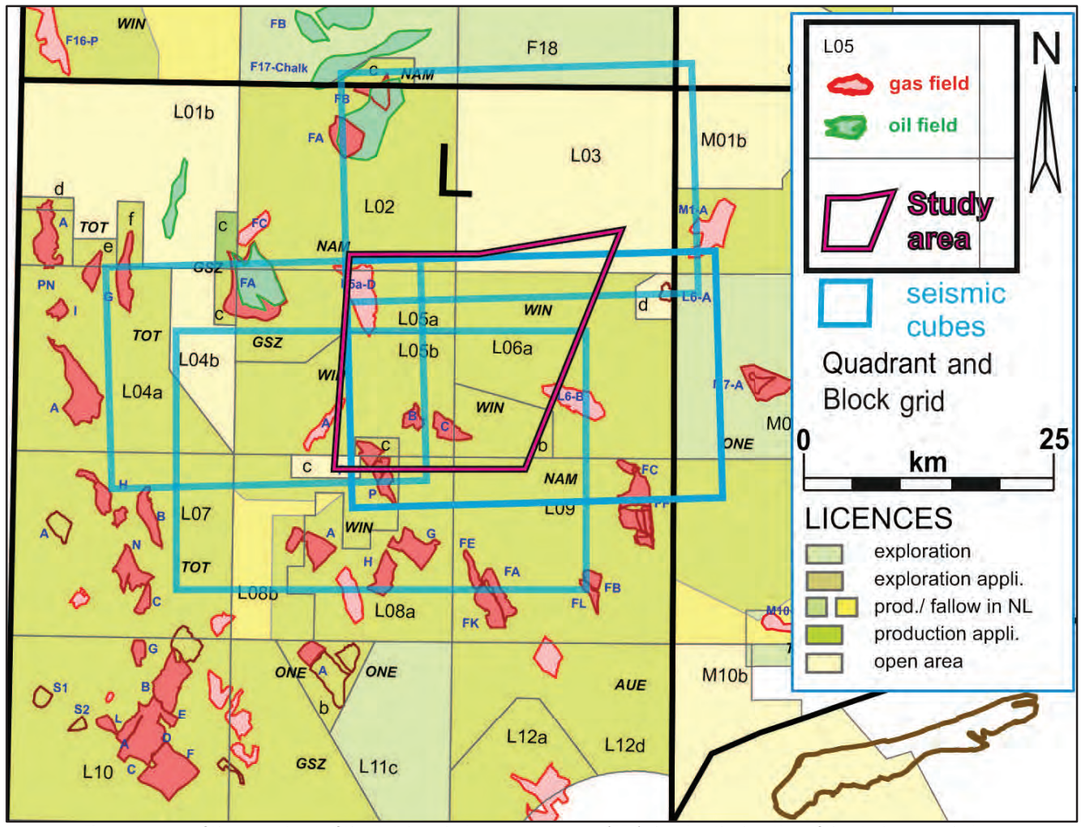

Figure 1. *Map of the L quadrant of the Dutch exclusive economic zone (EEZ) showing the location of the study area relative to the present hydrocarbon fields, licenses and sub- blocks. Also the outlines of four 3D seismic surveys that were used are indicated (modified after the CGG Gas & Oil Map©).*

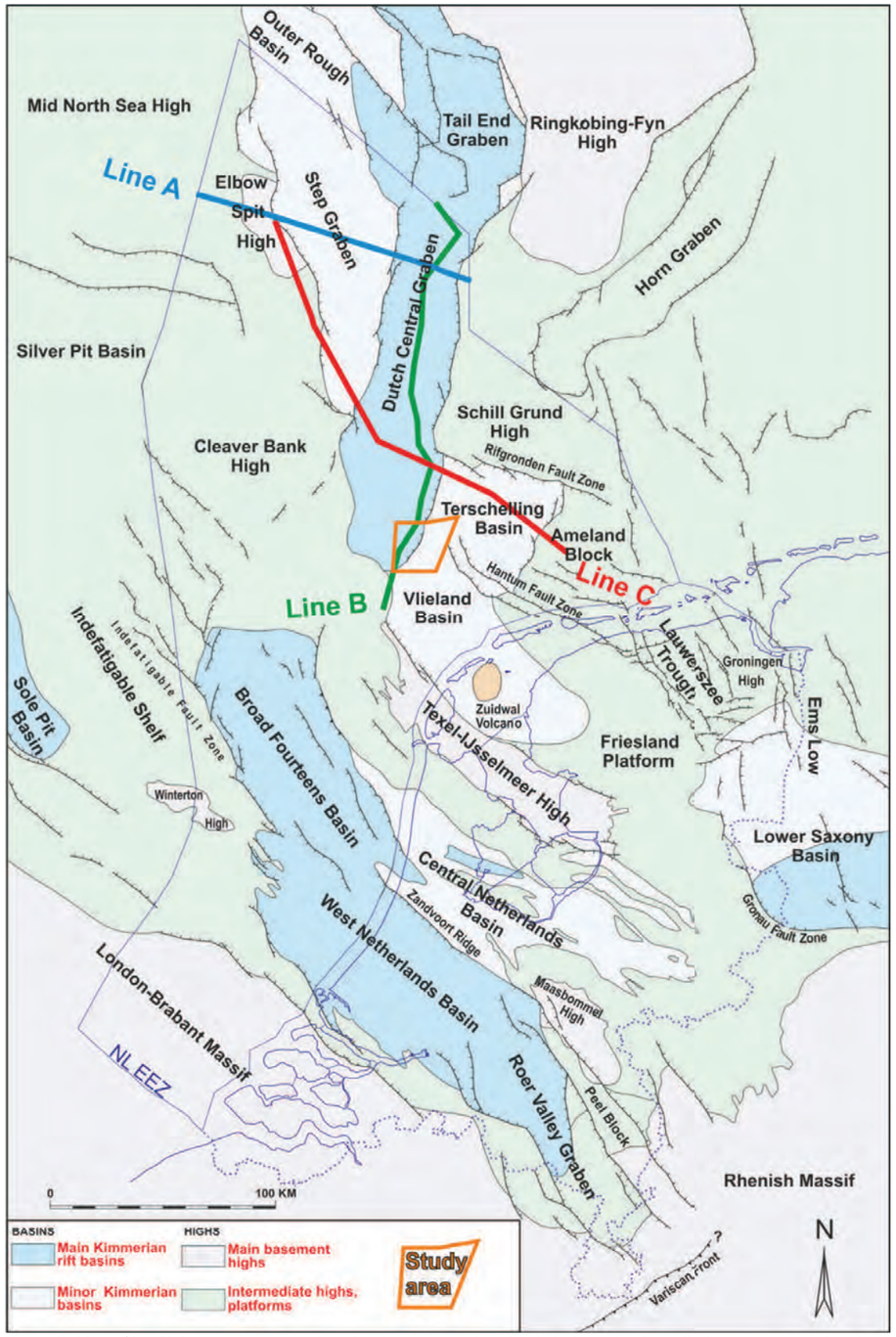

Figure 2. *Map of the Netherlands showing the structural elements in the Late Jurassic - Early Cretaceous period. Also the location of the study area of this research (orange polygon) together with the orientation of three regional transects (Line A in blue, Line B in green, Line C in red) are shown (modified after de Jager, 2007).*

Geological setting of the North Sea and previous work

Structural history of the Dutch North Sea

The following section summarizes the evolution of the Dutch North Sea, mainly focusing on the Late Jurassic period, as it is the main subject of this research. For a more comprehensive description of the geological development, the tectonic evolution and the deposited strata, the publications of Ziegler (1990a), Wong et al. (2007a), McCann (2008a), McCann (2008b), Doornenbal & Stevenson (2010) are recommended.

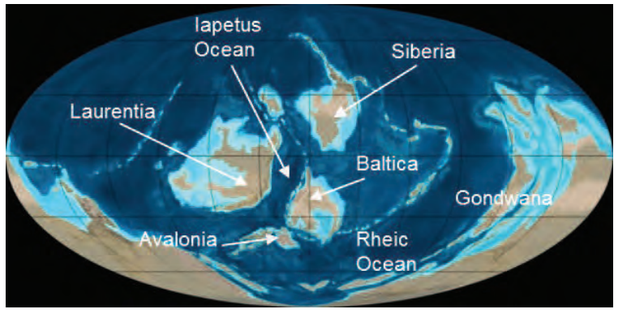

Figure 3. *The plate-tectonic setting at Late Ordovician time, ca. 450 Ma ago just before the Caledonian orogeny. The names of the individual terrains are indicated (after Blakey, 2009).*

At the end of the Precambrian, in Meso-proterozoic times, the assemblage of Rodinia, the oldest known supercontinent, took place (~1100 Ma; Scotese, 2003). During Neoproterozoic times (~750 Ma) Rodinia was split up into several continents: Gondwana, Laurentia, Baltica and Siberia (Ziegler, 1990). The area comprising the future North Sea and the Netherlands was situated on the eastern side of the Avalonian microplate (Glennie, 2005). In the Late Ordovician (~450 Ma) the Tornquist Sea was closed by the convergence of Avalonia towards Baltica (Figure 3).

During the mid-Silurian (~425 Ma) Laurussia, known as the 'Old Red Continent', assembled when the joined masses of Baltica and Avalonia collided with Laurentia, closing the Iapetus Ocean and creating the N-S trending Caledonian Fold Belt in the process (Glennie, 2005). In Figure 4 the timing of the tectonic phases are shown next to the orogenic phases and the geological time scale. It shows that the formation of the supercontinent of Pangea took place during the Caledonian and Variscan orogeny and underwent several tectonic phases.

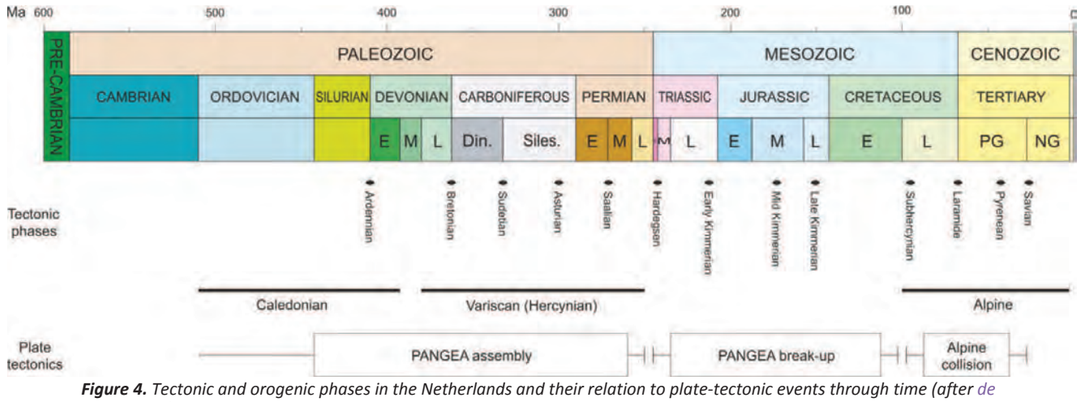

Figure 4. *Tectonic and orogenic phases in the Netherlands and their relation to plate-tectonic events through time (after de Jager, 2007).*

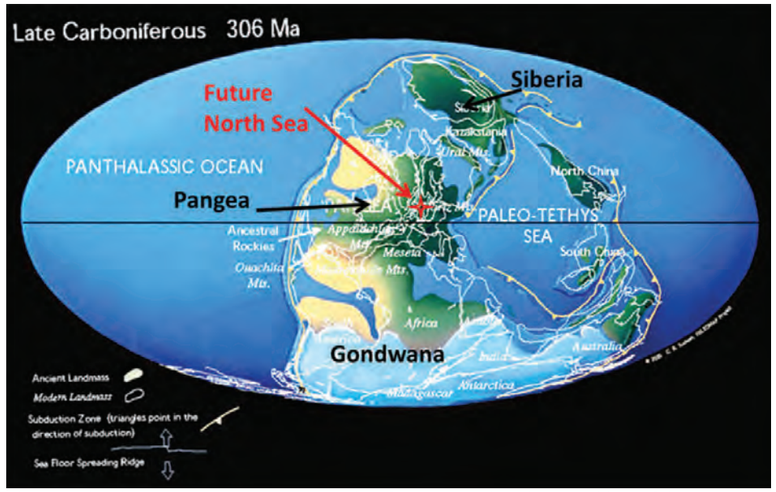

Figure 5. *The plate-tectonic setting at Late Carboniferous time when the assemblage of the supercontinent of Pangea was completed. The names of the individual terrains are indicated as well as the location of the future North Sea area (after Scotese, 2003).*

During the Early Devonian (~400 Ma) the area of the future North Sea and the Netherlands was located approximately 20° south of the equator on the southern margin of the Laurussian Plate (Scotese, 2003). Laurussia and Gondwana started to collide during the Middle Devonian (ca. 390 Ma) creating the active east-west oriented Variscan Fold Belt, which was located south of the Rheic Ocean (Glennie, 2005). The continents of the future European and North-American continental plates on one side of the Rheic Ocean and Gondwana on the other side continued to converge during the Variscan orogeny (Figure 5) and by Late Carboniferous times (~290 Ma) the formation of the supercontinent of Pangea was completed as the Armorican Terrane Assemblage and the Iberian microcontinents successively accreted against the southern margin of Laurussia (Soper et al., 1992; Glennie, 2005; Pharaoh et al., 2010; Doornenbal and Stevenson, 2010).

The area of the future Netherlands and the North Sea was located north of the Variscan Fold Belt and continued to drift further northward, as compression from the Variscan orogeny continued. The landlocked position close to the Equator where a humid and tropical climate prevailed was maintained (Scotese, 2003).

The latest Carboniferous (Gzhelian ~290 Ma) and Early Permian were marked by the final suturing phases of Pangea. The late-Variscan and post-orogenic evolution of the crust of the Southern Permian Basin was affected by wrench faulting associated with intrusive and extrusive magmatism (Ziegler, 1990a; Wilson et al., 2004). This caused profound thermal thinning of the lithosphere that and broad uplift that resulted in deep erosion (Ziegler et al., 2004; De Jager, 2007). The so-called Permo-Carboniferous tectonic-magmatic event formed large NW-SE trending swells and is now represented by the eroded Westphalian subcrop at the Base Permian Unconformity (De Jager, 2007 and Van Buggenum & Den Hartog Jager, 2007).

The dominant NW-SE fault set in the Netherlands, which can be seen, for instance, at the Hantum Fault, probably dates back to the Caledonian orogeny when Laurentia and Avalonia collided (De Jager, 2007). Early Permian reactivation of this mid-Paleozoic fault set was probably caused by the wrench faulting, whilst regionally a conjugate set of NE-SW to NNE-SSW faults developed (Ziegler, 1988). This is the second most common fault set in the Dutch subsurface (Ziegler, 1990a).

The Base Permian Unconformity represents a hiatus of around 40 to 60 Ma and plays an important role in the petroleum geology of the North-Sea area (De Jager & Geluk, 2007). Namurian

to Westphalian strata are overlain at this level by upper Rotliegend strata, which started to be deposited during the Permian in the large E-W trending Southern Permian Basin (Geluk, 2007a). Nowadays, the pre-Permian sedimentary succession reaches thicknesses of up to 10 km in large parts of the North Sea area (Nielsen et al., 2005). Due to poor well control there is only little direct information on the exact age of these deposits (Geluk et al., 2007).

Regional subsidence dominated the evolution of the southern North Sea Basin in Permian times, as the thermal anomaly decayed (Van Wees et al., 2000). The Permian period was a time of relative tectonic quiescence (Paul, 2006) of the area of the future Netherlands and the North Sea. Ongoing subduction of the Paleotethys Ocean beneath the southern margin of Europe caused the region of the study area to drift further northward (Stampfli & Borel, 2002). Here, at approximately 20° north of the equator, an arid climate prevailed (Glennie, 1998; Geluk, 2007a).

The outlines of the Proto-Dutch Central Graben, Broad Fourteens Basin and Lauwerszee Trough can already be recognized in the upper Rotliegend isopach patterns (De Jager, 2007).

Because the subsidence rates exceeded sedimentation rates, due to the profound thermal relaxation of the crust, a landlocked depression developed, which was located well below global sea-levels. The eustatic sea-level had risen due to the melting of the ice cap on the continent of Gondwana (Ziegler, 1990a). This resulted in the emergence of a seaway between the Southern Permian Basin and the Barents Sea during the late Permian. The rifting in the Arctic/North Atlantic region combined with the creation of this seaway resulted in the very rapid flooding of the Southern Permian Basin with saline sea-waters. This made it possible for the cyclic salt and anhydrite-dominated evaporites of the Zechstein group (~272 - 253 Ma) to be deposited (De Jager, 2007).

It is the post-burial migration of these evaporites that has greatly influenced the post-Permian structural evolution of the Netherlands and the North Sea area. A large part of the present study focuses on areas where Zechstein rock salt migrated.

Lithostratigraphy of the Upper Permian Zechstein Group

According to Ziegler, (1990a) the mechanism controlling the cyclicity of the Zechstein deposition has a glacio-eustatic origin. Seven cycles have been identified, from which five have been found in the Netherlands. The base of each cycle is marked by a transgressions (Figure 6).

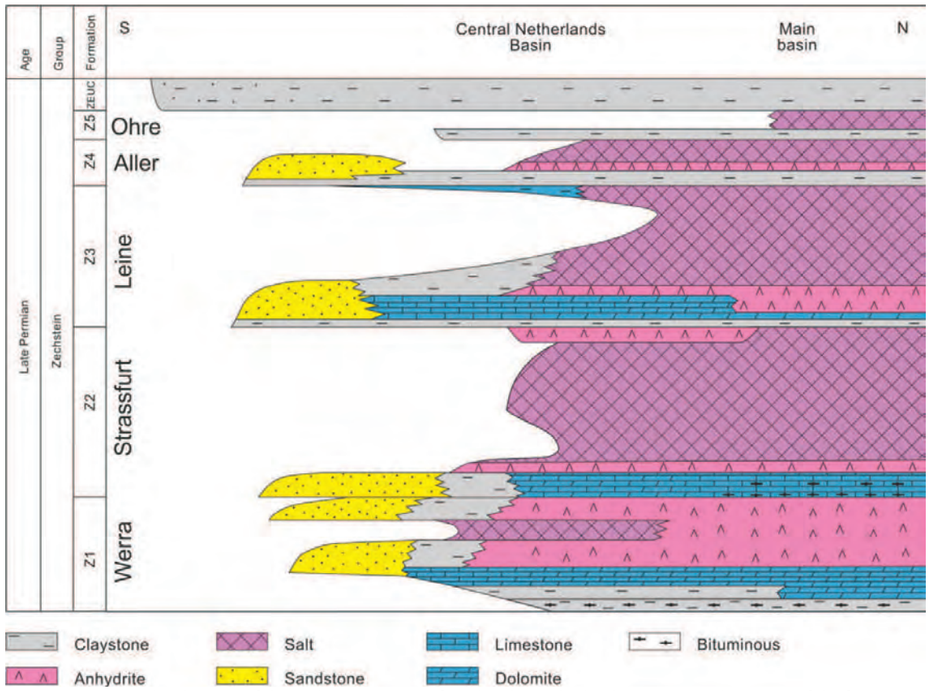

Figure 6. *Stratigraphic diagram of the Zechstein Group as found in the Netherlands. Z1 - Z5 are the names of the five evaporite cycle. In the study area the Z2, Z3 and Z4 salt members are the major salt intervals involved in salt mobilization and in the formation of diapirs (figure from Geluk, 2007).*

The total original depositional thickness of the Zechstein Group increases from 50 m in the southern Netherlands, to over 1200 m in the northern part of the Dutch North Sea. The exact depositional thickness of the Zechstein Group is still the subject of debate. A recent TNO in-house study conducted by van Winden (2015), concludes that a maximum thickness of up to 2000 m is more likely. In this case dissolution, erosion and redistribution processes during diapirism must have had a greater influence on the distribution of the Zechstein Group. Sequence stratigraphic models describe the cyclicity of Zechstein as governed by phases of initial marine transgression, followed by regressive phases with the deposition of evaporites as a result (Richter-Bernburg, 1955). The basal Z1 Werra, Z2 Strassfurt and Z3 Leine Formations follow the classic carbonate-evaporite cycle and associated clastics. The carbonate unit of each formation shows a basin, slope to platform facies transition, which confirms that these three formations were deposited in a marine environment.

The basal member of the Werra Formation (Z1) is a finely laminated claystone with a TOC (Total-Organic-Carbon) up to 5% (Lokhorst, 1998), followed by the Z1 Carbonate, Z1 Anhydrite, the Z1 Salt members with local sandstones in the southern part. The formation onlaps onto the London-Brabant Massif in the south-west, and has a constant thickness of around 50 m in the main basin of condensed strata due to low sediment supply. The thickness of the formation increases towards the eastern part of the Netherlands where, the Z1 Anhydrite Member reached 500 m of thickness in a platform facies.

The Stassfurt Formation (Z2) was deposited with a thickness of 50 m in the south and reached 700 m in the northern offshore and comprises a basal carbonate unit, followed by a Basal Anhydrite Member and Z2 Salt Member. Local sandstones occur in the western offshore and the southern limit is represented by an anhydrite-bearing claystone unit. The salt of the Z2 formation reached an original thickness of over 600 m, and is mainly composed of halite. It is strongly deformed due to halokinesis.

The strong movements of the Z2 Salt Member, caused the intense deformation of the upper Z3 Leine Formation that comprises relatively brittle layers consisting of anhydrite, carbonate and clay. The basal member is represented by grey shales with thickness variance from 5 to 10 m, followed by the Z3 Carbonate Member represented by a few meters of dark-colored limestone. The Main Anhydrite Member presents a significant thickness variability, increasing from 3 m in the shelf to a maximum of 100 m of depositional thickness. It was deposited only on the northern part of the carbonate platform, the slope, and in the basin. The upper part of the Leine Formation is the Z3 Salt Member that has an depositional thickness of 300-400 m and was only deposited in the north-western offshore and the north-eastern onshore of the Netherlands. It is mainly composed of halite in the lower part and has an upper part represented by layers of potassium-magnesium and 10 m thick beds of bischofite.

The Aller Formation is mainly composed of the basal Red Salt Clay Member and the Z4 Pegmatite Anhydrite Member. The Z4 salt occurs only in depocenter of the main basin where it reached 150 m of thickness.

The Ohre Formation, which occurs only in the north-eastern onshore and north-western offshore of the Netherlands comprises several meters of claystone and up to 15 m of halite. The absence of carbonate platform facies in the last two cycles attests the deposition in permanently hypersaline conditions (Geluk, 2007).

Due to extensive halokinesis in large areas of the North Sea it is difficult to determine the original depositional thickness of the Zechstein sequence. In the axial parts of the Southern Permian Basin the original thickness is estimated to be around 1500 m (Ziegler, 1988, 1990a). In ten Veen et al. (2012) a restoration of the depositional thickness in the Netherlands of the Z2, Z3 and Z4 salt members of approximately 200 to 900 m is presented (Figure 7a). The map of the present-day thickness of the Zechstein Group (Figure 7b) shows major thickness variations null to > 1800 m.

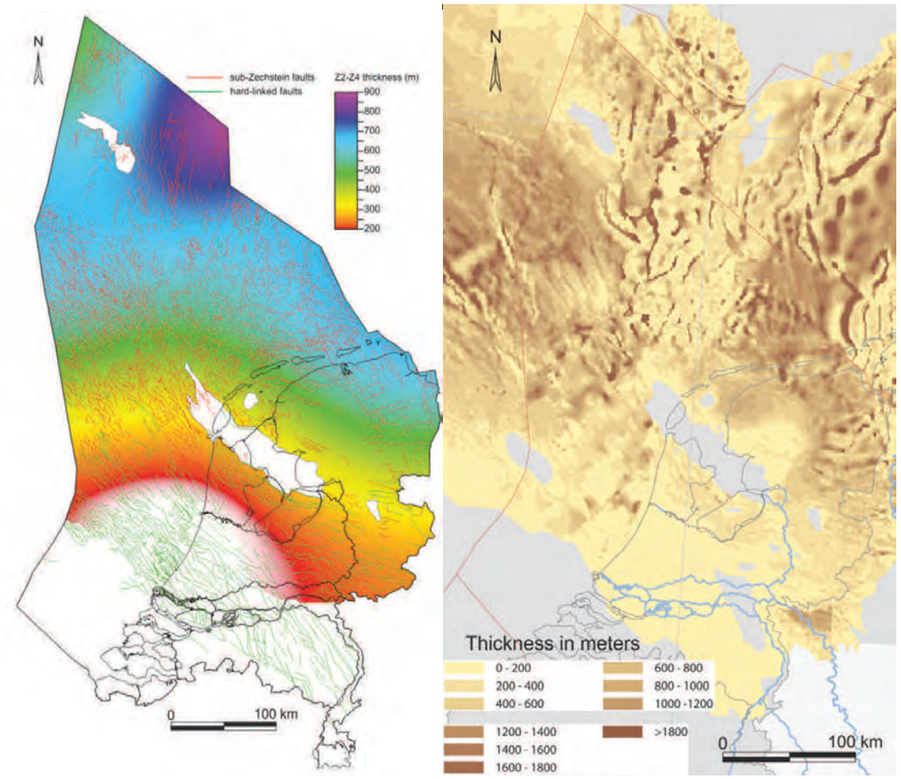

Figure 7. A) *Thickness distribution of the original Zechstein salt thickness (Z2, Z3 and Z4 salt cycles)in the Netherlands based on smoothing restoration (after ten Veen et al., 2012). Also the major faults offsetting the Zechstein Group are indicated.* ***B)*** *Present-day thickness and distribution of the Zechstein Group in the Netherlands (modified after Doornenbal & Stevenson, 2010).*

Mesozoic development

At the start of the Mesozoic, the area of the Netherlands was located in the arid climate zone but moved to the sub-tropical climate zone on the northern Hemisphere during the Kimmerian rift phase, in Triassic - Early Cretaceous times. The break-up of Pangea initiated in the Early Triassic times with the onset of rifting between Fennoscandia and Greenland (Lott et al., 2010). As the crustal extension slowly propagated southward, an eastern rift arm developed at the present day North Sea area. Although the rift intensity rapidly decreased southward, by Middle Triassic times rifting also took place in the southern North Sea area (Ziegler, 1990a). By the end of the Early Cretaceous rifting in the North Sea area stopped after crustal separation was achieved in the Central Atlantic.

Triassic and Early Jurassic strata show very regular and broad facies patterns, because, in the Netherlands, this period is characterized by relative tectonic quiescence and the sedimentation was mainly influenced by thermal subsidence (De Jager, 2007). After the deposition of the Zechstein Group, the oldest Triassic strata are the lacustrine sediments of the Lower Buntsandstein Formation, which are followed by the fluvio-eolian clastics of the Main Buntsandstein. Marine conditions prevailed during the Middle Triassic leading to the deposition of claystones, carbonates and evaporites of the Röt and Muschelkalk Formations and the fine-grained clastics of the coastal plain to marine Keuper Formation. The fine-grained, mainly argillaceous clastics of the Lower Jurassic Altena Group were deposited in an epicontinental sea that had developed during continued regional

subsidence. During the Middle Jurassic the Central North Sea thermal dome caused the uplift of wide area of the North Sea. Also much of the Dutch offshore was uplifted, which restrained sedimentation only to the active N-S trending rift basin of the Dutch Central Graben (Ziegler, 1990; Underhill & Partington, 1993).

The main structural elements in the Dutch subsurface were formed during the climax of the Kimmerian tectonic phase (Late Jurassic - Early Cretaceous) when rifting strongly accelerated. These Kimmerian extensional areas in the Dutch part of the North Sea, the Dutch Central Graben, the Step Graben and the Terschelling Basin, deepened and accommodated up to 2500 m of sediments mainly belonging to the largely continental Schieland Group, the predominantly marine Scruff Group and the continental to restricted marine Niedersachsen Group (De Jager, 2007). For a comprehensive description of the depositional environments and the stratigraphy of the Upper Jurassic strata in the Dutch North Sea the publication of Munsterman et al. (2012) is recommended. Figure 8 summarizes the complex sedimentary relationships of the Late Jurassic period in the study area.

At first, the extension direction was oriented E-W and only affected the narrow axis of the Dutch Central Graben, this phase is referred to as Sequence 1 in Abbink et al. (2006) (mid-Callovian, Oxfordian and early Kimmeridgian). The sediments associated with this phase belong to the Central Graben Subgroup, of the Schieland Group. It is mainly present in the Dutch Central Graben, but the latest occurrence is in the Terschelling Basin where the Friese Front Member is the lowest Upper Jurassic strata (Figure 8). According to Munsterman et al. (2012) these silty to clayey sandstones, claystones and distinct coal layers have been deposited during a transgression in a predominantly non-marine coastal to delta plain setting.

A more arid phase commenced during the Upper Jurassic, when a change in structural style also occurred in the southern North Sea. The E-W direction of extension changed to NE-SW (Zanella & Coward, 2003). NW-SE normal faulting developed, as the dominant Paleozoic NW-SE trending lineaments reactivated. As a result the Step Graben and the Terschelling Basin opened and subsidence in some parts of the Dutch Central Graben halted. During this phase, which is referred to as Sequence 2 in Abbink et al. (2006) (early Kimmeridgian - early Portlandian), the Terschelling Basin was filled with up to 2000 m of thick siliciclastic deposits, mainly belonging to the predominantly marine Skylge Formation (Duin et al., 2006), which is part of the Scruff Group. Following the nomenclature introduced by Munsterman et al. (2012), the Skylge Formation is subdivided into the Oyster Ground Member, the Terschelling Sandstone Member, the Noordvaarder Member and the Lies Member. In general, it can be stated that the Skylge Formation consists of alternating silty to sandy claystones and argillaceous and/or non-argillaceous glauconite sandstones (Munsterman et al., 2012). In the northern part of the Dutch Central Graben the fine-grained Kimmeridge Clay Formation was deposited during this phase (Figure 8).

During the last phase of rifting, which occurred around the Jurassic-Cretaceous boundary (early Portlandian - Ryazanian; Sequence 3 in Abbink et al., 2006), the NW-SE faulting decreased. The Terschelling Basin and the Step Graben further deepened whereas certain parts of the Dutch Central Graben were subject to erosion. The Scruff Greensand Formation and the Lutine Formation were deposited during this phase, after which the arid climate period came to an end.

The Scruff Greensand Formation, which comprises the Scruff Spiculite Member and the Stortemelk Member, consists of gray-green shallow marine fine-grained sandstones that are often intensely bioturbated. The glauconite content is generally high and locally spiculites are abundant at the base of the section. The sandstones may be slightly argillaceous and/or calcareous (Munsterman et al., 2012). The Clay Deep Member of the Lutine Formation consists of brownish, grey and black bituminous claystones. The Schill Grund Member consists of olive-grey to grey-brown very fine to silty sandstones (Munsterman et al., 2012).

Cretaceous and Paleogene development

Prior to Sequence 3 sensu Abbink et al. (2006) the adjacent platform areas of the rift basins were uplifted during the Kimmerian phase, which is represented by an unconformity of Early Cetaceous age. Following the erosion and deep truncation of the highs surrounding the rift basins, open marine conditions took over.

The rifting in the North Sea area ceased in the Early Cretaceous (late Ryazanian) and the faulting in the Graben area gradually came to a halt as the ocean spreading commenced westward of the Iberian Plate. During the subsequent post-rift sag phase thermal subsidence caused relative sea-level rise (Kombrink et al., 2012). Over 1400 m of claystones, shales marls, siltstones and fine-grained glauconitic sandstones of the largely argillaceous Rijnland Group were deposited in a shallow marine to coastal environment. The sedimentation took place in a broad area and stepped over onto the adjacent platform areas, like the Schill Ground High and the Cleaver Bank Platform, and effectively blankets the former graben and platform configuration.

During Late Cretaceous times the sea-level reached an all-time high and, together with regional subsidence, the conditions favored the deposition of relative uniform chalk lithologies with rhythmic bedding. Shallow seas even covered elevated structures such as the London-Brabant Massif. In areas located further offshore the deposits of Chalk Group reached up to 1500 m (De Jager, 2007). The present-day thickness of the Chalk Group is variable, but generally increases towards the southwards.

Northward directed compression originating from the early Alpine continental collision induced the inversion of the Kimmerian rift basins in the southern North Sea (Coward et al., 2003). Two major phases of inversion are recognized (De Jager, 2003; Total, 2007). The timing of these pulses is comparable for the involved areas, but the scale of the inversion has a great variability (De Jager, 2007). The first inversion phase, which started during the Late Cretaceous, was the Subhercynian to Laramide phase. Especially the Laramide pulse was well developed in the Dutch territories (De Jager, 2007; Total, 2007). The Pyrenean to Savian Phase was the second period of inversion in the North Sea, which was most pronounced in the UK offshore (Total, 2007). Between the two major inversion phases and parallel to the Cretaceous-Paleogene transition the extensional movements in the Atlantic system resumed (Coward et al., 2003). In the Terschelling basin some of the strain of the inversion pulses was accommodated by transpressional movement along the Hantum Fault Zone. This fault zone lies to the southeast of the study area and bounds the Terschelling Basin to the south. It was formed during Late Carboniferous times and consists of WNW-ESE trending synthetic strike slip faults and NW-SE antithetic strike slip faults (De Jager and Geluk, 2007).

It is important to note that in literature the term ‘inversion’ is used for several phenomena. Inversion structures are often associated with compressional strain affecting sedimentary basins, but three modes must be differentiated: Direction reversal of individual structures of faults; basin subsidence evolving into basin uplift; and apparent or relative movements of adjacent structures (Buchanan & Buchanan, 1995; Clausen et al., 2012). In this research the inversion of an extensional basin is defined as the accommodation of compressional or transpressional strain by reverse reactivation of existing normal faults or the development of reverse faults and folds (MacGregor, 1995; Turner & Williams, 2004; Jackson et al., 2013).

In large areas of the Dutch North Sea, due to the more than 1 km thick Zechstein salt package, the faults below and above the Zechstein are completely detached and reacted differently to the strains of the inversion pulses. This resulted in a broad uplift of the post-Zechstein deposits. For the purposes of the exploration and production industry it is very important to understand the processes involved with basin inversion, because it can play an important role in the development of hydrocarbon traps.

The Upper Cretaceous Chalk Group is overlain by the successive deposits of the siliciclastic Lower, Middle and Upper North Sea Group that filled the North Sea basin during the Cenozoic as a result of the ongoing thermal subsidence and sediment loading subsidence (Duin et al., 2006). In Paleogene times the sediments were the erosional products derived from areas uplifted by the Alpine orogeny. During the Miocene and Pleistocene the westward prograding deltas of the Eridanos River dominate the deposition in the southern North Sea (de Jager, 2007). It is likely that differential loading of the Mesozoic salt structures, due to increased sediment input, differential compaction of Mesozoic and Cenozoic strata and mid-Miocene tectonic rejuvenation caused Late Cenozoic salt movement (Clausen et al., 2012 and Harding & Huuse, 2015).

Principles of salt flow and previous work on diapirism in the Dutch North Sea

Most of the information in this section is taken from the publication of Hudec & Jackson (2007). This section provides a summary of some of the principles used when dealing with deformation involving evaporates.

Most salt tectonic literature uses the term 'salt' not only for the pure and crystalline halite (NaCl), but applies it in a much broader sense. The amount of halite in a salt body may vary and often a salt body contains other sorts of evaporites and even non-evaporitic lithologies. In the southern North Sea and in the Netherlands the Z2, Z3 and Z4 salt cycles of the Zechstein are the major salt intervals involved in salt withdrawal and the formation of diapirs.

In the study area, the Upper Triassic evaporite layers (Main Röt Evaporite Member, Upper Röt Evaporite Member, Muschelkalk Evaporite Member, Main Keuper Evaporite Member and Red Keuper Evaporite Member) are probably too thin to be involved in diapirism, but can accommodate extension and act as levels of detachment where faults sole upon. Penetration of Zechstein salt into these Triassic salt layers can be seen in the study area.

Salt can be considered to behave like a fluid over geologic time scales. Having a negligible yield strength, salt is usually the mechanically weakest part of any rock system. Deformation is often localized or accommodated by salt bodies. Evaporites typically deform by means of dislocation creep and diffusion creep. In general, salt is less dense than moderately to fully compacted overburdens. This density inversion makes the sedimentary succession gravitational unstable. At burial depths from 650 m to 1500 m, buoyant salt rise may commence. In the southern North Sea, it took until the Middle Triassic for the first salt swells to form and started to locally interrupt the broad nature of the facies patterns (de Jager, 2007; Pharaoh et al., 2010).

Three types of (differential) loading are known to drive salt flow: gravitational loading, displacement loading and thermal loading. The forces needed to deform the (brittle) overburden, and the force it takes to let salt flow take place within a buried layer, oppose salt movement. Hence, the strength of the sedimentary roof and the boundary drag along the edge of the salt layer play a role. It can be assumed that most diapirs have pierced brittle overburdens (Hudec & Jackson, 2007).

When differentially loaded, the rising movement of salt can be activated by one of four mechanisms: Reactive piercement, active piercement, erosional piercement and/or thrusting piercement. Passive diapirism may take place when the upwelling salt body has completely pierced the overburden and is exposed at the surface were sediments accumulate around it. Reactive diapirism takes place in response to regional extension when the brittle overburden of a salt layer is thinned and weakened, resulting in a rising motion of the salt that fills the space created in the developing graben. Reactive diapirism is considered to be the main mechanism of initiating salt flow (Vendeville & Jackson, 1993). Salt migration sometimes results in thinning of a salt layer in such a way that the top and the bottom contacts of the salt layer have merged resulting in a salt weld. When a salt weld forms, movement of the salt seizes, and the level does not act as an effective detachment anymore. Vertical salt welds may also develop when the sides of a former diapir meet. The formation of vertical salt welds is often caused by regional compression.

Regional shortening thickens and therefore strengthens the overburden of salt bodies. This may slow down the formation of new salt diapirs. However, regional shortening also may focus deformation at an already existing salt body. This is called diapir amplification and often is seen together with the phenomena of 'teardrop' diapir formation that have become detached from their source area. As a result a steep salt weld separates the salt pedestal and the allochthonous 'teardrop' shaped salt body. Further compression will often lead to reactivation of the salt weld as a thrust plain. Allochthonous salt sheets overlie stratigraphicaly younger strata. The sheets can be emplaced in one of four modes: extrusive salt sheet advance; open-toed advance; thrust advance and salt wing intrusion. Salt-wing intrusion is a special form of allochthonous salt emplacement where a salt body penetrates younger salt layers from the flank of a diapir. According to Hudec and Jackson (2007) salt wings are only known from the Zechstein salt basin. It is thought that during Late Cretaceous shortening these Zechstein wings intruded into the shallower Triassic evaporite layers as areas of lower pressure developed due to buckling (Hudec, 2004).

We have seen that the burial depth plays a role in initiating and driving salt flow, but also the total thickness of the salt layer has a large influence on the structural evolution of a basin. In the area of the southern North Sea this means that the distribution and the thickness of the deposits of the former Zechstein basin play a major role. Ten Veen et al. (2012) imply that where the depositional thickness of the Zechstein salt is less than 300 m the structural style is 'thick-skinned', meaning that the sub-Zechstein faults reflect the regional stress history and have propagated into the supra-salt layers. This explains why the fault patterns in 'thick-skinned' areas are similar in the sub- and supra-salt layers. When the depositional thickness of the salt layer is thicker than 300 m the structural style is 'thin-skinned'. This means that regional stresses will deform the sub-salt domain in a brittle way and sub-salt faults do not propagate through the salt layer. In terms of stress, the layers above the salt are detached from the sub-salt domain and are only indirectly related to the active stress field. In the rift basins of the Dutch North Sea almost all diapirs and salt walls seem to originate at major pre-Zechstein faults, and thus, are oriented along the strike of the structural grain (ten Veen et al., 2012). Salt mobilization was initiated during the Early Kimmerian (228-203 Ma), but the main phase of active diapirism and salt flow occurred during the Late Kimmerian extension (154-140 Ma), followed by some minor activity during the Subhercynian inversion pulse (Remmelts, 1995; ten Veen et al., 2012). Alternating movements of intersecting fault patterns caused isolated diapirs to rise up. These salt structures are probably younger than the larger salt walls in the region, which are oriented along single faults (ten Veen et al., 2012).

Previous research concerning the study area and current state of knowledge

Apart from finding a relation between salt structures, their thickness and underlying faults, ten Veen et al. (2012) also stress that the amount of dissolved and re-deposited salt during the extrusive phase of the salt bodies is still unclear. Koyi and Petersen (1993); Koyi et al. (1993) and Remmelts (1995, 1996) also identified relations between the position of sub-salt faults and salt bodies.

Detailed 3D seismic analysis on specific salt bodies have been carried out previously in the southern North Sea: In the UK sector of the southern North Sea Jenyon (1984; 1985 and 1988) studied individual salt structures and interpreted their movements, collapse structures and diapirs related to basin edge faulting and the deformation mechanisms of diapir roofs before piercement. Davison et al., (2000) studied, in the UK Central Graben, the mechanics of Zechstein salt piercement of the overburden. The structural evolution of specific salt walls and diapirs in the Danish Central Graben were studied by Rank-Friend & Elders (2004). One of their findings was that during the Kimmerian rifting, straight salt walls developed from the Zechstein salt level. In Early Cretaceous times the salt migrated along the axis changing the appearance of the salt into isolated diapirs. Harding & Huuse (2015) studied the timing and evolution of a specific diapir using thickness maps in

a small area (also the Terschelling Basin) approximately 70 km to the southeast of the study area of this work.

De Jager (2012) wrote about the discovery of the Fat Sand Play in the L9 block located in the northern sector of the Vlieland Basin, just southeast of the study area of this work. These syn-extensional aeolian sands were deposited in an early half-graben with a listric fault soling out on top of a Zechstein salt swell. It is also concluded that early salt flow led to the development of turtle structures in Triassic times during deposition of the Röt- and Muschelkalk Formations.

A lot of work has been done on inversion structures present in northern Germany and the southeastern part of the North Sea: Baldschuhn et al. (1991) reviewed hypotheses to explain the inverted salt structures of Mesozoic age in Northern Germany (Lower Saxony basin, Pompeckj block, Gifhorn trouth). They conclude that most inversion structures formed due to small scale readjustments in the graben areas rather than long distance stress regimes (e.g. Alpine compression). Mohr et al. (2005) studied the interaction between sedimentation and salt flow at the western flank of the Triassic Ems Low. Using 2D seismic interpretation and reconstruction they conclude that during the Late Cenozoic salt diapirs rejuvenated in specific episodes triggered by regional tectonic pulses.

A series of research projects by TNO - Geological Survey of the Netherlands focused on the so-called NCP-2A area. This area includes the Terschelling Basin and the southernmost part of the Dutch Central Graben. These studies had the objective of generating a comprehensive 3D subsurface model of the geology of the Dutch offshore (Verweij & Witmans, 2009). This included: Well log correlation, biostratigraphic analysis, sedimentological analysis, seismic interpretation, construction of a 3D time model, time-depth conversion, petrophysical analysis, maturity analysis, temperature analysis, hydrodynamic characterization, fluid composition analysis, construction 2D maps and cross-sections and basin modelling. The results of that work can be downloaded via the website of the Dutch Oil and Gas portal (http://www.nlog.nl/nl/pubs/maps/geologic_maps/NCP2_Subregions.html). Via this website TNO - Geological Survey of the Netherlands publishes updated reports on several of the previously mentioned subjects together with updated depth- and thickness maps of the major intervals present in the Dutch subsurface. Thus, the present state of knowledge about the Dutch subsurface can be found at the NLOG website.

The publication of Munsterman et al. (2012) that revises the nomenclature of the Upper Jurassic stratigraphy in the Dutch North Sea has already been mentioned when describing the Mesozoic development. The Wheeler diagram in Figure 8 summarizes the complex sedimentary history. The new lithostratigraphic relationships and names introduced by Munsterman et al. (2012) have also been applied in this research. Sequence 2 and 3 sensu Abbink et al. (2006) are named S1 and S2 respectively in this work.

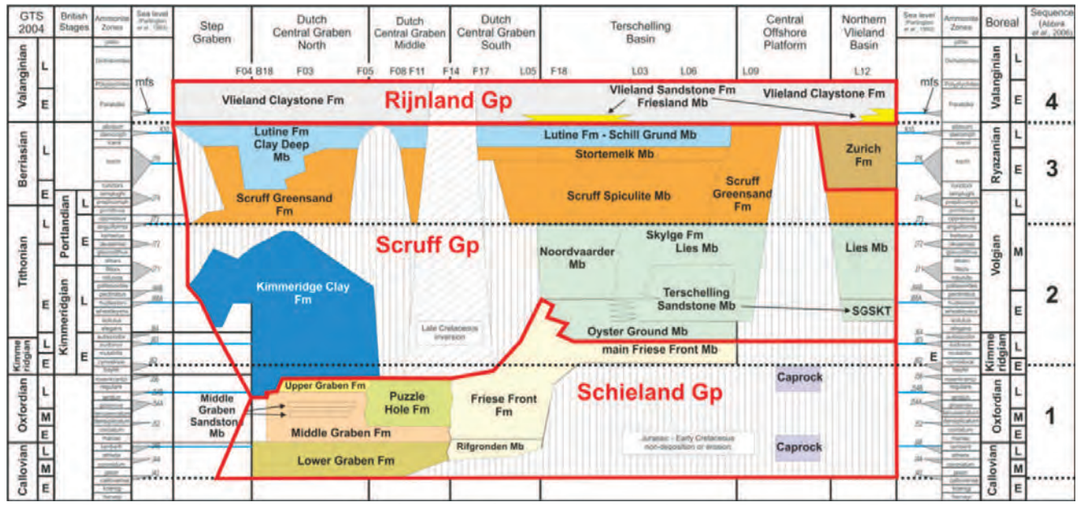

Figure 8. *N-S oriented lithostratigraphical framework of the Callovian - Ryazanian in the Dutch North Sea. The Schieland Group has mainly a continental origin, whereas the Schieland Group and the Scruff Group are predominantly of marine origin (from Munsterman et al., 2012).*

The burial graph of well M01-02, presented by Nelskamp et al. (2012) clarifies the burial history of the Terschelling Basin. This well is representative for the Terschelling Basin and is currently at its maximum burial depth. The graph shows four phases of rapid burial that coincide with main tectonic events of the basin as described by Ziegler (1990a). These phases are: Late Carboniferous, Late Permian to Early Triassic, Late Jurassic to Early Cretaceous and Pliocene to Quaternary. This basin modeling exercise had the objective to investigate the role of salt tectonics in the generation of over-pressures in the area of the southern Dutch North Sea. They found that overpressures in the Jurassic and Cretaceous rocks in the Terschelling Basin are the result of early compaction of Neogene mudstones. Over-pressurized drilling hazards in Triassic rocks are caused by lateral sealing and the timing of salt migration.

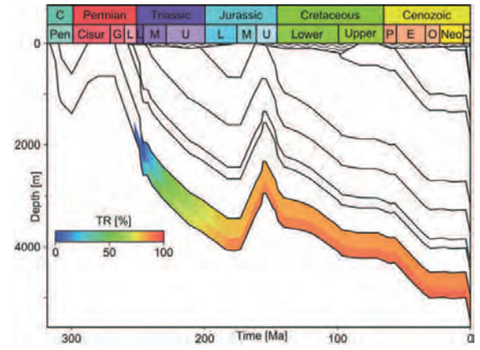

Figure 9. *Burial history diagram of well M01-02 from the Terschelling Basin. The transformation ratio of the Carboniferous source rocks is color coded. Figure from Nelskamp et al., 2012.*

The structural setting and the tectonic style of the southern Dutch North Sea are shown in Figure 10. These geological profiles are a result of the mapping and modeling exercise of Verweij & Witmans (2009) mentioned earlier. Cross section B-B' runs from north to the south across the Terschelling Basin. Cross section C-C' runs from west to east across the southern margin of the Dutch Central Graben and through the Terschelling Basin. It can be seen that Upper Jurassic strata are present in both sections and that this interval is thinned or terminated at the margins of the rift basins. Larger and smaller salt structures can be seen in both profiles that are oriented perpendicular to each other. An important difference between the domains of the Dutch Central Graben and the Terschelling Basin is that the Lower and Middle Jurassic strata are not present in the Terschelling Basin, and that Upper Jurassic strata seems to be thinner in the Dutch Central Graben.

Furthermore, the Upper Triassic succession is thicker in the Dutch Central Graben than in the Terschelling Basin. Intense faulting of the pre-Zechstein strata can be seen in both sections, whereas the Mesozoic strata show less faults. These faults are mostly salt related.

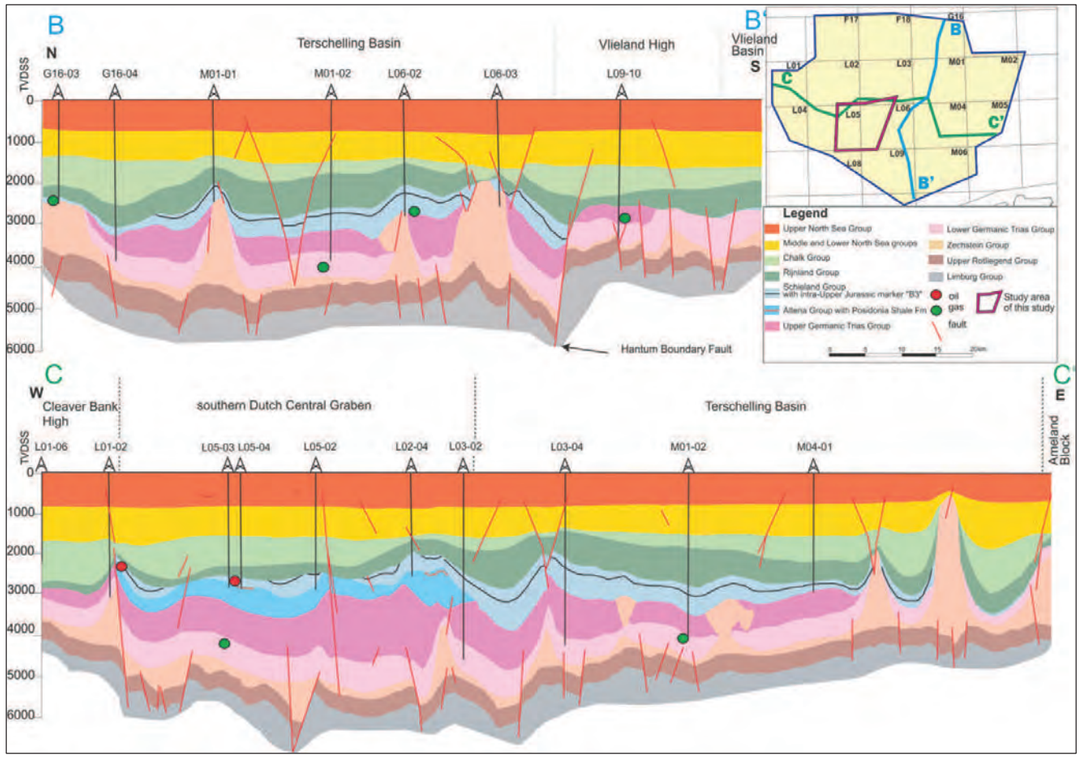

Figure 10. *Geological profiles through the Terschelling Basin. Above the N-S section between the points B-B'. Below the W-E section between the points C-C'. For a legend and a location map see top right. (Annex G2 and G3 from Verweij & Witmans, 2009). The study area of this study is indicated in the overview map with a pink polygon.*

Methods and data

Dataset

After the first oil show was found in the Dutch part of the North Sea in 1970, an impressive amount of geological data has been acquired by the oil and gas industry. The available dataset was provided by the 'Focus' research project (TNO), but most of the data is publicly available and accessible via the website of the Dutch Oil and Gas portal (http://www.nlog.nl). Except for the actual well cores that can be studied in the geological sample repository in Zeist, which is hosted by the DINOloket and TNO Geological Survey (GDN).

The area of interest for this research covers the area of the Dutch Central Graben, the Terschelling Basin and the Step Graben combined (Figure 2). 203 wells have been included into the Focus project's dataset, from which 45 have cored intervals. All wells within the area of interest and have been drilled for exploration or production purposes. Amongst other information, most of these data points contain information about the location of the well, total depth, deviation of the well trajectory and the presence of cored intervals. Most of the wells include well logs, for most wells, gamma ray, neutron, sonic and resistivity logs are available. A list of all the wells included in the dataset is available in Appendix A.1. Well markers from previous TNO research or mapping projects, from a 2009 study performed by the company 'Panterra', and from information gathered during the drilling process are also included into the dataset. These markers indicate the depth of either the top or the base for a certain stratigraphic interval at the location of a well. The scale of all well related data is provided in meters.

Additionally, a large number of seismic acquisition campaigns have been carried out in the Dutch part of the North Sea. In total 14 2D seismic surveys and 62 3D cubes are included in the Focus project dataset (Appendix A.2 and A.3). All of these surveys are publicly available (http://www.nlog.nl/nl/seismic/seismic.html). Most of the 2D surveys consist of older lines, with a wide spacing, which were shot for regional seismic studies. The most important data for this research are the 3D seismic cubes.

Previously interpreted and continuous surfaces are included in the dataset. These surfaces were made by the TNO mapping department for the 'NCP2' study and from a study from 2009 performed by the company 'Panterra'. They show a coarse regional interpretation for several key stratigraphic levels and acted as a guideline for further and more detailed seismic interpretation. The time-structure maps of the base and the top of the Zechstein Group are not a result of this work but were taken from the NCP2 dataset.

As mentioned earlier, the majority of this report covers a structural and seismic study that has been conducted in the area of the L5 and L6 blocks. The 3D seismic survey Z3NAM1990F, which covers parts of the L05, L06, L09 and M04 blocks, has been used for most of the seismic interpretation. Also the time-structure maps of several surfaces and the time-thickness maps, presented later, were produced with information obtained from this cube. For the purpose of extending the area in which a detailed interpretation was carried out and to do seismic to well ties with wells lying outside of the Z3NAM1990F cube, the seismic surveys Z3NAM-1990B, Z3WIN2003A and Z3NAM1994B were used (Figure 1).

Well markers and well logs of the following 24 wells were used to guide the detailed analysis:

L02-04	L02-08	L03-02	L03-03	L03-04
L05-01	L05-02	L05-03	L05-04	L05-05
L05-05	L05-06	L05-07	L05-C-03	L06-01
L06-02	L06-03	L06-04	L06-05	L06-07
L08-07	L08-P-01	L09-02	L09-04	

Methods

This chapter describes the methodology used in this work to determine how the distribution of the Upper Jurassic reservoir facies is related to salt migration. The methods include:

- Literature study
- Well-log analysis and correlation
- Core description
- Seismic to well-ties
- Seismic interpretation of 2D and 3D seismic surveys
- Integration of results

Well-log analysis and correlation

An example of the well log analysis is given in Figure 11.

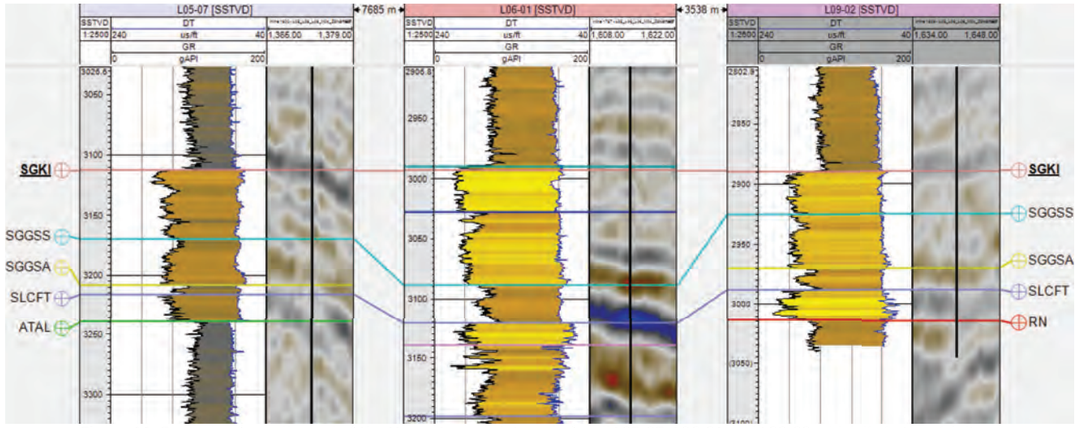

Figure 11. *Example of a well panel of the Upper Jurassic interval of well L05-07, L06-01 and L09-02 which lie in the vicinity of the study area, exported from Petrel.*

On the vertical axis the true vertical depth is shown in meters, on the horizontal axis several types of information are shown. Well markers for the given intervals are displayed with colored lines and are laterally correlated to corresponding intervals in the neighboring wells. The wiggle traces of the gamma ray log and the density log (derived from the neutron log) are displayed in such a way that the color code between the traces corresponds roughly to the type of sediment (yellow for sand, grey for shale). The actual seismic signals at the locations of these time-depth converted wells are also shown in order to determine which reflector corresponds to a specific lithological interface. It becomes immediately clear that some levels have a distinct seismic expression, whilst other levels do not display a distinct expression. There are also levels that have a clear expression at a certain location, whilst they are hardly recognizable in the seismic image on other locations. Especially unconformities are difficult to trace.

Core description

During the course of this project some time was spent on studying cored intervals of the Terschelling Sandstone Member and the Scruff Greensand Formation of the wells L06-02, L06-03 and M01-01. However, the findings of these efforts are not presented in this work, because the interpretation of the stratigraphy of the cores in the area is considered to be beyond the scope of this project.

Seismic interpretation

The software used in this work to handle seismic and well data is the Petrel E&P 2013 package. The interpretation of key horizons was done by manually tracking reflectors or using the guided auto-tracking tool. Faults visibly offsetting reflectors and other truncations of reflectors were marked. Key intervals that had a discordant relation resulting in unconformities were interpreted by hand.

The following intervals were distinguished and their bases were marked (Figure 16A). This was done for the regional transects, as well as for sections within the area where the detailed analysis has taken place:

	Groups	**Code**	**Age**
-	Upper North Sea Group	NU	(Miocene- Holocene)
-	Lower and Middle North Sea Group	N	(Paleo- Oligocene)
-	Chalk Group	CK	(Late Cretaceous)
-	Rijnland Group	KN	(Early Cretaceous)
-	Schieland Group and Scruff Group	S	(Late Jurassic)
-	Altena Group	AT	(Lower and Middle Jurassic)
-	Upper Germanic Trias Group	RN	(Middle and Late Triassic)
-	Lower Germanic Trias Group	RB	(Early Triassic)
-	Zechstein Group	ZE	(Late Permian)

All strata below the Late Permian Zechstein interval are labeled ‘pre-Zechstein’ and are treated as the Basement interval of the region and are not further subdivided. The Upper Jurassic interval is subdivided into two sequences and the sequence boundary of the younger sequence is placed at the base of the Scruff Greensand Formation. This level separates the two phases, which are referred to in Abbink et al. (2006) as Sequence 2 and 3. In this present study, the older interval is named ‘S1’ interval and consists of the Skylge Formation. The younger interval is named the ‘S2’ interval and consists of the Scruff Greensand Formation and the Lutine Formation.

In the study area located in the L5 and L6 blocks using the Z3NAM1990F 3D seismic survey the following horizons were interpreted three-dimensionally in a close spaced grid (Figure 12).

- The base S1 horizon represents the base of the Upper Jurassic strata in the study area (in other studies this level sometimes is called the ‘S’ level because it may coincides with the base of the Upper Jurassic Schieland Group). The ‘S1’ interval consists of the Main Friese Front Member of the Friese Front Formation and the Skylge Formation.
- The base S2 horizon resents the sequence boundary between the S1 and S2 intervals. It is placed at the base of the Scruff Greensand Formation.
- The top S2 horizon represents the interface between the top of the Upper Jurassic strata and the base of the lowermost Cretaceous present in the study area (in other studies this level sometimes is called the ‘KN’ level because it may coincides with the base of the Lower Cretaceous Rijnland Group). The ‘S2’ interval consists of the Scruff Greensand Formation and the Lutine Formation.

In Appendix C.1, a paragraph can be found that explains how seismic images are obtained from acoustic waves. Additionally the theory behind acoustic impedances is explained and the polarity convention used in this work is presented.

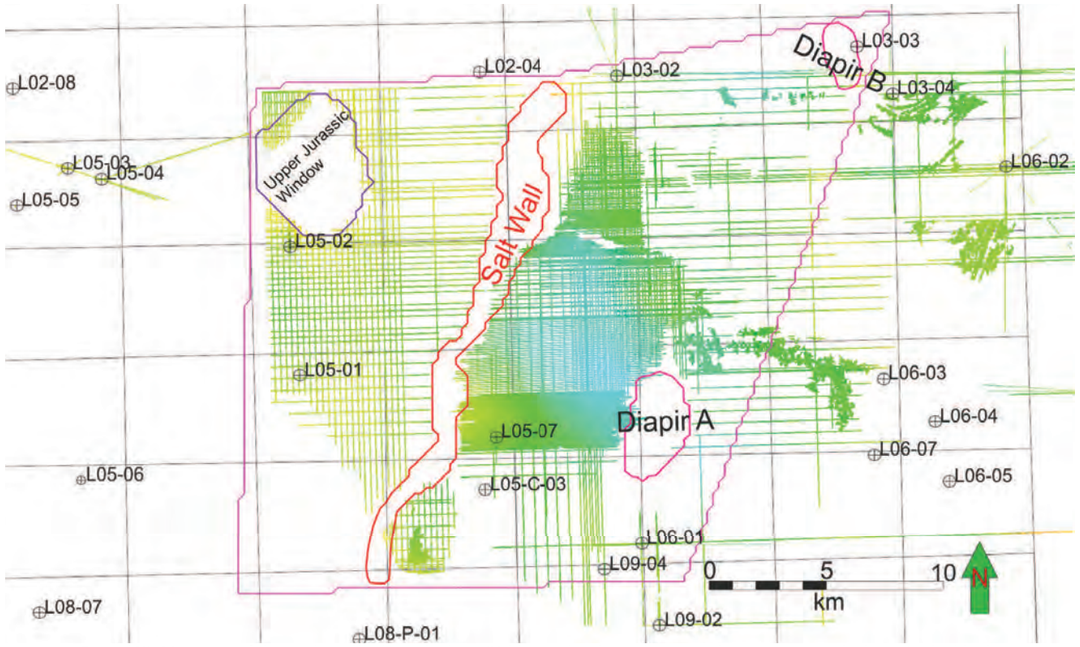

Figure 12. *Map view of the study area where the base S1 horizon has been interpreted using cross- and inlines. In the blank areas the reflector could not be followed. The interpretation was not pushed underneath the salt structures. The areas where salt bodies have penetrated this surface can already be seen (salt wall and Diapirs). For an explanation of the other features the legend in Figure 13 is needed.*

The following legend applies for Figure 12, all the time-structure maps and all time-thickness maps.

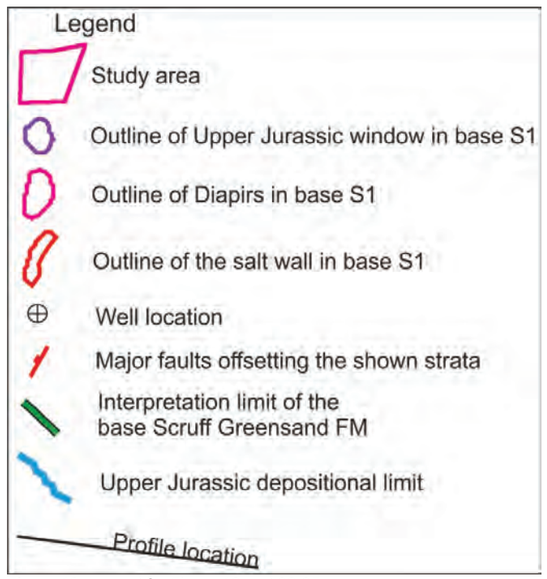

Figure 13. *Legend for Figure 12 and 28-35.*

The interpretation of these three horizons started at well locations and extended gradually into the study area so that the exact reflector could be determined that represents the stratigraphic interface of interest. In order to compare the well data measured in units of depth, to seismic data measured in units of time, seismic to well-ties were performed. For this 1D synthetic seismic profiles were constructed at the well locations and compared with the actual seismic data at those points. After the time-depth relation at the location of a wellbore is determined, the information from the well markers and from the well-logs can be used to pinpoint the seismic expression of a certain stratigraphic level. Often the well markers alone were not conclusive and the gamma ray-, neutron-, sonic- and resistivity logs were used to calibrate the interpretation.

Continuous and smoothed surfaces were extracted from the gridded horizons so that time-structure maps of the three horizons bounding the S1 and S2 intervals could be constructed (Figure 30 -32). The difference between these individual surfaces, measured in time, was calculated and used to create time-thickness maps of the S1 and S2 intervals (Figure 33 - 35). A correction was applied in order to display the stratigraphical thickness instead of the vertical thickness.

In addition to the three dimensional interpretation of Upper Jurassic intervals, six random lines within the same 3D cube (Z3NAM1990F) were interpreted in order to illustrate and explain the structure of the most important features. The interpretation of these sections was done using the Petrel software. The figures were graphically enhanced using the CorelDRAW drafting software (Figure 36 - 41).

Salt flow and sedimentation

As salt becomes mobile and the resulting structures evolve through different stages, the comparison of key surfaces and thickness maps helps elucidate their evolution. An important assumption is that thinner intervals develop over the crest of a rising salt structure while thicker packages (e.g. turtle structures) are representative of paleo-depocenters and salt withdrawal areas. The identification of allochthonous salt sheets and remobilized salt bodies proved to be difficult, because the salt is often not present at the allochthonous position and only strata related to the salt migration are left.

Reflector terminations and stratigraphic external forms

This section focuses on the way specific reflectors are terminated and overlain by other reflectors at unconformities. This information provides important implications on the origin of the layers. Also the shape of specific stratigraphic units and the external forms of, for instance, growth strata are important aspects to focus on during the seismic interpretation (Rowan and Weimer, 1998, Bouroullec et al., in press). To determine the stratigraphic relationships of different seismically visible units, key reflectors such as termination points of individual reflectors, sequence boundaries and unconformity surfaces are marked.

For this project it is important to distinguish between zones with onlapping reflectors and zones where reflectors drape over a certain structure or wedge out at the same position. Figure 14 schematically demonstrates the two scenarios.

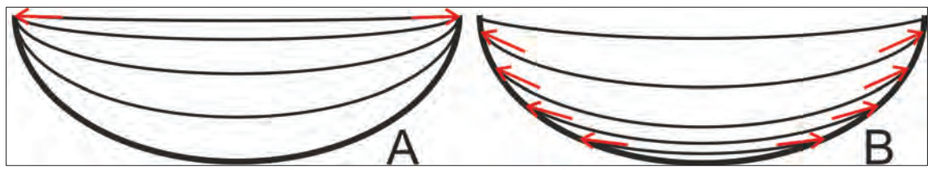

Figure 14. *Schematic representation of the relation between terminated reflectors and the basin margin. Red arrows indicate the points of reflector termination.* ***A)*** *Growth strata with successive reflectors that terminate at the same point and fan out.* ***B)*** *The points of reflector onlap successively changes position and become higher.*

In case A, all reflectors terminate at the same high location at the shoulders of the depocenter and fan out from that same position towards the center of the basin. Case B shows successive reflectors onlapping onto subsequently higher points of the margin of the basin. The different scenarios yield very different implications concerning the water depth and the creation of accommodation space at the time of deposition. For instance, in case A the creation of accommodation for each step was focused in the middle of the basin and the water depth may have stayed the same during the deposition of the entire succession. In case B a rising water level may have deposited successive layers that onlap onto successively higher positions of a paleo depth.

Reflector terminations at the top or bottom of stratigraphic units yield important information about the relation between two successive units. Truncated or incised bounding reflectors indicate erosion and the possible infill of a paleo-topography.
Additionally, thickness variations of individual stratigraphic units can provide useful information on syn-sedimentary salt migration and the creation of accommodation space.

Figure 15 shows five different endmembers of stratigraphic external forms that were encountered within the study area:

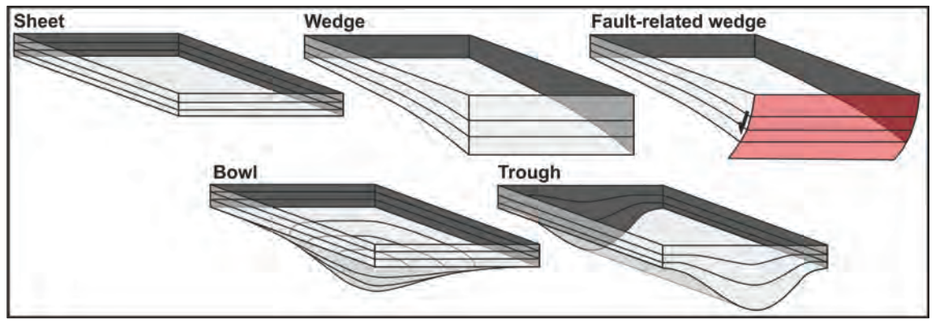

Figure 15. *Schematic representation of different modes of thickness variations of stratigraphic units also referred as stratigraphic external forms (from Bouroullec et al, in press).*

1) Sheet external form shows a stratigraphic unit that is the result of uniform sediment deposition and creation of accommodation space.
2) The wedge external form is the results of the creation of more accommodation space along an active diapir.
3) Wedge external form can also be fault-related
4) A bowl-external form has its thickest sedimentary succession in its center. These sediments were deposited in an area where accommodation space was focused in the basin axis and relate to salt flowing in all direction underneath this basin axis.
5) The accommodation space for the trough external form was created in a linear manner underneath the trough. Salt migrated bidirectional and in opposite directions away from the linear depocenter.

Results

In this chapter the results of this work are presented in three sections. In the first section a description of three regional transects is presented and an interpretation of the structures of each transect is provided. In the second section the results derived from the gridding exercise are described. The third section covers the results of the interpretation of six seismic sections crossing through the study area.

Interpretation of regional transects

Three regional transects have been constructed and studied in order to determine the characteristics of the main structures and most important features of the Dutch rift basins. The orientations of the transects were chosen in such a way that the cross-sections showed areas where interaction between Upper Jurassic strata and past salt migration could be identified.

The first transect, Line A, is shown in Figure 17 (for location see Line A in Figure 2 and 16B). It is composed of the 2D seismic line ABT-91-08 and a random line from the 3D seismic survey Z3NAM1989E. This transect is linearly orientated from WNW to ESE and has a total length of approximately 130 km. The line is oriented perpendicular to the strike of the main geological structures in the region. It cross cuts the area of the Elbow Spit High, the Step Graben, the Dutch Central Graben and covers the margin of the Schill Ground Platform. To show detailed structures two zoom-ins, one on the Step Graben and one on the Dutch Central Graben, are shown in Figure 18 and 19. Please note that the term ‘random line’ is the technical term for a seismic section from a 3D survey that does not lie on a specific in- or cross line. The orientation of the random lines used in this work was chosen deliberately.

The second transect, Line B, is shown in Figure 20 (for location see Line B in Figure 2 and 16B). It is composed of several random lines of various 3D seismic surveys. The path of this transect has been chosen to intersect with several wells in order to obtain reliable calibration of seismic and well data. This resulted in a non-linear transect with a roughly N-S trending direction starting in the north of the Dutch Central Graben and ending on the margin of the Central Offshore Platform. The locations of wells in the vicinity of the line are indicated on top of the profile. The total length of the transect is approximately 183 km. Three structural features are shown in greater detail: Figure 21 shows an area where listric faults can be seen; Figure 22 shows the south flank of Diapir 2 and the Triassic anticlinal Structure D in greater detail; and Figure 23 shows a zoom in of a feature that is possibly caused by compression or thrusting. The seismic data that contributes to this transect are taken from the following seismic surveys from north to south (all are random lines: Z3FUB-2002A, Z3NAM1982A, Z3NAM1989E, Z3PET1992F, Z3OXY1994, Z3WES2003A, Z3PGS2001A, Z3STA1985A, Z3NAM1992A, Z3NAM1994B, Z3NAM1990F, Z3WIN2003A and Z2WIN1995A.

The third transect, Line C, is shown in Figure 24 (see Line C in Figure 2 and 16B for location). It is composed of the 2D seismic lines SNSTI-87-29E and SNSTI-87-29D and of several random lines from four 3D seismic surveys, namely Z3NAM1992A, Z3NAM1993C, Z2NAM1990E and Z3PET1991B. This transect is oriented perpendicular to the strike of different salt bodies that are present within the three rift basins of the Dutch northern offshore. Therefore, the transect is not completely linear but displays a kink at point B. The first part of the transect from point A to point B, is NNW-SSE orientated and has a length of approximately 107 km. This part of the transect runs from the Elbow Spit High, through the Step Graben into the Dutch Central Graben. The second part of the transect from point B to point C, is NW-SE orientated and has a length of approximately 98 km, hence the total length of the third transect is approximately 205 km. This part of the transect runs from the Dutch Central Graben through the Terschelling Basin ending at the Ameland Platform. Three areas of Figure 24 are shown in greater detail below the section in separate figures. Figure 25 zooms in on Location 5 where a salt pillow formed above a pre-Zechstein basement high. Figure 26 shows the structure around a salt body that forms the boundary between the Dutch Central Graben and the

Terschelling Basin. The last detailed picture (Figure 27) shows an area of the Terschelling Basin, where a feature can be observed that is interpreted as a horizontal salt weld.

The legend in Figure 16a applies to the regional transects. In addition to the here presented interpretation, several inter Upper Jurassic markers are shown that originate from a study published by the company 'Panterra' in 2009. The vertical axes of all seismic profiles presented in this report are given in two way travel time (TWT in milliseconds) and shown with a 5x vertical exaggeration. The location of the transects are shown in Figure 2 and 16B. On the cover page of this report a 3-dimensional representation of these interpreted sections can be found as well.

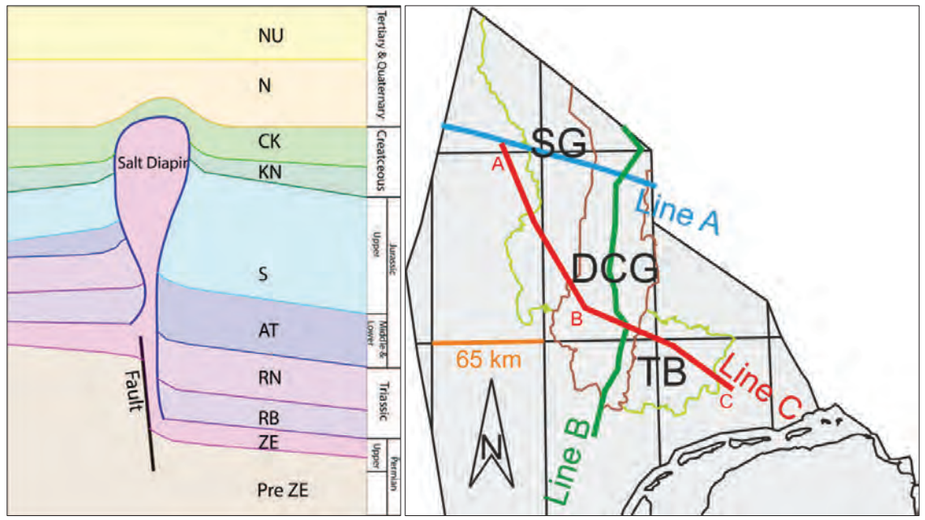

Figure 16. A) *Legend for the three regional transects and corresponding chronostratigraphy. Nu: Upper North Sea Group, N: Middle and Lower North Sea Group, CK: Chalk Group, KN: Rijnland Group, S: Schieland, Scruff and Niedersachsen Groups, AT: Altena Group, RN, Upper Germanic Trias Group, RB, Lower Germanic Trias Group, ZE: Zechstein Group, pre-ZE: basement interval* ***B)*** *Overview map of the Dutch Northern Offshore with the locations of the three transects and the outlines of the Step Graben, Dutch Central Graben and the Terschelling Basin indicated. SG: Step Graben, DCG: Dutch Central Graben, TB: Terschelling Basin.*

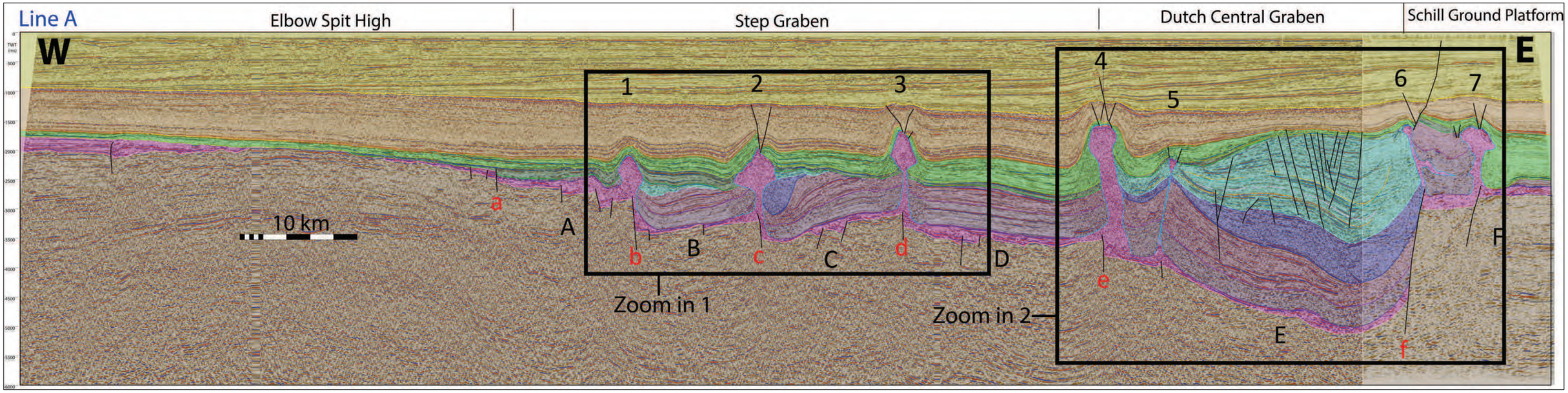

Figure 17. *W-E oriented line A, cross-cutting the area of the Elbow Spit High, the Step Graben, the Dutch Central Graben and covers the margin of the Schill Ground Platform. The areas indicated with the zoom-in boxes are shown in greater detail in Figure 18 and 19.The annotations are explained in the text below. The legend can be found in Figure 16A. A high resolution version of this figure can be found in Appendix B.1. In addition to the here presented interpretation, several inter Upper Jurassic markers are shown that originate from a study published by the company 'Panterra' in 2009.*

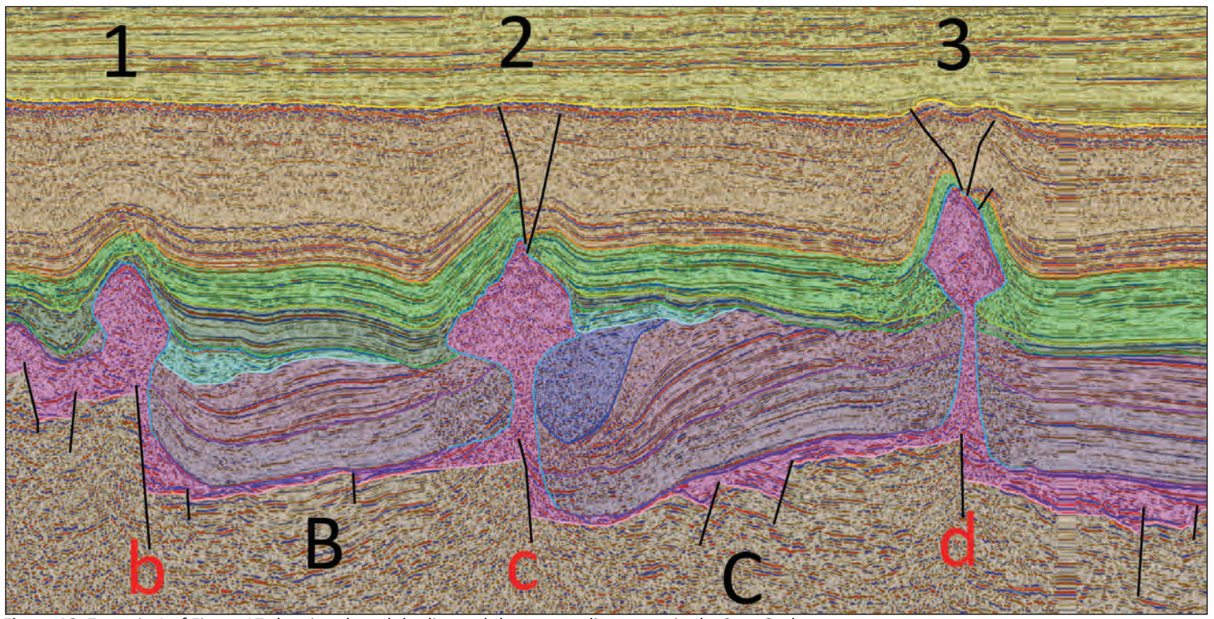

Figure 18. *Zoom-in 1 of Figure 17 showing the salt bodies and the surrounding strata in the Step Graben.*

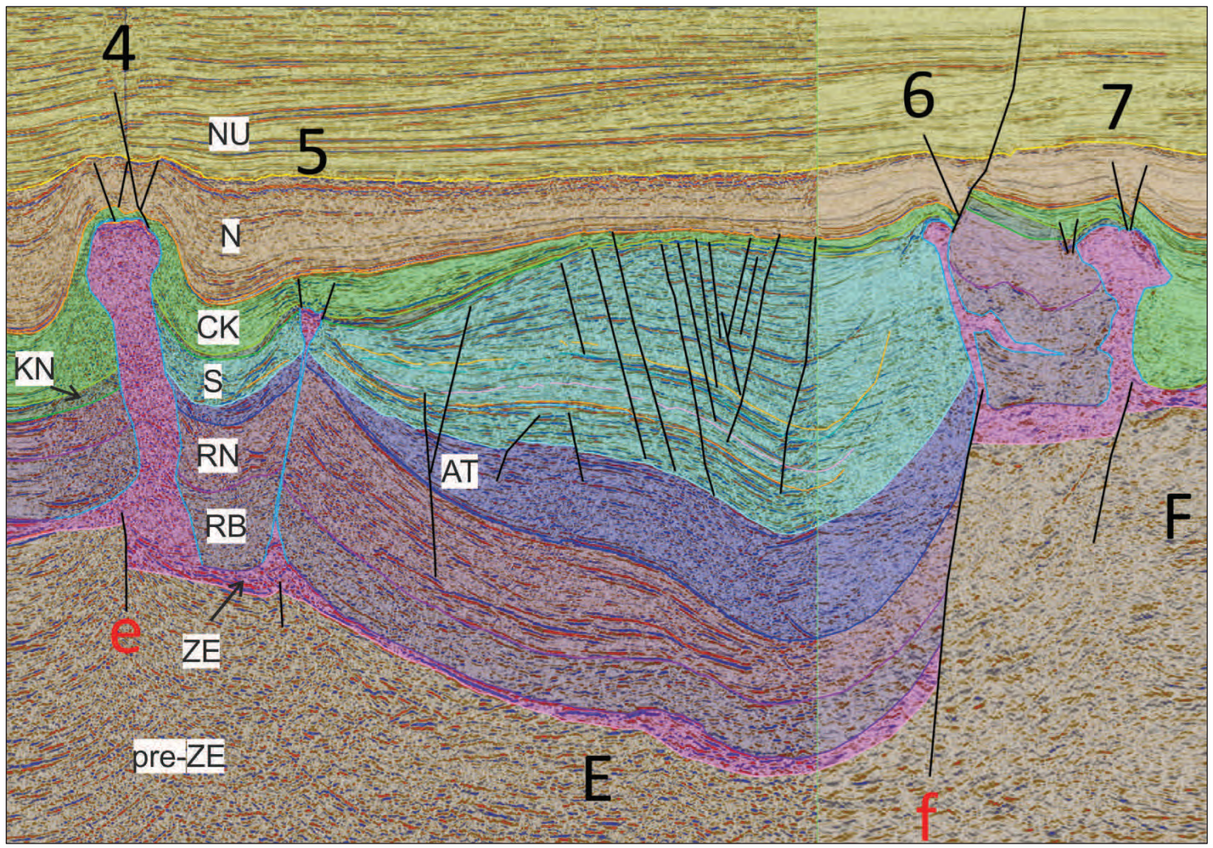

Figure 19. *Zoom-in 2 of Figure 17 showing the asymmetric basin of the northern part of the Dutch Central Graben and the surrounding salt bodies. In addition to the here presented interpretation, several inter Upper Jurassic markers are shown that originate from a study published by the company 'Panterra' in 2009.*

Line A - Elbow Spit High, Step Graben and Dutch Central Graben

A main observation from the interpreted version of line A is that the post Permian strata thicken from W to E, which correlates to a deepening of the pre-Zechstein basement. Between the Elbow Spit High in the west and the Schill Ground Platform in the east two asymmetric rift basins (Step Graben and Dutch Central Graben) are shown. In this section the extension of these two areas is largely accommodated by six normal faults with a large offset (Faults a-f, Figure 17), which divide the section in five distinct (tilted) Fault Blocks (A-E).

Block A is bound by Fault a and b and contains several normal faults with a steep eastern dip direction. These faults display an offset of the pre-Zechstein basement. Block B is bound by Fault b and c, minor faulting of the pre-Zechstein basement is caused by sub-vertical faults. Block C is bounded by Fault c and d and contains two major western dipping normal faults with significant offset of the pre-Zechstein basement. Block D is bound by Fault d and e and contains two small sub-vertical normal faults that offset the pre-Zechstein basement. Block E is bound by Fault e and f and spans the width of the Dutch Central Graben. In this section, the Dutch Central Graben has a half-graben geometry.

In block E a faulted turtle-back anticline structure has developed in the Upper Jurassic sequence. The top of the pre-Zechstein basement deepens gradually and is deepest close to the margin of the Schill Ground Platform. Only one normal fault with a small offset at the pre-Zechstein basement is recognized within block E. The vertical difference of the top of the pre-Zechstein basement within this block is mainly accommodated by Fault f. On the western side of Fault f and Salt Body 6 all Mesozoic layers are tilted steeply to the center of the basin. Block F is bound on the western side by Fault f. Within this part of the section, one additional western dipping normal fault with a relatively large offset of the pre-Zechstein basement is observed.

Line A shows seven salt bodies piercing the overburden. They formed above faults with significant pre-Zechstein offset, hence it is likely that these faults initiated salt migration. Most of these salt diapirs occur above the fault block bounding faults described above, this means that these faults were of great influence on the structural development of the section. Crestal normal faults, generally linearly shaped in a cross-section, have formed at the top of each salt diaper (e.g. above Diapir 2, 3 and 4). In map view these faults often are curved or circular (Hudec & Jackson, 2007).

When looking at the present day distribution of the Zechstein Group it becomes apparent that this layer has been subject to salt migration and thinning, especially at the deepest parts of the rift basins where the salt layer seems almost depleted. Eastward from Salt Body 1 the thickness of the Lower Germanic Trias Group shows a very regular distribution. Whereas the Upper Germanic Trias Group shows gradual thickness variations between Diapir 2 and 3 and in the western part of the Dutch Central Graben. The thickness of the interval stays relatively constant in the remaining segments of the profile.

The Lower to Middle Jurassic Altena Group is mainly present in the Dutch Central Graben. Additionally, in the area between the eastern flank of Diapir 2 and the thick sequence of the Upper Triassic, an isolated patch of Lower to Middle Jurassic strata of the Altena Group is present. Within the Dutch Central Graben, the interval is thinner in the western part. At this location the base of the Upper Jurassic strata seem to truncate the Altena Group. The isolated patch is quite thick and thins very rapidly to the east. The structure resembles a rim syncline. The Upper Jurassic is distributed very unevenly over the section. The thickest and deepest part, almost 2000 ms, is present in the Dutch Central Graben. Here, between diapirs 4 and 6, a spectacular turtle-back anticline has developed with thinning sequences towards the west. Around Salt Body 5 the base of the Upper Jurassic truncates the Altena Group. Two isolated slivers of Upper Jurassic strata are visible to the east of Diapir 1 and 2 respectively. Both patches thin towards the east and seem to incise into lower lying units.

The Lower Cretaceous Rijnland Group is very thin to absent in the eastern part of the Step Graben and the Dutch Central Graben. The top of the interval shows signs of erosion and is probably unconformably overlain by the Chalk Group. In the western part of the Step Graben, a slightly thicker succession of the Rijnland Group is present that thickens towards the western side of the Step Graben and onlaps onto the Elbow Spit High. Rim synclines have formed on both sides of the flanks of Diapir 1. Although the Chalk Group shows significant thickness differences, it is present over the complete length of the section.

At several locations the base of the Upper Cretaceous truncates older strata. This can be seen for instance in the Dutch Central Graben above the Upper Jurassic turtle-back anticline. Here only a thin layer of chalk from the Chalk Group is present. The Cenozoic sediments blanket all of the previously described structures. Some variation in thickness is observed throughout the section, although this is of lesser importance when focusing on the structures of the Upper Jurassic sequences. Even though Diapir 3 is the only salt body that has pierced completely through the Cretaceous strata in this section, crestal uplift and thinning of the Lower North Sea Group, and even the Upper North Sea Group, can be seen above all salt bodies. Diapir 1, 2 and 3 exhibit a diamond shaped head and a thin, or even completely squeezed feeder. In this section it seems as if Salt Body 5 has been detached completely from its pedestal, the exact location of the salt weld is not known and can only be approximated.

The interpretation of the marginal area of the Schill Ground Platform was somewhat problematic, but in general it can be stated that major salt evacuation in the Dutch Central Graben area resulted in the creation of Diapir 6 above Fault f. The sedimentation on the Central Offshore Platform was not significant during the rifting phase, but commenced during the Late Cretaceous.

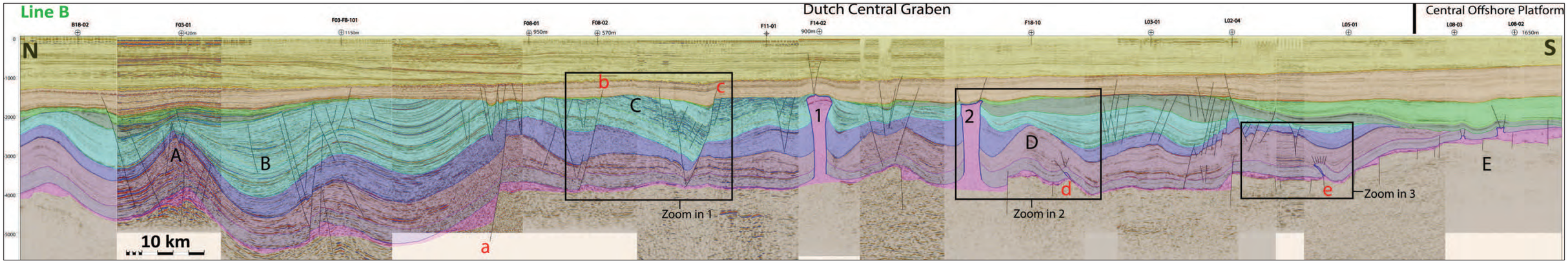

Figure 20. *N-S oriented line B across the Dutch Central Graben. The areas indicated with the zoom-in boxes are shown in greater detail in Figure 21, 22 and 23. The annotations are explained in the text below. The legend can be found in Figure 16A. A high resolution version of this figure can be found in Appendix B.2.*

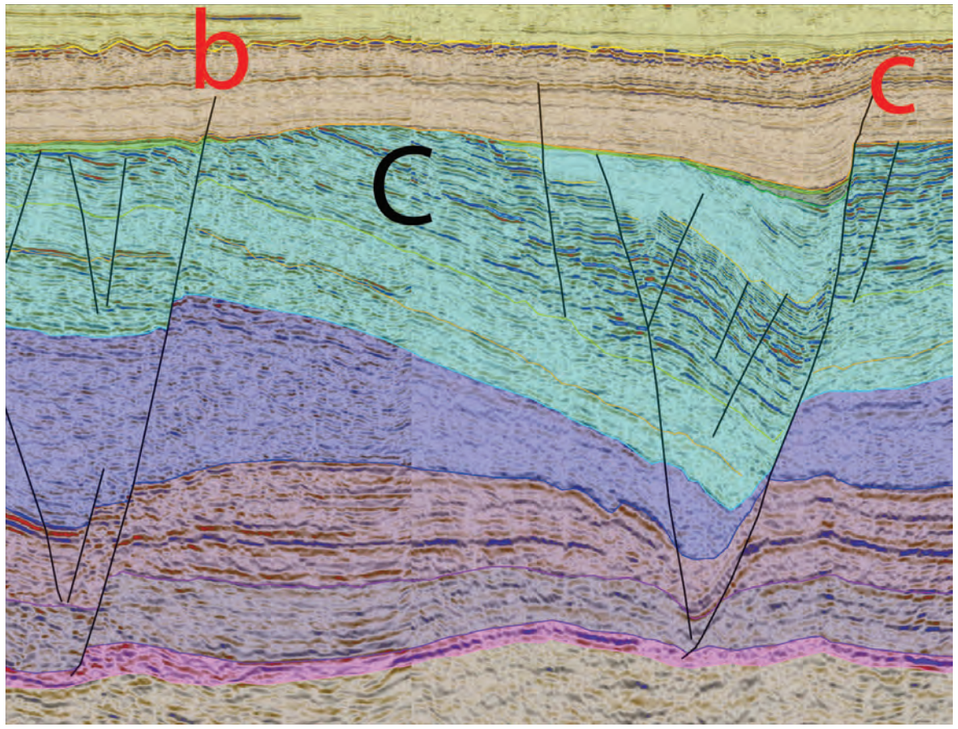

Figure 22. *Zoom-in 1 of Figure 20 showing two large northward dipping listric faults (b and c) that sole onto the Zechstein Group along these faults growth strata developed in the Upper Jurassic.*

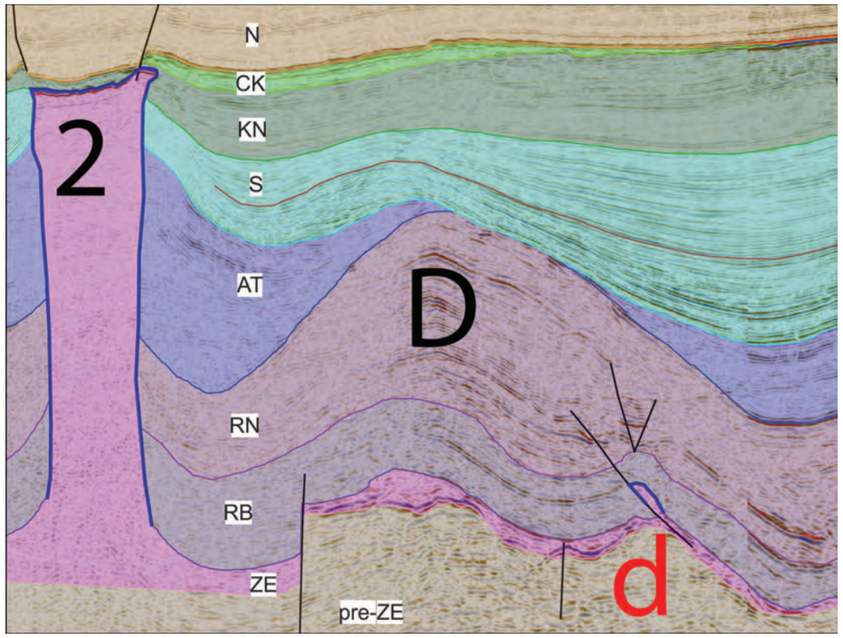

Figure 23. *Zoom-in 2 of Figure 20 showing the thickened Jurassic succession at the southern flank of Diapir 2 and the Triassic anticlinal Structure D that is truncated by the base of the Upper Jurassic. At Location d, a structure can be seen where Zechstein Salt was transported upward, possibly along a thrust plain.*

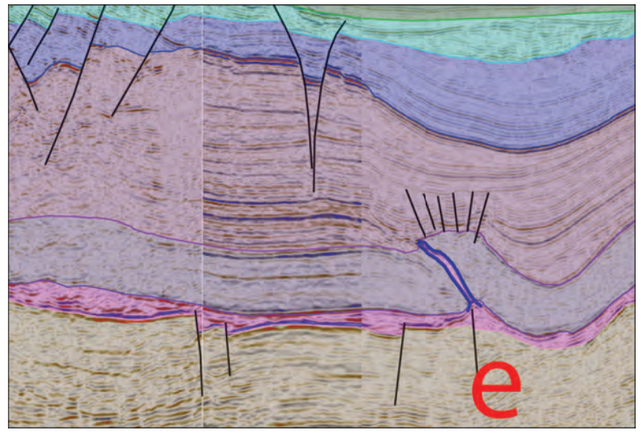

Figure 21. *Zoom-in 3 of Figure 20 showing feature e in the Lower Triassic resembling a thrust structure possibly caused by compression.*

Line B - Dutch Central Graben

Line B shows a profile from N to S along the axis of the Dutch Central Graben and onto the Central Offshore Platform showing how the phases of basin evolution (e.g. rifting, salt migration, inversion, erosion and blanketing off) have affected the different regions of this rift basin.

When looking at line B a few features stand out. The level of the pre-Zechstein basement deepens towards the north, which accommodated the deposition of a large package of Upper Jurassic strata especially on the northern side of the profile. The top of the pre-Zechstein basement reaches its deepest position in the northern part of the section. Here it lies at approximately 5500 ms. Due to along-strike orientation of this transect there are only a few faults that offset the pre-Zechstein basement. Nonetheless, large listric Faults (a-c) that seem to sole on the Zechstein salt are present. These faults show significant offset of the Mesozoic strata. The transect also shows a significant hiatus at the base of the Cretaceous.

This transect shows the result of intense salt evacuation along the axis of the Dutch central Graben. Hence, the thickness of the Zechstein Group in this transect is very limited to almost depleted. To allow for detailed descriptions of the structures of this transect, areas of interest are marked (A-E, a-e and 1-2 in Figure 20).

Two piercing diapirs (1 and 2) are present in the central part of the transect. At the base of the diapirs no faults are visible, therefore it is not known which faults triggered the formation of the diapirs. However, it is very likely that the diapirs originate from normal faults that are oriented perpendicular to this profile. Both diapirs seem to be isolated structures that are not connected to other salt bodies. Several anticlinal structures appear above salt swells of the Zechstein Group (e.g. A and D). The thickness of the Upper Triassic Group is increased as well within these anticlines. The origin of this thickening will be discussed later in this report.

The layer thickness of the Lower Germanic Trias Group stays relatively constant over the complete length of the transect. This is also observed for the Upper Triassic Group, except for local thickening above the anticlinal structures. The Upper Triassic Group is progressively eroded towards the Central Offshore Platform.

The Jurassic Altena Group shows variable thicknesses, from very thick in rim synclines around the flanks of the diapirs to very thin or completely eroded on top of the anticlinal structures (D). The Altena Group is not present on the Central Offshore Platform.

Everywhere along the axis of the Dutch Central Graben, Upper Jurassic sediments have been deposited that display significant thickness variations. The thickness increases rapidly northward and reaches its maximum thickness in the northern part of the transect (B). Here the Kimmerian extension and the salt migration enabled the fill of the basin with approximately 2000 ms of Upper Jurassic sediments. At some locations an erosional surface at the base of the Upper Jurassic truncates the underlying sequences.

The contact between the Lower Cretaceous and the Upper Jurassic seems to be concordant at most places throughout the section. The thickest succession of Lower Cretaceous sediments can be found in the southern part of the Dutch Central Graben. The present day distribution of the Chalk Group along the line is variable. Only in the northern most part of the section and near the Central Offshore Platform this interval has a continuous appearance. Also, small patches of the Chalk Group are recognized at other locations that are concordantly overlain by the Lower North Sea Group indicating that they were deposited in the latest Cretaceous, hence they appear to be post-inversional. A hiatus between the Upper Jurassic and Upper Cretaceous strata can be recognized for instance at Position C. This indicates that a large amount of sediment of the Upper Jurassic to Upper Cretaceous interval was removed during the Campanian Subhercynian inversion phases and the Paleocene Laramide pulse (De Jager, 2007). Burial graphs constructed for the south-western part of the Dutch Central Graben support these findings (Nelskamp et al., 2012). The siliciclastic deposits of the Cenozoic Lower and Upper North Sea Group fill the topography of the underlying structures and show a very even thicknesses distribution.

TNO innovation for life

The two diapirs show signs of (sub-) aerial exposure at their tops that must have occurred during the Late Jurassic for Diapir 1 and during the Early Cretaceous for Diapir 2. The major listric Faults, a, b and c, seem to subdivide the Dutch Central Graben into zones with differing amounts of subsidence at different times (see Rosendaal et al. (2014) for further reading on this topic). At Position d and e, structures that resemble compressional or thrusting features can be seen. Zechstein salt is present at the position of the faults and has transported the Lower Triassic Group upward. At the area of the Central Offshore Platform (E) the basement is at its highest position. Also the Zechstein layer has the largest thickness at this location. Two small salt bodies have pierced into the Lower Triassic strata. The Chalk Group dominated the Mesozoic deposition at this location.

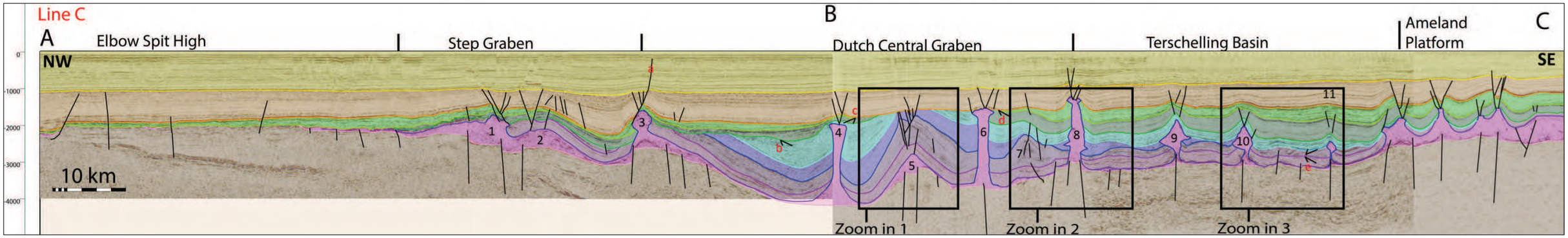

Figure 24. *From point A to point B line C is orientated NNW-SSE. From point B to point C is NW-SE orientated. The areas of the Elbow Spit High, the Step Graben, the Dutch Central Graben, the Terschelling Basin and the Ameland Platform are covered. The areas indicated with the zoom-in boxes are shown in greater detail in Figure 25, 26 and 27. The legend can be found in Figure 16A. A high resolution version of this figure can be found in Appendix B.3.*

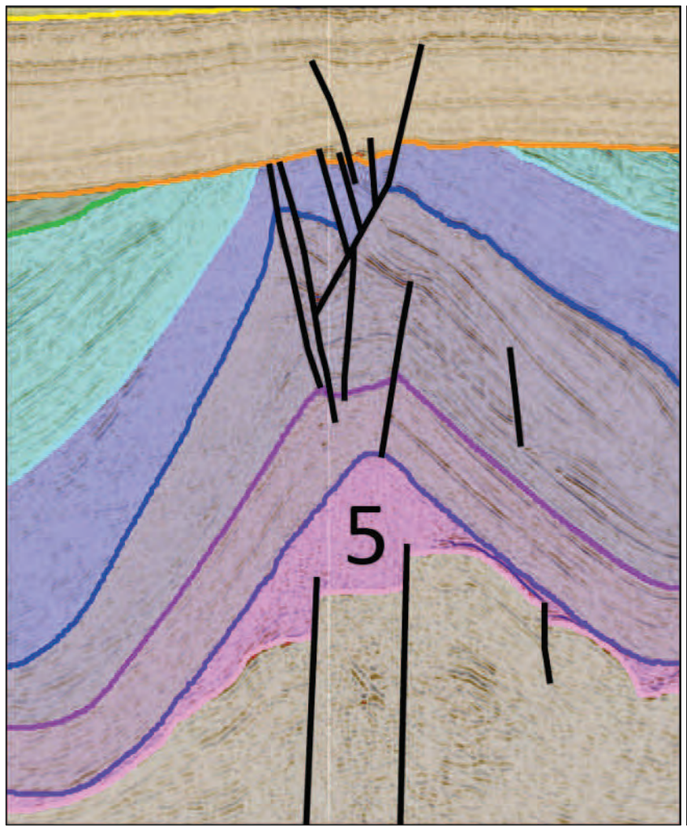

Figure 25. *Zoom-in 1 of Figure 24 showing a salt pillow at Position 5.*

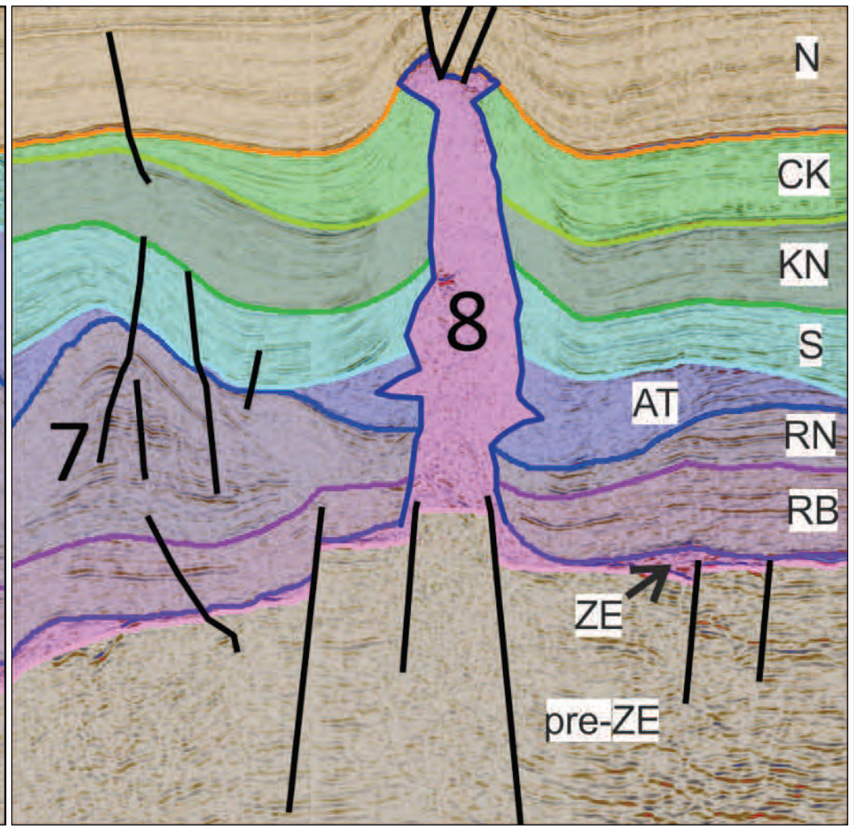

Figure 26. *Zoom-in 2 of Figure 24 showing Salt Body 8 and the surrounding strata. Thickness variations at almost all levels can be observed at this location that forms the margin of the Dutch Central Graben and the Terschelling Basin.*

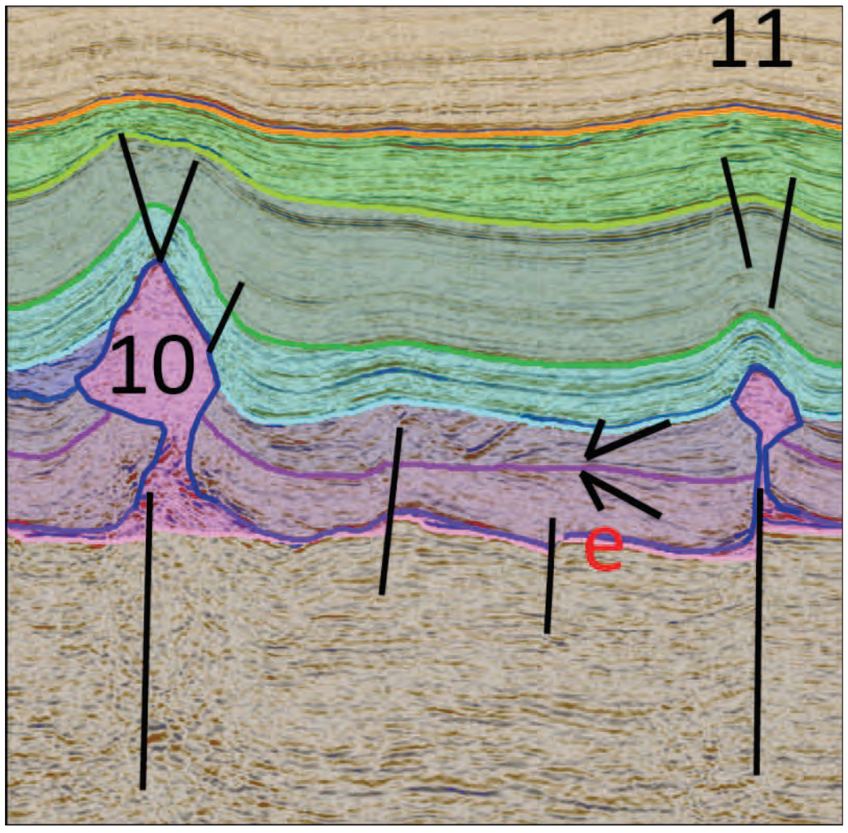

Figure 27. *Zoom-in 3 of Figure 24 showing Salt Body 10 and 11 that area located in the Terschelling Basin. Between these structures a possible horizontal salt weld can be observed at point e.*

Line C - Elbow Spit High, Step Graben, Dutch Central Graben, Terschelling Basin and Ameland Platform

This transect runs through all of the three rift basins with an orientation perpendicular to the structural grain of the northern Dutch offshore. When looking at the profile it becomes apparent that the expression of the different structural zones is different.

The platform area of the Elbow spit High shows no major pre-Zechstein basement level variations. In the SE the Zechstein Group onlaps onto the Paleozoic structure that is successively covered by the Chalk Group, the Lower North Sea Group and the Upper North Sea Group, which are deposited in broad facies patterns.

The Step Graben has an asymmetric appearance. The level of the basement deepens towards the SE and is offset by steep normal faults that terminates upward in the Zechstein salt. The Zechstein salt is thinned in the depocenter of the Step Graben located in the SW of the basin. A Salt Swell (2) and a piercing Salt Body (1) form thickened salt segments in the Step Graben. The Lower Triassic is present westward of Salt Body 1 and has a uniform thickness. The Upper Triassic is only present in the depocenter, eastward of Diapir 3, and thins towards Salt Swell 2. There are no Jurassic strata present in this part of the Step Graben, however the hiatus at the base of the Cretaceous might conceal Jurassic deposition, as the amount of erosion is not known. Overall the Lower Cretaceous thickens from NW to SE within the Step Graben. Salt body 1 has pierced up into this interval. The Chalk Group is quite thick at the marginal zone of the Elbow Spit High and the Step Graben and thins towards the depocenter in the SE. Only at the NW flank of Diapir 3 is the Chalk Group somewhat thicker, which suggests that a rim-syncline was formed at this location. The Lower North Sea Group has thinned slightly on the crests of Salt Body 1 and 2. In the depocenter of the Step Graben this interval rapidly thickens due to the creation of accommodation space during the deposition of the upper part of the Lower North Sea Group.

Rejuvenated salt migration into Diapir 3 and rise of Diapir 3 accommodated by Fault a, might have taken place, because fault a can be traced up into the Upper North Sea Group and the presence of a depocenter is also reflected in this youngest interval. This indicates continued subsidence in that area and remobilization of Diapir 3. Crestal normal faults have formed on top of the Salt Body 1 and 2.

Diapir 3 forms the boundary of the Step Graben and the Dutch Central Graben in this section. Diapir 8 lies on the transition from the Dutch Central Graben to the Terschelling basin. The pre-Zechstein basement gradually deepens towards the SE of the Dutch Central Graben and reaches its deepest position underneath Diapir 4 (approx. 4500 milliseconds). Between Diapir 4 and 6 the pre-Zechstein basement is elevated underneath Location 5. Further to the SE the basement deepens again. At the NW margin of the Dutch Central Graben and underneath Diapir 3 the Zechstein layer is thickened in respect to the depocenters, where the layer is almost depleted and has been evacuated. At Location 5, a thickened swell of Zechstein salt forms the core of an anticlinal structure. This salt body did not evolve into a piercing structure. The Upper Triassic seems to thicken on top of this structure, which indicates that Salt Swell 5 was collapsing during the Late Triassic. At Position 7 an Upper Triassic turtle structure can be seen. This indicates that during the Late Triassic lateral salt migration away from Position 7 occurred (e.g. into Diapir 6 and 8). During the deposition of the Altena Group the salt migration shifted further to the flanks of the diapirs and created rim-synclines within this interval. The Zechstein layer at this position is almost completely depleted.

The Lower Triassic has a uniform thickness across the Dutch Central Graben and follows the topography of the Zechstein Group. The Upper Triassic also exhibits uniform layering, except in the area around Salt Body 5 and Position 7. The Altena Group only shows minor thickness variations to the NW of Diapir 4. At Position 5 and 7 the Altena Group is severely thinned and even truncated at the base Cretaceous unconformity. Near the flanks of Diapir 4, 6 and 8 rim-synclines yield a thickened sequence of this interval.

A thick layer of Upper Jurassic strata has been deposited in the depocenter around Diapir 4. To the SE of Diapir 4 the Upper Jurassic strata displays a rim-syncline, which indicates that Diapir 4 was rising during the Late Jurassic. The rise was terminated near the top of the Upper Jurassic interval. The Upper Jurassic interval displays a very uniform thickness from the SE side of Salt Swell 5, almost up until the onlapping structures on the margin of the Ameland Platform, were it thins. The layer is pierced by Diapir 6 and 8 and is uplifted by Diapir 9, 10 and 11. At Location b the Upper Jurassic strata are truncated by the Lower Cretaceous strata. To the SE of this point the two intervals have a concordant boundary. To the NW of Salt Swell 5 the base of the Cretaceous is deposited after the erosional hiatus caused by the Alpine inversion.

Between points c and d the base of the Lower North Sea Group truncates older strata, even the Chalk Group is not present (anymore) in this location. This indicates that the Alpine inversion was most intense in this area. The Lower North Sea Group is slightly thinned on top of Structure 5. Diapir 8 completely penetrates the Chalk Group, offsets the Lower North Sea Group and even forms a slightly elevated point in the Upper North Sea Group. This means that Diapir 8 is the salt structure that has seen the youngest salt migration in this transect. Rim-synclinal shapes in the Chalk Group and Lower North Sea Group indicate post-inversion rejuvenation of this structure at both sides.

The pre-Zechstein basement level of the Terschelling Basin in this profile is relatively uniform and only gradually decreases SE of Diapir 11 to form the margin at het Ameland Platform. The Zechstein layer is very thin to absent throughout the entire basin and has migrated laterally and upward into several diapirs (8, 9, 10 and 11). The Lower Triassic is evenly distributed across the basin and follows the topography of the top of the thin Zechstein layer. Also the Upper Triassic is distributed evenly, although the thickness of the layer increases slightly in between the diapirs and is slightly thinned near the flanks of the diapirs. This indicates that turtle structures have formed, although they are not very well pronounced. The sedimentation shifted from the centers of the sub-basins to the flanks of the diapirs during the deposition of the Altena Group, this explains the rim-synclinal shapes in this interval.

Between the Upper Jurassic strata and its underlying units, a hiatus and an unconformable boundary can be seen in the entire Terschelling Basin, except for the SE flank of Diapir 8. At the crests of slightly thickened Upper Triassic turtle structures it can be observed that the base of the Upper Jurassic truncates older strata. Diapir 9, 10 and 11 have pierced upwards as far as the lower reflectors of the Upper Jurassic interval. The layers found above these diapirs have experienced different degrees of uplift due to the rise of the diapirs. The uplift propagates up to the base of the Upper North Sea Group. Diapir 9 and 10 show distinct squeezed feeder areas, broadened middle parts and thinner crests. The Upper Jurassic strata are evenly distributed across the Terschelling Basin, showing a uniform thickness. At the margin of the Ameland Platform this interval onlaps onto the structurally elevated area.

The Cretaceous intervals show a broad facies distribution. On top of the diapirs the layers thin slightly and exhibit slight thickening above the flanks of the diapirs, which might indicate salt migration at the time of deposition.

The Cenozoic sediments only show minor thickness variations in the Terschelling basin. Namely, above the crests of the diapirs the sediments are slightly thinned. Additionally, an interesting feature can be observed in the Triassic interval at Position e. Here the reflectors of both the Lower Triassic Group and the Upper Triassic Group terminate at the boundary layer of these two intervals. Possibly inter Upper Triassic (Main Röt Evaporite Member) salt was evacuated from this position. A salt weld remains at this position.

On the Ameland Platform the basement level is uniformly elevated in respect to the three rift basins. The thickness of the Zechstein Group best approximates depositional thickness, which can be seen in the outermost SW corner of the profile (almost 800 milliseconds). Compared to the diapirs in the three rift basins, the salt structures formed in the Ameland Platform are less vertically pronounced and show limited piercing into their overburden. It is clear that the salt structures have not evolved as far as earlier described diapirs.

The Lower Triassic Group was deposited on top of the Zechstein Group with an uniform thickness, but was eroded and pierced by later upward salt flow. Upper Triassic strata were not

deposited in this part of the transect. The earliest salt flow in this area probably dates back until the Late Jurassic, because this interval can be found in the sub-basins between the salt bodies were it onlaps onto the salt flanks. All these structures have formed on top of normal faults, which offset the pre-Zechstein basement and terminate upwards into the Zechstein salt. It is assumed that the depositional layer thickness of the Cretaceous intervals was rather uniform across the platform.

Present day the Cretaceous is faulted and offset by crestal faults that formed on top of the salt bodies. The Lower North Sea Group shows large thickness variations across these faults, indicating salt migration or salt body collapse during the time of deposition. The North Sea Group shows a regular and even distribution

Time-structure maps and time-thickness maps

In the following section the results derived from the gridding exercise using the Z3NAM1990F 3D seismic survey are described. In order to provide the reader with a better understanding of the structures present in the study area, two time-structure maps taken from the NCP2 dataset made by the TNO mapping department are presented first. The interpretation that was done to create these continuous surfaces is not the result of this work, but the structures displayed in the maps will be described briefly to aid further understanding and interpretation.

For all time-structure maps shown in this report the warm colors indicate shallower areas of a specific horizon and the cold colors indicate deeper areas. In the time-thickness maps warm colors indicate a thicker package of a certain interval and cold colors represent thinner areas. For several time-structure maps and time-thickness maps examples of the most pronounced fault systems present in a certain intervals are indicated by red fault lines. These faults were interpreted and traced using the Z3NAM1990F 3D seismic survey including six fully interpreted sections (Figure 36-41). The location and orientation of these sections are also indicated in the individual maps. The outlines of distinct and important features, which will be discussed later on in this report, are also shown (e.g. salt wall and Diapirs). The legend shown in Figure 13 applies for all the time-structure maps and all time-thickness maps.

Base Zechstein Group time-structure map

The base of the Zechstein Group coincides with the top of the pre-Zechstein 'Basement' of this region, thus the time-structure map of this horizon (Figure 28) indicates the arrangement of the pre-Zechstein structures that are seated underneath more recent structures described later in this report.

The most common fault set that offsets the pre-Zechstein basement in the study is oriented NW-SE. This coincides with the dominant fault set in this area of the Dutch northern offshore (e.g. Hantum Fault Zone). In the SW corner of the map, between two parallel and long faults belonging to this fault set, the base of the Zechstein Group has been faulted downward. These faults belong to the NW-SE fault set which is dominant in the Dutch northern offshore. Between the salt wall and Diapir A, two structural lows are present. Significant offset along two NW-SE oriented faults have created these structural lows. The yellow colored area close to well L05-C-03 forms a pre-Zechstein basement high. The interpreted base of the Zechstein Group also indicates the areas where the major salt bodies have formed. These areas are marked as higher locations, most likely because of pull up effects encountered underneath the salt during seismic imaging.

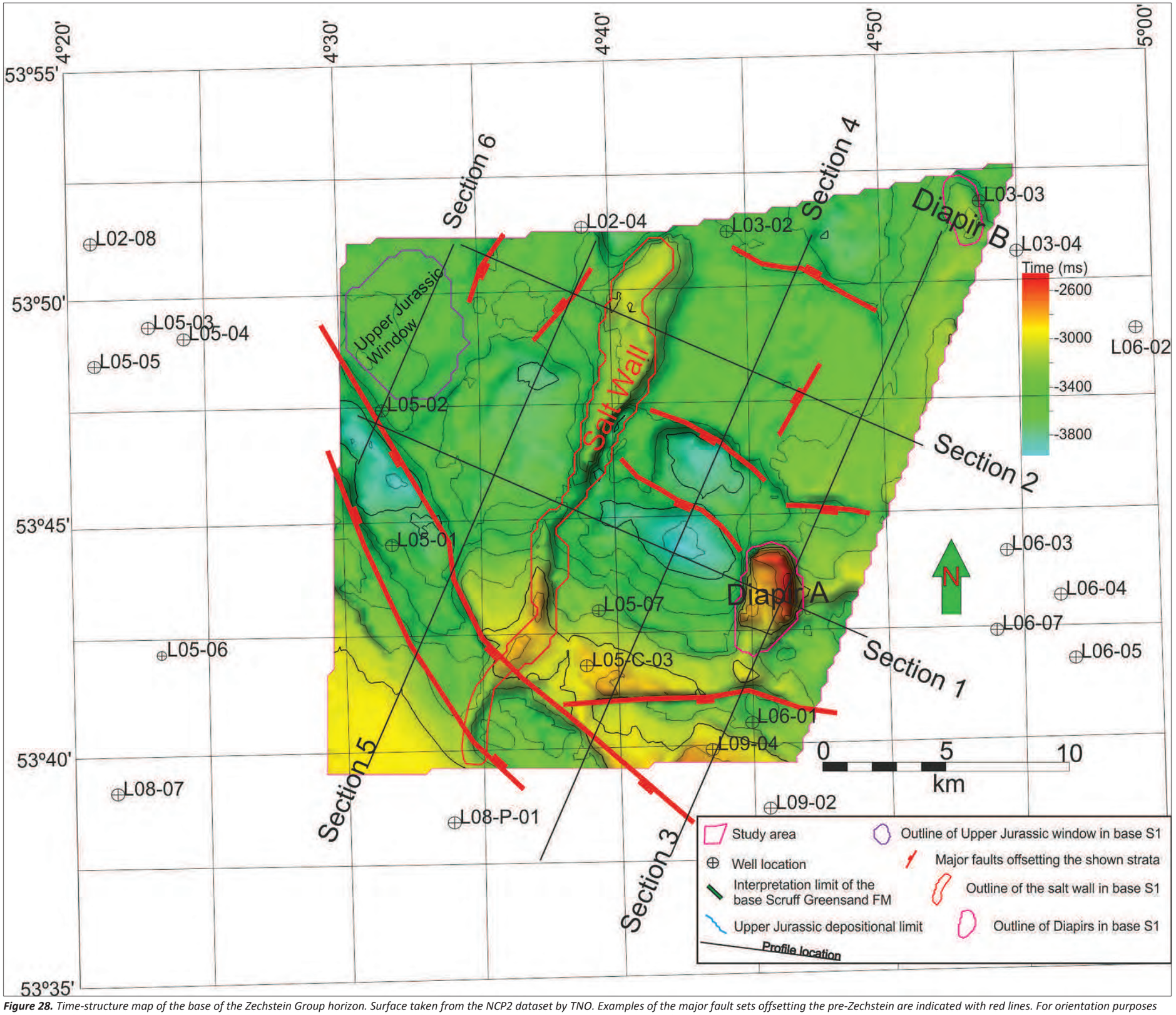

Figure 28. *Time-structure map of the base of the Zechstein Group horizon. Surface taken from the NCP2 dataset by TNO. Examples of the major fault sets offsetting the pre-Zechstein are indicated with red lines. For orientation purposes several other features are shown: locations of Section 1 - 6, well locations, outlines of salt bodies and a window in the Upper Jurassic defined for the base S1 horizon.*

Top Zechstein Group time-structure map

The most pronounced features of the time-structure map of the top Zechstein Group horizon (Figure 29) are the elevated salt bodies. The northern part of the NNE-SSW trending salt wall is broader and higher than the southern part of the structure. The isolated Diapir A has sub-circular appearance and represents the highest point of this horizon. In the NE corner of the study area the smaller Diapir B is visible. The areas that formed lows at the base Zechstein horizon also represent lows at the top of the Zechstein interval. Locations where Zechstein salt has intruded into Triassic layers are not imaged or cannot be distinguished in this picture. This subject will be evaluated more extensively in the discussion of this report (Figure 46).

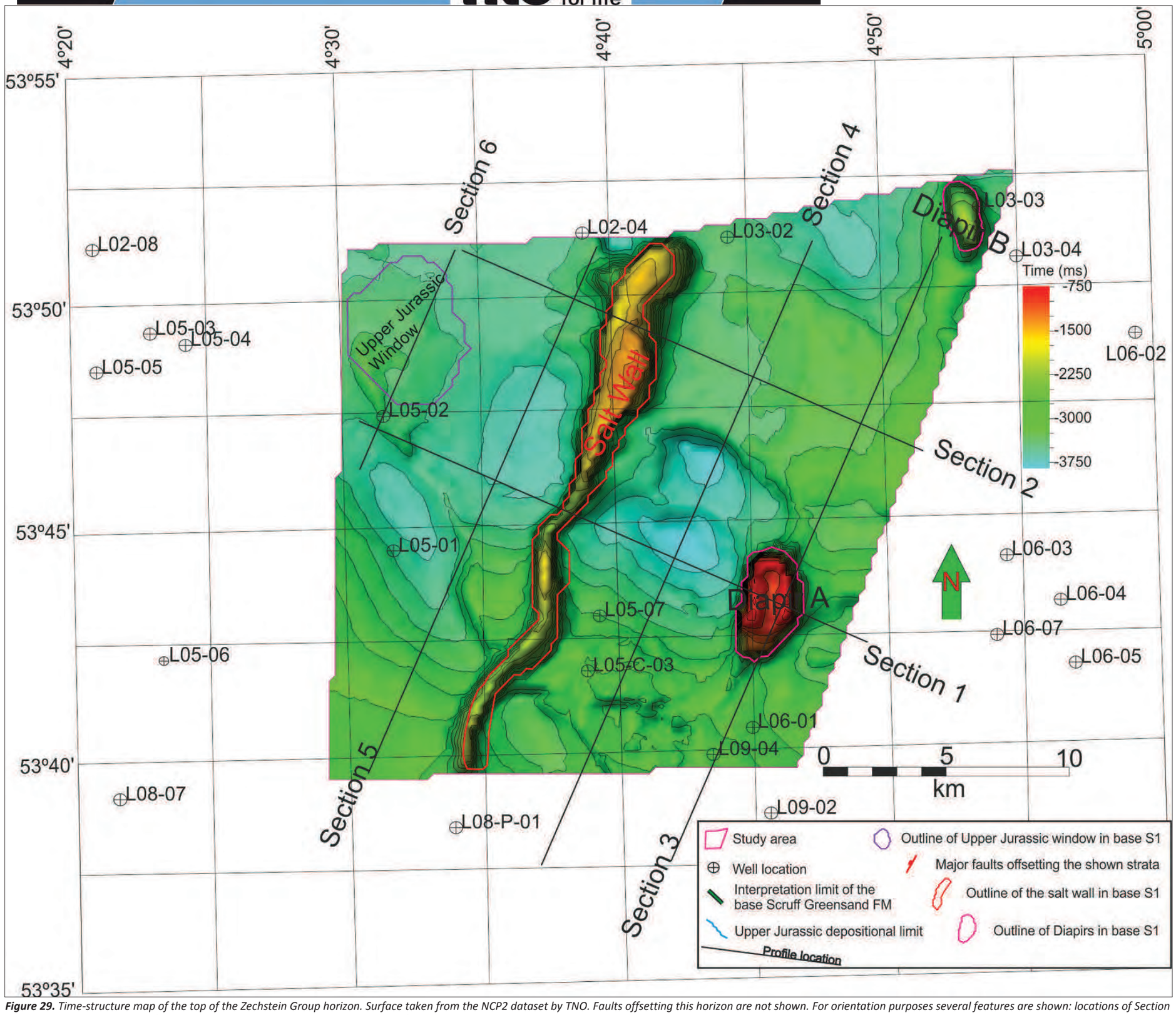

Figure 29. *Time-structure map of the top of the Zechstein Group horizon. Surface taken from the NCP2 dataset by TNO. Faults offsetting this horizon are not shown. For orientation purposes several features are shown: locations of Section 1 - 6, well locations, outlines of salt bodies and a window in the Upper Jurassic defined for the base S1 horizon.*

The literature study, the profiles and maps produced by the TNO mapping department for the NCP2 research area and the regional transects produced for this work indicate that the study area contains the following features relevant for this research:

Stratigraphy:

- Upper North Sea Group (Miocene- Holocene)
- Lower and Middle North Sea Group (Paleocene- Oligocene)
- Chalk Group (Late Cretaceous)
- Rijnland Group (Early Cretaceous)
- Schieland Group and Scruff Group (Late Jurassic)
- Altena Group (Lower and Middle Jurassic)
- Upper Germanic Trias Group (Middle and Late Triassic)
- Lower Germanic Trias Group (Early Triassic)
- Zechstein Group (Late Permian)

Pre-Zechstein stratigraphy (not further specified):

- Upper Rotliegend Group
- Limburg Group

Faults:

The main pre-Zechstein faults are NW-SE oriented. Regional a fault set of NE-SW to NNE-SSW oriented faults developed conjugate to the main fault set. Where the depositional thickness of the Zechstein Group was greater than 300 m the sub-, and supra salt units are mechanically detached. Furthermore, most of the faults offsetting the pre-Zechstein strata do not propagate into the supra salt domain, therefore the structural style can be classified as a thin-skinned tectonic setting,. The NW-SE trending lineaments became reactivated during the Late Jurassic as the extension direction changed from E-W to NE-SW and the Step Graben and the Terschelling Basin opened.

Salt structures:

Along with extension during the Triassic and Jurassic periods, Zechstein salt was mobilized. As a result NNE-SSW trending salt walls and isolated circular diapirs developed in the Terschelling Basin, resulting in severe thinning of the Zechstein salt. Accompanying growth strata formed in the Triassic, Jurassic and even Cretaceous periods. Salt movement during the early Late Triassic period and the influence of inter Triassic salt flow is still an unclear subject.

Basin inversion:

Northward directed compression caused by Alpine continental collision during the Late Cretaceous period inverted the structures that can be seen in the Kimmerian rift basins. The deformation typically focused at the areas where salt structures had formed above pre-salt faults.

Upper Jurassic horizons:

In the study area located in the L5 and L6 blocks using the Z3NAM1990F 3D seismic survey the following horizons were interpreted three-dimensionally:

- The base S1 horizon represents the base of the Upper Jurassic strata in the study area (in other studies this level sometimes is called the ‘S’ level because it may coincides with the base of the Upper Jurassic Schieland Group). The ‘S1’ interval consists of the Main Friese Front Member of the Friese Front Formation and the Skylge Formation.
- The base S2 horizon represents the sequence boundary between the S1 and S2 intervals. It is placed at the base of the Scruff Greensand Formation.

- The top S2 horizon represents the contact between the top of the Upper Jurassic strata and the base of the lowermost Cretaceous in the study area (in other studies this level sometimes is called the ‘KN’ level because it may coincides with the base of the Lower Cretaceous Rijnland Group). The ‘S2’ interval consists of the Scruff Greensand Formation and the Lutine Formation.

Base Sequence 1 time-structure map

The base S1 horizon (Figure 30) represents the base of the Upper Jurassic strata in the study area. The horizon has varying seismic expressions throughout the study area. At some locations a continuous reflector can be tracked, at other locations an unconformity marks this level. Due to non-deposition the Upper Jurassic is absent in the SW corner of the study area. In the NW corner of Figure 30 the Upper Jurassic strata are also absent in a circular area due to erosion. This area is indicated as the Upper Jurassic Window in the figure. In Figure 41, signs of an erosional interface and truncation can be seen. The salt wall and Diapir A have pierced the base S1 horizon, causing the holes in the surface at those locations. At the flanks of these salt bodies the horizon is bend upward. Diapir B has not pierced through this horizon, although the strata are uplifted at this position. The deepest point of this horizon lies between the salt wall and Diapir A directly next to the intersection of Section 1 and Section 4. This structural low seems to continue SE of Diapir A and has a NW-SE trend. To the west of Diapir B, a subtle structural low is visible.

The overall depth of the horizon in the area to the west of the salt wall is significantly higher than in the area to the east of the salt wall. Also the western area shows less vertical variation and is less faulted. The Upper Jurassic sequence is mainly affected by NNW-SSE to W-E trending faults. In the NE quadrant of the study area parallel faults have formed that offset the Upper Jurassic strata, although the offset is only minor for this horizon.

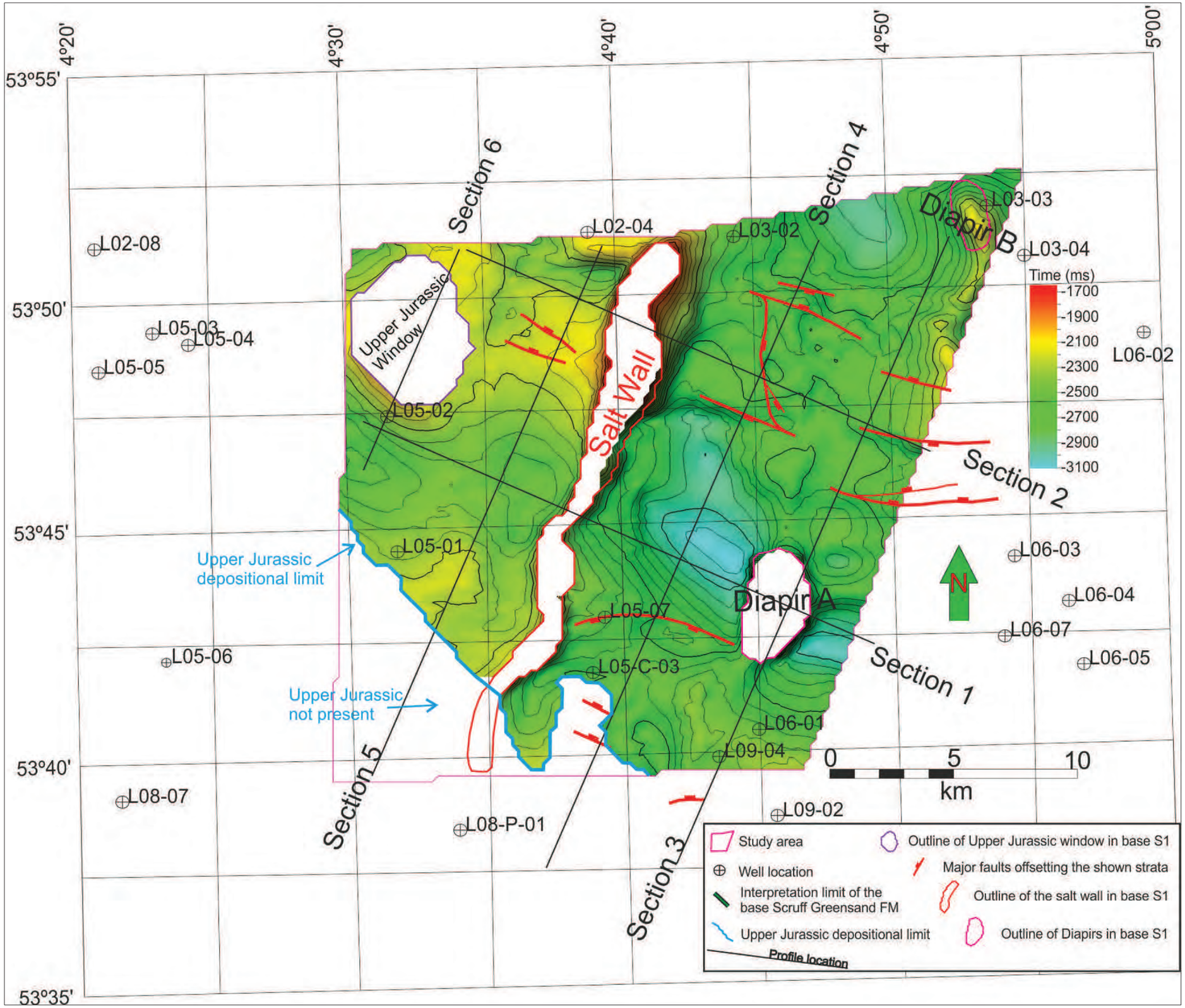

Figure 30. *Time-structure map of the base of S1. Examples of the major faults offsetting the Upper Jurassic are indicated with red lines. In the blank area in the SW corner of the figure, bounded by the blue line, no Upper Jurassic strata have been deposited. For orientation purposes several other features are shown: locations of Section 1 - 6, well locations, outlines of salt bodies and a window in the Upper Jurassic defined for this horizon.*

Base Sequence 2 time-structure map

This horizon shown in Figure 31 represents the sequence boundary between the S1 and S2 intervals. The horizon has varying seismic expressions throughout the study area. At some locations a continuous reflector can be tracked, at other locations an unconformity marks this level. The non-colored area to the SW of the blue line in the SW corner of the figure represents an area of non-deposition of the Upper Jurassic strata in the study area. The area marked as an Upper Jurassic Window represents an area where this horizon was eroded. The horizon of the boundary between S1 and S2 is absent at the locations of the salt wall and Diapir A. The remainder of the non-colored area, bounded by the green line at the edge of the interpreted area, represents an area where this inter Upper Jurassic horizon is not shown because it could not be interpreted adequately, although the interval is most likely present there. Because of the difficulty of interpreting this interval the estimated maximum extend of this interval is indicated for a small area with an orange (dotted) line in the southern part of Figure 30. This means that S1 does not extend further southward beyond this line whilst S2 does continue. This means that S2 extents further southward than S1 (Section 4 in Figure 39).

In general the horizon is shallower in the western part of the study area (westward of the salt wall) than in the eastern part. Also the structurally highest position can be found in the west. The structurally deepest position of the horizon can be found directly west of Diapir A. Approximately 7 km north of this position the contour lines are closely spaced directly south of a NNW-SSE trending fault. Here a structural low of this horizon is bound by this fault that has an offset of approximately 250 milliseconds. The other faults in the NE corner of the study area have only minor influence on this horizon.

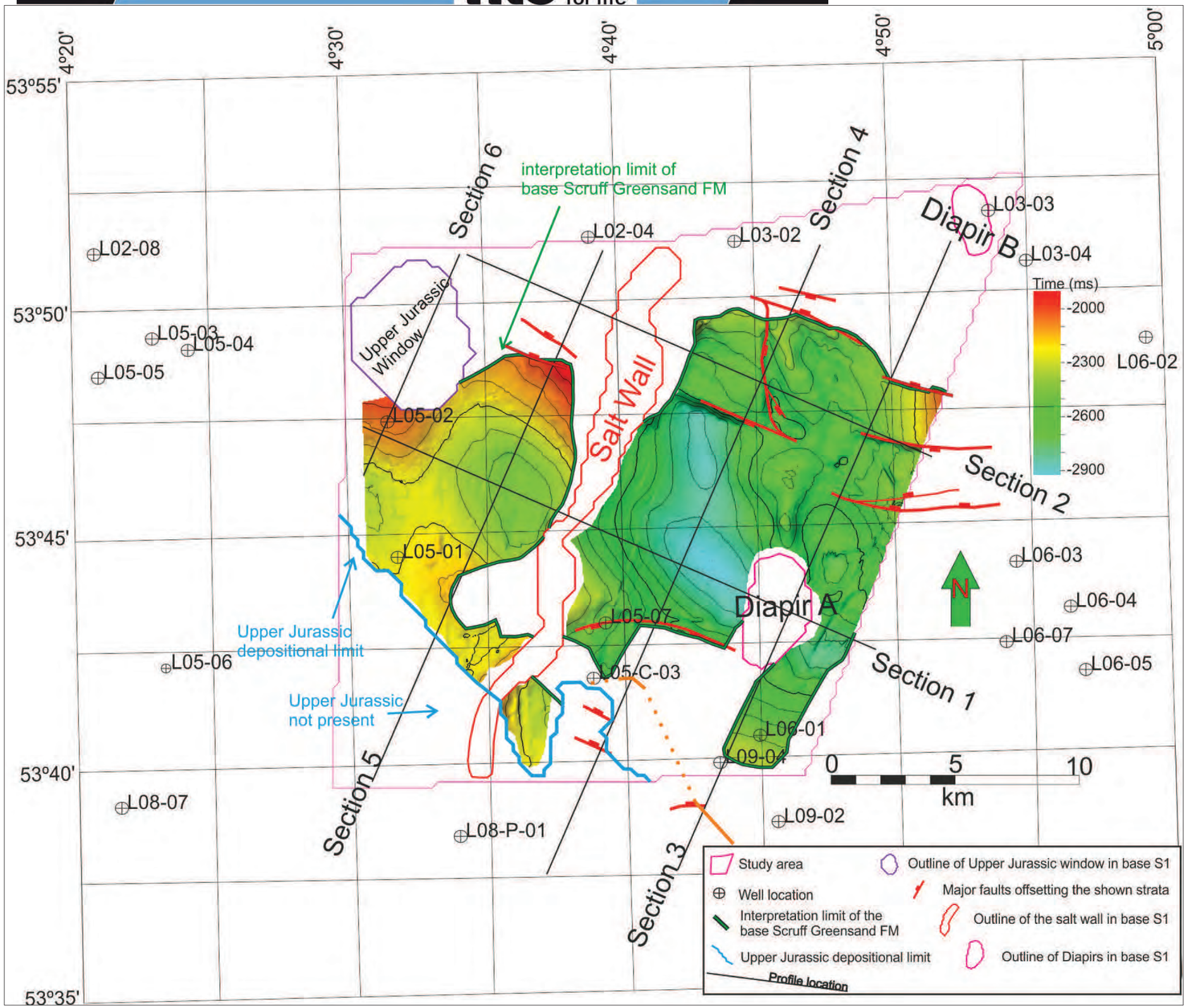

Figure 31. *Time-structure map of the boundary between S1 and S2. Examples of the major faults offsetting the Upper Jurassic are indicated with red lines. In the blank area in the SW corner of the figure, bounded by the blue line, no Upper Jurassic strata have been deposited. The rest of the blank area, bounded by the green line to the interpreted area, represents an area where this inter Upper Jurassic horizon is not shown because it could not be interpreted adequately, but the interface is most likely present at these locations. For orientation purposes several other features are shown: locations of Section 1 - 6, well locations, outlines of salt bodies and a window in the Upper Jurassic defined for this horizon.*

Top Sequence 2 time-structure map

The top S2 horizon (Figure 32) represents the interface between the top of the Upper Jurassic strata and the base of the lowermost Cretaceous present in the study area. The horizon has a varying seismic expression throughout the study area. At some places a continuous reflector can be tracked, at other locations an unconformity marks this level. The horizon is not pierced along the entire length of the salt wall, as was the case for the two horizons previously described. This horizon is pierced by the salt wall in the northern part of the study area, where the salt wall is broadest. Due to non-deposition the Upper Jurassic strata are absent in the SW corner of the study area. Also in the NW corner of the figure the Upper Jurassic strata are absent in a circular area due to erosion (Upper Jurassic Window). At the location of Diapir A the horizon is also absent. A general observation is that the changes in depth are more subtle than in the base S1 horizon and that the extremes are slightly less pronounced. To the west of the salt wall, the base S1 horizon displays only minor vertical variation, hence it has a regular geometry. Additionally, the structural low between the salt wall and Diapir A on the eastern side of the salt wall is also visible in this level and is bound by the same NNW-SSE trending fault mentioned for the base S2 horizon described previously. The other faults in the northeastern corner of the figure only cause minor disturbance of the contour lines. At the flanks of the salt bodies the horizon is bend upward. The uplifted zone at the location of Diapir B does not precisely coincide with the location of the diapir in the lower lying horizons.

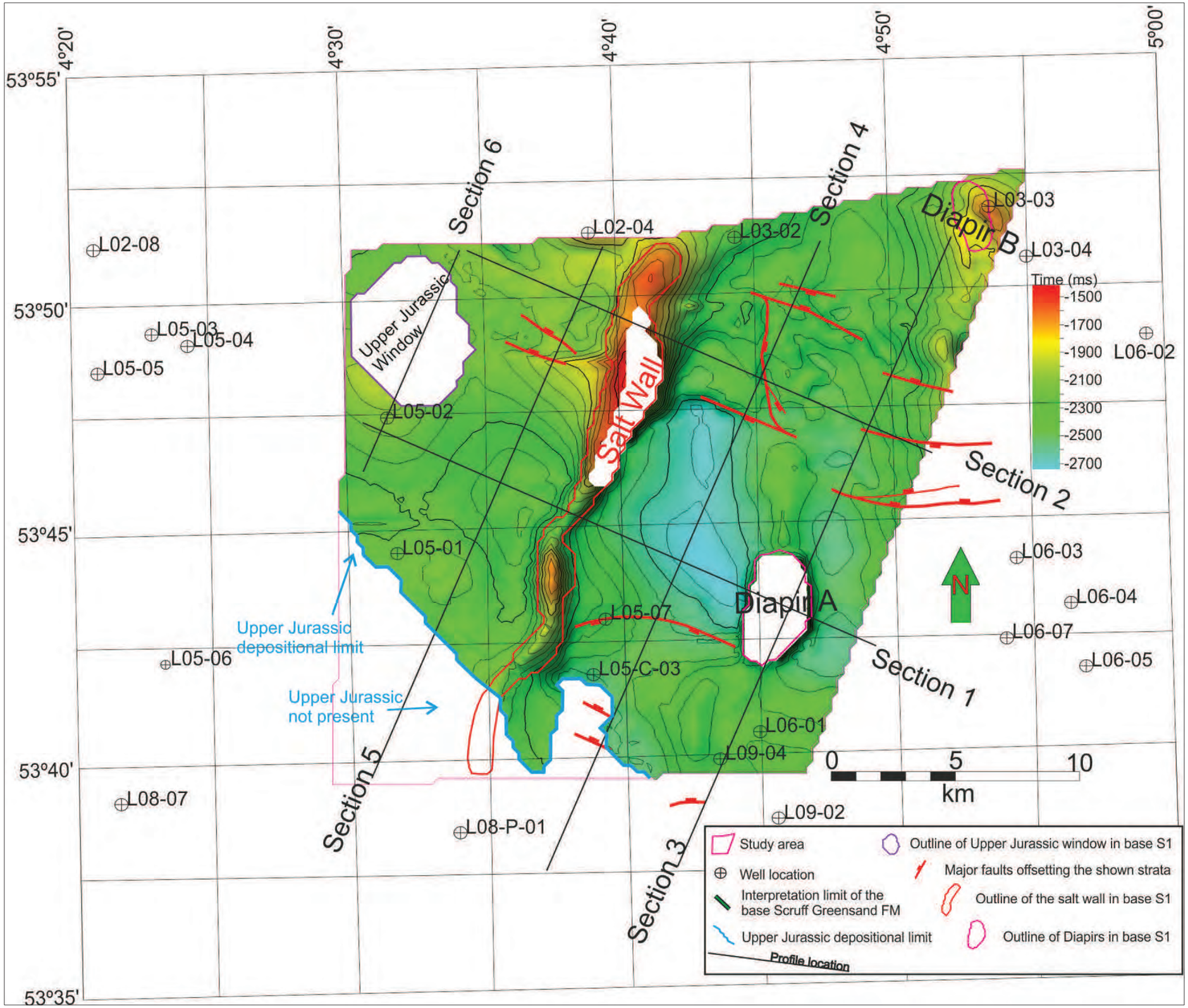

Figure 32. *Time-structure map of the top of S2. Examples of the major faults offsetting the Upper Jurassic are indicated with red lines. In the blank area in the SW corner of the figure, bounded by the blue line, no Upper Jurassic strata have been deposited. For orientation purposes several other features are shown: locations of Section 1 - 6, well locations, outlines of salt bodies and a window in the Upper Jurassic defined for this horizon.*

Sequence 1 + Sequence 2 time-thickness map

The horizons of the base S1 and top S2 have been combined to produce the time-thickness map of the two Upper Jurassic sequences present in the study area (Figure 33). The map shows the thickness of the combined Upper Jurassic strata measured in time. It can be seen that the faults offsetting the Upper Jurassic influenced the sedimentation in their direct surrounding. The areas that formed lows in time-structure maps of the individual horizons (base S1, base S2 and top S2) represent thickened areas in this map. For instance the area between the salt wall and Diapir A and the areas surrounding Diapir B show greater thicknesses than their surroundings. This means that these areas accommodated more sediments during the Late Jurassic. A likely scenario is that salt was withdrawn from underneath these areas creating accommodation space for the sedimentation of the Upper Jurassic strata. Alternatively these sequences experienced less erosion at these location. However, the amount of eroded Upper Jurassic strata cannot be inferred from this map alone. The proximity of these over thickened zones to surrounding salt bodies is a likely cause for the observed thickness changes. Another area where the Upper Jurassic strata are thicker, can be found southward of the Upper Jurassic Window. In SW corner of the time-structure map of the base Zechstein Group horizon (Figure 28), a zone is present that was faulted downward by two long parallel normal faults. This faulted zone lies beneath and parallel to the thickened area of Upper Jurassic strata described here.

The Upper Jurassic strata thin towards the western edge of the Upper Jurassic Window. Within the study area the Upper Jurassic strata generally thin towards the south.

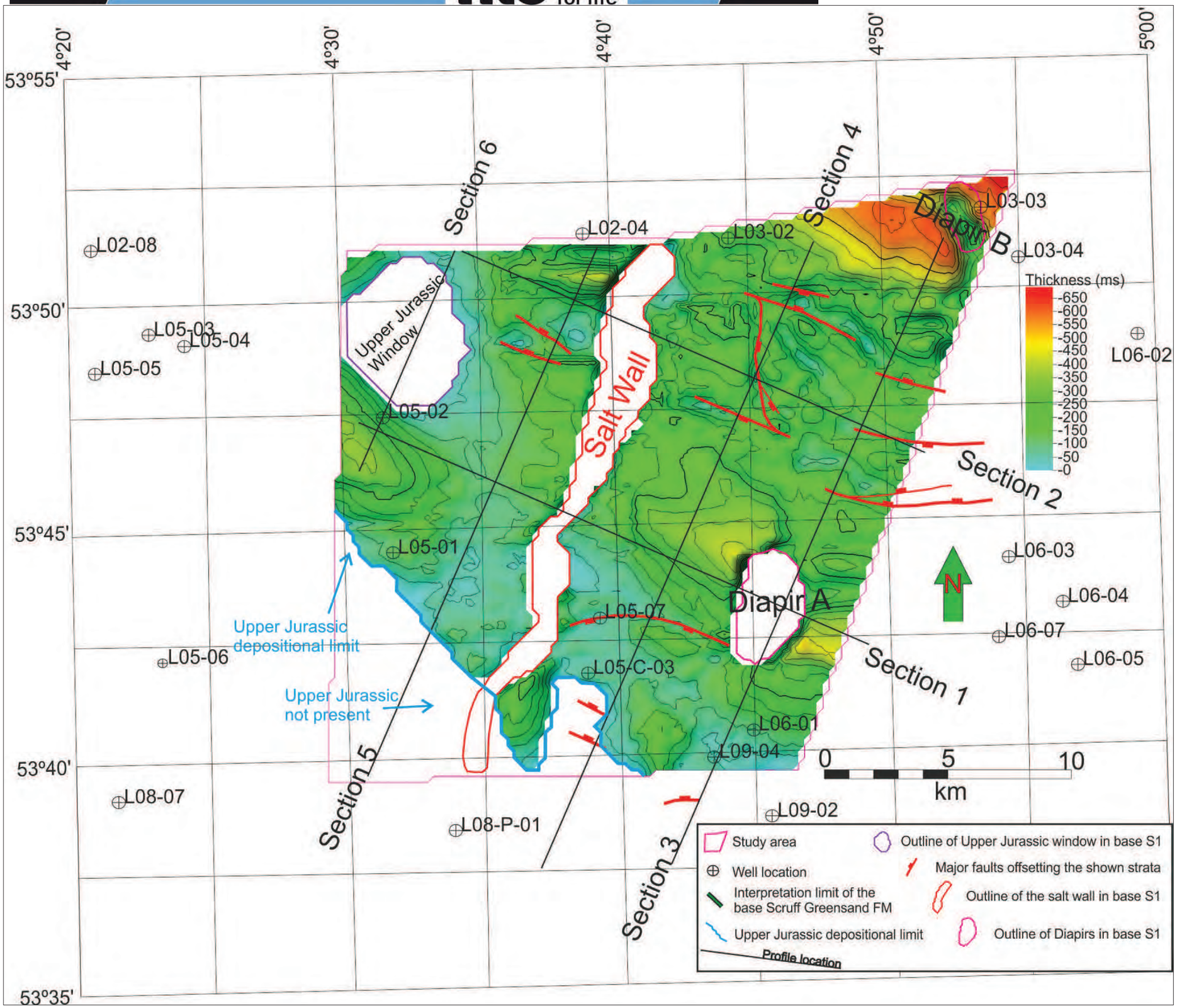

Figure 33. *Time-thickness map of the entire Upper Jurassic interval in the study area (S1 and S2). Examples of the major faults offsetting the Upper Jurassic strata are indicated with red lines. In the blank area in the SW corner of the figure, bounded by the blue line, no Upper Jurassic strata have been deposited. For orientation purposes several other features are shown: locations of Section 1 - 6, well locations, outlines of salt bodies and a window in the Upper Jurassic defined for this horizon.*

Sequence 1 time-thickness map

Unfortunately the thickness of the individual sequences are not known for the entire study area, because of interpretation difficulties of the S1 / S2 boundary horizon. The non-colored area to the SW of the blue line in the SW corner of the figure represents an area of non-deposition of the Upper Jurassic strata in the study area. The area marked as an Upper Jurassic Window represents an area where this interval was eroded. S1 is absent at the locations of the salt wall and Diapir A. The thickness of S1 is not known for the rest of the blank area, bounded by the green line to the interpreted area. Here the inter Upper Jurassic boundary could not be interpreted adequately. Nevertheless it can be seen that S1 (Figure 34) is thickened close to the flanks of Diapir A, at this location a low is visible in the time-structure maps. The thickest package of S1 is deposited in the western part of the study area. This thickened zone can be found southward of the Upper Jurassic Window. At several locations the thickness of S1 is close to 0 milliseconds (blue colors), for instance in the southern part of the area eastward of the salt wall. Adjacent to several faults in the northeastern part of the figure rapid thickness changes are displayed. Directly to the east of the N-S trending fault connecting two parallel NNW-SSE trending faults, S1 exhibits a thinned zone of approximately 1 km in width. 2 km further to the east of this fault, a thickened ridge has formed parallel to the N-S trending fault. For S2 these zones show opposite thicknesses.

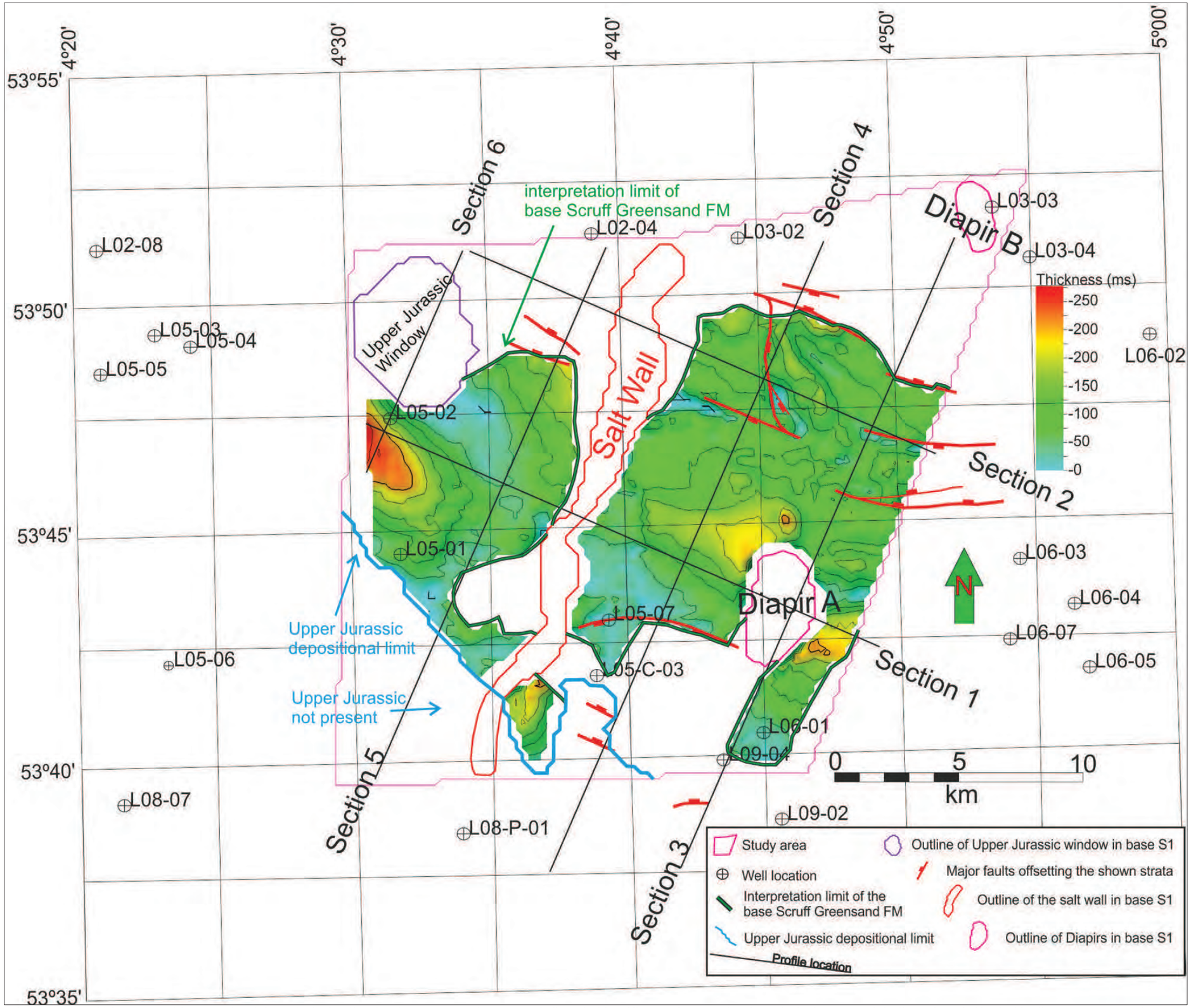

Figure 34. *Time-thickness map of S1. Examples of the major faults offsetting the Upper Jurassic strata are indicated with red lines. In the non-colored area in the SW corner of the figure, bounded by the blue line, no Upper Jurassic strata have been deposited. The rest of the blank area, bounded by the green line to the interpreted area, represents an area where the S1-S2 boundary horizon is not shown because it could not be interpreted adequately, but the interface is most likely present at these locations. For orientation purposes several other features are shown: locations of Section 1 - 6, well locations, outlines of salt bodies and a window in the Upper Jurassic defined for this horizon.*

Sequence 2 time-thickness map

In Figure 35, the thickness of the second Upper Jurassic sequence is presented. The non-colored area to the SW of the blue line in the SW corner of the figure represents an area on non-deposition of the Upper Jurassic. The area marked as an Upper Jurassic Window represents an area where this interval was eroded. S2 is not present any more at the locations of the salt wall and Diapir A. The thickness of S2 is not known for the rest of the blank area, bounded by the green line at the edge of the interpreted area. Here the inter Upper Jurassic boundary could not be interpreted adequately. It becomes clear that in general westward of the salt wall the sequence is very thin. To the east of the salt wall the overall thickness is greater than west of the salt wall. This means that the center of sedimentation shifted towards the east after S1 was deposited. The sequence is thickened at the position around Diapir A, where lows are visible in the time-structure maps of the Upper Jurassic horizons. Thus, this area accommodated more sediments than its surrounding during this sequence, indicating that salt was withdrawn from underneath these areas resulting in the creation of accommodation space. Rapid thickness changes near several faults in the northeastern part of the map can are also present in this sequence. Several areas where thicker packages formed in S1, show thinned zones for S2 and vice versa. This can be seen for instance to the east of the N-S trending fault connecting two parallel NNW-SSE trending faults. Here a thin package of S2 is present on top of a thicker package of S1 (Figure 34).

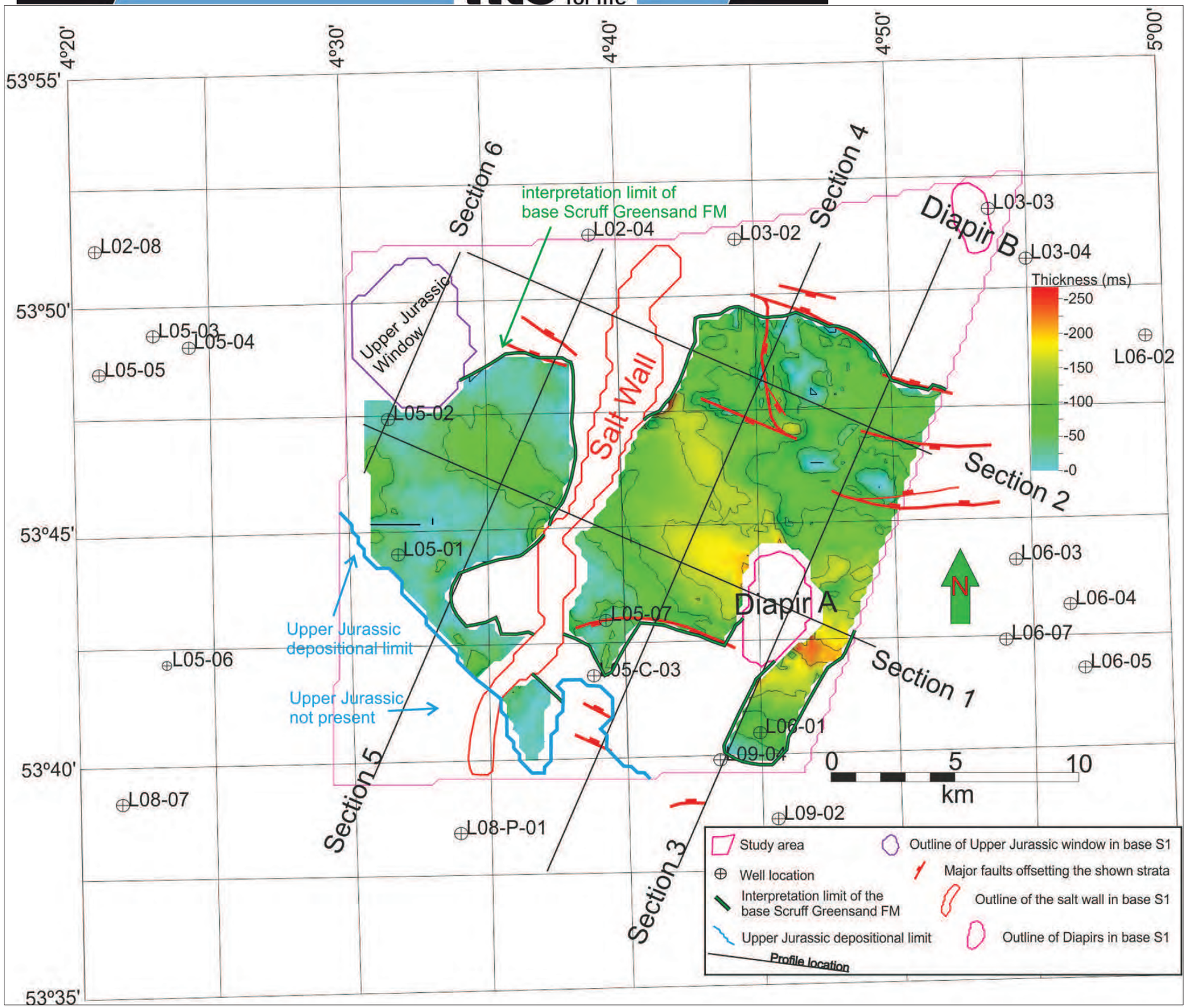

Figure 35. *Time-thickness map of S2. Examples of the major faults offsetting the Upper Jurassic strata are shown with red lines. In the blank area in the SW corner of the figure, bounded by the blue line, no Upper Jurassic strata have been deposited. The rest of the blank area, bounded by the green line to the interpreted area, represents an area where the base S2 horizon is not shown because it could not be interpreted adequately, but the interface is most likely present at these locations. For orientation purposes several other features are shown: locations of Section 1 - 6, well locations, outlines of salt bodies and a window in the Upper Jurassic defined for this horizon.*

Detailed sections

In the following section the results of the interpretation of six random lines is presented. These profiles were chosen to elucidate the most important structures and thickness changes that can be seen in the time-structure and time-thickness maps presented previously. The focus lies on the Upper Jurassic intervals and their genesis. The legend of these profiles can be found in Figure 41. The profiles are shown with a 5x vertical exaggeration. Only the position of the most important truncations and onlapping strata are shown, as otherwise the figures would become overcrowded.

Section 1 - in the Terschelling Basin

The profile in Figure 36 has a WNW-ESE orientation. This is perpendicular to the structural grain of the area. The profile crosscuts the salt wall at the position where it is least pronounced. Also Diapir A and the depocenter west of Diapir A are shown. Well L05-02 lies 600 m to the NNE, well L05-01 4,2 km to the SSW, well L05-07 3,3 km to SSW and well L06-01 4,9 km to SSW of the profile.

The pre-Zechstein basement is offset by several steeply dipping normal faults that terminate upward onto the Zechstein Group. The deepest point of the top of the pre-Zechstein basement lies in the most WNW part of the profile. The vertical difference of the top pre-Zechstein basement is mainly accommodated by a single fault that exhibits a large throw. Another structural low of the top of the pre-Zechstein is present to the ESE between the salt wall and Diapir A after which, the pre-Zechstein shallows towards the ESE edge of the profile. Overall the Zechstein Group is very thin. Only underneath Diapir A the layer has a considerable thickness. Both salt structures in this profile have completely pierced the Upper Jurassic strata in such a way, that in this orientation, no significant thickness changes can be observed at the location of the former flanks of the diapirs. Both salt bodies appear to have detached from their pedestal, so that only salt welds indicate the location of the former feeders. Thickened packages of the Upper Germanic Trias Group and the Altena Group are visible. Upper Triassic turtle structure have formed on both sides of the salt wall. Located closer to the position of salt wall, rim-synclines have formed in the Lower to Middle Jurassic. The Altena Group wedges out and is terminated against Upper Jurassic strata towards the ESE, between the two salt bodies. Viewing from the WNW the first 10 km of the interface between the Altena Group and the first Upper Jurassic sequence (S1) is concordant. Further to the ESE the contact is discordant and a hiatus at the base of S1 can be seen. The base of S2 slightly truncates the top of S1 west of the salt wall. Both S1 and S2 thicken in the most left part of the figure. From the salt wall to the ESE direction the entire Upper Jurassic interval thickens gradually and evenly. The depocenters present in the subsequent Mesozoic strata between the two salt bodies progressively shift towards Diapir A. There are no faults visible offsetting the Upper Jurassic. At the ESE flank of the salt wall the Upper Jurassic has been uplifted in such a way that the Lower Cretaceous sediments onlap onto the upturned flanks of S2. When going back to the time-thickness maps of the two Upper Jurassic sequences present in this study area, this profile crosscuts the depocenters to the eastern and western side of Diapir A. The profile shows that both S1 and S2 are thickened around Diapir A. Also at the WNW margin of the profile the thickening of S1 corresponds to a thickened area of the time-thickness map in Figure 34.

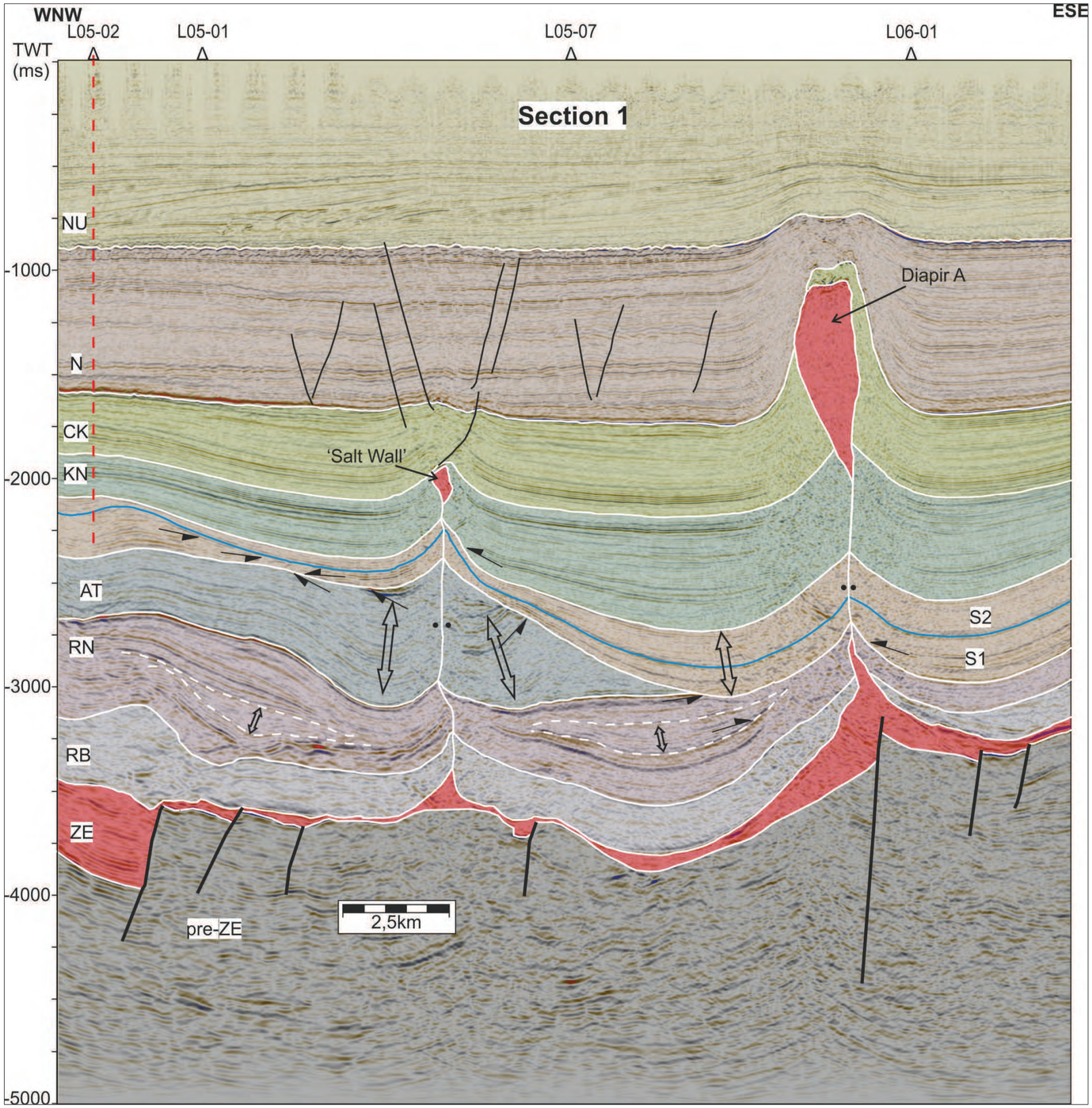

Figure 36. *Section 1. WNW-ESE oriented interpreted geological profile through the study area. For the legend see Figure 41. Inter Upper Triassic reflectors have been marked in order to highlight growth strata within that interval.*

Section 2 - in the Terschelling Basin

This profile (Figure 37) is WNW-ESE orientated as well. The profile crosscuts the salt wall at the position where it has a broad expression. Well L02-04 lies 2,6 km to the NNE, well L03-02 3,5 km to the NNE of the profile.

To the ESE of the salt wall the pre-Zechstein displays a uniform level. Directly left of the salt wall the pre-Zechstein is offset by a normal fault and continues on that level to the edge of the profile in the WNW. At the position of this fault, a small salt body has risen and has uplifted the Lower Triassic strata. The Upper Triassic is thinned above this small structure. There are no pre-Zechstein faults that propagate into the Mesozoic domain. Overall the Zechstein Group is quite thin, except for the impressive salt body that has risen from the Zechstein Group. It has pierced strata up to the Lower Cretaceous, has overturned all the Mesozoic strata and even the Upper North Sea Group has been affected. The Lower Triassic strata display an even thickness across the profile. An Upper Triassic turtle structure has formed to the WNW of the salt wall. To the ESE of the salt wall inter Upper Triassic truncations are present. This structure indicates the presence of a succession of an Upper Triassic withdrawal basin and a rim-syncline that moved closer to the salt body during the Upper Triassic. The Altena Group wedges out to the ESE and displays rim-synclinal features near the flanks of the salt body. Extensional faults are visible in the Upper Jurassic interval. The most pronounced faults terminate downwards onto the upper layers of the Upper Triassic. WNW of the salt wall, S1 shows a thickened succession within the faulted area. ESE of the salt wall, at the location of the extensional faults, the Lower Cretaceous and S2 are thickened. On the WNW margin of the figure, S2 is onlapping onto a high of the Altena Group. S2 is not present above this structure as it is unconformably overlain by Lower Cretaceous strata. The Upper Jurassic strata are uplifted spectacularly by the ESE flank of the salt wall. Here S1 is absent and only S2 is present in the uplifted flank. Further to the ESE the Upper Jurassic is distributed relatively evenly. At several positions along the profile the base of S1 is truncating and incising into lower lying units.

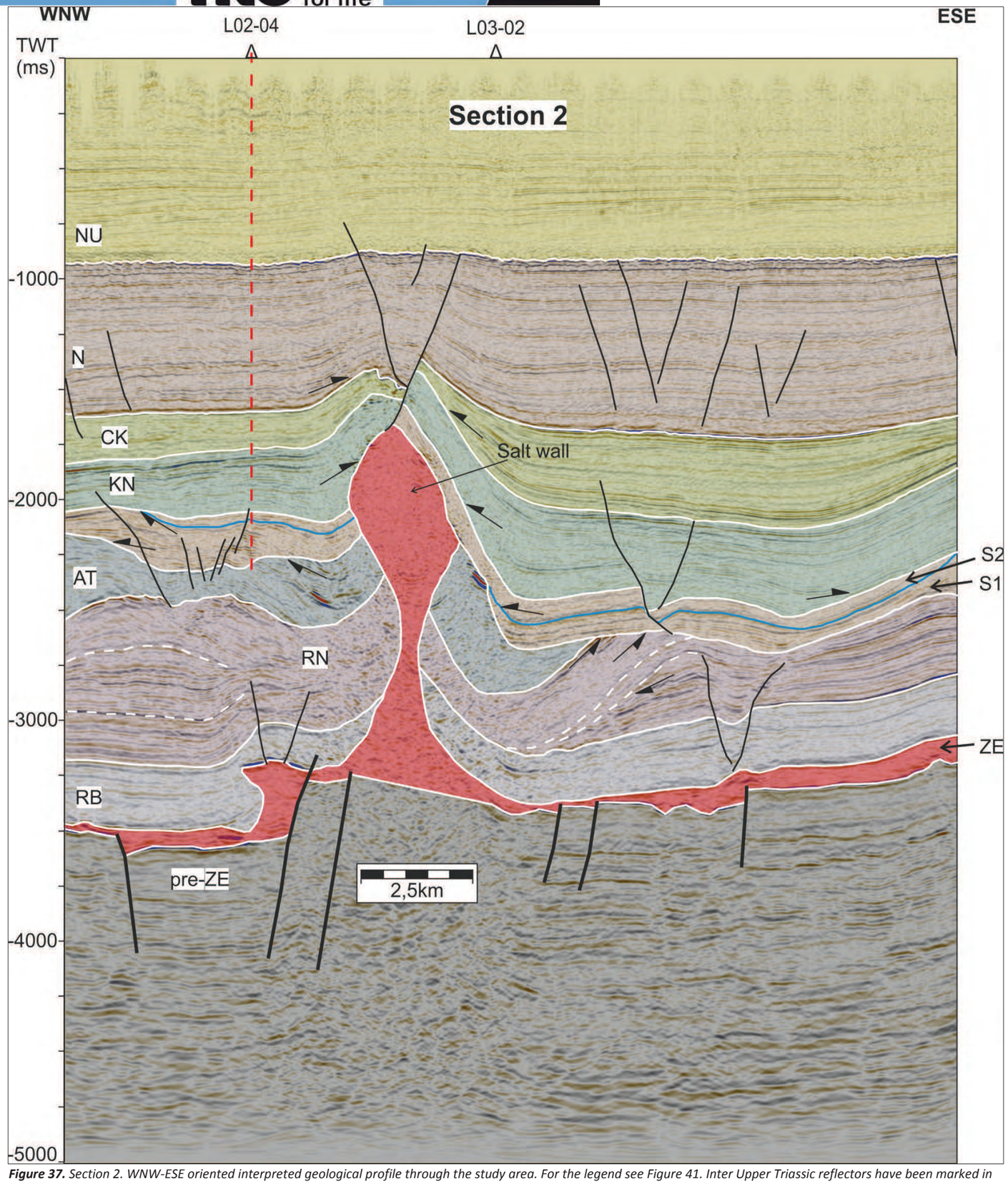

Figure 37. *Section 2. WNW-ESE oriented interpreted geological profile through the study area. For the legend see Figure 41. Inter Upper Triassic reflectors have been marked in order to highlight growth strata within that interval.*

Section 3 - in the Terschelling Basin

The profile in Figure 38 has a SSW-NNE orientation. This is along-strike with the structural grain of the area. The profile crosscuts Section 1 at the location of Diapir A and a zone with several faults offsetting the Upper Jurassic strata. Well L09-02 lies 2,8 km to the ESE, well L06-01 860 m to the ESE and well L03-04 3,2 km to the E of the profile.

Several normal faults offset the pre-Zechstein. The Zechstein Group is thicker at the hanging wall side of these faults. The overall depth of the top of the pre-Zechstein increases slightly to the NNE. The thickness of the Zechstein Group is variable as a result of lateral salt movement. Diapir A has risen from the level of the Zechstein Group and has pierced and upturned strata up to the Lower North Sea Group. Salt body C is a present day, very small, salt structure, which has risen at the NNE side of the profile. The structure shows signs of Zechstein salt being injected into shallower Upper Triassic salt layers. Remobilization of Salt Body C may have resulted in salt re-evacuation. The Upper Triassic strata show growth wedges at this location. The Lower Triassic strata are distributed relatively evenly, except the SSW edge of the profile, where the layer is thinned due to truncation of the Upper Triassic. The Upper Triassic thins from the NNE side of the profile towards the SSW flank of the diapir. From Diapir A towards the SSW edge of the profile, the layer slightly thickens again. Here the Upper Triassic is truncated and incised by S1.

When looking at Diapir A in this profile, both S1 and S2 show rim-synclines at the flanks of Diapir A. Although not as pronounced as the features present in Section 1. When looking at the time-structure maps, no pronounced thickness changes can be seen on the northern and southern side of Diapir A. This can be explained by the fact that the interpretation was not continued underneath the flanks of the salt bodies when the different horizons were gridded. The interpretation shown in Section 3 is therefore a more accurate representation of the structures near Diapir A. To the SSW of the rim-synclines at the flank of Diapir A, the Upper Jurassic strata are thinning. The Lower Cretaceous strata even incise into the Upper Jurassic strata in such a way that the Lower Cretaceous strata are in contact with S1. To the NNE of the right flank of Diapir A, the Upper Jurassic is thickening, this thickening is most pronounced in the S1 interval. This position coincides with the previously mentioned salt structure and Upper Triassic growth wedge. Several extensional faults offsetting the Upper Jurassic interval can be seen. It is assumed that these faults sole on intra Triassic salt layers. In the hanging wall side of these faults S1 displays the most pronounced thickening. Another interesting observation is that the Upper Cretaceous strata and the Lower North Sea Group thin towards the NNE.

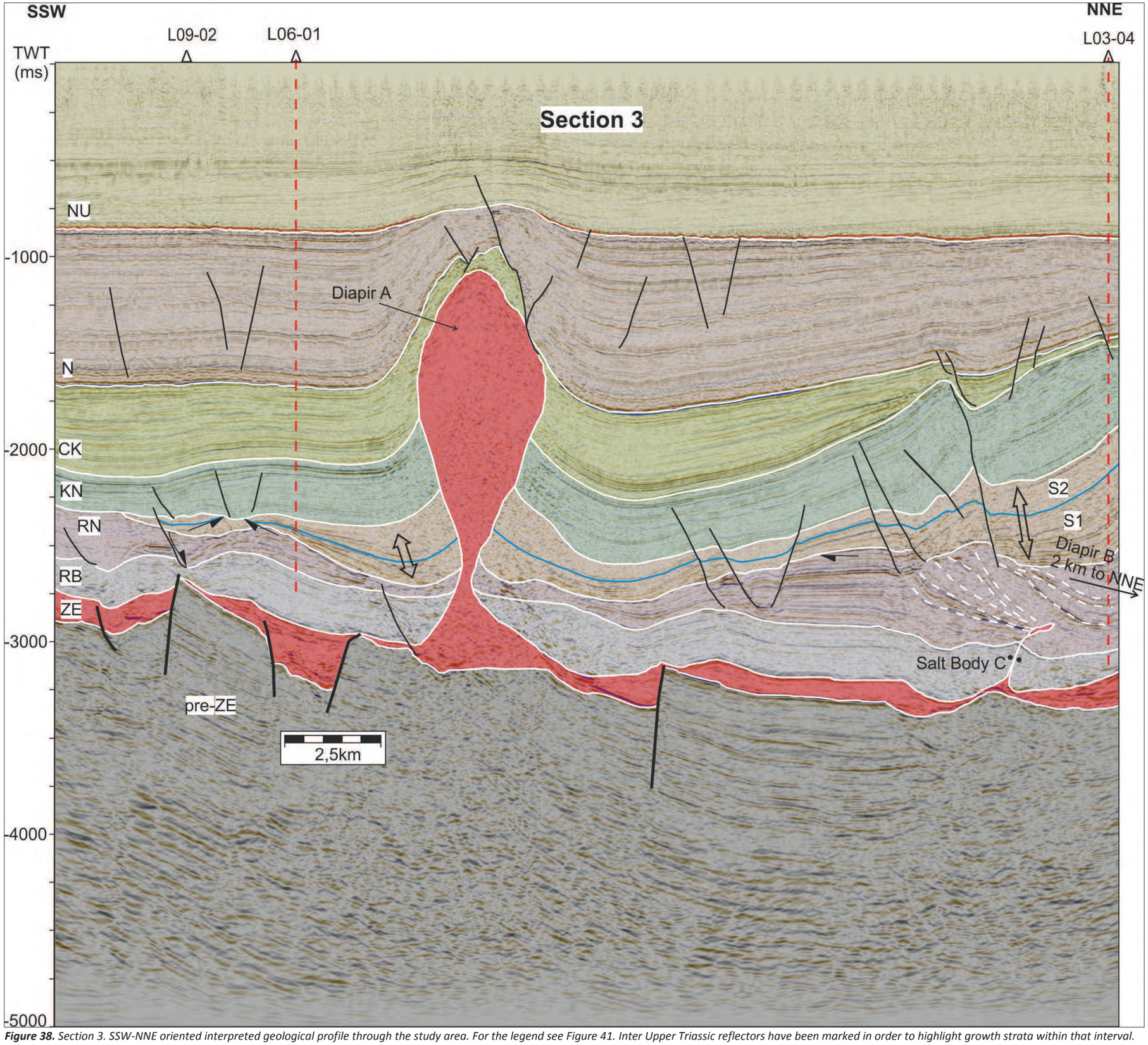

Figure 38. *Section 3. SSW-NNE oriented interpreted geological profile through the study area. For the legend see Figure 41. Inter Upper Triassic reflectors have been marked in order to highlight growth strata within that interval.*

Section 4 - in the Terschelling Basin

Section 4 (Figure 39) is oriented SSW-NNE, which is similar to the orientation of Section 3. The profile crosscuts the depocenter between the salt wall and Diapir A. Well L05-07 lies 3,7 km to the WNW and well L03-02 3,2 km to the WNW of the profile.

The top of the pre-Zechstein basement shows large vertical variations. Steeply dipping normal faults offset the pre-Zechstein basement. Several of these faults have also propagated upward into the supra salt domain. One fault even offsets the Lower Cretaceous strata. Especially the Upper Triassic interval is thickened at the hanging wall side of this fault. The deepest position of the top of the pre-Zechstein basement is visible in the center of the profile. In between two areas with a higher level of the pre-Zechstein basement, a structural low has developed. Here two large normal faults with a half-graben geometry created accommodation space, therefore the strata of the pre-Zechstein basement rotated resulting in NNE dip direction. The Zechstein Group is uniformly thin across the entire profile and at some locations the layer is even removed completely. The Lower Triassic strata are distributed evenly across the profile, but are thinned and eroded on top of the faulted pre-Zechstein high in the SSW. The Upper Triassic strata display a great thickness variation. The thickness of the interval is comparable at the right and left sides of the profile. However, in the central depocenter of the profile the thickness of the Upper Triassic is increased significantly, especially near the faults. Above the highest point of the pre-Zechstein, the Upper Triassic is thinner and the reflectors appear to be more chaotic. At this point there is no Lower Triassic left and listric faults seem to sole on inter Upper Triassic layers.

The Altena Group is not present over the entire length of the profile. Only a thin package of the Altena Group is present in the depocenter, thinning and onlapping onto both sides of the elevated shoulders. Also in between the extensional faults above the left pre-Zechstein basement high the Altena Group is present. The Upper Jurassic strata are also thickened in the central depocenter. Basal reflectors of S1 onlap onto the higher shoulders on both sides of the structural low. To the SSW S1 is even terminated completely. The S2 interval continues further to the SSW, although the package is increasingly thinned. The S2 interval terminates at the most distant listric fault on the SSW side of the profile. This shows that S2 extends further southward than S1, this was also illustrated in the time-structure map of Figure 31. To the NNE of the dominant basement fault, the thickness of the Upper Jurassic is influenced by the topography of the underlying Upper Triassic and several faults. S1 is thickening rapidly at the NNE side of the profile. Near the location of well L05-07 the top of S2 is truncated below the base of the Lower Cetaceous. At the NNE side of the profile, the Lower Cretaceous is onlapping onto S2. Furthermore, the Lower Cretaceous and the Chalk Group have blanketed the structures, creating more or less leveled horizons.

The thickness changes of the Upper Jurassic observed in this section can also be observed when looking at the time-thickness maps of the Upper Jurassic sequences. The area of the central depocenter shows thickening in Section 4 as well as in Figure 34 and 35. Also the thinning of the Upper Jurassic strata can be observed in both figures.

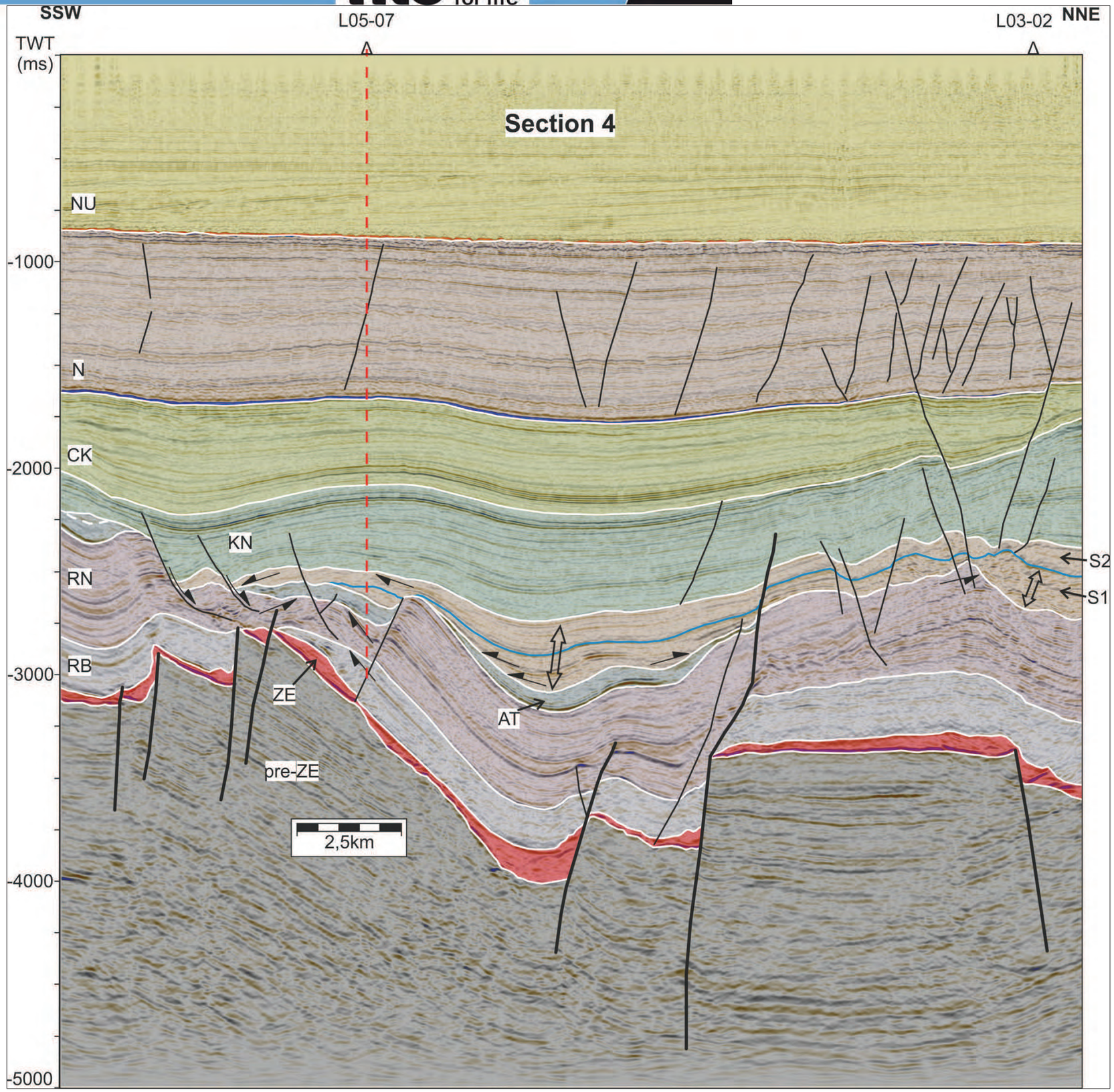

Figure 39. *Section 4. SSW-NNE oriented interpreted geological profile through the study area. For the legend see Figure 41.*

Section 5 - in the Terschelling Basin

Section 5 (Figure 40) is also oriented SSW - NNE and runs parallel to the salt wall on its western side. Well L05-01 lies 2,7 km to the WNW, well L05-02 5,2 km to the WNW and L02-04 800 m to the NW of the profile.

On both sides of the profile the top of the pre-Zechstein is higher than in the middle part of the profile. Steep normal faults offset the pre-Zechstein and have aided in creating the structural low in the middle of the profile. Overall the Zechstein Group is thin and seems almost depleted. Only at the hanging wall side of the sub-Zechstein faults, the layer is slightly thicker. None of these faults have propagated upwards through the Zechstein Group. The distribution of the Lower Triassic interval is generally regular although slightly thinning of the layers occurs on the NNE side of the profile. In the middle of the structural low, a remnant salt weld is interpreted. Zechstein salt has risen upward at this position and penetrated laterally into an inter Upper Triassic salt layer. The elongated allochthonous salt sheet (Salt Body D) is still in place. The Upper Triassic strata show the largest thickness variations present in this profile. Apart from the added thickness of the allochthonous salt the sequence also thickens from the SSW to the NNE. A growth wedge has formed on the right side of the structural low, probably due to salt withdrawal from underneath that position. On top of the NNE pre-Zechstein basement shoulder several faults crosscut the Mesozoic strata, mainly influencing the thickness of the Altena Group. The Altena Group thins and terminates towards the SSW above the pre-Zechstein basement shoulder. The thickest package can be found above the salt sheet. Here the youngest reflectors are somewhat irregular. These are probably reflections of the Posidonia Shale Formation. The youngest reflectors at the top of the Altena Group are truncated by successive layers of the Upper Jurassic and Lower Cretaceous. Further towards the NNE the Altena Group has a more regular expression and shows less thickness variation. The Upper Jurassic strata thin from the NNE towards the SSW. The layer has thinned above the location of the salt sheet and is terminated at the shoulder of the SSW pre-Zechstein basement shoulder. S1 of the Upper Jurassic interval slightly truncates the underlying Altena Group above Salt Body D. The sequence thickens from the deepest point in the structural low to the NNE edge of the profile. S2 truncates above Salt Body D against Lower Cretaceous strata. S2 has only a limited thickness in this profile, except for the deepest part of the Upper Jurassic strata where the sequence thickens slightly. This can also be observed in Figure 35 where the overall thickness of S2 is shown. The thickness of the Lower Cretaceous is significantly less than observed in Section 3 and Section 4. The lower reflectors of this interval truncate and onlap onto the highs of underlying sequences. The thickness is slightly increased in the central part of the profile. The Upper Cretaceous interval follows the topography of the underlying Lower Cretaceous package, thinning towards the NNE. The subsequent North Sea Groups blanket the older structures, creating an even topography.

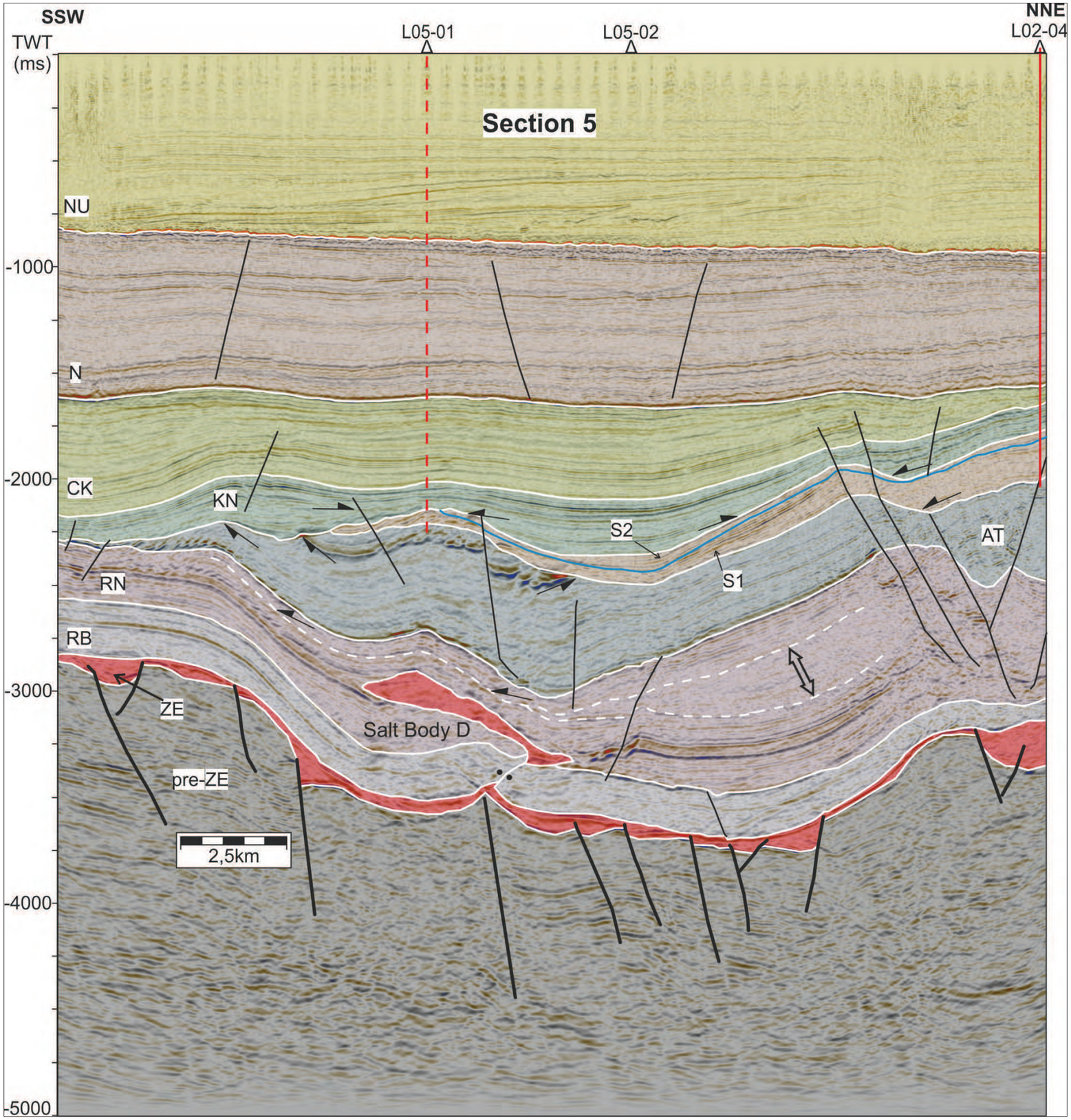

Figure 40. *Section 5. SSW-NNE oriented interpreted geological profile through the study area. For the legend see Figure 41. Inter Upper Triassic reflectors have been marked in order to highlight growth strata within that interval.*

Section 6 - in the Terschelling Basin

Section 6 (Figure 41) is the shortest and last profile described here. It runs across the area indicated as an Upper Jurassic Window and illustrates the along-strike (SSW-NNE) structures in the western part of the study area. Well L05-02 lies directly on the profile.

The reflectors of the pre-Zechstein basement are sub-horizontal and the top has a relatively uniform and horizontal character. At the SSW side of the profile the pre-Zechstein is downfaulted by large normal faults. The Zechstein Group is thicker at the lower and faulted location on the SSW side of the profile compared to the middle and NNE side of the profile. The Lower Triassic is distributed evenly and does not show significant thickness changes in this section. The allochthonous Salt Body E has penetrated the Upper Jurassic strata. Weak remnants of a salt feeder, that played a role during salt emplacement, can be seen between the Zechstein Layer and Salt Body E. Additionally, E-W lateral salt migration has probably played a role during the emplacement of the salt as well. The thickness of the Upper Triassic strata are constant as well. The upper part of this sequence is draping over Salt Body E, lifting the position of the reflectors. The Altena Group is also draping over the crest of Salt Body E, additionally, the thickness of the layer is not reduced at this location. To the NNE the Altena Group interval thickens slightly. The Upper Jurassic can only be found at the SSW and NNE sides of the profile. At the SSW side of the profile, this interval is bend upward and thinned towards the flank of Salt Body E. At the base, the reflectors are not onlapping onto the Altena Group. At the top, both S1 and S2 are truncated below Lower Cretaceous strata. At the NNE margin of the profile, a small sliver of Upper Jurassic strata (probably belonging to S1) is present. In between these two patches of Upper Jurassic strata, the Upper Jurassic is absent. This is the zone previously marked as the Upper Jurassic Window. At the base of the Lower Cretaceous strata an hiatus is present and signs of an erosional interface and truncation can be seen. The Lower Cretaceous is onlapping onto the crest above the salt body. This may indicate that the Upper Jurassic was deposited along the entire length of the profile, but has been eroded. The thickness difference of the two Upper Jurassic sequences in the SSW part of the profile are also observed in Figure 34 and 35.

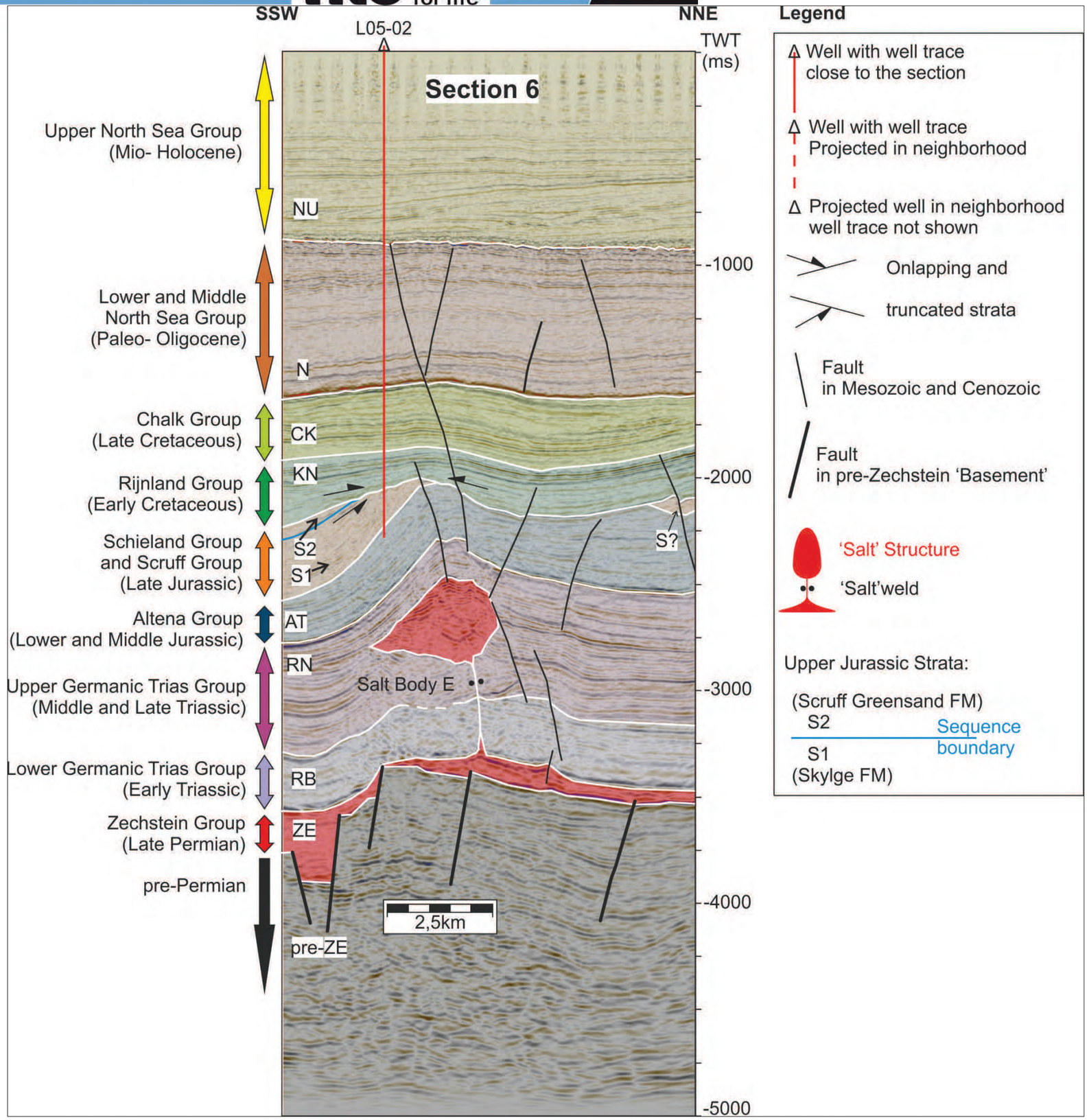

Figure 41. *Section 6. SSW-NNE oriented interpreted geological profile through the study area. Also the sedimentary groups and the legend for the detailed sections are shown.*

Discussion

In this chapter the results of this study are discussed. The focus lies on the explanation of the structures visible in the Upper Jurassic sequences and the salt migration that influenced the Upper Jurassic sedimentation. Additionally, growth strata related to the salt migration in other intervals and their implications will be discussed as well.

The larger study area within the Dutch North Sea

This section focuses on the salt structures, faults and sedimentary patterns of the regional transects, since the structural style in these sections may be analogous to the study area in the western part of the Terschelling Basin. Therefore, these observations may yield important implications for the interpretation of sedimentary and structural phenomena seen in the study area.

The seismic data used for this work, show that the pre-Zechstein interval in the Dutch North Sea area has its deepest position in the Dutch Central Graben, where the extensional deformation of the early Kimmerian rifting strongly downfaulted the relatively narrow zone of the Dutch Central Graben (Ziegler, 1990; Underhill & Partington, 1993). This resulted the creation of marginal faults that exhibit large offsets (e.g. Fault f in Line A, Figure 17)and the creation a large amount of accommodation space, allowing for sedimentation of a thick package of Upper Jurassic strata within the narrow N-S trending rift basin of the Dutch Central Graben (up to 2500 m, e.g. Position B in Line B, Figure 20). The extensional faults triggered flow of the Zechstein salt and initiated reactive diapirism, resulting in the formation of large salt pillows. In the southern North Sea, the first salt swells formed during the Middle Triassic (de Jager, 2007; Pharaoh et al., 2010). From the Late Triassic onward the salt pillows were further inflated and driven upward by continued salt migration that was caused by continued accumulation of sediments and differential loading of the Zechstein layer (Jackson et al. 1994; Davison et al., 2000; Rowan et al., 2003; Stewart, 2006; Hudec and Jackson, 2007). Active piercing diapirism commenced when the accumulated sediments loaded the salt layer sufficiently to drive upward salt migration.

Despite the fact that the Zechstein Group is at its deepest position in the Dutch Central Graben within the entire Dutch North Sea area, the related salt diapirs and salt walls that have risen in the Dutch Central Graben and at its margins, have developed into the tallest, shallowest and most pronounced salt bodies in the region. Although the present day shape of the salt bodies is influenced by a range of different factors, the height of the salt bodies within the Dutch Central Graben suggests that 1) the salt migration was stronger or more localized compared to other parts of the Dutch North Sea or 2) larger volumes of salt were available for withdrawal and migration.

Between the different salt bodies, the present day thickness of the autochthonous Zechstein salt layer, in all three basins (Dutch Central Graben, Step Graben and Terschelling Graben), is very thin. Especially at the locations of the deepest depocenters (e.g. locations B and E in Line A, Figure 17; B in Line B, Figure 20; around Diapirs 4 and 6 in Line C, Figure 24), where the Zechstein Group interval seems completely withdrawn, so that further salt flow was inhibited and further growth of the salt bodies ceased. Between Diapir 10 and 11 in Line C (Figure 24), the thickness of the Zechstein Group measures approximately 120 ms. As reported by Kombrink et al. (2012) and TNO - Geological Survey of the Netherlands http://www.nlog.nl/nl/pubs/maps/geologic_maps/DGM_deep_offshore.html (2010), the thickness of the salt at this position is no more than 150 to 200 m. Diapir 11 is significantly smaller than its neighboring salt bodies (Figure 24 shows the maximum height of the diapirs), this can be explained by the fact that the Zechstein layer welded out so that further salt migration and diapir growth ceased. Ferrer et al. (2012) made similar observations for Late Jurassic salt structures in the Parentis Basin in the eastern Bay of Biscay. Many of the salt structures they describe had stopped growing during the Mid-Cretaceous when their source layer had become depleted.

TNO innovation for life

After the first phase of Kimmerian rifting, that only affected the Dutch Central Graben in the Dutch North Sea, the direction of extension changed. A second phase of Kimmerian rifting commenced where the extensional deformation became less localized and affected a wider zone consisting of the Step Graben, the Dutch Central Graben and the Terschelling Basin This resulted in less localized and less pronounced deformational structures and the creation of a broad zone of accommodation space. Additionally, a portion of the deformational strain was accommodated by the reactivation of Paleozoic NW-SE trending lineaments. These factors explain why the pre-Zechstein sequence in the Step Graben and the Terschelling Basin are shallower than in the Dutch Central Graben. The burial graphs of the southern part of the Dutch Central Graben and the Terschelling Basin, as published by Verweij et al. (2009), also show the difference of the depth of the pre-Zechstein within the two basins. The relative timing of extension in the three basins in the Dutch North Sea explains why the deepest sequence of the Upper Jurassic (sensu Abbink et al., 2006) is only present within the Dutch Central Graben and why the youngest two sequences (sensu Abbink et al., 2006) are mostly found in the Step Graben and the Terschelling Basin.

The Zechstein Group in the Terschelling Basin and the Step Graben is situated shallower than in the Dutch Central Graben. This means that the salt bodies that have risen in these two peripheral rift basins, started to grow at a shallower depth and are not as tall as the salt bodies in the Dutch Central Graben. An explanation for this could be that less salt was available for salt migration into the salt bodies in the Terschelling Basin and Step Graben compared to the Dutch Central Graben, so that the resulting present day shape of the salt bodies is less vertically pronounced. Unfortunately, the amount of salt dissolution and redistribution that has taken place at the locations of the salt bodies is still unclear, but it is likely that the height of most diapirs within the Dutch North Sea is influenced by these processes.

The present day geometry of the different salt bodies throughout the three basins in the Dutch North Sea vary significantly. Salt pillows like the structures below positions A and D in Line B (Figure 20) and below positions 2 and 5 in Line C (Figure 24) have not evolved into piercing diapirs.

According to Hudec & Jackson (2007) it can be assumed that almost all present day diapirs have pierced brittle overburdens. This is also the case for the piercing salt bodies within the study area. Furthermore, all diapirs within the study area that have evolved into piercing diapirs have most likely experienced (sub) areal exposure or erosion (e.g. Diapirs 1-4 in Line A, Figure 17; Diapirs 1 and 2 in Line B, Figure 20; Diapirs 3,4 6, 8-11 in Line C, Figure 24). This is supported by a recent TNO in-house study conducted by van Winden (2015) in the Dutch northern offshore, which suggests that the original thickness of the Zechstein Group was much greater than previously assumed. In this case shallow processes such as dissolution, erosion and redistribution, that took place during diapirism, must have had a greater influence on the distribution of the Zechstein Group. However, only several of the largest diapirs within or at the margin of the Dutch Central Graben, (e.g. Diapir 1 and 2 in Line B, Figure 20), exhibit a flattened top where presumably caprocks have formed due to (sub) areal exposure. At other locations, like for instance at Diapir 10 in Line C (Figure 24), no caprocks are preserved due to ongoing upwards salt flow that removed and replaced possible leaching products with ‘fresh’ salt. At this position the lowest reflectors of the Upper Jurassic strata onlap onto the salt body. This indicates that the diapir was located near the surface at the time of deposition of the Upper Jurassic strata and that the diapir had a surface expression. Figure 42 shows two modes of reflector termination against diapirs. Almost all salt bodies within the study area experience onlapping of Upper Jurassic strata, as it is presented in case B.

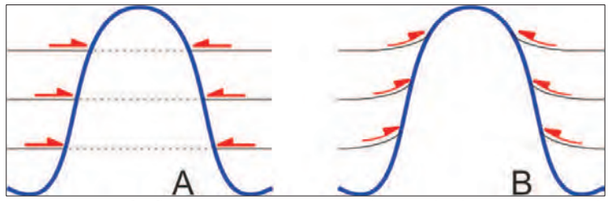

Figure 42. *Schematic representation of reflector terminations against diapirs. Blue lines indicate the diapirs, black lines represent the terminated layer and the red arrows indicate the point of termination. A) A horizontal and evenly stratified succession is pierced (brittlely) by the diapir after the deposition of the succession. No thickness differences of the sediments are observed and they display horizontally truncating reflectors. B) The sediments were deposited during the growth of the diapir. The surface expression of the diapir is indicated by the onlap of the reflectors and the fact that subtle thickness differences are visible in the deposits.*

After the active piercement phase, the salt bodies within the study area experienced a period of passive diapir growth, before being buried. It is possible that the sediment aggradation rate increased during the evolution of the diapirs, but that the sedimentary loading of the salt became a less important factor and caused the active piercing to cease. A possible mechanism for the ceasing of diapir growth is discussed by Hudec & Jackson (2007): When salt migration from the autochthonous salt layer slows down because the increased viscous resistance of the thinned salt layer has effectively immobilized the salt, the growth of the diapir ceases. However, only at a few locations within the study area, salt welds have been observed (e.g. directly next to the flanks of the diapirs 8 and 10 in Line C (Figure 24) or the ESE side of the salt wall in Section 2 (Figure 37)).

The lowest reflectors of the Upper Jurassic interval is the only reflector that onlaps onto Diapir 9 and 10 in line C (Figure 24) in the Terschelling Basin. This indicates that the autochthonous Zechstein salt layer became completely withdrawn just after the deposition of the lowest layers of the Upper Jurassic interval. The diapir growth slowed down and as a consequence the diapir became buried by the subsequent sedimentation.

Several salt bodies, especially in the Terschelling Basin (Diapir 9 and 10 in Line C, Figure 24), exhibit distinct wing-like geometries where the body of the diapir is significantly broader than the feeder area and the rest of the salt body. These wings have their maximum extend between the upper part of the Altena Group and the lower part of the Upper Jurassic interval. It is possible that the position of these wings indicate that during the deposition of these intervals, the diapir rise climaxed and the upward salt migration took place relatively fast.

The formation of an allochthonous salt sheet can be a possible explanation for these wing-like zones. There are no signs of dissolution or leaching of the salt observed in these wings, hence an extrusive advance of these sheets is unlikely. Open-toed or thrust advance (Hudec & Jackson, 2007) are more likely mechanisms of salt sheet formation that might have caused the wing like zones. According to Hudec & Jackson (2007) the formation of an allochthonous salt sheet is an extreme case of passive diapirism, in which the sediment aggradation rate is lower than the salt rise rate. The salt sheet spreads horizontally across a single bedding surface. The high rates of diapir growth can be induced by fast regional extension or by increased sedimentary loading of the salt. After the salt migration and diapir growth slow down and the relative sedimentation rate increases, the diapirs continue to rise, although they display a smaller diameter. Salt wings can also form by penetration of allochthonous salt into shallower, autochthonous salt layer. It is not likely that these specific wing-like zones were formed by this mechanism, because there are no known salt layers present at the upper part of the Altena Group and the lower part of the Upper Jurassic interval.

The shape of the salt bodies within the study area is greatly influenced by the basin inversion during the Alpine compression of the Dutch North Sea area. Salt is typically the weakest link in any rock system, and tends to accumulate most of the total strain, so that preexisting salt bodies usually deform first and display more deformation than the surrounding strata (Hudec & Jackson, 2007). The teardrop-shape of salt bodies, together with squeezed or pinched off feeder areas, are typical signs of diapir amplification due to regional compression (Hudec & Jackson, 2007). Diapirs 2 and 3 in line A

(Figure 17) exhibit such features and are good examples of the effects of the compression and rejuvenation of salt bodies.

Differential sedimentary loading is known to drive salt migration once a salt body has started to grow (Hudec & Jackson, 2007). The initial triggering of the diapirism in the Dutch North Sea is closely related to fault activity in the pre-Zechstein interval (e.g. ten Veen et al., 2012). The rise of isolated diapirs has been triggered by alternating movements of cross-cutting faults, whilst the rise of salt walls is triggered by movement along a single fault. At passive margin settings gravitational gliding above a salt detachment and sedimentary loading by delta progradation are known to initiate salt migration and resulting diapirism (Ge et al., 1997). However, the passive margin setting does not apply for the study area, therefore this scenario is not valid here. Additionally, nearly every salt body that has been studied has formed above normal faults located at the base Zechstein level. For some diapirs this can only be assumed, because the sub-salt seismic imaging underneath the salt structures is of poor quality. This indicates that the model of ten Veen et al. (2012) can be successfully applied to the results of this work, hence the initial diapirism in the study area has been triggered by movements of normal faults at the base Zechstein level.

Within the study area, only a very limited number of faults propagate from the sub-salt domain into the supra-salt domain. Figure 43 shows the different types of faults that are present within the study area.

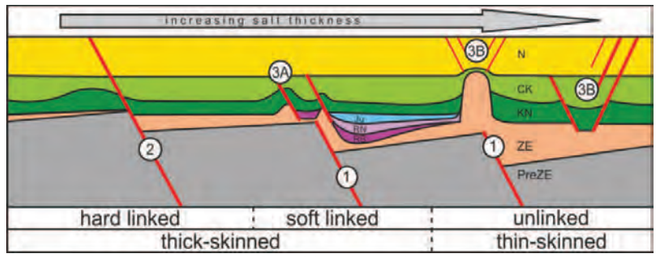

Figure 43. *Schematic N-S section in the Dutch North Sea with an increasing salt structure height and depositional salt thickness from left to right. The tectonic setting and the behavior of the faults are indicated below. The unlinked type 1 faults terminate upward in the Zechstein salt where the salt is thick. The hard linked type 2 faults originate below the Zechstein salt (as type 1) but also affect the supra-salt domain where the salt is thin or absent. The soft linked type 3A faults are spatially linked to salt structures and their associated sub-salt faults, but are not connected to them. The type 3B faults are not linked to sub-salt faults, but may be related to salt structures (figure from Ten Veen et al., 2012).*

Ten Veen et al. (2012) imply that when the depositional thickness before halokinesis, of the Zechstein salt is less than 300 m the structural style is 'thick-skinned', meaning that the sub-Zechstein faults reflect the regional stress history and have propagated into the supra-salt layers. This explains why the fault patterns in 'thick-skinned' areas are similar in the sub- and supra-salt layers. When the depositional thickness of the Zechstein salt is more than 300 m, the structural style is 'thin-skinned'. This means that regional stresses will deform the sub-salt domain in a brittle way and sub-salt faults do not propagate through the salt layer. In terms of stress, the layers above the salt are detached from the sub-salt domain and are only indirectly related to the active stress field. The fact that only a very limited number of faults propagate from the sub-salt domain into the supra-salt domain, combined with the assumption that the depositional thickness of the Zechstein salt was larger than 300 m lead to the observation that the tectonic style within the study area is thin-skinned. Faults that are situated underneath a thin layer of Zechstein salt that do not propagate from pre-Zechstein levels into the supra-salt layers must have been active before or during halokinesis and were not reactivated after halokinesis caused thinning of the original thickness of the salt.

On top of the crests of nearly every salt body in the study area, straight and relatively steep type 3B normal faults (Figure 43) can be seen (e.g. Diapirs 8 and 10 in Line C (Figure 24). These faults are caused by several processes: Vendeville and Jackson (1992) and Pascoe et al. (1999) demonstrate that these type of faults can be related to a reactive diapirism phase during regional extensional faulting and salt migration within rift basins. Another process that resulted in the formation of type 3B normal faults is diapir amplification and renewed growth of the salt bodies during the compressional phase in Late Cretaceous times (Ten Veen et al.,2012). The faults that have formed within the crests of turtle back structures (e.g. the Upper Jurassic interval in Line A (Figure 17), above Location E; the Upper Triassic interval on Line C (Figure 24), above Salt Pillow 5), also belong to the fault type 3B of (Figure 43). These faults have formed during the Late Cretaceous inversion (Lott et al., 2010).

Another interesting fault related feature can be seen in Line B. (Figure 20), where listric faults b and c seem to sole on the Zechstein salt layer and accommodate a huge amount of deformation, testified by the significant offset of the Mesozoic strata. Within this profile, these faults have an E-W orientation, parallel to the Jurassic extension direction and the basin bounding faults. Rosendaal et al., 2014, formulated the hypothesis that the main rifting in the Dutch Central Graben and the Step Graben took place during the Middle to Late Triassic and that the listric faults compartmentalize the basin into several areas that moved independent relative to each other. Unfortunately, in this research this hypothesis cannot be confirmed nor denied, therefore the source of the listric faults could not be determined.

The interplay between the deposition of the Mesozoic sediments and the migration of salt is the most challenging subject of this work. Sediments that were deposited in an area where accommodation space was created due to salt withdrawal also caused additional loading onto the salt, so that even more salt flow was initiated. Thus, it is important to carefully examine the shapes of the different salt bodies and the sediments in their vicinity, when drawing conclusions about their evolution through time.

Not only the height of the salt bodies is largest in the Dutch Central Graben, also the thickness of Upper Jurassic growth wedges and rim-synclines is greater in the Dutch Central Graben than in the Terschelling Basin and the Step Graben. For example, the Upper Jurassic rim-synclines around Diapir 4 and 6 in Line C (Dutch Central Graben) (Figure 24) show significantly thicker sediment packages compared to the same interval near Salt Body 9 and 10 in Line C (Terschelling Basin) (Figure 24). To allow for the deposition of thicker packages of sediment, more accommodation space must be created by means of salt evacuation. Higher rates of regional extension can be related to higher rates of salt migration (Jackson et al., 1994). Thus, the presence of thicker growth wedges and rim-synclines in the Dutch Central Graben compared to the Step Graben and the Terschelling Basin indicate that the extensional deformation during the Kimmerian rifting was more localized in the Dutch Central Graben than in the peripheral basins (Wong, 2007). The Upper Jurassic growth strata seem to be thickest in the Dutch Central Graben, but the effects of erosion during the Cretaceous uplift and inversion of the rift basins must be accounted for. Large areas of the Kimmerian rift basins experienced erosion after rifting ceased in the Dutch North Sea area. In many places a very pronounced hiatus can be observed between the syn-rift sediment and the post-inversion deposits (e.g. above position 5 in Line A, Figure 17). Hence, the depositional thickness of the Upper Jurassic is not preserved everywhere.

At several locations salt pillows with thickened packages of Upper Triassic strata can be identified (turtle-back structures). Location 7 in Line C (Figure 24) is a good example for this. These paleo-thick areas have likely been deposited with a bowl-shaped geometry at locations where early salt migration took place (Hudec et al., 2009). Sedimentary units with such an external shape were deposited in an area where accommodation space with a bowl-shaped geometry was created by salt migration into all directions away from the center of the depocenter (e.g. Hudec et al., 2009).

Progressive localization of the creation of accommodation space by sedimentary loading of a salt layer can be observed at rim-synclines. For instance at the SE flank of Diapir 4 in Line C (Figure 24 and 44) the depocenter of the successive layers can be seen to shift towards the diapir.

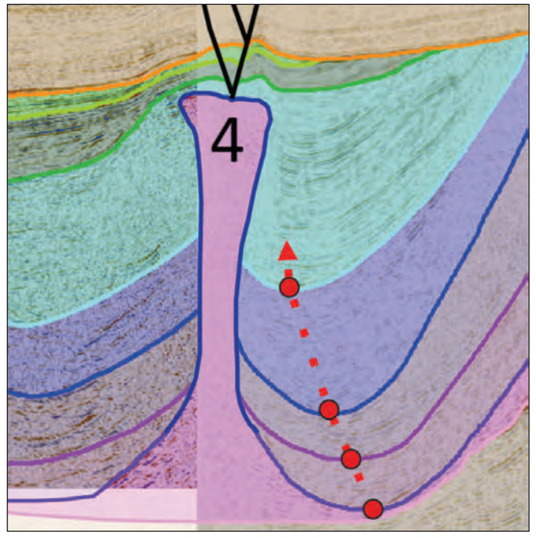

Figure 44. *Zoom in on Diapir 4 in Line C, Figure 24 showing the that depocenters of the successive layers shift towards the diapir.*

This means that the area of subsidence of the sedimentary depocenter became more localized as the salt layer was evacuated further.

Tectono-stratigraphy of the study area within in the Terschelling Basin

This section discusses the results of the seismic interpretation using the time-structure and time thickness (Figure 28-35) and the six detailed seismic sections (Figure 36-41), in the L5 and L6 blocks of the study area. The focus is the explanation of the structures visible in the Upper Jurassic sequences and the salt migration that influenced the Upper Jurassic sedimentation. However, growth strata related to the salt migration in other intervals and their implications will be discussed as well.

When looking at the detailed seismic sections (Figure 36-41), the time-structure maps and time thickness maps of the Upper Jurassic sequences (Figure 28-35), it is clear that the area westward of the N-S oriented salt wall shows structural and sedimentary differences compared to the area east of the salt wall. The most noticeable differences are: the distribution and stratigraphic thickness trends of several sedimentary intervals, the behavior of faults and the amount of erosion experienced by several intervals. In other studies and on regional maps of the area, the salt wall forms the margin between the Dutch Central Graben and the Terschelling Basin (e.g. Verweij & Witmans, 2009, Figure 10; De Jager, 2007, Figure 2; Pharaoh et al., 2010). The fact that the Altena Group disappears just to the east of the salt wall underlines the difference between these two zones. The study area is therefore subdivided into a western and an eastern domain, relative to the salt wall.

The time-structure and time-thickness maps (Figure 28-35) form the main result of this work, additionally seismic Sections 1-6 (Figure 36-41) have the purpose of highlighting the most

important structures and stratigraphic thickness changes that can be seen in the time-thickness maps. The time-thickness maps not only show where sediments are deposited during a certain period, but also indicate the thickness of the sediment packages. This means that these maps show at which locations the sedimentation predominantly took place and where sedimentation was restricted or even bypassed during the Late Jurassic period. If the condition was met that sediment supply was sufficient during a certain period, the over-thickened zones of this interval represent zones where accommodation space was created during the deposition. Differential erosion can also cause apparent thickness changes but cannot be quantified for this tectono-stratigraphic study. Thus, knowing that salt migration mainly took place during the Kimmerian period of extension, the formation of deposition centers is most likely the result of salt evacuation during that period. This is also confirmed by growth strata near the flanks of salt bodies that indicate that during the deposition, salt flowed into the neighboring structure.

From the time-thickness maps alone it is not possible to determine from which direction sediments entered the basin and to determine sedimentation rates. A seismic sequence stratigraphic analysis has not been conducted, but internal onlap/offlap relationships within S1 (seen in the seismic cube Z3NAM1990F) indicate that the influx was not directed from one specific direction. The work of Stegers (2006) where sand and clay percentages from core samples throughout the Terschelling Basin are correlated, suggests that the oldest Upper Jurassic sediments entered the basin from the south, the west and the northeast. However, that study did not discriminate between the two Upper Jurassic sequences that are present within the Terschelling Basin and several Upper Jurassic depositional environments were described on somewhat speculative arguments. Therefore, it is difficult to determine of the results published by Stegers (2006) are reliable. Therefore, the direction of sediment influx remains undetermined.

The diagram in Figure 45 has been constructed to summarize the evolution of several features within the study area and acts as a guide for the following discussion. The observed or most likely period of activity of the described features are indicated in the diagram.

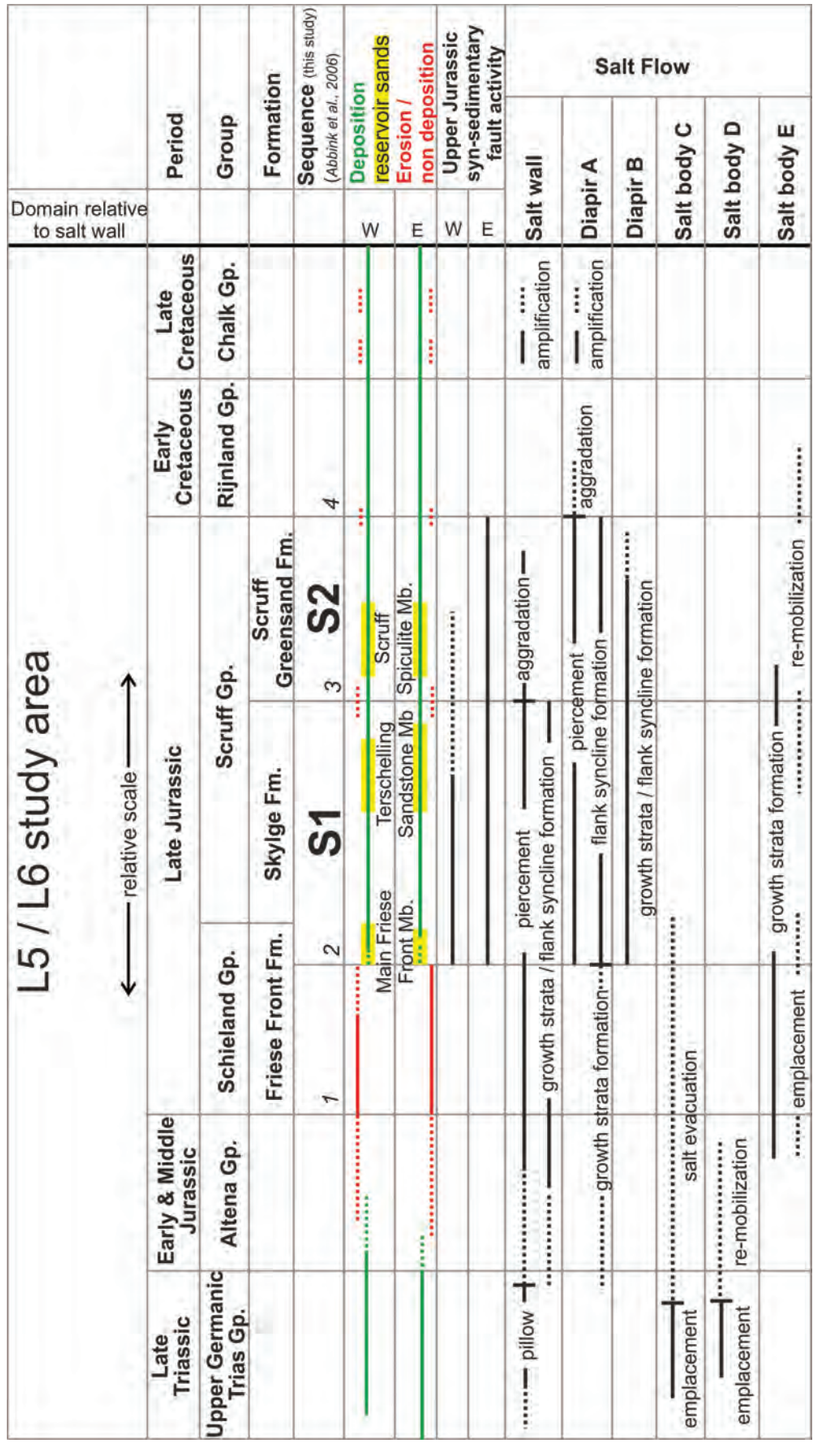

Figure 45. *Diagram showing the most likely period of activity of several features and processes within the study area. Dotted lines indicate that the level of confidence for a certain feature is limited compared to features and periods indicated with solid lines.*

Signs of early salt migration in the Upper Triassic and Lower and Middle Jurassic

When working with seismic data from the Dutch North Sea it becomes clear that the presence of Zechstein salt has influenced all aspects of the evolution of the region. Salt evacuation resulted in the creation of accommodation space in some areas, whereas the rise of impressive salt diapirs and walls took place elsewhere. Especially the Upper Jurassic displays spectacular growth strata and sedimentary thickness differences, but salt migration did not only take place during the Kimmerian rift climax. Signs of early salt migration in Triassic sequences can be seen in all three rift basins. The zones that contain Triassic growth strata, indicate the creation of accommodation space by salt withdrawal and rim-syncline formation before the Late Jurassic period started. Time-structure and time-thickness maps were constructed for the Upper Jurassic sequences but not for other intervals, because the focus of this project is explaining the structures visible in the Upper Jurassic sequences and the salt migration that influenced the Upper Jurassic sedimentation. Nevertheless the seismic interpretation carried out provided plenty of information to discuss early salt migration during the Late Triassic and Early and Middle Jurassic.

From regional observation it is known that the **Zechstein Group** has been deposited within the entire study area. Most faults that have offset the pre-Zechstein do not propagate upwards through the Zechstein Group, but only affect the base of the Zechstein Group. At the locations of these pre-Zechstein faults, thickness differences in the Zechstein Group are observed.

The **Lower Germanic Trias Group** contains only a few faults and no significant thickness differences across these faults can be seen. Minor thickness variations that are present on other locations within the interval seem to be unrelated to active salt migration during deposition. The average depositional thickness of the Lower Triassic interval within the study area of this study, is around 500 m (Verweij & Witmans, 2009). According to Hudec & Jackson (2007) buoyant salt rise may commence at burial depths from 650 m to 1500 m. In the southern North Sea, it took until the Middle Triassic for the first salt swells to form (de Jager, 2007; Pharaoh et al., 2010). The Lower Triassic has been uplifted and rotated by the different salt bodies that have pierced through this interval. (Section 1, Figure 36; Section 2, Figure 37; Section 3, Figure 38). In Section 1, (Figure 36) the Lower Triassic thins towards the feeder area of Diapir A. It is not visible if the Lower Triassic reflectors onlap onto the rising Zechstein salt due to the poor quality of the seismic image below the salt of Diapir A.

The oldest units that display growth strata, are found within the **Upper Germanic Trias Group**. In Section 1-6 (Figure 36-41) the areas that display Upper Triassic growth strata have been marked with white dotted lines. Above the top Upper Triassic surface a hiatus is present at many locations. The original depositional thickness of the Upper Triassic and the amount of erosion experienced by this interval is unknown. The uplift caused by the Central North Sea thermal dome is possibly related to the observed hiatus.

In Section 1 (Figure 36) the Upper Triassic interval displays significant thickness differences. To the WNW of the salt wall an over-thickened zone can be observed. These growth strata probably have the external form of a bowl in map view, but in Section 1 (Figure 36) only a trough is visible. Additionally, between the salt wall and Diapir A, an over-thickened trough external form is visible as well. The growth strata at these locations indicate that during the deposition, accommodation space was created within the area due of salt withdrawal. To the ESE of Diapir A the Upper Triassic is uniformly thin. It is possible that deposition was more limited in this area, but it is also possible that a significant part of the Upper Triassic has been eroded in the surrounding area of Diapir A. The Upper Triassic interval thins near the flanks of the salt wall and Diapir A and is crosscut by the salt bodies in a similar mode as described in Figure 42 A (straight truncation, no onlap visible). This indicates that a salt pillow formed at the locations of the salt wall and Diapir A during the Late Triassic.

In Section 2 (Figure 37) the Upper Triassic displays significant thickness differences. To the WNW of the salt wall an over-thickened turtle structure is visible. The Upper Triassic layers have been rotated and uplifted by the WNW flank of the salt wall when the salt pierced through the layer. The Upper Triassic in the ESE part of Section 2 (Figure 37) looks evenly stratified, but is truncated by younger Upper Triassic layers when converging to the salt wall. The thickness of the Upper Triassic in the ESE flank of the salt wall is less than elsewhere in Section 2 (Figure 37). The turtle structure in the WNW indicates that during the deposition, accommodation space was created within that area by salt migration away from the turtle structure. The fact that the Upper Triassic is thinner near the flanks of the salt wall indicates that a salt pillow formed at the locations of the salt wall during the Late Triassic. The top of the Upper Triassic shows signs of significant erosion, especially in the ESE part of Section 2 (Figure 37).

In Section 3 (Figure 38), signs of severe erosion at the top of the Upper Triassic interval can be seen as well. In the SSW area of in Section 3 (Figure 38) and near the flanks of Diapir A the thickness of the Upper Triassic is thin and growth strata are not observed. Only minor rotation and uplift of the Upper Triassic interval, near the flanks of Diapir A can be seen. Therefore, Diapir A was not subjected to active salt migration during the Late Triassic, assuming that the observed thickness of the Upper Triassic interval represents the depositional thickness. In the NNE part of Section 3 (Figure 38), growth wedges within the Upper Triassic interval can be seen. The successive reflectors of the growth strata, all seem to wedge out at the same stratigraphic interval. The Upper Triassic structures in the NNE of Section 3 (Figure 38) resemble the expulsion rollover structures demonstrated by Ge et al. (1997) with analogue models in a passive margin settings. Prograding deltaic settings are known to develop significant topographic relief and to exert sufficient loading to cause expulsion rollover structures. However, large prograding deltas did not develop in the Dutch North Sea during the Late Triassic. Additionally, the scale of the structures in the study area are much smaller than the structures studied by Ge et al. (1997), but a similar mechanism of salt loading and expulsion might explain the encountered growth wedge structures. It is possible that sediments coming from the SSW loaded the Zechstein salt and caused salt migration to the NNE which resulted into the expulsion of salt in front of the sedimentary wedge. It is likely that the emplacement of Salt Body C took place via this mechanism during the Late Triassic.

Thickness differences in Section 4 (Figure 39) of the Upper Triassic can be seen near the locations of faults. On top of the area where the basement displays its highest position, to the SSW of Well L05-07, the Upper Triassic is thinnest. At this location listric faults have been interpreted that seem to rotate several fault blocks. These listric faults sole onto intra-Upper Triassic layers, probably evaporitic layers of the Main Röt Evaporite Member, the Upper Röt Evaporite Member, the Muschelkalk Evaporite Member, the Main Keuper Evaporite Member or the Red Keuper Evaporite Member. Additionally, at this location the Lower Triassic and the Zechstein strata are partly missing. The cause for the removal of the strata is not known, therefore a more detailed study is needed to unravel the evolution of this specific zone. In the middle part of Section 4 (Figure 39), a paleo-deep can be seen. This is the only location within the study area where two basement faults have propagated into the Mesozoic domain. The Upper Triassic displays an over-thickened zone in the hanging wall of these faults. This variation in stratigraphic thickness against the fault provide evidence for syn-kinematic sedimentation, indicating that these two faults were active during the Late Triassic.

In Section 5 (Figure 40) the Upper Triassic interval displays significant thickness differences. Between wells L05-02 and L02-04, an over-thickened zone of Upper Triassic can be seen. In map view this zone has the external form of a bowl that thins towards the SSW. These growth strata indicate that the accommodation space that was created during deposition was caused by salt migration away from the thickened zone. Allochthonous Salt Body D has penetrated Upper Triassic layers. Salt migration from below the Upper Triassic growth strata in this section and additional sedimentary loading by the sediments of the growth strata (Hudec & Jackson (2007) might have

caused the emplacement of Salt Body D into the Upper Triassic layers. The Zechstein salt probably penetrated preexisting Upper Triassic evaporite layers (Lott, 2010).

Section 6 (Figure 41) displays allochthonous Salt Body E located within Upper Triassic layers. However, within this section the Upper Triassic interval does not show significant growth strata. Additionally, the Upper Triassic flanks on top of Salt Body E do not show thickness differences. This is a sign that the flanks were uplifted after deposition, therefore, the emplacement of Salt Body E took place after Late Triassic period.

The **Lower and Middle Jurassic Altena Group** was deposited during the Early and Middle Jurassic under the influence of continued regional subsidence (Ziegler, 1990; Underhill & Partington, 1993). In Section 1,2 and 4-6 (Figure 36, 37 and 39-41) it can be seen that the top of the Altena Group is truncated by an unconformity at the base of the Upper Jurassic and that a significant succession of this interval must have been eroded. This means that the original depositional thickness of this interval must have been significantly larger than the preserved sedimentary thickness.

Growth strata in the form of rim-synclines can be seen in Section 1 (Figure 36) near the flanks of the salt wall, indicating that during deposition accommodation space was created within the area by salt migrating into the salt wall. The zones where the growth strata can be found have shifted towards the salt wall in comparison to the Upper Triassic interval. This means that the area where accommodation space was created by salt migration was a localized process that migrated progressively closer to the salt wall. The reflectors of the Altena Group are terminated in a similar mode as described in Figure 42B (subtle thickness differences and signs of onlap onto the prior and shallower position of the salt body). This indicates that the salt wall had a surface expression during deposition of the Altena Group.

In Section 2 (Figure 37) the reflectors of the Altena Group are chaotic, but it can be seen that a rim-syncline formed near the flank of the salt wall in the Altena Group. The zones where the growth strata are present have shifted towards the salt wall in comparison to the Upper Triassic interval. This means that the area where accommodation space was created by salt migration, has been localized and took place closer towards the salt wall.

Only a thin sliver of the Altena Group is present in Section 4 (Figure 39).This interval disappears to the NNE as well as to the SSW. At the location of the depocenter in the middle of the profile the reflectors of the Altena Group are draped onto the shoulders surrounding the structural low. This indicates that the structural low deepened slightly during the deposition of the Altena Group and that the sedimentation rate could keep up with the subsidence rate. The accommodation space that was created for the sedimentation of the Altena Group in Section 4 (Figure 39) may result from salt migration at the Zechstein level.

The Altena Group in Section 5 (Figure 40) displays significant thickness differences. The strong reflectors in the top part of the Altena Group above Salt Body D probably represent the Posidonia Shale Formation; the youngest interval of the Altena Group in the study area. Above Salt Body D, the Altena Group is over-thickened compared to other locations in the profile. This zone has a bowl-shaped geometry and is interpreted as growth strata, because the reflector are wider spaced above Salt Body D and wedge out on either sides above the salt body. During the Early and Middle Jurassic continued regional subsidence that started in the Lower Jurassic prevailed (Wong, 2007). The additional accommodation space related to the growth strata in this profile can either originate from salt migration at the autochthonous Zechstein level or from salt remobilization of Salt Body D. The later scenario is favored. The fact that the Posidonia Shale Formation has been eroded in most parts of the study area indicates that significant regional uplift occurred after the deposition of the Altena Group (Ziegler, 1990; Underhill & Partington, 1993). The fact that the Posidonia Shale Formation is still present at the location above Salt Body D, indicates that additional local accommodation space must have been created to preserve these upper layers of the Altena Group. It is likely that Salt Body D was emplaced during the Late Triassic and that salt remobilization from

this position counteracted the uplift at this location during the phase of regional uplift. Sub-basins that were created above collapsing salt structures have been described by Stefanescu et al. (2000). To the SSW in Section 5, the Altena Group disappears.

In Section 6 (Figure 41), the thickness of the Altena Group is rather constant except for the NNE margin of the profile where the interval thickness increases slightly. Whether this increase can be classified as a growth wedge or that the increase is only apparent because of varying amounts of erosion along the profile is unknown. It is thought that salt migration that caused Salt Body E to rise was driven by the sedimentary loading of the Altena Group.

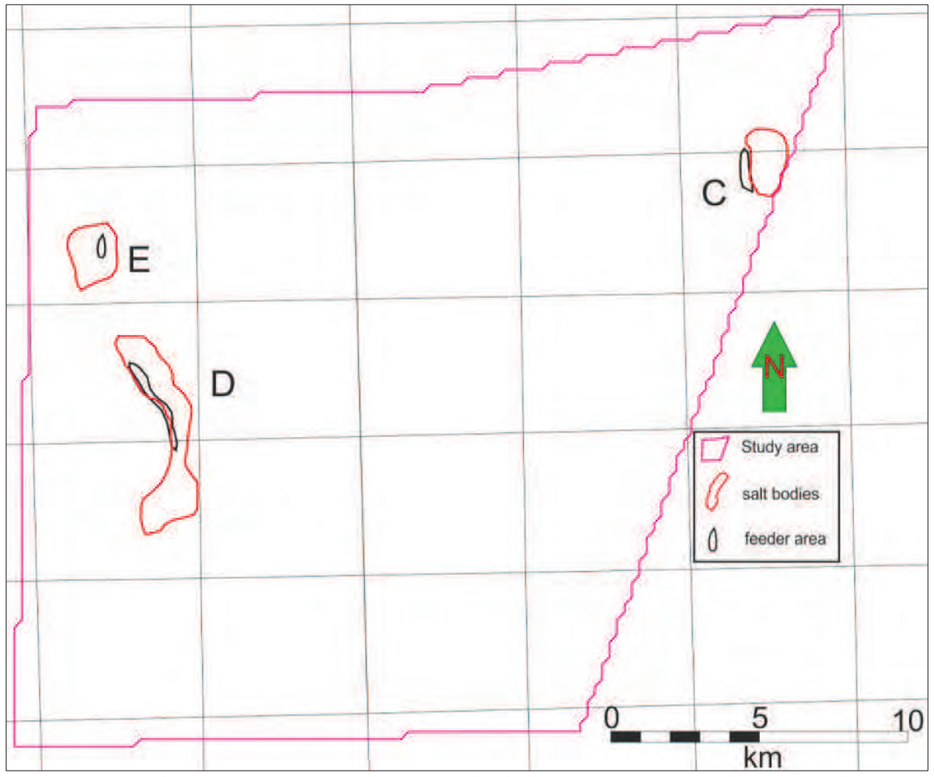

Figure 46. *Outlines of the intra-Upper Triassic salt bodies and their feeder areas that have been observed within the study area. Black lines represent the extent of the base of the feeder area; the red polygons indicate the extend of the salt bodies itself. The largest and pink bounding polygon indicates the study area in the L5/L6 block. For the location of the study area please see Figure 2 or 30.*

Figure 46 shows the intra-Upper Triassic salt bodies (Salt Bodies C-E) in the study area (Section 3, 5 and 6; Figure 38, 40 and 41). These salt bodies were initially formed by the processes that generally initiate diapirism (e.g. sedimentary loading and faulting in the pre-salt strata), but have not evolved into piercing structures. Remobilization of the salt swells, resulted locally in the creation of accommodation space on top of these structures. As a result, the formation of small sag areas in the Upper Triassic strata above the allochthonous salt levels and in the Upper Jurassic strata took place.

The two Upper Jurassic sequences

In the western domain, S1 of the Upper Jurassic interval shows some thickness variations (Figure 34), especially south of well L05-02. Here S1 thickens towards the WSW. This area is also shown in Section 1 (Figure 36) and Section 6 (Figure 41) on the left sides of both figures. This over-thickened zone has formed above an area where the base Zechstein is faulted downward between two parallel and long NW-SE trending faults (Figure 28). The over-thickened zone in S1 has the geometry of a growth wedge that thickens towards the WSW and thins towards the ENE. The growth strata at this location indicates that during the deposition, accommodation space was created within the area, most likely caused by salt migration away from the growth wedge and faulting at the at the Zechstein level. Although the top of S1 is truncated, the geometry of the wedge can still be identified. The additional depositional loading caused by the growth wedge resulted in salt migration in a NE-SW direction, contributing to the formation of Salt Body E (Figure 41 and 46). Between Well L05-01 and the salt wall in Section 1 (Figure 36) the thickness of S1 decreases. Truncated top reflectors indicate erosion at this level. The exact amount of eroded strata of S1 in the western domain is difficult to determine, however it is estimated that the original thickness of S1 is between 100 and 150 ms. Unfortunately, it is not possible to draw conclusions on the thickness distribution of S1 in the eroded areas. Near the flanks of the salt wall, no growth strata within S2 are visible and the thickness of the interval is uniformly thin.

Between the salt wall and the location of Well L05-01 in Section 1 (Figure 36) S2 also has a uniform thickness and does not exhibit growth structures. A minor thickening of S2 can be observed above the growth wedge of S1 at the location of well L05-02 in Section 1 (Figure 36). It is possible that the salt migration below this position, as was described for S1, still continued during the deposition of S2. The reflectors of S1 and S2 have a similar relation to the salt weld of the salt wall as described in Figure 42B (subtle thickness differences and signs of onlap onto the old position of the salt body). This suggests that the salt wall had a surface expression during the Upper Jurassic.

ESE of the salt wall, S1 and S2 show the same thickness trends as observed within Section 1 (Figure 36). Both units thicken gradually towards the ESE and exhibit over-thickened zones near the flank of Diapir A. The over-thickened zones resemble rim-synclines. These thickened zones are also observed in the time-thickness maps of S1 and S2 (Figure 34 and 35) to the west and east of Diapir A. The growth synclines at these locations indicate that during the deposition, additional accommodation space was created within the area. Salt migration away from the position of the growth strata into the Diapir A is a probable cause for the creation of the accommodation space. The reflectors of S1 and S2 have a similar relation to Diapir A as described in Figure 42B (subtle thickness differences and signs of onlap onto the old position of the salt body). This suggests that Diapir A had a surface expression during the Upper Jurassic.

Section 2 (Figure 37) shows a thickened package of S1, WNW of the salt wall. Along extensional normal faults thickness changes have developed that resemble a growth wedge. The growth strata at this location indicate that during deposition, accommodation space was created within the area. During the deposition of S2, salt migration away from the wedge is a probable cause for the creation of accommodation space. This salt flow was directed towards the SW and resulted in the formation of the salt wall and the formation of a smaller salt swell at the toe of the salt wall, which is visible in Section 2 (Figure 37). In the WNW part of Section 2 (Figure 37), S1 can be seen onlapping onto the Altena Group. This indicates that the area of salt withdrawal widened gradually during the deposition of S1. S2 does not show growth strata in Section 2 (Figure 37) and has an overall thin appearance westwards of the salt wall. The absence of growth strata of S2 and the overall limited thickness of this sequence westwards of the salt wall indicates that only minor accommodation space was created in the area. This indicates that salt migration slowed down within the western domain during the deposition of S2.

In Section 2 (Figure 37) to the ESE of the salt wall both S1 and S2 exhibit a uniform and evenly layered distribution. No significant growth strata or thickness differences are observed. This indicates that the accommodation space that was filled by S1 and S2 in Section 2 (Figure 37) does not result from local salt migration, but from regional subsidence. Furthermore, S2 on the eastern flank of the salt wall in Section 2 (Figure 37) is uplifted and rotated significantly by the rise of salt Diapir A. Additionally, the thickness of S2 does not change at this location. Therefore, it can be concluded that S2 was already deposited before it was uplifted and deformed by the rising salt wall.

In Section 2 (Figure 37) ESE of the salt wall both S1 and S2 are crosscut by a fault. No signs of syn-kinematic sedimentation within the Upper Jurassic strata can be seen.

In Section 3 (Figure 38) S1 and S2 exhibit rim-synclines near the flank of Diapir A. This diapir is fed by salt migration away from the growth strata. Due to the poor quality of the seismic image below the salt it is not possible to determine how the individual layers terminate against the salt body.

In the NNE part of Section 3 (Figure 38), S1 and S2 thicken towards the NNE. These over-thickened zones have formed above the area where expulsion rollover structures were described for the Upper Triassic interval. The over thickened zones of S1 and S2 are wedge-shaped and thicken towards the NNE. A probably source for these thickened zones is the formation of a rim-syncline during the rise of Diapir B, located 2 km to the N of Section 3 (Figure 38). The growth strata at this location indicate that during the deposition, accommodation space was created within the area. Salt migration away from the growth strata is a probable cause for the creation of the accommodation space. It is likely that the salt migrated into the direction of Diapir B.

In Section 4 (Figure 39), a series of listric faults can be identified in the southern part of the profile. These faults sole on Upper Triassic layers, as previously discussed. In the hanging walls of these faults growth strata have formed within S2 and in the Lower Cretaceous strata. Indicating that these faults were active during the deposition of these packages. These structures are possibly related to salt evacuation from underneath this position during this late stage of the rifting (Latest Jurassic-Earliest Cretaceous). This area forms a unique zone in the study area, because the Zechstein Group and the Lower Triassic strata are removed completely at several locations. The cause for the removal of the strata is not known, therefore a more detailed study is needed to unravel this area.

The sediments of S2 display a bowl-shaped over-thickened zone within the central part of Section 4 (Figure 39). The base of S1 onlaps onto the basement shoulders surrounding the structural low and the successive reflectors onlap onto subsequently higher points of the margin of the structural low (Figure 14B). The growth strata at this locations indicate that during the deposition, accommodation space was created within the area. Salt migration away from the bowl-shaped unit is a probable cause for the creation of the accommodation space. The salt flow was most likely directed towards Diapir A, because the time-thickness map of S1 (Figure 34) shows that these growth strata are directly adjacent to the diapir and also thicken towards the diapir. One explanation for the series of onlapping reflectors within the depocenter can be that salt withdrawal became less localized as S2 progressed. Another possibility is that a tectonic event changed the relative sea-level, resulting in the deposition of a series of onlapping strata. A southward progradation of S1 is another possibility. In order to determine which interpretation is most accurate, this zone needs to be studied in greater detail. The following figure explains the last two scenarios.

Figure 47. *Left: A prograding sequence. Right: Tectonic origin of onlapping strata.*

In Section 4, S2 is also thickened at within the structural low. The base of S2 does not onlap onto the shoulders of the structural low, but the entire sequence is thinned gradually towards the shoulders of the structural low, as shown in Figure 14A. Salt migration is the most probable cause for the created accommodation space. The salt most likely flowed towards Diapir A, which is confirmed

by the time-thickness map of S2 (Figure 35) that shows that these growth strata are directly adjacent to the diapir and also thicken towards the diapir.

In Section 5 (Figure 40) S1 thickens gradually towards the north and is terminated towards the south. The thickness of S2 in Section 5 (Figure 40) is generally very thin. However one thickened area can be distinguished at the location where well L05-02 is projected. At this position the entire Upper Jurassic interval forms a low. Above Salt Body D, both Upper Jurassic sequences are truncated and eroded. Due to the varying amounts of erosion of both Upper Jurassic sequences in Section 5 (Figure 40), it is not possible to interpret the visible thickness trends as syn-kinematic indicators. The fact that S1 thickens towards the north indicates that more accommodation space was created in the northern part of this profile during the deposition of S1, or that the northern part was less affected by erosion after the deposition of S1.

In Section 6 (Figure 41) towards the SSW flank of Salt Body E, the Upper Jurassic strata are thinning and are bend upward. Note, that this is not displayed very clearly because a large part of the Upper Jurassic strata have been truncated and eroded. From the top of Salt Body E to the NNE, the Upper Jurassic strata are eroded completely at the area indicated as an Upper Jurassic Window in the maps. No clear signs of onlap onto the Altena Group are present, so a possible explanation for this area is that the Upper Jurassic strata have been subjected to aerial exposure and erosion during the rise of Salt Body E.

Both S1 and S2 exhibit an overall thickening trend towards the north, whilst both intervals disappear towards the south. These trends represent the additional accommodation space that was created towards the north during the Upper Jurassic by means of salt migration. Furthermore, the salt wall is more pronounced in the northern part of the study area compared to the southern part. This indicates that the salt flow that resulted in the creation of additional accommodation space in the northern part of the study area, was directed towards the salt wall.

In the southern part of the study area, S1 onlaps onto older strata and is terminated (e.g. Section 4, Figure 39). This indicates that during the deposition of S1, the Terschelling Basin did not deepen and salt migration did not take place southward of the termination boundary of S1. Westwards of the salt wall, S2 shows only very little thickness variation combined with an overall thin appearance (Figure 35). This indicates that no localized salt flow took place during the deposition of S2 that contributed to the formation of the salt wall, and that the entire area westward of the salt wall subsided evenly during the latest sequence of the Upper Jurassic.
The time-thickness map of the entire Upper Jurassic interval (Figure 33) shows that, to the SW and NE of Diapir B, a very thick package of Upper Jurassic strata was deposited in a wedge or rim-synclinal geometry. Section 3 and 4 indicate that mainly S1 has been thickened during the creation of the accommodation space at this location. This creation of the accommodation space was caused by salt migration, therefore, it is very likely that the salt was evacuated in a NE-SW orientation and has been forced into Diapir B.

There are only a few faults that offset the two Upper Jurassic sequences in the western domain. Only at one location, westward of the salt wall in Section 2 (Figure 36), it can be seen that S1 is influenced by faulting. These extensional faults run oblique to the section and contribute to the thickening and faulting downward of S1 at this location. It is assumed that the additional sedimentary loading at this location has contributed to increased salt flow from this location and the accompanying formation of the salt wall. There are no other locations in the western domain where faults have propagated through the Upper Jurassic strata and have influenced the thickness or the distribution of these intervals.

The time-thickness maps of S1 (Figure 34) and S2 (Figure 35) show that both intervals are influenced by several faults in the northern part of the eastern domain. Section 3 and 4 (Figure 38 and 40) show their distribution in the most northern part of the study area. Several extensional faults that are oriented perpendicular to Section 3 and 4 (Figure 38 and 40), fault down through

Upper Jurassic strata and sole onto Upper Triassic layers. The sections reveal that the thickness changes of the individual sequences near these faults are limited and that the largest variations are probably caused by salt re-mobilization from Salt Body C in the direction of Diapir B or to a more eastern location.

Rapid thickness changes of S1 and S2 can be seen in the time-thickness maps of S1 and S2 (Figure 33-35) in the northern part of the study area to the east of the salt wall. Several areas, where thicker packages of S1 have formed, show thinned zones for S2 and vice versa. This can be seen, for instance, directly to the east of the N-S trending fault that connects two parallel trending faults (Figure 33, 34 and 35). Here S1 exhibits a thinned zone of approximately 1 km in width. Two kilometers further to the east of this fault, S1 forms a thickened ridge-shaped zone parallel to the fault N-S trending fault. For S2 these zones show opposite thicknesses. Also near other faults, thin packages of S2 are present on top of a thicker package of S1 and vice versa. These faults are oriented perpendicular to the direction of extension during the Late Jurassic and therefore may not be related to regional extension, but to salt withdrawal underneath the Upper Jurassic strata.

The phenomena that nearly every salt body present in the regional transects formed above normal faults located in the basement level, is also encountered in seismic sections of the detailed analysis in the L5/L6 area. For example, in Section 1 and 2 (Figure 36 and 37), normal faults can be seen underneath the salt wall and Diapir A. This means that all seismic data collected for this study show that the initial diapirism in the study area has been triggered by movements of normal faults at the base Zechstein level.

The shapes of the salt wall and Diapir A are greatly influenced by the inversion during the Alpine compression of the Dutch North Sea area. Salt is typically the weakest link in any rock system, and tends to accumulate most of the total strain, so that preexisting salt bodies usually deform first and display more deformation than the surrounding strata (Hudec & Jackson, 2007). The teardrop-shape of salt bodies, together with squeezed or pinched off feeder areas, are typical signs of diapir amplification due to regional compression (Hudec & Jackson, 2007). In Section 1 (Figure 36), the salt wall and Diapir A show squeezed feeder areas and remaining salt welds that can be traced upwards to the main salt bodies. The deformational strain was localized near salt structures and rejuvenated the upward salt flow. The present day height of the salt bodies is therefore influenced by this tectonic event.

During the course of this research project the decision was made to focus on the tectono-stratigraphy and the evolution of the salt migration within the study area rather than focusing on determining the properties and the exact distribution of the specific reservoir intervals within the Upper Jurassic. The distribution and the growth strata within S1 and S2 have been studied and can mostly be explained by Zechstein salt migration. It speaks for itself that the areas where Upper Jurassic growth strata have formed, discussed earlier in this chapter, represent the areas where the reservoir properties of these clastic, syn-sedimentary deposits are best. Three separate intervals with reservoir sands are recognized within the study area: The Main Friese Front Member is stratigraphically located at the base of S1. The Terschelling Sandstone Member is stratigraphically located near the top of S1. The Scruff Spiculite Member is stratigraphically located near the base of S2. The zones with reservoir sands are also indicated in Figure 45.

Conclusions

A tectono-stratigraphical and structural analysis of siliciclastic growth strata related to salt migration has been conducted for the areas of the Dutch Central Graben, the Terschelling Basin and the Step Graben. The following conclusions can be drawn from this research:

- Rifting resulted in the development of extensional faults. The initial triggering of the salt flow in the Dutch North Sea is closely related to fault activity in the pre-Zechstein basement interval. Differential sedimentary loading of the Zechstein salt, loaded the salt layer sufficiently to drive upward salt migration.
- The majority of the basement faults do not propagate through the Zechstein Group and are not linked to faults that occur above the Zechstein Group.
- Throughout the Dutch Central Graben, Step Graben and Terschelling Basin, the Zechstein Group has been affected by salt remobilization. At several locations the autochthonous salt welded out, which affected the ability of salt bodies to grow and rise further.
- All salt bodies within the study area that have evolved into piercing diapirs have most likely pierced a brittle overburden. It is likely that these piercing salt bodies experienced areal erosion or sub-areal exposure and that most diapirs had a surface expression at a certain time, indicated by onlapping reflectors against the diapirs and subtle thickness differences.
- The shape of the salt bodies within the study area is greatly influenced by the inversion during the Alpine compression of the Dutch North Sea area. The compression rejuvenated upward salt flow and squeezed the feeder areas.
- Salt migration did not only take place during the climax of the Kimmerian rifting. The first packages of growth strata that can be associated with salt migration, date back to the Late Triassic period.
- Salt migration from both sides of the salt wall towards the salt wall commenced during the Late Triassic. Salt migration towards the salt wall, took place closer to the salt wall on both sides, during the deposition of the Altena Group (Lower and Middle Jurassic). During the deposition of Sequence 1 (S1), piercing of the salt wall and associated salt migration continued. During the deposition of Sequence 2 (S2), salt migration slowed down and passive diapirism took over.
- The northern part of the study area accommodated more Upper Jurassic sediments than the southern part of the study area. Additionally, more salt flowed into the salt wall from the northern part of the study area than in the southern part.
- Growth strata that can be related to the rise of Diapir A can be seen in the Upper Triassic interval. During the deposition of Sequence 1 (S1) and 2 (S2), salt flow in the direction of Diapir A took place. This resulted in the formation of rim-synclines within these sequences around Diapir A.
- Salt migration into Salt body C took place during the Late Triassic. Salt expulsion due to differential sedimentary loading is a likely mechanism that caused the salt rise. Remobilization of Salt Body C started directly after the initial emplacement of the Zechstein salt. Remobilized salt from Salt Body C may have flown towards Diapir B.
- Growth strata that can be related to the rise of Diapir B can be seen in the Upper Triassic interval. During the deposition of Sequence 1 (S1) and 2 (S2), salt flow in the direction of Diapir B took place. This resulted in the formation of rim-synclines within these sequences to the NE and SW of the Diapir B.
- Salt flow into salt Body D took place during the Late Triassic. It is likely that penetration of Zechstein salt into an Upper Triassic evaporate layer took place. Remobilization of Salt Body D took place during the deposition of the Altena Group, creating additional accommodation space for this interval.
- Salt flow into Salt Body E started during the deposition of the Altena Group and continued during the deposition of Sequence 1 (S1). Salt flow into Salt Body E ceased during the deposition of Sequence 2 (S2) during the Late Jurassic.

Acknowledgements

I would like to use this opportunity to express my gratitude to everyone who supported me through the course of this master thesis project. I would like to thank The Dutch Organization for Applied Scientific Research (Nederlandse Organisatie voor toegepast-natuurwetenschappelijk onderzoek - TNO) for providing the internship opportunity and the financial support. Also I would like to acknowledge all the stakeholders of the 'Focus' project for providing this interesting challenge. I am thankful for the guidance, constructive criticism and friendly advice from my supervisors Renaud Bouroullec (TNO - Utrecht) and Jan de Jager (VU). I want to thank Kees Geel, Mart Zijp and Geert de Bruin for their advice and help on numerous subjects. I also would like to express gratitude towards the entire Petroleum Geoscience team for taking me onboard and creating an excellent working environment. Finally I would like to thank my family and friends for their support during the project.

References

Abbink, O.A., Mijnlieff, H.F., Munsterman, D.K. & Verreussel, R.C.M.H., 2006. New stratigraphic insights in the 'Late Jurassic' of the Southern Central North Sea Graben and Terschelling Basin (Dutch Offshore) and related exploration potential. Netherlands Journal of Geosciences 85: 221-238.

Baykulov, M., Brinka, H.-J., Gajewskia, D. & Yoon, M.-K., 2009. Revisiting the structural setting of the Glueckstadt Graben salt stock family, North German Basin. Tectonophysics 470: 162-172.

Beekman, F., 2011, 3D seismics and regional geology course, Shell Rijswijk and VU University, 2011.

Baldschuhn, R., Best, G., & Kockel, F., 1991. Inversion tectonics in the north-west German basin. Generation, accumulation and production of Europes hydrocarbons, Special Publication of the European Association of Petroleum Geoscientists, Oxford University Press 149-159.

Bouroullec, R., Weimer, P., & Serrano, O., in press. Petroleum Geology of the Mississippi Canyon, Atwater Valley, Western Desoto Canyon, and Western Lloyd areas, Northern Deep-Water Gulf of Mexico: Part 1, Traps, Reservoirs, and Tectono-Stratigraphic Evolution: AAPG Bulletin.

Buchanan, J.G. & Buchanan, P.G., 1995. Basin inversion. Basin inversion: In: Buchanan, J.G. & Buchanan, P.G. (Eds.), Geological Society Special Publication. 88, vii-ix.

CGG Gas & Oil Map, 26-01-2015. The Netherlands and adjacent areas. CGG Data Management©

Clausen, O.R., Nielsen, S.B., Egholm, D.L. & Goledowski, B., 2012. Cenozoic structures in the eastern North Sea Basin - a case for salt tectonics. Tectonophysics 514-517, 156-167.

Coward, M.P., Dewey, J., Hempton, M. & Holroyd, J., 2003. Tectonic evolution. In: Evans, D.J., Graham, C., Armour, A. & Bathurst, P. (Eds): The Millenium Atlas: Petroleum Geology of the Central and Northern North Sea. The Geological Society (London): 17-33.

Davison, I., Alsop, G.I., Evans, N.G. & Safaricz, M., 2000. Overburden deformation patterns and mechanisms of salt diapir penetration in the Central Graben, North Sea. Marine and Petroleum Geology 17: 601-618.

De Jager, J., 2003. Inverted basins in the Netherlands, similarities and differences. Netherlands Journal of Geosciences 82-4: 355-366.

De Jager, J., 2007. Geological development. In: Wong, T.E., Batjes, D.A.J. & de Jager, J. (eds): Geology of the Netherlands. Royal Netherlands Academy of Arts and Sciences (KNAW) (Amsterdam): 5-26.

De Jager, J., 2012. The discovery of the Fat Sand Play (Solling Formation, Triassic), Northern Dutch offshore-a case of serendipity. Netherlands Journal of Geosciences 91-04: 609-619.

De Jager, J. & Geluk, M.C., 2007. Petroleum geology. In: Wong, Th.E., Batjes, D.A.J. & de Jager, J. (eds): Geology of the Netherlands. Royal Netherlands Academy of Arts and Sciences (KNAW) (Amsterdam): 241-264.

Doornenbal, J.C. & Stevenson, A.G. (Eds.), 2010. Petroleum Geological Atlas of the Southern Permian Basin Area. EAGE Publications B.V., Houten.

Duin, E.J.T., Doornenbal, J.C., Rijkers, R.H.B., Verbeek, J.W. & Wong, T.E., 2006. Subsurface structure of the Netherlands; results of recent onshore and offshore mapping. Netherlands Journal of Geosciences 85: 245-276.

Ferrer, O., Jackson, M.P.A., Roca. E. & Rubinat, M., 2012. Evolution of salt structures during extension and inversion of the Offshore Parentis Basin (Eastern Bay of Biscay). Geological Society London Special Publications 363:361-379.

Ge, H., Jackson, M.P.A & Vendeville B.C., 1997, Kinematics and dynamics of salt tectonics driven by progradation: AAPG Bulletin 81: 398-423.

Geluk, M.C., 2007a. Permian. In: Wong, T.E., Batjes, D.A.J. & de Jager, J. (Eds): Geology of the Netherlands. Royal Netherlands Academy of Arts and Sciences (KNAW) (Amsterdam): 63-84.

Geluk, M.C., Dusar, M. & De Vos, W., 2007. Pre-Silesian. In: Wong, T.E., Batjes, D.A.J. & de Jager, J. (eds): Geology of the Netherlands. Royal Netherlands Academy of Arts and Sciences (KNAW) (Amsterdam): 27-42.

Glennie, K.W., 1998. Lower Permian - Rotliegend. In: Glennie, K.W. (ed.): Petroleum Geology of the North Sea, Fourth Edition. Blackwell Science (Oxford): 137-174.

Glennie, K. W., 2005. Regional tectonics in relation to Perm-Carboniferous hydrocarbon potential, Southern North Sea Basin. In*:* J. D. Collinson, D. J. Evans, D. W. Holliday & N. S. Jones. (eds): Carboniferous hydrocarbon geology - The southern North Sea and surrounding onshore areas. Yorkshire Geological Society. 1-12.

Harding, R. & Huuse, M., 2015. Salt on the move: Multi stage evolution of salt diapirs in the Netherlands North Sea, Marine and Petroleum Geology 61: 39-55.

Hudec, M.R., 2004. Salt intrusion: time for a comeback? In: Post, P.J., Olson, D.L., Lyons, K.T., Palmes, S.L., Harrison, P.F. & Rosen, N.C. (Eds.), Salt-Sediment Interactions and Hydrocarbon Prospectivity. 24th Annual Research Conference. GCSSEPM Foundation, Houston, Texas, pp. 11132.

Hudec, M.R. & Jackson, M.P.A., 2007. Terra infirma: understanding salt tectonics. Earth Science Reviews 82, 1-28.

Hudec, M.R., Jackson, M.P.A. & Schultz-Ela, D.D., 2009. The paradox of minibasin subsidence into salt: Clues to the evolution of crustal basins. Geological Society of America Bulletin 121(1-2): 201 221.

Jackson, C.A.- L., Chua, S. T., Bell, R. E. & Magee, C., 2013. Structural style and early stage growth of inversion structures: 3D seismic insights from the Egersund Basin, offshore Norway. Journal of Structural Geology 46: 167-185.

Jackson, M.P.A., Vendeville, B.C. & Schultz-Ela, D.D., 1994. Structural dynamics of salt systems. Annual Review of Earth and Planetary Sciences 22, 93-117.

Jenyon, M.K., 1984. Seismic response to collapse structures in the Southern North Sea. Marine and Petroleum Geology 1: 27-36.

Jenyon, M.K., 1985. Basin-edge diapirism and updip salt flow in Zechstein of Southern North Sea. American Association of Petroleum Geologists Bulletin 69: 53-64.

Jenyon, M.K., 1988. Overburden deformation related to the pre-piercement development of salt structures in the North Sea. Journal of the Geological Society of London 145: 445-454.

Kombrink, H., Doornenbal, J.C., Duin, E.J.T., Den Dulk, M., Van Gessel, S.F., Ten Veen, J.H. & Koyi, H., Jenyon, M.K. & Petersen, K., 1993. The effect of basement faulting on diapirism. Journal of Petroleum Geology 16-3: 285-312.

Koyi, H. & Petersen, K., 1993. Influence of basement faults on the development of salt structures in the Danish Basin. Marine and Petroleum Geology 10: 82-94.

Lott, G.K., Wong, T.E., Dusar, M., Andsbjerg, J., Mönnig, E., Feldman-Olszewska, A. & Verreussel, R.M.C.H., 2010. Jurassic. In: Doornenbal, J.C. & Stevenson, A.G. (eds): Petroleum Geological Atlas of the Southern Permian Basin Area. EAGE Publications b.v. (Houten): 175-193.

Macgregor, D., S., 1995. Hydrocarbon habitat and classification of inverted rift basins. Geological Society, London, Special Publications 88: 83-93.

McCann, T. (ed.), 2008a. The Geology of Central Europe. Volume 1: Precambrian and Paleozoic. The Geological Society (London), 748 pp.

McCann, T. (ed.), 2008b. The Geology of Central Europe. Volume 2: Mesozoic and Cenozoic. The Geological Society (London), 700 pp.

Mohr, M., Kukla, P. A., Urai, J. L., & Bresser, G., 2005. Multiphase salt tectonic evolution in NW Germany: seismic interpretation and retro-deformation. International Journal of Earth Sciences 94(5-6) 917-940.

Munsterman, D.K., Verreussel, R.M.C.H., Mijnlieff, H.F., Witmans, N., Kerstholt-Boegehold, S. & Abbink, O.A., 2012. Revision and update of the Callovian- Ryazanian Stratigraphic Nomenclature in the northern Dutch offshore, i.e. Central Graben Subgroup and Scruff Group. Netherlands Journal of Geosciences 91-4: 555-590.

Narkiewicz, M., Bitzer, F. & Scheck, M., 2000. On the origin of the Southern Permian Basin, Central Europe. Marine and Petroleum Geology 17: 43-59.

Nelskamp, S., Verweij, J.M. & Witmans, N., 2012. The role of salt tectonics and overburden in the generation of overpressure in the Dutch North Sea area. Netherlands Journal of Geosciences 91-4: 517-534.

Nielsen, L., Thybo, H. & Glendrup, M., 2005a. Seismic tomographic interpretation of Paleozoic sedimentary sequences in the southeastern North Sea. Geophysics 70 (4): R45-R56.

Paul, J., 2006. Der Kupferschiefer: Lithologie, Stratigraphie, Fazies and Metallogenese eines Schwarzschiefers. Zeitschrift der Deutschen Gesellschaft für Geowissenschaften 157: 57-76.

Pharaoh, T.C., Dusar, M., Geluk, M.C., Kockel, F., Krawczyk, C.M., Krzywiec, P., Scheck-Wenderoth, M., Thybo, H., Vejbæk, O.V. & Van Wees, J.D., 2010. Tectonic evolution. In: Doornenbal, J.C. & Stevenson, A.G. (editors): Petroleum Geological Atlas of the Southern Permian Basin Area. EAGE Publications b.v. (Houten): 25-57.

Rank-Friend, M. & Elders, C.F., 2004. The evolution and growth of Central Graben salt structures, Salt Dome Province, Danish North Sea. In: Davies, R.J., Cartwright, J.A., Stewart, S.A., Lappin, M. & Underhill, J.R. (Eds.), 3D Seismic Technology: Application to the Exploration of Sedimentary Basins, Geological Society, London, Memoirs 29: 149-163.

Remmelts, G., 1995. Fault-related salt tectonics in the southern North Sea, the Netherlands. In: Jackson, M.P.A., Roberts, D.G. & Snelson, S. (Eds.), Salt Tectonics: a Global Perspective, AAPG Memoir 65: 261-272.

Remmelts, G., 1996. Salt tectonics in the southern North Sea, the Netherlands. In: Rondeel, H.E., Batjes, D.A.J. & Nieuwenhuijs, W.H. (Eds.), Geology of Gas and Oil Under the Netherlands. Kluwer Academic Publishers, Dordrecht: 143-158.

Richter-Bernburg, G., 1955. Statigraphische Gliederung des deutschen Zechsteins. Zeitschrift deutschen geologischen Gesellschaft 105: 593-645.

Rosendaal, E.A., Kaymakci N., Wijker, D., Schroot, B.M., 2014. Structural development of the Dutch Central Graben: new ideas from recent 3D seismic.

Rowan, M. G., & Weimer, P.,1998. Salt-sediment interaction, northern Green Canyon and Ewing Bank (offshore Louisiana), northern Gulf of Mexico: AAPG Bulletin 82: 1055-1082.

Rowan, M.G., Lawton, T.F., Giles, K.A. & Ratliff, R.A., 2003. Near-salt deformation in La Popa basin, Mexico, and the northern Gulf of Mexico: a general model for passive diapirism. American Association of Petroleum Geologists Bulletin 87, 733-756.

Scotese, C. R., 2003. PALEOMAP/Earth History; http://www.scotese.com/earth.htm; 2 February 2003.

Soper, N.J., England, R.W., Snyder, D.B. & Ryan, P.D., 1992. The Iapetus suture zone in England, Scotland and eastern Ireland: a reconciliation of geological and deep seismic data. Journal of the Geological Society 149: 697-700.

Stampfli, G.M. & Borel, G.D., 2002. A plate tectonic model for the Paleozoic and Mesozoic constrained by dynamic plate boundaries and restored synthetic oceanic isochrons. Earth and Planetary Science Letters 196 (1-2): 17-33.

Stefanescu M., Dicea O. & Tari G., 2000. Influence of extension and compression on salt diapirism in its type area, East Carpathians Bend area, Romania. In: Salt, shale and igneous diapirs in and around Europe., Vendeville, B.C., Mart, Y., Vigneresse J.L. (eds). Geological Society Special Publications. 174:131-147.

Stegers, D.P.M., 2006. Sedimentary facies analysis of sequence 2 of the Upper Jurassic in the Terschelling Basin and the southern Dutch Central Graben. TNO report 2006-U-R0191/A. TNO - Built Environment and Geosciences, Business unit Geo energy and Geo information, Utrecht.

Stewart, S.A., 2006. Implications of passive salt diapir kinematics for reservoir segmentation by radial and concentric faults. Marine and Petroleum Geology 23, 843-853.

Ten Veen, J.H., Van Gessel, S.F., & Den Dulk M., 2012. Thin- and thick-skinned salt tectonics in the Netherlands; a quantitative approach. Netherlands Journal of Geosciences 91-4: 447-464.

Total E&P UK, 2007. A regional review of the Dinantian carbonate play: Southern North Sea & onshore UK. Total E&P UK, 1-64.

Turner, J.P., & Williams, G.A., 2004. Sedimentary basin inversion and intra-plate shortening. Earth-Science Reviews 65-3: 277-304.

Underhill, J.R. & Partington, M.A., 1993. Jurassic thermal doming and deflation in the North Sea: implications of the sequence stratigraphic evidence. In: Parker, J.R. (ed.) Petroleum Geology of Northwest Europe. Proceedings of the 4th Conference. Geological Society (London): 337-345.

Van Buggenum, J.M. & Den Hartog Jager, D.G., 2007. Silesian. In: Wong, Th.E., Batjes, D.A.J. & de Jager, J. (eds): Geology of the Netherlands. Royal Netherlands Academy of Arts and Sciences (KNAW) (Amsterdam): 43-62.

Van Winden, M., 2015. Master research project

Vendeville, B.C. & Jackson, M.P.A., 1993. Rates of extension and deposition determine whether growth faults or salt diapirms form. In: Proceedings of the Gulf Coast Section Society of Economic Paleontologists and Mineralogists Foundation 14th Annual Research Conference: 5-8.

Van Wees, J.D., Stephenson, R.A., Ziegler, P.A., Bayer, U., McCann, T., Dadlez, R., Gaupp, R., Verweij, J.M., Souto Carneiro Echternach, M. & Witmans, N., 2009. Terschelling Basin and southern Dutch Central Graben Burial history, temperature, source rock maturity and hydrocarbon generation - Area 2A. TNO report TNO-034-UT-2009-02065. TNO - Built Environment and Geosciences, Business unit Geo energy and Geo information, Utrecht

Verweij, J.M. & Witmans, N., 2009. Terschelling Basin and southern Dutch Central Graben Mapping and modeling - Area 2A. TNO report TNO-034-UT-2009-01569. TNO - Built Environment and Geosciences, Business unit Geo energy and Geo information, Utrecht.

Witmans, N., 2012. New insights into the geological structure of the Netherlands; results of a detailed mapping project. Netherlands Journal of Geosciences 91-4: 419-446.

Wilson, M., Neumann, E.-R., Davies, G.R., Timmerman, M.J., Heeremans, M. & Larsen, B.T., 2004. Permo-Carboniferous Magmatism and Rifting in Europe. In: Wilson, M., Neumann, E.-R., Davies, G.R., Timmerman, M.J., Heeremans, M. & Larsen, B.T. (Eds): Permo-Carboniferous magmatism and rifting in Europe. Geological Society Special Publication (London) 223: 1-10.

Wong, T.E., 2007. Jurassic. In: Wong, T.E., Batjes, D.A.J. & de Jager, J. (eds): Geology of the Netherlands. Royal Netherlands Academy of Arts and Sciences (KNAW) (Amsterdam): 107-125.

Wong, T.E., Batjes, D.A.J. & de Jager, J. (eds) 2007a. Geology of the Netherlands. Royal Netherlands Academy of Arts and Sciences (KNAW) (Amsterdam):354.

Zanella, E. & Coward, M.P., 2003. Structural framework. In: Evans, D., Graham, C., Armour, A. & Bathurst, P. (eds): The Millennium Atlas: Petroleum Geology of the Central and Northern North Sea. The Geological Society (London): 45-59.

Ziegler, P.A., 1988. Evolution of the Arctic-North Atlantic and the western Tethys. American Association of Petroleum Geologists, Memoir 43, 198 pp, 30 plates.

Ziegler, P.A., 1990a. Geological Atlas of Western and Central Europe (2nd edition). Shell Internationale Petroleum Maatschappij B.V.; Geological Society Publishing House (Bath), 239 pp.

Ziegler, P.A., Schumacher, M.E., Dèzes, P., van Wees, J.D. & Cloetingh, S.A.P.L., 2004. Post-Variscan evolution of the lithosphere in the Rhine Graben area; constraints from subsidence modelling. In: Wilson, M., Neumann, E.R., Davies, G.R., Timmerman, M.J., Heeremans, M. & Larsen, B.T. (Eds): Permo-Carboniferous magmatism and rifting in Europe. Geological Society Special Publication (London) 223: 289-317.

<**http://www.nlog.nl**> The Dutch Oil and Gas portal. September 2014. Dutch Ministry of Economic Affairs. Managed by TNO-DINO, Geological Survey of the Netherlands.
<http://www.nlog.nl/nl/seismic/seismic.html>
<http://www.nlog.nl/nl/pubs/maps/geologic_maps/NCP2_Subregions.html>
<http://www.nlog.nl/nl/pubs/maps/geologic_maps/DGM_deep_offshore.html>

Software:
Adobe, Illustrator; Photoshop
Corel, CorelDRAW
Schlumberger, Petrel E&P Software 2013
Microsoft, Word; Excel; PowerPoint
Weatherford, PreView Viewer

Appendices

A digital version of this report as well as all figures and appendices presented can be found here: https://www.dropbox.com/sh/om2l8sjlzmrkjr8/AABkqMLcDvqsBxp3jc6VKU4aa?dl=0

A.1 Wells in 'Focus' area

A11-01	A12-01	A12-02	A12-03
A14-01	A15-01	A17-01	A18-01
A18-02	A18-02-S1	B10-02	B10-03
B13-01	B13-02	B13-03	B13-04
B14-01	B14-02	B17-01	B17-02
B17-03	B17-04	B18-02	B18-03
E02-01	E02-02	E06-01	E09-01
E09-02	E12-01	E12-02	E12-03
E12-04	E18-01	F01-01	F02-01
F02-01-S1	F02-05	F02-06	F02-07
F03-01	F03-03	F03-04	F03-05
F03-05-S1	F03-06	F03-07	F03-08
F03-FB-101	F03-FB-102	F03-FB-103-S1	F03-FB-103-S2
F03-FB-104	F03-FB-104-S1	F03-FB-105-S3	F03-FB-105-S4
F04-01	F05-01	F05-02	F05-03
F06-01	F06-01-S1	F07-02	F08-01
F08-02	F09-01	F09-02	F10-01
F10-02	F11-01	F11-02	F11-03
F12-01	F12-02	F12-02-S1	F12-03
F12-03-S1	F13-01	F14-01	F14-02
F14-04	F14-05	F14-06	F14-06-S1
F14-07	F15-01	F15-02	F15-02-S1
F15-03	F15-05	F15-06	F15-07
F15-08	F15-A-01	F15-A-02	F15-A-03
F16-01	F17-01	F17-03	F17-04
F17-05	F17-06	F17-07	F18-01
F18-02	F18-03	F18-04	F18-05
F18-06	F18-07	F18-08	F18-08-S1
F18-09	F18-09-S1	F18-10	F18-10-S1
F18-10-S2	G10-01	G10-02	G10-03
G13-01	G13-02	G13-02-S1	G13-03
G16-01	G16-02	G16-03	G16-04
G16-06	G16-06-S1	G17-01	G17-02
G17-03	HOA-03	K06-01	L01-02
L01-03	L01-04-A	L01-05	L01-06
L02-01	L02-02	L02-03	L02-04
L02-05	L02-06	L02-07	L02-08
L03-01	L03-02	L03-03	L03-04
L04-01	L04-03	L04-05	L05-01
L05-02	L05-03	L05-04	L05-05
L05-06	L05-07	L05-C-03	L06-01
L06-02	L06-03	L06-04	L06-05
L06-07	L07-04	L08-02	L08-03

L08-07	L08-P-01	L09-01	L09-02
L09-04	L09-04-S1	L09-10	L12-01
L12-02	L12-03	L12-05	M01-01
M01-02	M03-01	M04-01	M04-02
M04-03	M05-01	M07-01	M07-02
M07-03	M08-01	M08-02	M09-01
M09-02	M10-01	M10-02	M10-03
M10-04	M11-01	NSN-01	

A.2 2D seismic surveys

ABT-91	N85	SNST-83	SNSTI-87
NSR08	stk16	Z2ARC1988C	Z2CGG1985A
Z2CON1987E	Z2GSI1986A	Z2NAM1981G	Z2NAM1990A
Z2WES1985C	Z2WES1988B		

A.3 3D seismic surveys

Z3CLY1998A	Z3FUG-2002A	Z3GDF2002A-3	Z3GDF2005A-1	Z3NAM1982A
Z3NAM1985A	Z3NAM1988A	Z3NAM1988D	Z3NAM1989B	Z3NAM1989C
Z3NAM1989E	Z3NAM-1990B	Z3NAM1990E	Z3NAM1990F	Z3NAM1990G
Z3NAM1991A	Z3NAM1991D	Z3NAM1991E	Z3NAM1992A	Z3NAM1993A
Z3NAM1993C	Z3NAM1994A	Z3NAM1994B	Z3NAM1995A	Z3NAM1996A
Z3NAM1997A	Z3NAM1998B	Z3NAM1998C	Z3NAM2006A-1	Z3NAM2008A-1
Z3OXY1994A	Z3OXY1996A	Z3PEN1985A	Z3PET1985A	Z3PET1987A
Z3PET1990A	Z3PET1991A	Z3PET1991B	Z3PET1991D	Z3PET1992A
Z3PET1992F	Z3PET1993A	Z3PET1994A	Z3PET1994B	Z3PGS_1999B
Z3PGS_2001A	Z3PLA1991B	Z3PLA1991D	Z3RWE1994A	Z3RWE1994E
Z3STA1985A	Z3UNC1987A	Z3WES1983A	Z3WES2003A	Z3WIN1992A
Z3WIN1995A	Z3WIN1997A	Z3WIN-2000A	Z3WIN2001B-1	Z3WIN2003A
Z3WIN2003B	Z3WIN2005B			

B.1 Line A

https://www.dropbox.com/s/fegmxrjs9bfzht7/Appendix%20B1%20Line%20A%20figure%2014.png?dl=0

B.2 Line B

https://www.dropbox.com/s/2w2sxisgh2xw3df/Appendix%20B2%20Line%20B%20figure%2017.png?dl=0

B.3 Line C

https://www.dropbox.com/s/cpotxrg31udtmd1/Appendix%20B3%20Line%20C%20figure%2021.png?dl=0

C.1 Theory of seismic waves and polarity

To obtain seismic reflection images, acoustic waves, traveling through the sub-surface are recorded and converted to images. So called compressional body waves (sometimes also called longitudinal, primary, or P-waves), which propagate as spherical fronts through the earth's surface, can also be seen as parcels of elastic strain energy. When a wave is transmitted into a medium with differing physical properties (acoustic impedance contrast) a portion of the wave's energy is reflected. The reflection coefficient at an interface can be derived when the amplitude and the polarity of the reflected wave is measured. In order to calculate the reflection coefficient of an interface the acoustic impedances of both layers must be known. The bulk density (ρ_{Bulk}) multiplied by the acoustic velocity (V_p) provides the acoustic impedances (Z) of a specific layer.

$$\boldsymbol{Z = \rho_{Bulk} * V_p} \qquad \text{eq.1} \qquad \text{Acoustic impedance}$$

The reflection coefficient (R) can be determined by the following equations. It describes the amplitude change of the reflected wave with respect to the incident wave. This transition must be calculated at the interface of two successive layers (Z1 and Z2) by using their acoustic impedances.

$$\boldsymbol{R = \frac{(Z_2 - Z_1)}{(Z_2 + Z_1)}} \qquad \text{eq.2} \qquad \text{Reflection coefficient}$$

An increasing acoustic impedance will result in a hard kick of the resulting amplitude. A decreasing acoustic impedance will result in a soft kick of the resulting amplitude. In this research the 0° European seismic convention is used where troughs are colored blue and represent hard kicks, peaks are colored red and represent soft kicks.

APPENDIX A6:
FIELD GUIDE
BOULONNAIS, FRANCE

Field Trip to the Upper Jurassic of the Boulonnais, France

24th - 28th June 2015

- Focus Project (TNO) -

Field Trip Leaders
Dr. Alain Trentesaux, Université de Lille 1 (alain.trentesaux@univ-lille1.fr)
Dr. Freek Busschers, TNO (freek.busschers@tno.nl)
Dr. Renaud Bouroullec, TNO (renaud.bouroullec@tno.nl)

Field Guide by Renaud Bouroullec and Isabel Millán (TNO)

ebn

ENGIE by people for people

ORANJE-NASSAU ENERGIE

STERLING RESOURCES

wintershall

TNO innovation for life

List of participants

First Name	Last Name	Company	Contact
Léna	Dauphin	ENGIE	Lena.Dauphin@gdfsuezep.nl
Danijela	Krizianic	ENGIE	Danijela.Krizanic@gdfsuezep.nl
Ruud	Lambert	Wintershall	ruud.lambert@wintershall.com
Raik	Bachmann	Wintershall	raik.bachmann@wintershall.com
Christoph	Börmann	Wintershall	christoph.boermann@wintershall.com
Rob	Lengkeek	ONE	lengkeek@onebv.com
Jeroen	Mullink	ONE	mullink@onebv.com
Peter	Matev	ONE	matev@onebv.com
Rutger	Gras	ONE	gras@onebv.com
Reinoud	Botman	ONE	botman@onebv.com
Eveline	Rosendaal	EBN	eveline.rosendaal@ebn.nl
Annelieke	Vis	EBN	annelieke.vis@ebn.nl
Renaud	Bouroullec	TNO	renaud.bouroullec@tno.nl
Roel	Verreussel	TNO	roel.verreussel@tno.nl
Freek	Busschers	TNO	freek.busschers@tno.nl
Alain	Trentesaux	University of Lille	alain.trentesaux@univ-lille1.fr
Thijs	Boxem	TNO	thijs.boxem@tno.nl
Dirk	Munsterman	TNO	Dirk.munsterman@tno.nl

Acknowledgements

We would like to thank the Focus Project team members, Thijs Boxem (Project Manager), Renaud Bouroullec (Research Lead), Geert de Bruin, Kees Geel, Nico Janssen, Isabel Millán, Dirk Munsterman, Roel Verreussel and Mart Zijp.

Our gratious thanks to Harmen Mijnlieff (TNO), Olivier Averbuch (Lilles Univ.) and Nicholas Tribovillard (Lilles Univ.) for their knowledge in the field and for contributing figures for this guide.

We would also like to thank the industrial sponsors of the Focus Project: EBN, Engie, Oranje-Nassau Energy, Sterling Resources and Wintershall.

Program and Safety

Program

Wednesday June 24rd

13:00	Meeting at TNO Utrecht. Travel by bus to Boulogne-sur-Mer
18:00	Arrival to Boulogne-sur-Mer and check-in at Hotel
18:30	Dinner in Boulogne-sur-Mer

Day 1. Thursday June 25th

9:00	Departure from Ibis parking lot
9:30	Cap de la Crèche outcrop
12:30	Lunch in the field
18:00	Back to Boulogne-sur-Mer
19:00	Dinner in Boulogne

Day 2. Friday June 26th

8:30	Departure from Ibis parking lot
9:00	Stop 1: Cran du Noirda
12:00	Lunch in Audresselles at L'Odyssee Restaurant.
13:00	Pointe de la Rochette outcrop
18:00	Back to Boulogne-sur-Mer
19:00	Dinner in Boulogne

Day 3. Saturday June 27th

8:30	Departure from Ibis parking lot
9:00	Stop1: Dunes de la Slack
11:00	Stop 2: Cap Gris Nez
13:00	Lunch in the field
18:00	Back to Boulogne-sur-Mer
19:00	Dinner in Boulogne

Sunday June 28th

8:00	Departure from Boulogne. ETA in Utrecht at 1 pm.

Emergency phone numbers

General emergency: 112
Medical helps/SAMU: 15
Police/Gendarmerie: 17
Fire Brigade: 18

Alain Trentesaux:	+33 601 80 26 33
Freek Busschers:	+31 650 65 68 88
Renaud Bouroullec:	+31 646 96 60 30
Thijs Boxem:	+31 646 96 60 68

Figure 1: Location map of the visited outcrops. Google map.

Content

Figure 2: Pointe de la Crèche outcrop located just north of Boulogne-sur-Mer. The sandy interval half way up the cliff is the Grès de Châtillon Unit and the upper sandy interval is the Grès de la Crèche Unit.

Regional Basin Overview

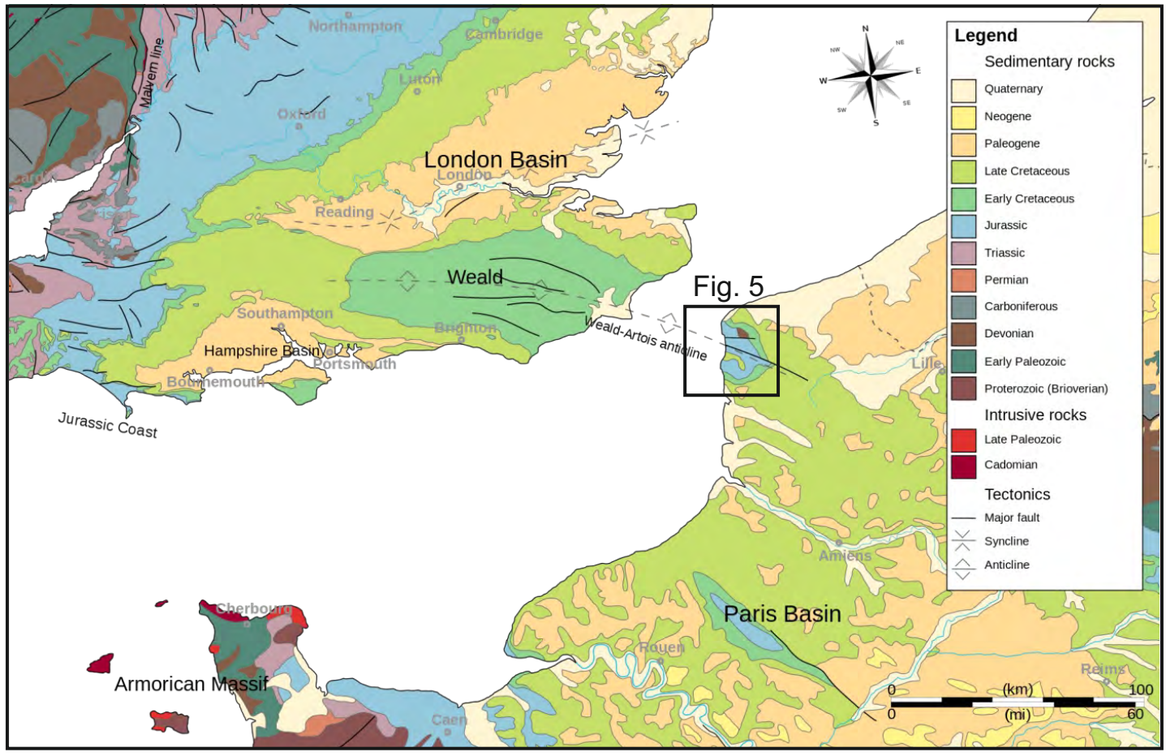

Figure 3: Simplified geological map of the Northern part of the Paris Basin and the London Basin.

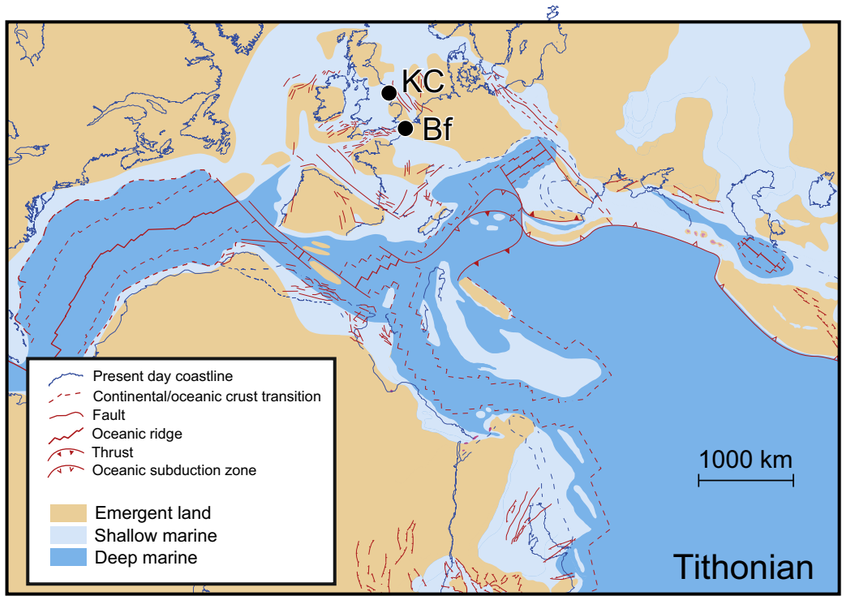

Figure 4: Paleogeographic reconstruction of the western Tethyan region during the Tithonian (Late Jurassic) showing the locations of the Kimmeridge Clay (KC; Yorkshire, United Kingdom), Boulonnais formations (Bf; northern France). Tribovillard et al. (2012b).

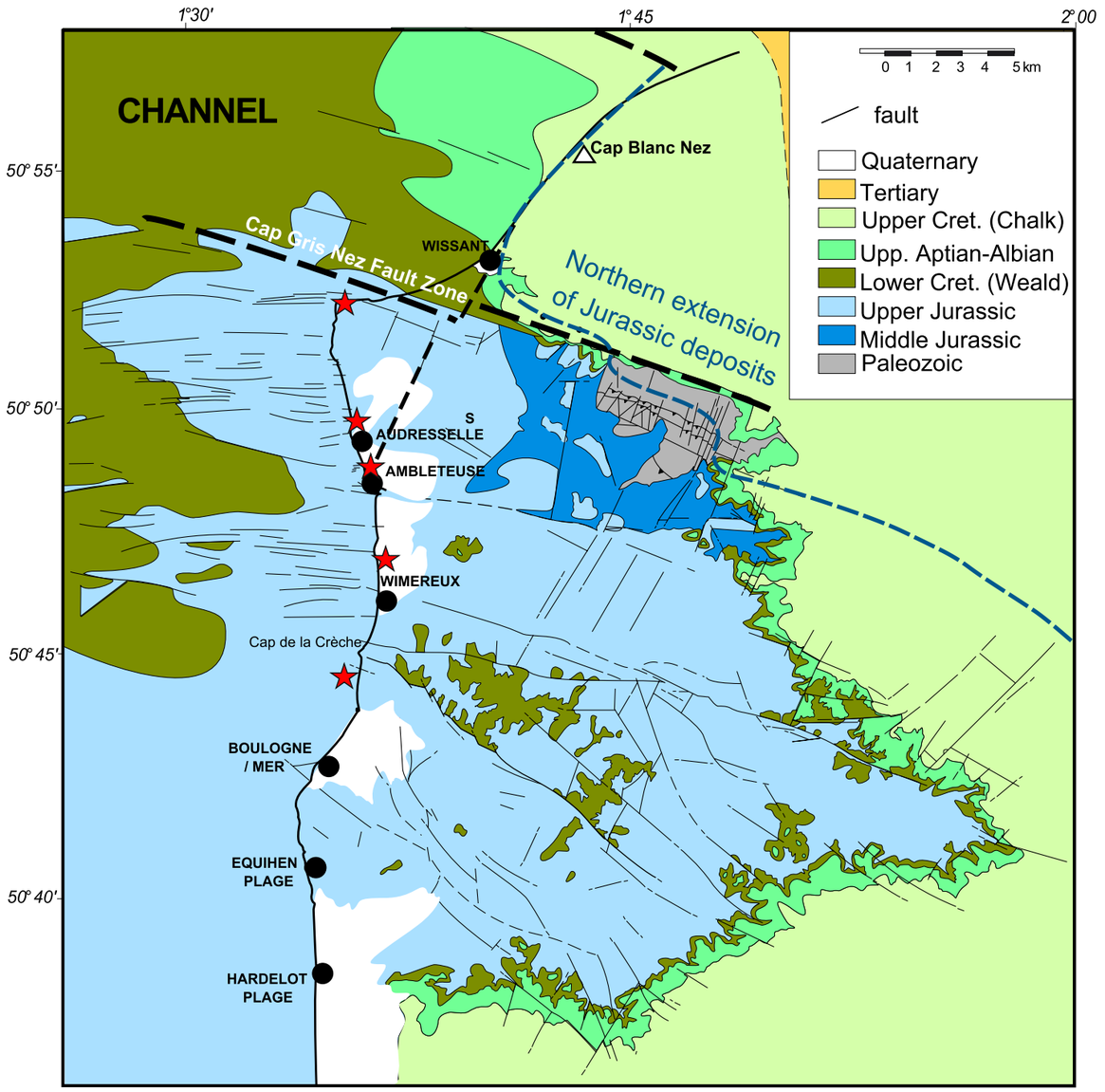

Figure 5: Mesozoic to Tertiary Geology of Northern France showing the Mezozoic Basin of the Boulonnais area. Modified after Mansy et al, (2003). Redrafted by O. Averbuch.

Tectonic Setting and Evolution

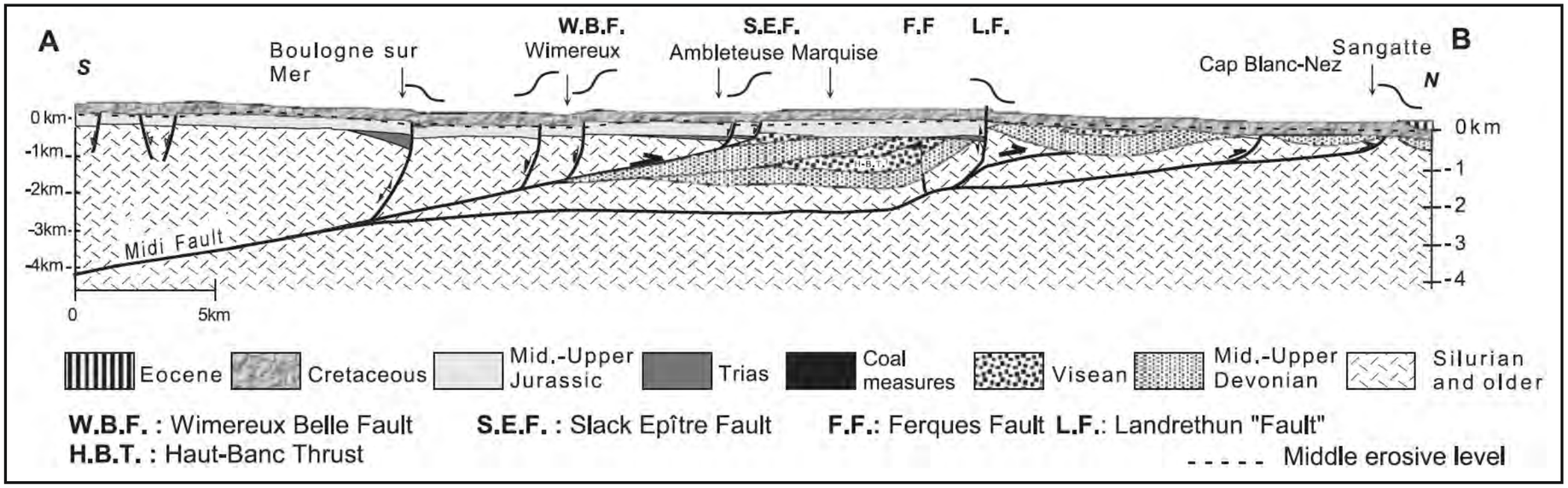

Figure 6: Geological cross section of the Boulonnais showing the relation of the inverted extensional faults to deeper Variscan thrust faults. Modified after Mansy et al. (2003).

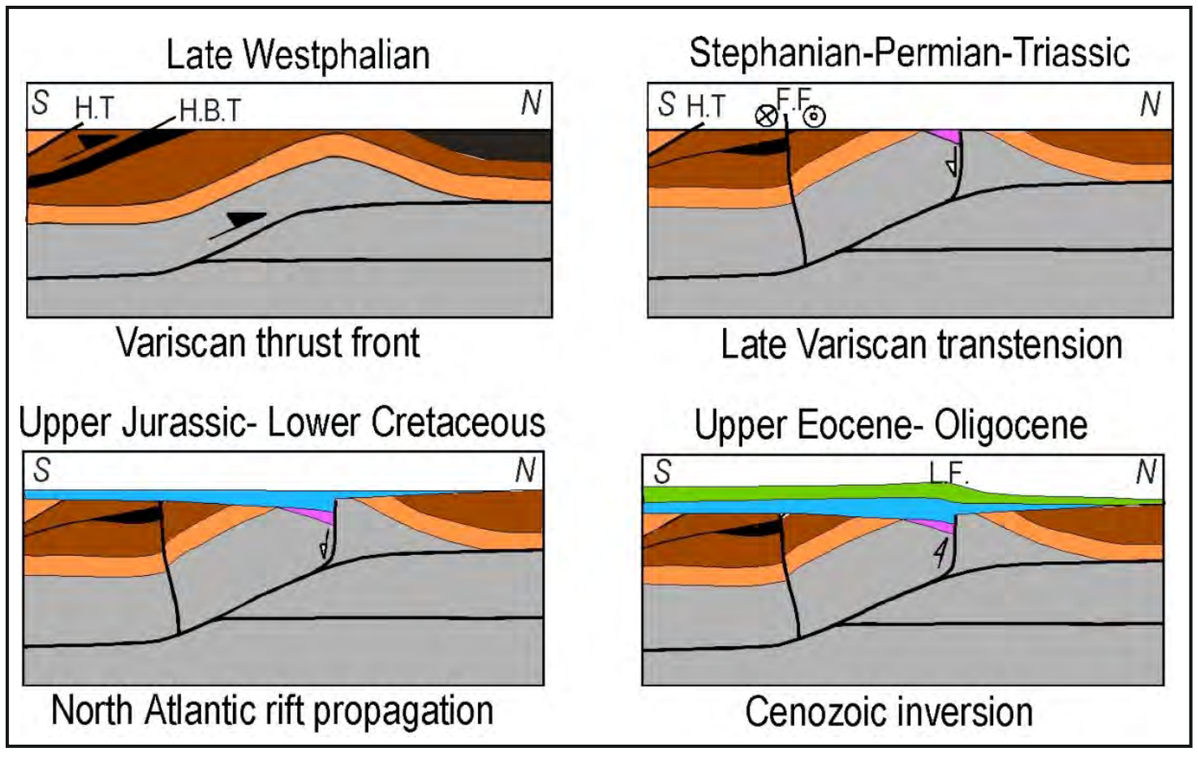

Figure 7: Reconstruction of extensional and inversion stages in the evolution of the Boulonnais part of the Weald-Boulonnais Basin. Modified after Mansy et al. (2003).

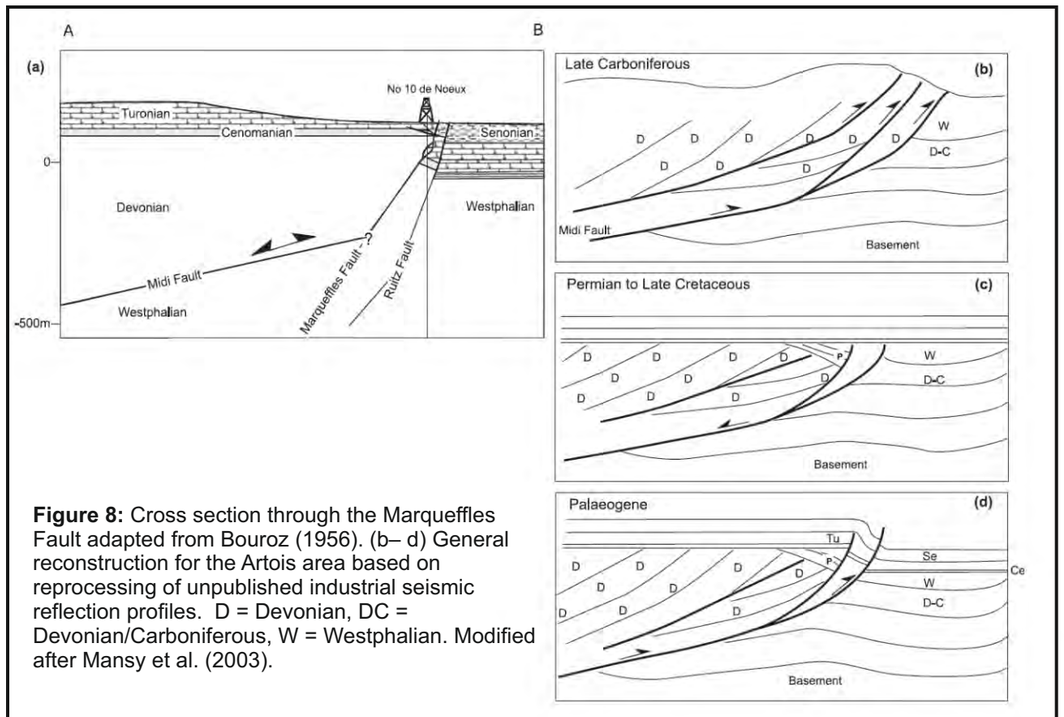

Figure 8: Cross section through the Marqueffles Fault adapted from Bouroz (1956). (b– d) General reconstruction for the Artois area based on reprocessing of unpublished industrial seismic reflection profiles. D = Devonian, DC = Devonian/Carboniferous, W = Westphalian. Modified after Mansy et al. (2003).

Stratigraphy

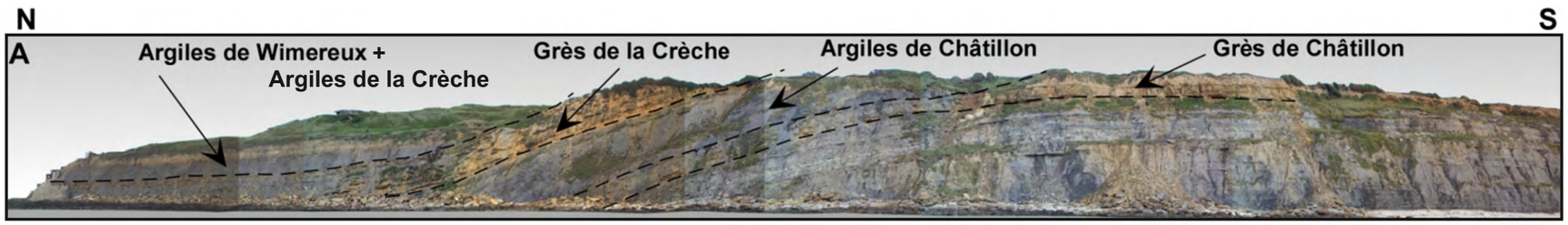

Figure 9: Interpreted outcrop photopanel of the Pointe de la Creche Anticline just north of Boulogne-sur-Mer (Braaksma, 2005).

Translation	
Grès	*Sandstone*
Argile	*Claystone*
Calciare	*Limestone*
Poudingue	*Conclomerate (old)*
Faille	*Fault*
Sable	*Sand*
Niveau	*Level*
Crèche	*Christ crib or nursery*
Boule	*Ball*
Bancs Jumeaux	*Twin beds*
Epaulards (Orque)	*Orca*
Courte-Dune	*Short-Dune*
Nez	*Nose*
Cap	*Cape*
Pointe	*Cape (or headland)*

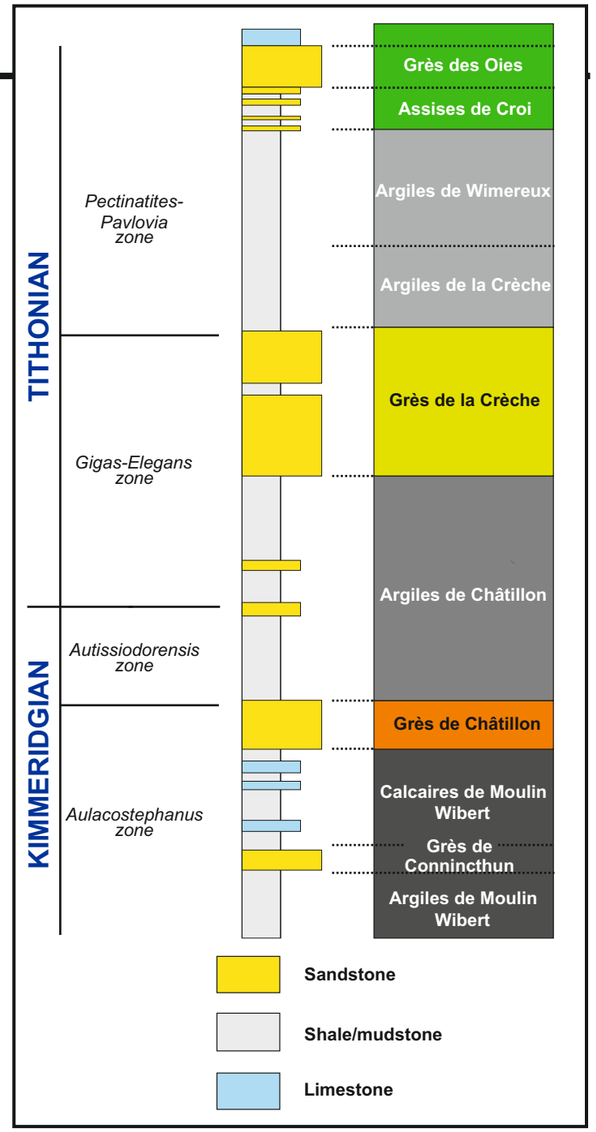

Figure 10: Lithostratigraphic, biostratigraphic and sequence stratigraphic framework of the Upper Jurassic rocks of the Boulonnais. Modified from Busschers (2015, unpublished).

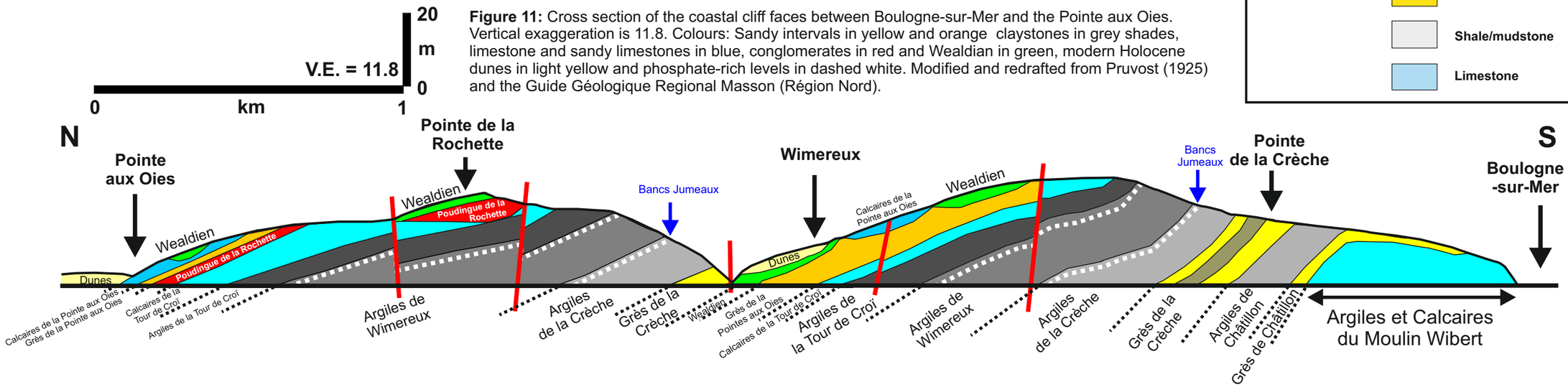

Figure 11: Cross section of the coastal cliff faces between Boulogne-sur-Mer and the Pointe aux Oies. Vertical exaggeration is 11.8. Colours: Sandy intervals in yellow and orange claystones in grey shades, limestone and sandy limestones in blue, conglomerates in red and Wealdian in green, modern Holocene dunes in light yellow and phosphate-rich levels in dashed white. Modified and redrafted from Pruvost (1925) and the Guide Géologique Regional Masson (Région Nord).

Subsurface Analogues in the Dutch Offshore (Regional Setting)

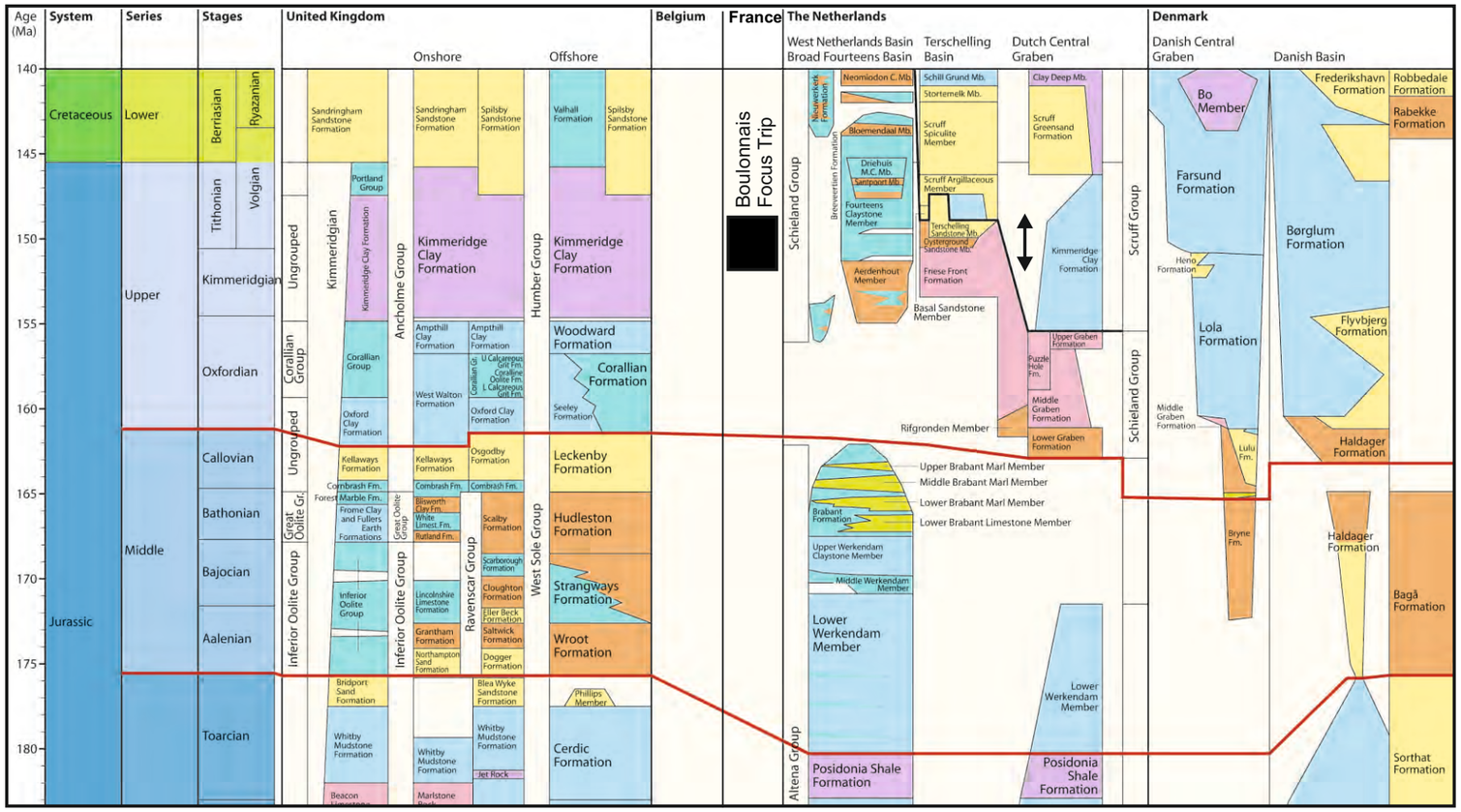

Figure 12: Tectonostratigraphic correlation chart of the Jurassic and Lower Cretaceous in the Southern Permian Basin. The Boulonnais outcrop section observed during this field trip has been added (Black box) for reference. Modified from Graham et al. (2010) - Southern Permian Basin Atlas.

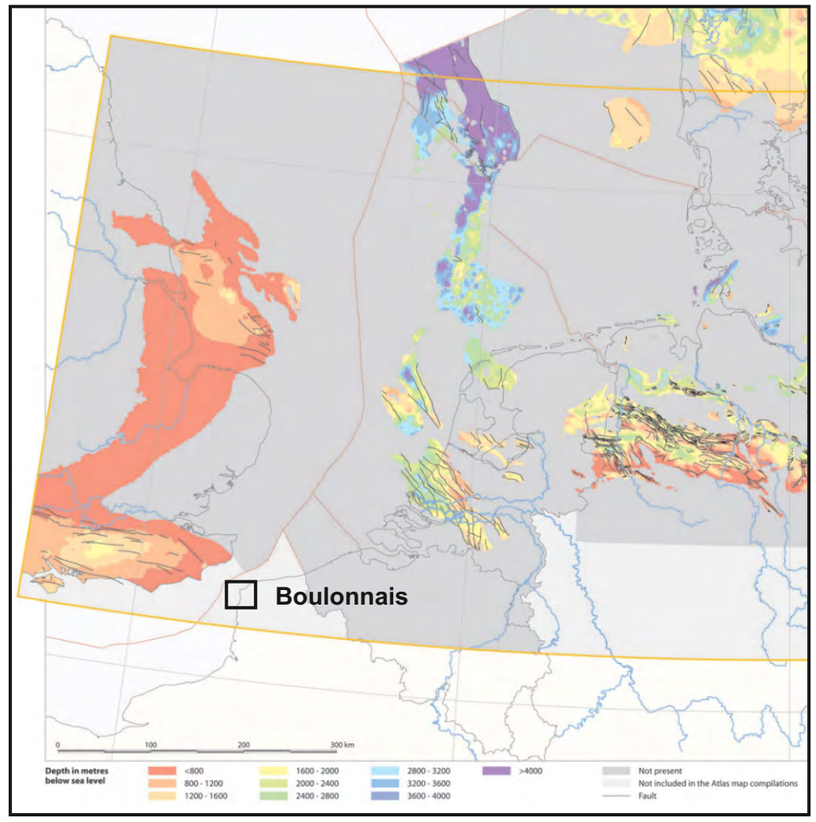

Figure 13: Base of Upper Jurassic map. From Graham et al. (2010) - Southern Permian Basin Atlas.

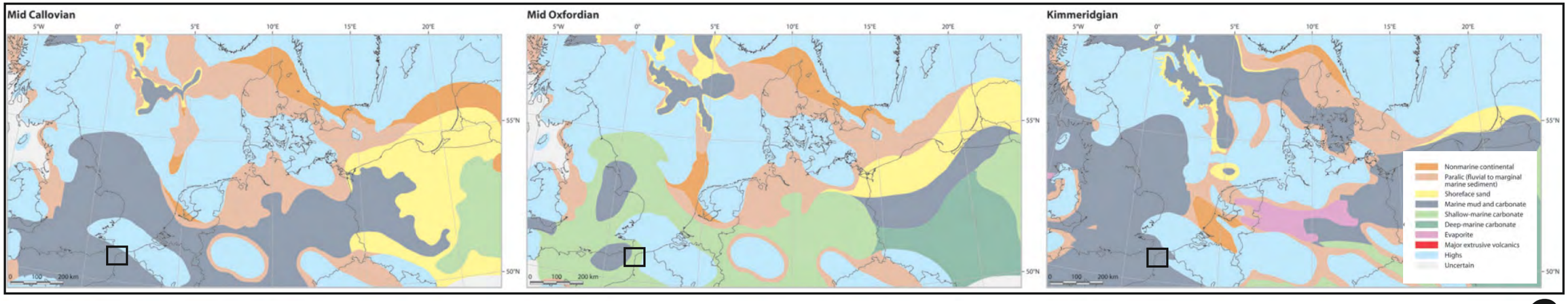

Figure 14: Palaeogeographic evolution in the Southern Permian Basin area during the Callovian, Mid Oxfordian and Kimmeridgian. Black boxes to highlight the Boulonnais area. Modified from Graham et al. (2010) - Southern Permian Basin Atlas.

Subsurface Analogues in the Dutch Offshore (Focus: Seismic)

Panel B
Terschelling Basin
- Focus Project -

Renaud Bouroullec (Lead Scientist),
Roel Verreussel, Kees Geel,
Dirk Munsterman, Geert de Bruin,
Mart Zijp, Nico Janssen,
Geert-Jan Vis, Dario Ventra
and Thijs Boxem (Project Manager)

v.3.0, 08-06-2015

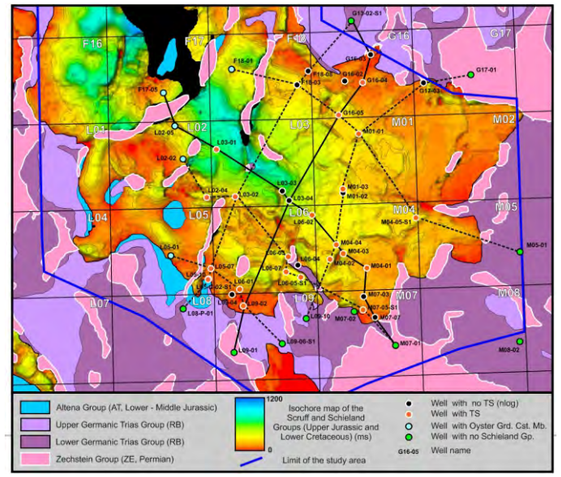

A

Figure 15: A few results from the Focus Project: A) Base Cretaceous subcrop map of the Terschelling Basin showing the location of the seismic transect in B and C. B) NNE-SSW oriented interpreted seismic section. C) same seismic section than shown in B but flattened on the top of Sequence 3. Unpublished, Bouroullec et al. (2015).

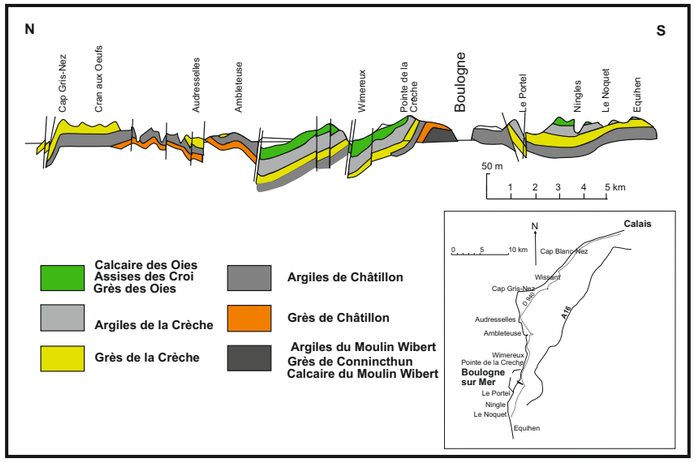

Figure 16: Cross section of the Boulonnais coastal outcrop belt between Equihen and Cap Gris Nez. This section is at the same scale (vertical and horizontal) as the Figures 15 B and C. Modified from Pruvost and Pringle, 1924; modified from Colbeaux, 1990; Modified by Busschers, 2015).

B

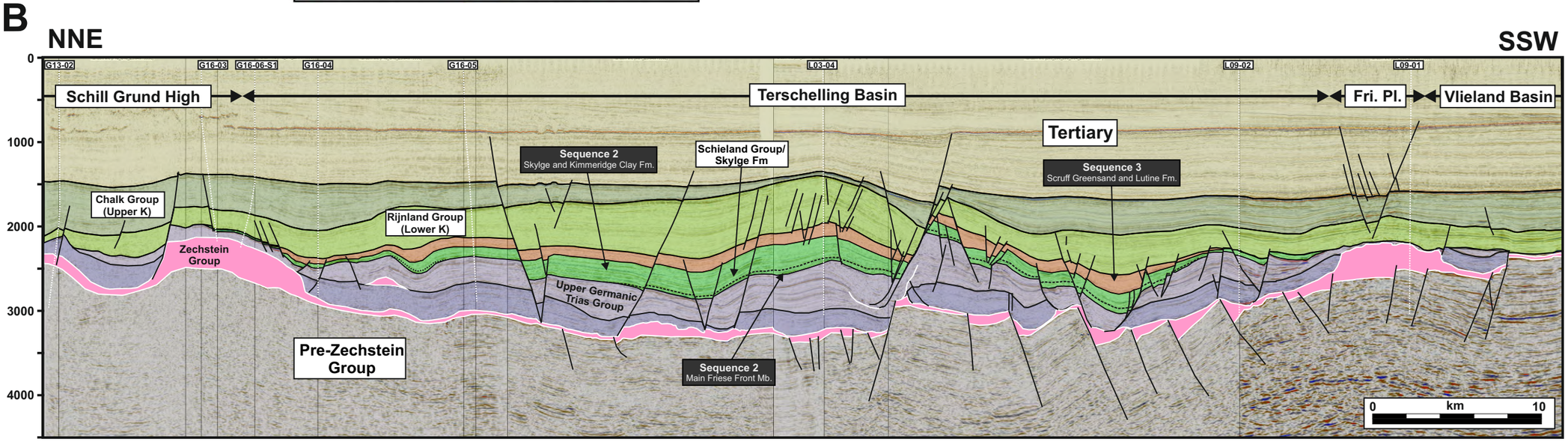

C

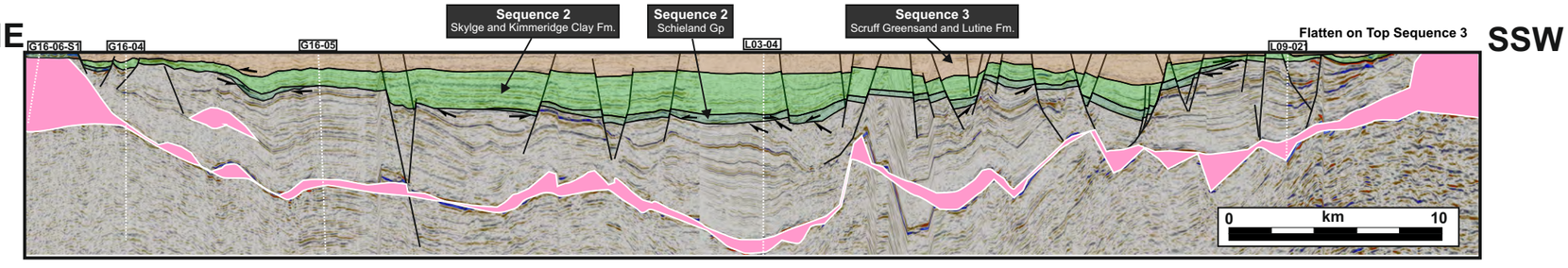

Subsurface Analogues in the Dutch Offshore (Focus: Well Correlation)

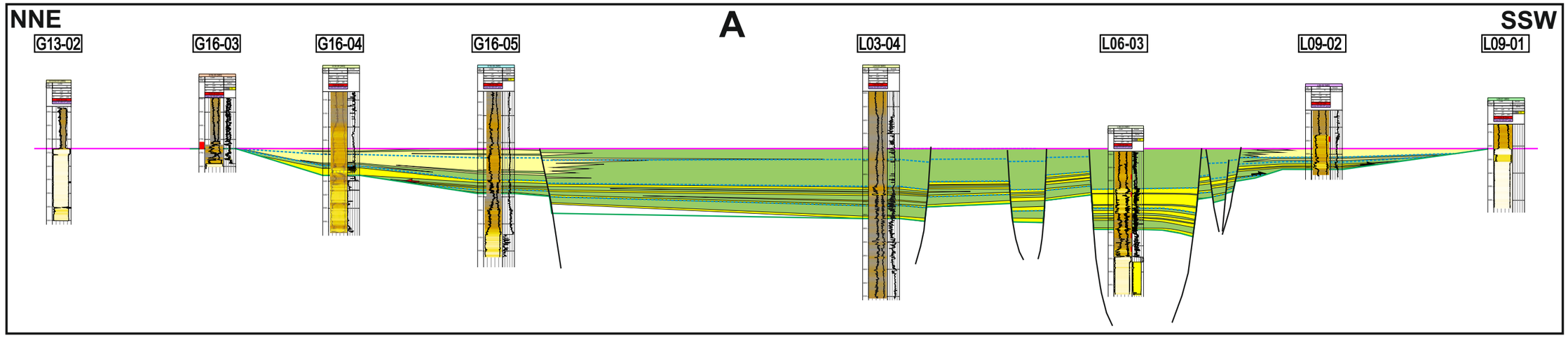

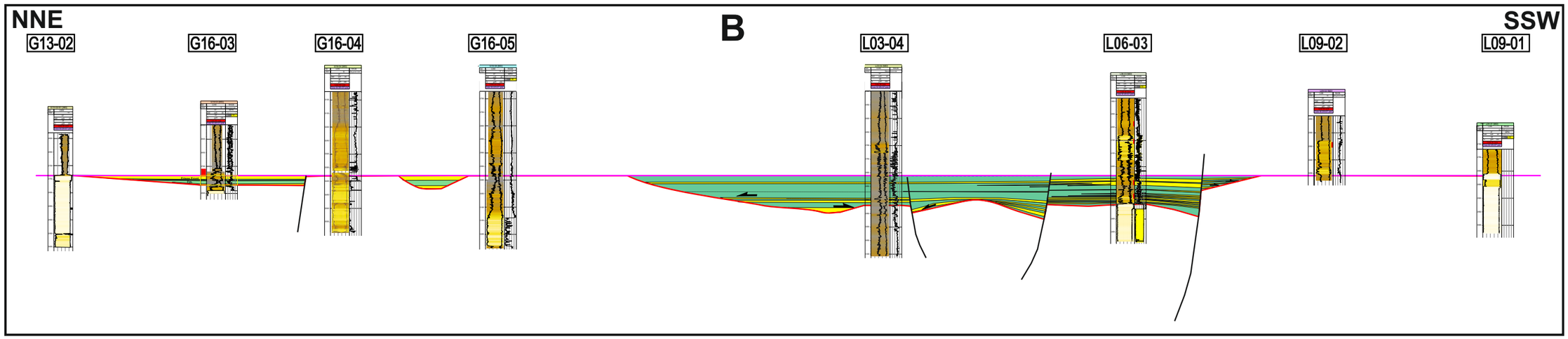

Panel B
Terschelling Basin
- Focus Project -

Renaud Bouroullec (Lead Scientist),
Roel Verreussel, Kees Geel,
Dirk Munsterman, Geert de Bruin,
Mart Zijp, Nico Janssen,
Geert-Jan Vis, Dario Ventra
and Thijs Boxem (Project Manager)

v.2.0, 02-04-2015

Figure 17: A few results from the Focus Project: A) Well correlation panel of the Upper part of Sequence 2 along the same transect shown in Figure 15. Flatten on an intra Lies Member marker. B) Well correlation panel of the lower part of Sequence 2 along the same transect shown in Figure 15. Unpublished, Bouroullec et al. (2015).

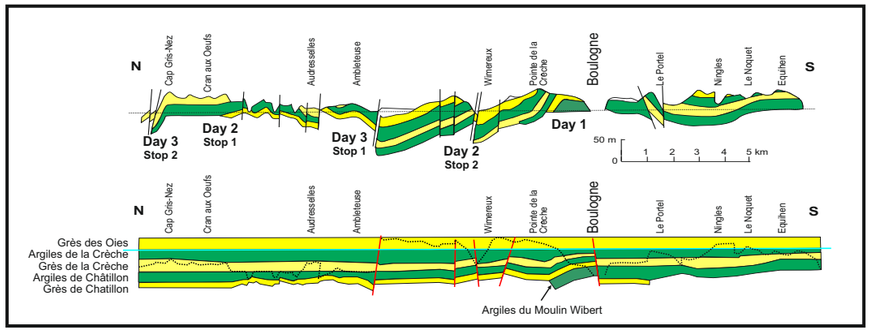

Figure 18: Cross section of the Boulonnais coastal outcrop belt between Equihen and Cap Gris Nez. This section is at the same scale (vertical and horizontal) as Figure 17 A) redrafted to highlight the high net-to-gross intervals (yellow), and the low net-to-gross intervals (green). B) Flattened on top of the Grès des Oies Unit to highlight the possible syn-sedimentary structures. Modified from Pruvost (1925).

Subsurface Analogues in the Dutch Offshore (Focus: Core Description)

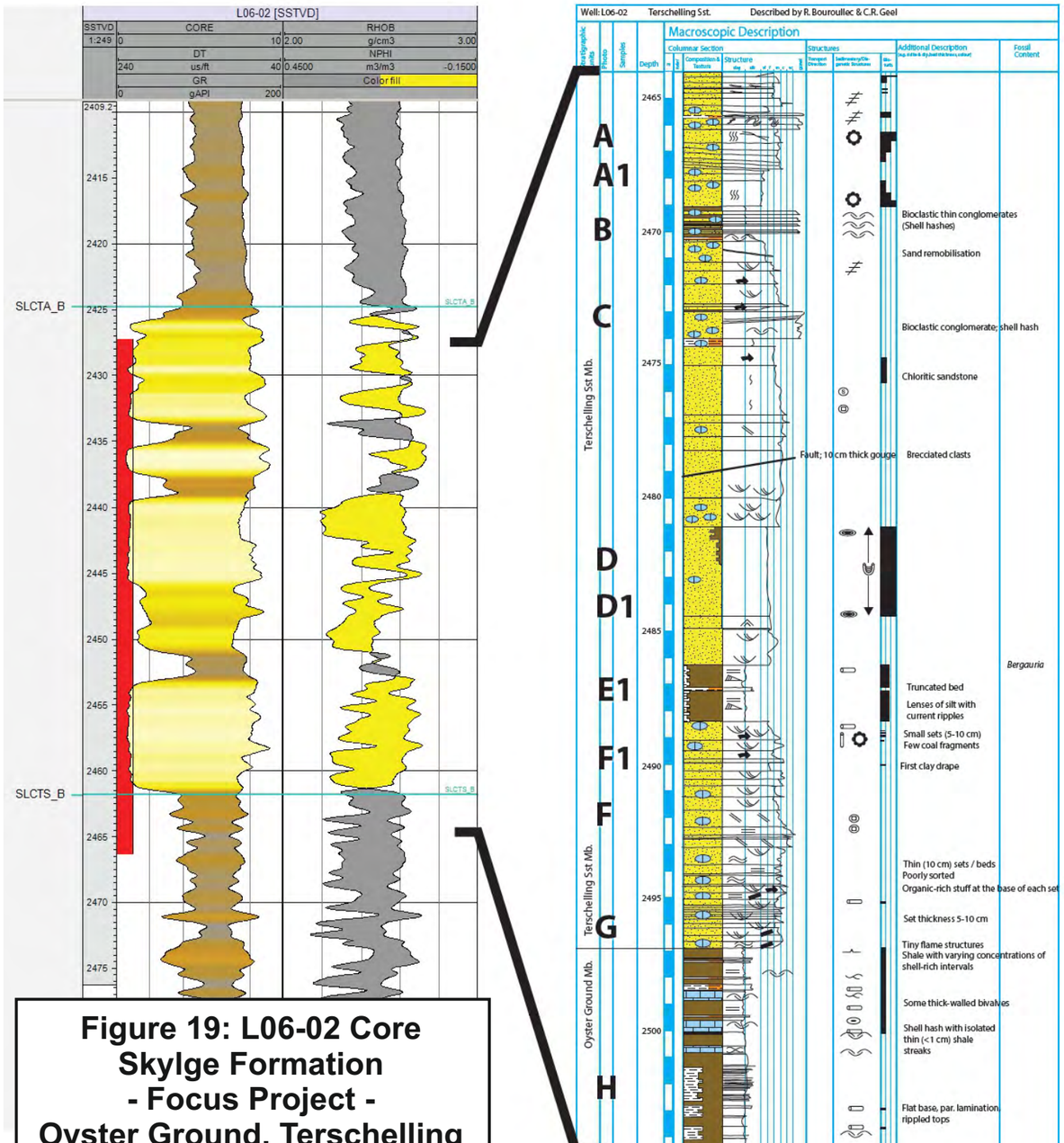

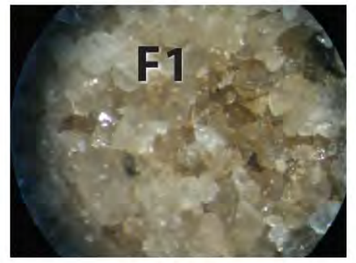

Figure 19: L06-02 Core Skylge Formation - Focus Project - Oyster Ground, Terschelling Sandstone and Lies Members

See legend next page. Compiled by K. Geel.

Subsurface Analogues in the Dutch Offshore (Focus: Core Description)

Figure 20: L06-02 Core
Skylge Formation
- Focus Project -
Oyster Ground, Terschelling
Sandstone and Lies Members

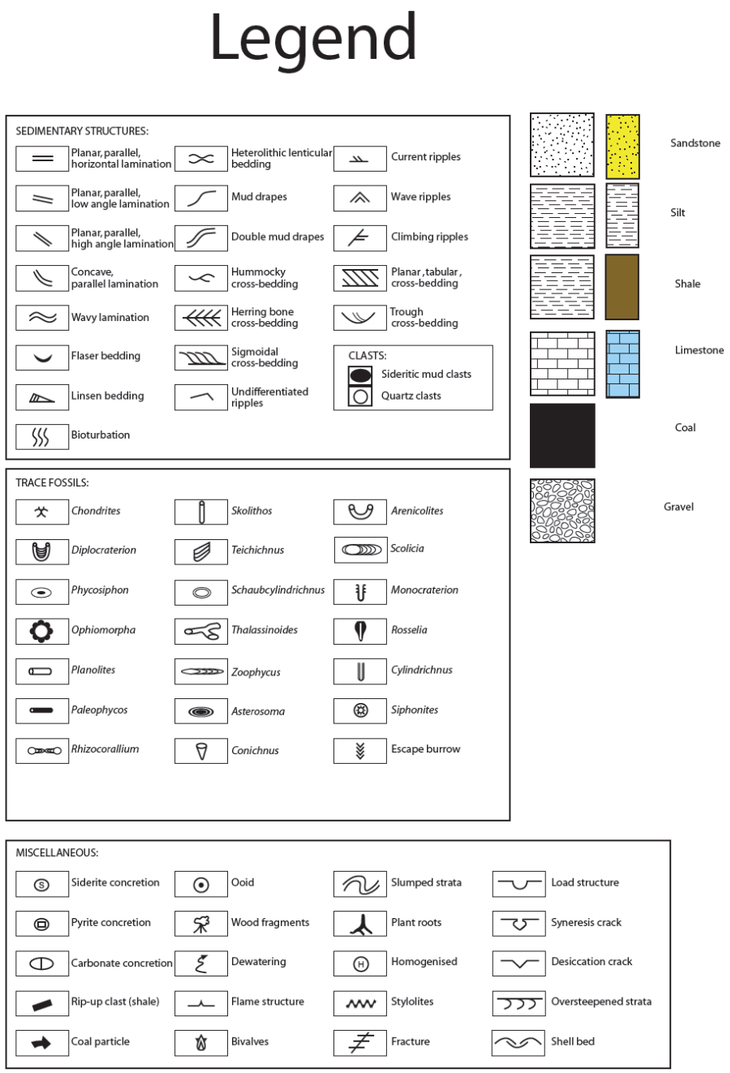

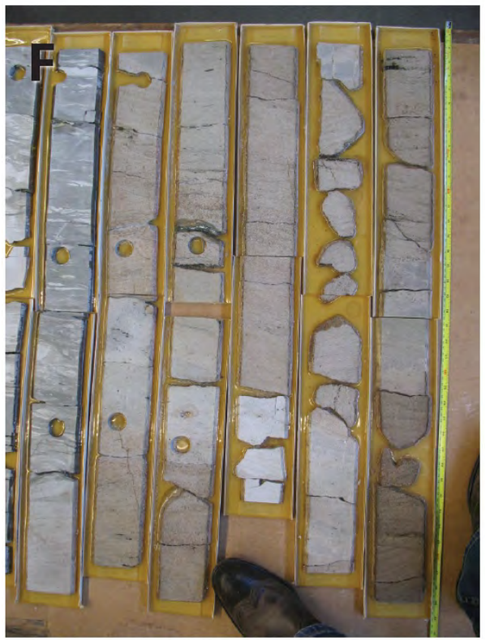

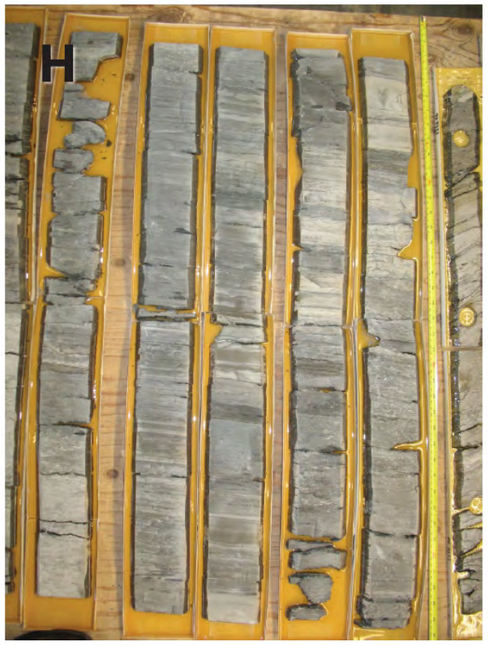

Compiled by K. Geel.

Day 1: Cap de la Crèche outcrop

Figure 20: Google Earth image of the Pointe de la Creche outcrop. Visited outcrop in the yellow box.

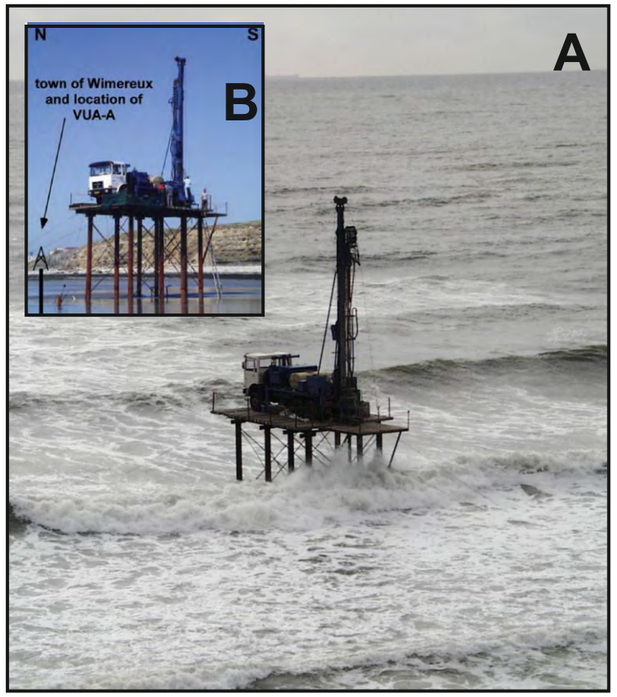

Figure 21: Platform used for drilling of well VUA . A). From Braaksma (2005), B) from Braaksma et al. (2006).

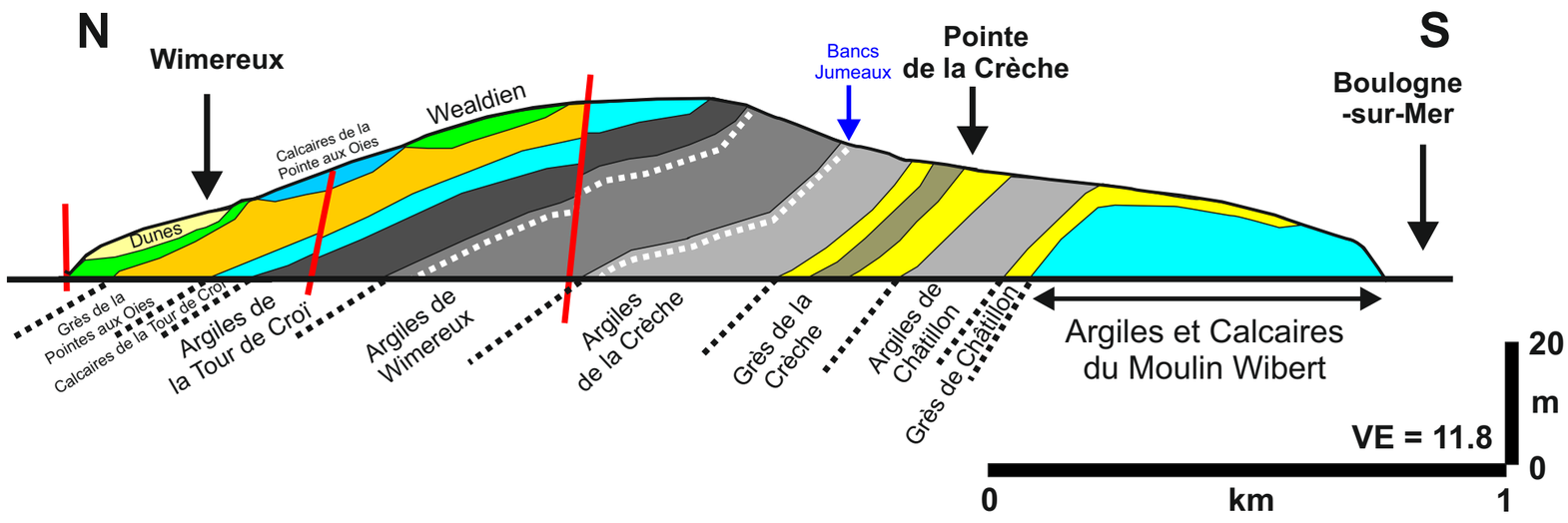

Figure 22: Cross section of the coastal cliff between Boulogne-sur-Mer and Wimereux. Vertical exaggeration is 11.8. Colours: Sandy intervals in yellow and orange, claystones in grey shades, limestone and sandy limestones in blue, conglomerates in red and Wealdian in green, modern Holocene dunes in light yellow and phosphate-rich levels in dashed white. Modified and redrafted from Pruvost (1925) and the Guide Géologique Regional Masson (Région Nord).

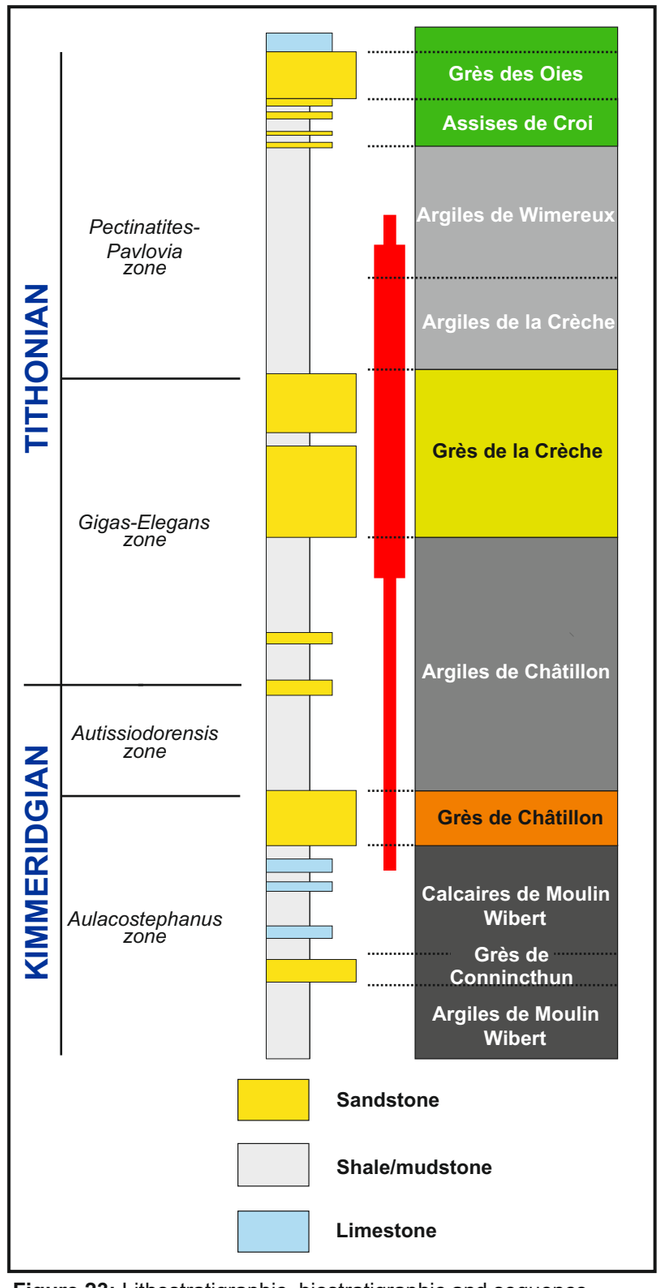

Figure 23: Lithostratigraphic, biostratigraphic and sequence stratigraphic framework of the Upper Jurassic rocks of the Boulonnais. Red bar shows the interval observed at this location. Modified from Busschers (2015, unpublished).

Day 1: Cap de la Crèche outcrop

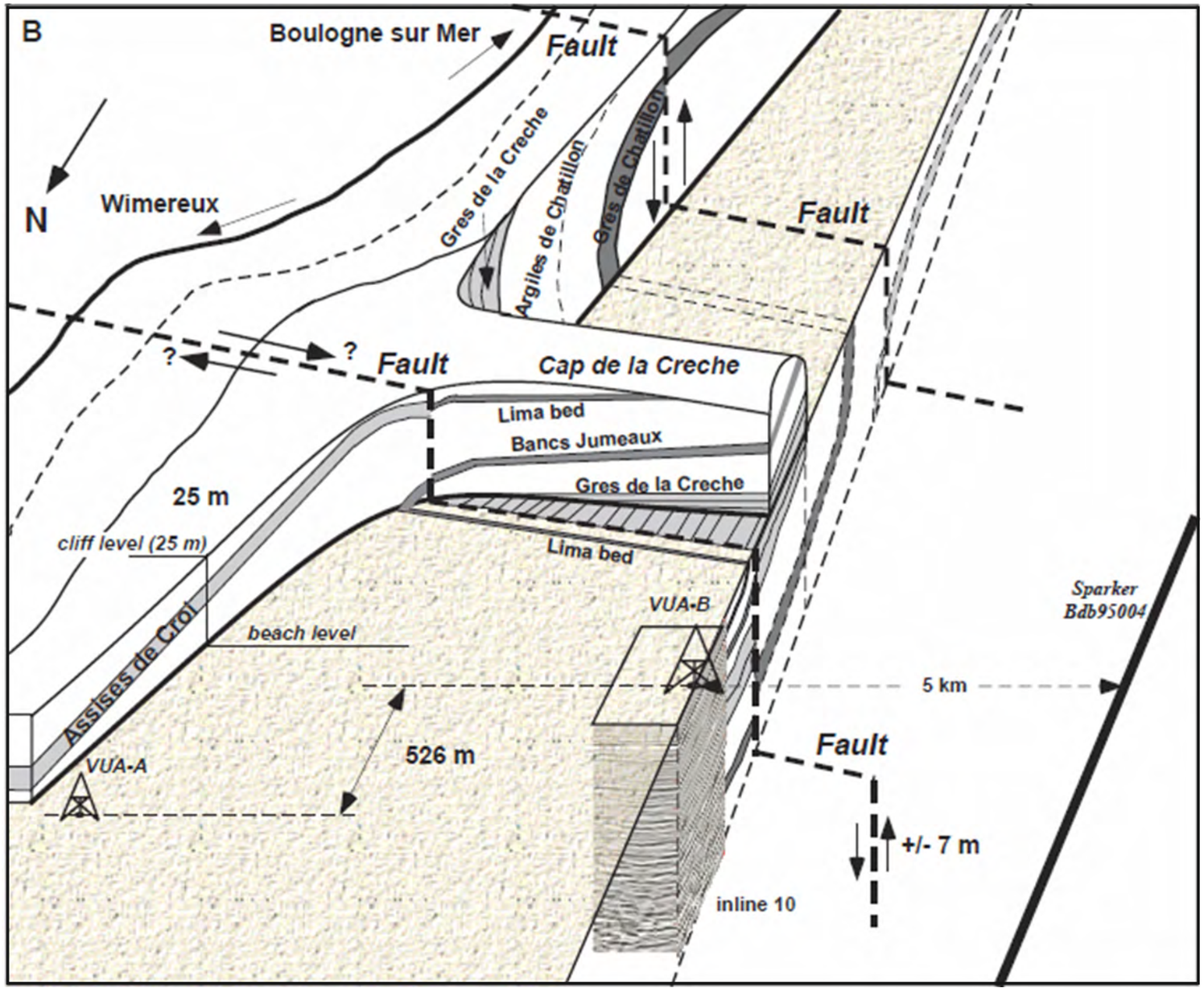

Figure 24: Bird's-eye view of the Boulonnais observatory along the English Channel coast in north-western France viewed from the NNW. Between the town of Wimereux and the city of Boulogne-sur-Mer, Upper Jurassic strata are folded into a monoclinal structure. At the beach level, a 3D seismic survey was performed (square) and borehole VUA-B was drilled. A second borehole (VUA-A) was drilled a year earlier and is located directly south of Wimereux (Braaksma et al, 2006).

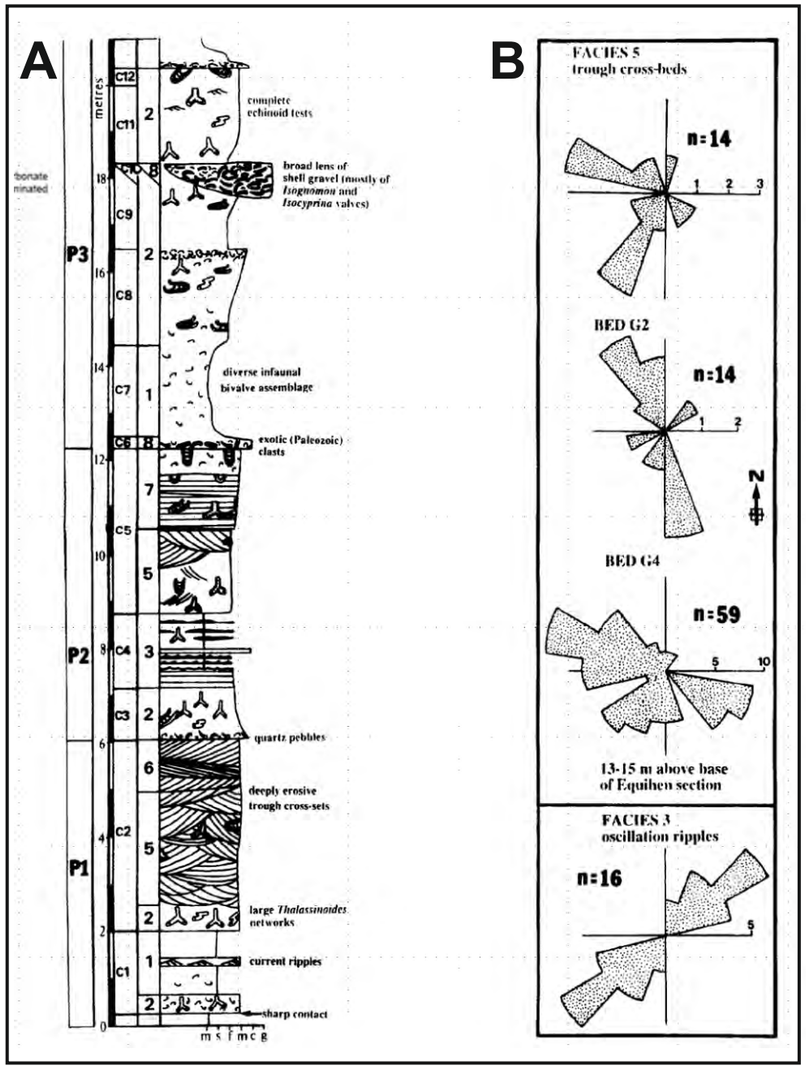

Figure 25: A) Measured section of the Grès de la Crèche at the Pointe de la Creche. B) Paleocurrent measurements from the Grès de la Crèche of trough cross-beds and oscillation ripples. Wignall et al. (1996)

Day 1: Cap de la Crèche outcrop

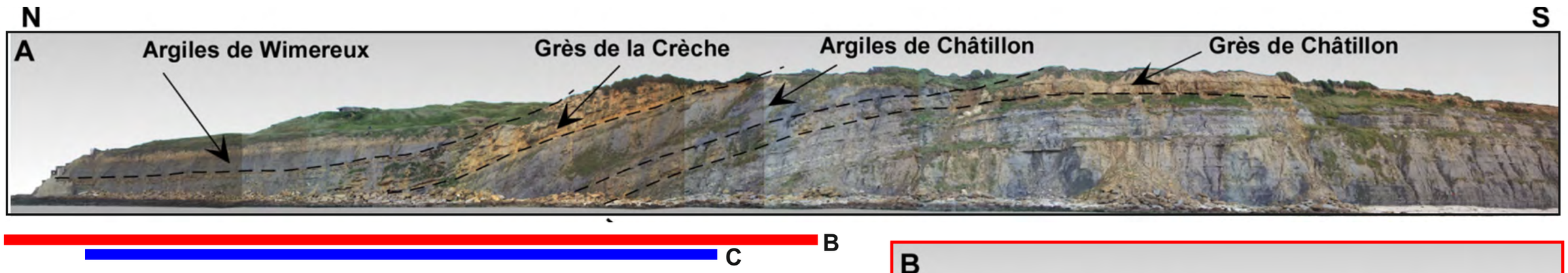

Figure 26: Photos of the Pointe de la Crèche outcrop. **A** and **B** are from Braaksma (2005) and **C** photo from K. Geel.

Day 1: Cap de la Crèche outcrop

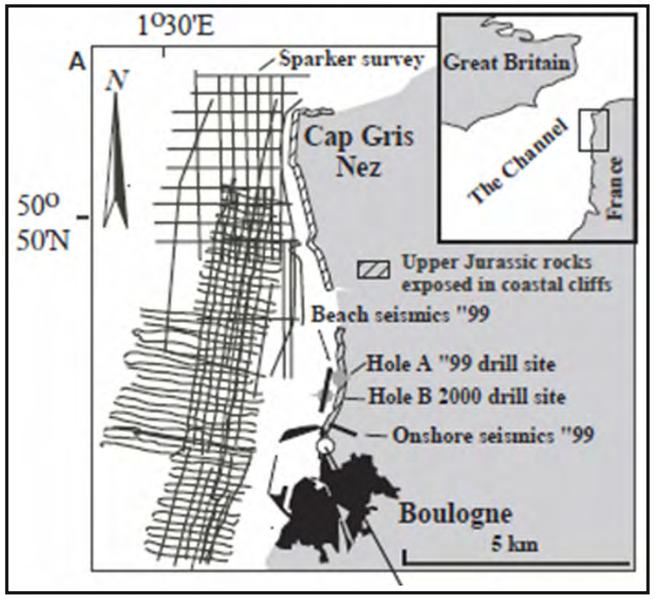

Figure 27: Subsurface data acquisition along the beach and offshore between Boulogne-sur-Mer and Cap Gris Nez. From Braaksma (2005).

Figure 28: 3D survey on the Pointe de la Crèche beach. From Braaksma (2005).

Figure 29: 3D survey on the Pointe de la Crèche beach. From Braaksma (2005).

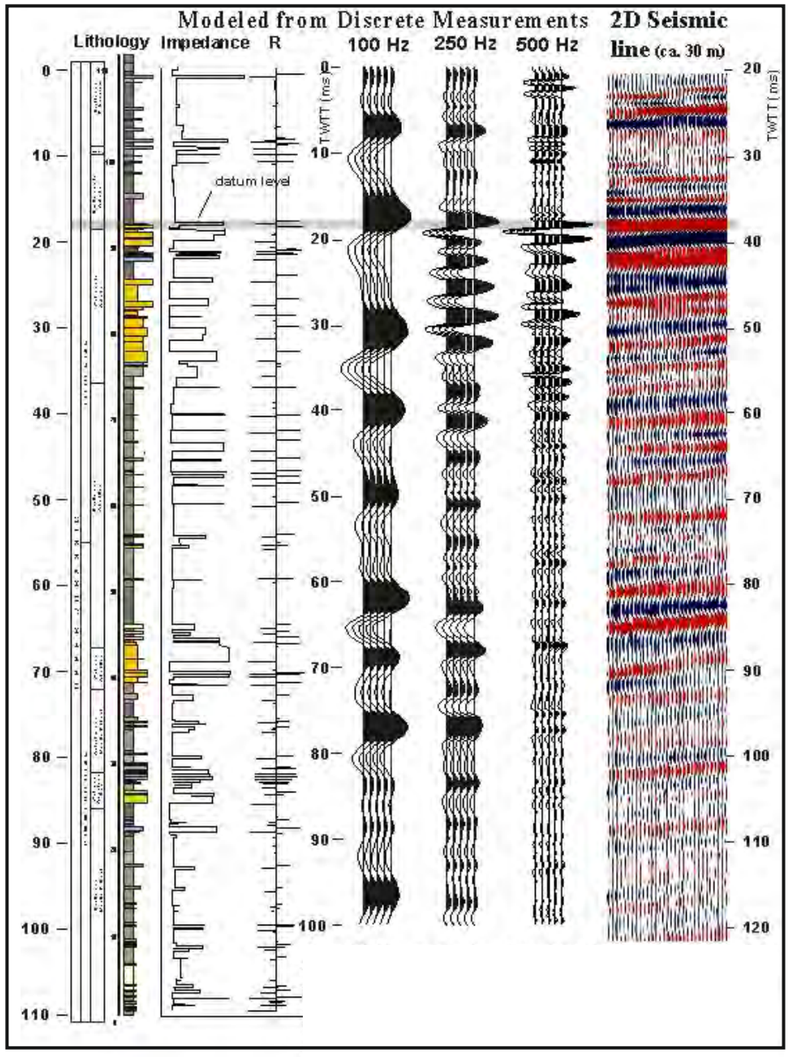

Figure 30: Well to seismic tie. Outcrop-derived impedance model, reflectivity trace, synthetic seismic traces (100, 250 and 500 Hz). Braaksma et al. (2005).

Day 1: Cap de la Crèche outcrop

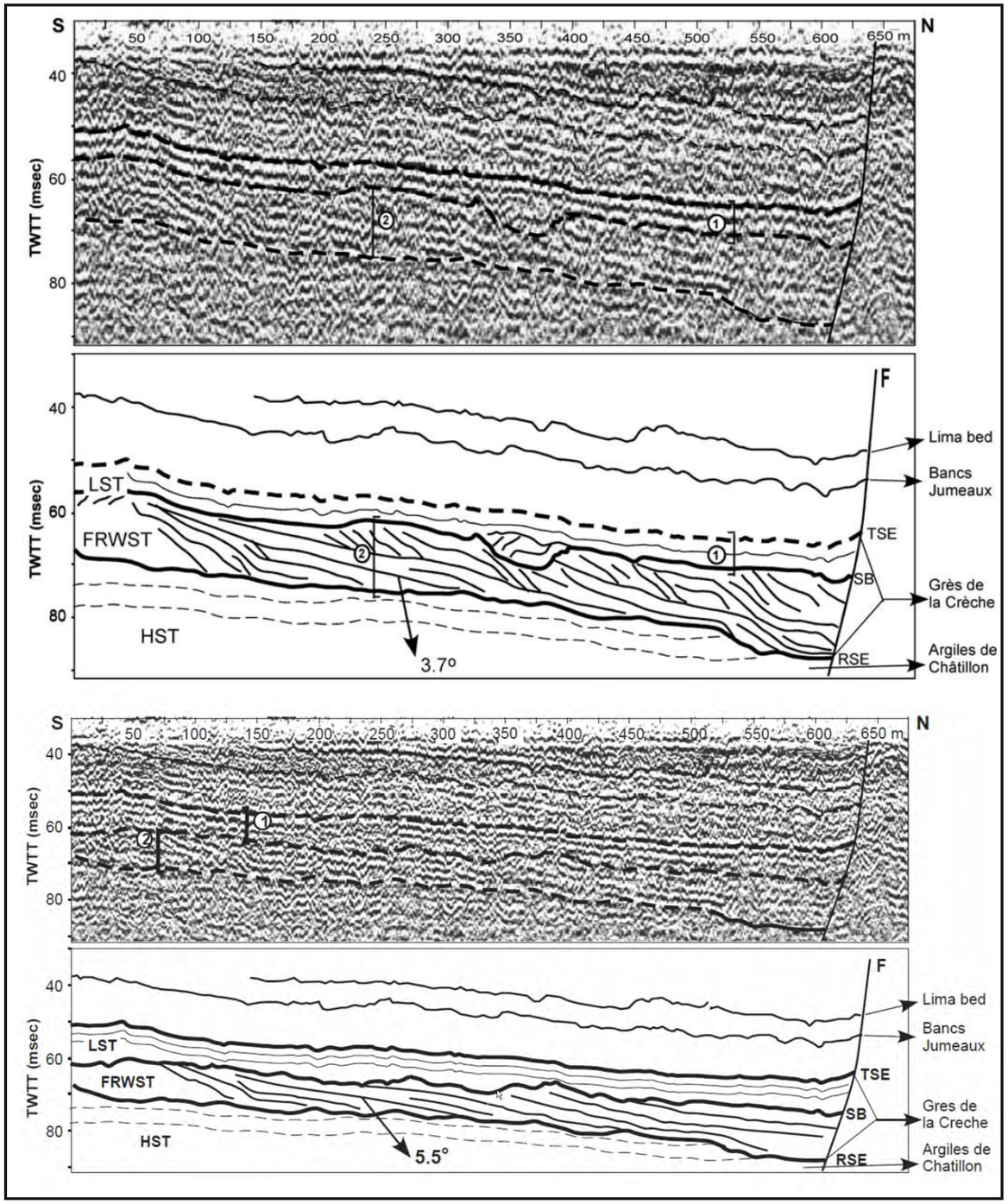

Figure 31: Offshore 2-D sparker seismic reflection profiles and line drawing interpretations. Peak frequency of the seismic line is approximately 500 Hz. Located offshore Wimereux. The parallel continuous bundle of high-amplitude reflections (indicated with number 1) is interpreted as the lowstand systems tract part of the composite sharpbased shoreface deposit. The interval indicated with the circle with number two shows progradational geometries (the angle of prograding clinoforms is approximately 3.7 degrees) and is interpreted as the forced regressive systems tract (FRWST) part of the composite sharp-based shoreface deposit. RSE = regressive surface of marine erosion; SB = sequence boundary; TSE = transgressive surface of marine erosion. From Braaksma et al. (2006).

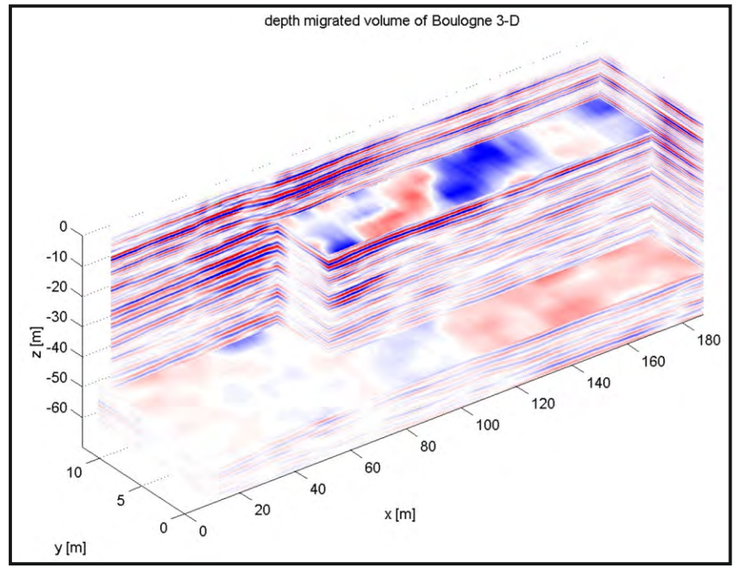

Figure 32: 3D seismic volume (Braaksma, 2005)

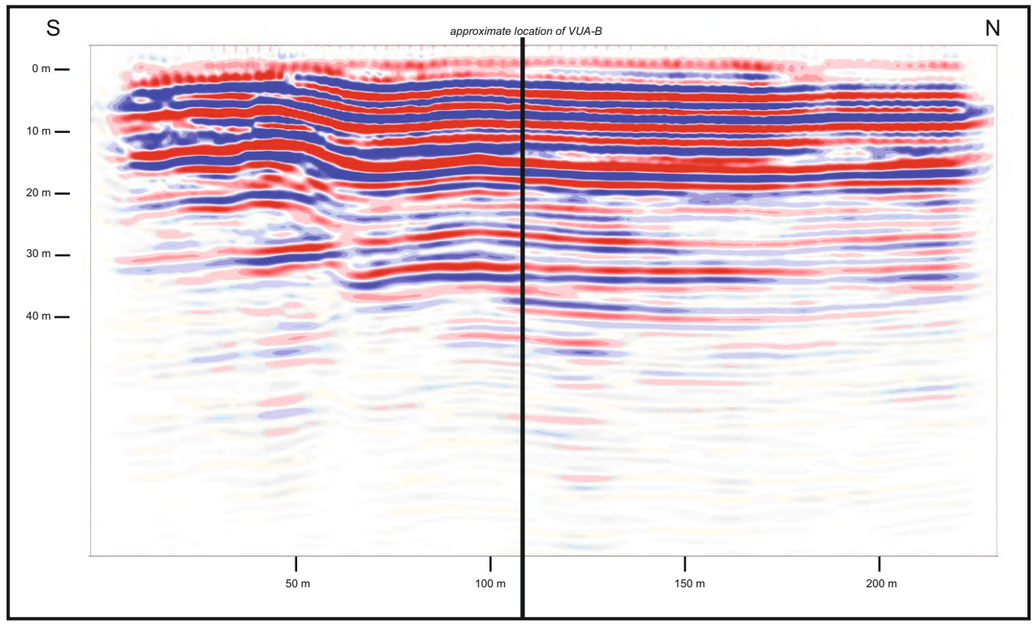

Figure 33: Seismic Line 10 from 2 D seismic survey (Braaksma, 2005)

Day 1: Cap de la Crèche outcrop - Excercise 1

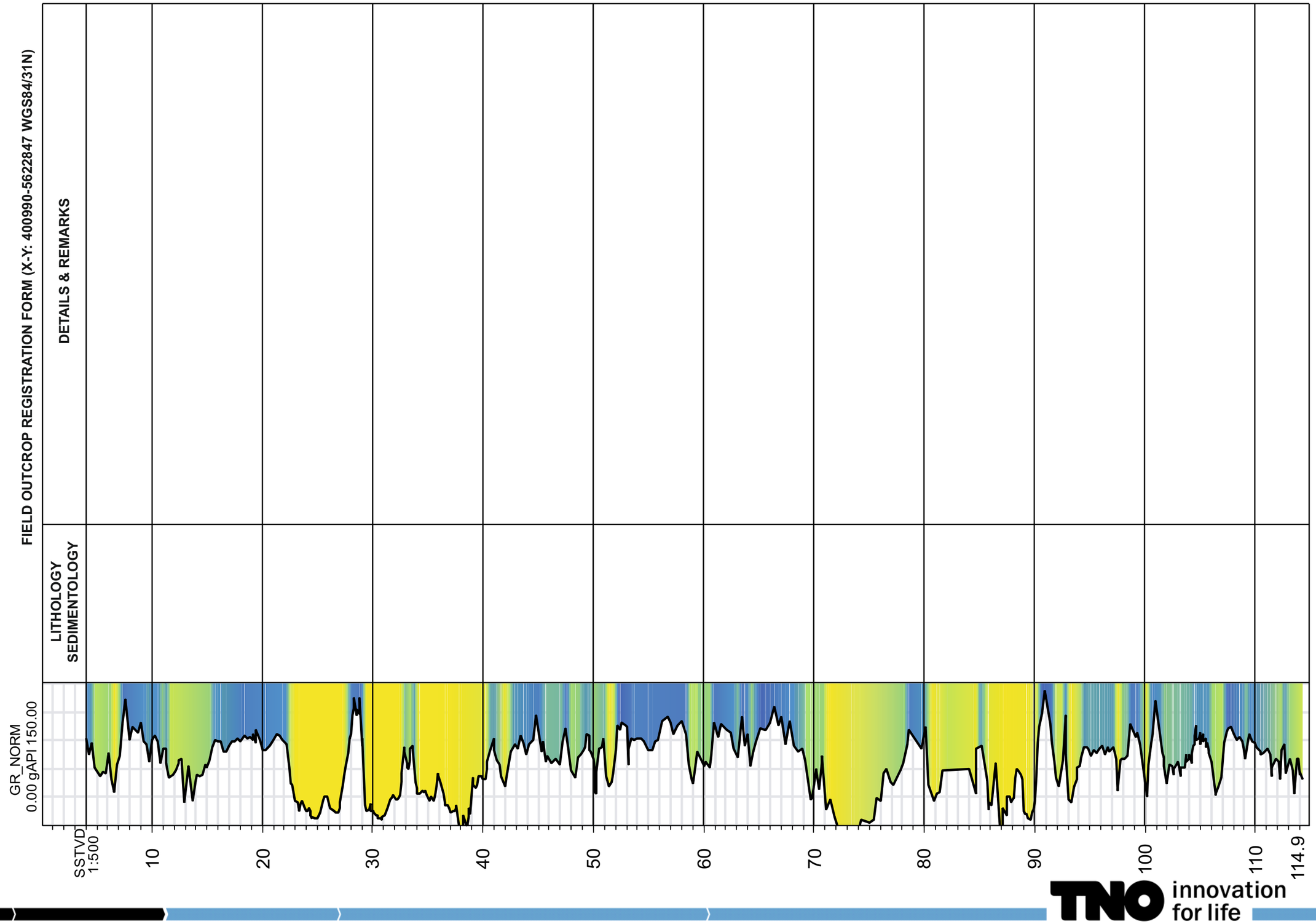

Figure 34: Gamma Ray log of the Pointe de la Crèche outcrop.

Day 1: Cap de la Crèche outcrop - Excercise 2

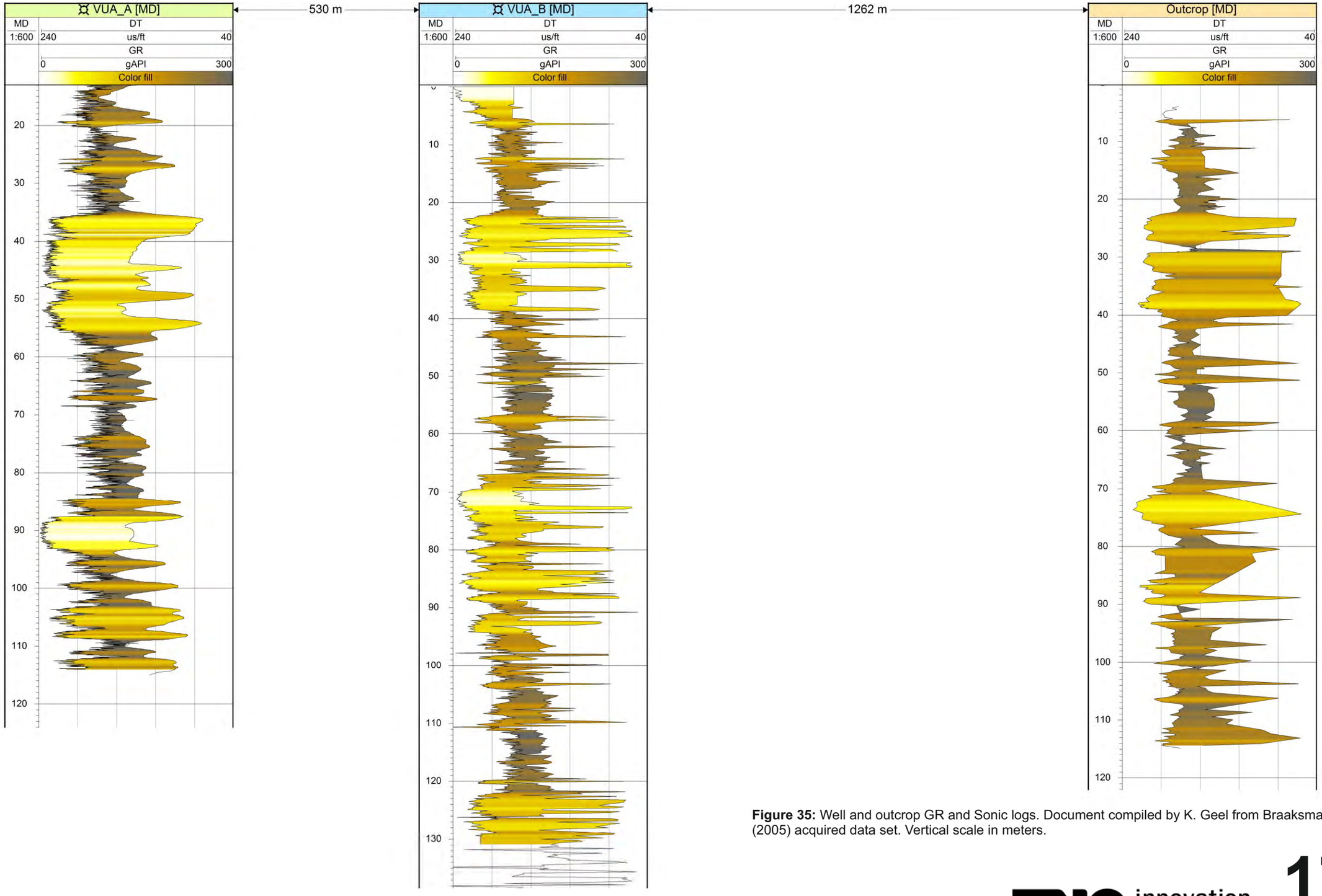

Figure 35: Well and outcrop GR and Sonic logs. Document compiled by K. Geel from Braaksma's (2005) acquired data set. Vertical scale in meters.

Day 2 - Stop 1: Cran du Noirda outcrop

Figure 36: Google Earth image of the Cran du Noirda outcrop. Visited outcrop in the yellow box.

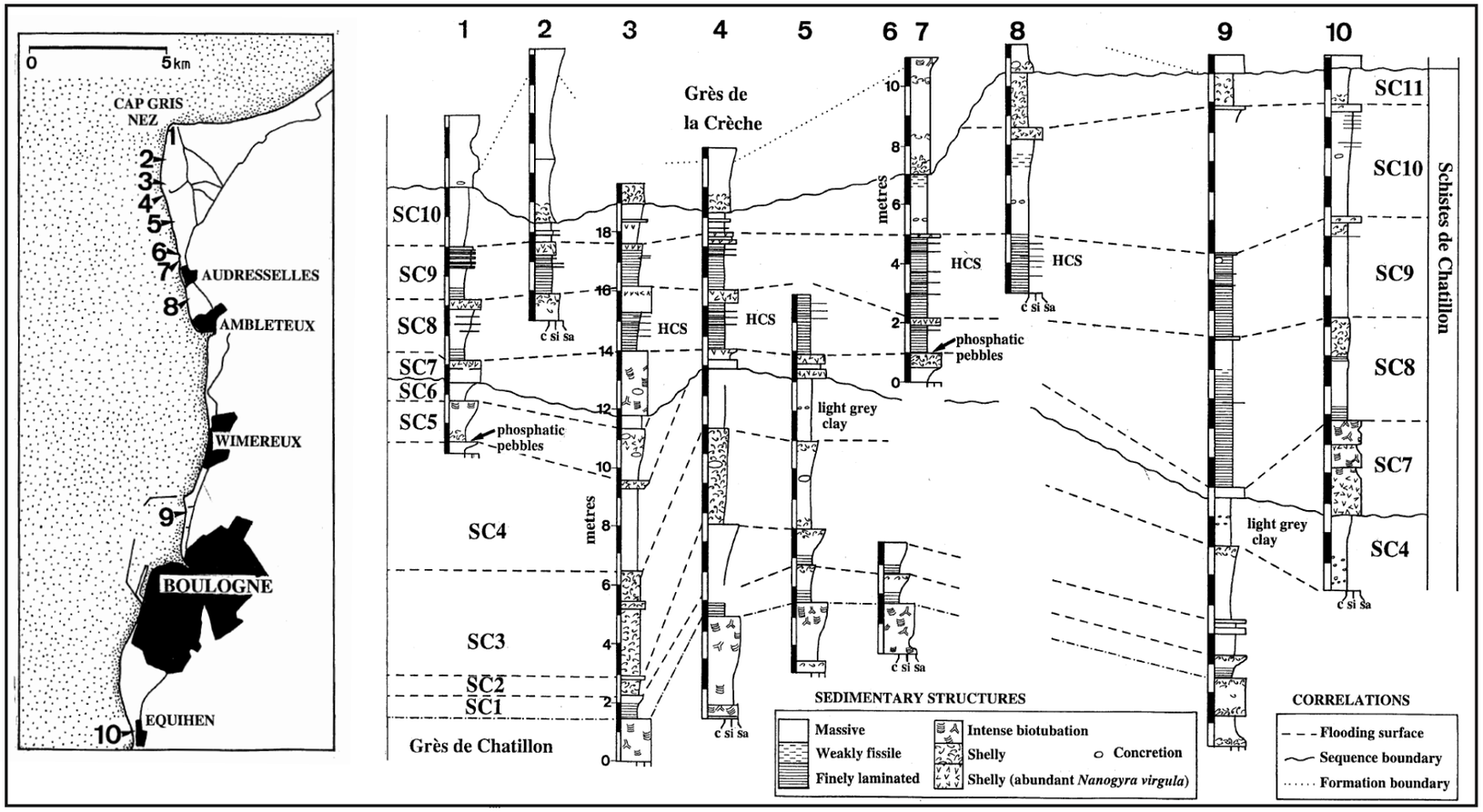

Figure 37: Correlation in the Argiles de Châtillon from the south of Boulogne sur Mer to Cap Gris Nez. See side map for location of the measured sectrions (Wignall and Newton, 2001).

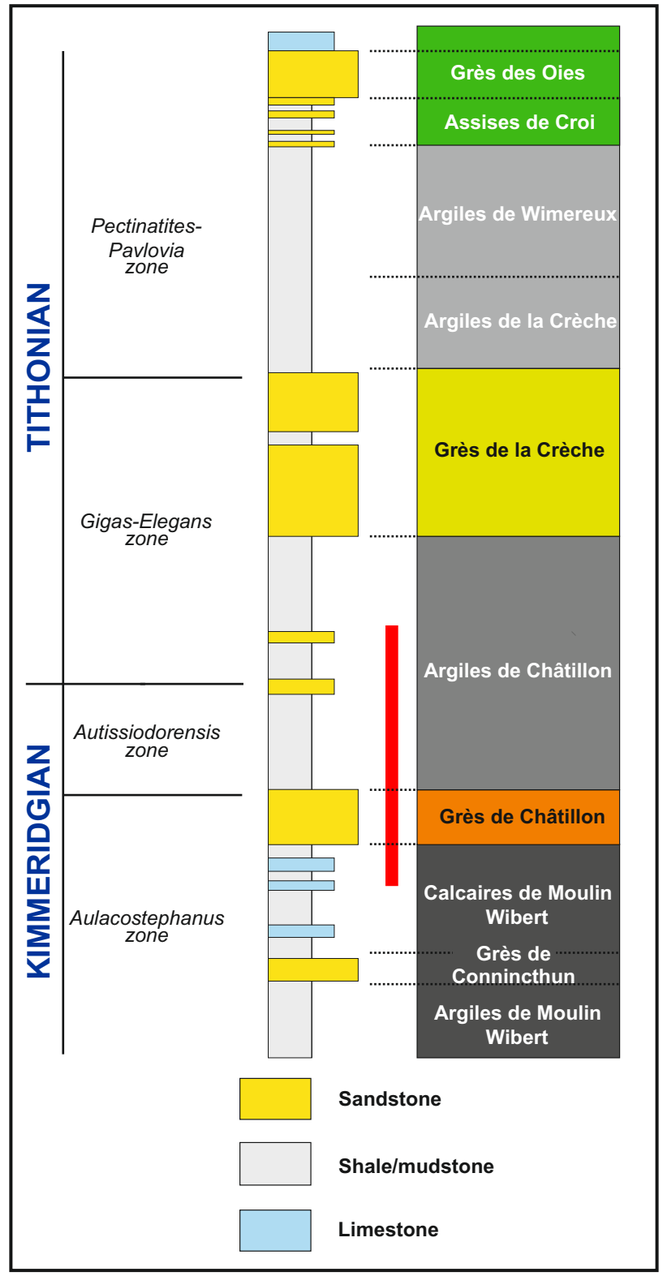

Figure 38: Lithostratigraphic, biostratigraphic and sequence stratigraphic framework of the Upper Jurassic rocks of the Boulonnais. Red bar shows the interval observed at this location. Modified from Busschers (2015, unpublished).

Day 2 - Stop 1: Cran du Noirda outcrop

Figure 39: Field photograph of the organic-rich shales at the base of the Argiles de Châtillon. The upper part of the Grès de Châtillon is exposed at the base of the cliff.

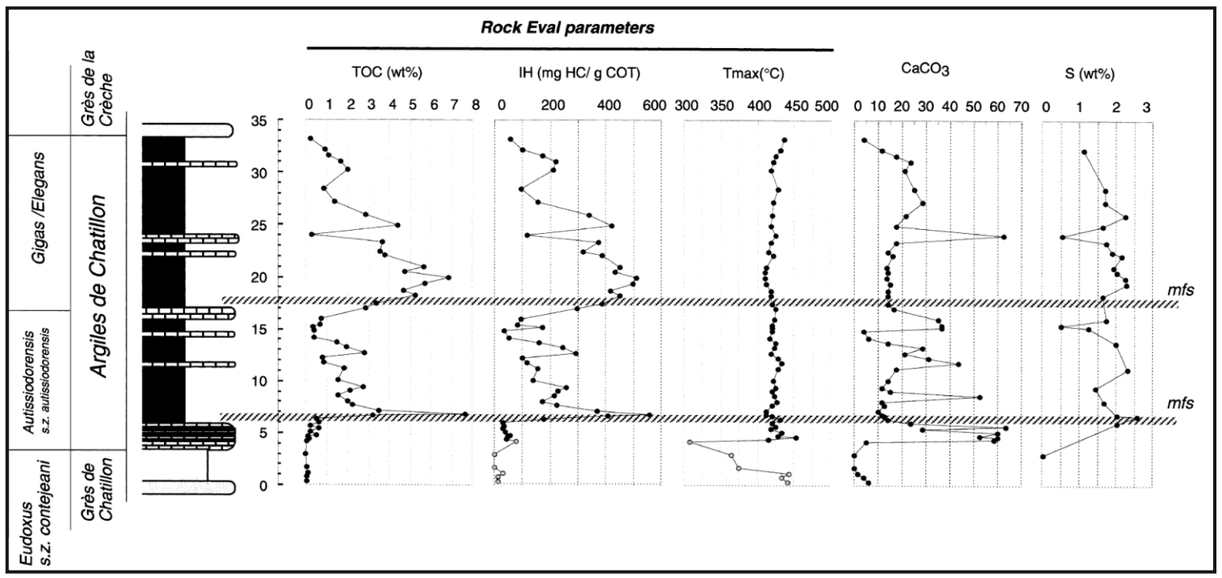

Figure 40: Stratigraphic variation in Rock Eval data and whole rock carbonate and sulphur content. From Tribovillard et al. (2001).

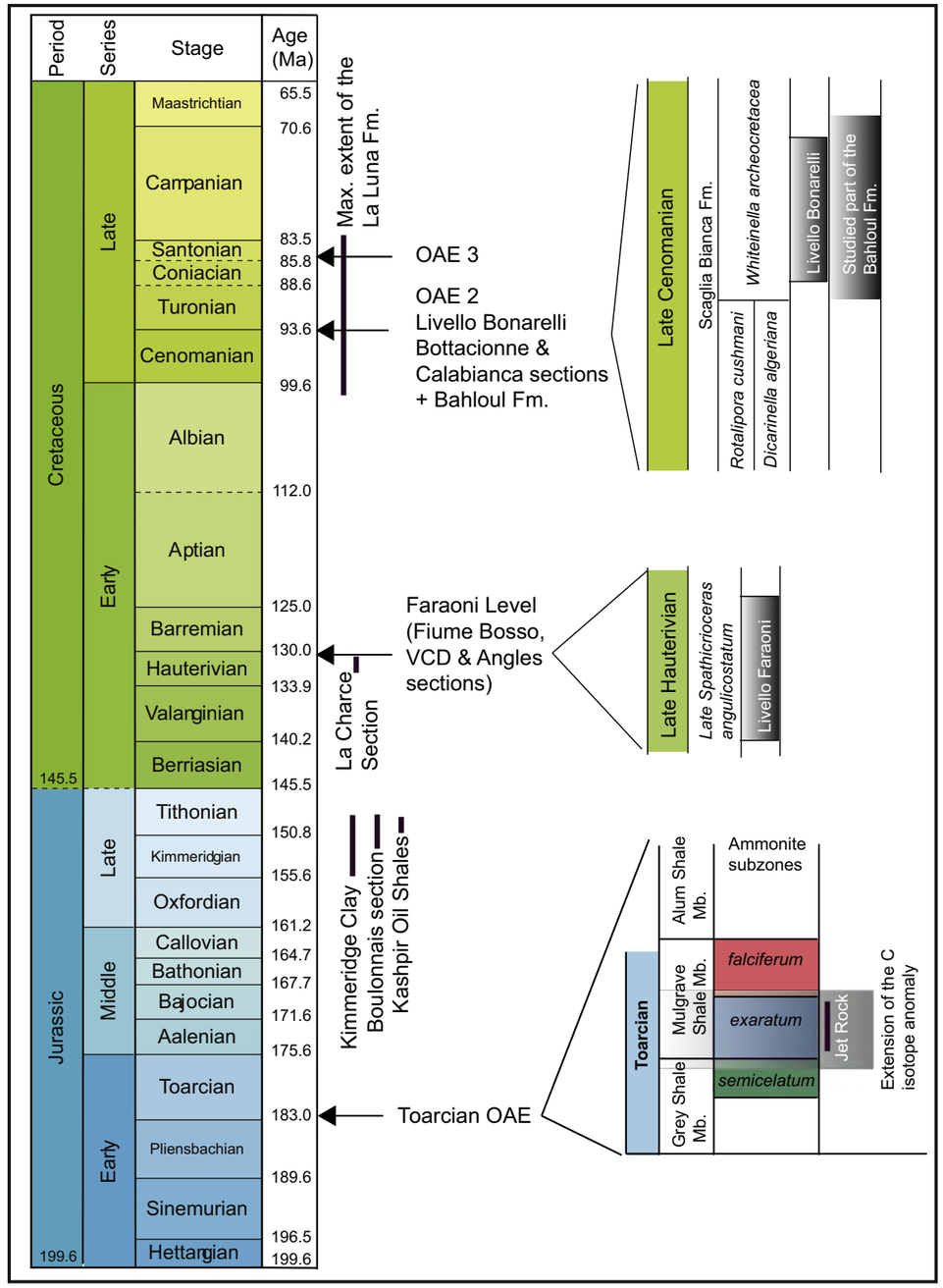

Figure 41: Stratigraphic distribution of the oceanic anoxic events (OAE) and organic matter-rich formations studied in the present paper. Time scale after the International Stratigraphic Chart 2009. From Tribovillard et al. (2012b).

Day 2 - Stop 1: Cran du Noirda outcrop

Figure 42: Ripple marks in the Grès de Châtillon (photo courtesy of A. Trentesaux).

Figure 43: U- shaped burrows (Rhyzocorrallium) in the Grès de Châtillon (photo courtesy of O. Averbuch).

Figure 44: Hummocky cross-stratifications in the Argiles de Châtillon (photo courtesy of A. Trentesaux).

Figure 45: Plan view of horizontal Ophiomorpha burrows (photo courtesy of I. Millan).

Figure 46: Ripple marks in the Grès de Châtillon (photo courtesy of I. Millan).

Figure 47: Cross bedding in the upper part of the Grès de Châtillon (photo courtesy of K. Geel).

Figure 48: Ophiomorpha burrows (photo courtesy of K. Geel).

Figure 49: Plan view of Ophiomorpha burrows (photo courtesy of K. Geel).

Figure 50: Fault plane (photo courtesy of I. Millan).

Day 2 - Stop 1: Cran du Noirda outcrop (New Palynological Results)

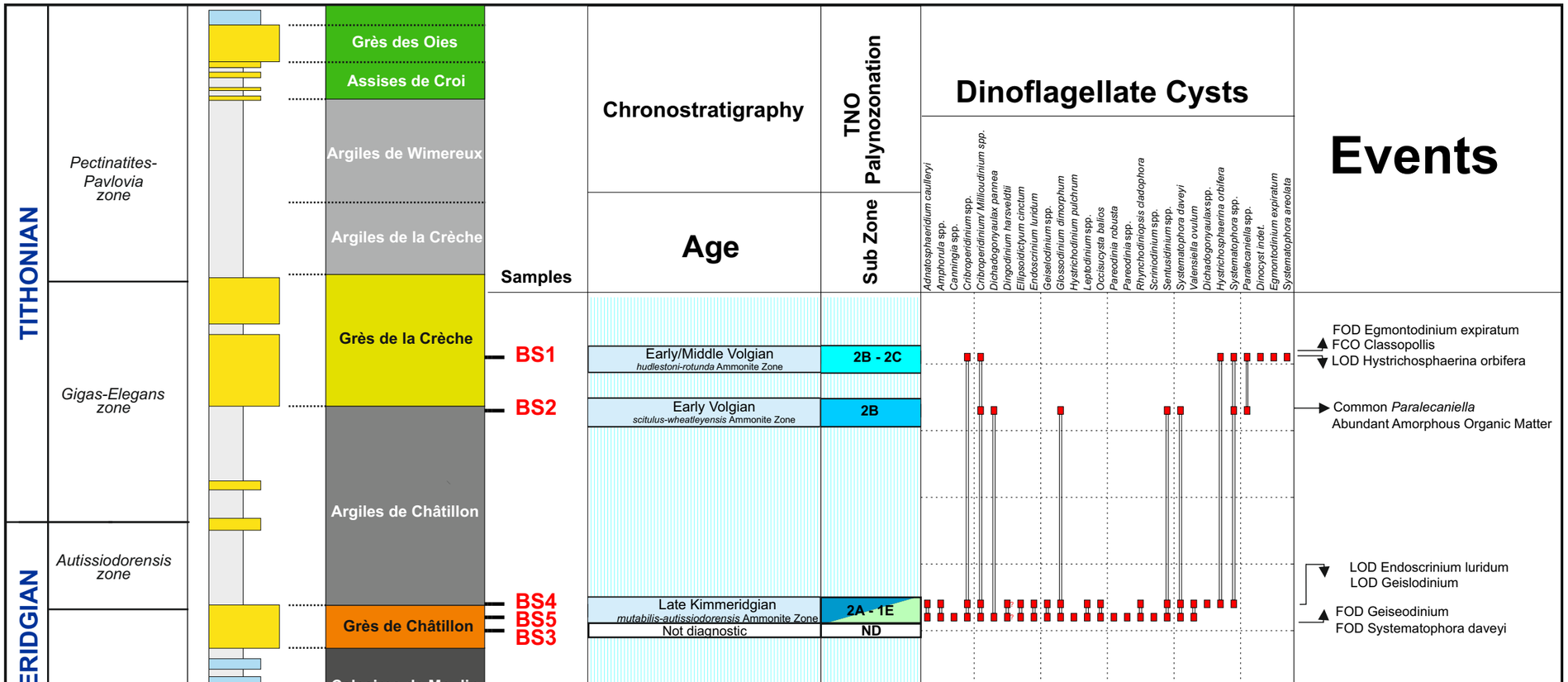

Figure 51: Palynological results of 5 outcrop samples from the Boulonnais: age-assessments based on First and Last Occurrences of dinoflagellate cysts and pollen and spores. Unpublished, Verreussel and Munsterman (2015).

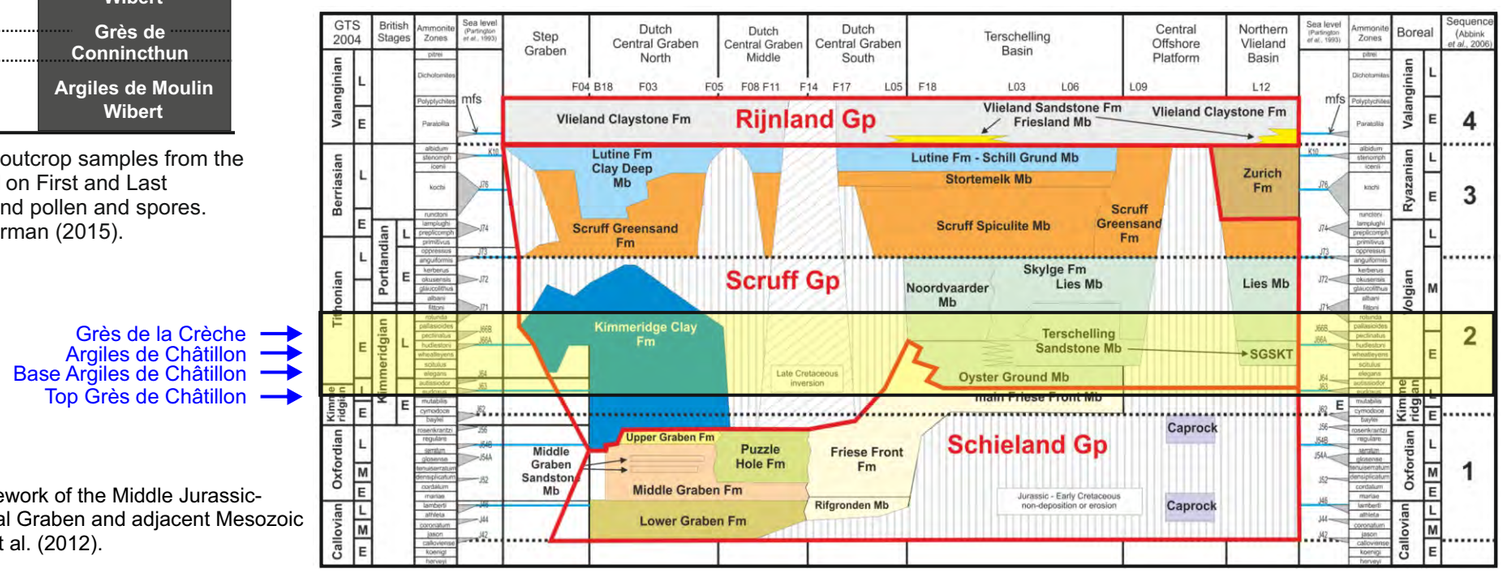

Figure 52: Lithostratigraphical framework of the Middle Jurassic-Early Cretaceous in the Dutch Central Graben and adjacent Mesozoic basins. Modified from Munsterman et al. (2012).

Day 2 - Stop 1: Cran du Noirda outcrop (New Palynological Results)

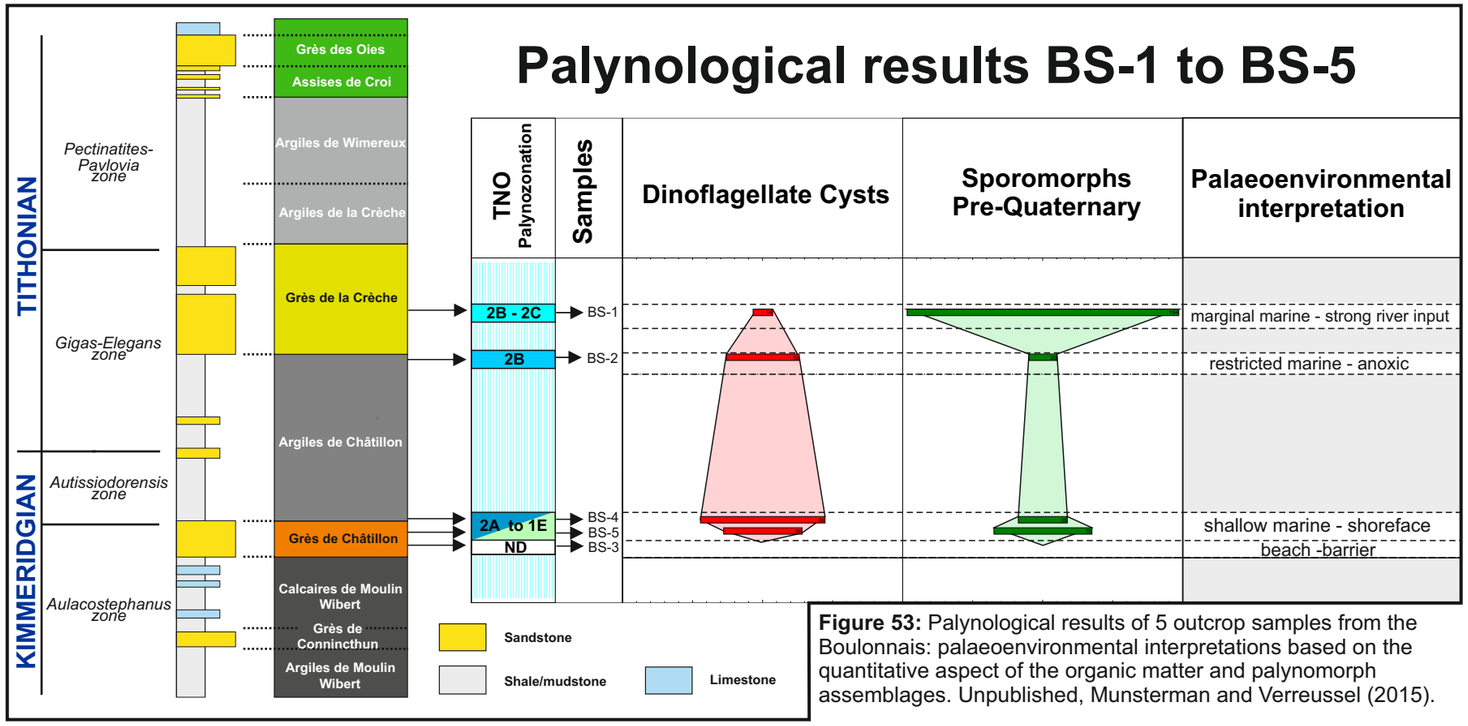

Figure 53: Palynological results of 5 outcrop samples from the Boulonnais: palaeoenvironmental interpretations based on the quantitative aspect of the organic matter and palynomorph assemblages. Unpublished, Munsterman and Verreussel (2015).

BS-1

Grès de la Crèche

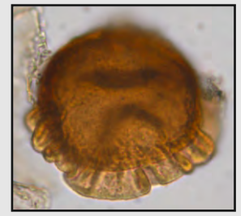

Callialasporites dampieri

Cicatricosiporites sp.

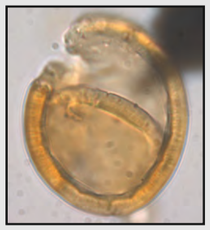

Tasmanaceae

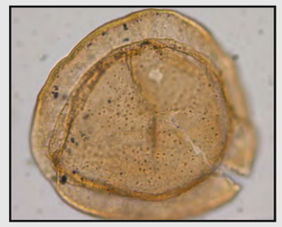

Callialasporites discoidalis

Abundant pollen and spores combined with rare dinocysts indicate a marginal marine environment with strong terrestrial input. The occurrence of the prasinophyte algae Tasmanaceae indicates influence of stratified water masses.

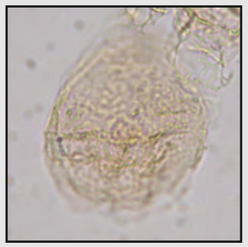

Geiselodinium sp.

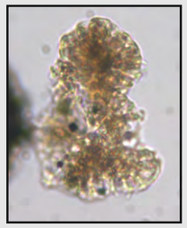

Botryococcus sp. [Transmitted light]

Botryococcus sp. [UV incident light]

BS-5

Grès de Châtillon

An upward increase in the amount of dinocysts indicates a transgressive trend from beach/barrier to shallow marine/shoreface. Rare occurrences of the freshwater algae *Botryococcus* indicate freshwater influence.

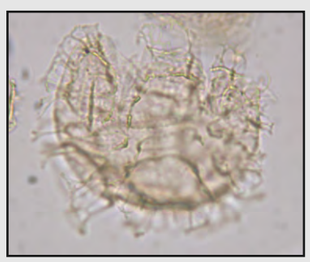

Amphorula metaelliptica

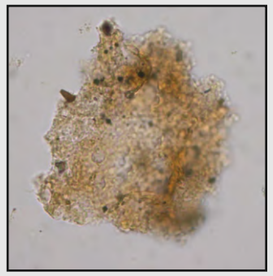

Amorphous Organic Matter [transmitted light]

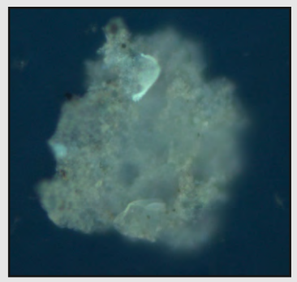

Amorphous Organic Matter [UV incident light]

Paralecaniella sp.

BS-2

Argiles de Châtillon

Abundant AOM indicates anoxic-dysoxic bottom conditions.
The common occurrence of the probable zygospore Paralecaniella sp. indicates restricted marine conditions with freshwater influence.

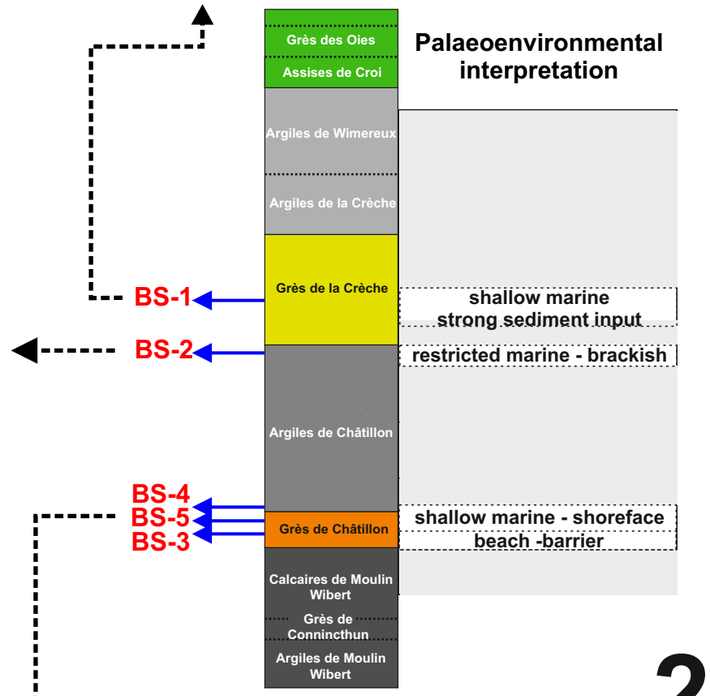

Day 2 - Stop 2: Pointe de la Rochette outcrop

Figure 54: Google Earth image of the Pointe de la Rochette outcrop. Visited outcrop in the yellow box.

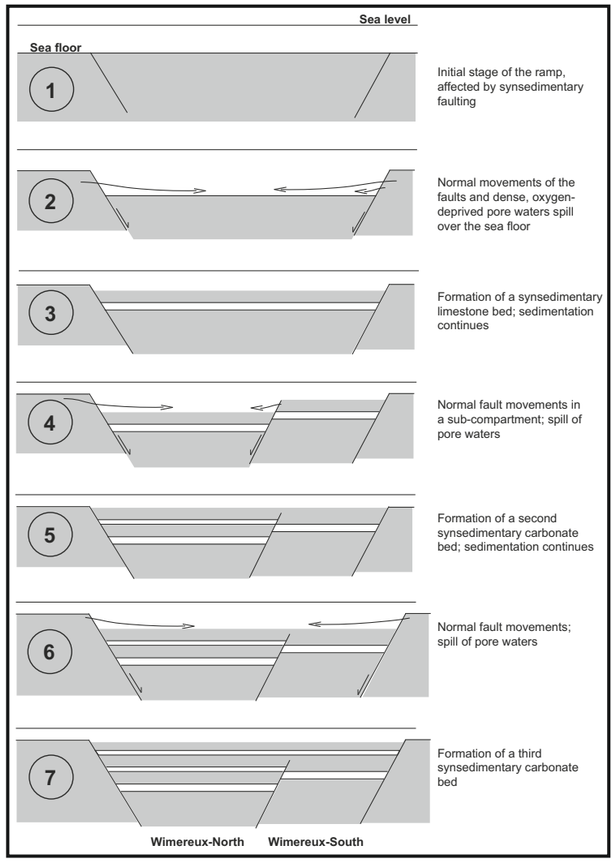

Figure 54: Schematic scenario of the synsedimentary early-diagenetic formation of the limestone beds, accounting for the fact that two beds are observed at Wimereux-South and three beds crop out at Wimereux-North. The model is scaleless and does not consider any role played by the sea level. The precise location of the synsedimentary faults is not known but their presence is demonstrated by the geometry of the sediment bodies and field evidences. From Tribovillard et al. (2012a).

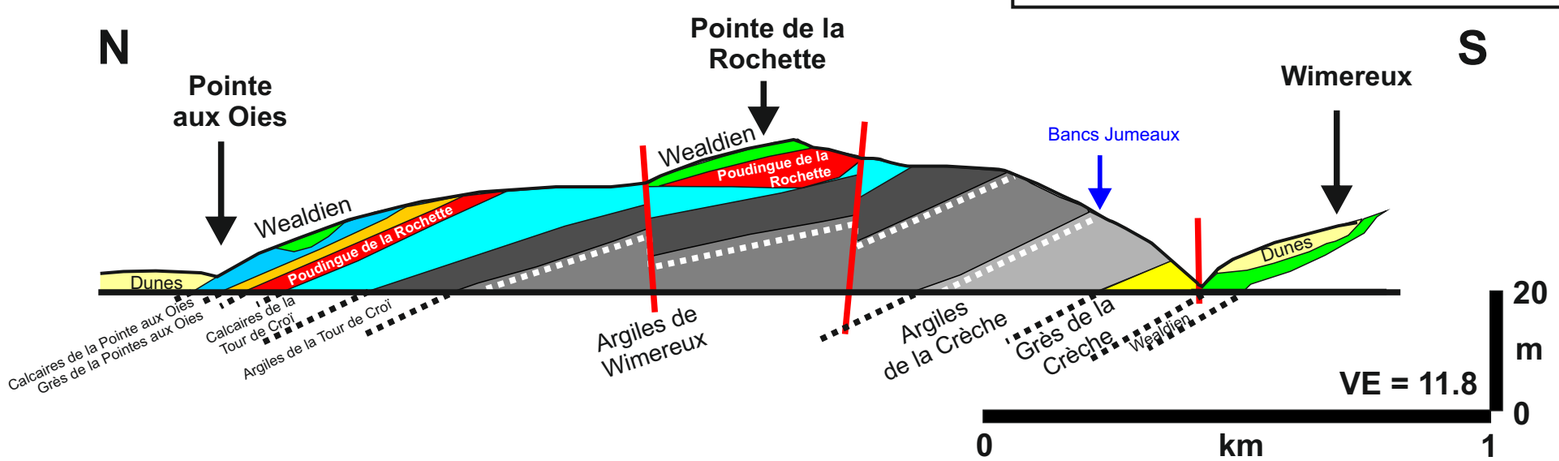

Figure 56: Cross section of the coastal cliff faces between Boulogne-sur-Mer and the Pointe aux Oies. Vertical exaggeration is 11.8. Colours: Sandy intervals in yellow and orange , claystones in grey shades, limestone and sandy limestones in blue, conglomerates in red and Wealdian in green, modern Holocene dunes in light yellow and phosphate-rich levels in dashed white. Modified and redrafted from Pruvost (1925) and the Guide Géologique Regional Masson (Région Nord).

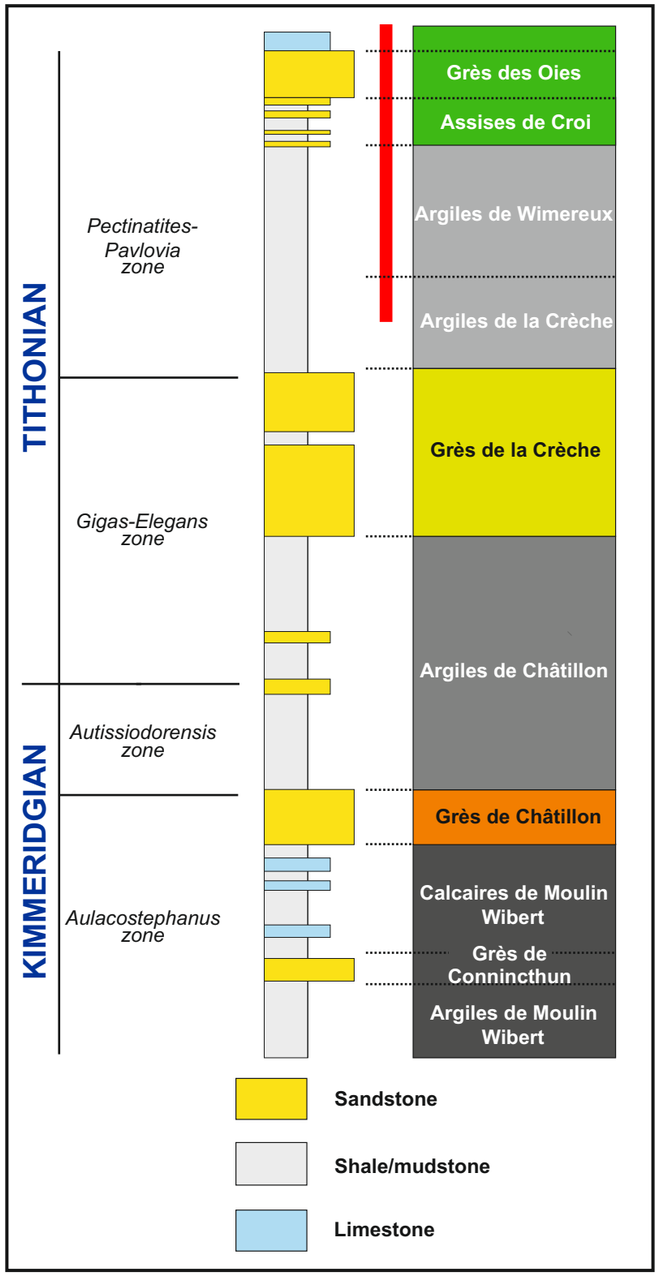

Figure 57: Lithostratigraphic, biostratigraphic and sequence stratigraphic framework of the Upper Jurassic rocks of the Boulonnais. Red bar shows the interval observed at this location. Modified from Busschers (2015, unpublished).

Day 2 - Stop 2: Pointe de la Rochette outcrop

Figure 58: Photopanels of the Pointe de la Rochette outcrop. Courtesy of K. Geel.

Day 3 - Stop 1: "Dune de la Slack"

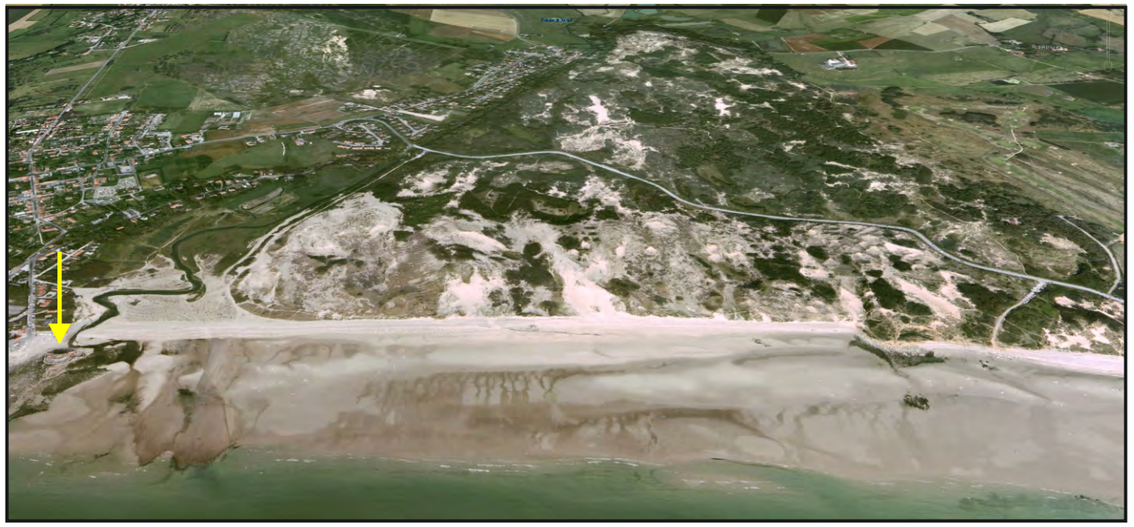

Figure 59: Google Earth image of the Pointe de la Rochette outcrop. Location of the stop at the yellow arrow (Fort Vauban, Fort d'Ambleteuse).

Figure 60: Postcards of Ambleteuse Fort and beach.

Figure 61: Aerial view of the Dune de la Slack (photography in http://france3-regions.francetvinfo.fr/nord-pas-de-calais/2013/07/11/dunes-de-la-slack-282421.html.

Figure 62: Semiconsolidated aeolian sandstones in Dune de la Slack (photography in http://commons.wikimedia.org/wiki/File:Ambleteuse_dunes_slack.jpg).

Day 3: Cap Gris Nez outcrop

Figure 63: Google Earth image of the Cap Gris Nez outcrop. Visited outcrop in the yellow box.

Figure 64: Anticline cropping out on the foreshore at Cap Gris Nez.

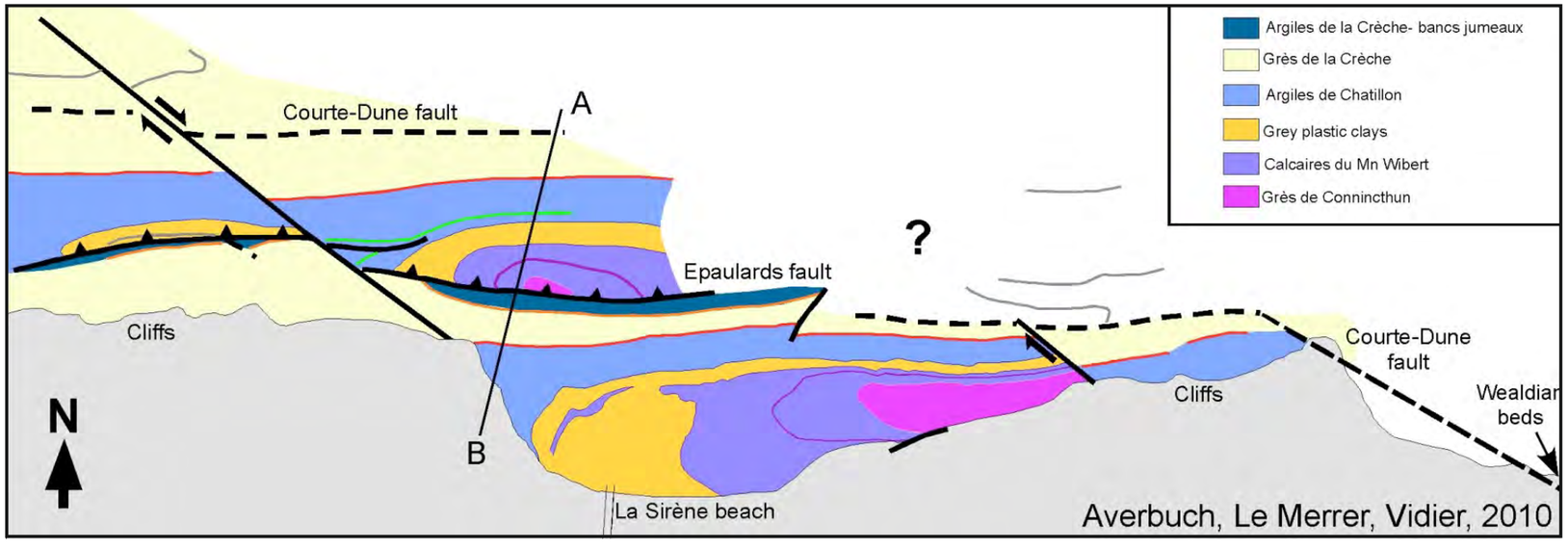

Figure 65 Geological map of the Cap Gris Nez fault zone along the shore (Averbuch et al., 2011).

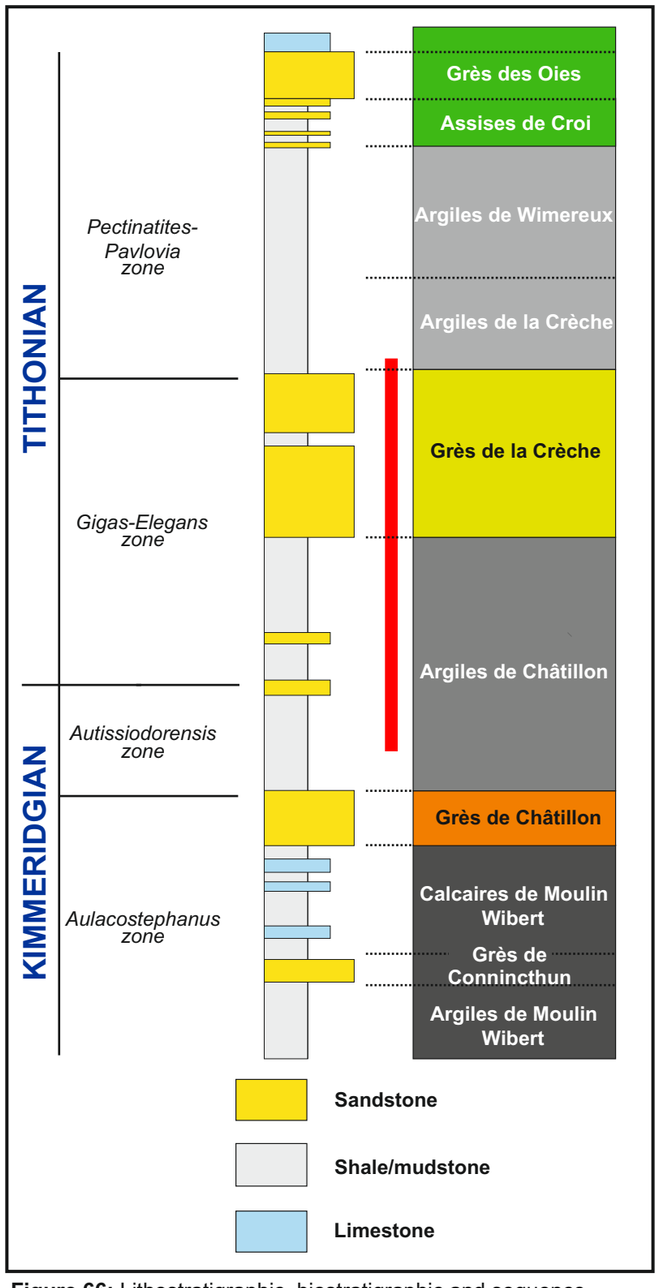

Figure 66: Lithostratigraphic, biostratigraphic and sequence stratigraphic framework of the Upper Jurassic rocks of the Boulonnais. Red bar shows the interval observed at this location. Modified from Busschers (2015, unpublished).

Day 3: Cap Gris Nez outcrop

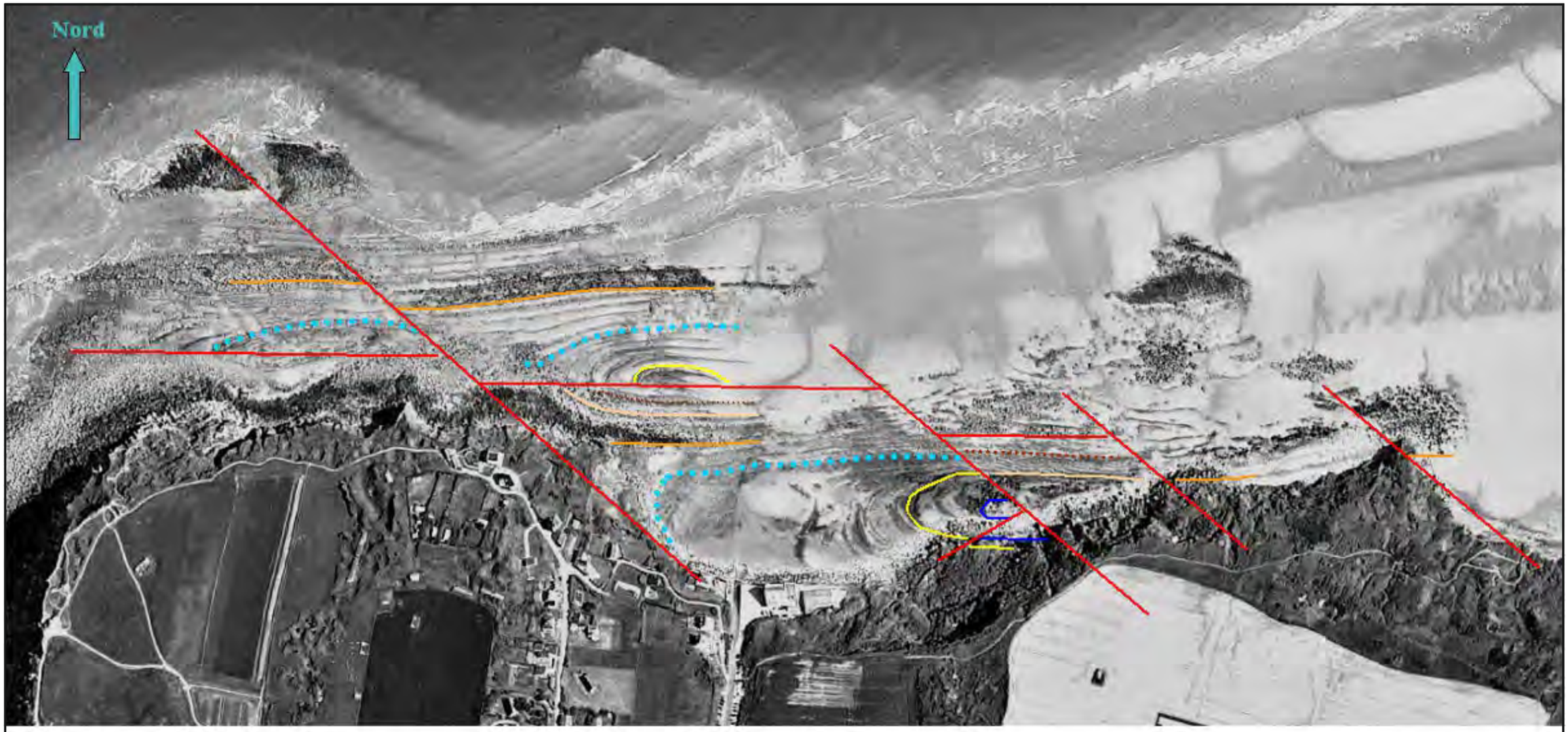

Schéma de la structure et localisation des principaux niveaux repère sur la plage du Cap Gris Nez
J.P. Vidier, A. Leduc et O. Averbuch en cours,

Légende : Failles ——— ; Sommet des Argiles du Moulin Wibert ——— ; Sommet des Sables de Connincthun ——— ;
Première lumachelle et petits récifs à huitres à la base des Argiles de Chatillon ▪▪▪▪; Base des Grès de la Crèche ——— ;
Sommet des Grès de la Crèche ——— ; Niveau phosphaté Ph1 .....

Figure 67: Structural framework and identification of the main faults and reference horizons at Cap Gris Nez. See figure for additional description. From (Vidier et al., unpublished).

Day 3: Cap Gris Nez outcrop

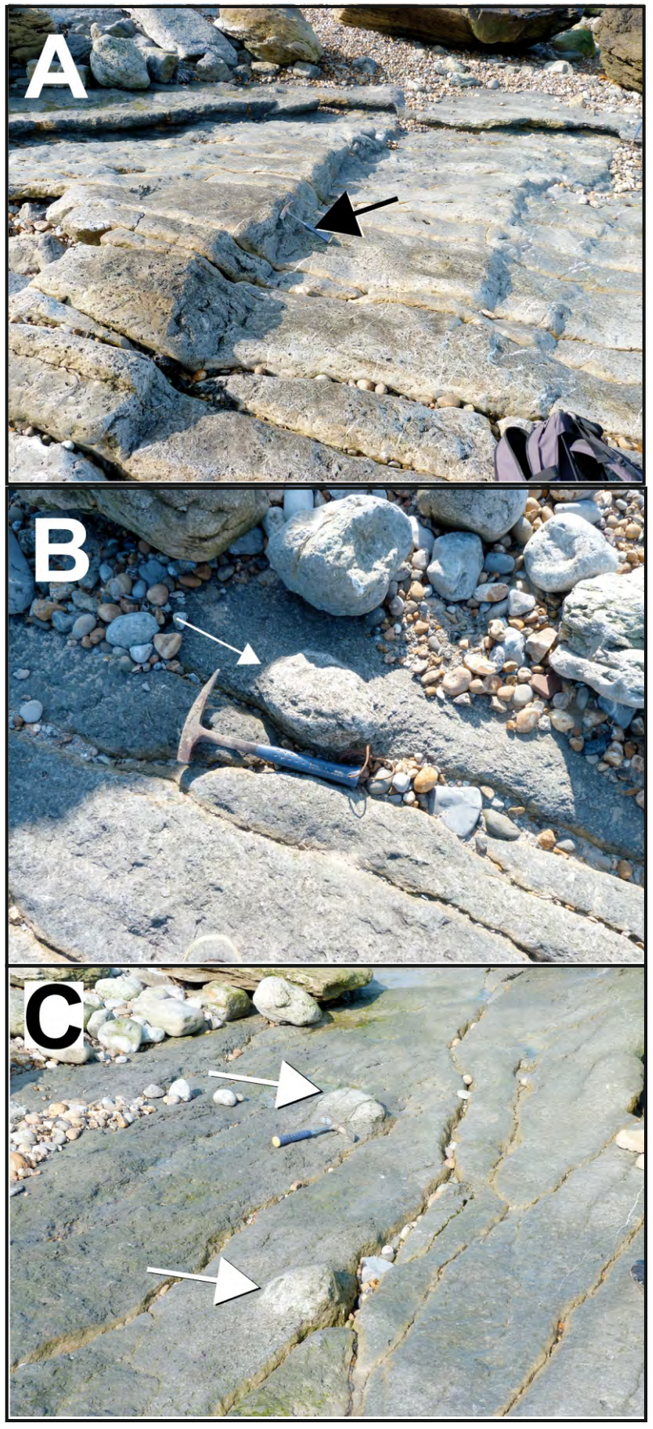

Figure 68: Synsedimentary soft deformations affecting the top bed of the Grès de Connincthun sandstones (A) and oyster patch reefs rooted on this bed (B and C) at La Sirène beach, Cap Griz Nez. photographs courtesy of O. Averbuch.

Figure 69: Photograph of one of the anticinal structure at the Cap Gris Nez, La Sirène beach. Photography courtesy of O. Averbuch.

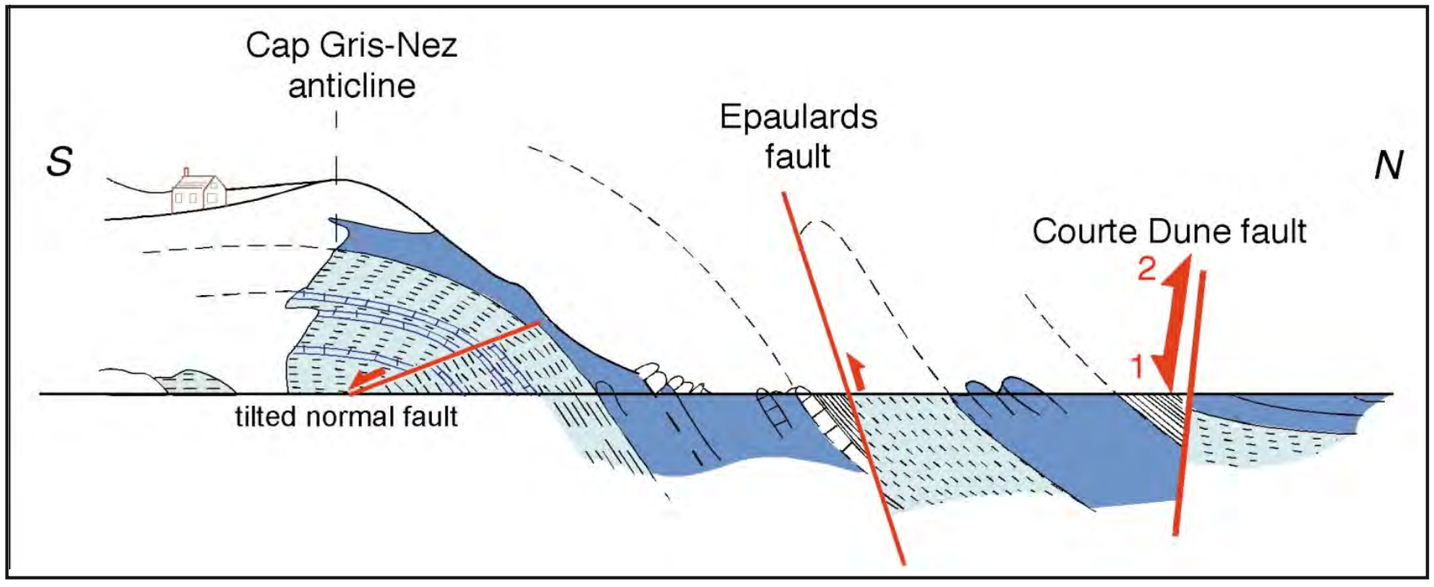

Figure 70: Section across the Cap Griz Nez fault zone on the Sirène beach (modified from Pruvost, 1925), O. Averbuch.

Day 3: Cap Gris Nez outcrop

Figure 71: Patch reef (photo courtesy of I. Millan).

Figure 72: Reworked, bioclasts-rich storm deposits, interbedded with sandy facies (photo courtesy of I. Millan).

Figure 73: Highly bioturbated sandstone bed (photo courtesy of I. Millan).

Figure 74: Highly bioturbated sandstone (photo courtesy of I.Millan).

Figure 75: Rhizocorarllium burrow (photo courtesy of I. Millan).

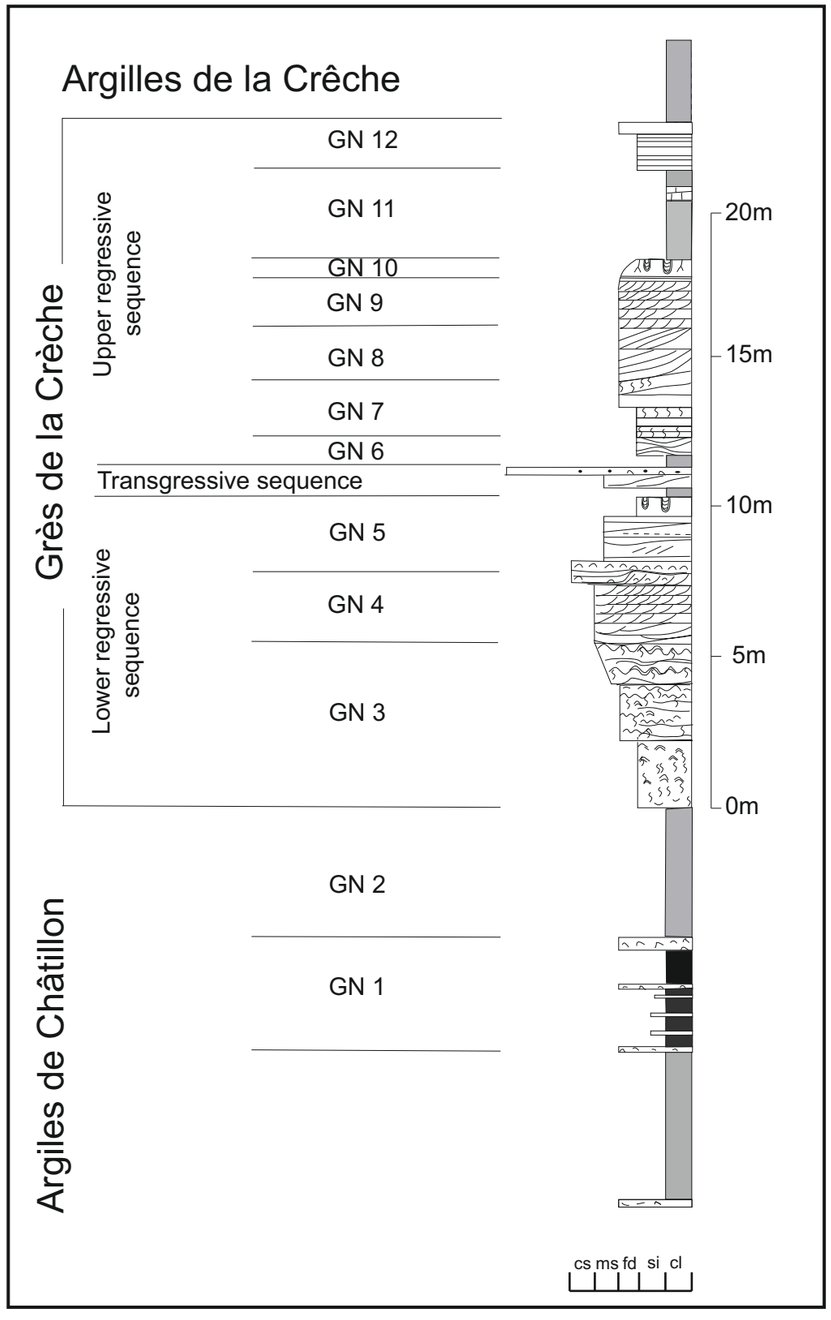

Figure 76: Synthetic stratigraphic column at the Cap Gris Nez outcrop (F. Busschers, unpublished).

Day 3: Cap Gris Nez outcrop

Figure 77: *Gyrochorte* burrows at the top of a sandy storm bed. Note double arched Spreiten. (photo courtesy of K. Geel).

Figure 78: *Diplocraterio*n burrows. The same block is show in Figure 80 from the side. See the double holes, which correspond to *Diplocraterion* (photo courtesy of I. Millan).

Figure 79: Carbonate concretions (Boules) in the Grès de la Crèche (photo courtesy of R. Bouroullec).

Figure 80: Side view of same block seen in Figure 76. Beautiful *Diplocraterio*n burrows observed (photo courtesy of I. Millan).

Figure 82: Cross-bedding in the sandstone and gravel beds of the Grès de la Crèche (photo courtesy of R. Bouroullec).

Figure 81: Sigmoidal and cross bedding in the Grès de la Crèche (photo courtesy of K. Geel).

References

Amedro F., Robaszynski F., 1999, Les craies cénomaniennes du Boulonnais. Comparaison avec l'Aube (France) et le Kent (Royaume Uni). Géologie de la France, 2, 33-53.

Averbuch O., Vidier J-P., Leduc A., Minguely B., 2011, Développement et inversion du bassin jurassique supérieur du Boulonnais : apport des affleurements côtiers entre Audresselles et Cap Gris-Nez. Georeg, Forum de la fédération française des géosciences. Géosciences des Régions de France et des pays environnants.

Braaksma, H., 2005, Geological and Petrophysical Calibration of Seismic Stratigraphy (Upper Jurassic Siliciclastics, Northern France. Phd Thesis Vrije Universiteit Amsterdam. ISBN 90-9019071-6.

Braaksma, H., Drijkoningen, G.G., Filippidou, N., Kenter, J.A.M. and Proust, J.N., 2006, The origin and nature of seismic reflections of sharp-based shoreface deposits (upper Jurassic Siliciclastics, northern France). Geophysical Prospecting, 2006, 54, 211–236.

Colbeaux, J. P., 1990, Analyse de structures post-cal6doniennes (Nord de la France, Sud de la Belgique), These Doct. Etat, Univ. Lille, 385 pp.

McEachern, J.A. and Bann, K.L., 2008, The role of ichnology in refining shallow marine facies models. In: Hampson, G.J. (ed) Recent Advances in Models of Siliclastic Shallow-Marine Stratigraphy, SEPM Special publication no. 90, p.73-116.

MacEachern, J.A., Bann, K.L., Pemberton, S.G. and Gingras, M.K., 2009, The ichnofacies paradigm: high-resolution paleoenvironmental interpretation of the rock record. In: MacEachern, J.A., K.L. Bann, S.G. Pemberton, and M.K. Gingras (Eds) Applied Ichnology, SEPM Short Course No 52, p.27-64.

Graham, L., Wong, T., Dusar, M., Andsbjerg, J., Monnig, E., Feldman-Olszewska, A., and Verreussel, R., 2010, Jurassic, Petroleum Geological Atlas of the Southern Permian Basin, eds. H. Doornenbal and A., Stevenson, Chapter 10, p. 175-193.

Mansy, J.L., Auffret, J.-P. and Guennoc, P., 2005, Carte géologique de la France, Feuille 5, Marquise, 2eme ediition, Echelle : 1/50 000, BRGM .

Mansy, J.-L., Manby, G., Averbuch, O., Everaerts, M., Bergerat, F., Van Vliet-Lanoe, B., Lamarche, J., & Vandycke, S., 2003, Dynamics and inversion of the Mesozoic basin of the Weald-Boulonnais area : role of basement reactivation. Tectonophysics, 373, 161-179.

Munsterman, D.K, Verreussel, R.M.C.H., Mijnlieff, H.F., Witmans, N., Kerstholt-Boegehold, S. and Abbink O.A., 2012, Revision and update of the Callovian-Ryazanian Stratigraphic Nomenclature in the northern Dutch offshore, i.e. Central Graben Subgroup and Scruff Group Netherlands Journal of Geosciences , Geologie en Mijnbouw, 91 – 4, p. 555 – 590.

Proust, J.N., Deconinck, J.F., Geyssant, J.R., Herbin, J. P. and Vidier, J.P., 1995, Sequence analytical approach to the Upper Kimmeridgian- Lower Tithonian storm-dominated ramp deposits of the Boulonnais (Northern France). A landward time equivalent to offshore marine source rocks. Geologische Rundschau 84, 255–271.

Proust J-N, Mahieux G., Tessier B., 2001, Field and seismic images of sharp-based shoreface deposits: implications for sequence stratigraphic analysis. Journal of Sedimentary Research 71, 6, 944-957.

Pruvost, P., 1925, Observations sur la structure du Cap Gris-Nez et sur les mouvements qui ont affecté le pays boulonnais après le dépôt du Jurassique. Bulletin des Services de la Carte Géologique de France et des topographies souterraines, N°156,Tome XXVIII,167-237.

Pruvost, P. and Pringle, J., 1924, A synopsis of the geology of the Boulonnais including a correlation of the Mesozoic rocks with those of England, with report of excursion. Proceedings of the Geologists' Association, 35, 29-67.

Schlirf, M., 2003, Palaeoecologic significance of Late Jurassic trace fossils from the Boulonnais, N France. Acta Geologica Polonica, Vol. 53 (2003), No. 2, pp. 123-142.

Tribovillard, N., Bialkowski, A., Tyson, R.V., Lallier-Verges, E. and Deconinck, J.-F., 2001, Organic facies variation in the late Kimmeridgian of the Bouilonnais area (northernmost France), Marine and Petroleum Geology, 18, p. 371-389.

Tribovillard, N., Sansjofre, P., Ader, M., Trentesaux, A., Averbuch, O. and Barbecot, F., 2012a, Early diagenetic carbonate bed formation at the sediment–water interface triggered by synsedimentary faults. Chemical Geology 300-301, p. 1–13.

Tribovillard N., Algeo, T.J., Baudin, F., Riboulleau, A., 2012b, Analysis of marine environmental conditions based on molybdenum–uranium covariation - Applications to Mesozoic Paleoceanography. Chemical Geology 324-325, p. 46–58.

Wignall, P.B., Sutcliffe, O.E., Clemson J. and Young E., 1996, Unusual shoreface sedimentology in the upper Jurassic of the Boulonnais, northern France. Journal of Sedimentary Research 66, p. 577–586.

Wignall, P. and Newton, R., 2001, Black shales on the basin margin : a model based on examples from the Upper Jurassic of the Boulonnais, northern France. Sedimentary Geology 144, 335-356.

Appendix 1: Ichnofacies in shallow marine rocks

Skolithos ichnofacies

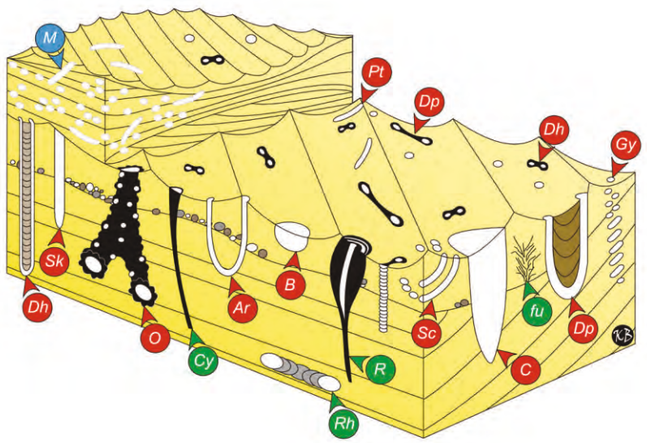

Appendix 1a: Schematic block diagram of the *Skolithos* Ichnofacies, Trace fossil abbreviations are as follows: *Arenicolites* (Ar), *Bergaueria* (B), *Conichnus* (C),*Cylindrichnus* (Cy), *Diplocaterium habichi* (Dh), fugichnia (fu), *Gyrolithes* (Gy), *Macaronichnus* (M), *Ophiomorpha* (O), *Palaeophycus* (Pt), *Rosselia* (R), *Rizocollarium* (Rh), *Schaubcylindrichnus* (Sc), and *Skolitus* (SK). Red labels reflect common constituents. Green labels show facies-crossing forms that are less common, and which occur in the *Cruziana* Ichofacies as well. Blue lavel marks assemblage that replaces *Skolithos* Ichonofacies in some settings.

Cruziana ichnofacies

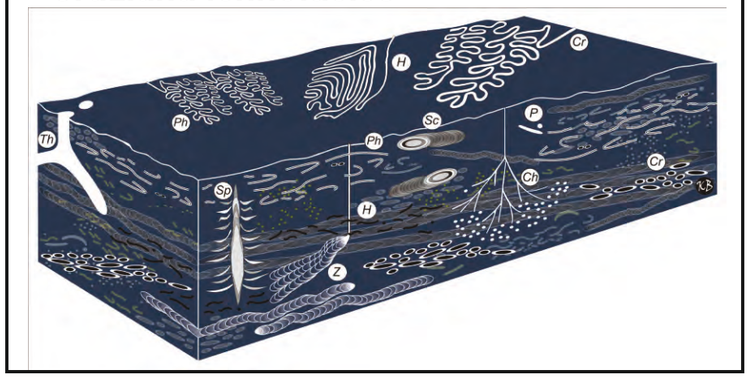

Appendix 1b: Schematic block diagram of the Cruziana Ichnofacies. Common traces include Arenicolites (Ar), Asterosoma (As), Chondrites (Ch), Cosmorhaphe (Cr), Cruziana (Cu), Cylindrichnus (Cy), Diplocraterion habichi (Dh), Gyrochorte (Gy), Helminthopsis (H), Lockeia (Lo), Ophiomorpha (O), Palaeophycus tubularis (Pt), Phoebichnus (Pb), Phycodes (Pc), Phycosiphon (Ph), Planolites (P), Psammichnites (Ps), Rhizocorallium (Rh), Rosselia socialis (Rs), Rosselia rotatus (Rr), Rusophycus (Ru), Siphonichnus (Si), Skolithos (S), Taenidium (Ta), Teichichnus (T), Thalassinoides (Th), and Zoophycos (Z).

Zoophycos ichnofacies

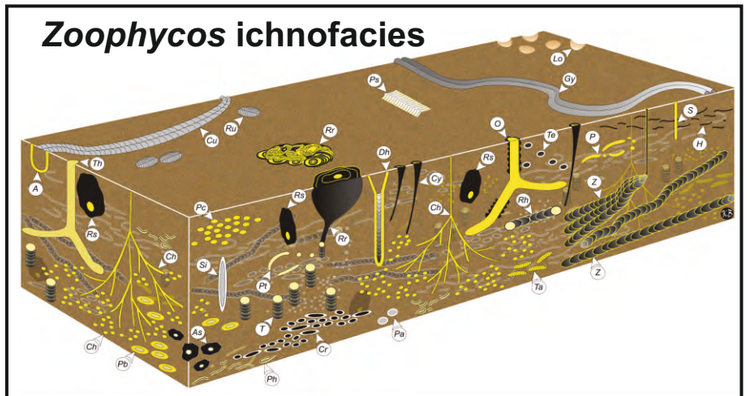

Appendix 1c: Schematic block diagram of the Zoophycos Ichnofacies. Traces include Chondrites (Ch), Cosmorhaphe (Cr), Phycosiphon (Ph), Planolites (P), Scolicia (Sc), Spirophyton (Sp), Thalassinoides (Th), and Zoophycos (Z).

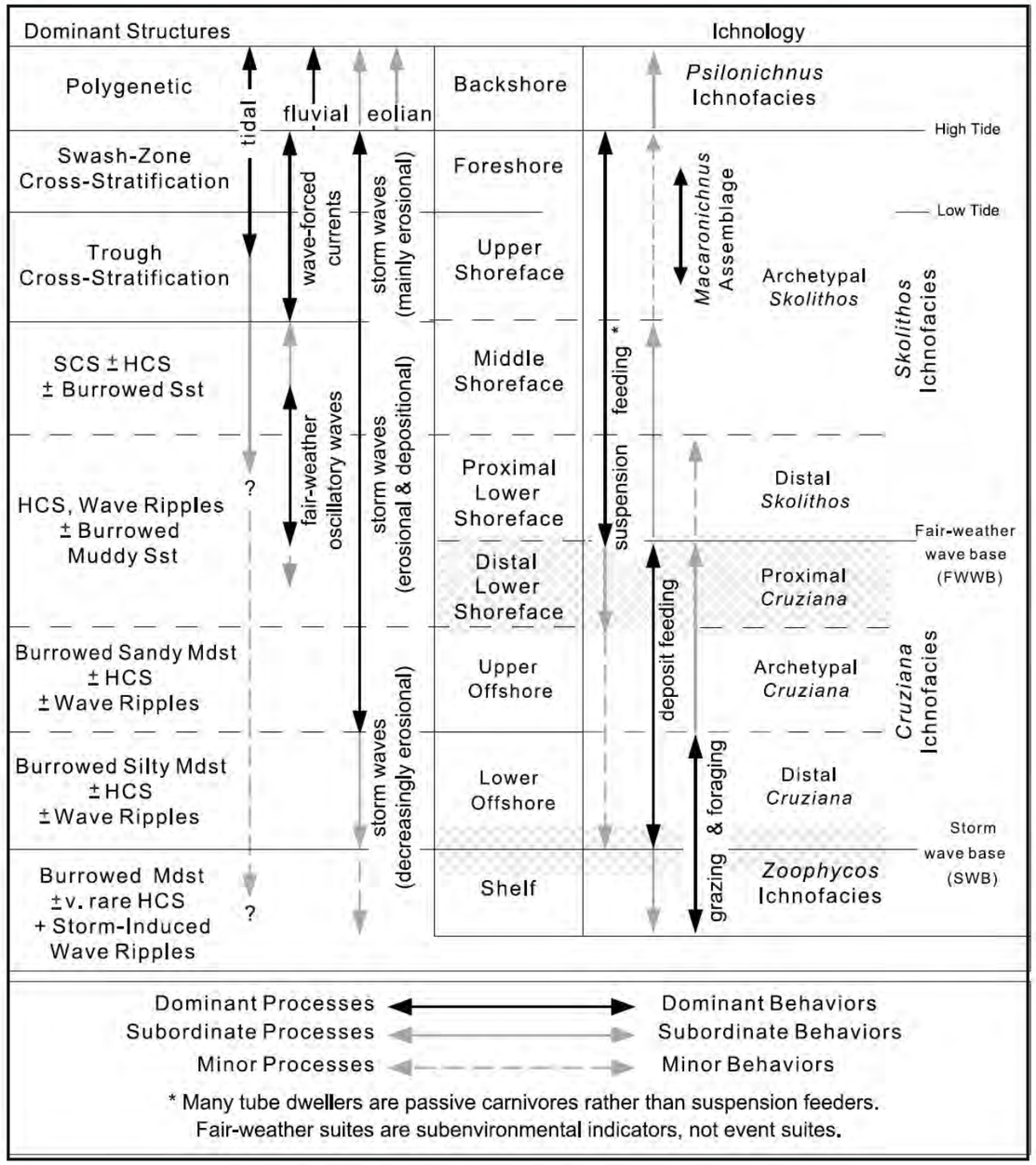

Appendix 1d: Integrated ichnological–sedimentological model for strandplain shoreface subenvironments, showing archetypal as well as proximal and distal expressions of ichnofacies. From McEachern & Bann (2008).

Compiled from Pemberton (2010), McEachern et al (2009), McEachern & Bann (2008)

Appendix 1: Ichnofacies in shallow marine rocks

Lower to middle shoreface

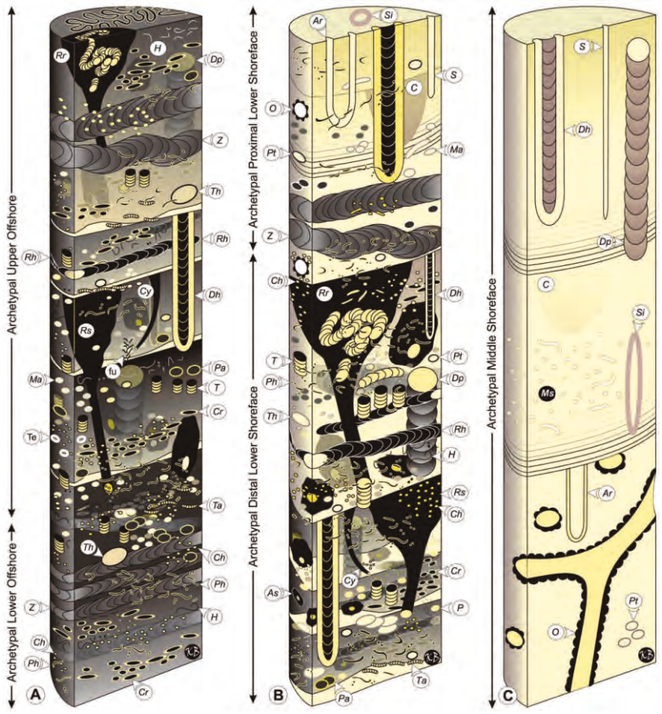

Appendix 1e: Schematic split-core diagrams of representative sections of a lower-oshore to middle-shoreface succession, showing the typical ichnogenera expected. Approximate core diameter 10 cm; core lengths not to scale. **A)** Lower-oshore to upper-oshore setting, showing an upward increase in sandstone and tempestite thickness and abundance, and a change from mainly grazing and deposit-feeding structures to predominantly deposit-feeding structures with subordinate grazing and suspension-feeding structures. **B)** Distal lower-shoreface to proximal lower-shoreface setting, showing an upward increase in sandstone and thickening of tempestites. Trace fossils show a change from predominantly deposit-feeding structures with subordinate grazing and suspension-feeding structures to equal proportions of deposit-feeding and suspension-feeding structures, with minor grazing structures. **C)** Middle-shoreface setting, showing stacked parallel-laminated sandstones (tempestites) and burrowed sandstones. Traces are dominated by dwelling structures of suspension feeders, passive carnivores, and Iterfeeders. Interstratal deposit-feeding structures are locally present. Trace-fossil codes are as follows: Arenicolites (Ar), Asterosoma (As), Conichnus (C), Chondrites (Ch), Cosmorhaphe (Cr), Cylindrichnus (Cy), Diplocraterion habichi (Dh), Diplocraterion parallelum (Dp), fugichnia (fu), Helminthopsis (H), Macaronichnus segregatis (Ms), Macaronichnus simplicatus (Ma), Ophiomorpha (O), Planolites (P), Palaeophycus heberti (Pa), Palaeophycus tubularis (Pt), Phycosiphon (Ph), Rhizocorallium (Rh), Rosselia rotatus (Rr), Rosselia socialis (Rs), Skolithos (S), Siphonichnus (Si), Taenidium (Ta), “Terebellina” (sensu lato) (Te), Teichichnus (T), Thalassinoides (Th), and Zoophycos (Z).

Brackish water - bay

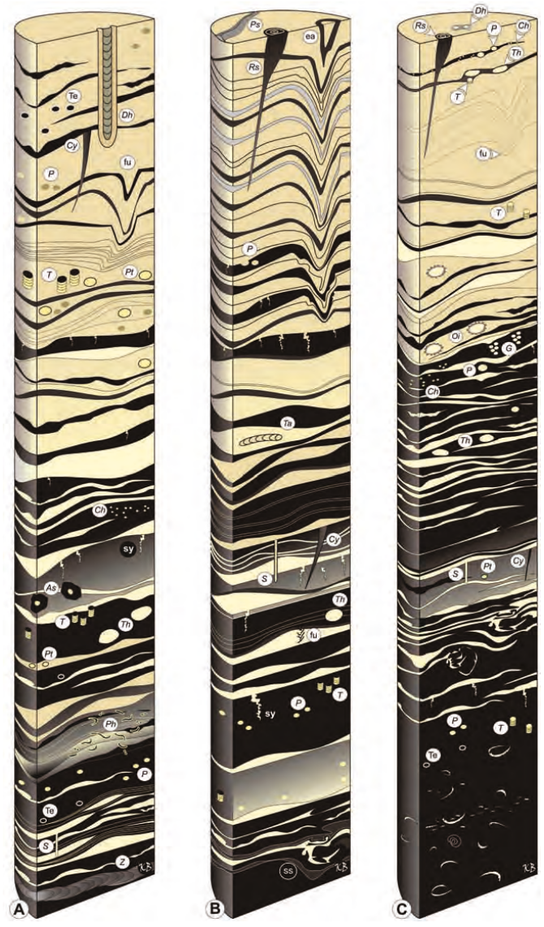

Appendix 1f: Schematic split-core diagrams of brackish-water-bay successions, showing the typical ichnogenera expected from distalbay (mud-prone) to bay-margin (sand-prone) facies. Approximate core diameter 10 cm; core lengths not to scale. **A)** Idealized succession of an open-bay deposit, based on observations of the Lower Cretaceous Viking Formation of the Jore Field, Alberta (cf. MacEachern et al., 1998; MacEachern et al., 1999a). **B)** Idealized succession of a restricted-bay succession, based on the Permian Pebbley Beach Formation, South Sydney Basin, Australia. **C)** Idealized succession of a central-bay deposit, based on wavedominated central basins of estuary complexes in the Lower Cretaceous Bluesky Formation, Paddy Member, and Viking Formation, Alberta. Trace-fossil codes are as follows: Asterosoma (As), Chondrites (Ch), Cylindrichnus (Cy), Diplocraterion (Dh), bivalve equilibrium-adjustment (ea), fugichnia (fu), Gyrolithes (G), Ophiomorpha irregulaire (Oi), Planolites (P), Palaeophycus tubularis (Pt), Phycosiphon (Ph), Psammichnites (Ps), Rosselia socialis (Rs), Skolithos (S), Taenidium (Ta), “Terebellina” (sensu lato Teichichnus (T), Thalassinoides (Th), and Zoophycos (Z). Sedimentologic symbols: synaeresis cracks (sy) and soft sediment deformation (ss).

Deltaic & strandplain shoreface

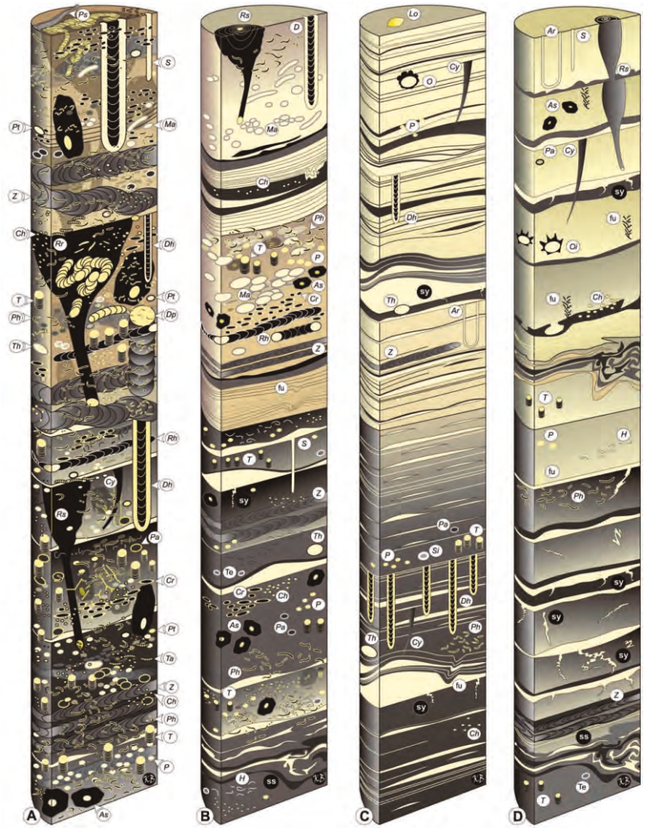

Appendix 1g: Schematic split-core diagrams of deltaic successions, compared to a strandplain shoreface, showing the typical ichnogener a expected. Approximate core diameter 10 cm; core lengths not to scale. **A)** Idealized onshore to lower-shoreface deposits of a nondeltaic strandplain shoreline. **B)** Idealized prodelta to delta-front succession of a wave-dominated to storm-inuenced delta, modeled after a number of Permian units of the Denison Trough, Australia. **C)** Idealized prodelta to delta-front succession of a tide-dominated delta, modeled after the Lower Jurassic Tilje Formation, Norway and Upper Cretaceous Frewens Sandstone, Wyoming. **D)** Idealized prodelta to delta-front succession of a river-dominated delta, modeled after the Middle Jurassic Oseberg Formation of Norway and Upper Cretaceous Dunvegan Formation (Allomember E), of Alberta. Trace-fossil codes are as follows: Arenicolites (Ar), Asterosoma (As), Chondrites (Ch), Cosmorhaphe (Cr), Cylindrichnus (Cy), Diplocraterion habichi (Dh), Diplocraterion parallelum (Dp), fugichnia (fu), Helminthopsis (H), Lockeia (Lo), Macaronichnus isp. (Ma), Ophiomorpha (O), Ophiomorpha irregulaire (Oi), Planolites (P), Palaeophycus heberti (Pa), Palaeophycus tubularis (Pt), Phycosiphon (Ph), Psammichnites (Ps), Rhizocorallium (Rh), Rosselia rotatus (Rr), Rosselia socialis (Rs), Skolithos (S), Siphonichnus (Si), Taenidium (Ta), “Terebellina” (sensu lato) (Te), Teichichnus (T), Thalassinoides (Th), and Zoophycos (Z). Sedimentologic symbols: synaeresis cracks (sy) and soft-sediment deformation (ss).

Compiled from McEachern et al (2009) and McEachern & Bann (2008)

Appendix 2: Sedimentary Facies and Architectural Elements

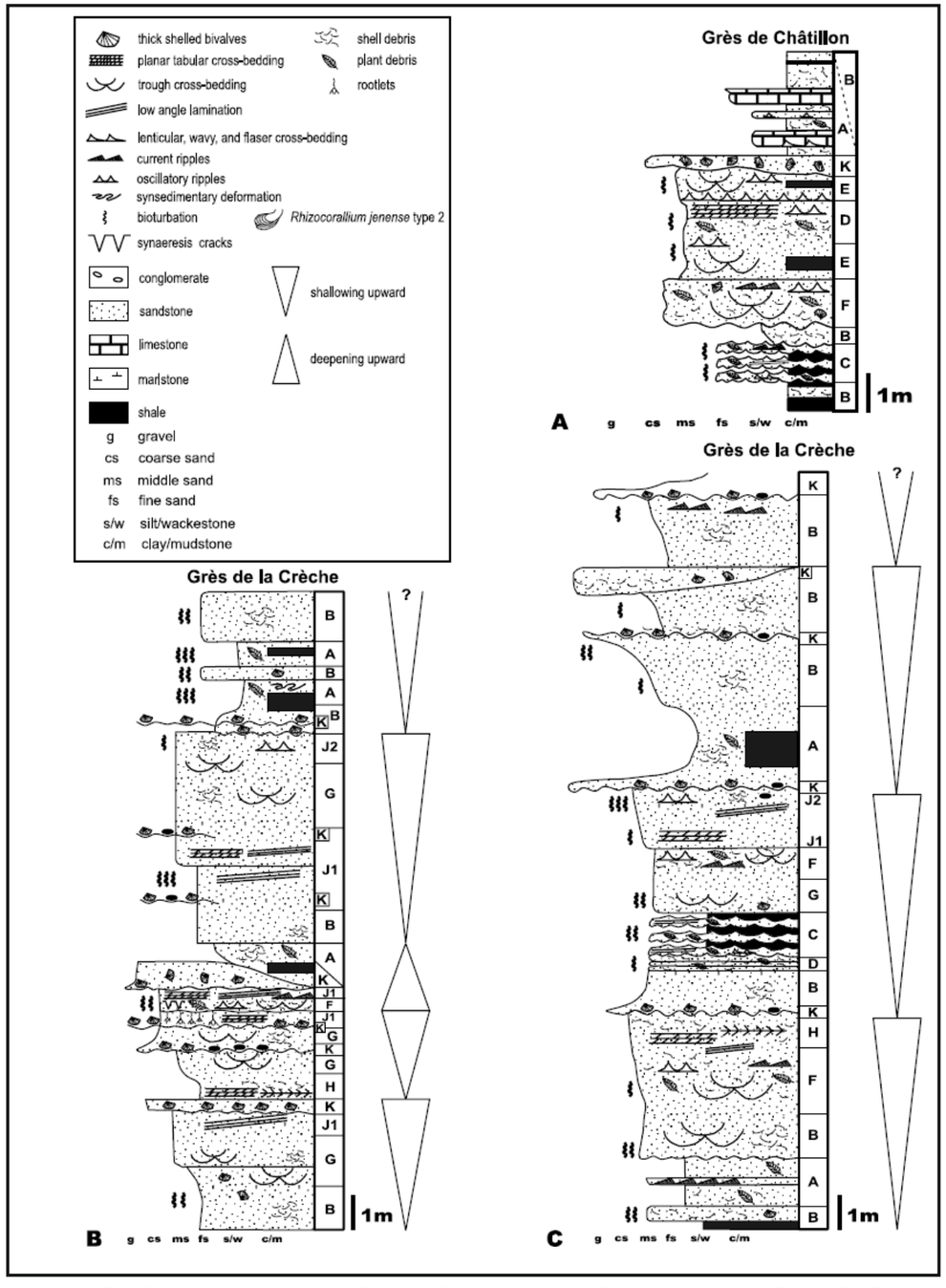

Appendix 2a: Generalized logs of the Grès de Châtillon (A) and Grès de la Crèche (B and C). B is a proximal section while C is a more distal section. Modified after Proust et al., (1995) and Wignall et al. (1996).

Facies Number	Description	Palaeoenvironment	Common Trace Fossils
Facies A	sharp based, highly bioturbated, shelly mudstone and siltstone; occasional plant remains; no primary sediment structures detectable due to high degree of bioturbation	unrestricted open marine conditions; storm influenced offshore deposits	difficult to assign due to high degree of bioturbation; occasionally *Palaeophycus tubularis* and *Planolites* determinable
Facies B	fine to medium sandstone, commonly argillaceous, with occasional shell gravel beds mostly made up of *Isognomon* and *Gervillella;* highly bioturbated	bioturbation dominated, storm influenced upper offshore	*Spongeliomorpha suevica* maze, *Rhizocorallium jenense* type 1, *Teichichnus*
Facies C	isolated lenses and thin-bedded, oscillation-rippled fine to medium sandstone; plant remains; erosional base showing tool marks; embedded in silty clay; low density bioturbation	tide, wave and storm influenced transition zone between shoreface and offshore	*Bolonia lata*, *Gyrochorte comosa, Chondrites intricatus*, *Rhizocorallium irregulare*, *Rh. jenense* type 1, *Lockeia siliquaria*
Facies D	thin- to medium-bedded (max. 20cm), oscillation-rippled, argillaceous, medium sandstone with erosional base showing tool marks and rare gutter casts; plant remains and shell debris common; low to high density bioturbation	wave and storm influenced lower to mid shoreface	*Teichichnus patens, Taenidium barretti*, *Asterosoma ludwigae*, *Spongeliomorpha suevica* type B, *Rosselia socialis*, concentrically laminated burrows, *S. nodosa* type C, *Rhizocorallium jenense* type 1, *Chondrites intricatus*
Facies E	decimetre-scale trough cross-bed sets (foreset angle app. 30°) of medium sandstone with mudstone intraclasts concentrated on the toesets; cross beds truncated by centimetre-thick medium, oscillation rippled sandstone with sharp base	wave and storm influenced lower shoreface to transition zone	*Rhizocorallium irregulare*, *Nereites missouriensis*, *Chondrites intricatus*
Facies F	oscillation- and current-ripple topped decimetre-scale, trough cross-bedded medium to coarse sandstones with shell and plant remains; occasional synaeresis cracks and flat topped ripple surfaces; partially completely bioturbated	tide, storm and wave influenced upper shoreface to foreshore	*Palaeophycus tubularis*, *Spongeliomorpha nodosa* type B, *Teichichnus*, *Planolites*, *Spongeliomorpha suevica* type B, *Rosselia*, *Treptichnus*
Facies G	trough cross-bedded medium sandstone with shell material, trough heights 30 to 50 cm; coset boundaries planar, marking abrupt increase in grain size, tool marks common	shoreface	*Diplocraterion parallelum*, *Spongeliomorpha nodosa* type B & C, *Rhizocorallium jenense* type 1, *Skolithos linearis*, *Spongeliomorpha suevica* type B, *Rosselia*
Facies H	tabular cross-bedded fine to medium sandstones with shell material; herringbone cross-stratification common	wave and tide dominated shoreface	
Facies J1	swash cross-stratified medium to coarse sandstones with very low angle cross- to planar-lamination	foreshore	*Diplocraterion parallelum*, *Rhizocorallium jenense* type 1, *Spongeliomorpha suevica* type B & C, rootlets
Facies J2	partially highly bioturbated, medium to coarse sandstone with low angle- to planar-cross stratification; shell debris (*Nanogyra*) and occasional quartz pebbles; surfaces with oscillation-ripple relics	wave influenced foreshore	*Rhizocorallium jenense* type 2, *Teichichnus*, *Palaeophycus*, *Spongeliomorpha nodosa* type B
Facies K	shell gravel, up to 70 cm thick, mainly made up of thick shelled bivalves (predominantly *Laevitrigonia*) and occasionally exotic clasts; reactivation surfaces present	upper offshore to foreshore	

Appendix 2b: Facies types and paleoenvironments of the Upper Jurassic rocks of the Grès de Châtillon and Grès de la Creche. Combined by Schlirf (2003) after Proust et al., (1995) and Wignall et al. (1996).

Notes

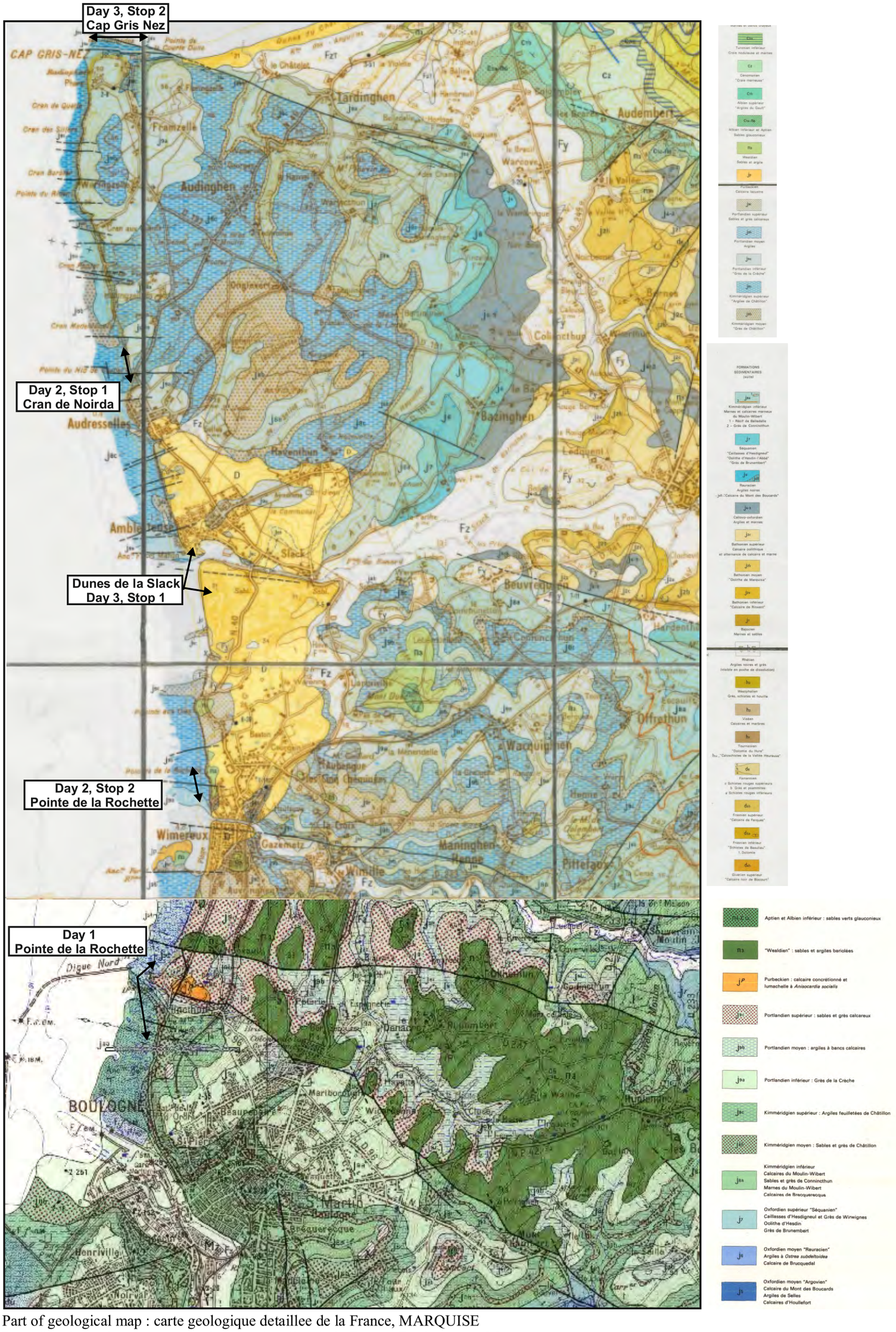

Part of geological map : carte geologique detaillee de la France, MARQUISE
Part of geological map : carte geologique detaillee de la France, Boulogne sur Mer

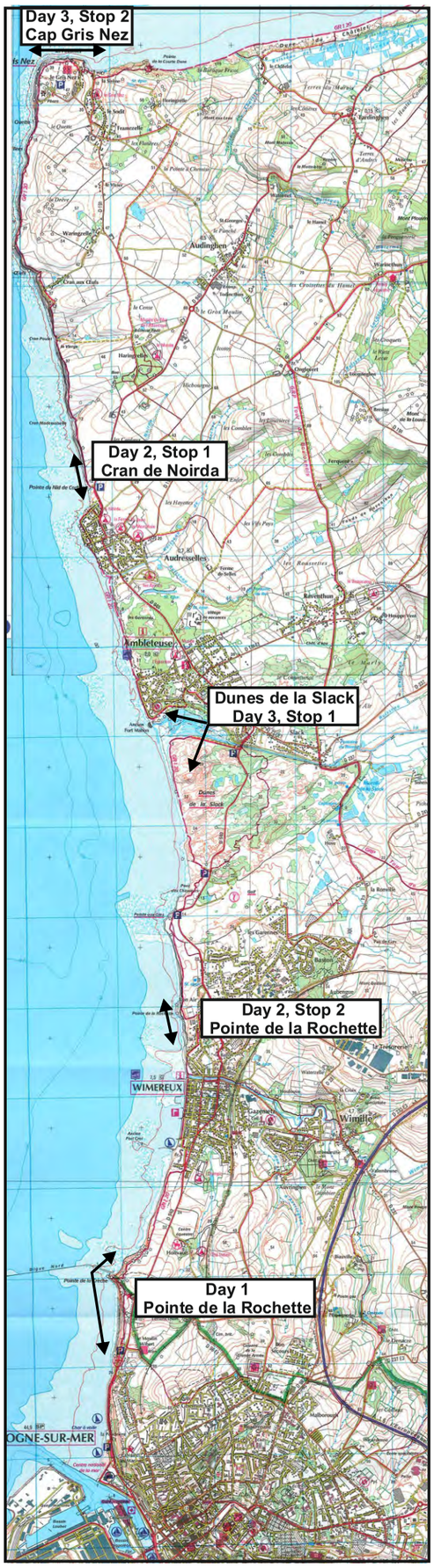

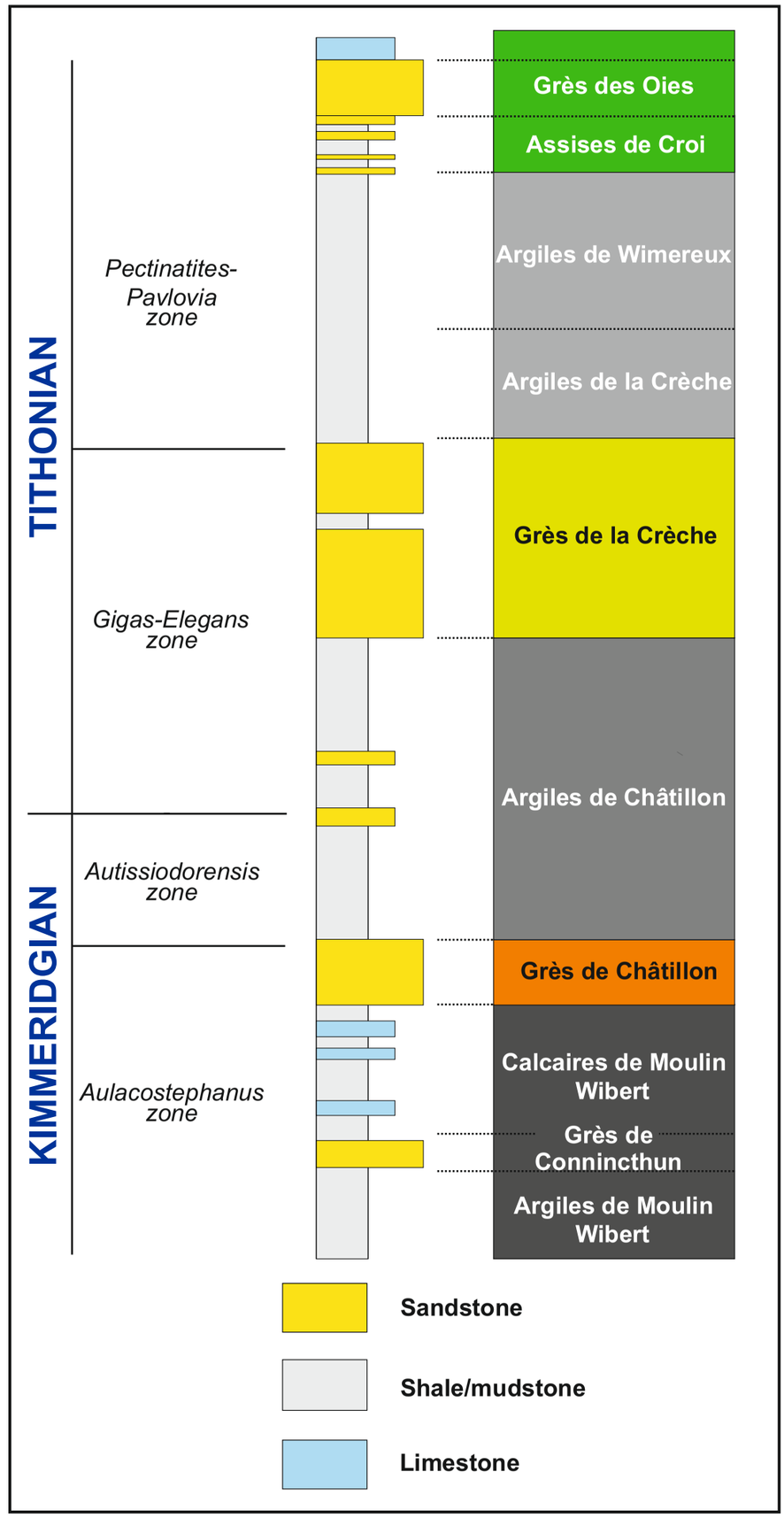

Lithostratigraphic, biostratigraphic and sequence stratigraphic framework of the Upper Jurassic rocks of the Boulonnais. RModified from Busschers (1995).

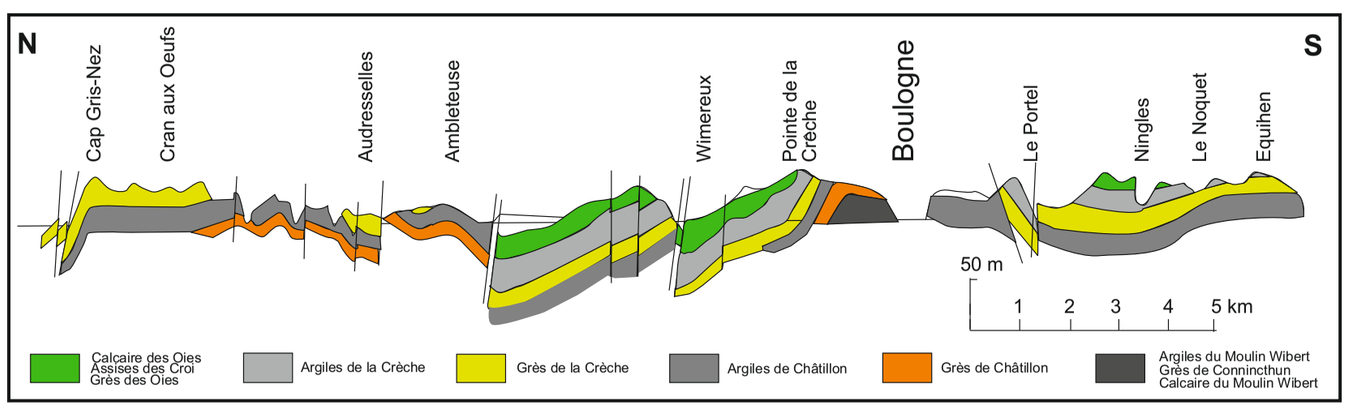

Cross section of the Boulonnais coastal outcrop belt between Equihen and Cap Gris Nez. Modified from Pruvost and Pringle, 1924; modified from Colbeaux, 1990; Modified by Busschers, 2015).

TNO innovation for life

For more information and questions, please contact:

Friso Veenstra
✉ friso.veenstra@tno.nl
✆ +31 (0) 88 866 53 55